

**SYNTHESES OF UNNATURAL AMINO ACIDS, PEPTIDES
AND NOVEL FLUORESCENT MOLECULES FROM
TROPOLONE**

By
CHENIKKAYALA BALACHANDRA

Enrolment No: **CHEM11201104010**

**National Institute of Science Education and Research (NISER)
Bhubaneswar**

*A thesis submitted to the
Board of Studies in Chemical Sciences
In partial fulfillment of requirements
for the Degree of
DOCTOR OF PHILOSOPHY
of
HOMI BHABHA NATIONAL INSTITUTE*



January, 2017

Homi Bhabha National Institute¹

Recommendations of the Viva Voce Committee

As members of the Viva Voce Committee, we certify that we have read the dissertation prepared by **Chenikkayala Balachandra** entitled **Syntheses of Unnatural Amino Acids, Peptides and Novel Fluorescent Molecules from Tropolone** and recommend that it may be accepted as fulfilling the thesis requirement for the award of Degree of Doctor of Philosophy.


Chairman – Prof. A. Srinivasan

Date: 24.11.17


Guide / Convener – Dr. Nagendra K. Sharma

Date:


Examiner – Prof. Santanu Bhattacharya

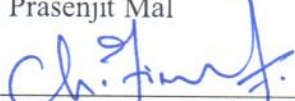
Date:


Member 1- Dr. Chidambaram Gunanathan

Date:


Member 2- Dr. Prasenjit Mal

Date:


Member 3- Dr. Tirumala Kumar Chowdary

Date:

Final approval and acceptance of this thesis is contingent upon the candidate's submission of the final copies of the thesis to HBNI.

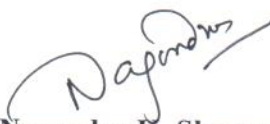
I/We hereby certify that I/we have read this thesis prepared under my/our direction and recommend that it may be accepted as fulfilling the thesis requirement.

Date: 24/11/2017

Place: Bhubaneswar

<Signature>

Co-guide (if applicable)


Dr. Nagendra K. Sharma
Guide

¹ This page is to be included only for final submission after successful completion of viva voce.

STATEMENT BY AUTHOR

This dissertation has been submitted in partial fulfillment of requirements for an advanced degree at Homi Bhabha National Institute (HBNI) and is deposited in the Library to be made available to borrowers under rules of the HBNI.

Brief quotations from this dissertation are allowable without special permission, provided that accurate acknowledgement of source is made. Requests for permission for extended quotation from or reproduction of this manuscript in whole or in part may be granted by the Competent Authority of HBNI when in his or her judgment the proposed use of the material is in the interests of scholarship. In all other instances, however, permission must be obtained from the author.

Chenikkayala Balachandra

DECLARATION

I, hereby declare that the investigation presented in the thesis has been carried out by me. The work is original and has not been submitted earlier as a whole or in part for a degree / diploma at this or any other Institution / University.

Chenikkayala Balachandra

List of Publications arising from the thesis

Journal

1. **Balachandra, C.;** Sharma, N. K. Synthesis and Conformational Analysis of New Troponyl Aromatic Amino Acid. *Tetrahedron* **2014**, 70, 7464-7469.
2. **Balachandra, C.;** Sharma, N. K. Instability of Amide Bond Comprising the 2-Aminotropone Moiety: Cleavable under Mild Acidic Conditions. *Org. Lett.* **2015**, 17, 3948-3951.
3. **Balachandra, C.;** Sharma, N. K. Novel Fluorophores: Synthesis and Photophysical Studies of Boron-Aminotroponimines. *Dyes and Pigments*, **2017** 137, 532-538.

Others (Manuscripts communicated and under preparation):

1. **Balachandra, C.;** Sharma, N. K. Direct/Reversible amidation of Troponyl alkylglycinates via Cationic Troponyl Lactones and Mechanistic Insights. (*Under Revision*).
2. **Balachandra, C.;** Sharma, N. K. Cyclic Aminotroponimines: pH and Solvent Dependent Fluorophores. (*Manuscript under preparation*).
3. **Balachandra, C.;** Sharma, N. K. Syntheses of *Hexa*-Peptides via alkyl linkers and their applications. (*Manuscript under preparation*).

Chapters in books and lectures notes: NA

Conferences

1. **Balachandra, C.;** Sharma, N. K. Presented a poster on "Synthesis and Conformational Analysis of New Troponyl Aromatic Amino Acid" in JNOST-2014, Department of Chemistry, IIT-Madras.
2. **Balachandra, C.;** Sharma, N. K. Oral presentation on "Introducing tropone moiety on aminoethylglycine backbone destabilizes the amide bond derived from *Traeg*: Cleavable in the presence of 5.0% TFA." Indian Peptide Society-2015, JNCASR, Bengaluru. Awarded Best Oral Presentation.
3. **Balachandra, C.;** Sharma, N. K. Presented a poster on "Cleavable Amide Bond in 5.0% TFA." in JNOST-2015, SCS, NISER-Bhubaneswar.

Chenikkayala Balachandra

To My Family

ACKNOWLEDGEMENTS

“Finally, I got opportunity to thank the people who are helped me to reach this stage of life. Yes, I do know that a simple thanks must not rebate, what they have done for me, but it makes me happy.

First, I must have to thank only one person, who made this thesis possible. Wait! wait! I want memorize some experiences before thanking him. I joined the NKS research group at NISER as a PhD student in January 2012 just after my master’s degree specialized in organic chemistry. In fact, I am second PhD student in NKS research group. When I joined the group, I had only theoretical knowledge and little bit of basic experimental knowledge. Today, if I look back, I have gained enormous professional experience. I already said, I am second student in NKS research group. My supervisor is also started his career with us and he is very dynamic. He used to work like us in his initial years. He was available for us all the time. This helped me a lot to learn most of the things from him. He taught us most of the professional skills from the scratch. I don’t know how do I begin to thank my supervisor Dr. Nagendra Kumar Sharma (NKS). As a research guide and teacher, he is an intellectual person. As a research supervisor, he has always been there to give valuable suggestions and important clues at difficult steps of my work. He has been always there to congratulate me and share his happiness during happy moments in our research. I spend more than five years of my life as his student. Undoubtedly, I am his student for the remainder of my life. Finally, I express my heartfelt gratitude to my supervisor Dr. Nagendra.

Most importantly, I started my education at the age of four years in our village elementary school. We had an excellent and wise teacher Mr S. Naganna. I also want to express my deepest gratitude to him.

In my intermediate (11 and 12th class), we also had an intellectual and smart teacher, who can teach chemistry like a tasty dish, he is who inspired me to take chemistry as my career. He is Mr. G. Naga Mallaya.

Throughout my student career, I am fortunate to have encouraging, wise and friendly teachers, they are Mr. Reddappa Reddy, Mr. Babu, Mr. Lakshimi Narayana, Mr. Kadhar Vali, Mr. Obul Reddy, Mr. Dasaradha Rami Reddy, I want to express my gratitude to all of them.

I express my sincere gratitude to my M.Sc., teachers Dr. K. Venkateswarulu, Dr. P. Vasugovardhan Reddy and Dr. Loka Subramanya Sharma.

I express my sincere thanks to Dr. Himansu S. Biswal for providing energy minimized structure for one of our peptides and Dr. Moloy Sarkar for his helpful discussions.

I want to express my heartfelt thanks to my friends Mr. Raviteja Nanabala, Mr. Ashok Kumar Reddy, Mr. Manohar Naidu, Mr. Dasthagiri and Mr. Sanjeeva Reddy. A special thanks to Mr's. Prasanthi Reddy.

I extend my gratitude to our founder director Prof. T. K. Chandrasekhar and present director Prof. V. Chandrasekhar for providing infrastructure.

I want to thank Prof. A. Srinivasan, Dr. C. Gunanathan (course work teacher also), Dr. Prasenjit Mal and Dr. Tirumal Kumar Choudhry (SBS) for being as my doctoral committee members.

I also want to thank my course work teachers Dr. Sudip Barman, Dr. V. Krishnan, Dr. Arindam Gosh and Prof. T. K. Chandrasekhar.

A special thanks to Dr. S. Peruncheralathan (SCS-NISER)

I also want to thank our past and present lab members, Ujwal, Chandrasekhar, Amar, Saikat, Amiya, Bhibuthi, and Dr. Smitha.

Further, I want to thank all friends and colleagues in common lab, Giriteja, Manoj, Adhi, Saikat, Tapas, Subbu, Venkat, Mriganka and Tirupathi.

I want to memorise help and co-operation of my family members during my hurdles, my father, mother, grandmother, aunt, younger brother and sister. I should not thank them, but a five minutes chatting with them over phone was a great relief during hurdles.

I am happy to remind my uncle, my friend and my philosopher Mr. V. Sanjeeva. Finally, I want to remind the almighty 'GOD' for giving me energy to overcome hurdles and to do hard work."

SYNOPSIS

Synthesis of Unnatural Amino Acids, Peptides and Novel Fluorescent Molecules from Tropolone

Chapter 1. Introduction

Tropolone: In 1942, Horald Raistrick isolated the natural products such as puberulonic acid, puberulic acid and stipitatic acid, though he proposed the chemical formula of these compounds and unable to propose a chemical structure.^{1a,b} After three years, Michael Dewar proposed a seven membered ring tropolonoid structure for Stipitatic acid.^{1c,d} Since then, many tropolonoid natural products were isolated and explored their biological activities.^{1f} Among them Thujaplicins, Colchicine, Manicol, β -Thujaplicinol, and Pycnidione are a few examples. In addition, tropolone forms dimeric metal complexes with metals like Be, Cu (II) and Zn (II) etc.^{1e} Aminotroponimines and their metal complexes were extensively synthesized as structural analogues of tropolone.^{1h}

Peptidomimetics: Peptides from natural amino acids are extensively synthesized and their secondary structures are studied. The secondary structure of peptides are responsible for the execution of their specific biological function.² The formation of secondary structure of any peptide is governed by the conformational preference of individual amino acid residue and hydrogen bonding.^{2g} Though natural synthetic peptides are potential to perform the biological functions, but these are less stable towards proteolytic enzymes.² To overcome these issues unnatural amino acids and peptides were developed. To date, several unnatural amino acids and their peptides with established secondary structures and biological functions are reported.²

Inspired from the biological importance of tropolonyl moiety and peptidomimetics, we planned to use the troponyl moiety as a conformation guiding substituent in the peptidomimetics. So far, there are no such reports, where tropone moiety is used as a conformation guiding substituent in the synthetic peptides.

Chapter 2. Synthesis and Conformational Analysis of New Amino acid- Troponyl aminoethylglycine (*Traeg*): This chapter explains the synthesis of rationally designed unnatural amino acid, Troponyl aminoethyl glycine (*Traeg*, **Figure 2.1A**) and role of the troponyl moiety in conformational preference/hydrogen bonding in its *Traeg*-aa (δ/α)-hybrid peptides.⁴ Synthesis of *Traeg* amino acid was achieved by following the **Scheme 2.1A**. Then, we attempted to synthesize the *Traeg* homologous peptides (**Figure 2.1B**) from the *Traeg* amino acid through the Standard Solid and Solution Phase Peptide Synthesis. Unfortunately, these attempts were unsuccessful. Then, we have synthesized the hybrid peptides from *Traeg* and α -amino acid derivatives by following **Scheme 2.1B**.

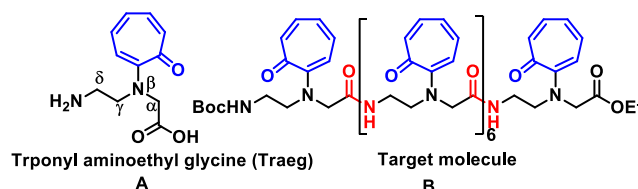
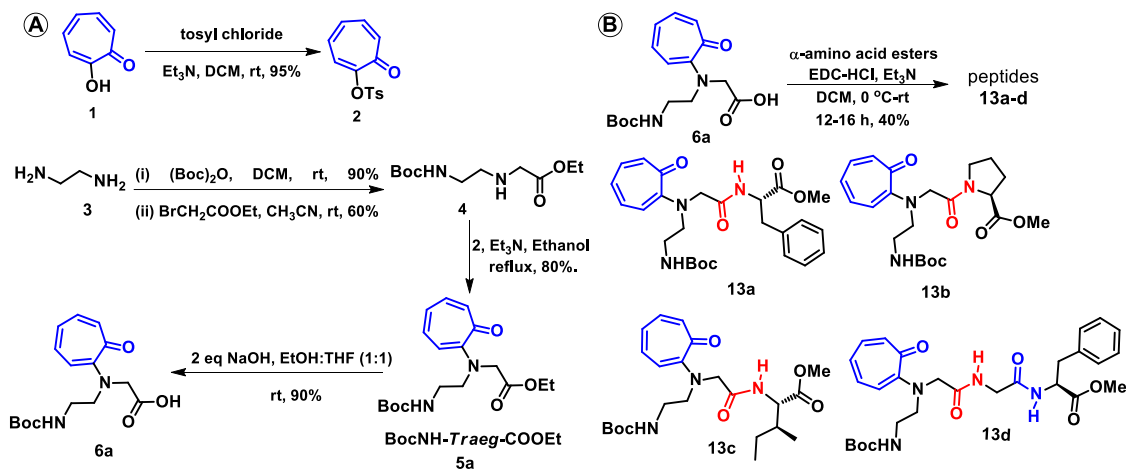


Figure 2.1. Hypothesis and objective

Synthesis of Traeg monomer and Traeg-aa heterologous peptides:



Scheme 2.1 (A) Synthesis of *Traeg* monomer. (B) Synthesis of *Traeg*-aa (δ/α)-hybrid peptides.

Conformational Analysis: To investigate the conformation of *Traeg* residue in *Traeg*-aa hybrid peptides, we performed the 2D NMR experiments (COSY, HSQC and NOESY). From 2D NMR studies, the troponyl (T3H) hydrogen is spatially interacting with aminoethyl backbone hydrogens (**Figure 2.2B**) and also confirmed that the troponyl carbonyl oriented towards the adjacent amide NH. The same orientation of troponyl carbonyl was found in monomer X-ray

structure (**Figure 2.2A**). Then, hydrogen bonding between the troponyl carbonyl and adjacent amide NH was established by following the $^1\text{H}/^{13}\text{C}$ NMR DMSO titration experiments and their titration profiles are depicted in **Figure 2.3C&D**. Similar orientation of troponyl carbonyl and hydrogen bonding were further supported by DFT studies and energy minimized structure of dipeptide **9** is provided in **Figure 2.2E**.⁴

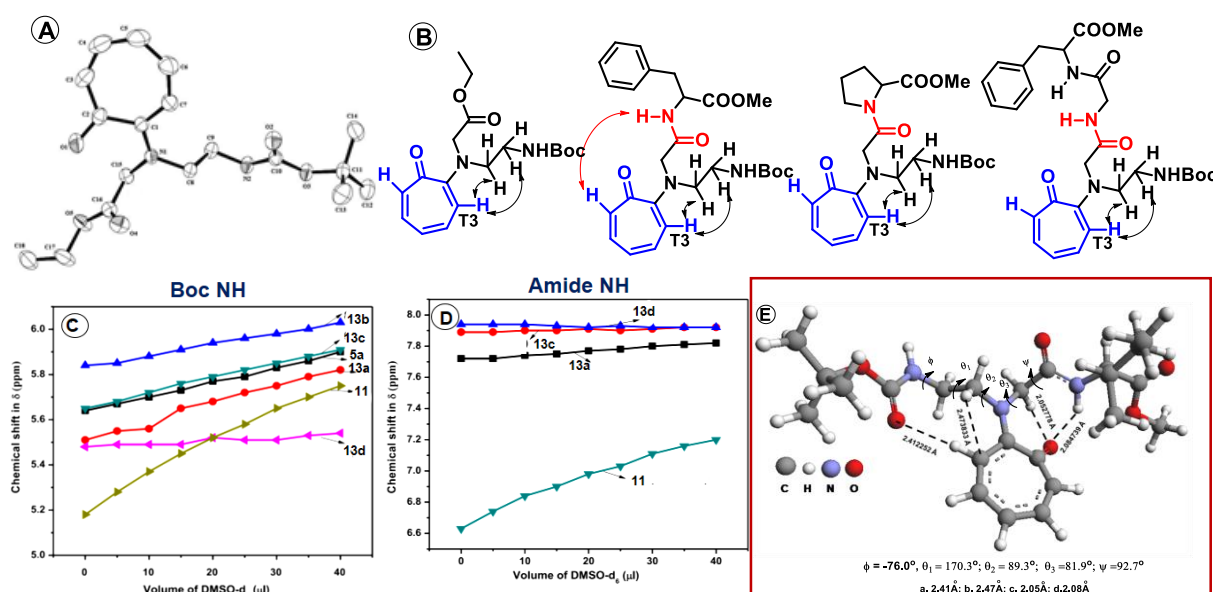
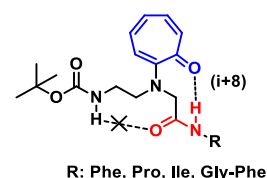


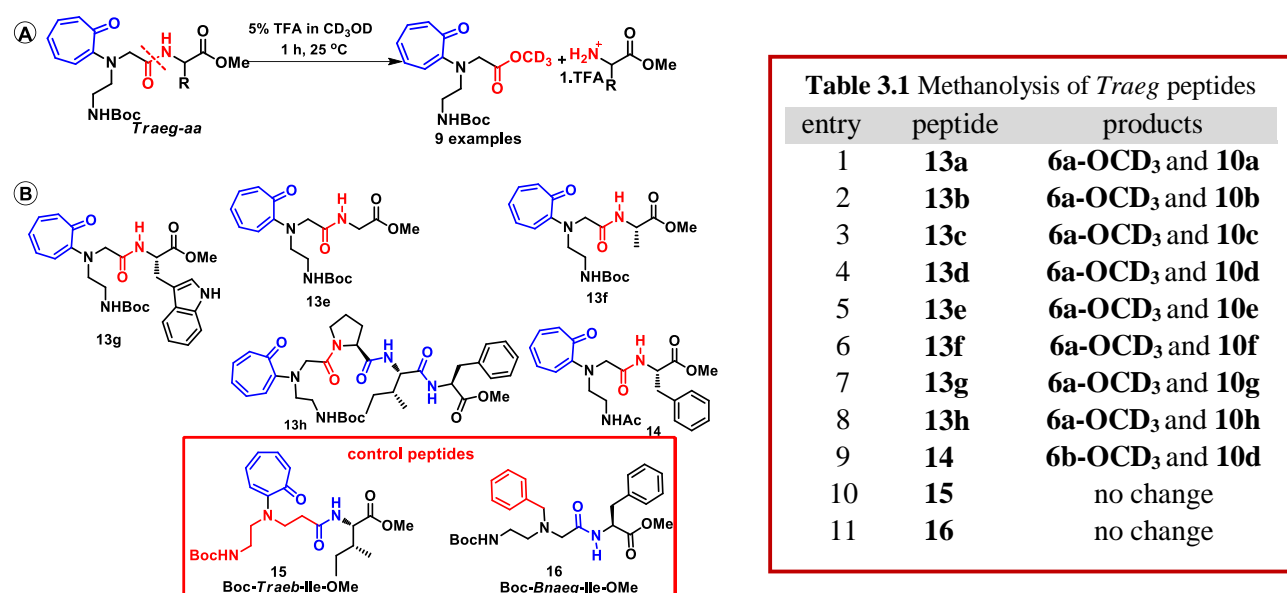
Figure 2.2. A) ORTEP diagram of **5a**. B) Observed NOESY interactions in **5a** and *Traeg* (δ/α) hybrid peptides C) DMSO titration profile of Boc NH of **5a/13a/b/c/d/11**. D) DMSO titration profile of amide NH **13a/c/d/11**. E) Energy minimized structure of dipeptide **9**.

In summary, the synthesis of *Traeg* monomer and *Traeg-aa* (δ/α)-hybrid peptides, the formation of eight membered ring hydrogen bonding between troponyl carbonyl and adjacent amide NH were explored.



Chapter 3. Instability of Amide Bond Derived from *Traeg* Amino Acid: This chapter explains an unusual cleavage of the amide bond derived from *Traeg*.⁵ Since the syntheses of *Traeg* homologous peptides were unsuccessful *via* both Solid and Solution Phase Peptide Synthesis. Also, the extension of the *Traeg* heterologous peptide length at the N-terminus end was unsuccessful. Surprisingly, during the Boc deprotection of *Traeg* hybrid peptides with 20% TFA in DCM, we found the hydrolysis of *Traeg* amide bond. We started investigating the hydrolysis/cleavage of *Traeg* amide bond systematically. First, we optimized the amide hydrolysis/cleavage conditions with different concentrations of TFA

and in different solvents. The optimized reaction conditions for amide methanolysis are 5.0% TFA in methanol for one hour (**Scheme 3.1A**).

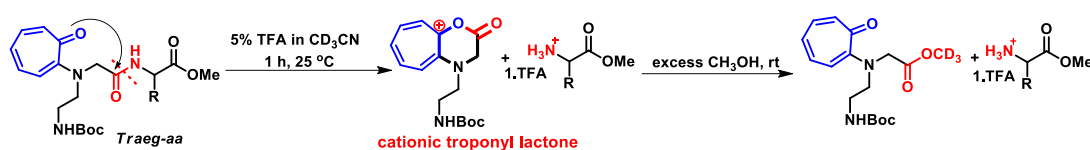


Scheme 3.1. A) Methanolysis of *Traeg* peptides. B) Synthesized *Traeg* peptides.

We also observed the cleavage of *Traeg* amide in 1.0 N *aqueous* HCl and 4 *equiv.* of PTSA in MeOH. The *Traeg* peptides (**13a-h**) were subjected to methanolysis in 5.0% TFA (~6 *equiv.*) in CD₃OD (Table 3.1) and monitored by NMR and ESI-MS. As expected, in case of *tri/tetra*-peptides **13d/h**, a regioselective methanolysis of *Traeg* amide was characterized and rest of the non-*Traeg* amide bonds were unaffected. For control studies, we synthesized the peptides **15** (Boc-*Traeb*-Ile-OMe) and **16** (Boc-*Bnaeg*-Phe-OMe). These peptides subjected for amide cleavage reaction, found that these non-*Traeg* amides are stable in presence of 5.0% TFA and Boc deprotection was observed. These results strongly suggests that only *Traeg* amide is cleavable under these conditions.

Mechanistic studies: To investigate the role of troponyl carbonyl, we attempted to cleave the amide bond in CD₃CN, a non-nucleophilic solvent, in presence of 5.0% TFA. From mass analysis, we characterized the formation of cationic troponyl lactone, which further

converted into *Traeg* methyl ester after the addition of the excess nucleophilic solvent, methanol (**Scheme 3.2**).



Scheme 3.2 Synthesis of cationic troponyl lactone

The formation of cationic lactone was an unprecedented reaction and interesting to investigate further. Hence, we have synthesized various troponyl glycinate peptides with different substituents at troponyl glycinate nitrogen atom (**Figure 3.2**).

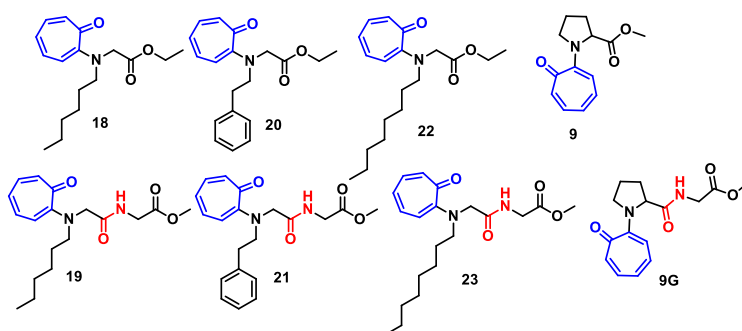
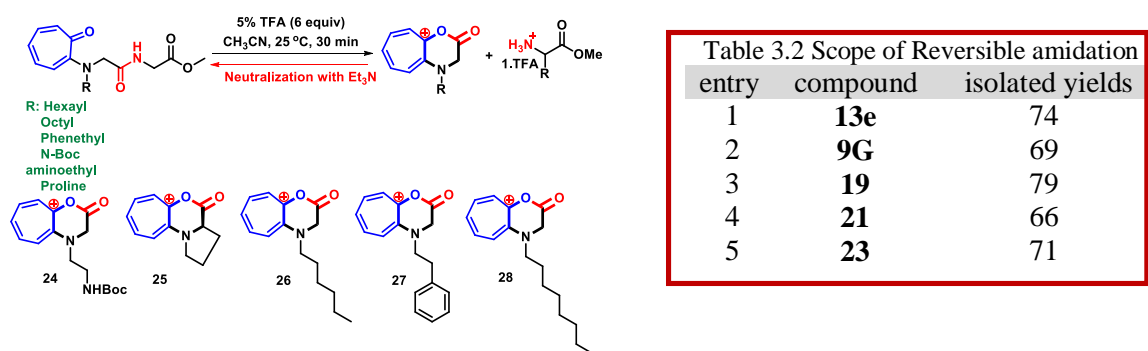


Figure 3.2. Synthesized monomers and dipeptides with different substituents at troponylglycinate nitrogen

The synthesized dipeptides were subjected for the synthesis of cationic troponyl lactones in presence of 5.0% TFA. From NMR and ESI-MS studies, the formation of cationic lactones were consistently observed with all those peptides. Interestingly, when the cationic troponyl lactone reaction mixture was neutralized with Et₃N, the cationic cyclic

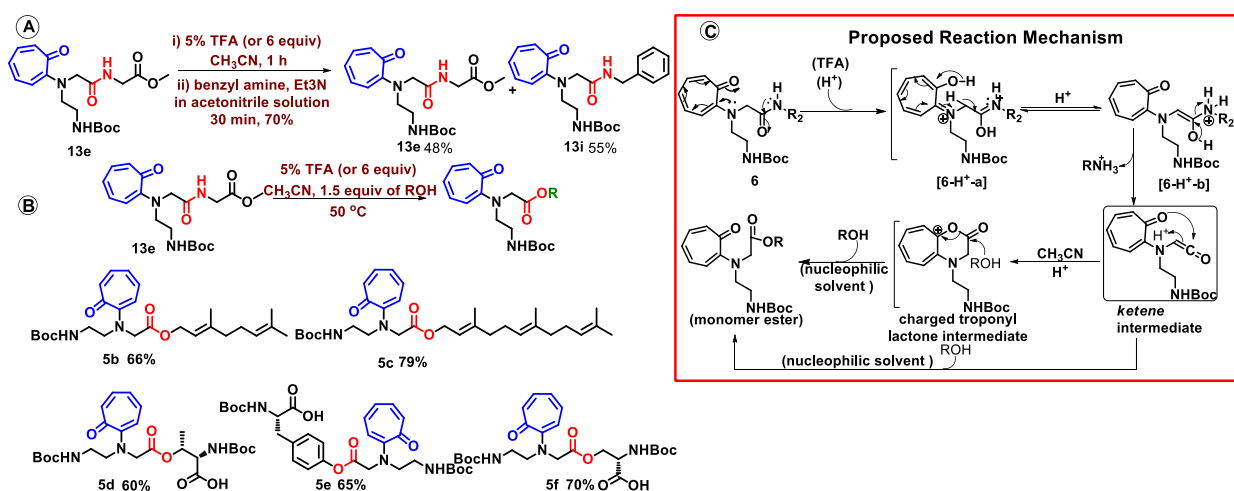


Scheme 3.2 Scope of the cationic troponyl lactone formation and isolated yields after reversible amidation

lactone exclusively converted into starting material (**Scheme 3.2**). So far, no such reversible amidation is known.

Further, we wanted to investigate the reactivity of cationic troponyl lactone with other nucleophiles. Hence, cationic troponyl lactone was treated with benzyl amine and Et₃N in acetonitrile to test the transamidation. After 30 minutes, dipeptides **13e** (starting material) and expected transamide **13i** were isolated in almost same ratio (**Scheme 3.3A**). On the other hand, we also performed the esterification reaction with 1.5 *equiv.* of other alcohols at 50 °C and respective products were isolated in good yields (**Scheme 3.3B**).

Based on the above experimental results we also proposed a plausible reaction mechanism (**Scheme 3.3C**).⁵



Scheme 3.3 A) Transamidation and Esterification. B) Esterification. C) Proposed reaction mechanism

In summary, the regioselective cleavage of *Traeg* amide bond, formation of the cationic troponyl lactone and its further conversion into ester was explored. For the first time, we have demonstrated the reversible amidation. We have performed the control experiments and proposed a plausible reaction mechanism for *Traeg* amide cleavage.

Chapter 4. Synthesis and Photophysical Studies of Novel Fluorescent Molecules from

Tropolone: Tropolone fluorescence properties were studied in cyclohexane, acidic and

basic water.^{3a} Inspired from the fluorescence properties of tropolone, we attempted to synthesize the cyclic aminotroponimines from *Traeg* amino acid. The Boc group of *Traeg* ester **5a** was deprotected with TFA and then allowed for cyclization in presence of Et₃N. We tested the fluorescence of obtained cyclic aminotroponimine and interestingly, it was a green fluorescent molecule with emission maxima at λ_{em} 482 nm.

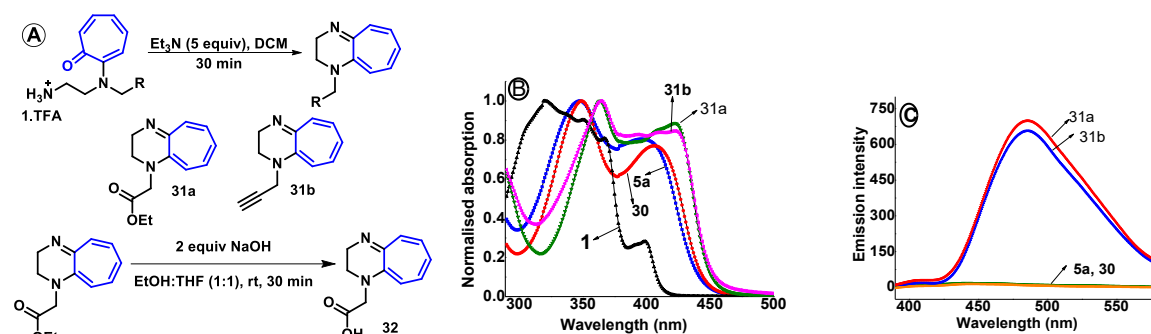
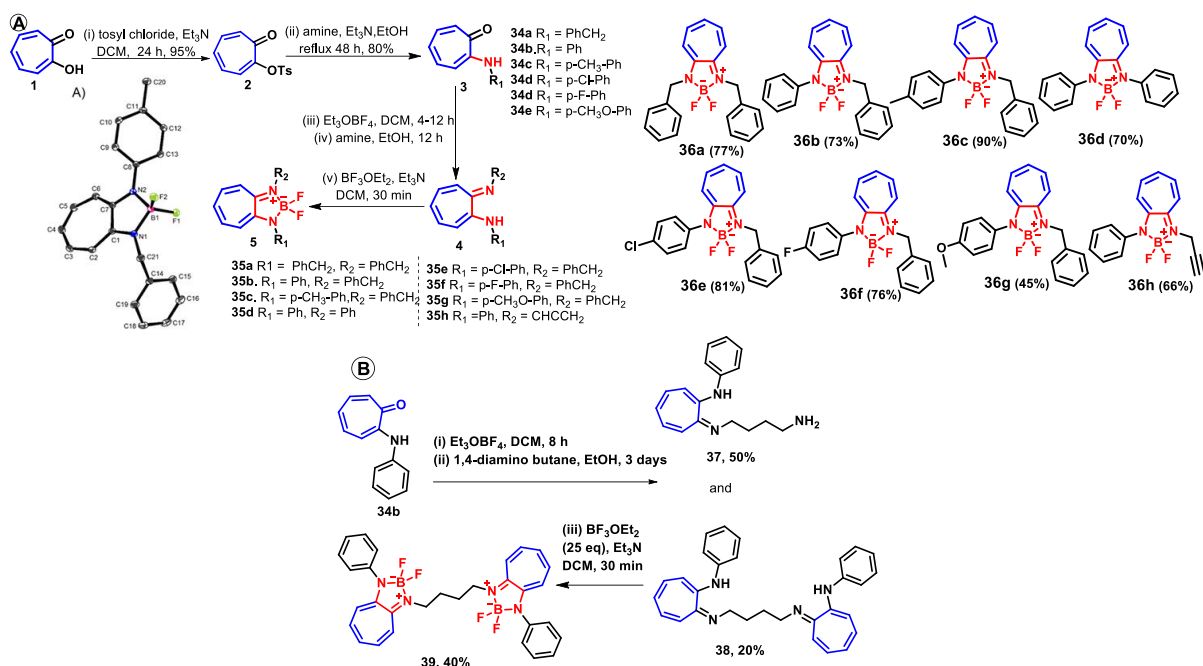


Figure 4.1 A) Normalized absorption spectra of **5a/30** and **31a/b** in methanol. B) Emission spectra of **5a/30** and **31a/b** in methanol at λ_{ex} 362 nm **5a** = 90 μ M; **30** = 150 μ M; **31a** = 60; **31b** = 70.

We have synthesized another cyclic aminotroponimine (**31b**) containing propargyl substituent. These are stable in acidic and basic medium. Absorption and emission of tropolone, aminotropones and cyclic aminotroponimines were recorded in methanol (**Figure 4.1 B&C**). From tropolone (320 nm) to cyclic aminotroponimines (362 nm), a red shift in absorption maxima was observed. The calculated quantum yields for these molecules (**31a/b**) are 0.05 (Φ_f). The fluorescence intensity enhancement in acidic medium and quenching in basic medium was observed and also sensitive towards the nature of solvent system.

Boron-Aminotroponimines: Boron dipyrromethene (BODIPY) fluorescent molecules are well known.^{3b,c} Inspired from the fluorescence properties of cyclic aminotroponimines, we have synthesized the boron-aminotroponimine complexes as analogues of boron dipyrromethane. Boron-aminotroponimine complexes (**36a-i**) were synthesized from tropolone in four steps by following **Scheme 4.1** and characterized by ¹H, ¹³C, ¹¹B, ¹⁹F and ESI-MS. The chemical structure of one of the boron complex **36c** was confirmed by single crystal X-analysis. In addition, dimeric boron-aminotroponimine complex **36i** was also synthesized (**Scheme 4.1B**).



Scheme 4.1 A) Syntheses of monomeric boron-aminotroponimine complexes. B) Syntheses of dimeric boron-aminotroponimine complex.

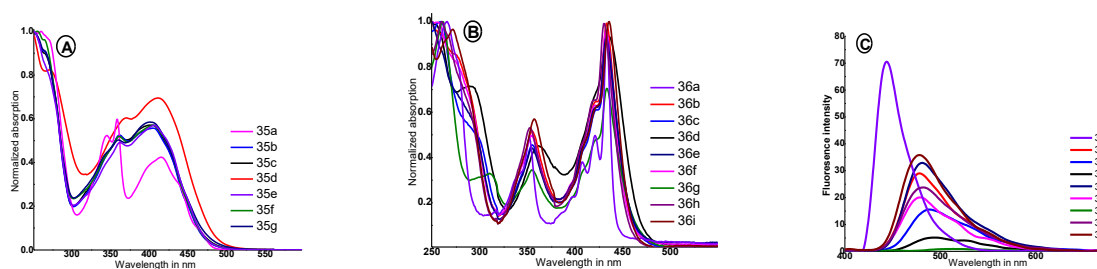


Figure 4.2 A&B) Absorption spectra of aminotroponimines and boron-aminotroponimines in cyclohexane. C) Emission spectra of boron-aminotroponimines in cyclohexane at $\lambda_{\text{ex}} = 350$ nm (20.0 μM).

After synthesis of boron-aminotroponimine complexes, we performed the photophysical studies in cyclohexane. The absorption (**Figure 4.2A**) and emission spectra of aminotroponimine ligands was recorded as control experiments and which indicates these are non-fluorescent. The boron-aminotroponimine complexes shows absorption maxima from 430 to 437 nm (**Figure 4.2B**), a red shift was observed from aminotroponimines absorption maxima (~412 nm). The boron-aminotroponimine complexes shows emission maxima from 445 to 540 nm (**Figure 4.2C**). Then, we calculated the quantum yields of these complexes such as **36a/b/e** = 0.17, **36c** = 0.07, **36d** = 0.05, **36g** = 0.006, **36f/h** = 0.15, **36i** = 0.28. (Quinine sulphate in 0.1 M H_2SO_4 is used as reference standard, $\lambda_{\text{ex}} = 350$ nm).

In summary, syntheses and photophysical properties of cyclic aminotroponimines and boron-aminotroponimines are explored. Our initial studies provide enormous opportunities to construct the better fluorescent molecules from boron-aminotroponimine core structure via a fine derivatization.

Chapter 5. Synthesis of β -hairpin type of *Hexa*-Peptides via Alkyl Linkers: β -hairpin secondary structure is one of the widely observed secondary structures in proteins.^{2a} The formation of hairpins are facilitated by the connecting loops (**Figure 5.1A**). Synthetic β -hairpin peptides with the connecting loop sequences ^DPro-Xxx (Xxx = Gly, ^LAla, ^DAla, Aib) and ^DPro-^LPro are well studied.^{2j}

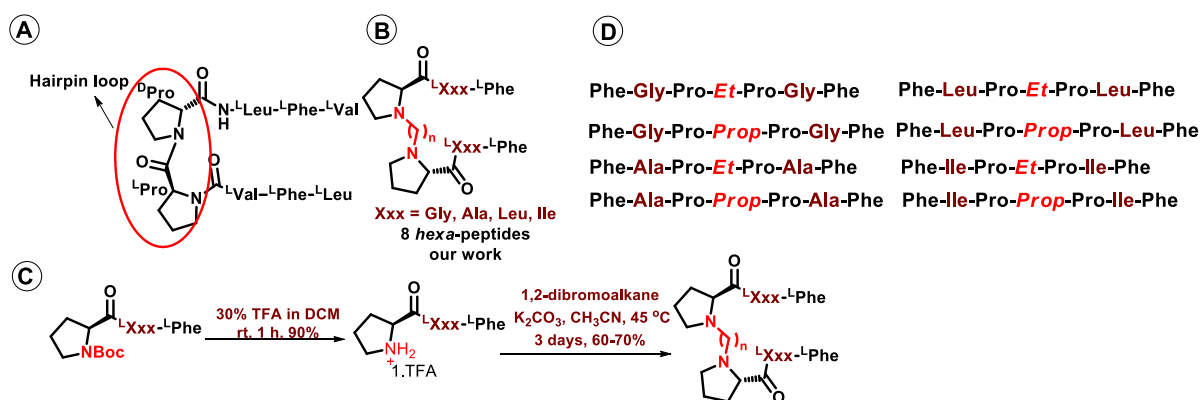


Figure 5.1 A&B) Reported hairpin peptide sequence and this work. C) Synthetic route to alkyl linker hexa-peptides. D) Synthesized hexa-peptides with ethyl and propyl alkyl linker.

Inspired from the known peptide hairpin secondary structures, we have designed the hexa-peptides, where two tri-peptides are connected by an alkyl linker instead of amide bond. These peptides were synthesized through Solution Phase Peptide Synthesis (**Figure 5.1C**) and characterized by NMR and ESI-MS. Then the secondary structure of the peptides were studied by CD spectropolarimeter.

In summary, the synthesis of hexa-peptides is completed successfully. CD studies reveals that these hexa-peptides (Phe-Gly/Ala-Pro-linker-Pro-Gly/Ala-Phe) are adopting hairpin type secondary structure in methanol.

References:

1. (a) Raistrick, H. *Biochem. J.*, **1932**, 26, 441. (b) Birkinshaw, J. H.; Chambers, A. R. Raistrick, H. *Biochem. J.*, **1942**, 36, 242. 4 (c) Dewar, M. J. S. *Nature*, **1945**, 155, 50. (d) Dewar, M. J. S. *Nature*, **1945**, 155, 141. (e) Pauson, P. L. *Chem. Rev.* **1955**, 55, 9. (f) Bentley, R. *Nat. Prod. Rep.* **2008**, 25, 118. (h) Roesky, P. W., *Chem. Soc. Rev.* **2000**, 29, 335.
2. (a) Branden, C.; Tooze, J. *Introduction to Protein Structure*; Garland: New York, NY, **1991**. (b) Seebach, D.; Matthews, J. L. *Chem. Commun. (Camb.)* **1997**, 21, 2015. (c) Gellman, S. H. *Acc. Chem. Res.* **1998**, 31, 173. (d) Hill, D. J.; Mio, M. J.; Prince, R. B.; Hughes, T. S.; Moore, J. S. *Chem. Rev.* **2001**, 101, 3893. (e) Kotha, S. *Acc. Chem. Res.* **2003**, 36, 342. (f) Foldamer: Structure, Properties and Applications; Hecht, S., Huc, I., Eds.; Wiley-VCH: Weinheim, Germany, **2007**. (g) Horne, W. S.; Gellman, S. H. *Acc. Chem. Res.* **2008**, 41, 1399. (h) Vasudev, P. G.; Chatterjee, S.; Shamala, N.; Balaram, P. *Chem. Rev.* **2011**, 111, 657. (i) Roy, A.; Prabhakaran, P.; Baruah, P. K.; Sanjayan, G. J. *Chem. Commun.* **2011**, 47, 11593. (j) Rai, R.; Raghothama, S.; Balaram, P. *J. Am. Chem. Soc.* **2006**, 128, 2675. References are therein.
3. (a) Breheret, E.F.; Martin, M. M. *Journal of Luminescence* **1978**, 49. (b) Loudet, A.; Burgess, K., *Chem. Rev.* **2007**, 107, 4891. (c) Ulrich, G.; Ziessel, R.; Harriman, A., *Angew. Chem., Int. Ed.* **2008**, 47, 1184.
4. Synthesis and Conformational Analysis of New Troponyl Aromatic Amino Acid. **Balachandra, C.**; Sharma, N. K. *Tetrahedron* **2014**, 70, 7464.
5. Instability of Amide Bond Comprising the 2-Aminotropone Moiety: Cleavable under Mild Acidic Conditions. **Balachandra, C.**; Sharma, N. K. *Org. Lett.* **2015**, 17, 3948.
6. Novel Fluorophores: Synthesis and Photophysical Studies of Boron-Aminotroponimines. **Balachandra, C.**; Sharma, N. K. *Dyes and Pigments*, **2017**, 137, 532.

List of Schemes

Scheme 2.1	Synthesis of <i>Traeg</i> amino acid monomer	44
Scheme 2.2	Synthesis of <i>Traeg</i> homologous dipeptide through solution phase	47
Scheme 2.3	Synthesis of <i>Traeg</i> homologous <i>di</i> -peptide through designed alternative method.	48
Scheme 2.4	Synthesis of heterologous peptides.	49
Scheme 3.1	Syntheses of AcNH- <i>Traeg</i> -COOH (6b)	103
Scheme 3.2	Syntheses of BocNH- <i>Traeb</i> -COOH (7)	104
Scheme 3.3	Syntheses of BocNH- <i>Bnaeg</i> -COOH (8).	104
Scheme 3.4	Syntheses of N-Boc aminoethyl aminoisobutyric acid (<i>aeaib</i>) and N-Boc amino ethyl alanine (<i>aeala</i>).	105
Scheme 3.5	Reported conversion of lactone into amide	112
Scheme 3.6	Synthesis of N-alkyl troponyl glycinate monomers (18/20/22/9), and their <i>di</i> -peptides (19/21/23/9G) with glycine and <i>Trpro-Phe-OMe</i> di-peptide (9F).	114
Scheme 3.7	Synthesis of cationic troponyl lactones from troponyl glycinate peptides 19/21/23/9G/F	115
Scheme 3.8	Reversible amidation reaction.	121
Scheme 3.9	Transamidation reaction with benzyl amine.	122
Scheme 3.10	Transesterification with Geraniol and Farnesol.	123
Scheme 3.11	Conversion of troponylglycinate esters into cationic troponyl lactones <i>via</i> protonated esters, followed by base mediated amidation of cationic troponyl lactones.	126

Scheme 3.12	Conversion of troponylglycinate esters into cationic troponyl lactones via protonated esters, followed by base mediated amidation of cationic troponyl lactones.	133
Scheme 4.1	(A) Synthesis of monomer S30 . (B) Synthesis of cyclic aminotroponimines 31a/b ; (C) hydrolysis of cyclic aminotroponimine ester.	301
Scheme 4.2	Synthesis of boron-aminotroponimine complexes	309
Scheme 4.3	Synthesis of dimeric aminotroponimine 35i and its boron complex 36i .	310
Scheme 5.1	Scheme 5.1 Syntheses of <i>hexa</i> -peptides via alkyl linkers.	406

List of Tables

Table 2.1	Chemical shift value of amide NH and troponyl C=O	54
Table 3.1	Optimization of reaction conditions	101
Table 3.2	Synthesis of hybrid peptides from <i>Traeg</i> / <i>Traeb</i> / <i>Bnaeg</i> peptides	105
Table 3.3	Regioselective methanolysis of <i>Traeg</i> derived amide bond	107
Table 3.4	¹³ C NMR chemical shift values of troponyl ring in peptides (19/23/9G) and troponyl lactones (25/26/28)	118
Table 3.5	Isolated yields of reverse amidation reaction	122
Table 3.6	Observed absorption peaks of <i>Traeg</i> peptides, <i>Traeb</i> peptide and monomers after addition of TFA and methanol.	123
Table 4.1	photophysical parameters of compound 31a and b	303
Table 4.2	Selected bond lengths and bond angles of boron complex 36c in solid state.	313
Table 4.3	Absorption parameters of aminotroponimine ligands	315

List of Figures

Figure 1.1	Tropolonoid natural products isolated by Horald Raistrick (A) and Tetsuo Nozoe (B).	1
Figure 1.2	A) Tropone and tropolone chemical structures and polarization representation B) Tautomeric forms of tropolone.	3
Figure 1.3	Pictorial representation of a few bioactive tropolonoid natural products and their biological activities.	4
Figure 1.4	Chemical structures of Purpurogallin and Theaflavins.	6
Figure 1.5	Chemical structures of Tropoisoquinolines	7
Figure 1.6	Chemical structures of Pycnidione and Epolone A	7
Figure 1.7	Chemical structures of hydroxyl tropolones.	7
Figure 1.8	Chemical structures of Aminotroponimines, tropocoronands and their metal complexes.	9
Figure 1.9	A) General structure of α -amino acids and peptide backbone; B) Three dimensional structures of proteins.	11
Figure 1.10	Secondary structures of natural synthetic peptides.	12
Figure 1.11	A) General representation of solution phase syntheses of peptides B) coupling reagents and additives C) Mechanism of carbodiimide mediated peptide coupling.	14
Figure 1.12	General representation of solid phase peptide syntheses, Boc strategy	15
Figure 1.13	Chemical structures of a few peptide therapeutic drugs.	17

Figure 1.14	Developed alternative for efficient peptide therapeutics	19
Figure 1.15.	General chemical structures of depsipeptides and thiodepsipeptides	20
Figure 1.16	General representation of different types of unnatural amino acids.	21
Figure 1.17.	General chemical structures of Aza-peptides and Azatides	21
Figure 1.18	General representation of backbone extended amino acids	22
Figure 1.19	(A) Syntheses of β -amino acids from α -amino acids through Arndt-Estert homologation. (B) Syntheses of γ -amino acids from β -amino acids through Arndt-Estert homologation. (C) Nomenclature of β -amino acids based position of substituents on backbone.	23
Figure 1.20	Chemical structures of Octreotide peptide (natural peptide hormone) B) A cyclic β -tetrapeptide to minmic the function of Octreotide.	24
Figure 1.21	Solid state secondary structures of poly- β 3-hAla (A) and α/β -peptide containing given sequence (B).	25
Figure 1.22	Representative examples of reported conformationally constrained cyclic natural and unnatural amino acids.	26
Figure 1.23	Peptides synthesized from the natural and unnatural amino acids (aromatic)	28
Figure 2.1	(A) Chemical Structure of tropolone; (B) Designed amino acid. (C) Representation of hydrogen bonding in <i>Traeg</i> peptides; (D) Target <i>Traeg</i> peptide.	43

Figure 2.2	ORTEP diagram of <i>Traeg</i> monomer 5a and molecular packing diagram.	45
Figure 2.3	Observed NOESY interactions of di and tri peptides 13a/b/d .	50
Figure 2.4	¹ H NMR titration experiments of dipeptide 13a	52
Figure 2.5	NMR titration profile: (A) Boc-NH at N'-end of 5a/13a-d, 11 ; (B) Adjacent amide NH at C'-end of 13a/c/d, 11 .	53
Figure 2.6	Stacked ¹³ C NMR spectra of tri-peptide 13d in given solvent system. All the spectra were characterized with respect to DMSO solvent residual peak.	55
Figure 2.7	Energy minimized structure of dipeptide 9 from DFT calculations.	56
Figure 2.8	Schematic representation of summary.	57
Figure 3.1	A) Representation of resonance stabilization in acyclic amide bond; B) Decreasing order of reactivity of carbonyl carbon in aldehydes, ketones, esters, amide and carboxylates.	94
Figure 3.2	Conventional hydrolysis of acyclic amide bond under basic and acidic conditions, respectively.	95
Figure 3.3	A) Non-planarity of the amide bond prevents the delocalisation of electrons. B) Iconic examples of strained cyclic lactams; C) Synthesis of 2-quinuclidone via non-classical pathway.	96
Figure 3.4	(A) Recent literature reports on hydrolysis of amide bonds under unconventional conditions.	98

Figure 3.5	Representation of present work. A) Cleavage of <i>Traeg</i> amide into cationic troponyl lactone followed by reversible amidation in acetonitrile, and <i>Traeg</i> ester in methanol. B) Conversion of esters into cationic troponyl lactone followed by amidation. C&D) control peptides, <i>Traeb</i> -aa & <i>Bnaeg</i> -aa. E) Reported peptide nucleic acids derived from aminoethyl glycine backbone.	99
Figure 3.6	<i>Traeg</i> amino acid (A, 6) and Designed control amino acids for <i>Traeg</i> amide cleavage studies: <i>Traeb</i> (B, 7), <i>Trpro</i> (D, 9).	102
Figure 3.7	Chemical structures of synthesized <i>Traeg</i> peptides for amide cleavage studies	106
Figure 3.8	Chemical structures of synthesized control peptides for amide cleavage studies	106
Figure 3.9	a) Time dependent ¹ H-NMR spectra of <i>di</i> -peptide 6b .	109
Figure 3.10	b) ESI-MS spectrum of dipeptide 13f after time dependent NMR; c) ESI-MS spectrum of <i>tetra</i> -peptide 13h after time dependent NMR.	110
Figure 3.11	Representation of possible nucleophilic addition reactive centres in tropylium cation (*); nucleophile addition is represented with arrows.	111
Figure 3.12	A & B) ¹ H & ¹³ C NMR of <i>Trhg</i> -Gly-OMe in CD ₃ CN, represents formation of tropylium cation and the reverse amidation; A) # are triethyl amine peaks; B) # are Trifluoroacetate peaks.	117

Figure 3.13	^{13}C NMR chemical shifts of troponyl ring in synthesized lactones (25/26/28)	119
Figure 3.14	ESI-MS spectra of troponyl lactone 24 .	121
Figure 3.15	(A) Absorption spectra of BocNH- <i>Traeg</i> -Pro-Ile-Phe-OMe (13h , black) and lactone (24 , green). (B) Conversion of troponyl lactone into methyl ester (7-22; each spectra recorded with two minutes time intervals). (C) Absorption studies of BocNH- <i>Traeb</i> -Ile-OMe (15). (d) Absorption studies of BocNH- <i>Traeg</i> -OEt (5a). All spectra were recorded with two minutes time intervals.	124
Figure 3.16	A) ^1H NMR of cationic troponyl lactone (26) obtained from peptide in CD_3CN . B) ^1H NMR of <i>Trhg</i> -Gly peptide (19) in CD_3CN . C) ^1H NMR of <i>Trhg</i> monomer 18 after addition of TFA (containing protonated form of monomer and cationic troponyl lactone) D) ^1H NMR of <i>Trhg</i> monomer 18 in CD_3CN . (*represent cationic troponyl lactone peaks, solid circles represents protonated monomer peaks).	127
Figure 3.17	A) ^{13}C NMR of cationic troponyl lactone (26) obtained from peptide in CD_3CN . B) ^{13}C NMR of <i>Trhg</i> -Gly peptide (19) in CD_3CN . C) ^{13}C NMR of <i>Trhg</i> monomer 18 after addition of TFA (peaks represents protonated form of monomer and cationic troponyl lactone (26)). D) ^{13}C NMR of <i>Trhg</i> monomer 18 in CD_3CN .	128
Figure 3.18	^1H and ^{13}C NMR signals considered for comparative studies.	128

Figure 3.19	Time dependent ^1H NMR spectra of BocNH- <i>Traeb</i> -Ile-OMe in CD_3OD .	129
Figure 3.20	Scheme of Boc deprotection and ESI-MS spectrum of NH_2 - <i>Traeb</i> -Ile-OMe.	130
Figure 3.21	A) ^1H NMR spectra of Troponylglycinate 20 in CD_3CN after addition of TFA after 8 h. B) ^1H NMR spectra of Troponylglycinate 20 in CD_3CN after addition of TFA after 1 h. C) ^1H NMR spectra of Troponylglycinate 20 in CD_3CN after addition of TFA-D after 6 h. (* represents cationic troponyl lactone peaks; solid circles represents protonated monomer and <u>solid triangle represents the CHD peak</u>)	134
Figure 3.22	A) ^{13}C NMR spectra of <i>Trpeg</i> undeuterated lactone (obtained spectra after addition of TFA after 8 h). B) ^{13}C NMR spectra of <i>Trpeg</i> deuterated and undeuterated lactone. (obtained spectra after addition of TFA after 7 h)	134
Figure 3.23	A) ^{13}C DEPT135 NMR spectra of deuterated and undeuterated <i>Trpeg</i> lactone in CD_3CN [green highlighted box represents triplet appeared due to CHD carbon]. B) ^{13}C DEPT135 NMR spectra of deuterated and undeuterated <i>Trpeg</i> and benzylamine dipeptide in CD_3CN [green highlighted box represents triplet appeared due to CHD carbon].	135
Figure 3.24	A) HRMS spectra of <i>Trpeg</i> and benzylamine deuterated peptide. B) HRMS spectra of <i>Trpeg</i> and benzylamine undeuterated peptide.	136

Figure 3.25	Possible mechanism of <i>Traeg</i> amide bond cleavage	139
Figure 3.26	Possible mechanism of conversion of <i>Troponylglycinate</i> esters into cationic troponyl lactone and amide.	140
Figure 3.27	Schematic summary of this chapter.	142
Figure 4.1	Chemical structures of A) tropolone. B) Colchicine C) 2-hetaryl-1,3-tropolones	297
Figure 4.2	Chemical structures of A) aminotroponimine ligand and metal complexes B) tropocoronands and its metal complexes.	299
Figure. 4.3	Chemical structures of A) boron-dipyrromethene core. C&D) cyclic aminotroponimine and boron-aminotroponimine core (this work).	300
Figure 4.4	(A) ORTEP diagram of monomer 30 . (B) Molecular packing diagram of 30 .	302
Figure 4.5	A) Normalized absorption spectra of tropolone, 5a/30 and 31a/b in methanol. B) Emission spectra of 5a/30 and 31a/b in methanol at λ_{ex} 362 nm (concentration is given 5a = 90 μM , 30 = 150 μM , 31a = 60 μM , 31b = 70 μM).	304
Figure 4.6	A) Absorption spectra 31a (160.0 μm) in different mediums. B) Emission spectra 31a (60.0 μM) in different mediums. C) Absorption spectra 31b (160.0 μm) in different mediums. D) Emission spectra 31b (60.0 μM) in different mediums.	306
Figure 4.7	(A) pH dependent fluorescence measurements of 31a (A), 31b (B).	307

Figure 4.8	(A) Emission of 31a with concentration (10.6 μ M); (B) Emission spectra of 31b with concentration of (7.5 μ M) in in different solvents systems using same instrument parameters.	308
Figure 4.9	^1H NMR (first), ^{11}B NMR (second), ^{19}F NMR (third) of 36c in CDCl_3 . HRMS spectrum of 36c (last).	311
Figure. 4.10	A) ORTEP diagram of 36c with 25% probability of ellipsoids, hydrogen atoms are deleted for clarity; B) Asymmetric unit of 36c .	313
Figure 4.11	A) Absorption spectra of aminotroponimate ligands (35a-g) in cyclohexane. B) Normalized absorption spectra of boron-complexes (36a-i) in cyclohexane. C) Normalized absorption spectra of aminotroponimine ligands (35a-g) in acetonitrile. D) Normalized absorption spectra of boron-aminotroponimines in acetonitrile (36a-e).	314
Figure 4.12	A) Emission spectra of boron-aminotroponimine complexes (36a-i) in cyclohexane at 20.0 μ M concentration. B) Normalized emission spectra of boron complexes (36a-i) in cyclohexane.	318
Figure 4.13	(A) Photographs of solid boron complexes. (B) Photograph of boron complexes in cyclohexane under hand hold UV lamp illumination.	319
Figure 5.1	A) Chemical structures of L-proline and 4-hydroxyproline. B) Structural representation of <i>trans/cis</i> -Proline amide bond. C) Structural representation of <i>exo/endo</i> ring puckering. D) Representation of $n \rightarrow \pi^*$ interaction in <i>trans</i> -Pro amide.	401
Figure 5.2	Reported hairpin nucleating sequence derived from L-Proline and D-Proline.	402

Figure 5.3	A) Designed <i>tri</i> -peptides for this work. B) Designed <i>hexa</i> -peptides containing alkyl linkers.	404
Figure 5.4	Synthesized <i>tri</i> -peptides.	406
Figure 5.5	Chemical structures of synthesized peptides.	407
Figure. 5. 6	¹ H NMR and mass spectra of Phe-Gly-Pro- <i>Propyl</i> -Pro-Gly-Phe and Phe-Gly-Pro- <i>Ethyl</i> -Pro-Gly-Phe, respectively.	408
Figure 5.7	¹ H- ¹ H NMR COSY spectra of <i>hexa</i> -peptide 38b in CDCl ₃	409
Figure 5.8	¹ H- ¹ H NMR ROESY spectra of <i>hexa</i> -peptide 39a in CDCl ₃	410
Figure 5.9	Observed ROESY interactions of <i>hexa</i> -peptide 39a in CDCl ₃	410
Figure 5.10	CD spectra of <i>tri</i> -peptides (37) and <i>hexa</i> -peptides (38-39) at 0.33 mM (A) and 1.33 mM (B) in methanol	412
Figure 5.11	CD spectra of <i>tri</i> -peptides (37) and <i>hexa</i> -peptides (38-39) at 0.33 mM (A) and 1.33 mM (B) in acetonitrile.	413
Figure 5.12	CD spectra of <i>tri</i> -peptides (37) and <i>hexa</i> -peptides (38-39) at 0.33 mM (A) and 1.33 mM (B) in 2,2,2-trifluoroethanol.	414

List of abbreviations

Å	angstrom
aa	amino acid
Ac	acetyl
app.	apparent
aq.	aqueous
Bn	benzyl
Boc	<i>tert</i> -butoxycarbonyl
BODIPY	boron-dipyrromethene
<i>Bnaeg</i>	Benzylaminoethyl glycine
br	broad
°C	degrees Celsius
calc'd	calculated
CCDC	Cambridge Crystallographic Data Centre
CSD	Cambridge Structural Database
CD	Circular Dichroism
d	doublet
DMF	<i>N,N</i> -dimethylformamide
DCM	Dichloromethane
DMSO	dimethyl sulfoxide
DCE	dichloroethane
DIPEA	diisopropylethylamine
DIPCDI	diisopropylcarbodiimide
EC50	50% effective concentration
EDC.HCl	<i>N</i> -(3-Dimethylaminopropyl)- <i>N'</i> -ethylcarbodiimide hydrochloride

<i>equiv.</i>	equivalent
ESI	Electrospray Ionization
Et	ethyl
EtOAc	Ethylacetate
Epo	Erythropoietin
FDA	Food and Drug Administration
Fmoc	Fluorenyl methoxy carbonyl
g	gram(s)
COSY	Correlation Spectroscopy
h	hour(s)
HIV	Human Immunodeficiency Virus
HRMS	High Resolution Mass Spectroscopy
HSQC	Heteronuclear Single Quantum Coherence Spectroscopy
Hz	hertz
IR	infrared (spectroscopy)
<i>J</i>	coupling constant
K	kelvin
λ	wavelength
L	liter
m	multiplet or milli
<i>m/z</i>	mass to charge ratio
μ	micro
Me	methyl
mg	milli gram
MHz	megahertz

min	minute(s)
mol	mole(s)
mL	milli litre
μL	micro litre
μM	micro molar
mM	milli molar
mp	melting point
NMR	Nuclear Magnetic Resonance
NOE	Nuclear Overhauser Effect
NOESY	Nuclear Overhauser Enhancement Spectroscopy
nm	nanometers
<i>p</i>	para
Ph	Phenyl
pH	hydrogen ion concentration in aqueous solution
ppm	parts per million
Prop	propyl
q	quartet
PTSA	<i>p</i> -toluene sulfonic acid
rt	room temperature
s	singlet
t	triplet
TFA	Trifluoroacetic acid
THF	Tetrahydrofuran
TFE	trifluoroethanol
TLC	thin layer chromatography

TMS	trimethylsilyl
Ts	<i>p</i> -toluenesulfonyl (tosyl)
<i>Traeg</i>	Troponyl aminoethylglycine
<i>Traeb</i>	Troponyl aminoethyl- β -alanine
<i>Trpeg</i>	Troponyl phenethylglycine
<i>Trhg</i>	Troponyl hexylglycine
<i>Trog</i>	Troponyl octylglycine
<i>Trpro</i>	Troponyl prolinyl
UV	ultraviolet
w	weak

TABLE OF CONTENTS

ACKNOWLEDGEMENTS	v
SYNOPSIS.....	viii
List of Schemes	xviii
List of Tables	xix
List of Figures	xix
List of abbreviations	xxix

Chapter 1

1.1 Introduction of tropolone	1
1.1.1 History of tropolone discovery	1
1.1.2 Structure and general properties of tropolone	2
1.1.3 Bioactive tropolonoid natural products.....	4
1.1.4 Structural analogues and synthetic derivatives of tropolone	8
1.1.5 Photophysical properties tropolone moiety.....	10
1.2 Introduction of Peptidomimetics	11
1.2.1 General peptide synthetic approach.....	13
1.2.2 Peptide therapeutic drugs	16
1.2.3 Peptide therapeutic drugs - advantages and limitations.....	18
1.2.4 Alternative approaches to overcome the limitations of natural peptide therapeutics	18
1.2.5 Unnatural amino acids and peptidomimetics	20
1.2.6 Backbone expanded amino acids.....	22
1.2.7 Peptide nanomaterials	29
1.3 Summary and Outlook	30
1.4 References and Notes	33

Chapter 2

2.1 Introduction	41
2.1.1 Hypothesis and Objective	43
2.2 Results and Discussion	44
2.2.1 Synthesis of Troponyl aminoethyl glycine (<i>Traeg</i>) amino acid.....	44
2.2.2 Synthesis of <i>Traeg</i> peptides	46
2.2.3 Conformational analysis and hydrogen bonding studies	49
2.3 Conclusions	56
2.4 Experimental Section	57
2.5 References and Notes	67
2.6 Appendix	71

Chapter 3

3.1 Introduction	94
3.1.1 Structure and Reactivity of amide bond	94
3.1.2 Exceptions.....	96
3.1.3 Reported acyclic amide solvolysis under non-conventional conditions	97
3.1.4 Present work.....	99
3.2 Results and discussion	100
3.2.1 Design and synthesis of amino acid monomers and their peptides for amide cleavage studies	102
3.2.2 Synthesis of peptides	105
3.2.3 Methanolysis of <i>Traeg</i> amide bond.....	107
3.2.4 Methanolysis studies of <i>Traeg</i> -aa peptides (13a-h/14) by NMR and ESI-MS:..	108
3.2.5 Cleavage of <i>Traeg</i> amide into cationic troponyl lactone in acetonitrile	110
3.2.6 Synthesis of monomers and peptides with variety of substituents at troponyl glycinate nitrogen.....	114

3.2.7 Synthesis and characterization of cationic troponyl lactones	115
3.2.8 Cationic troponyl lactone facilitated reversible amidation	121
3.2.9 Transamidation.....	122
3.2.10 Transesterification:	122
3.2.11 UV-Visible studies	123
3.2.12 Comparative control studies of lactone formation with monomers and peptides:	125
3.2.13 Control studies	129
3.2.14 Deuterium entrapment at α -methylene group:	130
3.2.15 Proposed <i>Traeg</i> amide cleavage reaction mechanism:	137
3.3 Conclusions	141
3.4 Experimental Section	143
3.5 References and Notes	164
3.6 Appendix	168

Chapter 4

4.1 Introduction	297
4.1.1 Present work.....	299
4.2 Results and Discussion	301
4.2A Cyclic aminotroponimines: Synthesis and photophysical studies	301
4.2A.1 Syntheses	301
4.2A.2 Photophysical studies of cyclic aminotroponimines.....	302
4.2A.3 pH and solvent effects on fluorescence properties	307
4.2B Boron-Aminotroponimine complexes: Syntheses and photophysical studies	309
4.2B.1 Syntheses and characterization	309
4.2B.2 Photophysical studies of aminotroponimines and boron-aminotroponimines	313
4.3 Conclusions	321
4.4 Experimental Section	321

4.5 References and Notes	338
4.6 Appendix.....	342
Chapter 5	
5.1 Introduction.....	400
5.1.1 Importance of Proline and Hydroxyproline in peptides	400
5.1.2 Peptides as molecular building blocks in nanomaterial fabrication	403
5.1.3 Rational of Present Work	403
5.2 Results and discussion	405
5.2.1 Syntheses and characterization.....	405
5.2.2 NMR and Circular Dichroism (CD) spectroscopic studies	409
5.3 Conclusions.....	415
5.4 Experimental Section	416
5.5 References and Notes	422
5.6 Appendix.....	425
6. Thesis Summary	440

CHAPTER ONE

Introduction

Chapter 1: Introduction

1.1 Introduction of tropolone

1.1.1 History of tropolone discovery

Colchicine, a tropolonoid natural product, occupied the first page in the historical pages of tropolonoids (**Figure 1.1A**). And, still Colchicine remains as a sole drug for the treatment of acute gout flares since ancient days. In 1820s itself Pelletier and Caventou isolated the Colchicine from the *Colchicum autumnale* (Meadow saffron/autumn crocus).^{1,2} However, the arena of tropolonoids started in 1945 when Horald Raistrick, an eminent natural product chemist, isolated three tropolonoid natural products such as Stipitatic acid, puberulonic acid and puberulic acid from *Penicillium* species.^{3,4} Puberulonic acid ($C_9H_4O_7$) and Puberulic acid ($C_8H_6O_6$) are isolated from the *Penicillium puberulum* in 1932, and in 1942, Stipitatic acid ($C_8H_6O_5$) is isolated from *Penicillium stipitatum* (**Figure 1.1B**). He proposed the chemical

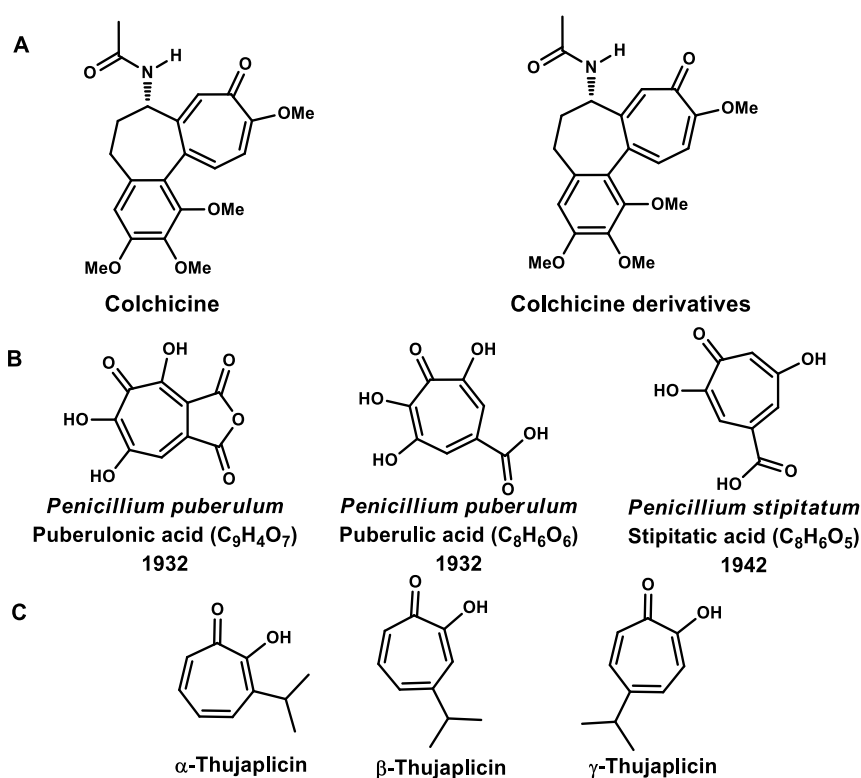


Figure 1.1 Tropolonoid natural products isolated by Horald Raistrick (A) and Tetsuo Nozoe (B).

formula for all these compounds, but was unable to determine the chemical structure with the obtained data.^{3,4} Because, the seven-membered ring tropolonoid structure was not known by that time. However, this uncertainty was cracked by Michael Dewar in 1945, who proposed a seven-membered ring aromatic structure for Stipitatic acid and Colchicine.^{5,6} This discovery leads to the classification of aromatic compounds into benzenoids and non-benzenoids. In the same period, Thujaplicins were isolated from the heartwood of western red cedar and from the leaves of taiwanhinoki, individually by two renowned scientists, Erdtman and Tetsuo Nozoe.⁷⁻¹³ Thujaplicins are isopropyl substituted tropolones and on the basis of position of the isopropyl substituent on the seven-membered ring these are called as α,β,γ -Thujaplicins (**Figure 1.1C**). However, afterwards several tropolonoid natural products have been isolated and explored their utilities in different fields.¹⁷⁻²¹ Later on, tropolone itself is isolated from the bacterial species called *Pseudomonas plantarii* ATCC 43733 and *Pseudomonas lindbergii* ATCC 31099 in 1980.^{22,23} Most of the reported tropolonoid natural products were isolated from the plants and fungi as secondary metabolites.¹⁷⁻¹⁹

1.1.2 Structure and general properties of tropolone

Tropolone and tropones (**Figure 1.2A**) are the seven-membered ring, non-benzenoid aromatic compounds. Tropolone (2-hydroxy-2,4,6-cycloheptatrien-1-one) contains carbonyl and hydroxyl functional groups adjacent to each other.¹⁰⁻¹³ As mentioned above, troponyl aromatic ring is first discovered non-benzenoid aromatic system. The carbonyl functional group present on the tropolone ring is relatively more polarized, as a result the partial positive charge at carbonyl carbon is more stabilized when compare to aliphatic ketones and aldehydes, and further it is stabilised by aromaticity in tropolone.¹⁰ The positively charged carbon enables the delocalization of π -electrons over seven-membered ring.¹⁰ Due to the existence of positive charge, tropolone ring exhibits aromaticity. Importantly, in tropolone the hydroxyl proton

transfers rigorously between the carbonyl and hydroxyl functional groups, as a result, tropolone exists in two highly mobile tautomeric forms (**Figure 1.2B**).¹⁰ Whereas, in case of isomeric tropolones such as 3-hydroxytropolone and 4-hydroxytropolone, since the hydroxyl and carbonyl groups of these isomers are separated by more than one bond, as a result, proton transfer is not possible.¹⁰

In addition, in the literature it has been mentioned that tropolone is a vinylog of acetic acid. Tropolone has shown superior acidity than phenols with dissociation constant $pK = 6.8$ (pK of phenol, 10) but less acidic than acetic acid ($pK = 4.8$).¹⁰

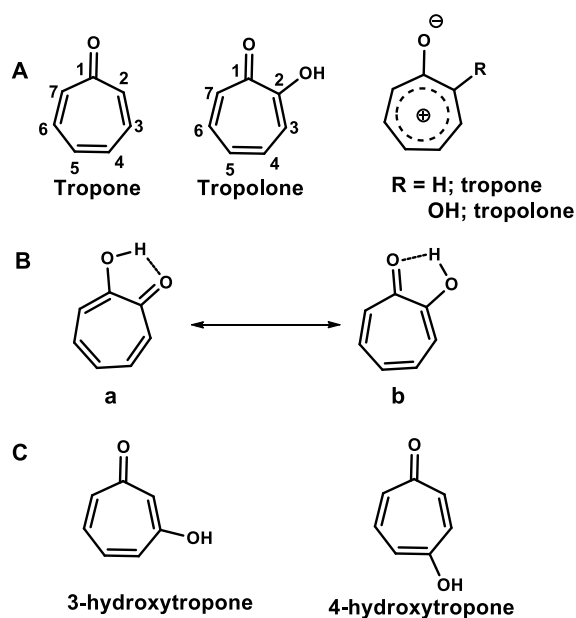


Figure 1.2 A) Tropone and tropolone chemical structures and polarization representation B) Tautomeric forms of tropolone.

Since the tropolone hydroxyl group is an enolic hydroxyl. Hence, it exhibits characteristic properties of enols and phenols. Tropolone also forms dimeric metal complexes with metals like Be, Cu, Zn, Ni, Co, Pb, Mg, Ca etc.¹⁰

1.1.3 Bioactive tropolonoid natural products

To date, approximately 200 tropolonoid natural products have been identified in the nature and isolated.¹⁷ A few examples of important tropolonoid natural products which are reported in the literature are pointed out and their biological properties are briefly described here. Along with explanation, a graphical representation of their biological properties are given in **Figure 1.3**. However, since two decades, tropolonoid natural products attracted the scientific community due to their interesting biological activities such as anti-bacterial, anti-fungal, anti-viral and anti-tumour activities (see examples later in this chapter).¹⁷⁻¹⁹ It is worth mention that,

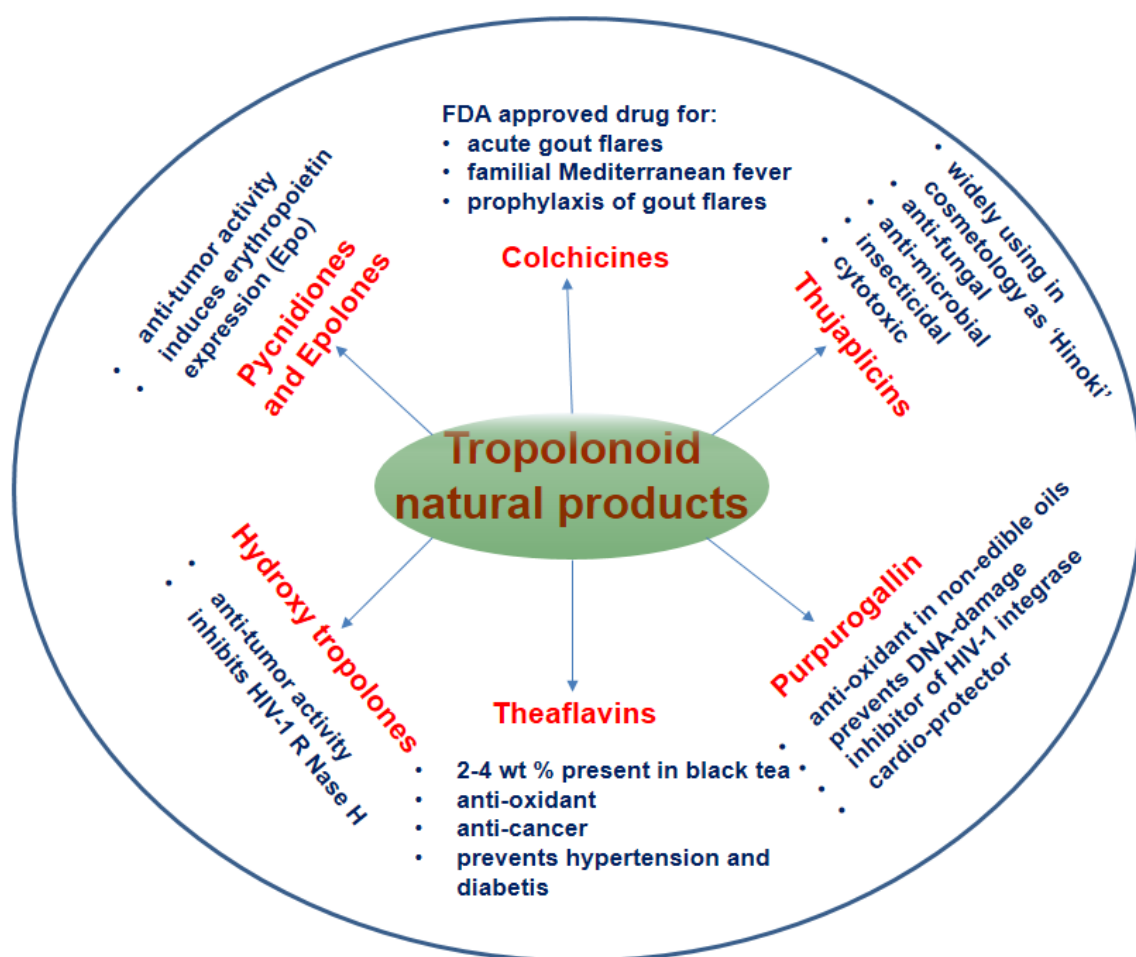


Figure 1.3 Pictorial representation of a few bioactive tropolonoid natural products and their biological activities.

tropolone itself is bacteriostatic and bacteriosidal. Puberulic acid has shown potential antimalarial activity.³⁰ From the literature, it has been learnt that the tropolonoids acts as selective inhibitors of enzymes by chelating with metal ion co-factors (Zinc, Magnesium and Manganese).¹⁷ Interestingly, most of the tropolonoid natural products are the secondary metabolites of either plants or fungi and their biosynthesis is well established.¹⁷

As discussed earlier, colchicine is known since ancient days and one of the most extensively studied member of tropolonoids (**Figure 1.1A**). The chemical structure of Colchicine was proposed by Dewar in 1945 along with the Stipitatic acid chemical structure.^{5,6} Literature revealed that colchicine is in existence in Europe and North Africa since 2000 years.¹⁷ In ancient days, it was used as poison and treatment of gout arthritis.¹⁸ And surprisingly, to date, it is the only drug which is using for the treatment of acute gout arthritis.¹⁷⁻¹⁹ In 2009, FDA approved the colchicine for treating the acute gout flares,²⁴ familial Mediterranean fever in childrens,²⁴ prophylaxis of gout flares, secondary amyloidosis and scleroderma.^{17,18} Though colchicine is well-known since 1940s but recent FDA approval is due to its general toxicity, which means an intake of colchicine more than 7 mg in a day is not suggested.¹⁷⁻¹⁹ On the other hand, colchicine has been known to bind with tubulin protein and prevents the formation of micro tubules during cell division. As a result, the cell division at the mitotic phase will be stopped.^{20,21} Moreover, colchicine has shown excellent cytotoxicity but its general toxicity became a major disadvantage for the use of colchicine in anti-tumour chemotherapy.^{20,21} Later on, numerous colchicine analogues have been synthesized to enhance cytotoxicity and to lower the general toxicity, but none of them were have shown cytotoxicity as effective as colchicine for treatment of cancer.^{17,18}

Thujaplicins (**Figure 1.1C**) are well-known with the trivial name ‘hinokitiol’ in eastern Asia countries such as Japan, Taiwan and Russia.¹⁷ These are isopropyl-tropolones. These have been using as preservatives for mushrooms, flowers, and vegetables owing to their anti-fungal

activity. It is worth to mention that, in Japan and Russia ‘hinoki’ oil (hinokitiol) products are widely using in cosmetic products as hair fall protectors and thinning of hair.^{17,28} The ‘Hinoki Clinical’ is one of the deluxe cosmetology services in Russia and Japan.^{17,28} They have also shown interesting biological activities such as anti-fungal, anti-microbial, anti-tumour, anti-inflammatory and insecticidal.¹⁹ β -Thujaplicin/hinokitiol is broadly useful in cosmetology.^{26,27} Moreover, β -dolabrinol and 4-acetyl tropolone are analogues of Thujaplicins, which have shown potential cytotoxic activity and metalloprotease inhibition.^{29,31}

Purpurogallin is a benzotropolone (**Figure 1.4A**), which is isolated from the nutgalls and oak bark.^{13,32,33} It was used as anti-oxidant in non-edible oils, fuels and lubricants.^{32,33} Recently, potential inhibition of HIV-1 integrase activity was observed by purpurogallin through metal chelation.³⁴

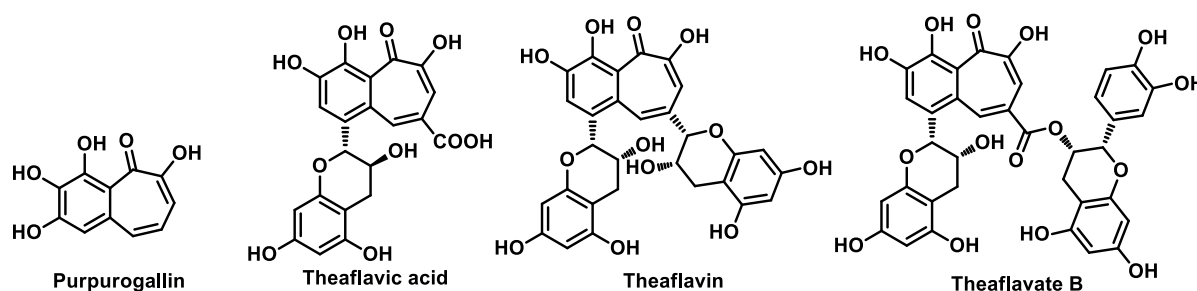


Figure 1.4 Chemical structures of Purpurogallin and Theaflavins.

Theaflavins were first isolated from black tea leaves in 1957 and they are also having a benzotropolone moiety (**Figure 1.4B**).³⁵ They have shown numerous biological activities such as anti-oxidant properties, anti-pathogenic, anti-cancer, preventing heart diseases, hypertension and diabetes. Theaflavins have also shown potential anti-HIV-1 activity.^{37,38}

Grandirubrine, imerubrine, isoimerubrine, pareirubrine A and pareirubrine B are another class of tropolonoids (**Figure 1.5**).³⁹⁻⁴¹ They are generally called as tropoisoquinolines and isolated from the Menispermaceae plants. They have also shown cytotoxic activity against selective cell-assays. Pareitropone is a tropoisoquinoline, isolated

from the plants of same family, which has shown superior cytotoxicity in leukemia P388 cells ($IC_{50}=0.8\text{ng/mL}$).⁴¹

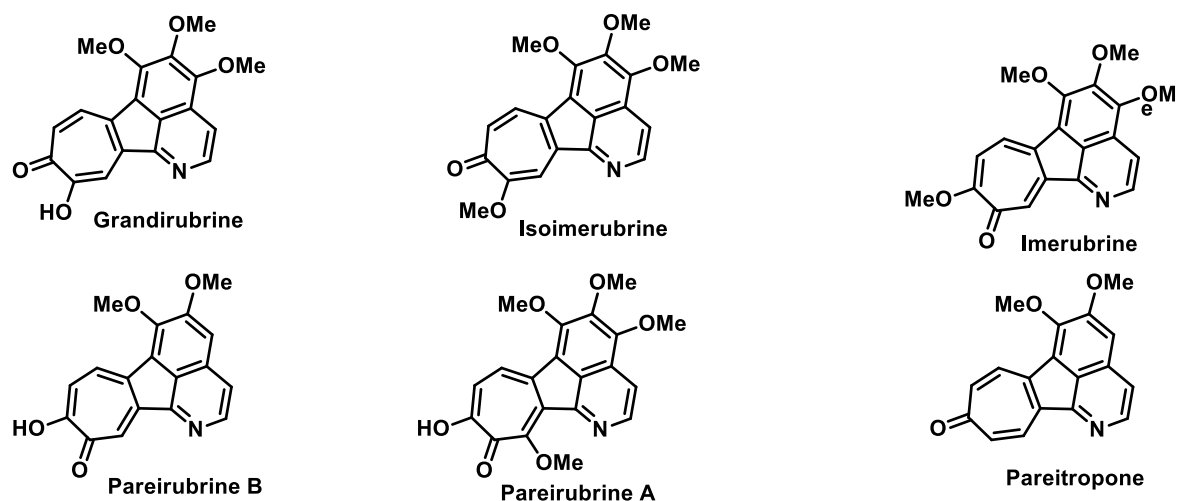


Figure 1.5 Chemical structures of Tropoisoquinolines

Epolones and Pycnidiones are polycyclic sesquiterpene-tropolones, containing eleven-membered humulene ring (**Figure 1.6**).⁴²⁻⁴⁴ These are isolated from the fungal species.

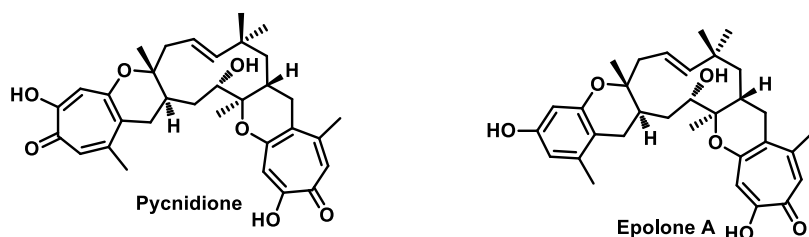


Figure 1.6 Chemical structures of Pycnidione and Epolone A

Epolone contains one tropolone unit whereas Pycnidione has two tropolone units. They have also shown notable anti-tumor activity.⁴² Moreover, the important application of pycnidione and epolones are, they induces erythropoietin (Epo) expression. Therefore, these may be possible alternatives for the treatment of anaemia, instead of recombinant Epo.⁴⁴

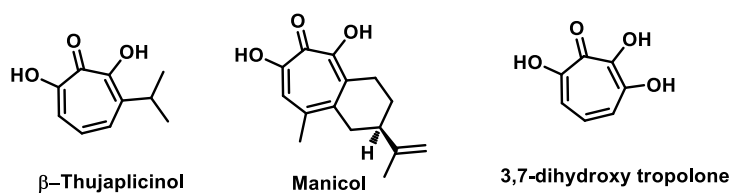


Figure 1.7 Chemical structures of hydroxyl tropolones.

Another important class is Hydroxy tropolones (**Figure 1.7**), β -Thujaplicinol and manicol are selective inhibitors of HIV-1 ribonuclease H enzyme with Mn^{2+} as co-factor.⁴⁷ 3,7-dihydroxy tropolone has shown strong anti-tumor activity against B16 melanoma.^{45,46}

Overall, it is worth mention that the biological activity of most of the tropolonoids is due to the presence of tropolone moiety and which helps to bind with target site through non-covalent interactions to execute specific biological function. In some cases, the specific enzyme activity (inhibition or promotion) of tropolonoids is due to the chelation of tropolone moiety with respective enzyme metal ion co-factors. Generally, in the literature, it has been widely discussed that the ketone and hydroxyl functional groups or one of them of tropolone moiety in tropolonoids are playing key role for the execution of specific biological activity.^{17,18}

1.1.4 Structural analogues and synthetic derivatives of tropolone

Structural analogues of tropolone such as aminotropone and thiotropolone have also been synthesized by replacing the oxygen atoms of tropolone with nitrogen and sulfur (**Figure 1.8**).⁴⁸ Thiotropolnes are sulfur analogues of tropolone, which have shown distinctive properties from tropolone. Thiotropolone has shown tautomerism in even low temperatures also, which is not exhibited by tropolone.⁵⁰ Thiotropolone also known to form metal complexes like tropolone.⁴⁹

On the other hand, tropolone is well known to form metals complexes (**Figure 1.8**).¹⁰ The presence of carbonyl and hydroxyl functional groups adjacent to each other on the seven-membered ring tropolone, made it as a worthy ligand for the formation of metal complexes with variety of metal ions.¹⁰ So far, several tropolonate metal complexes have been synthesized, and their chemical and physical properties were studied.¹⁰ Chelation of tropolone with metals results in formation of five membered metallacycle. Though they have shown

characteristic properties, but tuning them in desired manner for different applications by introducing substituents at chelating atom ‘oxygen’, is impossible.⁵¹ Hence, to overcome these difficulties, replacing the oxygen atom with another chelating atom which can facilitate the suitable derivatization is important. In this way, aminotroponimines (**Figure 1.8**) were synthesized.⁵¹⁻⁵⁵ Aminotroponimines are synthetic aza-derivatives of the tropolone and bidentate nitrogen chelating ligands. Where oxygen atoms are replaced by the trivalent nitrogen atom.⁵¹⁻⁵⁵ Importantly, the nitrogen atom is trivalent, therefore, there is wide scope to derivatize the aminotroponimines with various types of substituents at nitrogen atom.

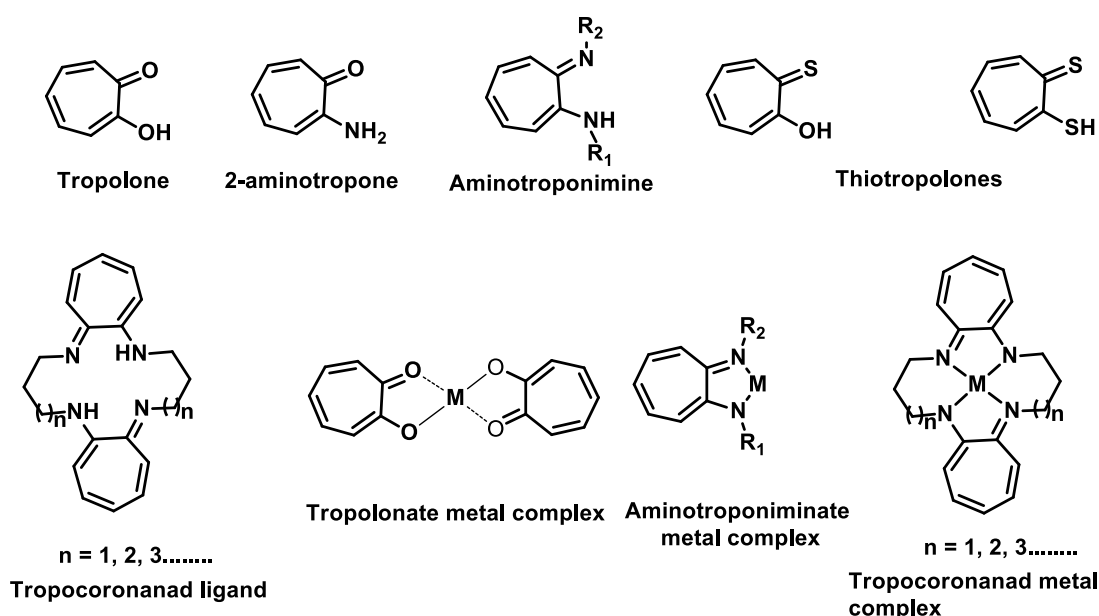


Figure 1.8 Chemical structures of Aminotroponimines, tropocoronands and their metal complexes.

To date, wide variety of aminotroponimines and their metal complexes have been synthesized. Aminotroponimine is a one of the ubiquitous ligands and forms metal complexes with almost all the metals.⁵¹⁻⁵⁵ They form five-membered ring metallacycles. The advantage with the aminotroponimine ligands is their feasibility to design in required manner by introducing variety of substituents at *N*-atom of ligand.⁵¹⁻⁵⁵ Tropocoronands are the best examples to explain the flexibility in designing the variety of ligands with aminotroponimine core structure (**Figure 1.8**). Tropocoronands are the macrocyclic aminotroponimine chelating ligands, where, they can provide opportunity to tune the macrocyclic ring size.⁵³⁻⁵⁵

Overall, to date, aminotroponimine complexes with most of the metals and non-metals have been synthesized and their structural properties are well described. And on the other hand, the synthesis of tropocoronands and their metal complexes are also elaborated, which are derived from cyclic aminotroponimines and metals. A few of the aminotroponimine metal complexes are known to catalyse selective organic transformation reactions.^{51,52}

1.1.5 Photophysical properties tropolone moiety

Since the electronic structure of tropolonoids is distinctive from benzenoids, hence they are known to exhibit characteristic photophysical properties.⁵⁶⁻⁶² Absorption and emission properties of tropolonoids are elucidated after the discovery of its chemical structure.⁵⁶⁻⁵⁹ Absorption properties of tropolone and its few derivatives are described in different mediums. In the literature, absorption properties of 5-nitrosotropolone and 5-tropolonediazonium salts have also been reported.⁶³ More interestingly, the fluorescence properties of tropolone moiety came into limelight in 1970s when Aria and Okuyama found the fluorescence of Colchicine after binding with tubulin protein.⁶⁰⁻⁶² After their report, fluorescence properties of tropolone and its few derivatives are also elucidated in different mediums.

Tropolone and colchicine have shown very low quantum yields at room temperature.⁵⁸ Interestingly, tropolone and colchicine have shown reportedly greater quantum yields at low temperature (77.0 K).⁵⁸ The fluorescence properties of dimeric tropolone derivatives linked by phenyl group and suitable connecting linkers and substituted tropolone derivatives (2-hetaryl-1,3-tropolones) have been also explored. Among them 2-hetaryl-1,3-tropolones have shown enhanced quantum yields at room temperature.⁶⁴ Overall, the constructed fluorescent molecules from tropolonoid aromatic system are very few in the literature.

1.2 Introduction of Peptidomimetics

Proteins and peptides are the ubiquitous structural and functional macromolecules occurs in living system. Proteins/peptides perform several physiological and biological functions in the living system as enzymes, hormones etc.^{65,66} The natural proteins and peptides are constructed from 20 proteinogenic α -amino acid building blocks which are connected through amide linkage.^{65,66} They are known to form specific and well-ordered three-dimensional structure.^{65,66} The three dimensional structures of few proteins (Pop2P, green fluorescent protein, myoglobin) existing in the literature are depicted in **Figure 1.9B**.¹¹⁴ The three dimensional structure of proteins is the combination of variety of secondary structural

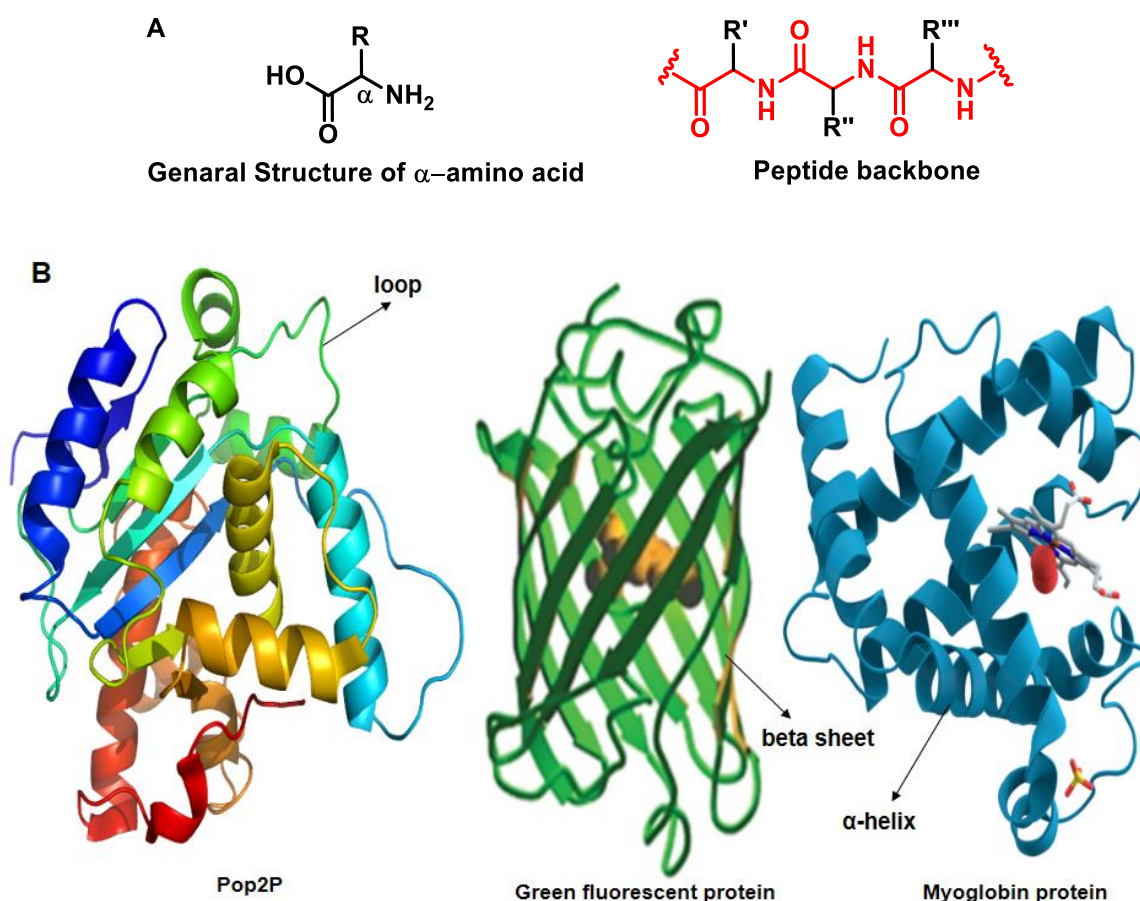


Figure 1.9 A) General structure of α -amino acids and peptide backbone; B) Three dimensional structures of proteins.

elements such as helix, turn, hairpin and sheet secondary structures (**Figure 1.9B**).⁶⁵⁻⁷⁸ This three dimensional structural organization leads to the precise spatial arrangement of functional groups in three dimensional space.⁶⁵⁻⁷⁸ Conformationally well-defined structural organization of proteins and peptides is responsible for the execution of their specific function.⁶⁵⁻⁷⁸ It is worth mention that the driving force for well-defined structural organization in proteins/peptides is, the favorable conformational preference of individual amino acid residue and hydrogen bonding interaction between NH and CO functional groups of polypeptide backbone. The conformational preference of every amino acid is different from the other. The conformational preference of each amino acid is mostly depends on the substituent at α -carbon atom and conformational preference of neighboring amino acid and rest of the sequence. However, it can be explained by taking the general structure of α -amino acids (**Figure 1.9A**), where 20 standard natural α -amino acids are structurally similar other than the substituent at α -carbon. Hence, it is clear that the conformational preference of individual amino acid residue is governed by the substituent present at its α -carbon and rest of the sequence. As a result, specific amino acid

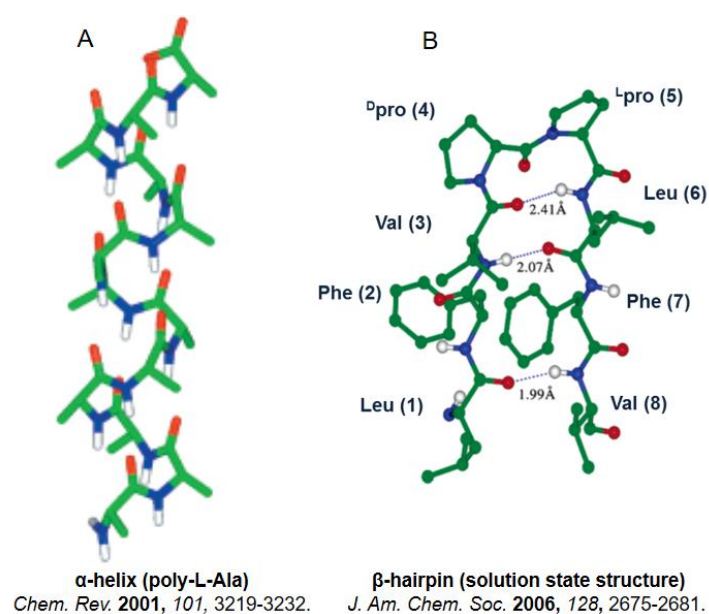


Figure 1.10 Secondary structures of natural synthetic peptides.

sequence is responsible for formation of specific 3D structural organization.⁶⁵⁻⁷⁸ In the literature, synthetic peptides with natural α -amino acids were extensively studied to understand the conformational preference of individual amino acid residues in their peptides.⁶⁹⁻⁷⁸ The natural synthetic peptides have shown well-ordered secondary structures depends on the sequence. For example, poly-L-alanine peptide forms α -helical structure in solid state (**Figure 1.10A**, 3.6 residues per turn, i+4 to i hydrogen bonding)⁸⁶ and an octapeptide of Leu-Phe-Val-^DPro-^LPro-Leu-Phe-Val has shown a β -hairpin secondary structure in solution (**Figure 1.10B**).⁸⁶ These are two representative examples for α -helix and β -hairpin, but countless number of natural synthetic peptides have been synthesized and explored their structural properties and today, this area of research is well-established and synthetic peptides are proved to be potential to mimetics of the function of biomolecules and currently they are in use as therapeutic drugs and for other biomedical applications.^{70-79, 98, 101}

Conformation governing factors in peptides/proteins:

- conformational preference of individual amino acid residue.
- Substituent/s on the amino acid backbone.
- non-covalent interactions: hydrogen bonding, vanderwalls interactions and π - π interactions.

1.2.1 General peptide synthetic approach

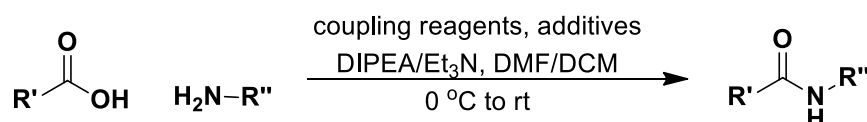
Syntheses of peptides in the laboratory is an important task to study their structural and biological properties. However, peptide syntheses is well established area in the organic chemistry.⁶⁸⁻⁷³ Majorly, there are two different standard protocols for the syntheses of peptides in laboratory these are

1. Standard Solid Phase Peptide Syntheses
2. Standard Solution Phase Peptide Syntheses

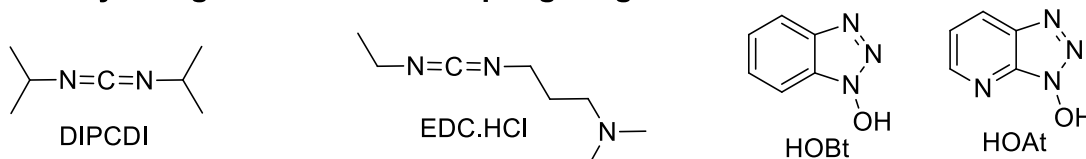
Any of these methods can be followed for the syntheses of desired target peptide. Selecting a particular synthetic protocol for the syntheses of desired peptide depends on the length of peptide sequence and ease of purification. For the syntheses of small peptides in more quantity, solution phase peptide syntheses is more preferable and for syntheses of larger peptides solid phase peptide syntheses is preferable.

In solution phase peptide syntheses, amine protected carboxylic acid (PG-NH-aa-COOH) and carboxylic acid protected free amine (NH₂-aa-COOPG) starting materials were dissolved in suitable solvent (DCM/DMF) in presence of coupling reagents/additives

A) General representation of solution peptide syntheses:



B) Widely using carbodiimide coupling reagents additives:



C) Mechanism of carbodiimide mediated solution phase peptide syntheses:

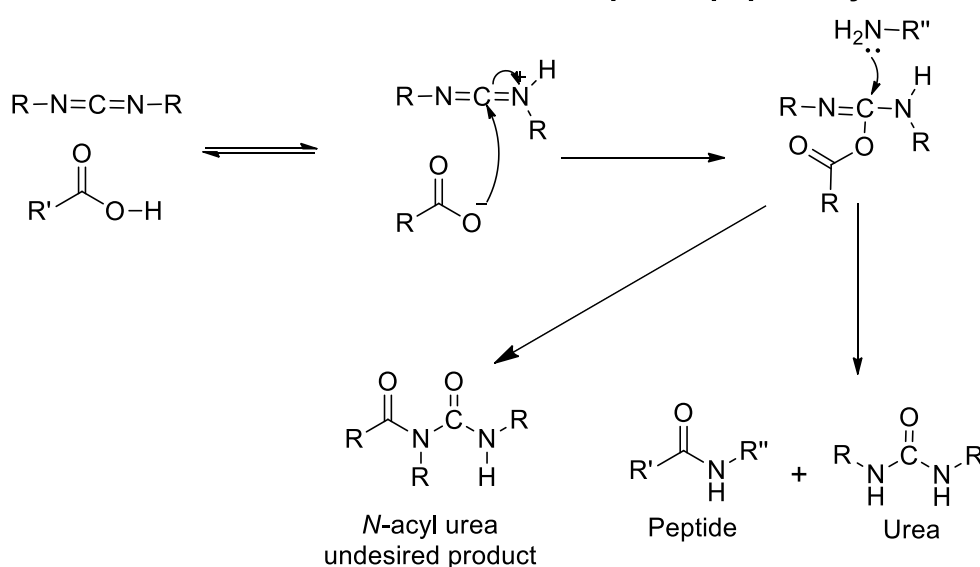


Figure 1.11 A) General representation of solution phase syntheses of peptides B) coupling reagents and additives C) Mechanism of carbodiimide mediated peptide coupling.

(DIPCDI or EDC.HCl and HOBt or HOAt) and an organic base (DIPEA). After completion of the reaction, the obtained peptide can be purified by following general purification

methods in synthetic organic chemistry (column chromatography). General solution phase peptide syntheses reaction and mechanism of carbodiimide mediated peptide coupling is presented in **Figure 1.11**.

On the other hand, in case of solid phase peptide syntheses, the growing peptide chain is attached to a solid support and unreacted starting materials and reagents are washed out. After completion of the syntheses desired peptide sequence, the peptide chain has to be cleaved from the solid support by following suitable methods and purified by preparative HPLC. Pictorial representation of solid phase peptide syntheses is depicted in **Figure 1.12**.

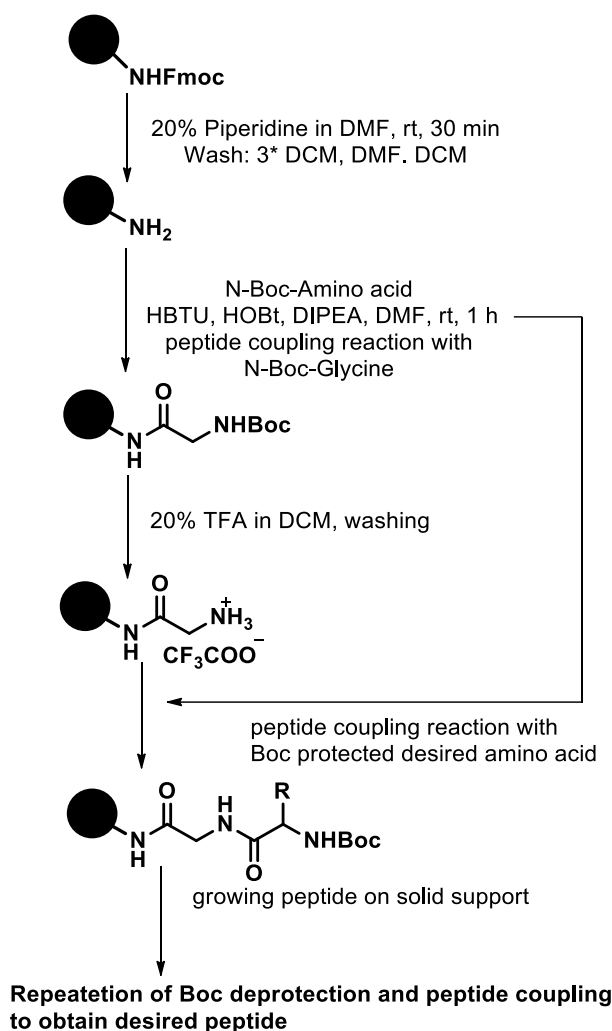


Figure 1.12 General representation of solid phase peptide syntheses, Boc strategy

Applications of peptides:

- Therapeutic drugs and vaccines of various diseases, and peptide hormones
- Selective binding ligands
- Organocatalysts
- Nanomaterials

1.2.2 Peptide therapeutic drugs

Synthetic peptides have wide range of applications such as therapeutic drugs, organocatalysts, and to fabricate functional nanomaterials. Peptide therapeutic drugs are one of the widely growing class of therapeutic drugs for various diseases.⁷⁹⁻⁸¹ Here, chemical structures of a few peptide therapeutic drugs available in market are presented in **Figure 1.13** (obtained from reference 79). Enalapril maleate is a *tri*-peptide which is currently in the market for the treatment of hypertension. Lisinopril is another *tri*-peptide for the treatment of hypertension and congestive heart failure. Sincalide is an *octa*-peptide of H-Asp- Tyr(OSO₃H)-Met-Gly-Trp-Met-Asp-Phe-NH₂ which is using for the treatment of diagnosis of the functional state of the gallbladder and pancreas and stimulant of the gastric secretion. Buserelin and histrelin acetates are the gonadotropin releasing hormone agonists, both are nona-peptides containing almost same sequence except the sixth residue. Buserelin is having D-serine whereas histrelin contains D-histidine. These are currently using for the treatment of advanced prostate cancer and central precocious puberty. Argipressin, lypressin and phenypressin are also *nona*-peptides and are vasopressin analogues used for the treatment of central diabetes and stomatitis. ADH-1 is a *penta*-peptide of Ac-c[Cys-His-Ala-Val-Cys]-NH₂, a FDA approved drug for the treatment of malignant melanoma. Glutathion is a *tri*-peptide of H-γ-Glu-Cys-Gly-OH and in use for the treatment of hepatic insufficiency and wound healing. Spaglumat magnesium salt is a dipeptide of Ac-Asp-Glu-OH is using for the treatment of allergic rhinitis

and conjunctivitis. Thymopentin is a *penta*-peptide of H-Arg-Lys-Asp-Val-Tyr-OH which is using for the treatment of primary and secondary immune system.

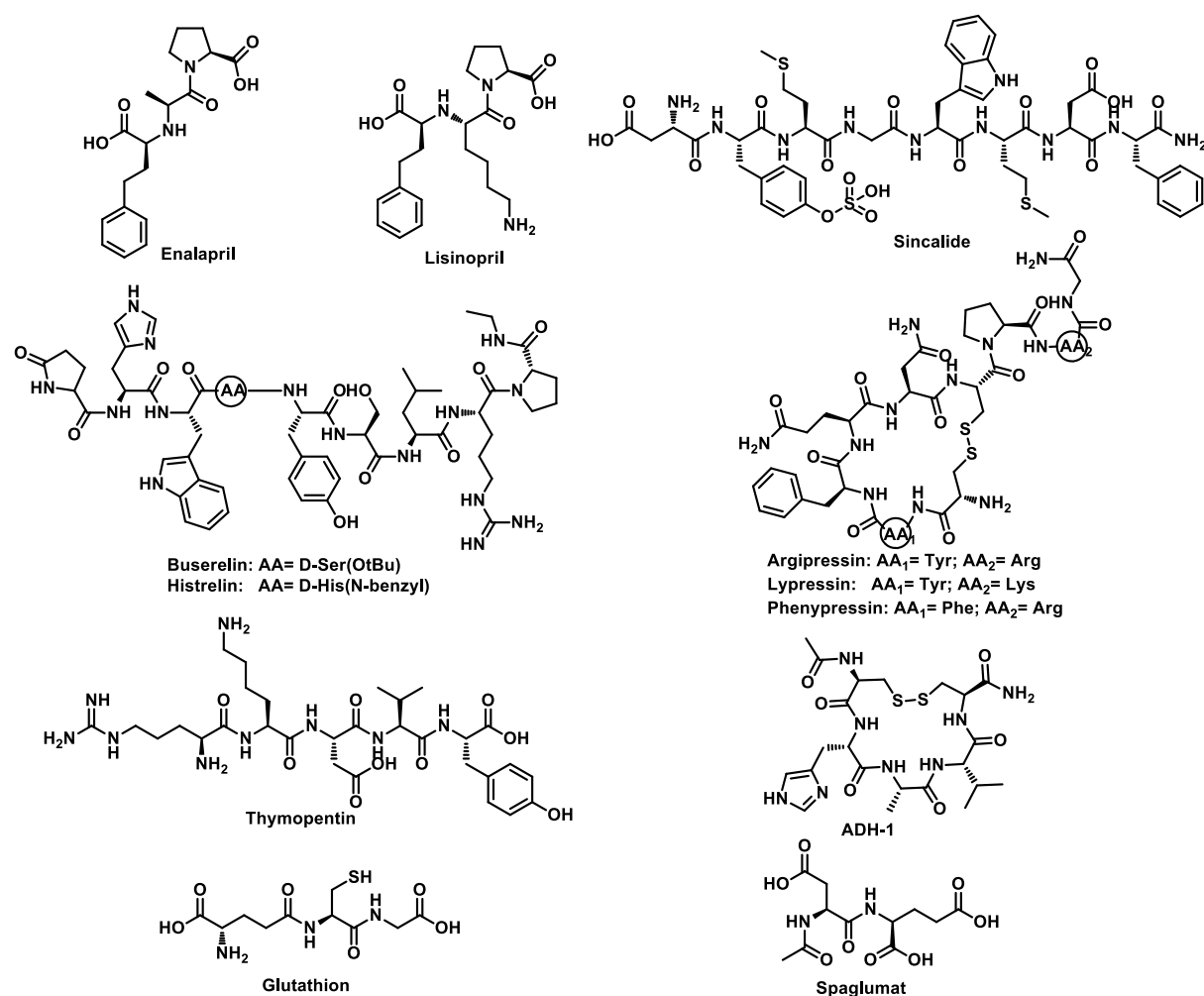


Figure 1.13 Chemical structures of a few peptide therapeutic drugs.

Some of the presented peptide therapeutics in **Figure 1.13** contains unnatural amino acid residues. For example, Enalapril and Lisinopril contains Phenethyl glycine, a structural analogue of phenyl alanine. Buserilin contains D-amino acid residue. Whereas Sincalide contains sulfonlated tyrosine. Argipressin and ADH-1 are cyclized through disulfide linkages.

1.2.3 Peptide therapeutic drugs - advantages and limitations

Advantages of peptide therapeutic drugs:

Peptide therapeutic drugs are currently in the pharmaceutical market for the treatment of various diseases. In most cases peptide therapeutic drugs acts as receptor agonists.⁷⁹⁻⁸¹ They have various advantages over small organic molecule drugs such as (i) greater efficacy (ii) specificity and (iii) less toxicity. Most importantly, high speed of action and less side effects of peptide based therapeutic drugs made them best alternatives over small organic molecule drugs in case of emergency treatments.⁷⁹⁻⁸¹

Limitations of peptide therapeutic drugs:

Though peptide therapeutic drugs have shown several advantages over small molecule drugs but they also have major limitations. These are, peptide therapeutic drugs derived from natural amino acids have shown notable limitations such as (i) low oral bioavailability and (ii) susceptibility towards proteolytic enzymes present in the gastrointestinal tract and plasma.^{79, 80} As a result, the oral administration of a peptide drug causes low bioavailability due to high concentration of proteolytic enzymes in the gastrointestinal tract which leads to the degradation of active drug.⁷⁹⁻⁸¹ Further threat to peptide therapeutic drugs is plasma, which also has high concentration of proteolytic enzymes and as a result, plasma residence time of active drug molecule decreases.⁷⁹⁻⁸¹

1.2.4 Alternative approaches to overcome the limitations of natural peptide therapeutics

To overcome the above mentioned limitations of peptide therapeutics derived from natural amino acids, structural modifications of active core of particular protein or existing lead peptide compound (drugs) are necessary without altering the pharmacokinetic properties of the native drug to enhance the plasma residence time and to facilitate the oral drug

administration.^{70,75,79-81,101} However, the execution of specific function of peptide based therapeutics depends on the secondary structure (conformation) of the molecule, therefore chemical modifications must provide similar structural and conformational properties of native peptide drug.⁷⁹⁻⁸¹ So far, various chemical modifications have been introduced which can be achieved through chemical synthetic strategies.^{68-78, 101}

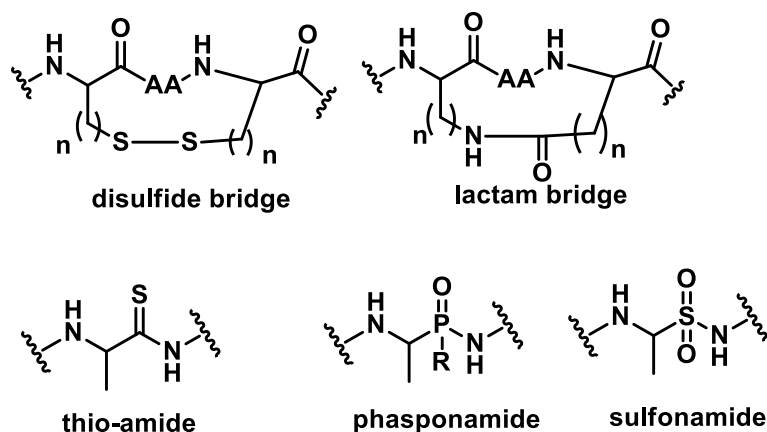


Figure 1.14 Developed alternative for efficient peptide therapeutics

These modifications include cyclization of the linear peptide between two ends or side chains *via* disulfide linkage, dicarba, lactam or hydrazine bridges to enhance the proteolytic stability and affinity.¹⁰¹

The other alternatives are (i) replacement of selective amide bond by CH_2 ($-CH_2-NH-$) or replacing the amide carbonyl with thio-amide or phosphonamide or making retro-inverso amide bond, (ii) isosteric replacement, (iii) introducing unnatural amino acid residues (non-proteinogenic amino acids) in place of natural amino acid residues.¹⁰¹ Or developing peptide therapeutic drugs from unnatural amino acid residues (**Figure 1.14**).

Isosteric replacement is the replacement of specific amide functional group by an isosteric functional groups such as esters, thioesters, thioamides, alkenes and fluoroalkenes.

The obtained peptides where amide bond is replaced by ester and thioester are called as depsipeptides and thiodepsipeptides, respectively (**Figure 1.15**).¹⁰¹

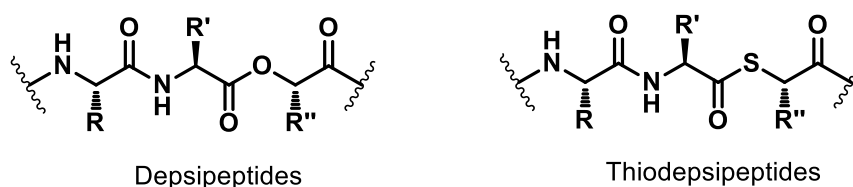


Figure 1.15. General chemical structures of depsipeptides and thiodepsipeptides

The peptides obtained after these chemical modifications of an existing native peptide can be generally called as peptidomimetics. Among all above mentioned chemical modifications, the development of unnatural amino acids as alternatives of natural amino acids attained special interest by the scientific community in the development of potential peptide therapeutic drugs.

1.2.5 Unnatural amino acids and peptidomimetics

Unnatural amino acids are those which doesn't coded by ribosomes during the syntheses of proteins through translation phenomenon in living system.⁶⁹⁻⁷² To date, different types of unnatural amino acids are reported in the literature. Importantly, either they may be derivatives of natural α -amino acids or they may be the designed novel amino acids with diverse chemical composition and can be achieved through chemical synthetic strategies. The different types of unnatural amino acids include, backbone extended amino acids, D-amino acids, C_{α} -substitution of natural amino acids, C_{α} replacement of natural amino acid residue by nitrogen, and *N*-alkylation of natural amino acids (peptiods, **Figure 1.16**).¹⁰¹

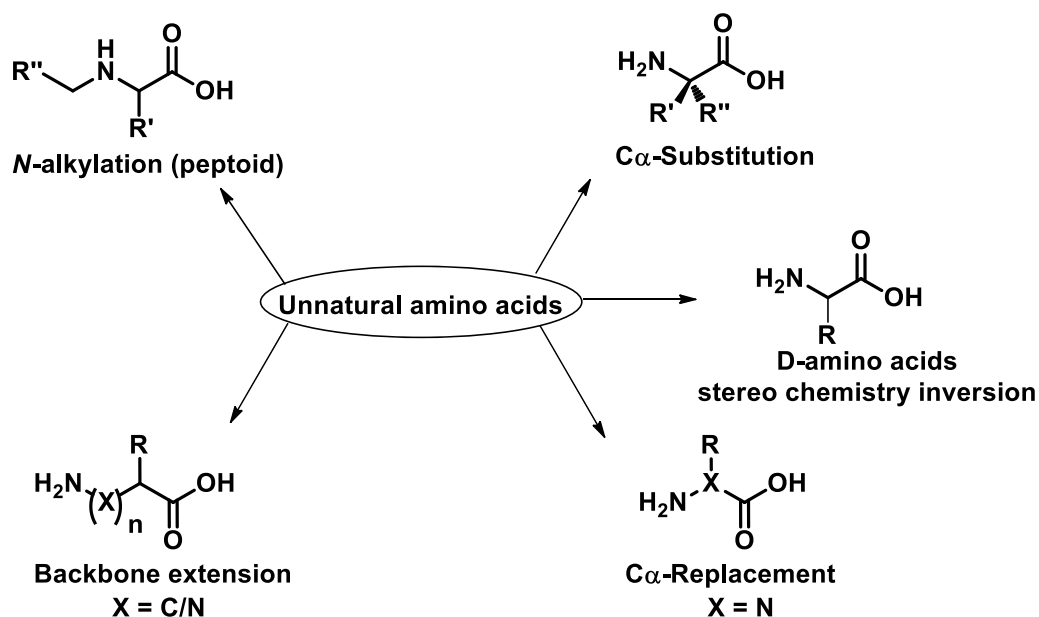


Figure 1.16 General representation of different types of unnatural amino acids.

C α replacement of natural amino acid residue by hetero atom like nitrogen gives unnatural aza-amino acids. The peptides obtained from these amino acids are called as aza-peptides and azitides (**Figure 1.17**).¹⁰⁰⁻¹⁰³ In the literature, the syntheses and conformational analysis of aza-peptides and azatides are also well-explored.¹⁰¹ Atazanavir, an FDA approved anti-HIV drug, which is an azapeptide inhibitor of the HIV-protease.¹⁰¹

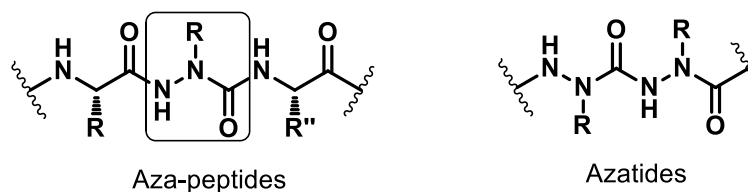


Figure 1.17. General chemical structures of Aza-peptides and Azatides

However, among these unnatural amino acids, herein, different types of backbone extended amino acids and their peptides are explained briefly.

1.2.6 Backbone expanded amino acids

Backbone expanded amino acids are homologative derivatives of natural α -amino acids.⁷⁷ To meet the growing requirement of applications of synthetic peptides in various fields such as potential peptide therapeutics, organo catalysts and to fabricate functional nanomaterials backbone expanded unnatural amino acids are developed as one of the alternatives for natural α -amino acids.⁷⁰⁻⁷⁷ They can be synthesized from α -amino acids by inserting methylene groups or hetero atoms through various chemical strategies.⁷¹ Otherwise, they can also be synthesized with diverse chemical composition through various chemical synthetic strategies.^{83-88,104} Based on the number of methylene groups/hetero atoms inserted between the amino and carboxyl functional groups, they are named as following (**Figure 1.18**).

- β -amino acids: one $-\text{CH}_2-$ insertion
- γ -amino acids: two $-\text{CH}_2-$ insertions
- δ -amino acids: three $-\text{CH}_2-$ insertions and so on

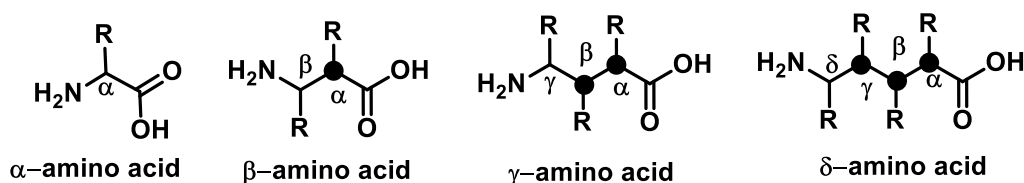


Figure 1.18 General representation of backbone extended amino acids

So far, β and γ -amino acids and their peptides explored enormously. The exploration of backbone extended amino acids started in 1990s.^{83,84} Since then several backbone expanded amino acids and peptides have been synthesized and studied their properties. In the literature, there are various methods for the synthesis of β -amino acids.¹⁰⁴ First time, Dieter Seebach and co-workers have synthesized β -amino acid derivatives of all 20 natural α -amino acids through Arndt-Estert homologation (**Figure 1.19A**).¹⁰⁴ The obtained β -amino acids through homologation of α -amino acids are called as β^3 -amino acids.⁸⁶

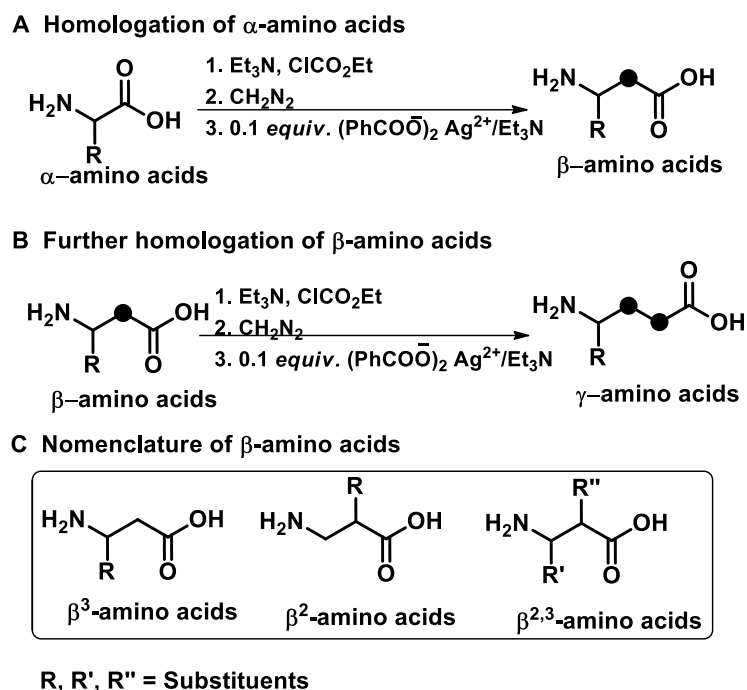


Figure 1.19 (A) Syntheses of β -amino acids from α -amino acids through Arndt-Estert homologation. (B) Syntheses of γ -amino acids from β -amino acids through Arndt-Estert homologation. (C) Nomenclature of β -amino acids based position of substituents on backbone.

On the other hand, β -amino acids with unnatural substituents on the backbone are also extensively reported.^{69-72, 82-89} A few examples are, amino cyclopentyl carboxylic acid (ACPC) and amino cyclohexyl carboxylic acid (ACHC).⁷⁵ To note very few, but countless number of β -amino acids and their peptides have been synthesized and their secondary structures are exploited. And hybrid peptides containing both β and α -amino acid residues are also synthesized, their secondary structures and biological properties are reported.⁹¹⁻⁹³ Based on the position of substituent on the backbone of β -amino acids, they are named as shown in the **Figure 1.19C**. Interestingly, the unnatural β -peptides and $\alpha\beta$ -hybrid peptides have shown similar or enhanced biological properties with respect to that of natural peptides and greater resistance towards the proteolytic enzymes.^{69-72, 82} For example, Octreotide (brand name SANDOSTATIN) is a cyclic α -octapeptide which can mimic the function of Somatostatin and is in clinical use to treat the acromegaly and intestine cancers.⁸² This is synthesized from α -amino acids containing the following residues, Phe-Cys-Phe-Trp-Lys-Thr-Cys-Thr and the

cyclization is done between two cysteine residues via disulfide linkage. The biological half-life of this drug is found to be 1.7-1.9 hours, which is very short. To mimic the function of this drug Seebach and co-workers synthesized a cyclic β -tetrapeptide containing the β^3 -Lys-Thr-Phe-Trp amino acids. This β -peptide has shown similar affinity towards human somatostatin receptors (**Figure 1.20**).⁸²

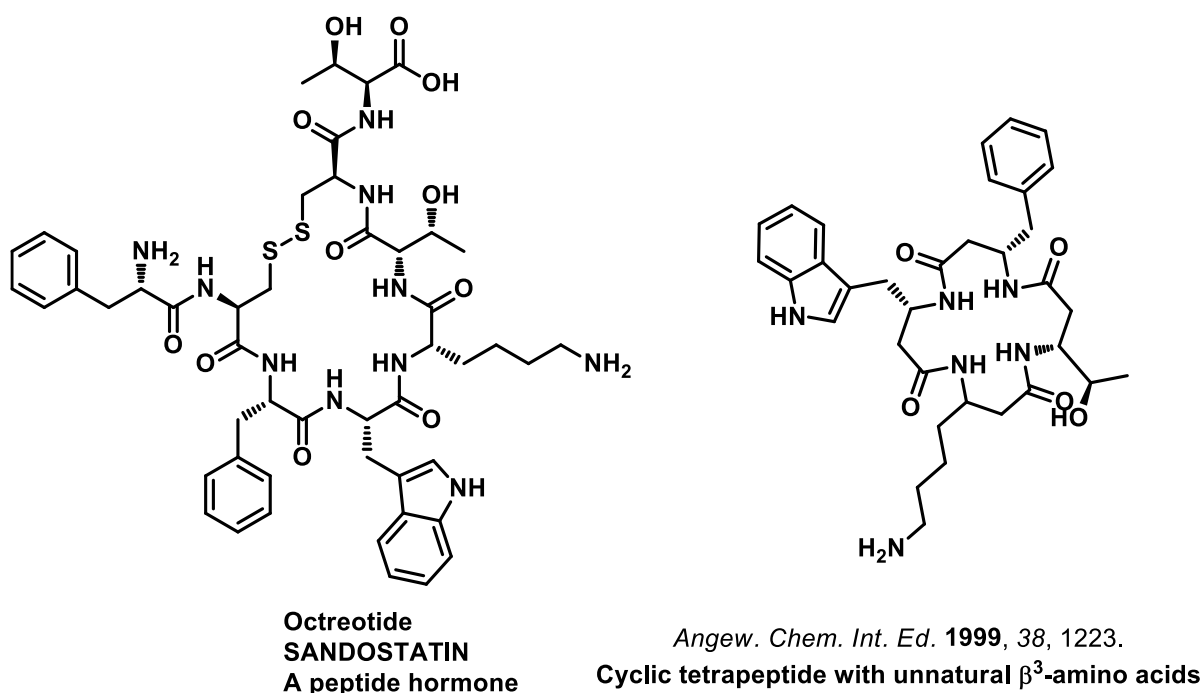


Figure 1.20. Chemical structures of Octreotide peptide (natural peptide hormone) B) A cyclic β -tetrapeptide to mimic the function of Octreotide.

In addition to β -amino acids and peptides, the syntheses and structural studies of unnatural γ , δ -amino acids and their peptides have also been exploited.^{90, 104, 105}

The evolution of unnatural peptides as potential mimics of naturally occurring peptides and proteins leads to the development of novel backbone extended amino acids as one of the alternatives of α -amino acids and their peptides.^{77, 79-81}

Moreover, as described previously, the biological action of peptides depends on the three dimensional structure and arrangement of active functional groups on the surface of the structure of the peptide. The three dimensional conformation of a peptide depends on the

conformational preference of individual amino acid residue and sequence. Hence, backbone extended amino acids provide enormous scope to restrict the allowed conformational space of the individual amino acid residue by introducing various conformational constraints on the extended backbone in the form of substituents.⁷⁷ And, it has been proved that the substituents on the amino acid backbone plays key role in the formation of novel and stable secondary structures.⁶⁹⁻⁷⁷ This can be explained by an example, oligomers of β -alanine have shown unordered secondary structures in solution and sheet like packing was reported in the solid state,⁸³ whereas modification of two backbone carbon atoms of β -alanine by introducing substituents at β^2 , β^3 , $\beta^{2,3}$ positions leads to the formation of helical structures in the solution and solid state.^{71,72} More interestingly, synthetic poly β^3 -hAlanine forms a 14-helical structure in solid state (**Figure 1.21A**) unlike poly-L-Alanine, which readily forms a α -helix (reference 86). In Figure 1.21B, a synthetic α/β -peptide of Ala, ACPC and Aib (aminoisobutyric acid) containing the given sequence is able to form 14/15-helical structure.⁸⁷

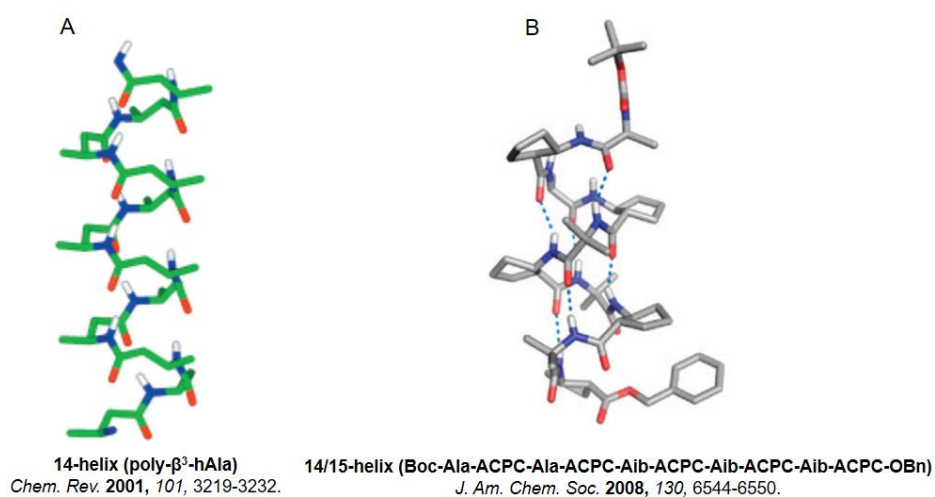


Figure 1.21. Solid state secondary structures of poly- β^3 -hAla (A) and α/β -peptide containing given sequence (B).

However, the effect of substituents on the conformation was enormously reviewed.⁶⁹⁻⁷⁷ Overall, the careful selection of substituent on expanded backbone will govern the secondary

structure formation of a peptide by restricting the allowed conformational space and which is responsible for formation of different secondary structural elements.⁷⁷

Conformationally constrained amino acids (natural and backbone expanded): Another interesting part of backbone extended amino acids is, introducing conformational constraints by modifying backbone into a cyclic ring or by bulky substituents (**Figure 1.22**).^{77,86} The amino acids in which ‘the possible number of conformations are reduced by introducing the conformationally rigid or cyclic substituents on the backbone’ are called as conformationally constrained amino acids.⁸⁵⁻⁸⁹ Proline and hydroxyl proline are the notable examples for conformationally constrained natural α -amino acids (**Figure 1.22A**). However, several conformationally constrained unnatural amino acids are reported and majority of them

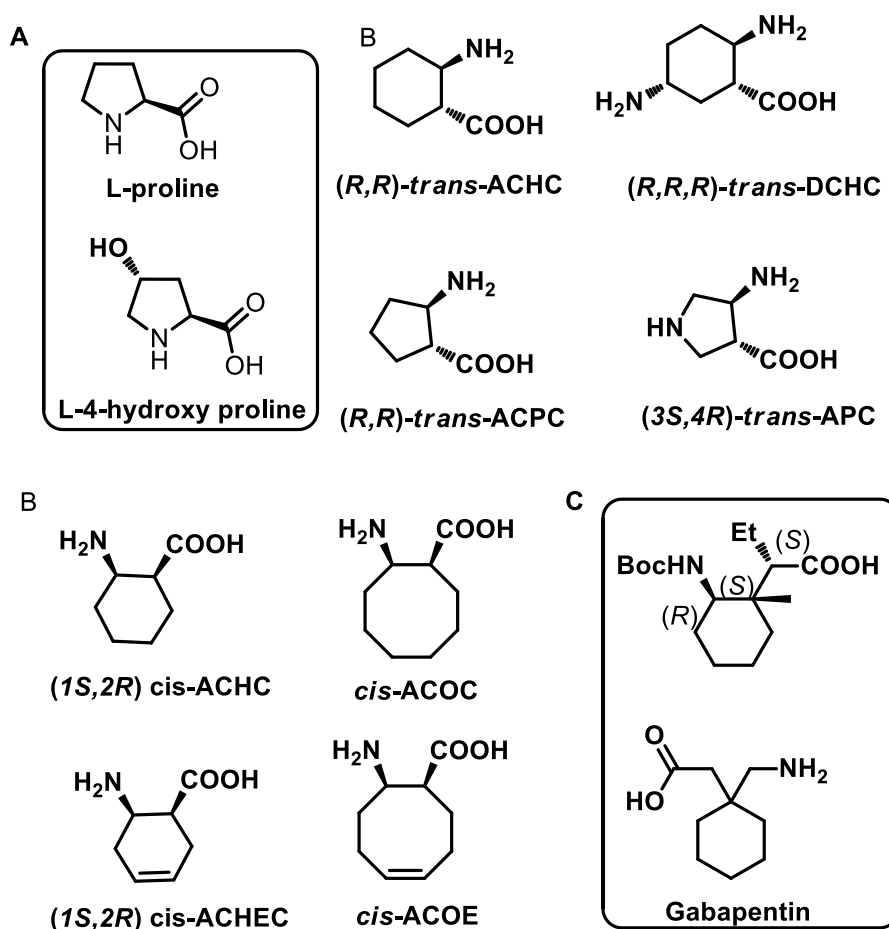


Figure 1.22 Representative examples of reported conformationally constrained cyclic natural and unnatural amino acids.

are amino acids with cyclic backbones or with sterically bulky substituents on the backbone (**Figure 1.22B&C**). In general, cyclic backbone containing amino acids are less flexible when compare to acyclic amino acids due to the presence of rigid cyclic ring. The conformation of the backbone cyclic ring depends on the stability of its conformational isomer which are formed due to ring puckering.⁸⁶ The formation of more stable conformational isomer depends on the nature of the ring and positions of substituents on the ring and their contribution to steric crowding in the conformational isomer. In general, the conformational isomer having less steric crowding is more stable.

A few examples for conformationally constrained amino acids are shown in the **Figure 1.22**.⁸⁵⁻⁹³ The peptides synthesized from conformationally constrained amino acids have shown novel and well-ordered secondary structures with superior stability.

Unnatural aromatic amino acids: On the other hand, in the repertoire of peptidomimetics, unnatural aromatic amino acids (**Figure. 1.23**) and their peptides attained the special interest by the scientific community.⁹⁴ Mostly, natural and unnatural aromatic amino acids are containing benzene ring as aromatic system. The natural aromatic amino acids such as phenyl alanine, tyrosine, tryptophan contains the aromatic ring at the side chain.⁶⁵ In case of most of the unnatural aromatic amino acids, it was observed that the aromatic ring is acting as backbone of the amino acid, where amino and carboxyl groups are attached to the ring system.⁹⁴⁻⁹⁹ Hence most of the unnatural aromatic amino acids explored so far are distinctive from natural aromatic amino acids. As a result, the planar backbone of the unnatural aromatic amino acids provides less conformational flexibility. Owing to this advantage, synthesis of peptides from the unnatural aromatic amino acid building blocks and their structural studies are extensively explored. They have shown well-ordered novel secondary structures in solid and solution states.⁹⁴⁻⁹⁶ As mentioned earlier, the high order in the secondary structure of these peptides is due to the rigidity and planarity of the backbone aromatic ring of amino acid residue. To date,

various peptidomimetics containing benzenoid unnatural aromatic amino acids have been reported with interesting novel secondary structures.⁹⁴⁻⁹⁹

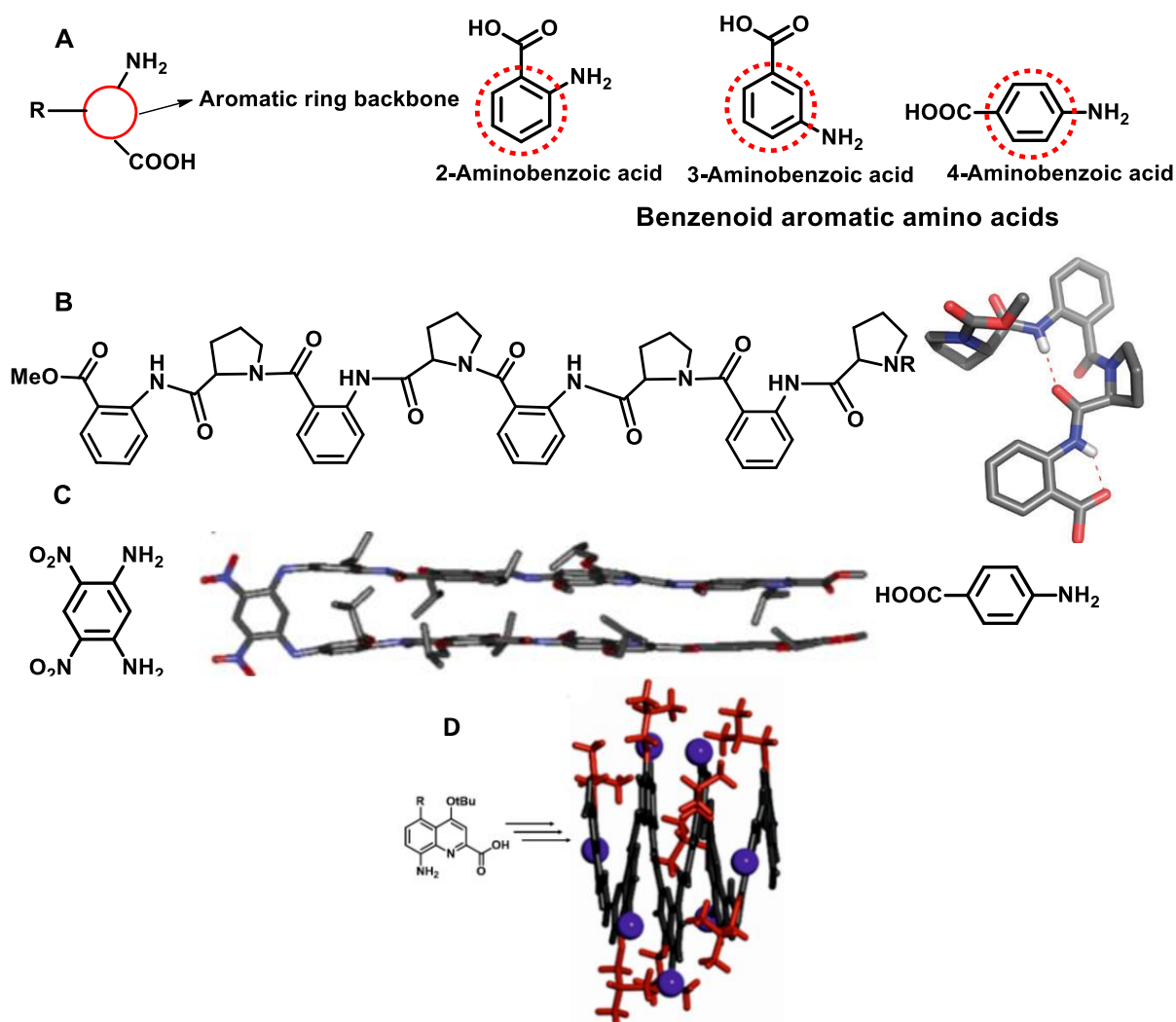


Figure 1.23 Peptides synthesized from the natural and unnatural amino acids (aromatic)

A few examples are given in **Figure 1.23**. (i) In **Figure 1.23C** represents the artificial hairpin type of secondary structure, where two strands of the hairpin are synthesized from 4-aminobenzoic acid derivative and these are connected with the help of 1,3-diamino-5,6-dinitrobenzene via amide bond.¹⁰⁷ (ii) In **Figure 1.23D**, a highly ordered helical secondary structure of peptide synthesized from 2-carboxy-8-aminoquinolone derivatives is presented.¹⁰⁸ (iii) Hybrid peptides of various benzenoid aromatic amino acids and natural α -amino acids are also synthesized and studied. Anthronilic acid and proline α/β -hybrid peptides displayed a new

right-handed helical structure containing repeated pseudo β -turns with nine membered ring hydrogen bonding (**Figure 1.23B**).⁹⁹

1.2.7 Peptide nanomaterials

Nanomaterials found to have wide range of applications for biomedical use (biomaterials) and in electronic devices.¹⁰⁹⁻¹¹¹ It is well studied that, a few proteins/polypeptides in the living system aggregates (self-assembly) to form fibril like structures (nanostructures) called amyloid fibrils. The aggregation phenomenon of naturally occurring proteins/peptides encouraged the researchers to fabricate the nanostructures from synthetic peptides in the laboratory.¹⁰⁹⁻¹¹¹ Non-covalent interactions induces the aggregation/self-assembly process, which is a key factor for the formation of nanostructures. Highly effective non-covalent interactions those favors the formation of nanostructures include hydrogen bonding, van der Waals and stacking interactions. Peptide nano-materials drawn the interest of scientists, because of their chemical stability, opportunities to tune the nanostructure by altering the sequence, well established and high yielding synthetic methods, easy in incorporation of hydrophilic and hydrophobic groups in the molecule.¹⁰⁹⁻¹¹¹ Interesting advantages of peptide nano-materials are biocompatible and biodegradable.¹⁰⁹⁻¹¹¹

The application of peptides as catalysts for the enantioselective organic transformation reactions is an interesting and growing area of research. Less toxicity to the living system and chirality in the molecules made them as promising catalysts for enantioselective synthesis.^{112,113}

Overall, unnatural backbone extended amino acids gained great interest by the scientific community due to their importance in the peptide therapeutic drug design to overcome the

limitations of natural peptide therapeutics. The advantages of unnatural backbone extended amino acids is syntheses of peptidomimetics with well-defined secondary structures for the applications in various fields by introducing various substituents on the extended backbone. The peptides synthesized from unnatural backbone extended amino acids have shown relatively stable towards proteolytic enzymes, easy to tune the active molecular conformation with minimum number of residues.

1.3 Summary and Outlook

In summary, proteins and polypeptides are synthesized by nature to perform several biological functions. They made up of 20 natural α -amino acids with diversity in the sequence. They form specific three dimensional structural organization which is responsible for their function. To understand the structural aspects and functions of proteins/polypeptides, peptides from natural α -amino acids have been synthesized broadly. On the way to develop the synthetic peptides as structural and functional mimetics of natural proteins, enormous research had took place on the synthesis, structural and functional properties of synthetic peptides. As a result synthetic peptides transformed into therapeutic drugs, specific binding ligands, hormones and as catalysts, and now peptide therapeutic drugs are available in the market for treatment of various diseases. As described already, peptide therapeutics have various advantages over small molecule drugs, but they also have considerable major limitations. To overcome these limitations researchers developed various structural changes in the lead natural active peptide sequence which are discussed briefly.

Tropolone moiety was found in many biologically active natural products. A few tropolone natural products and their derivatives are using as drugs for various diseases. And some other tropolonoids have shown interesting biological properties. Colchicine and Thujaplicins are now in the market as drugs for acute gout arthritis and as antifungal agents.

Thujaplicinol as ‘Hinokitiol or Hinoki’ oil is one of the widely using component in the cosmetology. In most of the cases, it was concluded that the tropolonoids excute biological action through chelation mechanism or through non-covalent interactions and which is facilitated by carbonyl and hydroxyl functional groups. Overall, tropone/tropolone moieties play vital role in the execution of biological function, due to the presence of carbonyl and hydroxyl functional groups.

The syntheses of various types of unnatural amino acids, their peptides, and their structures and biological functions have been exploited. And unnatural benzenoid aromatic amino acids and their peptides are also extensively explored in terms of syntheses, structural aspects and properties.

Now the question is *‘Is there any amino acid/peptide derived from tropolonoid aromatic rings? To our knowledge the answer is ‘No!’*

Surprisingly, though tropolonoids are known since 1940s, but so far there are no reports on tropolonoid aromatic amino acids. Therefore, the syntheses and properties of aromatic amino acids and peptides containing tropolonoid aromatic system are yet be explored. Interestingly, both peptidomimetics and tropolonoids have great applications in the field of therapeutics. Moreover, troponyl moiety can provide an extra hydrogen bonding acceptors site as troponyl carbonyl other than amide carbonyl. Hence, if we could make amino acids containing troponyl moiety as substituent on the backbone, it might be possible to obtain peptides with novel secondary structure and biological properties.

Rest of the thesis explains, the design and syntheses of unnatural amino acids containing troponyl moiety, syntheses of heterologous peptides, conformational analysis of synthesized heterologous peptides, difficulties in the syntheses of homologous peptides, unusual and regioselective cleavage of amide bond derived from Troponyl aminoethylglycine,

formation of cationic troponyl lactone in acetonitrile after amide cleavage, cleavage of Troeg amide into troponyl lactone and reformation of amide bond after neutralization. We have also demonstrated acid and base mediated amidation and de-amidation via cationic troponyl lactone intermediate of N-alkyl troponylglycinate esters as recyclable esters for protection of amine. The syntheses of novel fluorescent molecules, as cyclic aminotroponimines and boron-aminotroponimines from tropolone. And on the other hand, the syntheses of sequence symmetric hexa-peptides through alkyl linkers.

1.4 References and Notes

1. Pelletier, P. J.; Caventou, J. B. *Ann. Chim. Phys.* **1820**, *14*, 69.
2. Geiger, P. L. *Ann. Pharm.* **1833**, *7*, 269.
3. Birkinshaw, J. H.; Raistrick, H. *Biochem. J.*, **1932**, *26*, 441–453.
4. Birkinshaw, J.H.; Chambers, A. R.; Raistrick, H. *Biochem. J.*, **1942**, *36*, 242–251.
5. Dewar, M. J. S. *Nature*, **1945**, *155*, 50–51.
6. Dewar, M. J. S. *Nature*, **1945**, *155*, 141–142.
7. Erdtman, H.; Gripenberg, J. *Nature*, **1948**, *161*, 719.
8. Erdtman, H.; Gripenberg, J. *Nature*, **1949**, *164*, 316.
9. Cook, J. W.; Loudon, J. D. *Q. Rev. Chem. Soc.*, **1951**, *5*, 99–130.
10. Pauson, P. L. *Chem. Rev.*, **1955**, *55*, 9–136.
11. Nozoe, T. *Seventy Years in Organic Chemistry*, American Chemical Society, Washington, DC, **1991**.
12. Nozoe, T. *Sci. Rep. Tohoku Univ., Ser. 1: Phys., Chem., Astron.*, **1950**, *34*, 199–236.
13. Nozoe, T. *Nature*, **1951**, *167*, 1055–1056.
14. Merling, G. *Chem. Ber.* **1891**, *24*, 3108.
15. Doering, W. V. E.; Knox, L. H. *J. Am. Chem. Soc.* **1954**, *76*, 3203.
16. Dauben, H. J.; Gadeckt, F. A.; Harmon, K. M.; Pearson, D. L. *J. Am. Chem. Soc.* **1957**, *79*, 4557.
17. Bentley, R. *Nat. Prod. Rep.* **2008**, *25*, 118.
18. Liu, N.; Song, W.; Schienebeck, C. M.; Zhang, M. Tang, W. *Tetrahedron*, **2014**, *70*, 9281.

19. Zhao, J. *Curr. Med. Chem.*, **2007**, *14*, 2597–2621.
20. Brossi, A.; Yeh, H. J. C.; Chrzanowska, M. Wolff, J.; Hamel, E.; Lin, C. M.; Quin, F.; Suffness, M. ; Silverton, J. *Med. Res. Rev.*, **1988**, *8*, 77–94.
21. Brossi, A.; *J. Med. Chem.*, **1990**, *33*, 2311–2318.
22. Lindberg, G. D.; Larkin, J. M.; Whaley, H. A. *J. Nat. Prod.* **1980**, *43*, 592.
23. Azegami, K.; Nishiyama, K.; Kato, H. *Appl. Environ. Microbiol.* **1988**, *54*, 844.
24. Zhang, W. *et al.*, *Ann. Rheum. Dis.*, **2006**, *65*, 1301–1311 and 1312–1324.
25. Kallinich, T.; Haffner, D.; Niehues, T.; Huss, K.; Lainka, E.; Neudorf, U.; Schaefer, C.; Stojanov, S.; Timmann, C.; Keitzer, R.; Ozdogan, H.; Ozen, S. *Pediatrics*, **2007**, *119*, e474–e483.
26. Arima, Y.; Nakai, Y.; Hayakawa, R.; Nishino, T.; *J. Antimicrob. Chemother.* **2003**, *51*, 113–122.
27. Imai, N.; Doi, Y.; Nabae, K.; Tamano, S.; Hagiwara, A.; Kawabe, M.; Ichihara, T.; Ogawa, K.; Shirai, T. *J. Toxicol. Sci.*, **2006**, *31*, 357–370.
28. <http://www.hinoki.com/>, Obtained from the internet sources and Thujaplicin products are available in the market as ‘Hinoki’ shampoo, conditioner, soap and so on (prevents hair fall, provides fair skin tone).
29. Morita, Y.; Matsumura, E.; Tsujibo, H.; Yasuda, M.; Sakagami, Y.; Okabe, T.; Ishida, N.; Inamori, Y. *Biol. Pharm. Bull.*, **2001**, *24*, 607–611.
30. Sennari, G.; Hirose, T.; Iwatsuki, M.; Omura, S.; Sunazuka, T. *Chem. Commun.*, **2014**, *50*, 8715.

31. Morita, Y.; Matsumura, E.; Okabe, T.; Fukui, T.; Shibata, M. Sugiura, M.; Ohe, T.; Tsujibo, H.; Ishida, N.; Inamori, Y. *Biol. Pharm. Bull.*, **2004**, 27, 899–902.
32. Prasad, K.; Kapoor, R.; Lee, P. *Mol. Cell. Biochem.* **1994**, 139, 27.
33. Wu, T. W.; Wu, J.; Zeng, L. H.; Au, J. X.; Carey, D.; Fung, K. P. *Life Sci.* **1994**, 54, 123.
34. Wu, T.W.; Zeng, L. H.; Wu, J.; Fung, K. P.; Weisel, R. D.; Hempel, A.; Camerman, N. *Biochem. Pharmacol.* **1996**, 52, 1073.
35. Roberts, R. A. C. *J. Sci. Food Agric.* **1957**, 8, 72.
36. Lin, J. K. *Arch. Pharmacol Res.* **2002**, 25, 561.
37. Mukamal, K. J.; Maclure, M.; Muller, J. E.; Sherwood, J. B.; Mittleman, M. A. *Circulation* **2002**, 105, 2476.
38. MacKenzie, T.; Comi, R.; Sluss, P.; Keisari, R.; Manwar, S.; Kim, J.; Larson, R.; Baron, J. A. *Metabolism* **2007**, 56, 1694.
39. Silverton, J. V.; Kabuto, C.; Buck, K. T.; Cava, M. P. *J. Am. Chem. Soc.* **1977**, 99, 6708.
40. Morita, H.; Matsumoto, K.; Takeya, K.; Itokawa, H.; Iitaka, Y. *Chem. Pharm. Bull.* **1993**, 41, 1418.
41. Morita, H.; Takeya, K.; Itokawa, H. *Bioorg. Med. Chem. Lett.* **1995**, 5, 597.
42. Mayerl, F.; Gao, Q.; Huang, S.; Klohr, G. E.; Matson, J. A.; Gustavson, D. R.; Pirnik, D. M.; Berry, R. L.; Fairchild, C.; Rose, W. C. *J. Antibiot.* **1993**, 46, 1082–1088.
43. Cai, P.; Smith, D.; Cunningham, B.; Brown-Shimer, S.; Katz, B.; Pearce, C.; Venables, D.; Houck, D. *J. Nat. Prod.* **1998**, 61, 791–795.
44. Wanner, R. M.; Spielmann, P.; Stroka, D. M.; Camenisch, G.; Camenisch, I.; Scheid, A.; Houck, D. R.; Bauer, C.; Gassmann, M.; Wenger, R. H. *Blood*, **2000**, 96, 1558–1565.

45. Tomita, K.; Hoshino, Y.; Nakakita, Y.; Umezawa, S.; Miyaki, T.; Okiand, T.; Kawaguchi, H. *J. Antibiot.* **1989**, *42*, 317–321.
46. Budihas, S. R.; Gorshkova, I.; Gaidamakov, S.; Wamiru, A.; Bona, M.K.; Parniak, M. A.; Crouch, R. J.; McMahon, J. B.; Beutler, J. A.; Le Grice, S. F. J. *Nucleic Acids Res.* **2005**, *33*, 1249–1256.
47. Freed, E. O. Mouland, A. J. *Retrovirology*, **2006**, *3*, 77–88.
48. Imafuku, K.; Kobayashi, T.; Matsumura, H. *Bull. Chem. Soc. Jpn.*, **1985**, *58*, 181.
49. Forbes, C. E.; Holm, R. H. *J. Am. Chem. Soc.* **1968**, *90*, 6884.
50. Machiguchi, T.; Hasegava, T.; Saitoh, H.; Yamabe, S.; Yamazaki, S. *J. Org. Chem.* **2011**, *76*, 5457.
51. Roesky, P. W., *Chem. Soc. Rev.* **2000**, *29*, 335.
52. Zulys, A.; Dochnahl, M.; Hollmann, D.; Löhnwitz, K.; Herrmann, J.-S.; Roesky, P. W.; Blechert, S., *Angew. Chem. Int., Ed.* **2005**, *44*, 7794.
53. Davis, W. M.; Roberts, M. M.; Zask, A.; Nakanishi, K.; Nozoe, T.; Lippard, S. J. *J. Am. Chem. Soc.* **1985**, *107*, 3864.
54. Imajo, S.; Nakanishi, K.; Roberts, M.; Lippard, S. J.; Nozoe, T., *J. Am. Chem. Soc.* **1983**, *105*, 2071.
55. Villacorte, G. M.; Gibson, D.; Williams, I. D.; Lippard, S. J., *J. Am. Chem. Soc.* **1985**, *107*, 6732.
56. Hosoya, H.; Tanaka, J.; Nagakura, S.; *Tetrahedron* **1962**, *18*, 859.
57. Yamaguchi, H.; Amako, Y.; Azumi, H.; *Tetrahedron* **1968**; *24*, 267.

58. Croteau, R.; Leblanc, R. M.; *Journal of Luminescence* **1977**, *15*, 353. (b) (d) Breheret, E.F.; Martin, M. M. *Journal of Luminescence* **1978**, 49.
59. Hojo, M.; Hasegawa, H.; Yoneda, H.; *J. Chem. Soc. Perkin. Trans. 2.* **1994**, 1855.
60. Arai, T.; Okuyama, A. *Seikagaku.* **1973**, *45*, 19.
61. Weisenberg, R. C.; Borisy, G. G.; Taylor, E. W. *Biochemistry*, **1968**, *7*, 4466.
62. Bhattacharyya, B.; Wolff, J. *Proc. Nat. Acad. Sci. USA*, **1974**, *71*, 2627.
63. Ito, A.; Muratake, H.; Shudo, K. *J. Org. Chem.* **2013**, *78*, 5470. (b) Ito, A.; Muratake, H.; Shudo, K. *J. Org. Chem.* **2009**, *74*, 1275.
64. Sayapin, Y. A.; Tupaeva, I. O.; Kolodina, A. A.; Gusakov, E. A.; Komissarov, V. N.; Dorogan, I. V.; Makarova, N. I.; Metelitsa, A. V.; Tkachev, V. V.; Aldoshin, S. M.; Minkin, V. I. *Beilstein J. Org. Chem.* **2015**, *11*, 2179–2188.
65. Branden, C.; Tooze, J. *Introduction to Protein Structure*; Garland: New York, NY, **1991**.
66. Alberts, B.; Johnson, A.; Lewis, J.; Raff, M.; Roberts, K.; Walter, P. *Molecular Biology of the Cell*, 4th ed.; Garland Science: New York, NY, 2002.
67. *Foldamer: Structure, Properties and Applications*; Hecht, S., Huc, I., Eds.; Wiley-VCH: Weinheim, Germany, **2007**.
68. Lubell, W. D. Editorial. *J. Org. Chem.* **2012**, *77*, 7137.
69. Seebach, D.; Hook, D. F.; Glattli, A. *Biopolymers* **2006**, *84*, 23.
70. Seebach, D.; Gardiner, J. *Acc. Chem. Res.* **2008**, *41*, 1366.
71. Seebach, D.; Matthews, J. L. *Chem. Commun. (Camb.)* **1997**, *21*, 2015.
72. Gellman, S. H. *Acc. Chem. Res.* **1998**, *31*, 173.

73. Hill, D. J.; Mio, M. J.; Prince, R. B.; Hughes, T. S.; Moore, J. S. *Chem. Rev.* **2001**, *101*, 3893.
74. Sunanda, C.; Rituparna, S. R.; P. Balaram.; *J. R. Soc. Interface.* **2007**, *4*, 587.
75. Horne, W. S.; Gellman, S. H. *Acc. Chem. Res.* **2008**, *41*, 1399.
76. Kotha, S. *Acc. Chem. Res.* **2003**, *36*, 342.
77. Vasudev, P. G.; Chatterjee, S.; Shamala, N.; Balaram, P. *Chem. Rev.* **2011**, *111*, 657.
78. Pattabiraman, V. R.; Bode, J. W. *Nature*, **2011**, *480*, 471.
79. Vlieghe, P.; Lisowski, V.; Martinez, J.; Khrestchatisky, M. *Drug Discov. Today* **2010**, *15*, 40.
80. Fosgerau, K.; Hoffmann, T. *Drug Discov. Today* **2015**, *20*, 122. (c) Hruby, V. J.; Cai, M. *Annu. Rev. Pharmacol. Toxicol.* **2013**, *53*, 557.
81. Pelay-Gimeno, M.; Glas, A.; Koch, O.; Grossmann, T. N. *Angew. Chem. Int., Ed.* **2015**, *54*, 8896. References are therein.
82. Gademann, K.; Ernst, M.; Hoyer, D.; Seebach, D. *Angew. Chem. Int., Ed.* **1999**, *38*, 1223.
83. Narita, M.; Doi, M.; Kudo, K.; Terauchi, Y. *Bull. Chem. Soc. Jpn.* **1986**, *59*, 3553.
84. Appella, D. H.; Christianson, L. A.; Karle, I. L.; Powell, D. R.; Gellman, S. H. *J. Am. Chem. Soc.* **1996**, *118*, 13071;
85. Hanessian, S.; Luo, X.; Schaum, R.; Michnick, S. *J. Am. Chem. Soc.* **1998**, *120*, 8569.
86. Cheng, R. P.; Gellman, S. H.; DeGrado, W. F. *Chem. Rev.* **2001**, *101*, 3219-3232.
87. Choi, S. H.; Guzei, I. A.; Spencer, L. C.; Gellman, S. H. *J. Am. Chem. Soc.* **2008**, *130*, 6544.

88. Lee, W.; Kwon, S.; Kang, P.; Guzei, I. A.; Choi, S. H. *Org. Biomol. Chem.* **2014**, *12*, 2641.
89. Kwon, S.; Kang, P.; Choi, M.-G.; Choi, S. H. *New J. Chem.* **2015**, *39*, 3221.
90. Venkatraman, J.; Shankaramma, S. C.; Balaram, P. *Chem. Rev.* **2001**, *101*, 3131.
91. Guo, L.; Almeida, A. M.; Zhang, W.; Reidenbach, A. G.; Choi, S. H.; Guzei, I. A.; Gellman, S. H. *J. Am. Chem. Soc.* **2010**, *132*, 7868.
92. Guo, L.; Chi, Y.; Almeida, A. M.; Guzei, I. A.; Parker, B. K.; Gellman, S. H. *J. Am. Chem. Soc.* **2009**, *131*, 16018.
93. Balaram, P. *Biopolymers* **2010**, *94*, 733. (e) Fisher, B. F.; Gellman, S. H. *J. Am. Chem. Soc.* **2016**, *138*, 10766.
94. Roy, A.; Prabhakaran, P.; Baruah, P. K.; Sanjayan, G. J. *Chem. Commun.* **2011**, *47*, 11593.
95. Zhang, D.-W.; Zhao, X.; Hou, J.-L.; Li, Z.-T. *Chem. Rev.* **2012**, *112*, 5271. (c) Guichard, G.; Huc, I. *Chem. Commun.* **2011**, *47*, 5933.
96. Zhang, D.-W.; Zhao, X.; Li, Z.-T. *Acc. Chem. Res.* **2014**, *47*, 1961.
97. Ramesh, V. V. E.; Priya, G.; Kotmale, A. S.; Gonnade, R. G.; Rajamohanan, P. R.; Sanjayan, G. J. *Chem. Commun.* **2012**, *48*, 11205.
98. Prabhakaran, P.; Priya, G.; and Sanjayan, G. J. *Angew. Chem. Int. Ed.* **2012**, *51*, 4006.
99. Prabhakaran, P.; Kale, S. S.; Puranik, V. G.; Rajamohanan, P. R.; Chetina, O.; Howard, J. A.; Hofmann, H. J.; Sanjayan, G. J. *J. Am. Chem. Soc.* **2008**, *130*, 17743.
100. Spiegel, J.; Mas-Moruno, C.; Kessler, H.; Lubell, W. D. *J. Org. Chem.* **2012**, *77*, 5271 – 5278.
101. Avan, I.; Hall, C. D.; Katritzky, A. R. *Chem. Soc. Rev.* **2014**, *43*, 3575.

102. Khashper, A.; Lubell, W. D. *Org. Biomol. Chem.* **2014**, *12*, 5052.
103. Góngora-Benítez, M.; Tulla-Puche, J.; Albericio, F. *Chem. Rev.* **2014**, *114*, 901.
104. Seebach, D.; Kimmerlin, T.; Sebesta, R.; Campo, M. A.; Beck, A. K. *Tetrahedron* **2004**, *60*, 7455.
105. Seebach, D.; Beck, A. K.; Bierbaum, D. J. *Chem. Biodivers.* **2004**, *1*, 1111.
106. Frackenpohl, J.; Arvidsson, P. I.; Schreiber, J. V.; Seebach, D. *ChemBioChem.* **2001**, *2*, 445.
107. Sebaoun, L.; Kauffmann, B.; Delclos, T.; Maurizot, V.; Huc, I. *Org. Lett.* **2014**, *16*, 2326.
108. Li, X.; Qi, T.; Srinivas, K.; Massip, S.; Maurizot, V.; Huc, I. *Org. Lett.* **2016**, *18*, 1044.
109. Reches, M.; Gazit, E. *Science*, **2003**, *300*, 625.
110. Gazit, E. *Chem. Soc. Rev.* **2007**, *36*, 1263.
111. Mandal, D. Shirazi, A. N.; Parang, K. *Org. Biomol. Chem.* **2014**, *12*, 3544.
112. Lewandowski, B.; Wennemers, H. *Curr. Opin. Chem. Biol.* **2014**, *22*, 40.
113. Duschmale, J.; Kohrt, S.; Wennemers, H. *Chem. Commun.* **2014**, *50*, 8109.
114. <https://upload.wikimedia.org/wikipedia/commons/6/60/Myoglobin.png>,
http://www.biotek.com/assets/tech_resources/11596/figure2.jpg and
http://upload.wikimedia.org/wikipedia/commons/e/e6/Spombe_Pop2p_protein_structure_rainbow.png

CHAPTER TWO

Synthesis and Conformational Analysis of New Troponyl Aromatic Amino Acid

Chapter 2: Synthesis and Conformational Analysis of New Troponyl Aromatic Amino Acid

2.1 Introduction

Proteins/peptides, play key role in the biochemical operations such as catalysis, specific binding and direct flow of electrons. Functional protein attains a specific three dimensional compact conformation.¹⁻³ The tertiary structure of protein is responsible for the generation of “active site” via precise arrangement of functional groups.¹⁻³ The well-defined three dimensional structural organization of proteins is governed by the favourable conformational preference of individual amino acid and non-covalent interactions. The tertiary structure of a protein is a combination of several secondary structural elements such as helix, turns, and sheets. Formation of a specific secondary structural element associated with the conformational preference of amino acid residue and the type of hydrogen bonding.¹⁻³

To mimic the function of natural proteins/peptides, countless number of natural and unnatural peptides have been synthesized.⁴⁻¹² The backbone extended unnatural peptides, such as β and γ -peptides are one of the extensively studied class of unnatural peptides in terms thier syntheses and secondary structures.¹³⁻¹⁹ The backbone extended amino acids are able to form stable secondary structures even with four suitable residues and these are potential to inhibit protein-protein interactions.³⁻¹² For example, a cyclic tetra- β -peptide, containing β^3 -Lys-Thr-Phe-Trp amino acid residues is able to mimic the function of Octreotide, an octapeptide synthesized from natural amino acids.¹⁰ Moreover, unnatural peptides are relatively stable towards enzyme degradation.³⁻¹⁰

From the literature, it has been learnt that the careful design of amino acid residue with suitable substituents is important.³⁻¹⁹ Where, the substituent can contribute to the stable secondary structure formation either by restricting the allowed conformational space or by noncovalent interactions. For example, β -alanine oligomers forms unordered structures in

solution and sheet like packing was reported in the solid state.²⁹ In contrast, substituents at backbone carbon atoms of the β -alanine generates oligomers with stable helix conformation. For an example, formation of stable 14-helix by homo oligomer of *trans*-2-amino cyclohexane carboxylic acid (ACHC) is reported, where cycloalkane ring facilitates the formation of helical structure.^{30,31}

Overall, synthetic peptides are in huge demand in expansion of potential peptide mimetics, which may have improved or similar functional properties as natural proteins/peptides and to overcome the major limitation of natural synthetic peptides, which is proteolytic instability.⁶⁻¹² With these concerns, natural/unnatural amino acids and their peptides have been extensively explored.⁶⁻¹⁹ It is worth mention that aromatic amino acids and peptides bearing phenyl residue are one of the extensively explored class of unnatural amino acids.¹³⁻¹⁸ Because phenyl residue has high probability in forming stable secondary structure, owing to the presence of an extra stabilizing factor as π - π non-covalent interactions.¹³⁻¹⁶ Tropolone and related non-benzenoid aromatic rings are in existence since 1940s as described in chapter one. But troponyl containing amino acids and peptides not yet explored fully. Importantly, troponyl derivatives contains carbonyl functional group, which provides an extra hydrogen bonding site and as a result binding with target site is possible via non-covalent interactions. On the other hand the presence of an extra carbonyl on substituent of amino acid residue provides a novel and stable conformation in peptide.

It is important to discuss the structural and biological importance of tropolone (**Figure 2.1, A**). Tropolone is a seven membered ring aromatic compound which comprises carbonyl and hydroxyl groups adjacent to each other and belongs to class of non benzenoids, where the delocalization of 6 π -electrons over seven *p*-orbitals takes place.^{36,37} The carbonyl group on this ring is highly polarized and stabilized by aromaticity. In the literature, a large number of natural products are reported which contain tropolone, after isolation and characterization of β -

thuzaplicinol (hinokitiol) in 1940s.³⁸⁻⁴¹ Some of the natural products are listed in Chapter I. Recently, tropolone derivatives are investigated as potential therapeutic agents as antibacterial,⁴² antifungals,⁴³ anticancer drugs,⁴⁴⁻⁴⁵ and α -hydroxy tropolone has reportedly shown antiviral activity with Human Immunodeficiency Virus (HIV) reverse transcriptase⁴⁶ and on the other hand, it is also reported that it is strongly chelating to metals like Be, Cu (II) and Zn (II) etc.,^{47,48}

2.1.1 Hypothesis and Objective

Inspired from the importance of unnatural oligomers, we designed an unnatural amino acid, troponyl aminoethyl glycine (*Traeg*, **Figure 2.1B**). This amino acid contains a tropone ring connected to the nitrogen atom of the aminoethylglycine backbone. Tropolone moiety is a 7-membered aromatic ring containing carbonyl functionality.

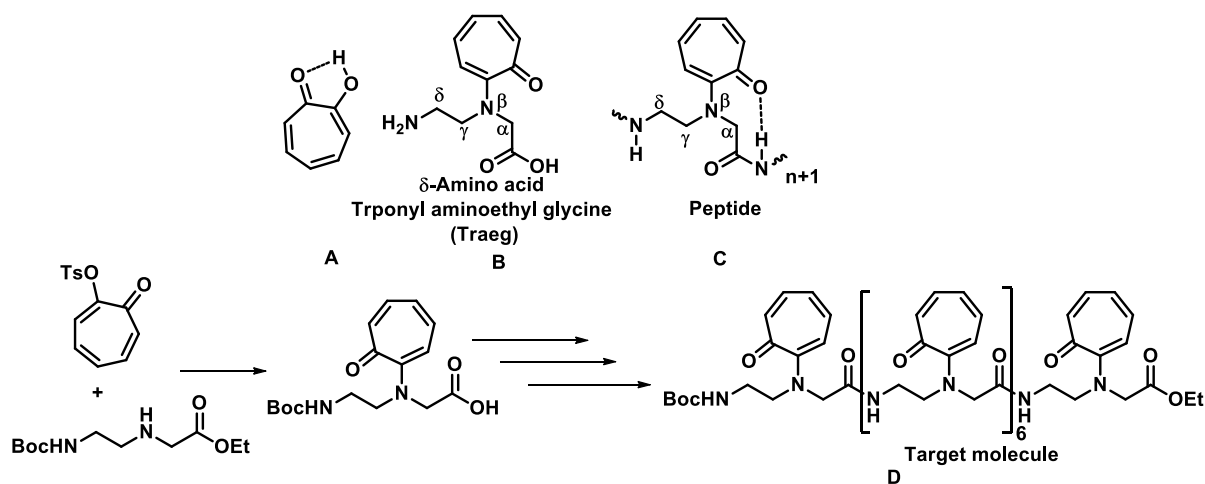


Figure 2.1 (A) Chemical Structure of tropolone; (B) Designed amino acid. (C) Representation of hydrogen bonding in *Traeg* peptides; (D) Target *Traeg* peptide.

We envisioned that the carbonyl group of the tropone moiety may take part in the formation of a stable secondary structure of its peptides. So far, tropolone is not explored as conformational guiding substituent in backbone expanded amino acids. On the other hand

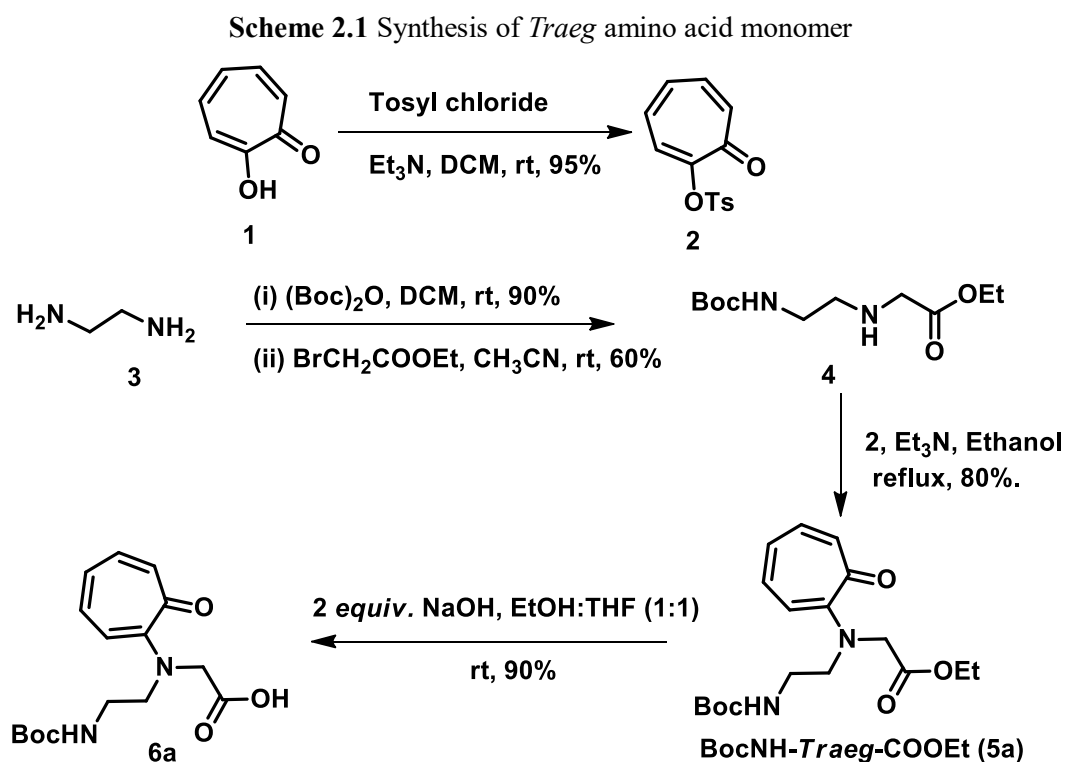
several unnatural benzenoid aromatic amino acids are used for the synthesis of stable foldamers.^{3b-g}

This chapter explains about the syntheses of δ -amino acid (Troponyl aminoethyl glycine, **Figure 2.1, B**), difficulties in the synthesis of homologous peptides (**Figure 2.1, D**) and successful synthesis of heterologous peptides (**Figure 2.1, C**). We performed the systematic conformational analysis by experimental and theoretical methods and illustrated the formation of 8-membered ring hydrogen bond between troponyl carbonyl and adjacent amide NH in *Traeg-aa* (δ/α) hybrid peptides.

2.2 Results and Discussion

2.2.1 Synthesis of Troponyl aminoethyl glycine (*Traeg*) amino acid

The synthesis of δ -amino acid was started from commercially available material tropolone **1** and ethylenediamine **3** (**Scheme 2.1**). The tropolone (**1**) was converted into



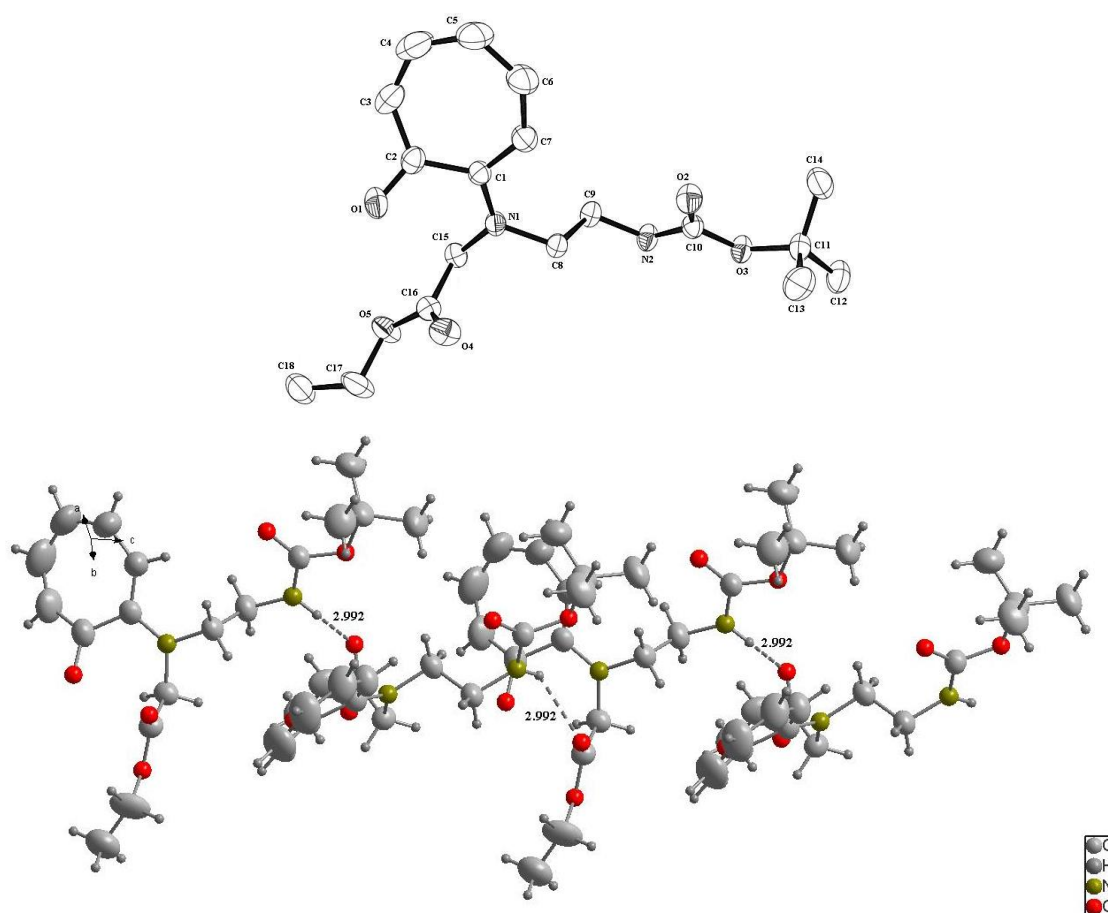


Figure 2.2 ORTEP diagram of *Traeg* monomer **5a** and molecular packing diagram.

2-tosyloxypyrone (**2**) by following the literature procedure.⁵¹ While *N*-Boc-aminoethyl glycinate (**4**) backbone was prepared from ethylenediamine (**3**) in two steps from our reported procedure.³⁵ In next, 2-tosyloxypyrone (**2**) and *N*-Boc-aminoethyl glycinate backbone (**4**) were refluxed for 48 hours in ethanol in the presence of triethyl amine which gave δ -amino acid monomer **5** in 80% yield after column purification. The structure of **5** was established by $^1\text{H}/^{13}\text{C}$ NMR, ESI-MS and single crystal X-ray analysis, the ORTEP diagram and molecular packing diagram obtained from single crystal x-ray analyses is depicted in **Figure 2.2**. In further, the ethyl ester of monomer **5** was hydrolyzed into carboxylic acid functionalized monomer **6** under given conditions (Scheme 1.1). Boc group was deprotected with 20% TFA in DCM to obtain free amine of monomer **NH₂-5a** for peptide coupling.

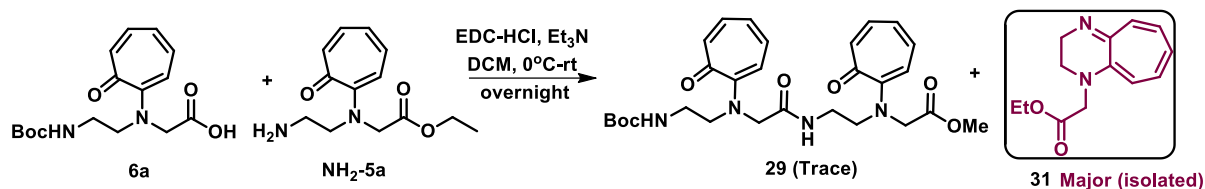
2.2.2 Synthesis of *Traeg* peptides

Synthesis of Traeg homologous peptides (Solid Phase Peptide synthesis): After synthesizing the *Traeg* carboxylic acid monomer, the synthesis of *Traeg* homologous hexapeptides were attempted through Standard Solid Phase Peptides synthesis.³⁵ The Fmoc protected MBHA resin was used as solid support. The synthetic protocol is presented in the Scheme 1.2. First, the resin was soaked in dichloromethane and Fmoc protecting group was deprotected. The Fmoc deprotected free amine on resin is allowed to peptide coupling with *Traeg* carboxylic acid monomer. The reaction proceeded successfully and was witnessed by Kaiser test. For further coupling, the Boc protecting group of *Traeg* monomer was deprotected by using 20.0% TFA in DCM (detailed procedure is provided in experimental section). To our surprise, the Kaiser test was negative. We tried three times, by following the same procedure same procedure, every time after first coupling a negative Kaiser test was observed. Unfortunately, we failed to synthesize the *Traeg* homologous hexapeptides after several trails. Though we were unable to find the exact reason for this failure, later on, we found that an unusual cleavage of amide bond derived from *Traeg* is happening. In Chapter III this unusual solvolysis of amide bond is explained clearly with several examples and suitable control experiments.

Syntheses of Traeg homologous peptides (solution phase):

Next, we attempted to synthesize the homologous dipeptide through Standard Solution Phase Peptide synthesis. For this purpose, we deprotected the Boc protecting of *Traeg* monomer in presence of 20% TFA in DCM. Afterwards, the peptide coupling reaction was carried out under given conditions (**Scheme 2.2**). The TLC analysis of the reaction mixture revealed that only trace amount of product was formed. ESI-MS

analysis of the reaction mixture revealed that the *Traeg* free amine is unstable after neutralization, which instantly cyclized into cyclic imine (**31**, **Scheme 2.2**).

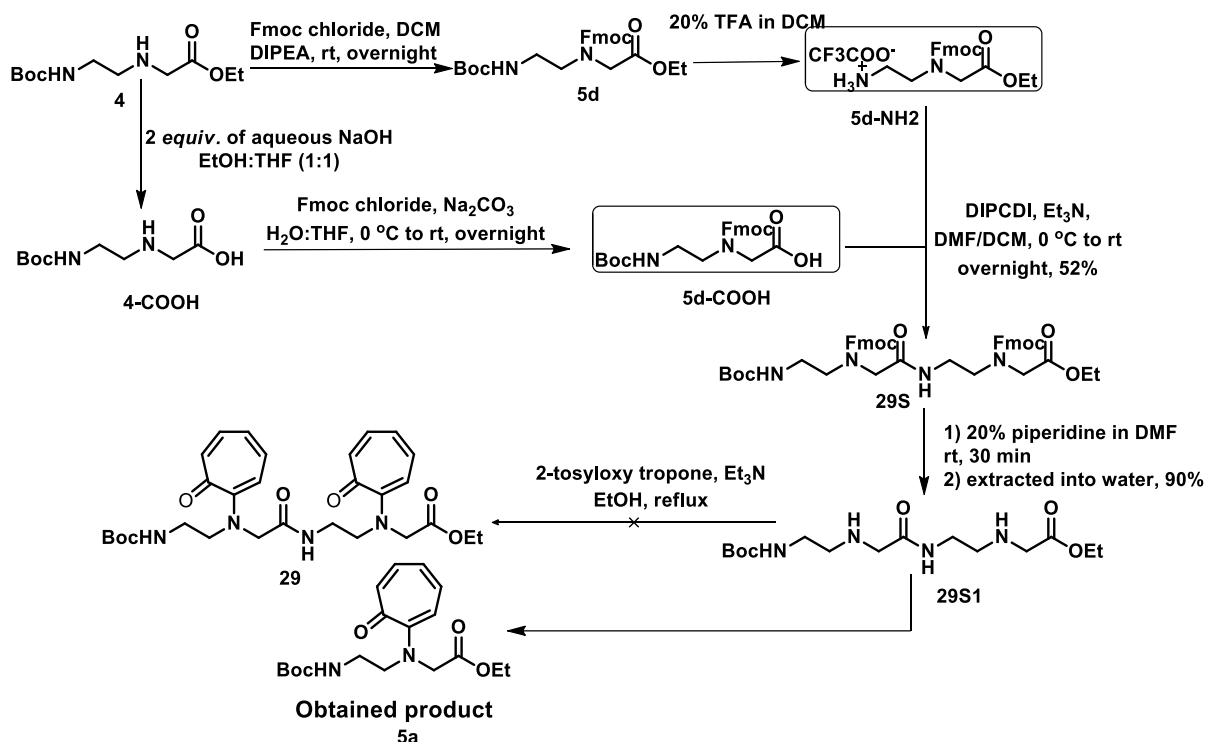


Scheme 2.2 Synthesis of *Traeg* homologous dipeptide through solution phase

Syntheses of Traeg homologous di-peptides through alternative synthetic route:

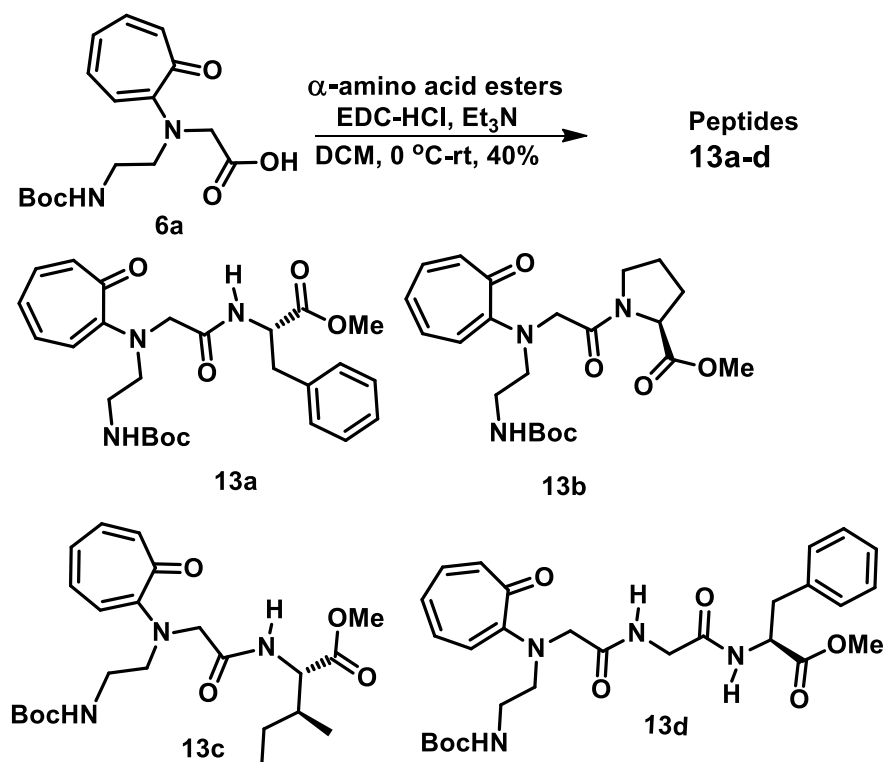
In this synthetic route, first we prepared the backbone dipeptide (**29S1**) and that was allowed to troponylation under the optimized conditions. The backbone dipeptides was synthesized by following the **Scheme 2.3** (detailed procedures are provided in experimental section). First, the Fmoc protected aminoethylglycine (*aeg*) monomers (**5d-NH₂**, **5d-COOH**) have been synthesized by following the **Scheme 2.3**. These Fmoc protected monomers were employed for the syntheses of Fmoc-protected amino ethylglycine dipeptide (**29S**). The Fmoc group of the dipeptide was deprotected by using 20.0% piperidine in DMF. The obtained free amine diamine peptide was extracted and then allowed to troponylation. To our surprise, the purification and characterization of the reaction mixture revealed that the obtained product was *Traeg* monomer. Through this method also we failed to synthesize the *Traeg* homologous dipeptide.

Scheme 2.3 Synthesis of *Traeg* homologous *di*-peptide through designed alternative method.



Synthesis of Traeg heterologous peptides: After realizing the difficulties in the syntheses of *Traeg* homologous peptides. The other alternative we had was, the syntheses of *Traeg* heterologous peptides, explore the role tropone carbonyl in hydrogen bonding, and in controlling the conformation of resultant peptide, before finding another suitable backbone to incorporate tropone moiety as a substituent on the backbone of amino acid residue. Hence, we strategically designed two types of hybrid *dipeptides*: one having amide NH and another without amide NH at *C'*-end to investigate the role troponyl carbonyl in hydrogen bonding. For these reasons we selected following naturally α -amino acid residues: L-phenylalanine (Phe), L-Isoleucine (Ile), and L-proline (Pro). In **scheme 2.4**, BocNH-*Traeg*-COOH monomer **6** was coupled with free amino group of α -amino acid ester derivatives to obtain hybrid dipeptides (**13a-d**). The hybrid dipeptide **13a** was prepared from L-phenylalanine methyl ester, dipeptide **13b** from L-proline

Scheme 2.4 Synthesis of heterologous peptides.



methyl ester, and dipeptide **13c** from isoleucine methyl ester with moderate yields in presence of peptide coupling reagent EDC.HCl. We also synthesized dipeptide **11** having only α -amino acid residues for control studies. In further a hybrid tripeptide **13d** was also synthesized from the free amine of dipeptide **11**. All these synthesized *di/tri*-peptides **13a-d** were characterized by $^1\text{H}/^{13}\text{C}$ NMR and Mass (ESI-MS) analysis. For structural confirmation and to predict the conformation of peptides, 2D NMR (COSY, NOESY, and HSQC) of hybrid peptides (**13a/b/d**) were recorded and then analyzed systematically.

2.2.3 Conformational analysis and hydrogen bonding studies

Aggregation studies: Before investigating the conformation of Troponylglycinate amino acid (*Traeg*) and its hybrid peptides (*Traeg*-aa), and hydrogen bonding studies, we examined the aggregation of these peptides at different concentration.⁵² For that reason,

^1H NMR experiments of these peptides at different concentrations was performed. The amide NH chemical shift was constant at all the concentration from 2.0 mM to 106.0 mM. However, slight down field shift of Boc NH was noticed at 106.0 mM concentration. These experimental results revealed that the *Traeg* peptides are not self-aggregating in CDCl_3 . From this experimental results, we confirmed that the down field shift of amide NH is not due the intermolecular hydrogen bonding, which generally observed as a result of aggregation of molecules. Overall, these studies supported that *Traeg* derived peptides are not involving in aggregation in CDCl_3 .

2D NMR analysis

^1H - ^1H NMR COSY experiments were carried out to assign the chemical shifts of all protons, while chemical shifts of all carbons having hydrogen atoms are assigned from ^1H - ^{13}C HSQC NMR experiment. In **Table 2.1**, the hydrogen resonance of carbamate NH and amide NH in monomer **5a** and peptides **13a-d** are summarized. Similarly the carbon resonance of troponyl carbonyl $\text{C}=\text{O}$ are also extracted from their respective ^{13}C NMR. This 2D NMR analysis confirmed the structure of dipeptides.

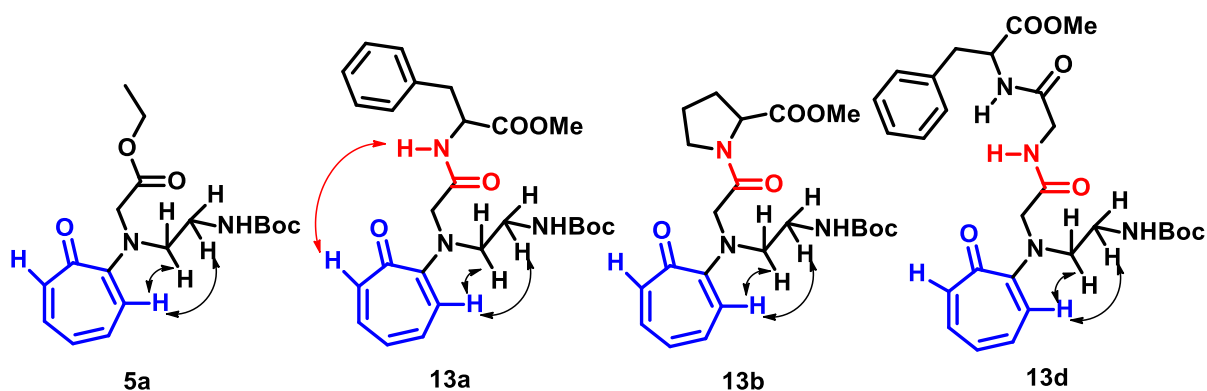


Figure 2.3 Observed NOESY interactions of di and tri peptides **13a/b/d**.

After assignment of protons and carbons of *di/tri*-peptides, their ^1H - ^1H NOESY spectrum helped to extract the non-vicinal proton coupling interactions. The NOESY spectral analysis of dipeptide **13a** has shown NOE interactions between troponyl ring

protons (t7H) with adjacent amide NH of phenylalanine residue and t3H with aminoethyl protons met₁/met₂ (γ H/ δ H, **Figure 2.3**). These results suggest that the similar orientation of troponyl carbonyl in dipeptide **7** toward *C'*-end, like in monomer **5a**. The similar 2D-NMR experiments and analyses were performed on other *Traeg* derived peptides (**13b/d**). In peptides **13b/d**, similar NOE interaction were observed (**Figure 2.3**) and it concludes that the troponyl ring oriented towards *C'*-end in all hybrid peptides including monomer in solution. This orientation of troponyl ring in **5a/13a/b/d** might be opted due to the steric conflict between aminoethyl protons and troponyl carbonyl group. Overall, similar NOE interactions were observed for monomers and all peptides, which means, troponyl ring orientation and conformation of the *Traeg*, in monomer and peptides is most probably similar.

¹H NMR DMSO titration experiments: In this method, a sequential addition of external strong hydrogen bond acceptor takes place. The addition of external hydrogen bond acceptor disturbs the intra/intermolecular hydrogen bonds to some extent present in the peptide solution, which can be observed in ¹H and ¹³C NMR spectra of respective solution. The free amide/Boc-NH protons of peptide forms an intermolecular hydrogen bond with external hydrogen bond acceptor. As a result, the chemical shift of that particular NH causes downfield. The amide/Boc-NH protons involving in strong intramolecular hydrogen bonding could not be affected with the addition of external hydrogen bond acceptor. In some cases little upfield or down field shift of intramolecularly locked NH due to interruption of the intramolecular hydrogen bonding with external hydrogen bond acceptor.^{21-25,32}

After establishing the orientation of troponyl ring towards *C'*-end, we started investigating the role of troponyl carbonyl in hydrogen bonding with adjacent amide

NH by following NMR titration methods.^{21-25,32} The similar ^1H NMR titration experiments were performed with hybrid *di/tri*-peptides **13a-d**. Stacked ^1H NMR spectra of dipeptide **13a**, generated during the titration experiments are depicted in **Figure 2.4**. All ^1H NMR spectra of di/tri-peptides, which generated during DMSO- d_6 titration experiments are provided in appendix. NMR titration profiles, chemical shift vs volume of DMSO- d_6 , for amide NH and Boc NH of hybrid peptides are extracted from respective ^1H NMR titration experiments and plots are depicted in **Figure 2.5**. From NMR titration experiments it is learnt that Boc NH peak (δ 5.5 ppm) of all hybrid peptides and monomer is showing significant downfield shift of with the addition of DMSO- d_6 (**Figure 2.5A**), while very little upfield shifting in amide NH peak (δ 7.8 ppm) was observed with the addition of DMSO- d_6 (**Figure 2.5B**). Whereas, the amide

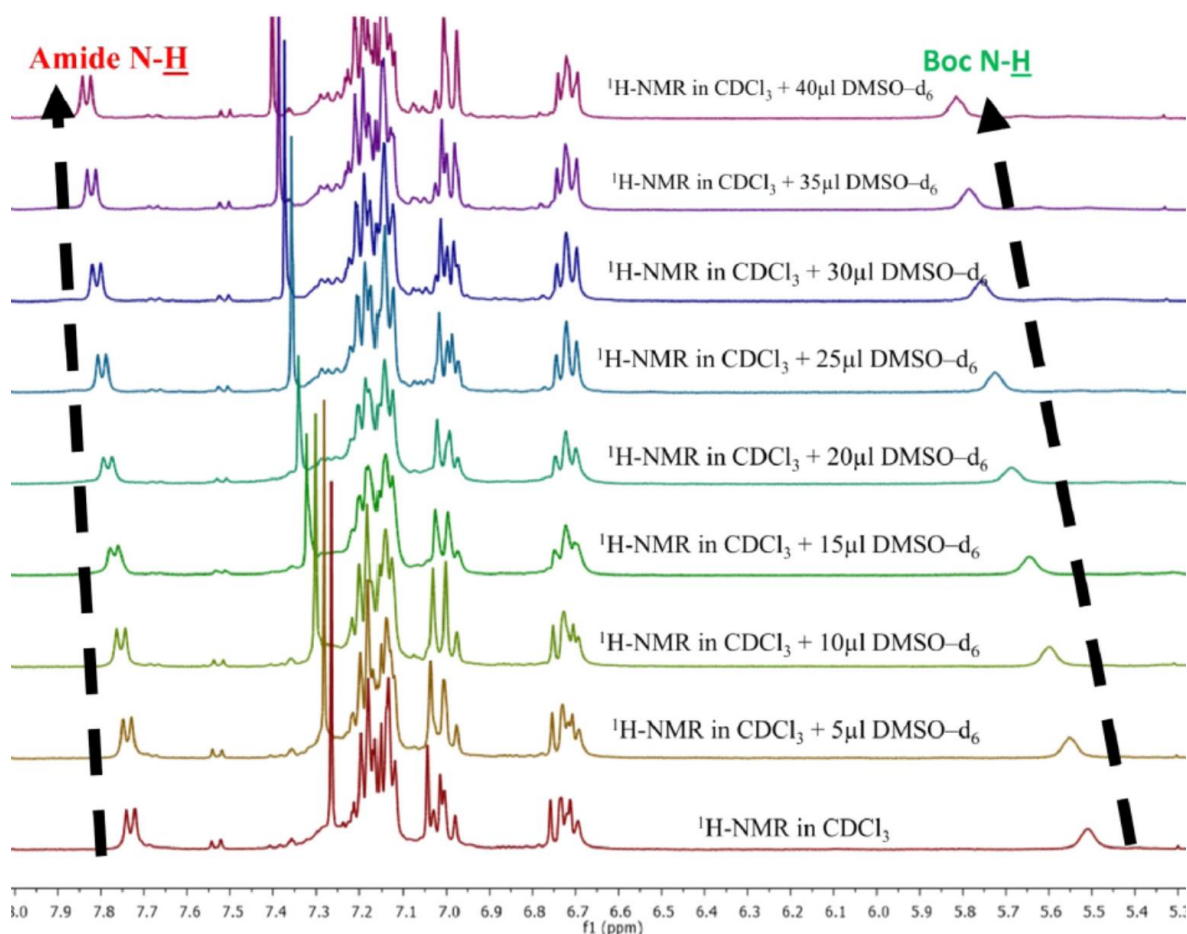


Figure 2.4 ^1H NMR titration experiments of dipeptide **13a**

NH and Boc NH of control dipeptide **11** has shown considerable downfield shift with the addition of DMSO- d_6 . This experiment suggest that these amide protons are exposing to the solvent equally.

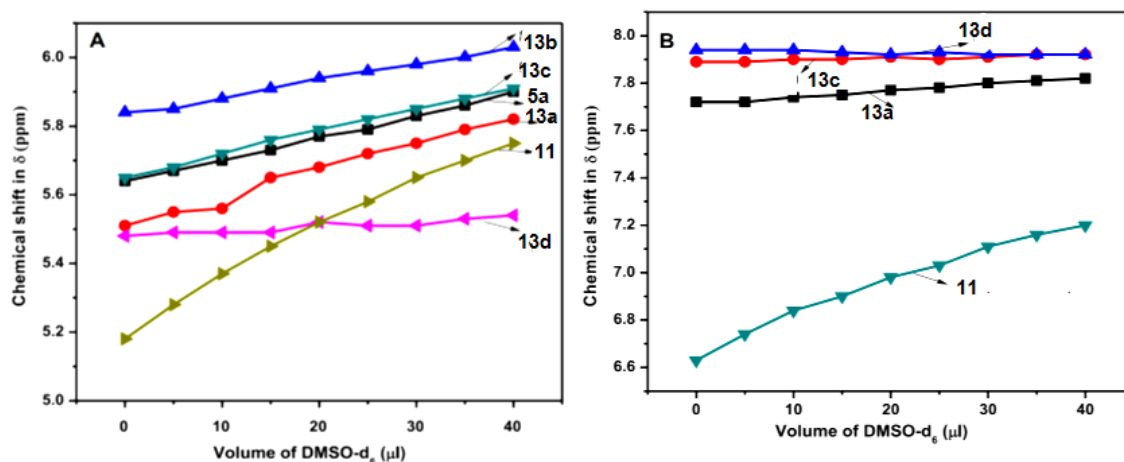


Figure 2.5 NMR titration profile: (A) Boc-NH at N'-end of **5a/13a-d**, **11**; (B) Adjacent amide NH at C'-end of **13a/c/d**, **11**.

Overall, DMSO- d_6 titration experiments revealed that the adjacent amide NH (n+1) in *Traeg* derived peptides **13a/c/d** is involving in hydrogen bonding with troponyl carbonyl.

¹³C NMR DMSO titration experiments: At first we noted the chemical shift of troponyl carbonyl carbon of all peptides **13a-d**, and monomer **5a** (Table 2.1). Though, ¹³C NMR of all compounds were recorded in CDCl₃ but the chemical shift of troponyl carbonyl carbon for each compound is varied. In case of monomer **5a** and dipeptide **13c** the troponyl carbonyl carbon is resonating at δ 181.7, whereas in case of other peptides **13a/c/d**, the down field shift was observed. Maximum down field shift was observed in dipeptide **13c** (δ 183.2). This down field shift may be because of hydrogen bonding, which drives the electron density along C=O π -bond towards oxygen.

Table 2.1 Chemical shift value of amide NH and troponyl C=O

entry	compound	carbamate NH (ppm)	amide NH (ppm)	troponyl carbonyl (C=O) group (ppm)
1	5a	5.6	no	181.7
2	13a	5.5	7.7	182.5
3	13b	5.8	no	181.7
4	13c	5.6	7.9	183.2
5	11	5.1	6.6	no <i>Traeg</i>
6	13d	5.5	7.9	182.7

Further, we investigated the increased down field shift of troponyl carbonyl carbon in peptides **13a/c/d** is because of whether hydrogen bonding or its primary structure.³³ For this reason we recorded ¹³C NMR of tripeptide **13d** in CDCl₃ (100%), DMSO-d₆ (100%) and CDCl₃:DMSO-d₆ (3:1, 1:1). All the four spectra are calibrated with respect to DMSO-d₆ solvent residual peak provided in **Figure 2.6**. In the stacked ¹³C NMR spectra of tripeptide **13d** depicted in **Figure 2.6**, troponyl ring and adjacent amide carbonyl carbon chemical shifts are showing clear shifts in two different solvents, whereas chemical shifts of phenyl ring carbons and other carbons like ester, Boc carbonyl remains same in both the solvents. As per our interest, we keenly examined the shift in the troponyl carbonyl chemical shift in given solvent systems. Interestingly, the troponyl carbonyl appeared at ~ δ 182.9 in CDCl₃ and at δ 180.69 in DMSO-d₆ as well as in the mixture of DMSO-d₆:CDCl₃, which has shown upfield shift. The upfield shift is due to the existing of free carbonyl in the solvent system containing DMSO-d₆. It is known that, in CDCl₃ the hydrogen bond remain undisturbed. Whereas, in DMSO-d₆, the intramolecular hydrogen bond is replaced by the intermolecular hydrogen bond with DMSO-d₆.³³ Overall, these results further supports the participation of troponyl carbonyl in hydrogen bonding with adjacent amide NH.

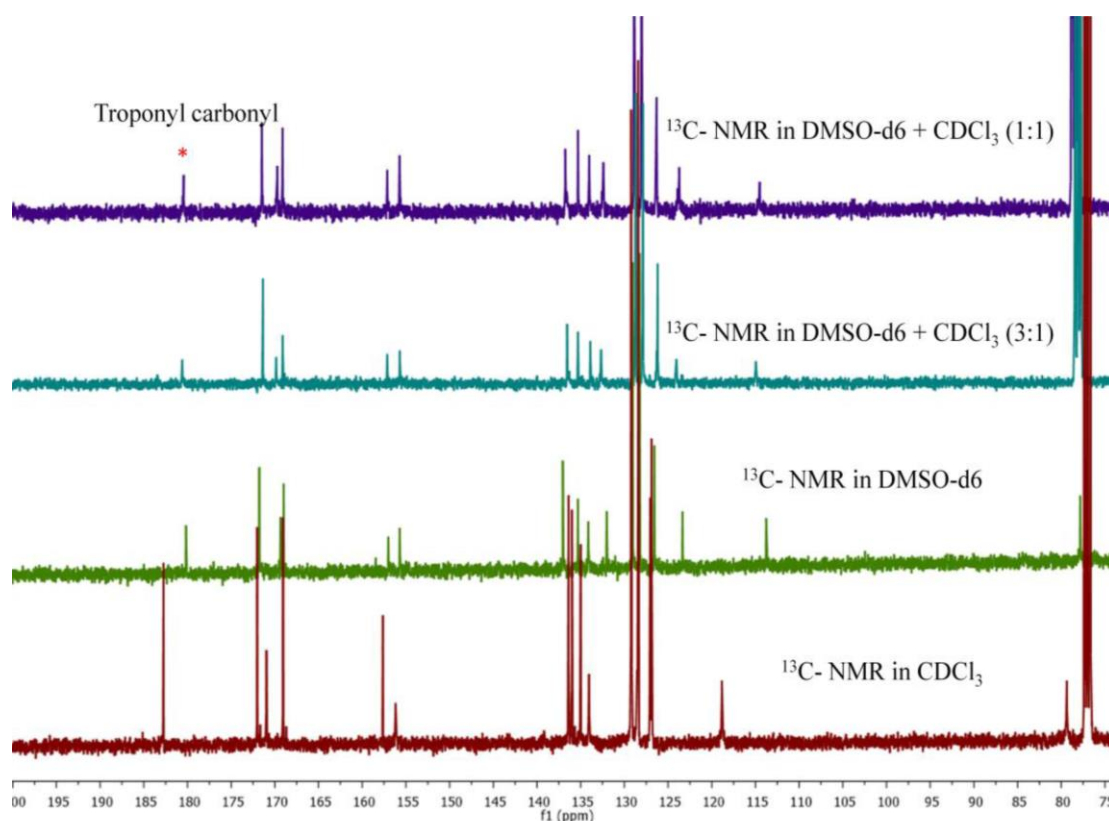


Figure 2.6 Stacked ^{13}C NMR spectra of tri-peptide **13d** in given solvent system. All the spectra were characterized with respect to DMSO solvent residual peak.

DFT Calculations: DFT calculation was performed with B97 TROBOLONE Software on dipeptide **13c** in gas phase to acquire geometrically optimized structure of **13c**. The optimized geometry of **13c** is provided in **Figure 2.7** which also indicate the troponyl carbonyl orientation toward C' -end of peptide **13c**. The theoretical pdb files of peptide **13c** are provided in appendix. This optimized structure of **13c** has following strong non-covalent hydrogen bond interaction: $\text{C}=\text{O} \cdots \text{H}-\pi\text{C}$ (2.41Å); $\pi\text{C} \cdots \text{H}-\text{C}$ (2.47Å); $\text{C}=\text{O} \cdots \text{H}-\text{C}$ (2.05Å); and $\text{C}=\text{O} \cdots \text{H}-\text{N}$ (2.08Å). These results also support the formation of 8-membered ring hydrogen bond motif between Troponyl carbonyl and $(i+1)^{\text{th}}$ amide NH, which may afford interesting helical structure in longer peptide.

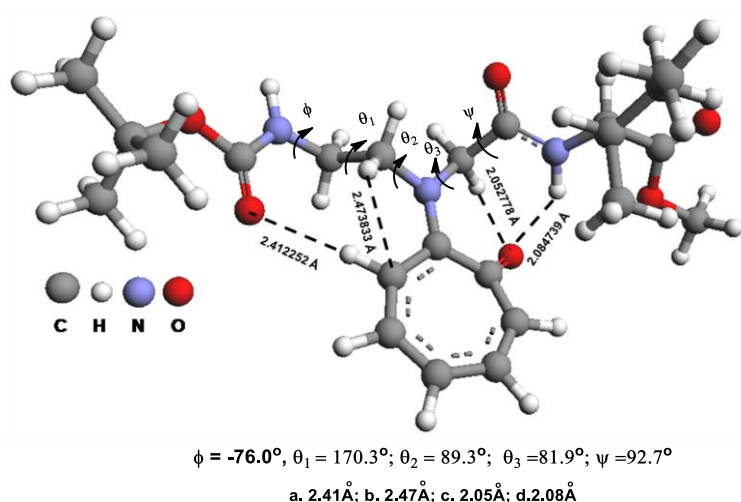
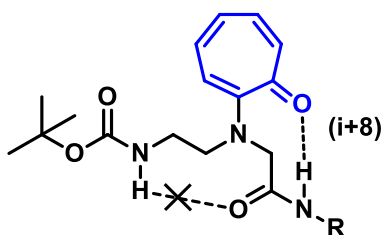


Figure 2.7 Energy minimized structure of dipeptide **9** from DFT calculations.

2.3 Conclusions

In summary, we have successfully synthesized the designed new unnatural δ -amino acid, Troponyl aminoethylglycine (*Traeg*) and their δ/α hybrid peptides. All compounds were thoroughly characterized. From the 2D NMR spectral analysis, we established that the troponyl ring is oriented towards the C-terminal end in *Traeg* monomer **5a** and its peptides **13a-d**. Further, the hydrogen bonding interaction between the troponyl carbonyl and adjacent amide NH is investigated by the ^1H & ^{13}C NMR DMSO- d_6 titration experiments. These experimental results revealed that troponyl carbonyl is in hydrogen bonding with adjacent amide NH. Further, these experimental results are supported with the energy minimized structure from DFT calculations. Overall, for the first time, we have used the troponyl aromatic ring as a substituent in backbone extended δ -amino acid. Unfortunately, the synthesis of *Traeg* homologous peptides are unsuccessful. However, we have demonstrated the hydrogen bonding ability of troponyl carbonyl and the formation of eight-membered ring hydrogen bond between the troponyl carbonyl of *Traeg* residue and its adjacent amide NH in heterologous peptides (**Figure 2.8**).



R: Phe, Pro, Ile, Gly-Phe

Figure 2.8 Schematic representation of summary.

2.4 Experimental Section

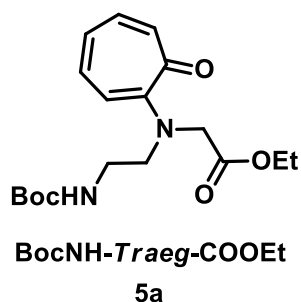
Materials and instrumentation: All required materials were obtained from commercial suppliers and used without further purification. Dry dichloromethane was freshly prepared by distilling over KOH and Calcium hydride sequentially. Reactions were monitored by thin layer chromatography, visualized by UV and Ninhydrin. Column chromatography was performed in 100-200 mesh silica. NMR spectra were recorded on Bruker AV-400 (^1H : 400 MHz, ^{13}C : 100.6 MHz). ^1H and $^{13}\text{C}\{^1\text{H}\}$ NMR chemical shifts were recorded in ppm downfield from tetramethyl silane. Splitting patterns are abbreviated as: s, Singlet; d, doublet; dd, doublet of doublet; t, triplet; q, quartet; dq, doublet of quartet; m, multiplet. Mass spectra were obtained from Bruker micrOTOF-Q II Spectrometer.

Syntheses of N-Boc-ethylenediamine: N-Boc-ethylene diamine was synthesized by following the previously reported procedure.³⁵

Syntheses of ethyl-N(2-Boc-aminoethyl)glycinate (4): Ethyl-N(2-Boc-aminoethyl)glycinate was synthesized by following the reported procedures.³⁵

Procedure for the syntheses of 2-tosyloxypone (2): Tropolone (1.0 equiv.) and tosylchloride (1.2 equiv.) was dissolved in anhydrous methylene chloride under inert atmosphere and allowed to stir. To the resultant mixture 2.5 equiv. of triethylamine was added slowly. The addition of triethylamine results in formation of yellow viscous liquid, to this further added anhydrous methylene chloride to decrease viscosity of the solution. The resultant mixture is allowed to stir at room temperature until completion of the reaction as judged by TLC. After completion all volatiles were evaporated to obtain crude product. To the crude product ethanol or methanol was added. This results in precipitation of the desired product as white solid. The precipitate was filtered by using vacuum filtration and dried. The obtained product was used for next step.

Syntheses of ethyl-(2-N-Boc-aminoethyl)tropolonyl)glycinate (5a):



To a solution of 2-tosyloxy tropone (**2**) (1.2g, 4.34 mmol) in ethanol (25 mL) was added ethyl (2-N-Boc-aminoethyl) glycinate (**4**) (3.2 g, 13.04 mmol) and refluxed. Reaction was monitored using thin layer chromatography (TLC) and found the completion of reaction after two days. After cooling to room temperature, reaction mixture was concentrated under vacuum on rota vapour. The reaction residue was redissolved in DCM (50 mL) and washed with water three times and then with brine solution (10 mL) by using separating flask. The organic layer was kept over Na₂SO₄ for 30 min and then concentrated to dryness under vacuum. The concentrated residue was subjected for purification on silica gel by column chromatographic methods. The major component of reaction residue was purified with solvent mixture ethyl acetate:hexane (1:3) and characterized as desired product (1.2 g, 80%) by ¹H/¹³C-NMR and Mass spectrometric method. ¹H NMR (400 MHz, CDCl₃) δ (ppm) 7.12 – 6.96 (m, 2H), 6.92 (d, J = 11.8 Hz, 1H), 6.75–6.55 (m, 2H), 5.60 (s, 1H), 4.20 (s and q, 4H), 3.59 (t, J = 6.1 Hz, 2H), 3.45-

3.31 (m, 2H), 1.40 (s, 10H), 1.26 (t, $J = 7.1$ Hz, 3H). ^{13}C -NMR (101 MHz, CDCl_3): δ (ppm) 181.69, 170.41, 157.93, 156.21, 135.62, 133.92, 133.78, 125.10, 115.79, 79.37, 61.15, 53.57, 52.37, 37.57, 28.33, 14.11. HRMS (ESI-TOF) m/z : $[\text{M}+\text{H}]^+$ calcd. for $\text{C}_{18}\text{H}_{26}\text{N}_2\text{O}_5$ 351.1914, found 351.1922. Summary of X-ray data of monomer 5 is deposited to the Cambridge Structural Database (CSD) and their deposition number is CCDC 975954.

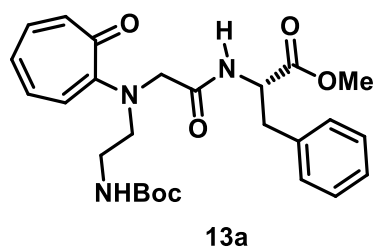
General procedure for the ester hydrolysis of monomers: Hydrolysis of monomers (**5a**, **4**) were carried out by following the reported literature procedures.^{9b} *Traeg* monomer (**5a**) was dissolved in ethanol and tetrahydrofuran (1:1) mixture. To this 2 *equiv.* of sodium hydroxide aqueous solution was added by dissolving by dissolving in very little amount of water. Then reaction mixture is stirred for 30 min to 1 h, as judged by TLC. After completion of the reaction all volatiles were evaporated under reduced pressure. To the crude product 1.0 N HCl was added and extracted with DCM. The combined organic layers were evaporated in *vacuo* and dried completely. The obtained product was used for the peptide synthesis without any further purification and charecterization.

Note: In case of hydrolysis of *aeg* monomer **4**, after completion of the reaction all volatiles were evaporated and the resultant residue containg NaOH was gently neutralized with 1.0 N HCl to almost neutral pH (pH = 6.0-7.0, pH of the solution was tested by pH paper). Water was evaporated under reduced pressure and obtained product was used for Fmoc protection.

Procedure for solid phase peptide syntheses: Fmoc protected MBHA (Rink amide 4-methylbenzhydrylamine, polymer-bound) resin was taken in manual peptide syntheses flask, added dichloromethane and allowed to swell at room temperature for two hours under nitrogen atmosphere. After swelling of the resin, Fmoc was deprotected by using 20.0% Piperidine in DMF and washed the resin with 3*DCM, 3*DMF and 3*DCM. Then the resin was purged with nitrogen to create inert atmosphere. After this, a solution of

Traeg amino acid (3.0 *equiv.*), DIPEA (3.0 *equiv.*) and HOTU (3.0 *equiv.*) in DMF is added to the free amine resin and left at room temperature for two hours. To check the completion of the reaction, we performed the Kaiser test with resin. After confirming the completion of the reaction, the undesired starting materials present in the reaction mixture are washed out. Again, resin was washed by following the above procedure. After washing, capping of any unreacted free amine was done by using acetic anhydride and triethyl amine solution in DCM. Again, resin was washed and for further coupling, the Boc protecting group removed and repeated the above procedure.

Syntheses of dipeptide (13a):



A solution of *N*-(2-amioethyl)troponylglycine (**6a**) (200 mg, 0.62 mmol) in anhydrous dichloromethane (10 mL) was cooled to 0°C, and then EDC-HCl (142 mg, 0.744 mmol, in some cases diisopropyl carbodiimide was also used as coupling reagent) was added to the solution and stirred for 5 minutes at 0°C. Then L-phenylalanine methyl ester hydrochloride (160 mg, 0.744 mmol) and triethylamine (0.26 mL, 1.86 mmol) was added together. This reaction mixture was continued to stir at room temperature (rt) for overnight (reaction temperature was raised to 45-50 °C to obtain good yield of product in case of less conversions). After completion of the reaction, the volatiles were evaporated under reduced pressure. Concentrated reaction residue was re-dissolved in DCM (30 mL) and then washed with water thrice (3*30mL) followed by saturated sodium bicarbonate (20 mL) by following extraction method. The washed organic layers were combined together and concentrated under reduced pressure and then loaded on silicagel column for purification by EtOAc/Hexane to obtain desired product (**7**). The major component was isolated with EtOAc/Hexane (30:70) and characterized as desired product (120 mg, 40%) by ¹H/¹³C-NMR and Mass spectrometric method. ¹H NMR (400

MHz, CDCl₃) δ (ppm) 7.76 (d, J = 7.9 Hz, 1H), 7.24 – 7.06 (m, 7H), 7.05 – 6.92 (m, 2H), 6.72 (dd, J = 21.4, 13.0 Hz, 2H), 5.59 (s, 1H), 4.78 (dd, J = 14.0, 6.7 Hz, 1H), 3.93 (d, J = 16.7 Hz, 1H), 3.88 – 3.75 (m, 1H), 3.72 – 3.60 (m, 3H), 3.55 – 3.37 (m, 1H), 3.36 – 3.12 (m, 4H), 3.05 – 2.93 (m, 1H), 1.38 (s, 9H). ¹³C NMR (101 MHz, CDCl₃): δ (ppm) 182.52, 171.78, 169.39, 157.22, 156.02, 135.87, 134.34, 133.79, 129.02, 128.91, 128.27, 126.75, 126.38, 118.09, 79.02, 55.60, 53.25, 52.12, 51.18, 37.65, 37.46, 28.19. HRMS (ESI-TOF) m/z : [M+H]⁺ calcd for C₂₆H₃₃N₃O₆ 484.2442, found 484.2486.

Syntheses of BocNH-Fmoc-aeg-OEt (5d): N-Boc, ethyl, amino ethylglycinate (**4**) was dissolved in dichloromethane, to this 1.2 *equiv.* of Fmoc-Cl was added. To the resultant mixture 3.0 *equiv.* of DIPEA is added and allowed to stir at room temperature (12 h). Reaction was monitored by TLC. After completion of the reaction, all volatiles were evaporated under *vacuo*. The obtained crude product was dissolved in DCM and washed with water thrice. Combined organic layers after extraction were dried over sodium sulphate and concentrated. The crude product is loaded on silica gel column and purified by using ethyl acetate and hexanes mobile phases. Obtained product was characterized by mass and used for further step.

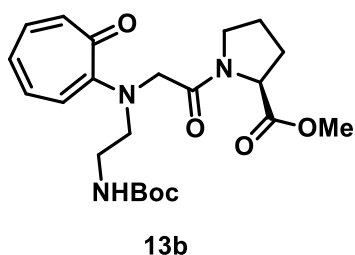
Synthesis of BocNH-Fmoc-aeg-COOH (5d-COOH): To a solution of BocNH-aeg-COOH and sodium bicarbonate (2.0 *equiv.*) in water and dioxane (1:1) mixture, Fmoc-chloride (1.2 *equiv.*) was added in portion wise at 0 °C. The reaction mixture is allowed to stir at room temperature for 6 h. After completion of the reaction, the reaction mixture pH was adjusted to pH 2.0 by using 1.0 N HCl and extracted with ethyl acetate thrice. Organic layers are combined together, dried over sodium sulphate and concentrated to dryness. The obtained product was used for peptide syntheses without any further purification.

Synthesis of BocNH-Fmoc-aeg-Fmoc-aeg-OEt (29S): BocNH-Fmoc-aeg-COOH (**5d-COOH**) was taken in anhydrous DMF and cooled to 0 °C. To the cooled solution,

diisopropyl carbodiimide is added (use of EDC-HCl as coupling reagent caused the deprotection of Fmoc groups) and allowed to stir at 0 °C. After five minutes, neutralized solution of $\text{NH}_2\text{-Fmoc-aeg-OEt}$ (**5d-NH₂**) in DMF and 3 equiv. of Et_3N was added slowly at 0 °C. The resultant reaction mixture is allowed to stir at room temperature for 12 h. After completion of the reaction, all volatiles were evaporated and obtained residue was redissolved in DCM and washed with 1.0 N HCl and water. Combined organic layers were dried over sodium sulphate and concentrated to obtain crude product. The crude product was purified through silica gel column chromatography by using ethyl acetate and hexanes as mobile phase. Obtained product was characterized by mass and used for next step.

Synthesis of BocNH-aeg-aeg-OEt (29S1): The dipeptide **29S**, was added 20.0% piperidine in DMF and allowed to stir at room temperature for two hours. After completion of the reaction, DMF was evaporated under reduced pressure. The obtained residue was redissolved in water and filtered to remove precipitated fluorenyl by products. The obtained water filtrate was concentrated in rota evaporatory under reduced pressure and at 50 °C. The obtained product was characterized by mass spectrometry and used for troponylation under optimized conditions for monomer troponylation.

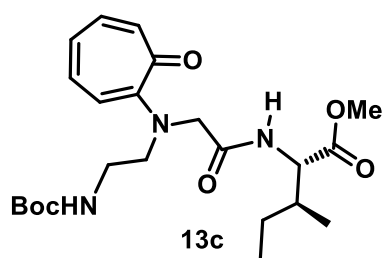
Syntheses of dipeptide (13b):



Similarly the dipeptide **13b** was synthesized from Traeg (6) and L-proline methyl ester. (150 mg, 41%). ^1H NMR (400 MHz, CDCl_3) δ 7.15 – 6.98 (m, 3H), 6.92 (dd, J = 11.7, 5.5 Hz, 1H), 6.78 (t, J = 11.6 Hz, 1H), 6.70 – 6.58 (m, 1H), 5.91 – 5.77 (m, 1H), 4.72 (d, J = 17.2 Hz, 1H), 4.49 (dd, J = 8.4, 4.0 Hz, 1H), 4.20 (t, J = 13.9 Hz, 1H), 3.90 – 3.81 (m, 1H), 3.79 (s, 1H), 3.74 (dd, J = 11.2, 5.9 Hz, 1H), 3.69 (s, 3H), 3.64 (dd, J = 12.7, 5.5 Hz, 1H), 3.55 (dt, J = 17.1, 8.8 Hz, 2H), 3.40 (d, J = 5.7 Hz, 3H), 2.35 – 2.27 (m, 1H), 2.27 – 2.15 (m, 2H), 2.13 – 1.94 (m, 4H), 1.44 (d, J = 19.3 Hz, 9H).

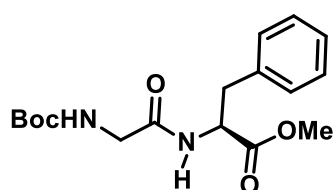
^{13}C NMR (101 MHz, CDCl_3): δ (ppm) 181.71, 172.49, 167.89, 157.49, 156.37, 135.66, 134.02, 133.72, 124.99, 116.67, 79.07, 58.92, 53.37, 52.49, 52.26, 46.21, 37.87, 28.83, 28.42, 24.89, (cis and trans isomers are existing around secondary amide bond in 1:4, not predicted due to overlapping signals). HRMS (ESI-TOF) m/z : $[\text{M}+\text{H}]^+$ calcd. for $\text{C}_{22}\text{H}_{31}\text{N}_3\text{O}_6$ 456.2105, found 456.2123.

Syntheses of dipeptide (13c):



Similarly the dipeptide **13c** was synthesized from Traeg (6) and L-Isoleucine methyl ester. (45 mg 36%) ^1H NMR (400 MHz, CDCl_3) δ in ppm 7.90 (d, $J = 8.2$ Hz, 1H), 7.24 – 7.12 (m, 1H), 7.11 – 7.00 (m, 2H), 6.92 – 6.81 (m, 1H), 6.79 – 6.70 (m, 1H), 5.65 (s, 1H), 4.65 – 4.43 (q, 1H), 4.18 – 4.05 (m, 1H), 3.72 (d, $J = 5.3$ Hz, 1H), 3.69 (s, 3H), 3.63 – 3.50 (m, 1H), 3.47 – 3.24 (m, 4H), 2.32 (dd, $J = 17.1, 9.6$ Hz, 1H), 2.02 – 1.85 (m, 1H), 1.52 (dd, $J = 1.0, 6.1$ Hz, 1H), 1.47 – 1.34 (m, 9H), .21 – 1.12 (m, 1H), 0.96 – 0.82 (m, 6H). (cis and trans isomers are existing around carbamate amide bond in 1:4, not predicted due to overlapping signals). ^{13}C -NMR (101 MHz, CDCl_3) δ in ppm 183.22, 172.43, 169.79, 157.71, 156.27, 136.95, 136.41, 136.18, 135.01, 133.83, 132.73, 127.70, 119.33, 113.09, 79.21, 64.92, 56.65, 56.25, 52.06, 51.39, 37.81, 37.28, 28.33, 24.94, 22.64, 15.68, 14.24, 11.53. (cis and trans isomers are existing around carbamate amide bond in 1:4). HRMS (ESI-TOF) m/z : $[\text{M}+\text{H}]^+$ calcd. for $\text{C}_{23}\text{H}_{35}\text{N}_3\text{O}_6$ 472.2418, found 472.2428.

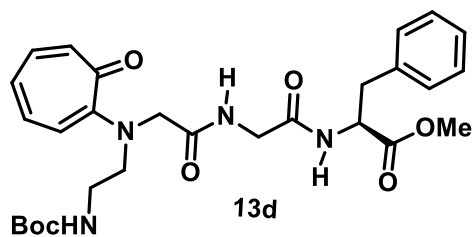
Syntheses of dipeptide (11):



Similarly the dipeptide **11** was synthesized from N-Boc glycine and L-Phenylalanine methyl ester. ^1H NMR (400 MHz, CDCl_3) δ 7.36 – 7.17 (m, 3H), 7.16 – 7.03 (m, 2H), 6.59 (s, 1H), 5.14 (s, 1H), 4.94 – 4.82 (m, 1H), 3.78 (dd, $J = 18.7, 5.5$ Hz, 2H), 3.71 (s, 3H), 3.20 – 3.06 (m,

2H), 1.44 (s, 9H). ^{13}C NMR (101 MHz, CDCl_3) δ in ppm 171.70, 169.12, 155.91, 135.61, 129.17, 128.56, 127.09, 80.16, 77.00, 53.04, 52.29, 44.10, 37.83, 28.22. HRMS (ESI-TOF) m/z : $[\text{M}+\text{H}]^+$ calcd. for $\text{C}_{17}\text{H}_{24}\text{N}_2\text{O}_5$ 337.1758, found 337.1723.

Syntheses of tri-peptide (13d):



Similarly the tripeptide **13d** was synthesized from *Traeg* (**6**) and $\text{NH}_2\text{-Gly-Phe-OMe}$. (138 mg, 41%).

^1H NMR (400 MHz, CDCl_3) δ 7.91 (s, 1H), 7.29 (d, $J = 7.7$ Hz, 1H), 7.27 – 7.16 (m, 3H), 7.15 – 7.01 (m,

4H), 6.94 (dd, $J = 25.0, 10.4$ Hz, 2H), 6.81 – 6.68 (m, 1H), 5.55 (s, 1H), 4.81 (dd, $J = 13.4, 6.5$ Hz, 1H), 4.08 (dd, $J = 16.7, 6.2$ Hz, 1H), 3.97 – 3.73 (m, 3H), 3.75 – 3.54 (m, 4H), 3.53 – 3.34 (m, 2H), 3.29 (d, $J = 5.3$ Hz, 2H), 3.09 (qd, $J = 13.8, 6.4$ Hz, 2H), 1.39 (s, 9H). ^{13}C NMR (101 MHz, CDCl_3) δ in ppm 182.74, 172.02, 170.96, 169.07, 157.65, 156.18, 136.39, 136.00, 135.01, 134.05, 129.19, 128.48, 126.97, 118.83, 79.37, 56.85, 53.42, 52.13, 42.90, 37.58, 37.09, 28.30. HRMS (ESI-TOF) m/z : $[\text{M}+\text{H}]^+$ calcd. for $\text{C}_{28}\text{H}_{36}\text{N}_4\text{O}_7$ 541.2657, found 541.2565.

Crystal data of monomer 5a:

Table S12. Crystal data and structure refinement for agr : (CCDC file No:975954)

Identification code:	agtr
Empirical formula:	$\text{C}_{18}\text{H}_{26}\text{N}_2\text{O}_5$
Formula weight:	350.41
Temperature:	296(2) K

Wavelength:	0.71073 Å
Crystal system:	Monoclinic
Space group:	P2(1)/c
Unit cell dimensions:	$a = 11.1125(4) \text{Å}$; $\alpha = 90.0$. $b = 15.3001(7) \text{Å}$; $\beta = 112.3460$. $c = 12.2394(5) \text{Å}$; $\gamma = 90.0$.
Volume:	1924.70(14) Å ³
Z:	4
Calculated density:	1.209 Mg/m ³
Absorption coefficient:	0.088 mm ⁻¹
F(000):	752
Crystal size:	0.06 x 0.041 x 0.032 mm
Theta range for data collection:	2.49 to 26.770.
Limiting indices:	-14 ≤ h ≤ 14, -19 ≤ k ≤ 19, -15 ≤ l ≤ 14
Reflections collected / unique:	25584 / 4071 [R(int) = 0.0609]
Completeness to theta:	26.77 99.2 %
Absorption correction:	Semi-empirical from equivalents
Max. and min. transmission:	0.7454 and 0.6864
Refinement method:	Full-matrix least-squares on F ²

Data / restraints / parameters:	4071 / 0 / 230
Goodness-of-fit on:	F^2 1.013
Final R indices [$I > 2\sigma(I)$]:	$R_1 = 0.0484$, $wR_2 = 0.1217$
R indices (all data):	$R_1 = 0.0990$, $wR_2 = 0.1457$
Largest diff. peak and hole:	0.247 and -0.199 e. \AA^{-3}

2.5 References and Notes

1. Branden, C.; Tooze, J. *Introduction to Protein Structure*; Garland: New York, NY, **1991**.
2. Alberts, B.; Johnson, A.; Lewis, J.; Raff, M.; Roberts, K.; Walter, P. *Molecular Biology of the Cell*, 4th ed.; Garland Science: New York, NY, **2002**.
3. *Foldamer: Structure, Properties and Applications*; Hecht, S., Huc, I., Eds.; Wiley-VCH: Weinheim, Germany, **2007**.
4. Seebach, D.; Matthews, J. L. *Chem. Commun. (Camb.)* **1997**, 21, 2015.
5. Gellman, S. H. *Acc. Chem. Res.* **1998**, 31, 173.
6. Horne, W. S.; Gellman, S. H. *Acc. Chem. Res.* **2008**, 41, 1399.
7. Kotha, S. *Acc. Chem. Res.* **2003**, 36, 342.
8. Lelais, G.; Seebach, D. *Biopolymers*. **2004**, 76, 206.
9. Seebach, D.; Hook, D. F.; Glattli, A. *Biopolymers*. **2006**, 84, 23.
10. Seebach, D.; Gardiner, J. *Acc. Chem. Res.* **2008**, 41, 1366.
11. Vasudev, P. G.; Chatterjee, S.; Shamala, N.; Balaram, P. *Chem. Rev.* **2011**, 111, 657.
12. Hill, D. J.; Mio, M. J.; Prince, R. B.; Hughes, T. S.; Moore, J. S. *Chem. Rev.* **2001**, 101, 3893.
13. Roy, A.; Prabhakaran, P.; Baruah, P.K.; Sanjayan, G. J. *Chem. Commun.* **2011**, 47, 11593.
14. Prabhakaran, P.; Priya, G.; Sanjayan, G. J. *Angew. Chem., Int. Ed.* 2012, 51, 4006.
15. Zhang, D. W.; Zhao, X.; Hou, J. L.; Li, Z. T. *Chem. Rev.* **2012**, 112, 5271.
16. Zhang, D. W.; Zhao, X.; Li, Z. T. *Acc. Chem. Res.* **2014**, 47, 1961.
17. Ramesh, V. V. E.; Roy, A.; Vijayadas, K. N.; Kendhale, A. M.; Prabhakaran, P.; Gonnade, R.; Puranik, V. G.; Sanjayan, G. J. *Org. Biomol. Chem.* **2011**, 9, 367.

18. Ramesh, V. V. E.; Priya, G.; Kotmale, A. S.; Gonnade, R. G.; Rajamohanan, P. R.; Sanjayan, G. J. *Chem. Commun.*, **2012**, 48, 11205–11207.
19. Hicks, R. P.; Russell, A. L. *Methods Mol. Biol.* **2012**, 794, 135.
20. Sengupta, A.; Aravinda, S.; Shamala, N.; Raja, K. M. P.; Balaram, P. *Org. Biomol. Chem.* **2006**, 4, 4214;
21. Rai, R.; Vasudev, P. G.; Ananda, K.; Raghothama, S.; Shamala, N.; Karle, I. L.; Balaram, P. *Chem.-Eur. J.* **2007**, 12, 3295.
22. Bandyopadhyay, A.; Jadhav, S. V.; Gopi, H. N. *Chem. Commun.*, **2012**, 48, 7170–7172.
23. Mali, S. M.; Jadhav, S. V.; Gopi, H. N. *Chem. Commun.*, **2012**, 48, 7085-7087.
24. Bandyopadhyay, A.; Gopi, H. N. *Org. Lett.*, **2012**, 14, 2270-2273.
25. Basuroy, K.; Dinesh, B.; Reddy, M. B. M.; Chandrappa, S.; Raghothama, S.; Shamala, N.; Balaram, P. *Org. Lett.* **2013**, 15, 4866.
26. Fremaux, J.; Kauffmann, B.; Guichard, G. *J. Org. Chem.* **2014**, 79, 5494.
27. Peng, Y.; Gong, T.; Cui, Y. *Chem. Commun. (Camb.)* **2013**, 49, 8253.
28. Schramm, P.; Sharma, G. V. M.; Hofmann, H.-J. *Biopolymers.* **2010**, 94, 279.
29. Narita, M.; Doi, M.; Kudo, K.; Terauchi, Y. *Bull. Chem. Soc. Jpn.* **1986**, 59, 3553.
30. Narita, M.; Doi, M.; Kudo, K.; Terauchi, Y. *Bull. Chem. Soc. Jpn.* **1986**, 59, 3553.
31. Appella, D. H.; Christianson, L. A.; Karle, I. L.; Powell, D. R.; Gellman, S. H. *J. Am. Chem. Soc.* **1996**, 118, 13071.
32. Hanessian, S.; Luo, X.; Schaum, R.; Michnick, S. *J. Am. Chem. Soc.* **1998**, 120, 8569.
33. Rai, R.; Raghothama, S.; Balaram, P. *J. Am. Chem. Soc.* **2006**, 128, 2675.
34. Urry, D. W.; Mitchell, L. W.; Onishi, T. *Proc. Natl. Acad. Sci. U.S.A.* **1974**, 71, 3265.
35. Dochnahl, M.; Lohnwitz, K.; Pissarek, J. W.; Biyikal, M.; Schulz, S. R.; Schon, S.; Meyer, N.; Roesky, P. W.; Blechert, S. *Chem.-Eur. J.* **2007**, 13, 6654.
36. Sharma, N. K.; Ganesh, K. N. *Chem. Commun. (Camb.)* **2005**, 34, 4330.

37. Bentley, R.; Thiessen, C. P. *Nature*, **1959**, *184*, 552 Suppl. 8.
38. Dewar, M. J. *Nature*, **1950**, *166*, 790.
39. Bentley, R. *Nat. Prod. Rep.* **2008**, *25*, 118.
40. Byeon, S. E.; Lee, Y. G.; Kim, J. C.; Han, J. G.; Lee, H. Y.; Cho, J. Y. *Planta. Med.* **2008**, *74*, 828.
41. Koufaki, M.; Theodorou, E.; Alexi, X.; Nikoloudaki, F.; Alexis, M. N. *Eur. J. Med. Chem.* **2010**, *45*, 1107.
42. Sanz, P.; Mo, O.; Yanez, M.; Elguero, J. *Chem.-Eur. J.* **2008**, *14*, 4225.
43. Morita, Y.; Sakagami, Y.; Okabe, T.; Ohe, T.; Inamori, Y.; Ishida, N. *Biocontrol Sci.* **2007**, *12*, 101.
44. Morita, Y.; Matsumura, E.; Okabe, T.; Shibata, M.; Sugiura, M.; Ohe, T.; Tsujibo, H.; Ishida, N.; Inamori, Y. *Biol. Pharm. Bull.* **2003**, *26*, 1487.
45. Narita, T.; Suga, A.; Kobayashi, M.; Hashimoto, K.; Sakagami, H.; Motohashi, N.; Kurihara, T.; Wakabayashi, H. *Anticancer research* **2009**, *29*, 1123.
46. Chung, S.; Himmel, D. M.; Jiang, J. K.; Wojtak, K.; Bauman, J. D.; Rausch, J. W.; Wilson, J. A.; Beutler, J. A.; Thomas, C. J.; Arnold, E.; Le Grice, S. F. *J. Med. Chem.* **2011**, *54*, 4462.
47. Fullagar, J. L.; Garner, A. L.; Struss, A. K.; Day, J. A.; Martin, D. P.; Yu, J.; Cai, X.; Janda, K. D.; Cohen, S. M. *Chem. Commun. (Camb.)*, **2013**, *49*, 3197.
48. Nishinaga, T.; Aono, T.; Isomura, E.; Watanabe, S.; Miyake, Y.; Miyazaki, A.; Enoki, T.; Miyasaka, H.; Otani, H.; Iyoda, M. *Dalton Trans.* **2010**, *39*, 2293.
49. Miyake, Y.; Watanabe, S.; Aono, S.; Nishinaga, T.; Miyazaki, A.; Enoki, T.; Miyasaka, H.; Otani, H.; Iyoda, M. *Chem. Commun. (Camb.)* **2008**, *46*, 6167.
50. Kofoed, T.; Hansen, H. F.; Orum, H.; Koch, T. *J. Peptide Sci.* **2001**, *7*, 402.
51. Erdmann, R. S.; Wennemers, H. *J. Am. Chem. Soc.* **2010**, *132*, 13957.

2.6 Appendix

1. NMR ($^1\text{H}/^{13}\text{C}$) and HRMS spectra of <i>BocNH-Traeg-OEt</i> (5a).....	72
2. Characterization data $^1\text{H}/^{13}\text{C}$ NMR and HRMS of <i>BocNH-Traeg-Phe-OMe</i> (13a).....	74
.....	75
3. Characterization data $^1\text{H}/^{13}\text{C}$ NMR and HRMS of <i>BocNH-Traeg-Phe-OMe</i> (13b).....	76
4. Characterization data $^1\text{H}/^{13}\text{C}$ -NMR and HRMS of <i>BocNH-Traeg-Ile-OMe</i> (13c).....	78
5. Characterization data $^1\text{H}/^{13}\text{C}$ NMR and HRMS of <i>BocNH-Traeg-Gly-Phe-OMe</i> (13d).....	80
6. COSY and NOESY spectra of <i>Traeg</i> monomer 5a :.....	82
7. COSY, HSQC and NOESY spectra of dipeptide 13a :	83
8. COSY, HSQC and NOESY spectra of dipeptide 13b :	85
9. COSY, HSQC and NOESY spectra of tripeptide 13d :.....	87
10. Stacked ^1H NMR of dipeptide 13a :.....	89
11. Stacked ^1H NMR of <i>Traeg</i> monomer 5a :	89
12. Stacked ^1H NMR of dipeptide 13b :.....	90
13. Stacked ^1H NMR of tripeptide 13d :	90
14. Stacked ^1H NMR of dipeptide 13c :.....	91
15. Stacked ^1H NMR of dipeptide 11 :.....	91
16. Stacked ^1H NMR of tripeptide 13d :	92
17. DFT calculated electron density map of dipeptide 13c	92
18. Theoretical Ramachandran map	93
19. Crystal packing diagram of monomer 5a	93

1. NMR ($^1\text{H}/^{13}\text{C}$) and HRMS spectra of *BocNH-Traeg-OEt* (**5a**)

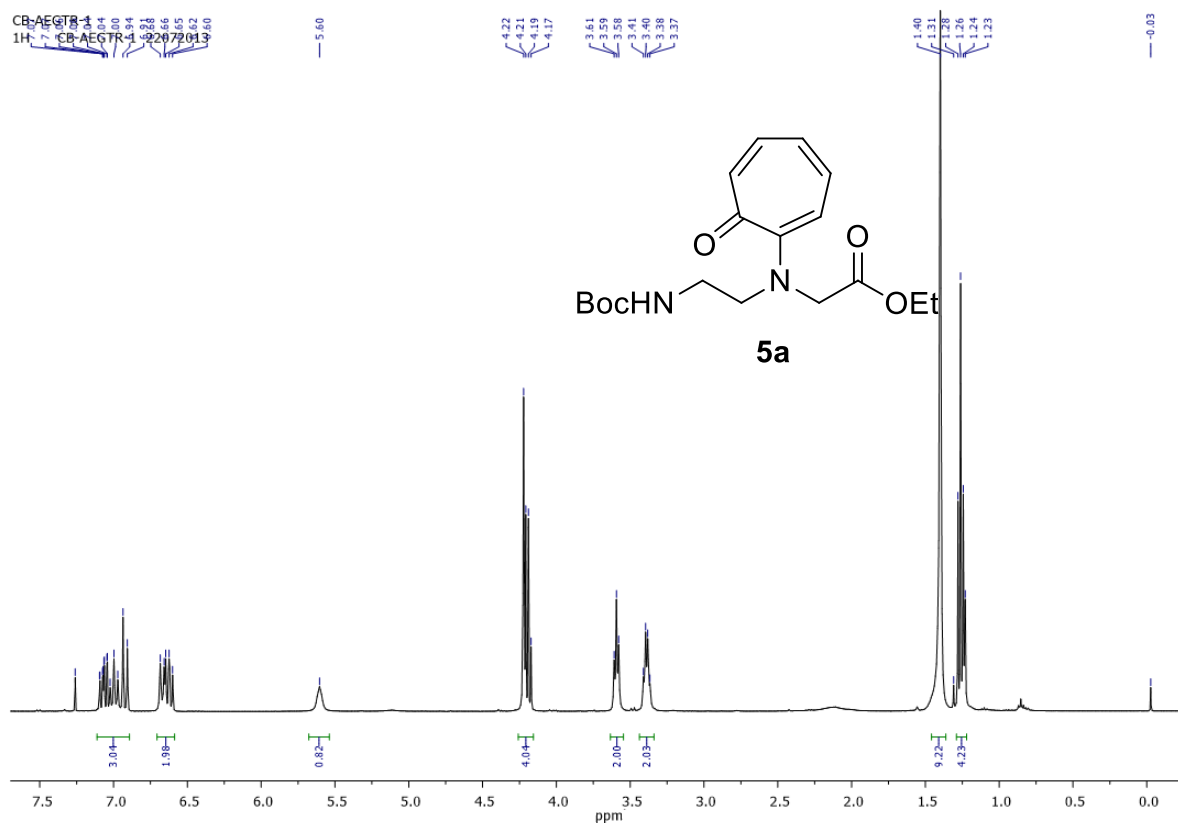


Figure A1. ^1H -NMR spectrum of *BocNH-Traeg-OEt* (**5a**) in CDCl_3

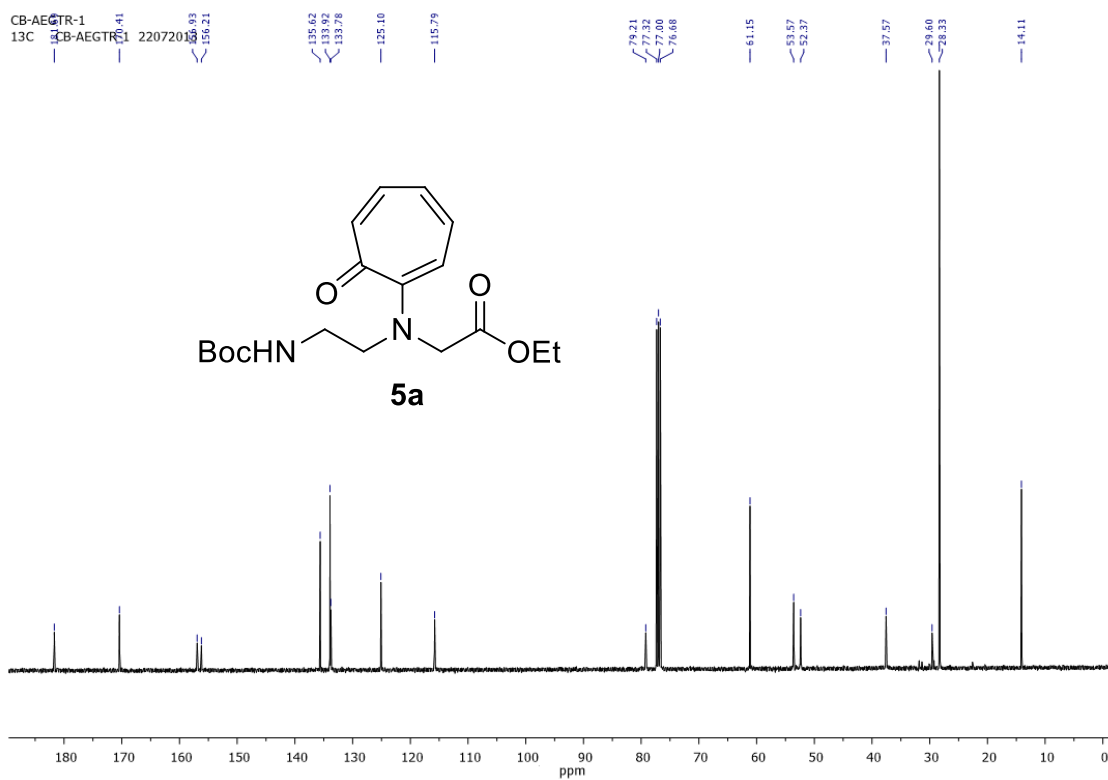


Figure A2. ^{13}C -NMR spectrum of *BocNH-Traeg-OEt* (**5a**) in CDCl_3

Display Report

Analysis Info

Analysis Name D:\Data\JULY-2013\NKS\22072013-CB_aegtram_LOW.d
Method Pos_tune_low.m
Sample Name CH3CN
Comment

Acquisition Date 7/22/2013 2:50:52 PM

Operator Amit-Rajkumar
Instrument microTOF-Q II 10337

Acquisition Parameter

Source Type	ESI	Ion Polarity	Positive	Set Nebulizer	0.4 Bar
Focus	Not active	Set Capillary	4500 V	Set Dry Heater	180 °C
Scan Begin	50 m/z	Set End Plate Offset	-500 V	Set Dry Gas	4.0 l/min
Scan End	3000 m/z	Set Collision Cell RF	130.0 Vpp	Set Divert Valve	Waste

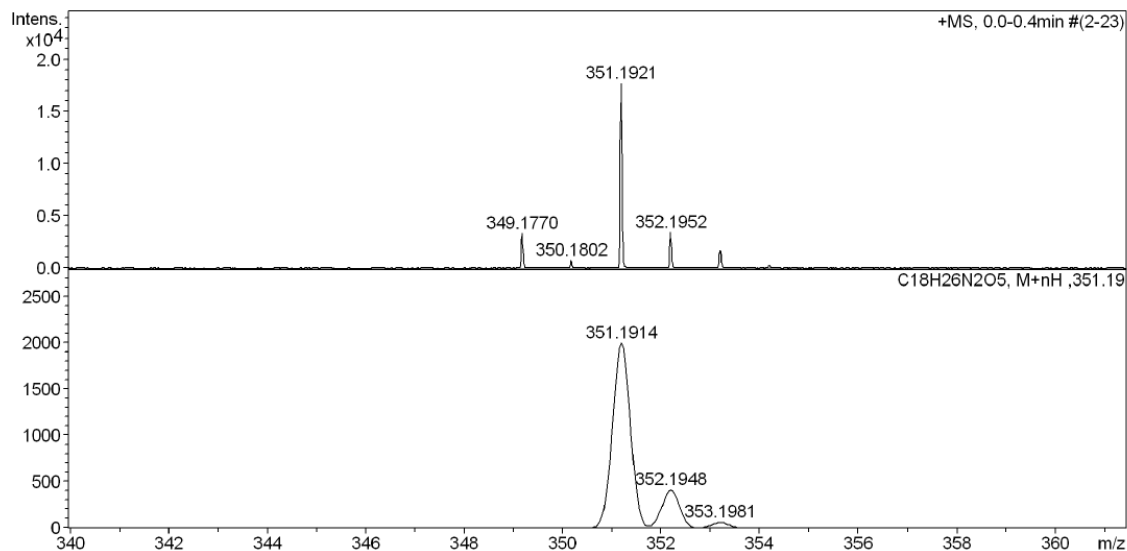
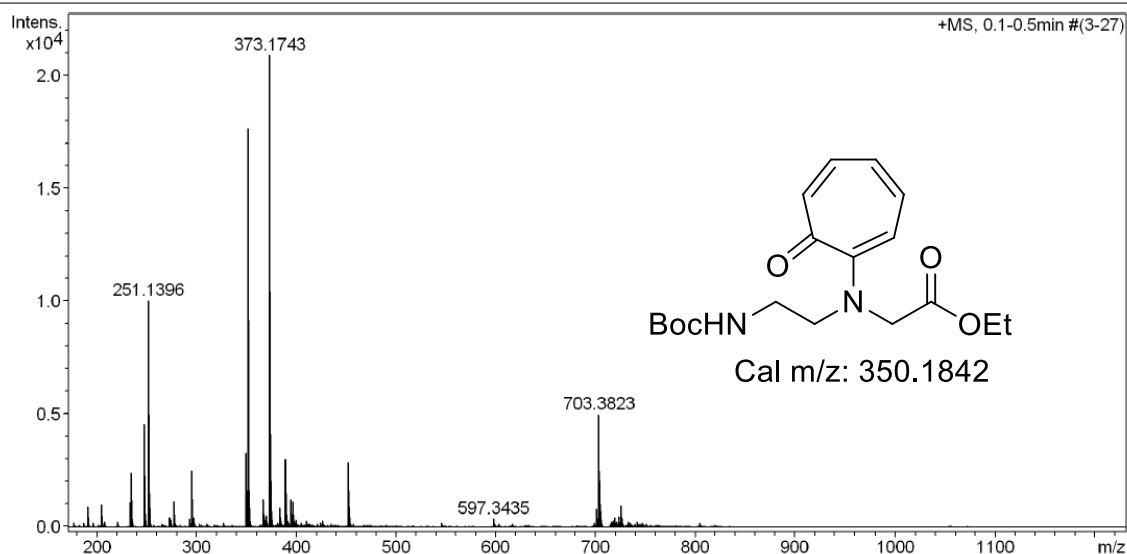


Figure A3. Mass spectrum of *BocNH-Traeg-OEt* (**5a**)

2. Characterization data $^1\text{H}/^{13}\text{C}$ NMR and HRMS of *BocNH-Traeg-Phe-OMe* (**13a**)

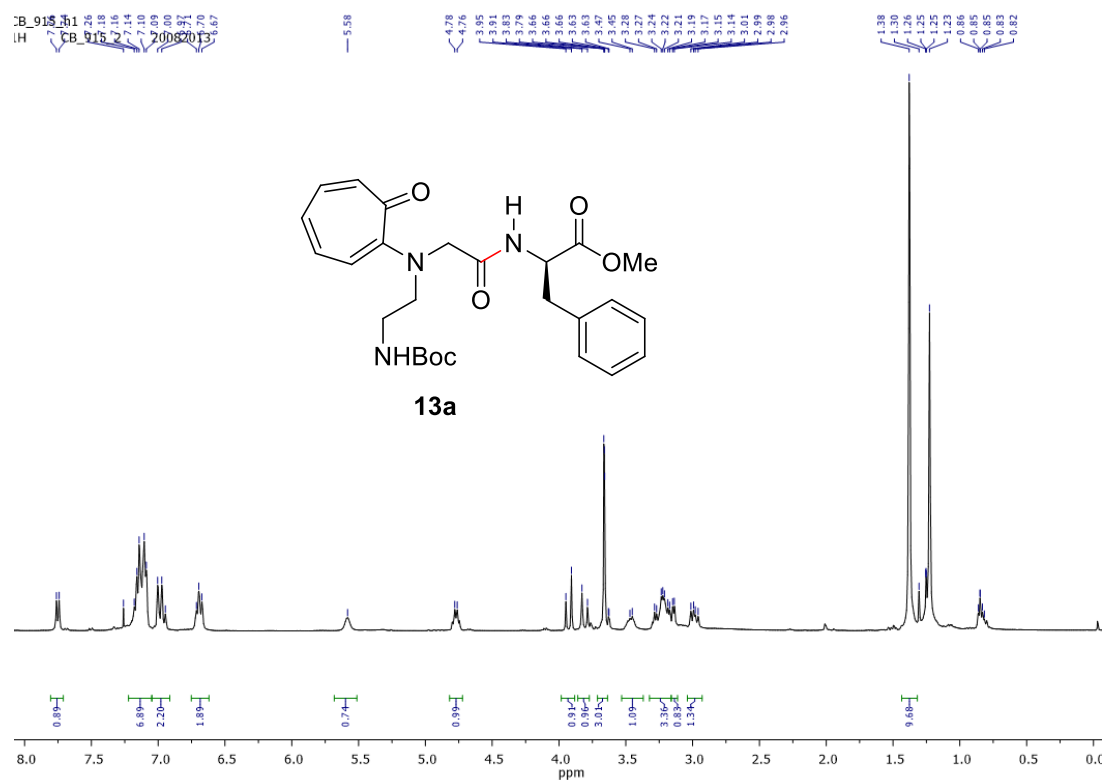


Figure A4. ^1H NMR spectrum of *BocNH-Traeg-Phe-OMe* (**13a**) in CDCl₃

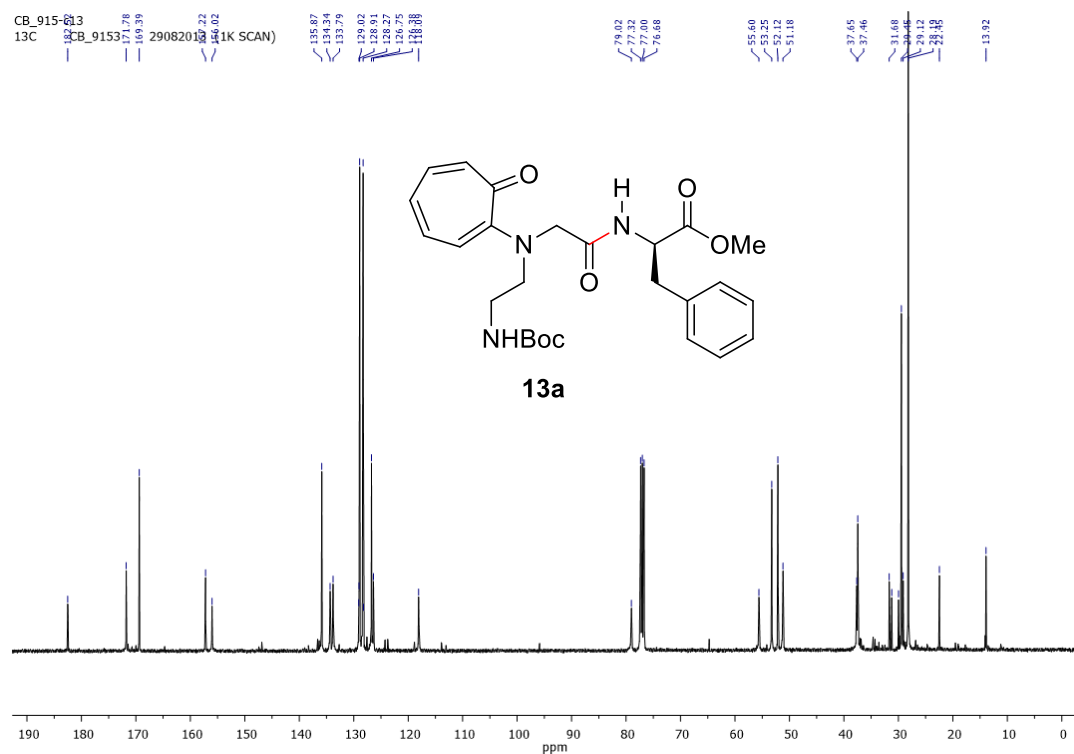


Figure A5. ^{13}C NMR spectrum of *BocNH-Traeg-Phe-OMe* (**13a**) in CDCl₃

Display Report

Analysis Info

Analysis Name D:\Data\AUG-2013\NKS\05082013_NKS_BC_9150G_RE.d
 Method Pso_tune_wide.m
 Sample Name CH3CN
 Comment

Acquisition Date 8/5/2013 5:15:45 PM

Operator Amit-Rajkumar
 Instrument micrOTOF-Q II 10337

Acquisition Parameter

Source Type	ESI	Ion Polarity	Positive	Set Nebulizer	0.4 Bar
Focus	Not active	Set Capillary	4500 V	Set Dry Heater	180 °C
Scan Begin	50 m/z	Set End Plate Offset	-500 V	Set Dry Gas	4.0 l/min
Scan End	3000 m/z	Set Collision Cell RF	650.0 Vpp	Set Divert Valve	Waste

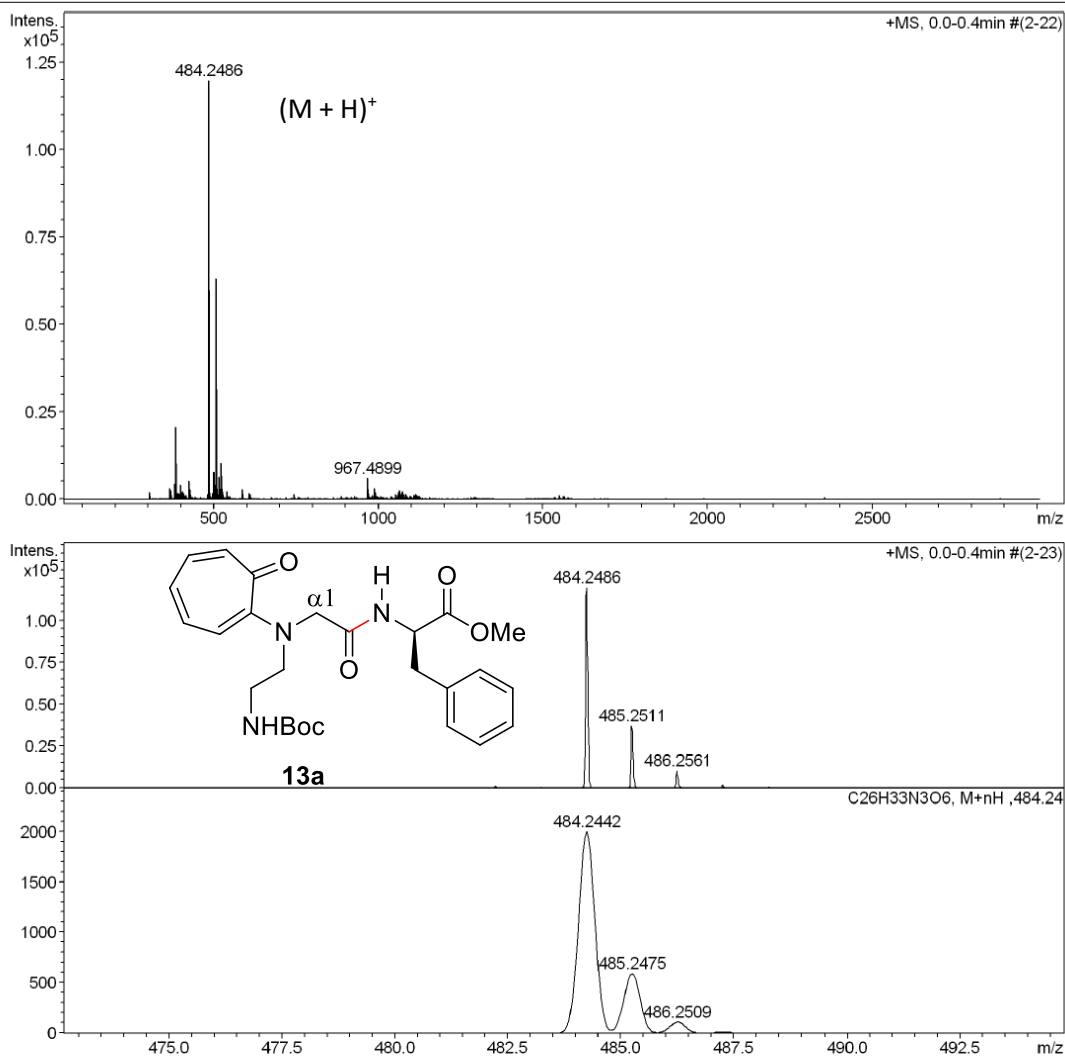


Figure A6. HRMS spectrum of dipeptide **13a**.

3. Characterization data $^1\text{H}/^{13}\text{C}$ NMR and HRMS of *BocNH-Traeg-Phe-OMe* (**13b**)

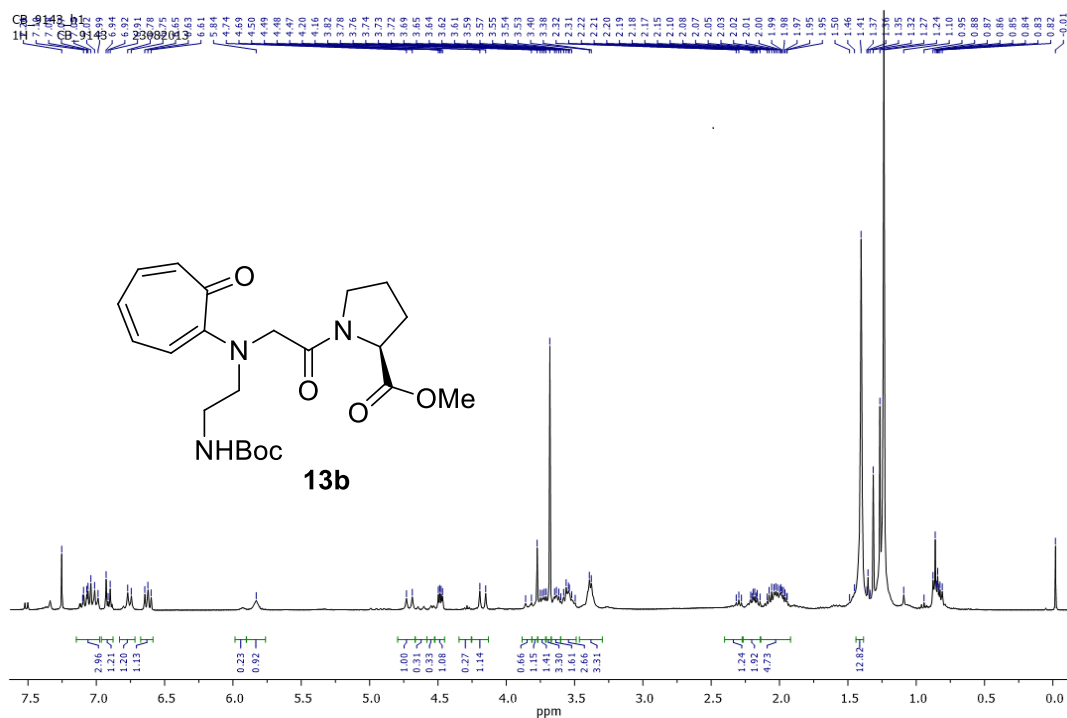


Figure A7. ^1H NMR spectrum of *BocNH-Traeg-Pro-OMe* (**13b**) in CDCl₃

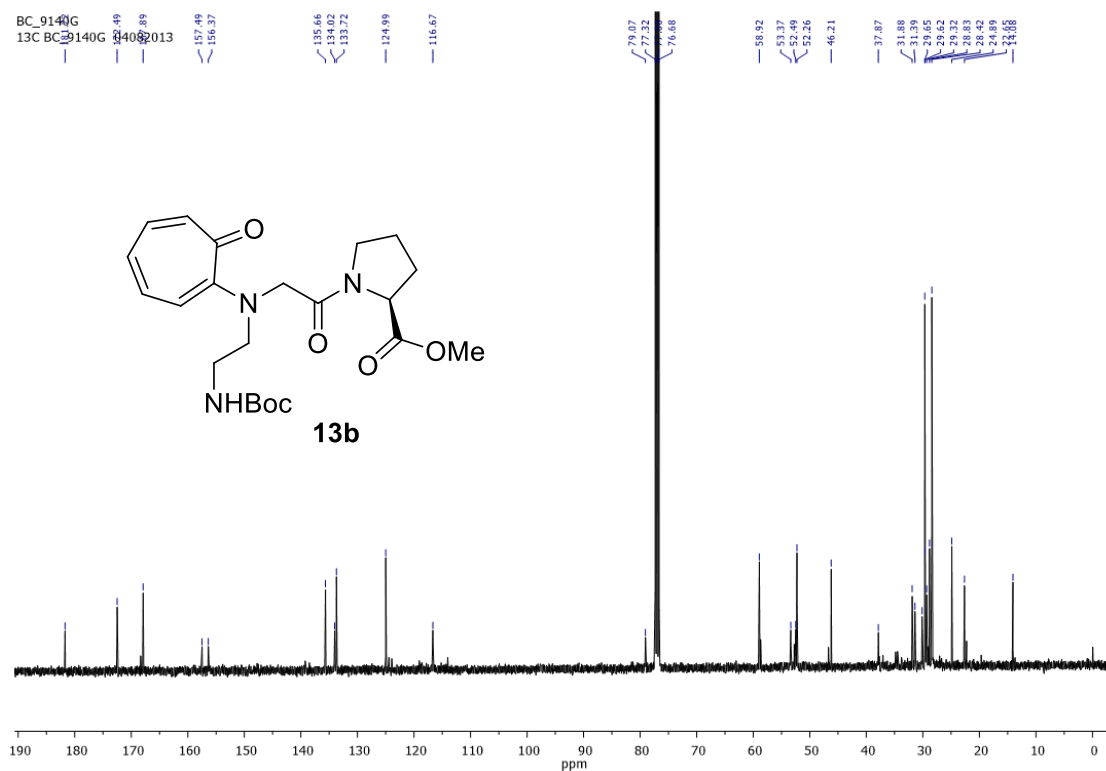


Figure A8. ^{13}C NMR spectrum of *BocNH-Traeg-Pro-OMe* (**13b**) in CDCl₃

Display Report

Analysis Info

Analysis Name D:\Data\JULY-2013\NKS\29072013_NKS-CB-aegtrproDP.d
Method Pos_tune_low.m
Sample Name CH3CN
Comment

Acquisition Date 7/29/2013 11:34:05 AM

Operator Amit-Rajkumar
Instrument micrOTOF-Q II 10337

Acquisition Parameter

Source Type	ESI	Ion Polarity	Positive	Set Nebulizer	0.4 Bar
Focus	Not active	Set Capillary	4500 V	Set Dry Heater	180 °C
Scan Begin	50 m/z	Set End Plate Offset	-500 V	Set Dry Gas	4.0 l/min
Scan End	3000 m/z	Set Collision Cell RF	130.0 Vpp	Set Divert Valve	Waste

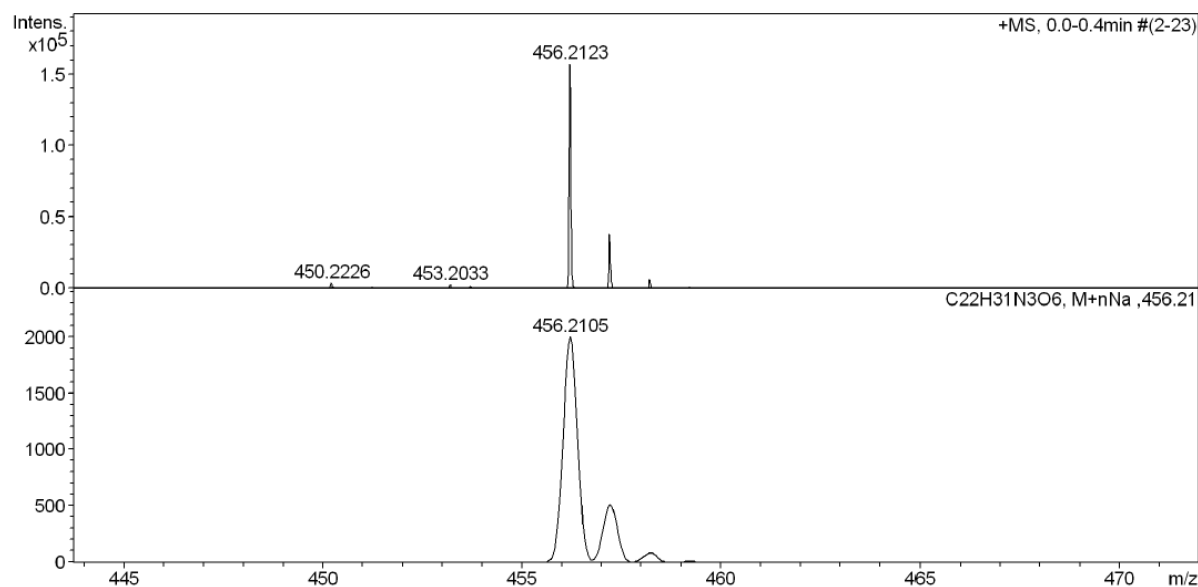
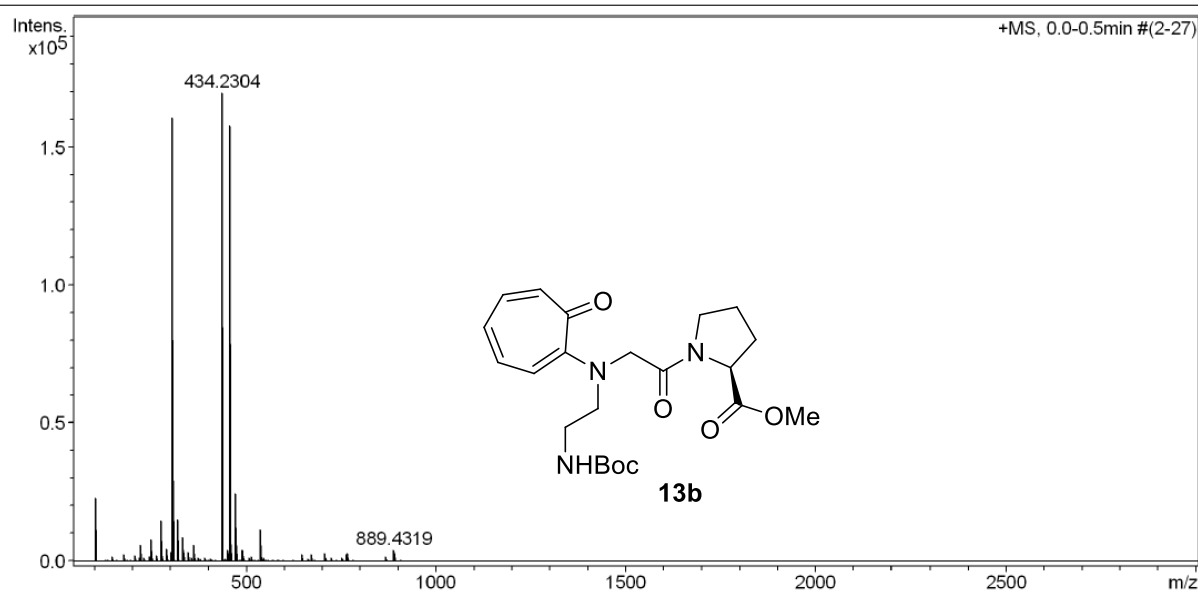


Figure A9. HRMS mass spectrum of *BocNH-Traeg-Pro-OMe* (**13b**)

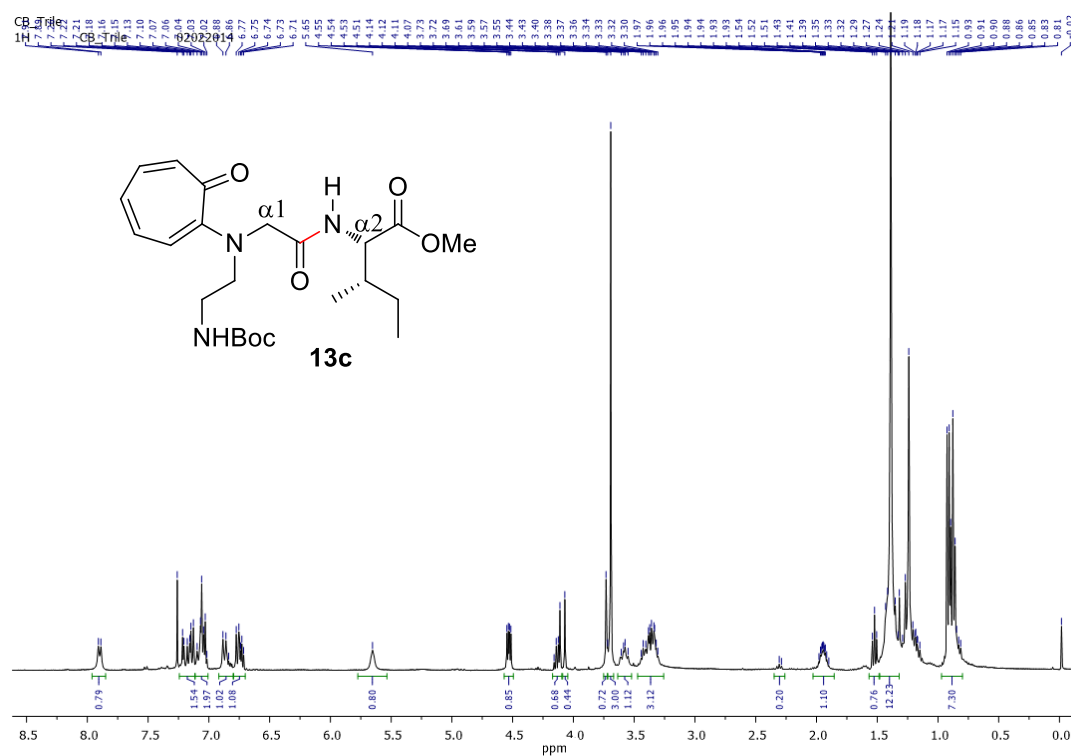
4. Characterization data $^1\text{H}/^{13}\text{C}$ -NMR and HRMS of *BocNH-Traeg-Ile-OMe* (**13c**)

Figure A10. ^1H -NMR spectrum of *BocNH-Traeg-Ile-OMe* (**13c**) in CDCl_3

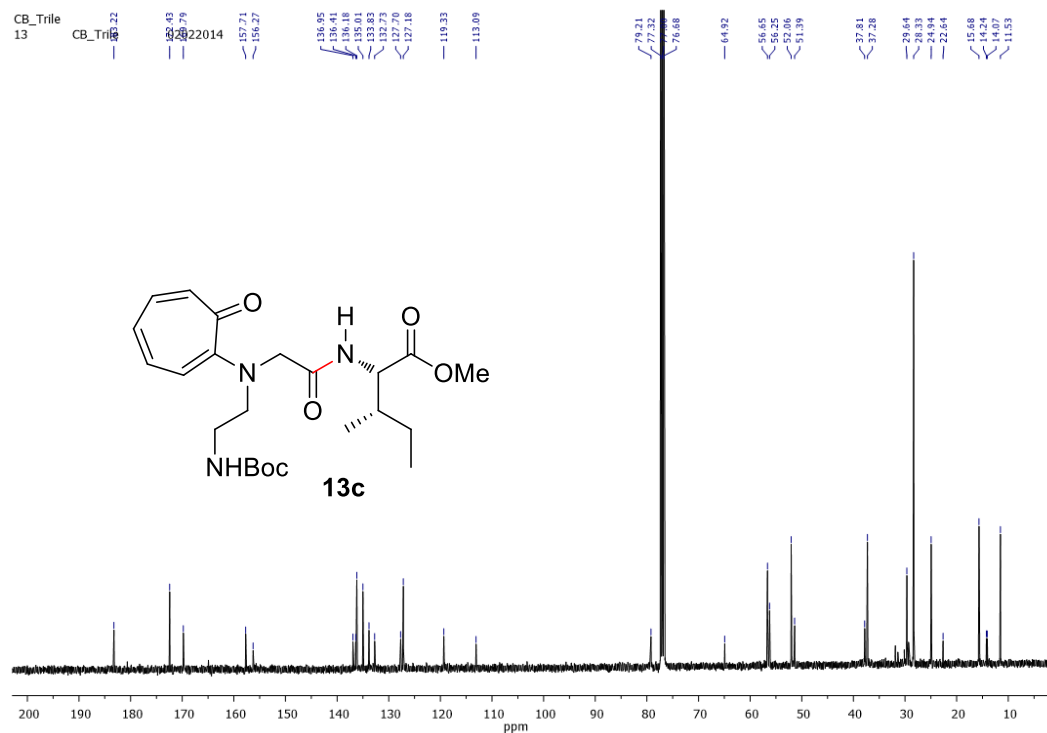


Figure A11. ^{13}C -NMR spectrum of *BocNH-Traeg-Ile-OMe* (**13c**) in CDCl_3

Display Report

Analysis Info

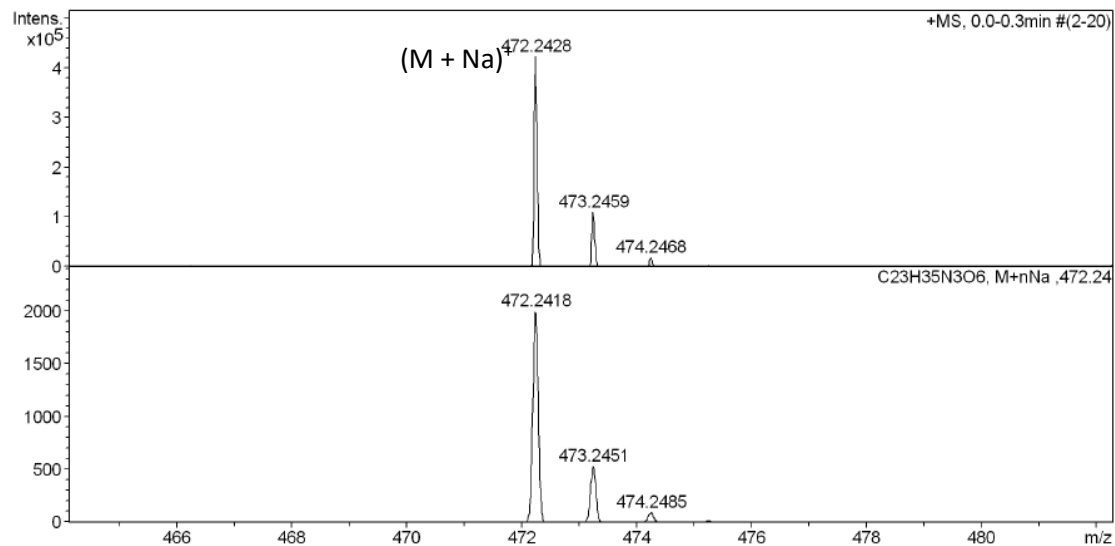
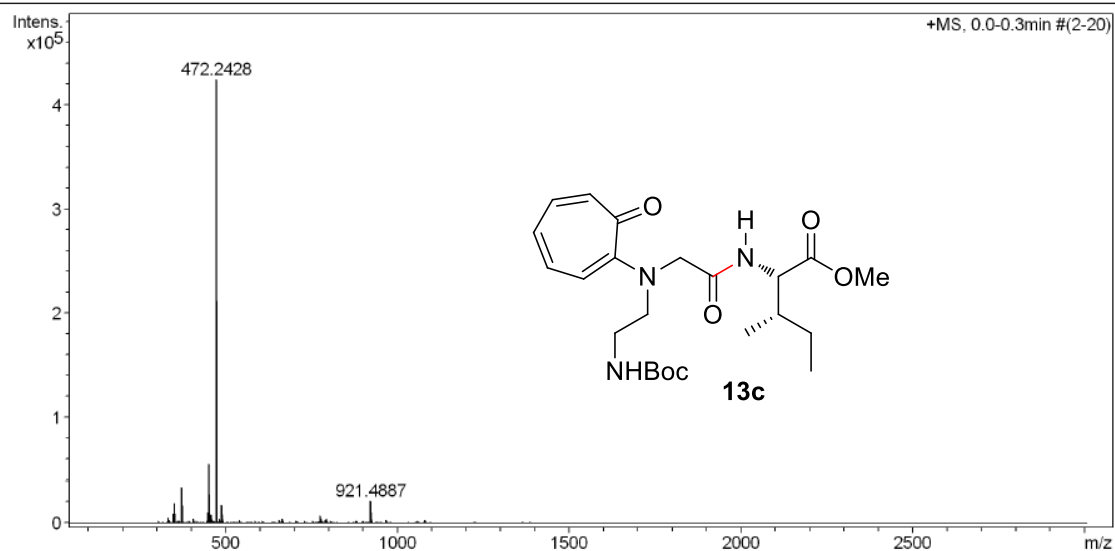
Analysis Name D:\Data\FEB-2014\NKS\03022014_NKS_CB_TRILE.d
 Method Pso_tune_wide.m
 Sample Name
 Comment

Acquisition Date 2/3/2014 11:03:21 AM

Operator A.S.Sahu
 Instrument micrOTOF-Q II 10337

Acquisition Parameter

Source Type	ESI	Ion Polarity	Positive	Set Nebulizer	0.4 Bar
Focus	Not active	Set Capillary	4500 V	Set Dry Heater	180 °C
Scan Begin	50 m/z	Set End Plate Offset	-500 V	Set Dry Gas	4.0 l/min
Scan End	3000 m/z	Set Collision Cell RF	650.0 Vpp	Set Divert Valve	Waste



Bruker Compass DataAnalysis 4.0

printed: 2/4/2014 12:31:24 PM

Page 1 of 1

Figure A12. ¹H-NMR spectrum of *BocNH-Traeg-Ile-OMe* (**13c**)

5. Characterization data $^1\text{H}/^{13}\text{C}$ NMR and HRMS of *BocNH-Traeg-Gly-Phe-OMe* (**13d**)

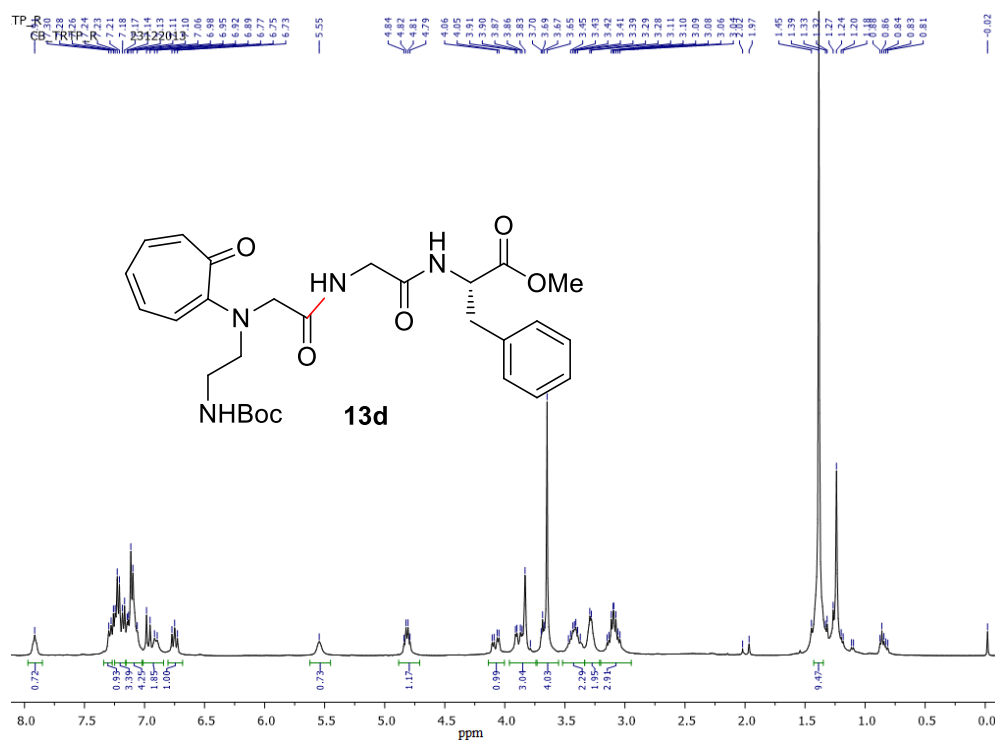


Figure A13. ^1H NMR spectrum *BocNH-Traeg-Gly-Phe-OMe* (**13d**) in CDCl_3

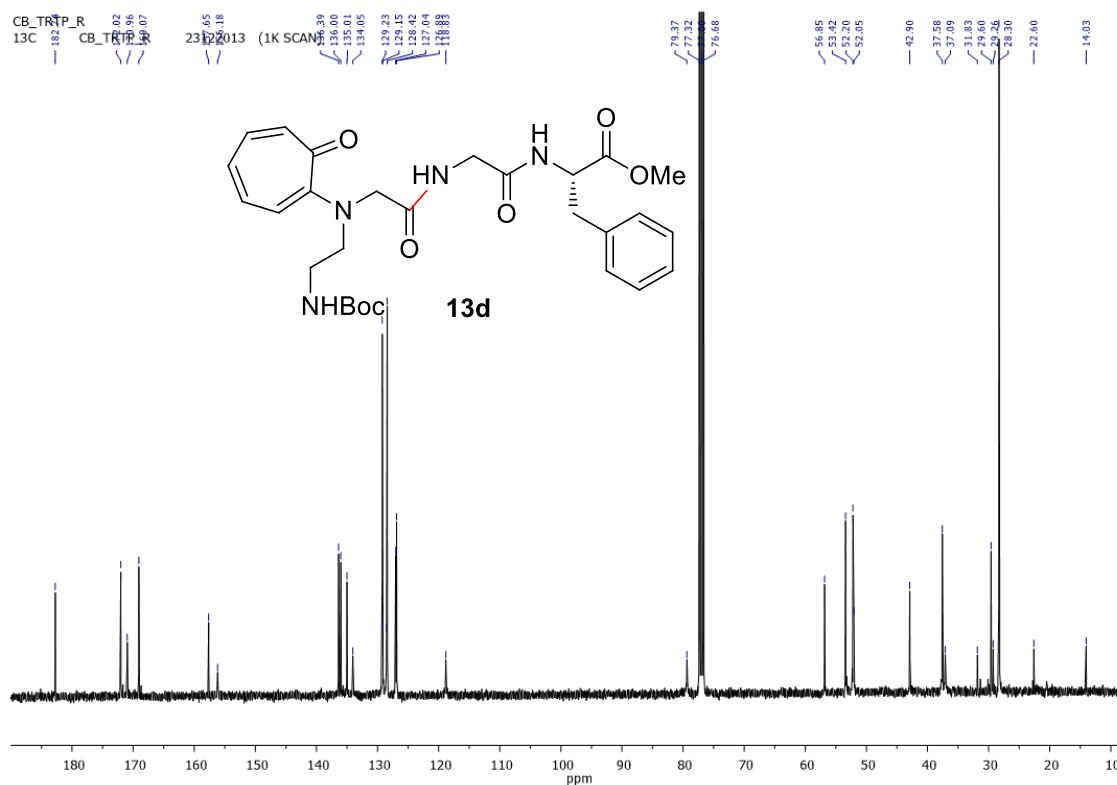


Figure A14. ^{13}C NMR spectrum *BocNH-Traeg-Gly-Phe-OMe* (**13d**) in CDCl_3

Display Report

Analysis Info

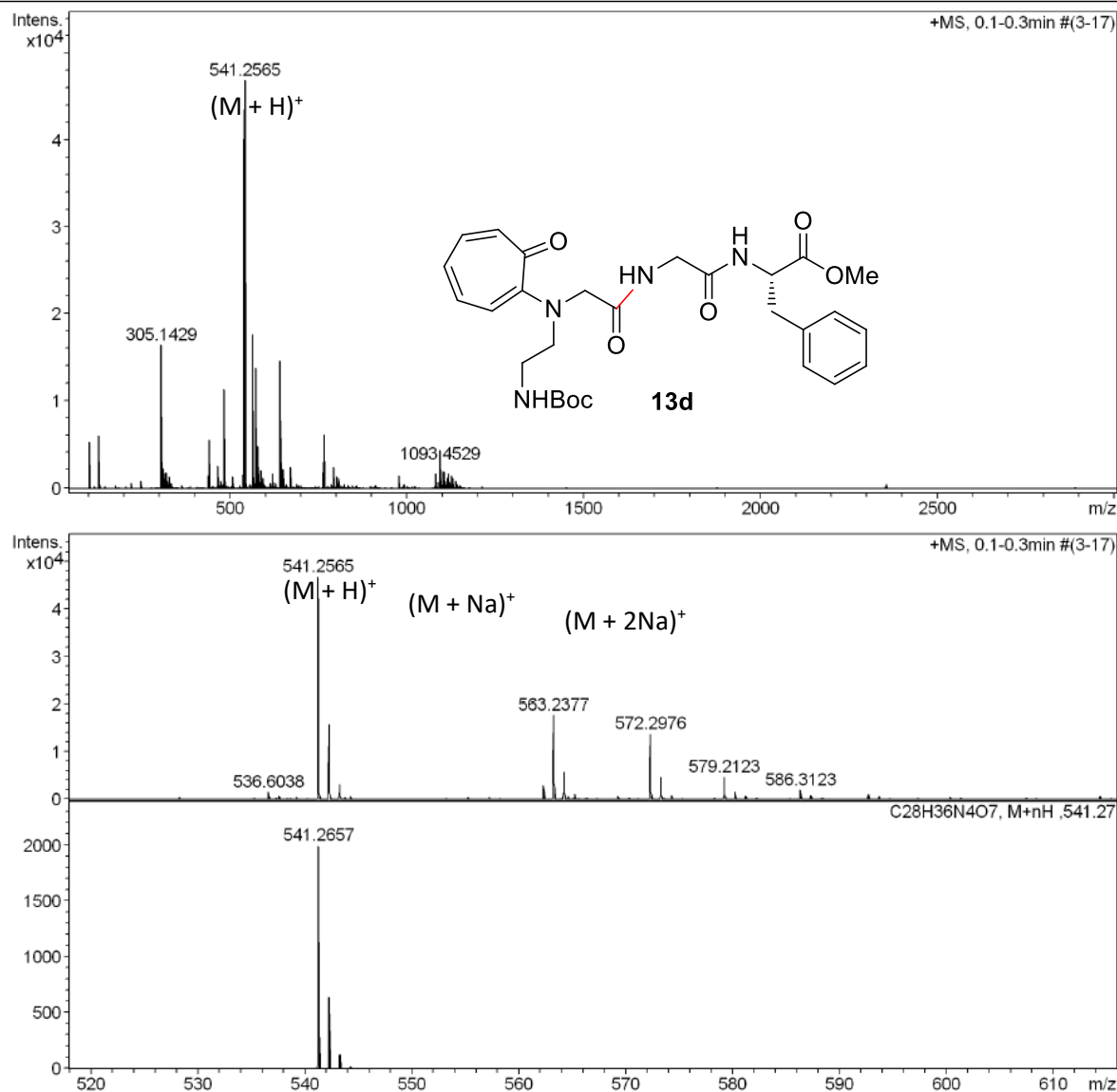
Analysis Name D:\Data\DEC-2013\NKS\26122013_NKS_CB_TRTP.d
 Method Pos_tune_low.m
 Sample Name < No Sample >
 Comment

Acquisition Date 12/26/2013 1:25:06 PM

Operator A.S.Sahu
 Instrument micrOTOF-Q II 10337

Acquisition Parameter

Source Type	ESI	Ion Polarity	Positive	Set Nebulizer	0.4 Bar
Focus	Not active	Set Capillary	4500 V	Set Dry Heater	180 °C
Scan Begin	50 m/z	Set End Plate Offset	-500 V	Set Dry Gas	4.0 l/min
Scan End	3000 m/z	Set Collision Cell RF	130.0 Vpp	Set Divert Valve	Waste



Bruker Compass DataAnalysis 4.0

printed: 1/4/2014 12:59:59 PM

Page 1 of 1

Figure A15. HRMS mass spectrum of *BocNH-Traeg-Gly-Phe-OMe* (**13d**)

6. COSY and NOESY spectra of *Traeg* monomer **5a**:

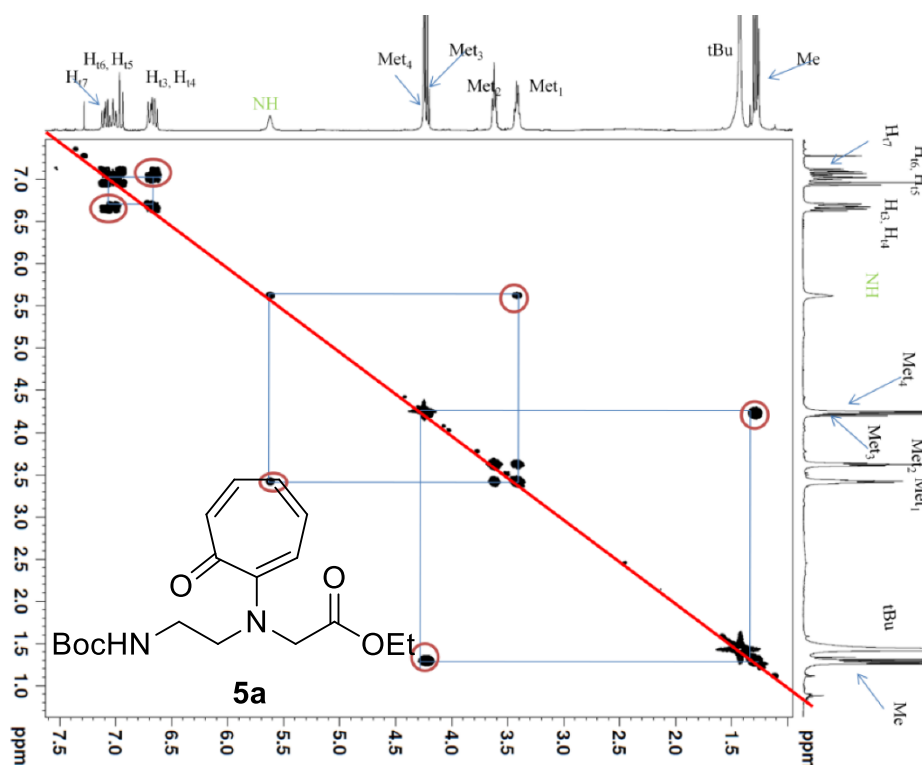


Figure A16. COSY spectrum of *Traeg* monomer **5a**.

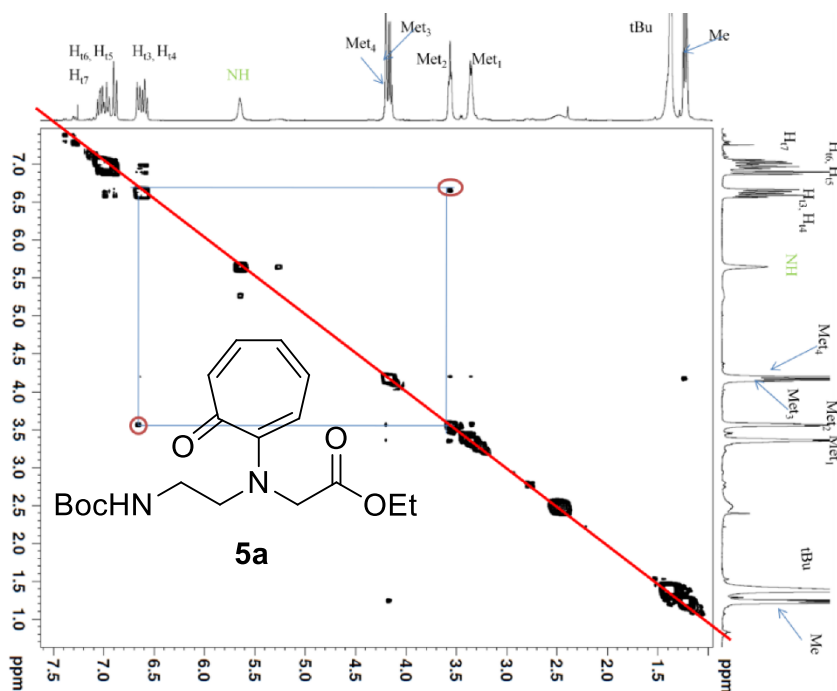


Figure A17. NOESY spectrum of *Traeg* monomer **5a**.

7. COSY, HSQC and NOESY spectra of dipeptide **13a**:

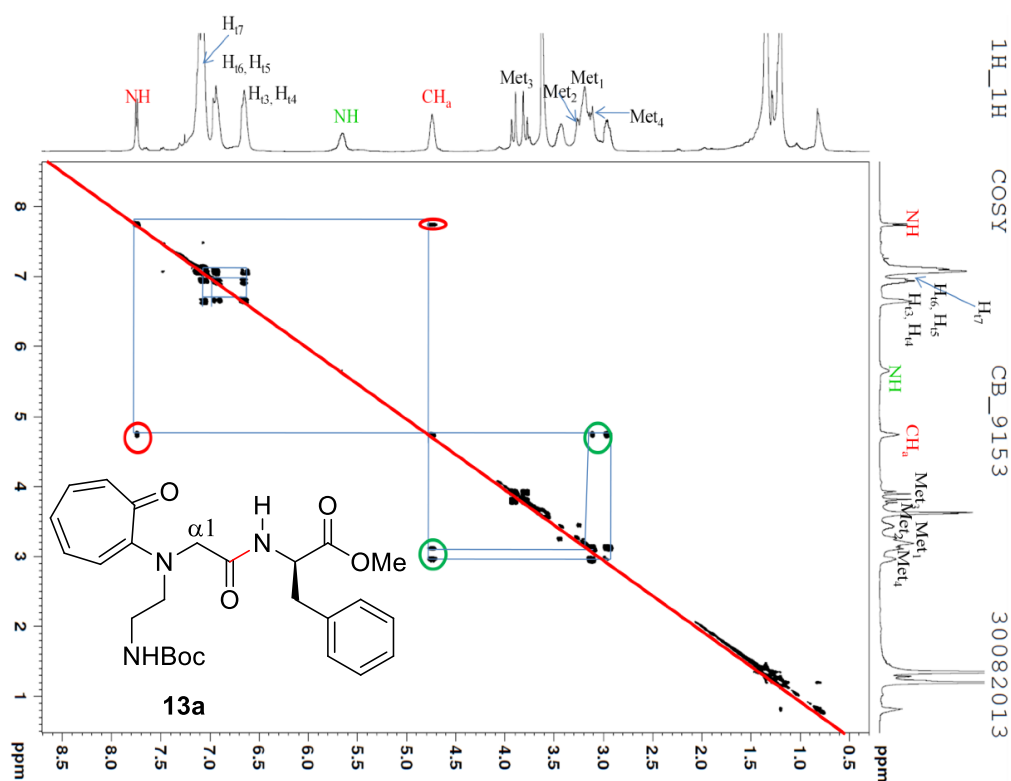


Figure A18. COSY spectrum of dipeptide **13a**.

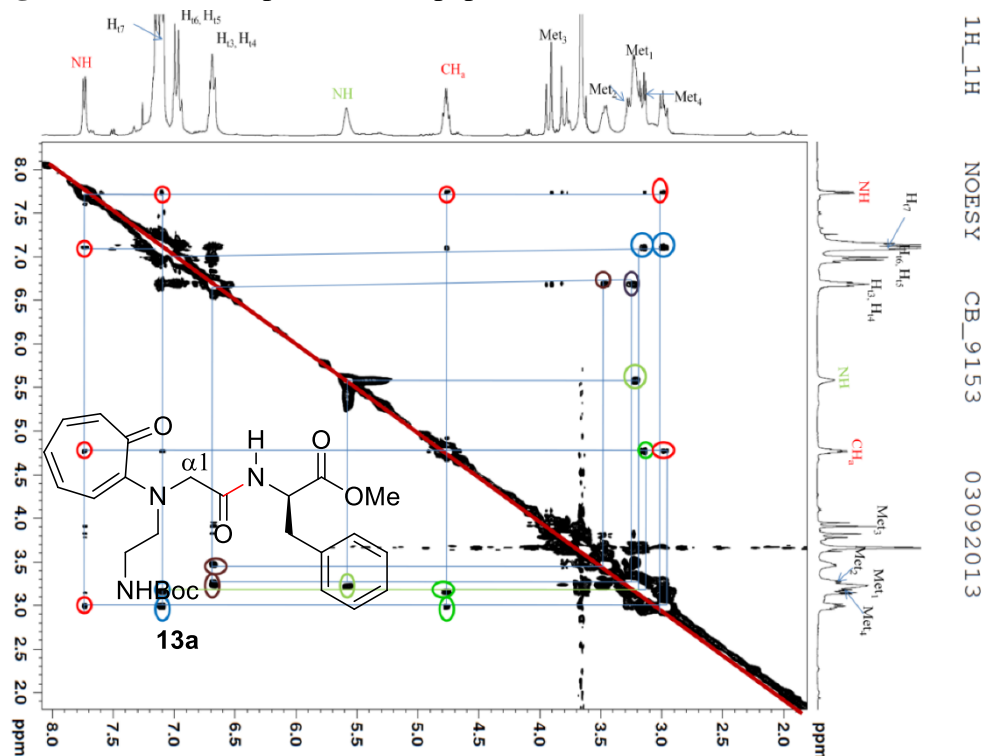


Figure A19. NOESY spectrum of dipeptide **13a**.

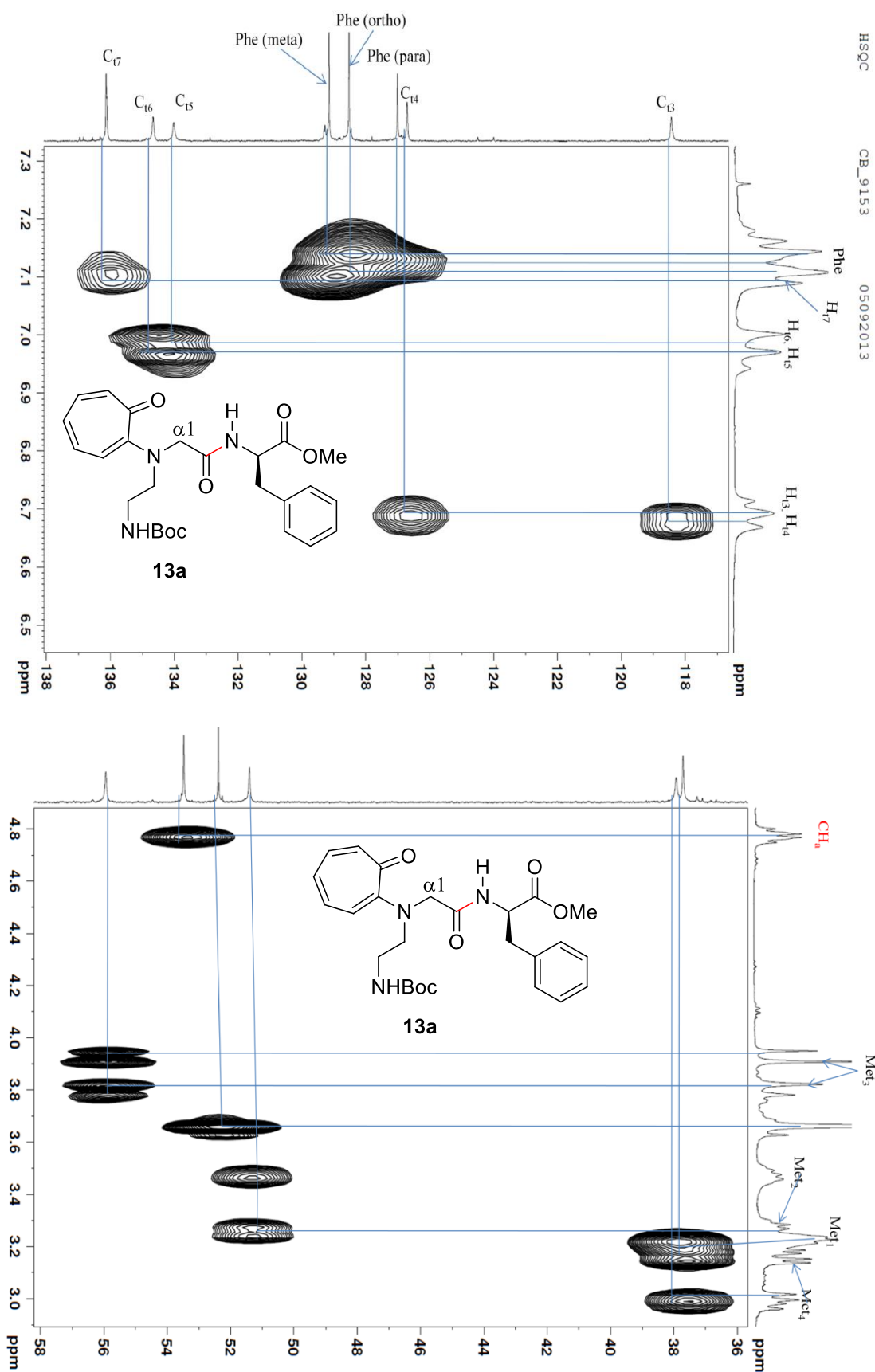


Figure A20. HSQC spectrum of dipeptide **13a**

8. COSY, HSQC and NOESY spectra of dipeptide **13b**:

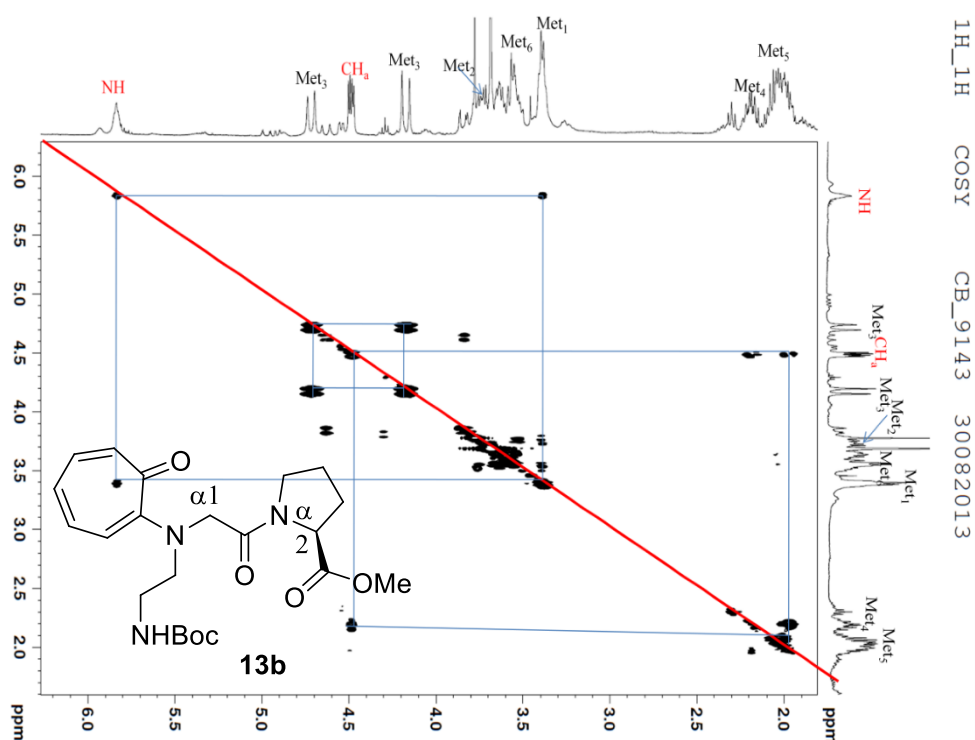


Figure A21. COSY spectrum of dipeptide **13b**.

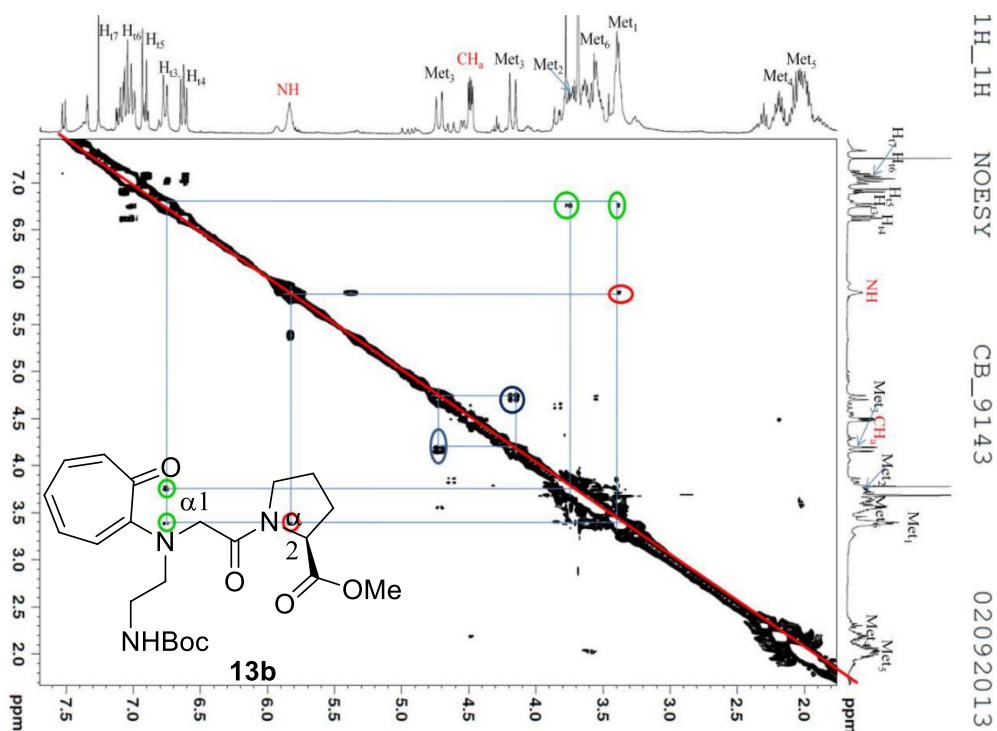


Figure A22. NOESY spectrum of dipeptide **13b**.

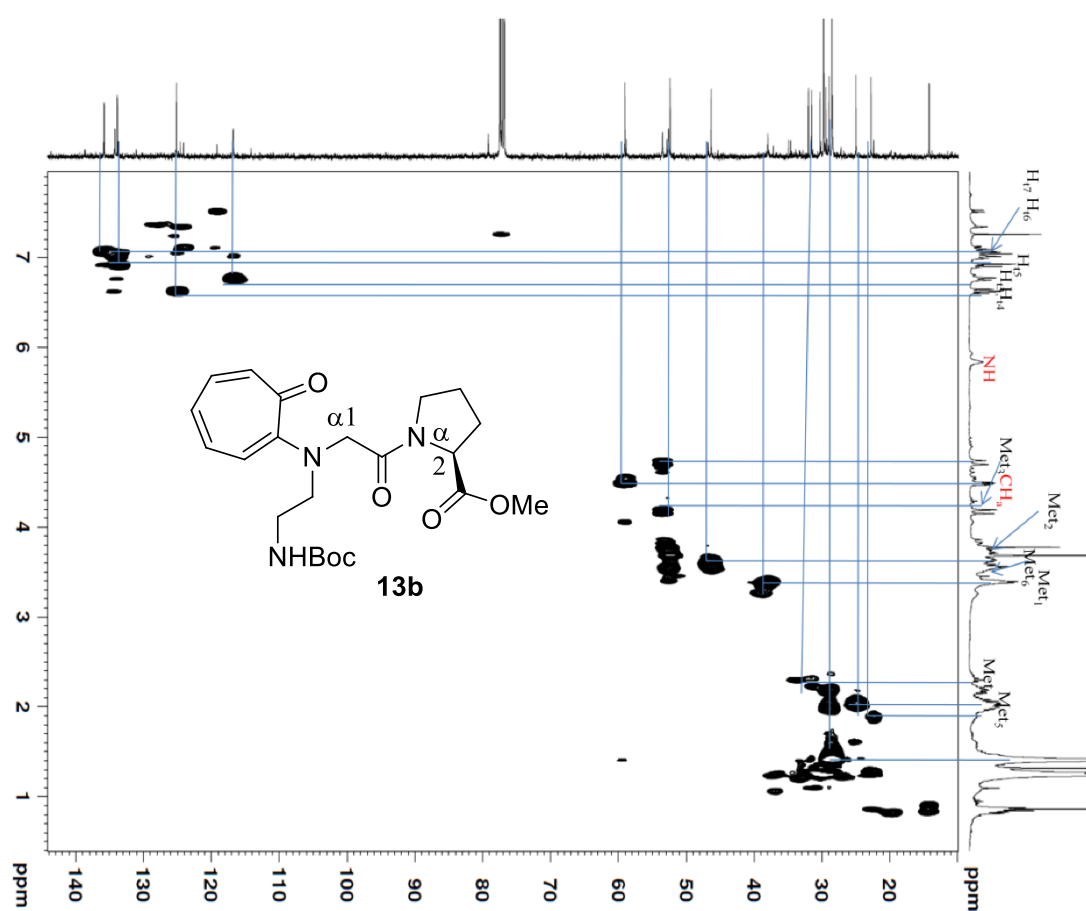


Figure A23. HSQC spectrum of dipeptide **13b**.

9. COSY, HSQC and NOESY spectra of tripeptide **13d**:

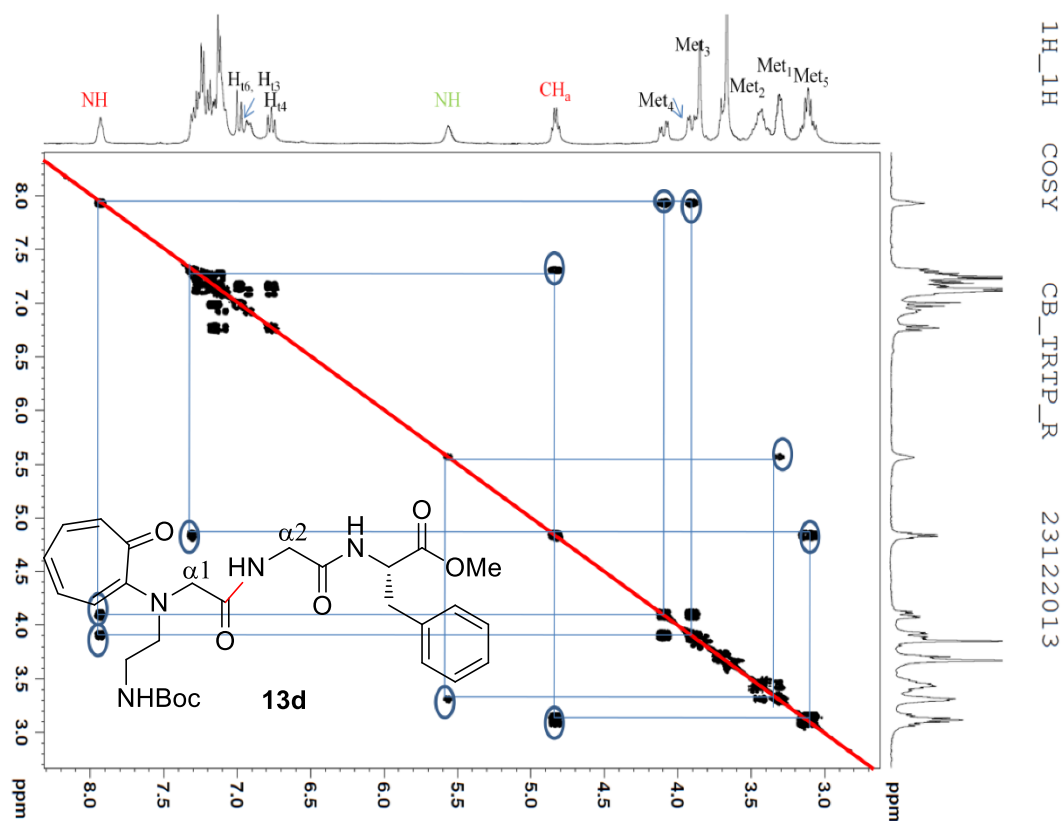


Figure A24. COSY spectrum of tripeptide **13d**.

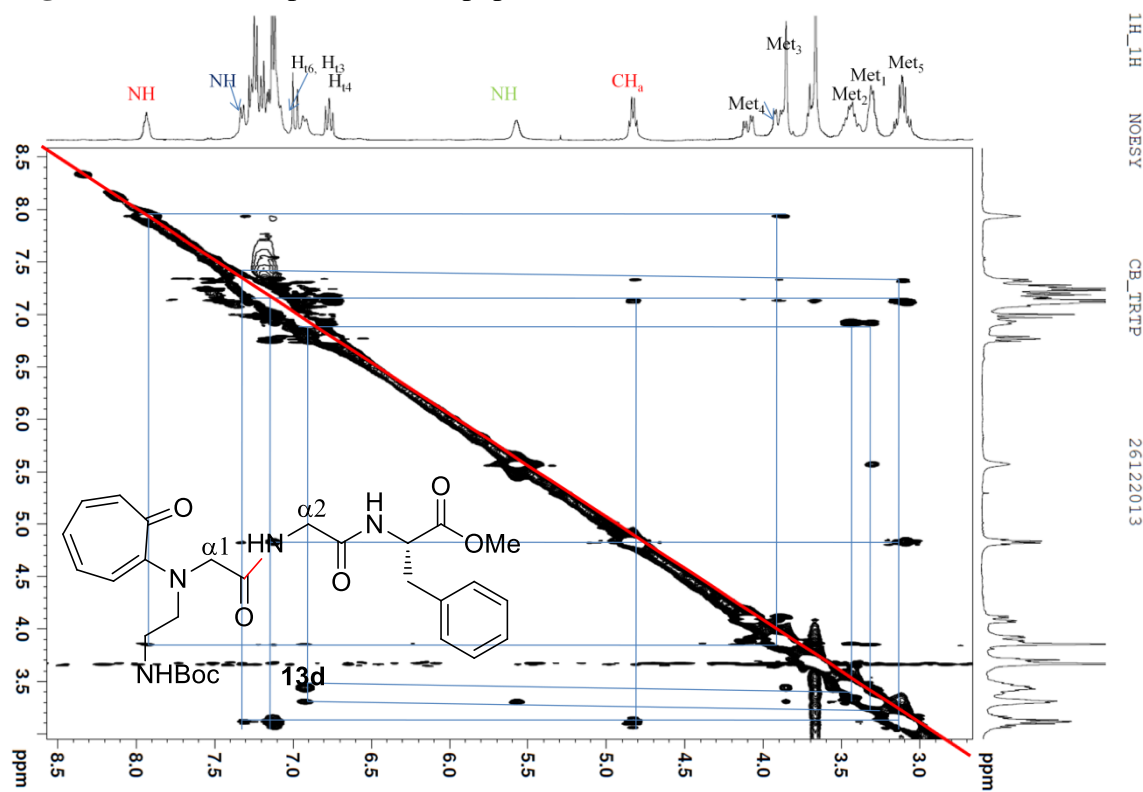


Figure A25. NOESY spectrum of tripeptide **13d**.

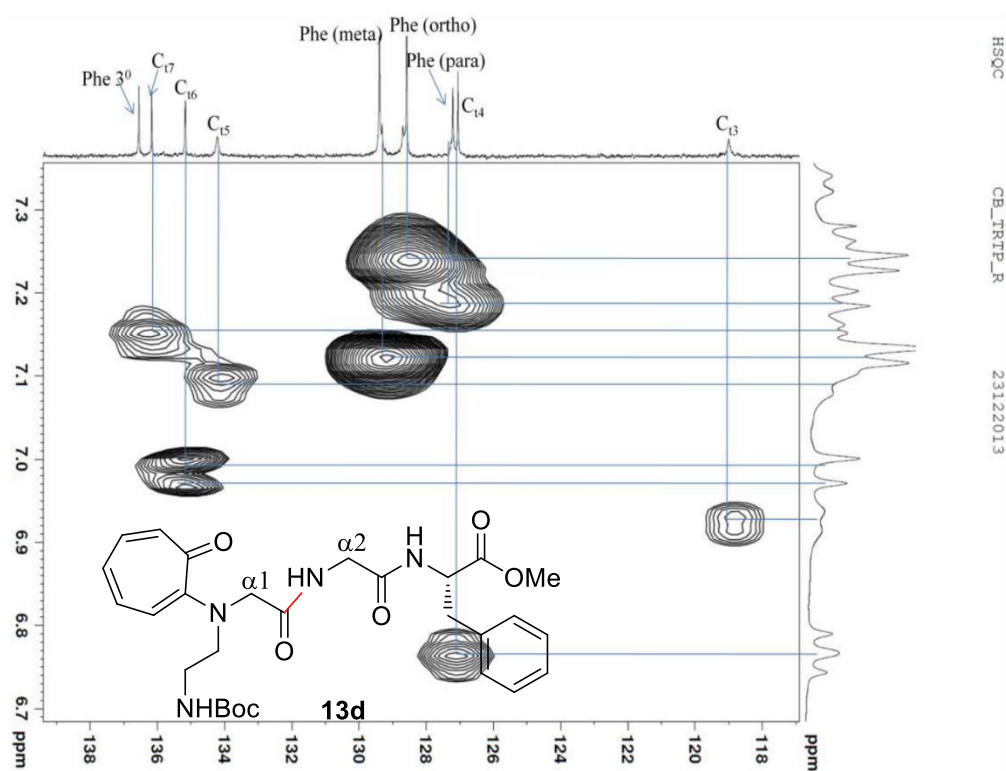
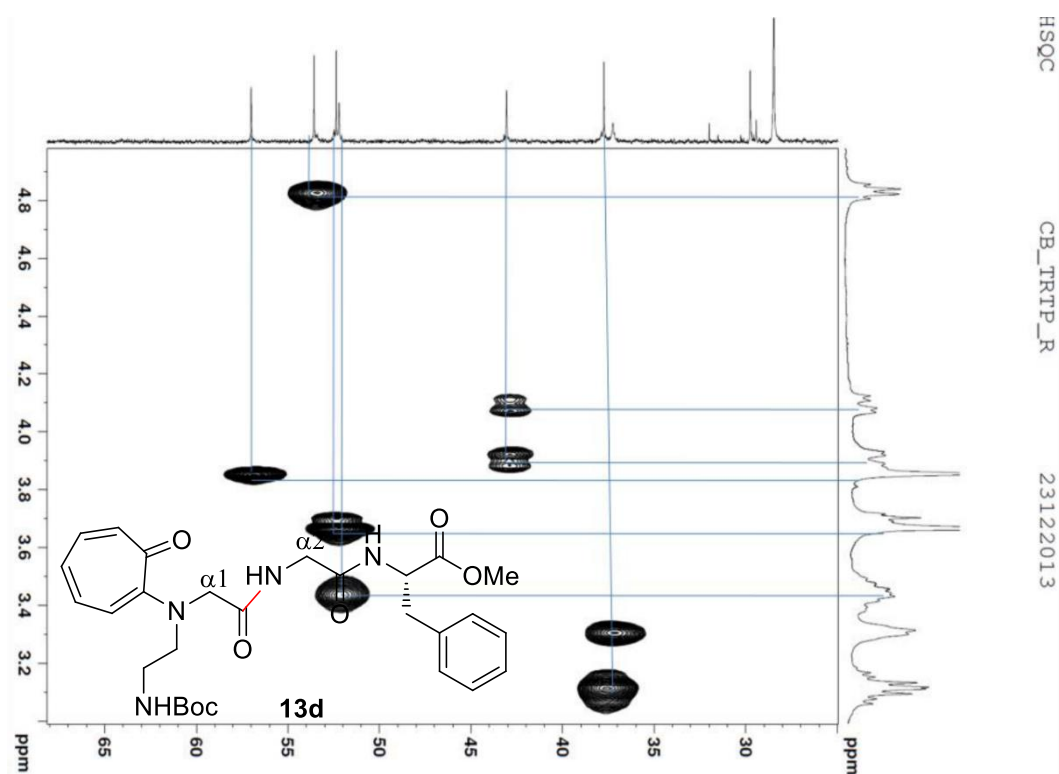


Figure A26. HSQC spectrum of tripeptide **13d**.

10. Stacked ^1H NMR of dipeptide **13a**:

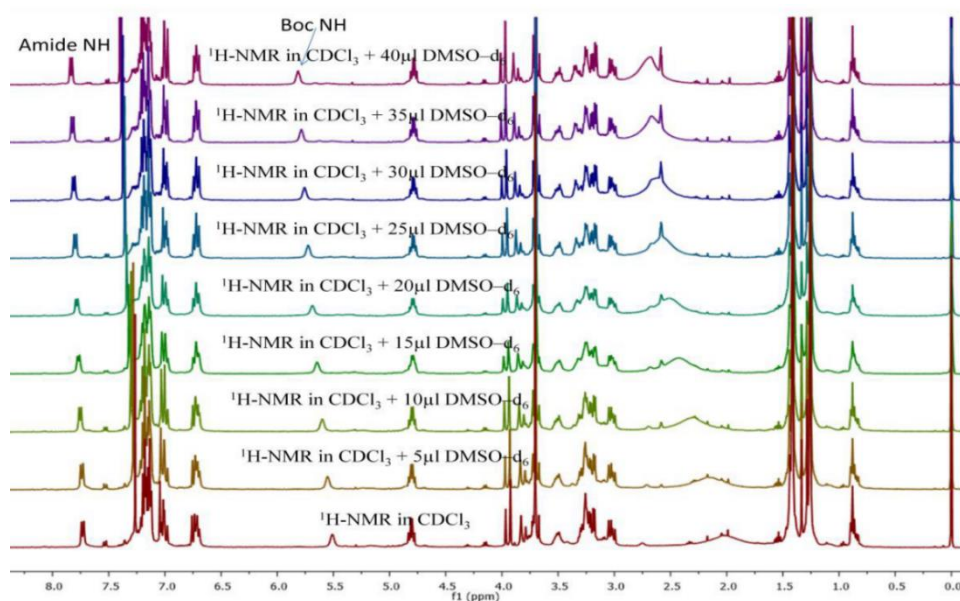


Figure A27. Stacked ^1H NMR spectra of dipeptide **13a** generated with the sequential addition of 5 μL $\text{DMSO}-d_6$.

11. Stacked ^1H NMR of *Traeg* monomer **5a**:

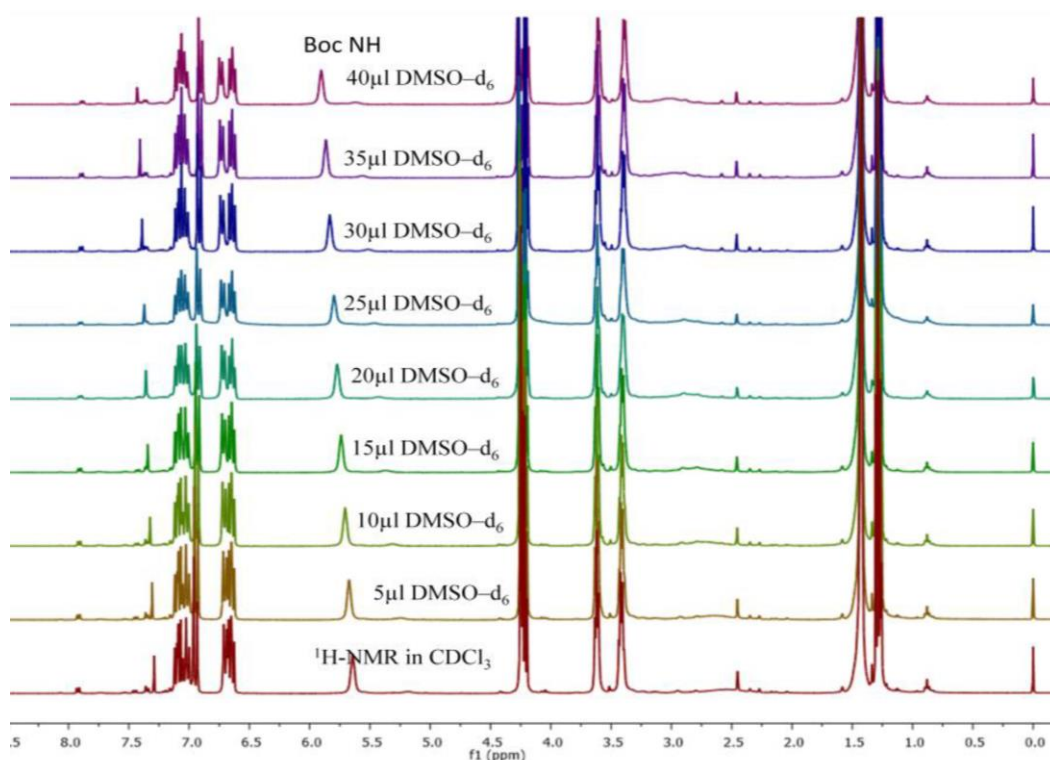


Figure A28. Stacked ^1H NMR spectra of dipeptide **5a** generated with the sequential addition of 5 μL $\text{DMSO}-d_6$.

12. Stacked ^1H NMR of dipeptide **13b**:

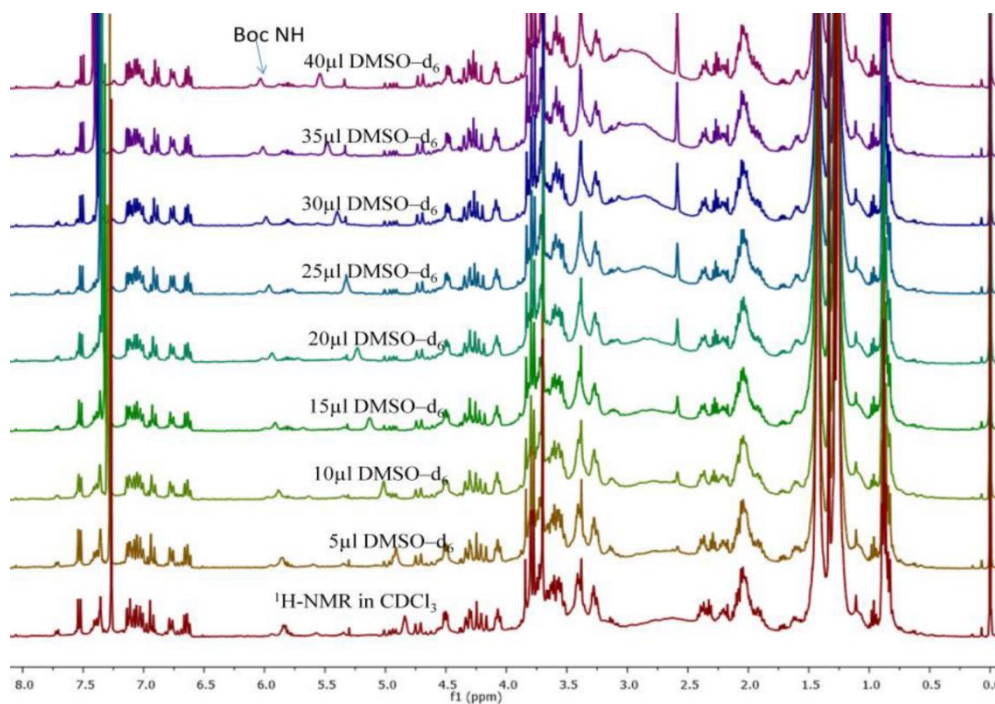


Figure A29. Stacked ^1H NMR spectra of dipeptide **13b** generated with the sequential addition of 5 μL DMSO- d_6 .

13. Stacked ^1H NMR of tripeptide **13d**:

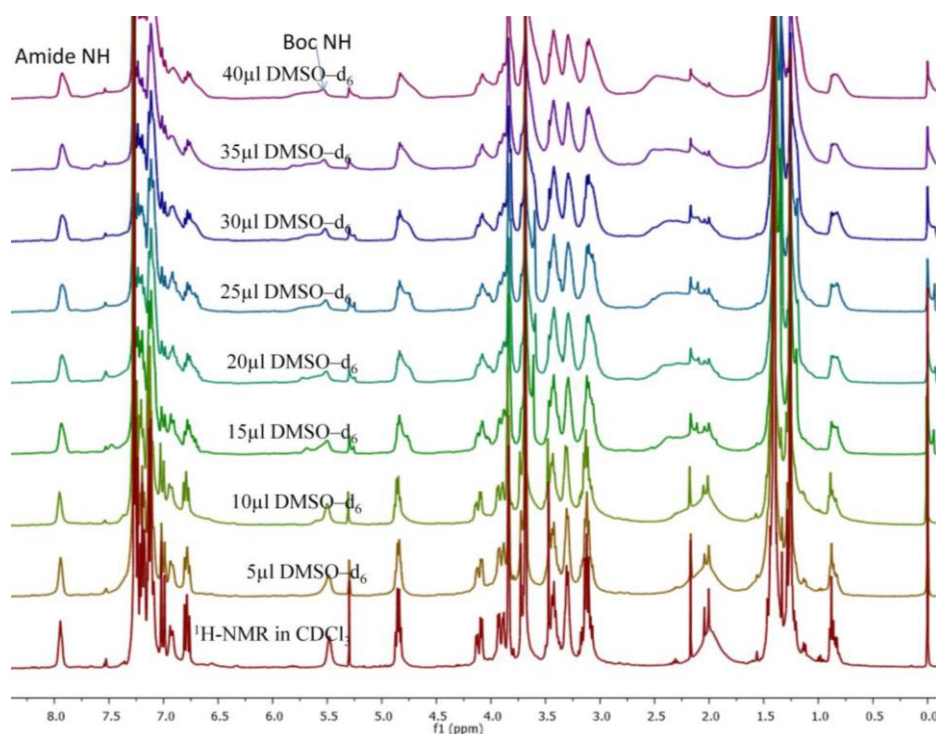


Figure A30. Stacked ^1H NMR spectra of dipeptide **13d** generated with the sequential addition of 5 μL DMSO- d_6 .

14. Stacked ^1H NMR of dipeptide **13c**:

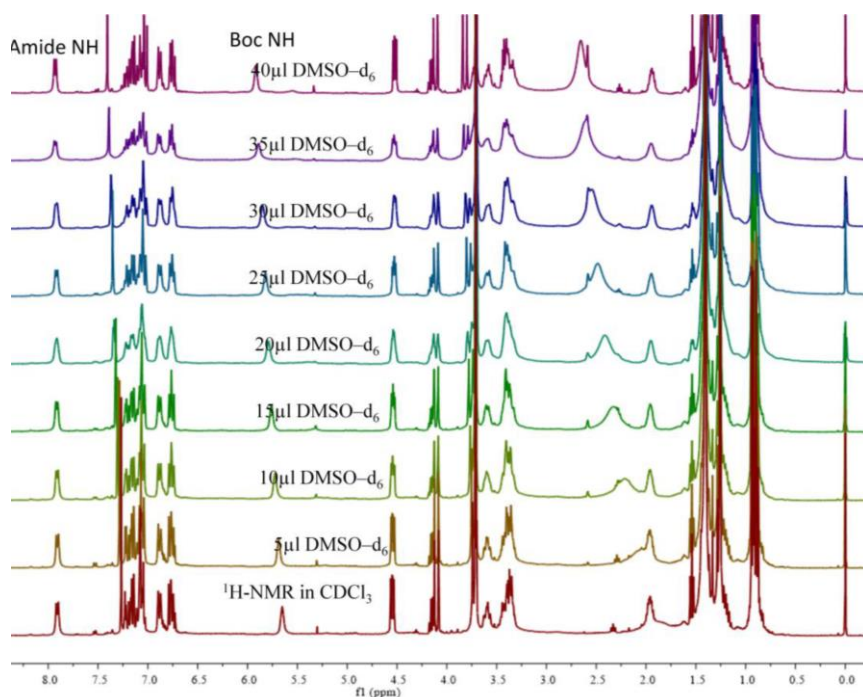


Figure A31. Stacked ^1H NMR spectra of dipeptide **13c** generated with the sequential addition of 5 μL $\text{DMSO}-d_6$.

15. Stacked ^1H NMR of dipeptide **11**:

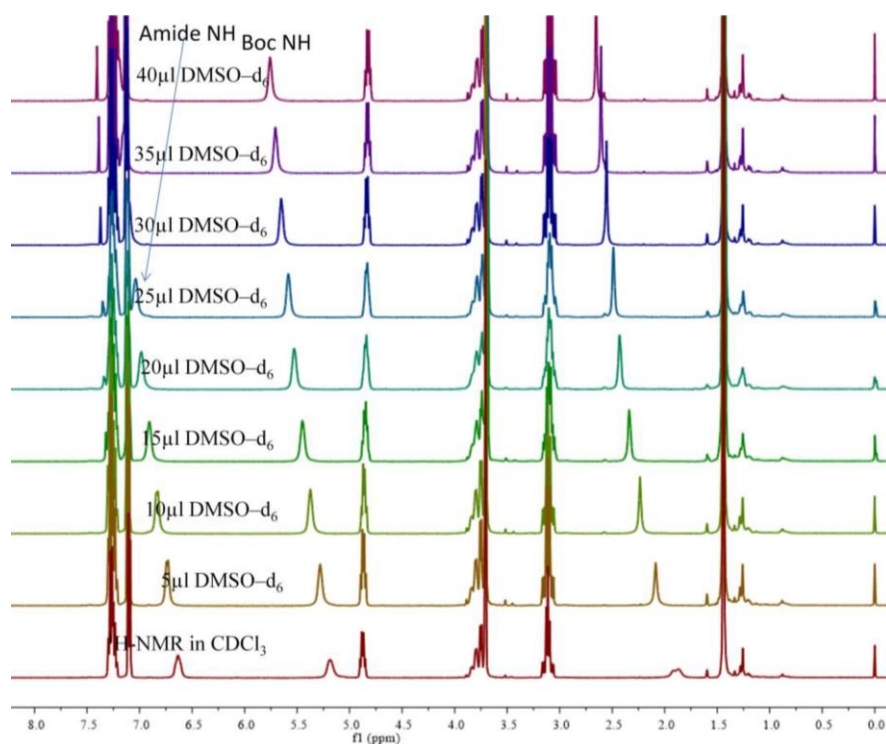


Figure A32. Stacked ^1H NMR spectra of dipeptide **13c** generated with the sequential addition of 5 μL $\text{DMSO}-d_6$.

16. Stacked ^1H NMR of tripeptide **13d**:

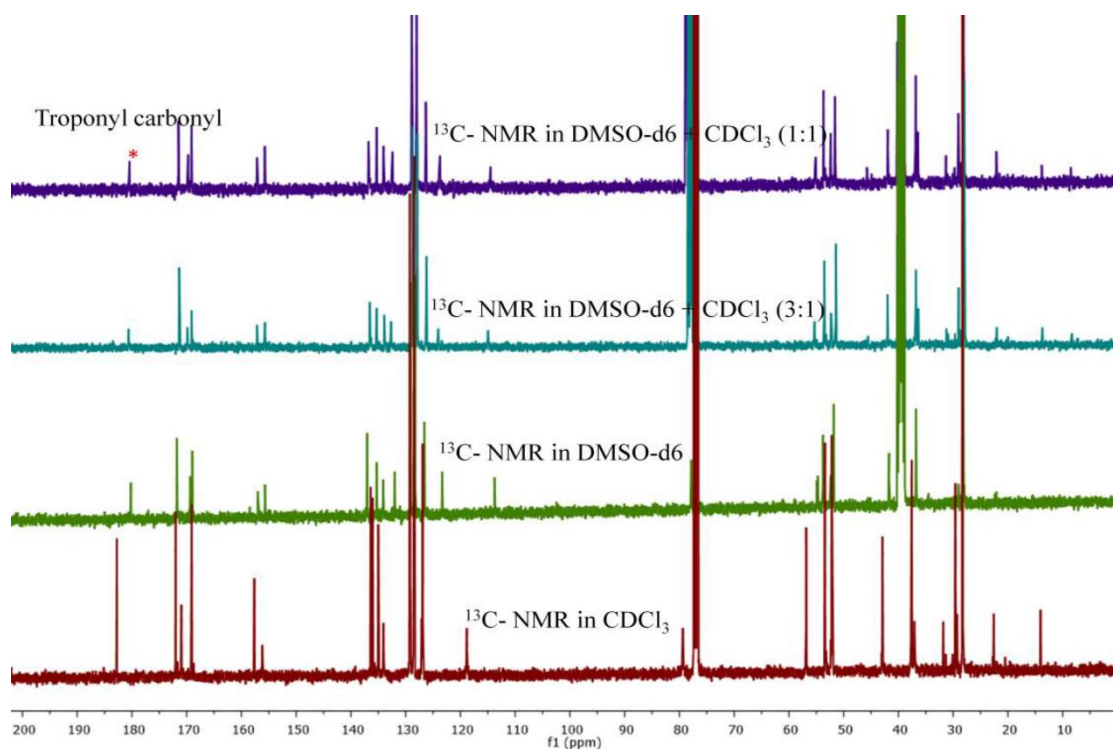


Figure A33. ^{13}C NMR DMSO titration experiments of tripeptide **13d**

17. DFT calculated electron density map of dipeptide **13c**

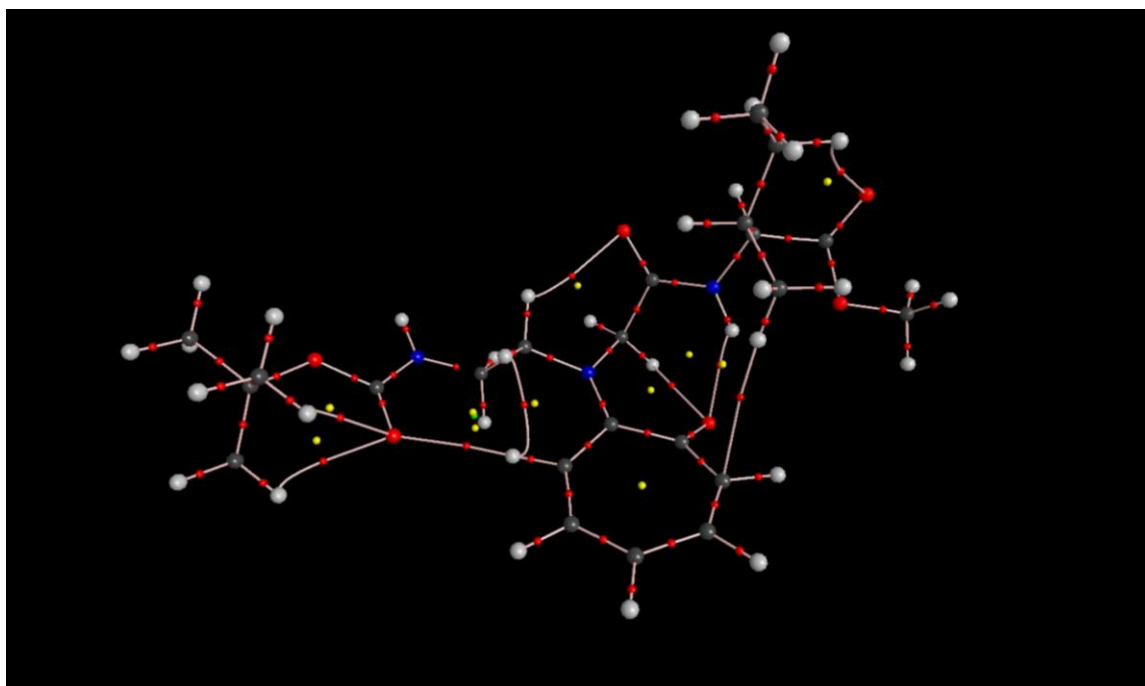


Figure A34. DFT calculated electron density map of dipeptide **13c**.

18. Theoretical Ramachandran map

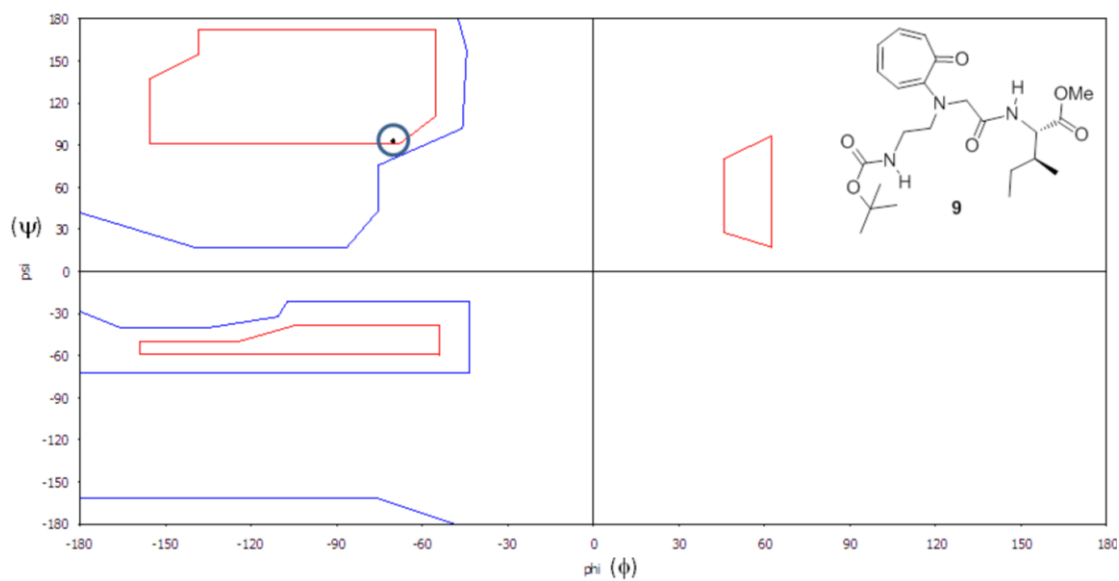


Figure A35. Theoretical Ramachandran plot of dipeptide **13c**.

19. Crystal packing diagram of monomer **5a**

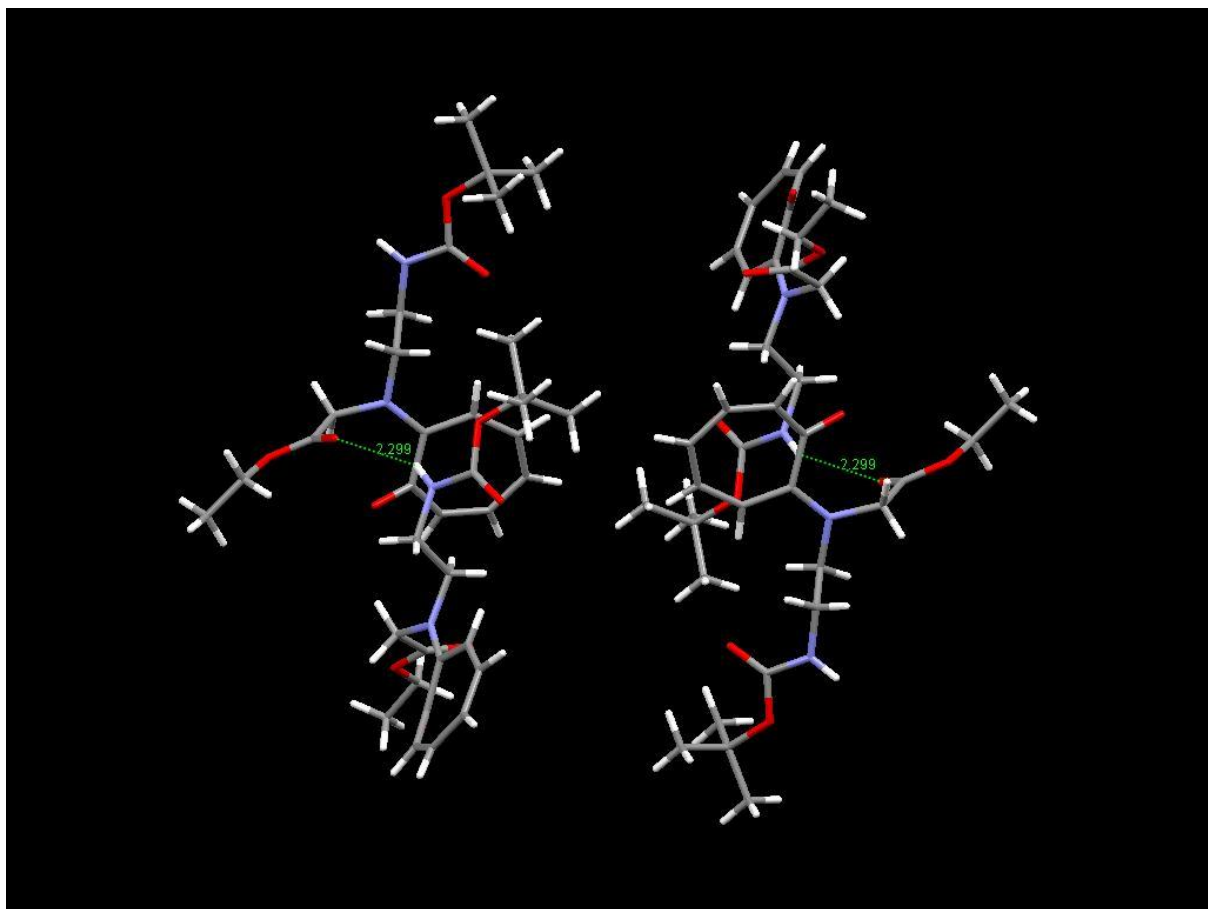


Figure A36. Molecular packing diagram of *Traeg* monomer **5a**.

CHAPTER THREE

Instability of Amide Bond Comprising the 2-Aminotropone Moiety: Cleavable under Mild Acidic Condition

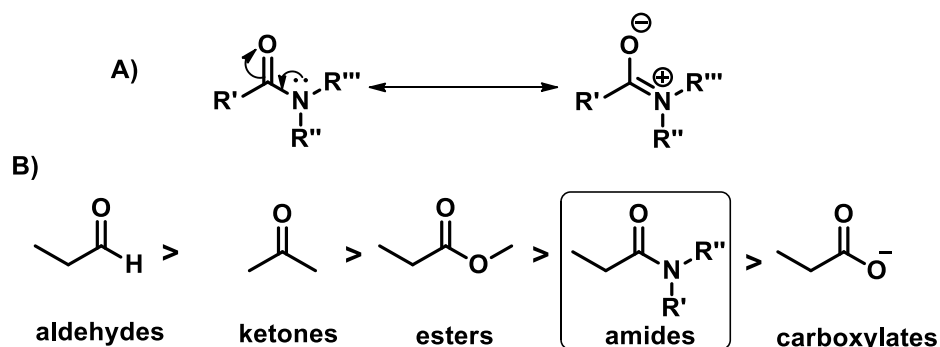
Chapter 3. Instability of Amide Bond Comprising the 2-Aminotropone Moiety: Cleavable under Mild Acidic Condition

3.1 Introduction

3.1.1 Structure and Reactivity of amide bond

The amide bond is a ubiquitous functionality present in many natural products, proteins/peptides and drugs, importantly, the building blocks of proteins/peptides (amino acid residues) are connected by amide bonds.¹⁻³ Most of the amide bonds has been known to be stable at neutral pH and room temperature for many years.²⁻⁸ However, enzymes (peptidases) hydrolyses the amide bond specifically under physiological conditions.¹

Since the amide functional group is one of the widely present functionalities in biomacro molecules, the structural and chemical properties are very well-understood.⁷ In general, the amide bond is carboxylic acid derivative, which can be obtained through coupling reaction between carboxylic acid and free amine under standard coupling conditions.²⁻⁹



Decreasing reactivity order of carbonyl carbon towards nucleophilic substitution

Figure 3.1 A) Representation of resonance stabilization in acyclic amide bond; B) Decreasing order of reactivity of carbonyl carbon in aldehydes, ketones, esters, amide and carboxylates.

Another carboxylic acid derivative is alkyl carboxylates (esters), these can be obtained by reacting carboxylic acid with alcohol.⁷ The difference between the amide and ester is the connected atom to the carbonyl carbon. Amides and esters have shown distinctive structural

and chemical properties. The decreasing reactivity order of few carbonyl compounds are provided in the **Figure 3.1**. Among all, amide is least reactive (high stability) when compare to aldehydes, ketones, and esters towards nucleophilic substitution.⁷

The high stability of amide bonds arises due to delocalization of nitrogen lone pair electrons towards amide carbonyl. Structurally, acyclic amide bond (-NHCO-) is planar in nature, which is favourable for delocalization of nonbonding electrons of nitrogen towards the π -orbital of carbonyl and as a result, the partial double bond character as $^+N=C-O^-$ arises in the amide bond (**Figure 3.1A**). This partial double bond nature decreases the electrophilicity of the amide carbonyl group.^{2,7} Hence, acyclic amide bonds are highly stable under those conditions where esters can be easily hydrolysed. This stability of amide bond is one of the great advantage in peptide syntheses, where ester can be easily and selectively hydrolysed in presence of amide.³

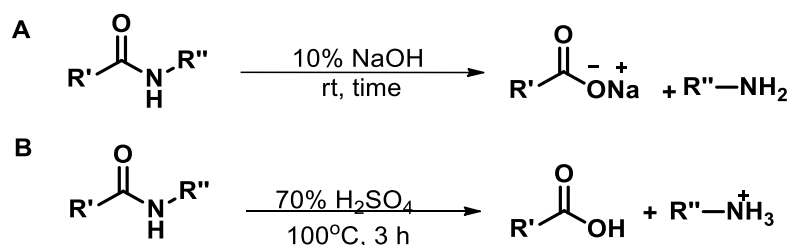


Figure 3.2 Conventional hydrolysis of acyclic amide bond under basic and acidic conditions, respectively.

In the laboratory, hydrolysis of the amide bond requires drastic conditions such as elevated temperatures and extreme pH (**Figure 3.2**).⁷ At high pH, the direct nucleophilic addition at amide carbonyl followed by elimination of amine occurs. While at low pH, protonation of amide carbonyl is followed by nucleophilic addition with pronounced elimination of amine. In both cases, the reaction proceeds through the formation of tetrahedral intermediate at the C-atom of amide carbonyl.⁷

3.1.2 Exceptions

However, in literature, there are some exceptional amides which undergoes solvolysis easily. The instability of these amides depends on the steric and electronic properties of the constituent atoms of amide bond and α -carbon.^{2,9}

Strained cyclic lactams: Strained cyclic lactams are relatively more reactive towards solvolysis.¹ The more reactivity of these amides is due to non-existence of resonance stabilization (**Figure 3.3A**). The reason behind this is that the constituent atoms of the amide bond in strained cyclic lactams are non-planar due to steric effects.^{2,7,9} The non-planarity of the constituent atoms of the amide bond, prevents the delocalisation of electrons.

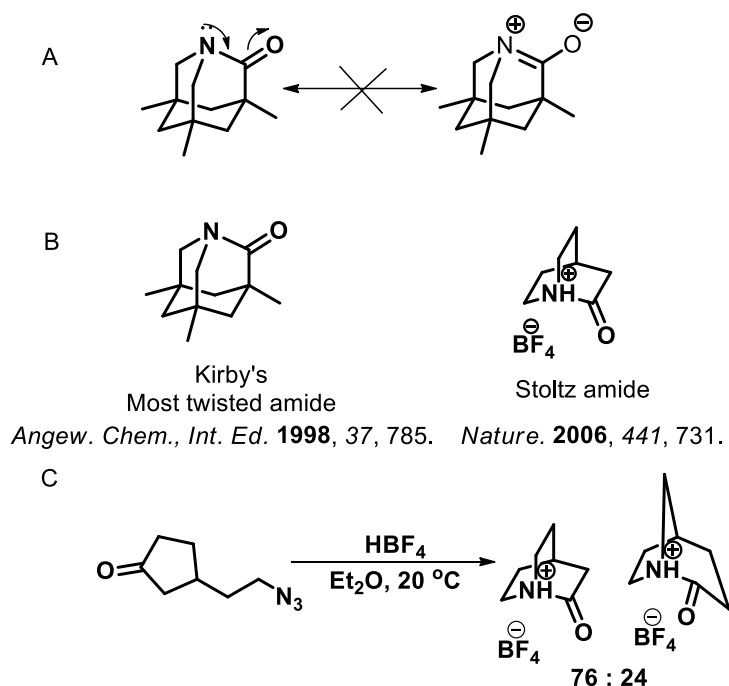


Figure 3.3 A) Non-planarity of the amide bond prevents the delocalisation of electrons. B) Iconic examples of strained cyclic lactams; C) Synthesis of 2-quinuclidone via non-classical pathway.

As a result, the amide bond does not exist as a partial double bond. Hence, amide carbonyl reactivity increases dramatically. Steric and electronic effects influence the hydrolysis/solvolysis of bridged bicyclic lactams.^{2,10}

In the literature, several strained cyclic lactams are reported which undergoes solvolysis abnormally. Some of the iconic examples of the strained cyclic lactams are discussed here.¹¹⁻¹³ In the late 1990s, Anthony J. Kirby and co-workers reported the hydrolysis of the amide bond of *1-aza-2-adamantanone* in presence of water within a minute, where the amide *N*-atom is at the bridgehead of the bicycle which prevents the amide resonance and diminishes the stability of the amide bond (**Figure 3.3B**).¹³

Another interesting example is the synthesis and characterization of 2-quinuclidone, which is a bridged bicyclic lactam. In the literature it has been mentioned that several attempts were made for the synthesis of 2-quinuclidone since 1938 via classical amide synthesis, but all of these trails were unable to provide sufficient characterization data.¹¹ Finally, Stoltz and his co-workers reported the synthesis and characterization of *2-quinuclidone* in 2006 via non classical amide synthesis as a salt of tetrafluoroborate (**Figure 3.3C**).¹¹ These difficulties in the synthesis of 2-quinuclidone are due to the high reactivity of amide as a free base and undergoes decomposition very quickly. Now a days, studies on the reactivity of strained lactams are increasing and providing enormous data to understand fundamental factors that govern the reactivity.¹¹⁻¹⁸

3.1.3 Reported acyclic amide solvolysis under non-conventional conditions

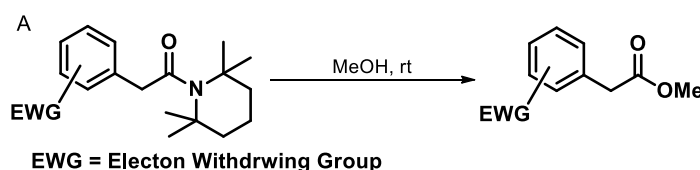
In contrast to the strained cyclic lactams, acyclic amide bonds are highly stable towards solvolysis due to the resonance stabilisation as described in **Figure 3.1A**. But, either incorporation specific characteristic groups at α -carbon atom or at amide nitrogen can destabilise the amide bond towards solvolysis, or otherwise a suitable metal catalyst can make a specific amide bond labile towards solvolysis.¹⁹⁻⁴² The activation of amides towards the solvolysis or utilising the amides as synthetic precursors for functionalization of organic molecules is emerging as an interesting area in recent days.²⁹⁻³³ Moreover, there are notable

reports on metal free¹⁹⁻²³ and metal mediated^{24-33,57} acyclic amide solvolysis. Few examples of recently reported amide solvolysis reactions are presented in **Figure 3.4**. The amide solvolysis of benzamides presented in **Figure 3.4A** is one of the fascinating examples of amide solvolysis. Where, the α -carbon of the amide bond is activated with electron withdrawing groups and on the other hand, the amide nitrogen is sterically hindered, which means both electronic and steric factors together activated the amide bond towards solvolysis.⁴¹ Therefore, steric and electronic factors play a prominent role in activating the acyclic amide bond.

In case of metal mediated amide solvolysis (**Figure 3.4B&C**), both reported examples follow a different mechanism. Zinc catalysed amide solvolysis (**Figure 3.4B**) facilitated by the

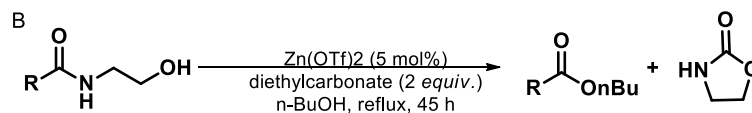
Previous reports

I) Transition metal free amide cleavage

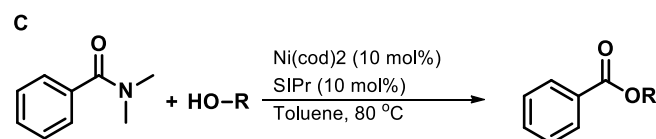


Angew. Chem., Int. Ed. **2012**, 51, 548.

II) Transition metal mediated amide cleavage



Angew. Chem., Int. Ed. **2012**, 51, 5723.



Nature, **2015**, 524, 79.

Figure 3.4 (A) Recent literature reports on hydrolysis of amide bonds under unconventional conditions.

chelation of Zn^{2+} ion with the amide carbonyl oxygen, followed by N,O-acyl rearrangement and transesterification and hence the presence of β -hydroxyl group is compulsory.²⁵ Nickel catalysed amide solvolysis presented in **Figure 3.4C** proceeds through the well-known mechanism, i.e., oxidative addition, ligand exchange and reductive elimination.²⁹

3.1.4 Present work

In expansion of repertoire of unnatural amino acids and peptides, we have reported the syntheses of new troponyl δ -amino acid, troponyl aminoethylglycine (*Traeg*) and its hybrid

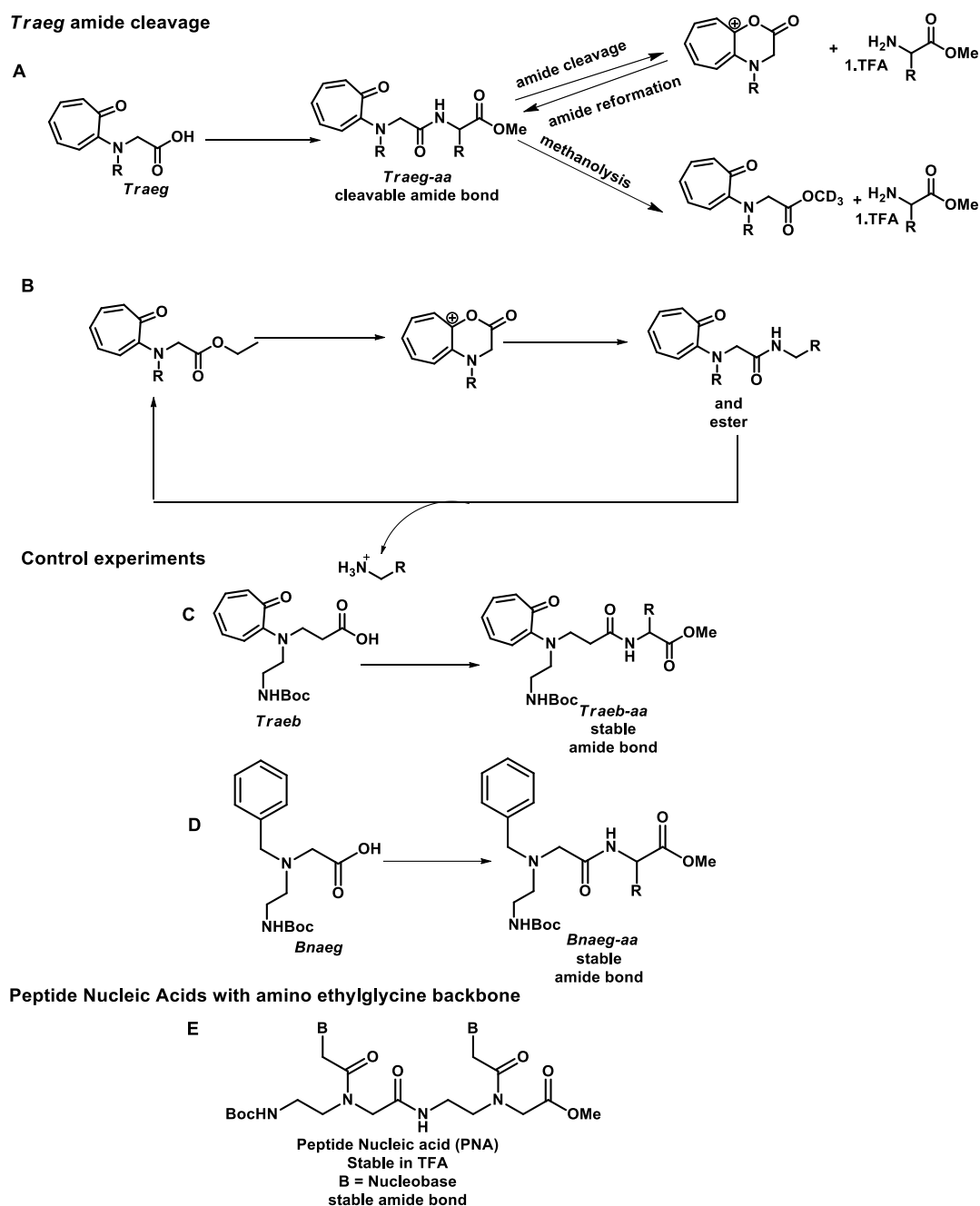


Figure 3.5 Representation of present work. A) Cleavage of *Traeg* amide into cationic troponyl lactone followed by reversible amidation in acetonitrile, and *Traeg* ester in methanol. B) Conversion of esters into cationic troponyl lactone followed by amidation. C&D) control peptides, *Traeb*-aa & *Bnaeg*-aa. E) Reported peptide nucleic acids derived from aminoethylglycine backbone.

di/tri-peptides (*Traeg*-aa; aa = α -amino acid esters).⁴⁴ Further, we have attempted to increase the chain length of those peptides at *N*-terminus, during this process we found an unusual cleavage of amide bond in presence of 5.0% TFA (6.0 *equiv.*) derived from *Traeg*.⁴⁵

Further, we have carried out a systematic investigation of the unusual instability of *Traeg* amide, during this process of investigation, each and every step revealed most surprising results.

In this chapter, we have explained the regioselective cleavage of the *Traeg* amide bond, derived from *Traeg* and natural α -amino acid derivatives (**Figure 3.5A**), in presence of 5.0% TFA (6 *equiv.*). During mechanistical investigation, it was found that in absence of external nucleophiles, in anhydrous acetonitrile and TFA (6 *equiv.*), 1,2-disubstitued cationic troponyl lactone (tropylium cation) was obtained instead of *Traeg* carboxylic acid derivatives. Where the troponyl ketone group is acting as nucleophile. The obtained tropylium cation was highly stable for long time in acetonitrile. Even though after addition of 1.5 *equiv.* of hydroxyl nucleophile (alcohols), the conversion of cationic troponyl lactone into *Traeg* ester was considerably less after two hours and in presence of excess alcohols, conversion was enhanced. To our surprise, the neutralization of the reaction mixture with triethylamine, containing cationic troponyl lactone and TFA salt of amine results in the instant reformation of starting material. In the literature, so far there are no reports on such reversible amidation phenomenon. Most interesting and exciting part of this work is reversible amidation and recyclable troponylglycinate ester via amide bond (**Figure 3.5B**). For control studies, the rationally designed peptides *Traeb*-aa (**Figure 3.5C**) and *Bnaeg*-aa (**Figure 3.5D**) are synthesized.

3.2 Results and discussion

During our work on the synthesis of troponyl aminoethylglycine amino acid (*Traeg*) and its peptides (chapter I, where we synthesized the *Traeg* peptides at C-terminus), we

attempted to extend the peptide sequence at *N*-terminus. Hence, the *N*-Boc group of peptides **6** were attempted to remove with 20% TFA in DCM. To confirm the formation of Boc deprotected peptide **6** after reaction, we performed ESI-MS analysis. We observed a strange cleavage of *Traeg* derived amide bond along with Boc deprotection. At the moment, the results were surprising, because the amide bonds of structurally related peptide nucleic acids (PNA) are stable like other acyclic amide bonds even in neat TFA.^{42,43} Hence, to make sure, we performed the reaction several times, under same conditions and analyzed the reaction mixture with ESI-MS (Electrospray Ionization Mass Spectrometry). These experiments clearly revealed the cleavage of amide bond derived from *Traeg*. For example, to explain, when the peptide **13e** was treated with 20% TFA in DCM, the formation of *Traeg* amino acid (NH₂-*Traeg*-OH) and methyl ester of glycine (Gly-OMe, **10e**) was observed along with Boc deprotection. Next, we optimized the concentration of TFA required for the cleavage of *Traeg* derived amide bond.

Table 3.1 Optimization of reaction conditions

entry	compound	reaction conditions	products
1	13e	20% TFA (24 <i>equiv.</i>) in DCM, 1h, 25 °C	NH ₂ - <i>Traeg</i> -OH, NH ₂ -Gly-OMe
2	13e	15% TFA (18 <i>equiv.</i>) in DCM, 1h, 25 °C	NH ₂ - <i>Traeg</i> -OH, NH ₂ -Gly-OMe
3	13e	5% TFA (6 <i>equiv.</i>) in DCM, 1h, 25 °C	BocNH- <i>Traeg</i> -OH, NH ₂ -Gly-OMe
4	13e	5% TFA (6 <i>equiv.</i>) in MeOH, 1h, 25 °C	BocNH- <i>Traeg</i> -OMe, NH ₂ -Gly-OMe
5	13e	1.0 N HCL + Ethyl acetate solution of peptide 13e (bilayer), 15 min, rt	BocNH- <i>Traeg</i> -OH, NH ₂ -Gly-OMe
6	13e	4 <i>equiv.</i> of PTSA in methanol, rt, 1h	BocNH- <i>Traeg</i> -OMe, NH ₂ -Gly-OMe

With successive trial experiments (reaction conditions provided in **Table 3.1**), we found that only 5.0% TFA in DCM (~6.0 *equiv.*) is sufficient to cleave the *Traeg* derived amide bond selectively. Interestingly, Boc protecting group (carbamate bond) was quite stable under above optimized conditions (5.0% TFA). The same reaction when we performed in methanol instead of dichloromethane, we obtained the methyl ester of *Traeg* (BocNH-*Traeg*-OMe, **6a-OMe**) and α -amino acid ester. Later on, we tested several acids to cleave the amide bond. The *Traeg* derived amide bond would be cleavable selectively with 1.0 N HCl, PTSA (para-toluene sulfonic acid). Curiously, the peptide **13e** was treated with neat acetic acid and found that the amide bond was stable in acetic acid.

3.2.1 Design and synthesis of amino acid monomers and their peptides for amide cleavage studies

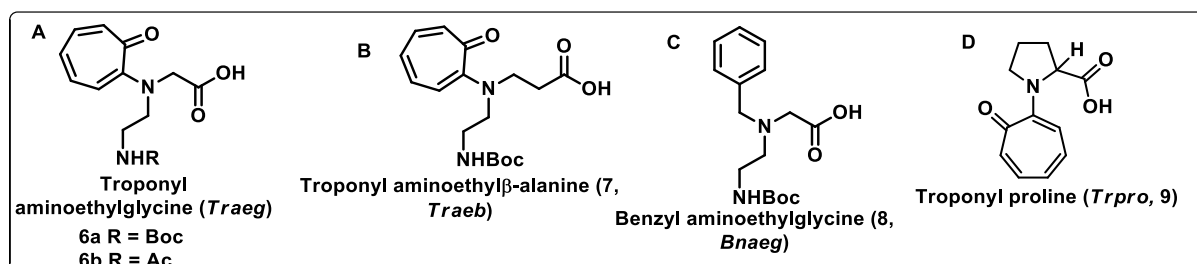


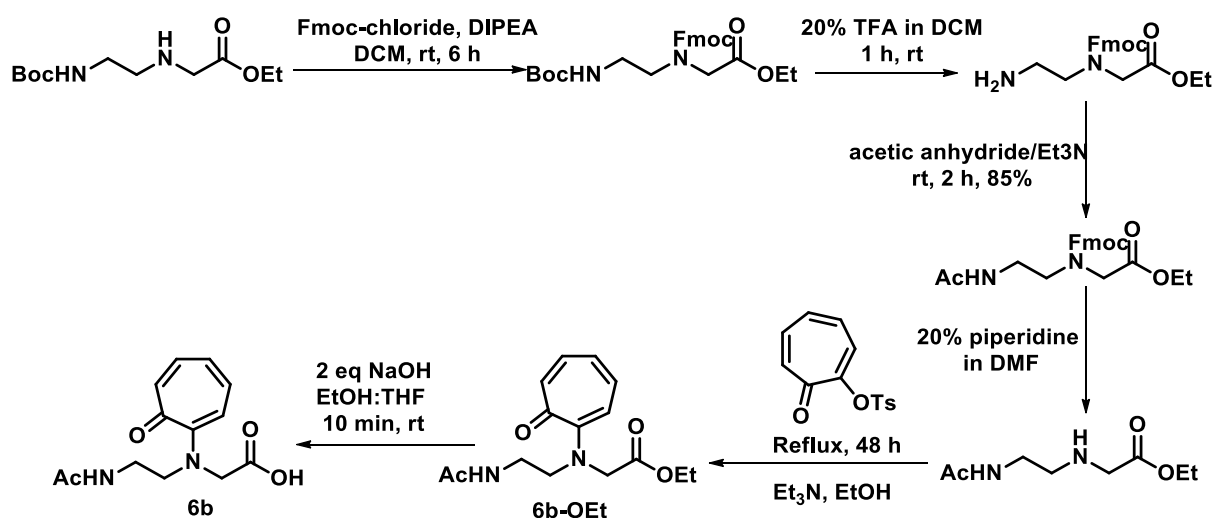
Figure 3.6 *Traeg* amino acid (A, **6**) and Designed control amino acids for *Traeg* amide cleavage studies: *Traeb* (B, **7**), *Trpro* (D, **9**).

The presented amino acids in the **Figure 3.5** are the designed amino acids to investigate the role of troponyl moiety and α -methylene group in the regiselective cleavage of amide bond derived from *Traeg* amino acids. Among these designed control amino acids (**Figure 3.5**, B-D), we have successfully synthesized the *Traeb*, *Trpro* and *Bnaeg* amino acids and their peptides by following the established procedures.

We began with the syntheses of unnatural aromatic amino acid derivatives **6-8** (Figure 3.5). The synthesis of *Traeg* amino acid, BocNH-*Traeg*-OH (**6a**), was accomplished by following the presented procedure in chapter one.⁴⁴⁻⁴⁹ The syntheses of other derivatives such as AcNH-*Traeg*-OH (**6b**), BocNH-*Traeb*-OH (**7**) and BocNH-*Bnaeg*-OH (**8**) are described in Scheme 3.1-3.3.

Synthesis of AcNH-*Traeg*-COOH

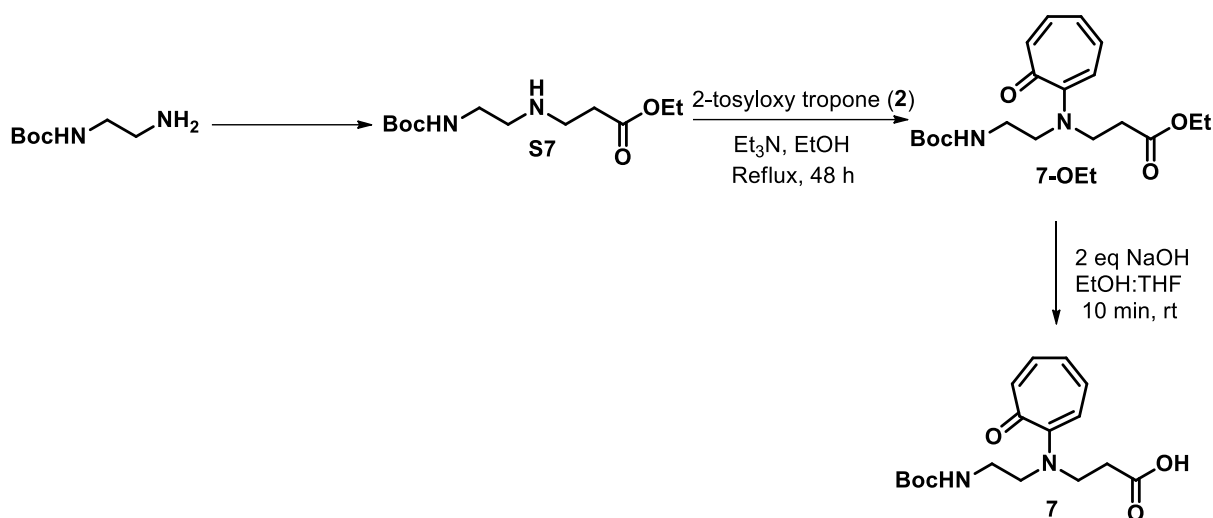
Scheme 3.1 Syntheses of AcNH-*Traeg*-COOH (**6b**)



The synthesis of monomer **6b**, AcNH-*Traeg*-OH, was carried out by following the reported literature procedures presented in scheme 2. We were unable to synthesize the monomer **6b** from *Traeg* monomer 1-OEt. The problem accompanied with this is that the cyclization of obtained free amine from *Traeg* into cyclic aminotroponimine (described in Chapter II). Hence, we followed the synthetic route given in Scheme 3.1. Where, AcNH-*aeg*-OEt was prepared from BocNH-*aeg*-OEt backbone in four steps: Fmoc protection of *aeg* NH, Boc deprotection, acylation and Fmoc deprotection. This *N*-acylated *aeg* ester (AcNH-*aeg*-OEt) was tropolonylated with 2-tosyloxy tropone. The obtained AcNH-*Traeg*-OEt was then subjected for hydrolysis with NaOH to prepare AcNH-*Traeg*-COOH (**6b**).

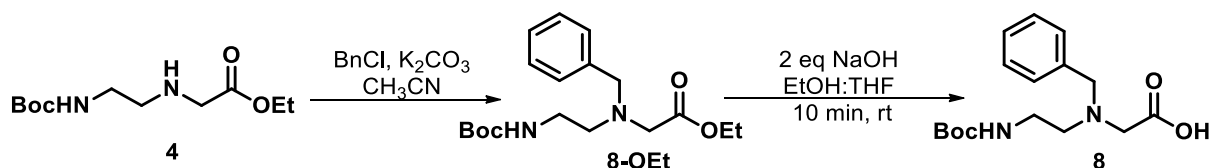
Synthesis of BocNH-Traeb-COOH: *N*-Boc-ethylenediamine was treated with ethyl bromo propanoate in presence of potassium carbonate in acetonitrile to obtain *N*-Boc aminoethyl β -alanate. This backbone further treated with 2-tosyloxy tropone by following the general procedure to obtain troponyl aminoethyl β -alanate (*Traeb*), which is a homologative derivative of *Traeg*. The protected amino acid was hydrolysed to obtain BocNH-*Traeb*-COOH (Scheme 3.2, **7-OEt**).

Scheme 3.2 Syntheses of BocNH-*Traeb*-COOH (**7**)



Synthesis of BocNH-Bnaeg-COOH:

Scheme 3.3 Syntheses of BocNH-*Bnaeg*-COOH (**8**).

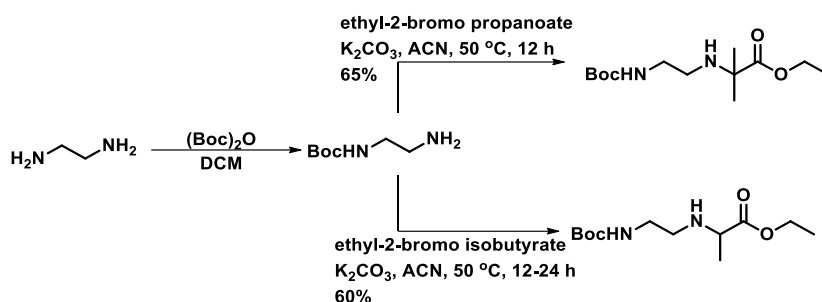


N-Boc aminoethylglycine backbone was treated with benzyl bromide in presence of potassium carbonate in acetonitrile to obtain Benzyl aminoethylglycinate (*Bnaeg*). The protected amino acid was hydrolysed into carboxylic acid (Scheme 3.3, **8**).

Designed synthetic route to Traeala, Traeaib: We attempted to synthesize *Traeala*, *Traeaib* monomers and their peptides, but was unsuccessful. Though we succeeded in the

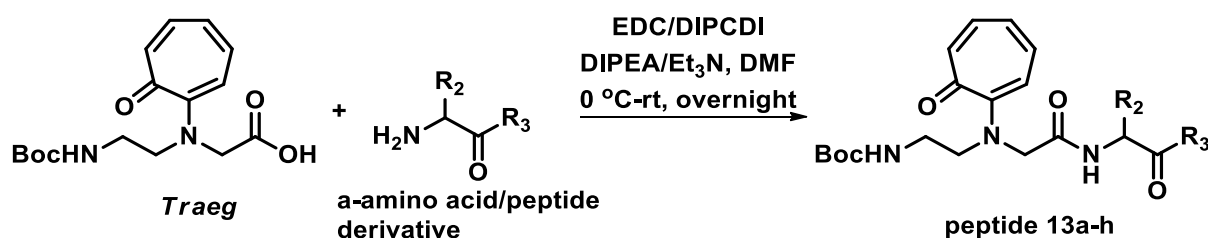
syntheses of *N*-Boc aminoethyl aminoisobutyric acid (*aeaib*) and *N*-Boc aminoethylalanine (*aeala*) backbones, unfortunately, troponylation reaction of these backbones given only trace amount of product (Scheme 3.4). Experimental procedure for backbone syntheses is given in experimental section

Scheme 3.4 Syntheses of *N*-Boc aminoethyl aminoisobutyric acid (*aeaib*) and *N*-Boc amino ethyl alanine (*aeala*).



3.2.2 Synthesis of peptides

Table 3.2 Synthesis of hybrid peptides from *Traeg*/*Traeb*/*Bnaeg* peptides



entry	carboxylic acid derivative	ester of α-amino acid/peptide derivative	peptide
1	6a	10a (Phe-OMe)	13a
2	6a	10b (Pro-OMe)	13b
3	6a	10c (Ile-OMe)	13c
4	6a	10d (Gly-Phe-OMe)	13d
5	6a	10e (Gly-OMe)	13e
6	6a	10f (Ala-OMe)	13f
7	6a	10g (Trp-OMe)	13g
8	6a	10h(Pro-Ile-Phe-OMe)	13h
9	6b	10a (Phe-OMe)	14
10	7	10c (Ile-OMe)	15
11	8	10a (Phe-OMe)	16
12	5d-COOH	10e (Gly-OMe)	17

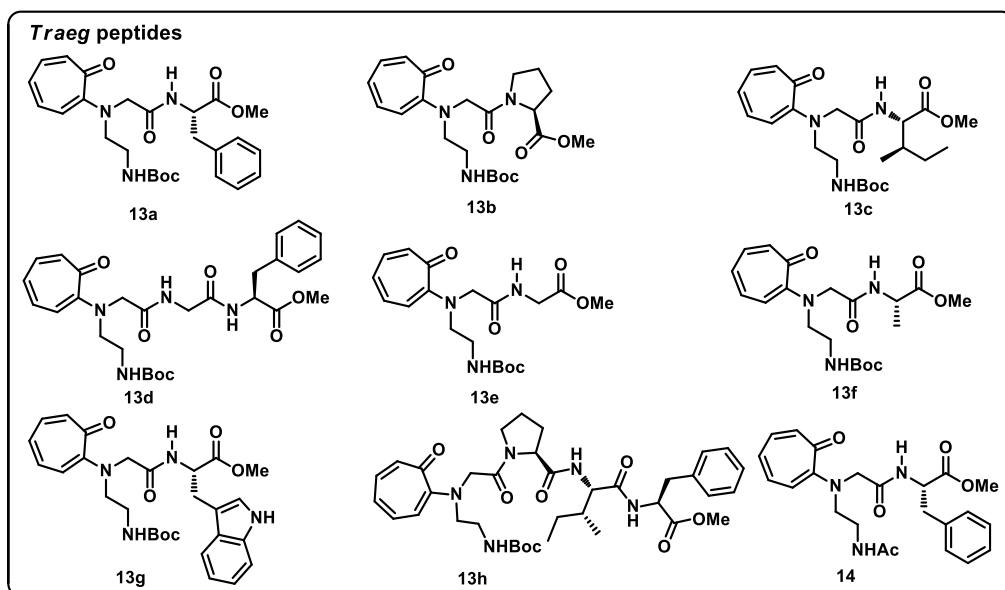


Figure 3.7 Chemical structures of synthesized *Traeg* peptides for amide cleavage studies

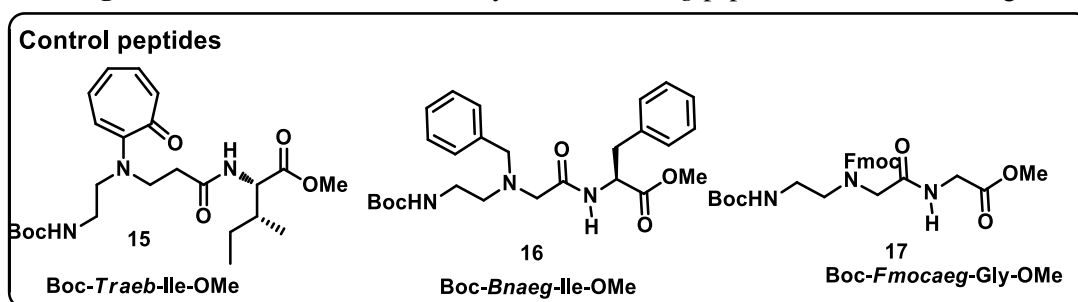


Figure 3.8 Chemical structures of synthesized control peptides for amide cleavage studies

These amino acids were employed for the synthesis of hybrid peptides **13-16** with natural α -amino acid ester derivatives (**13a-h**) (Table 3.2, entry 1-11) by using standard peptide coupling reaction conditions. Reactions were carried out in anhydrous DMF or DCM by using DIPCDI (diisopropyl carbodiimide) or EDC-HCl as coupling reagents, in presence of triethylamine. The *Traeg* derived hybrid peptides **13a-h** were synthesized from BocNH-*Traeg*-OH (**6a**) and respective α -amino acid ester derivatives **10a-h** (Table 3.2, entry 1-8). The *N*-acylated hybrid peptide **14** was accomplished from AcNH-*Traeg*-OH (**6b**) and α -amino acid ester **10a** (Table 2.2, entry 9). For control studies, the dipeptide **15** was synthesized from BocNH-*Traeb*-OH (**7**) and α -amino acid ester **10c** (Table 3.2, entry 10), while the other

dipeptide **16** was synthesized from BocNH-*Bnaeg*-OH (**8**) and α -amino acid ester **10a** (Table 3.2, entry 11). Obtained pure products were characterized with NMR and ESI-MS. Relevant spectra are given in appendix. Chemical structures of all the synthesized peptides are provided in **Figure 3.7** and **3.8**.

3.2.3 Methanolysis of *Traeg* amide bond

All the synthesized *Traeg* peptides **13a-h** & **14** were employed for the methanolysis of amide bond in the presence of 5% TFA in CD₃OD. In case of all the peptides **13a-h** & **14**, Regioselective methanolysis of *Traeg* derived amide bond was confirmed and the conversion is >95%, within one hour (**Table 3.3**). The methanolysis experiments were also performed with control peptides **15/16** under same conditons, we did not observe any change in their characterization data in the given time.

Table 3.3 Regioselective methanolysis of *Traeg* derived amide bond

<p>peptides 13a-h $\xrightarrow[1\text{ h, } 25\text{ }^{\circ}\text{C}]{5.0\% \text{ TFA in CD}_3\text{OD}}$ <i>BocNH-Traeg-OCD₃</i> (6a-OCD₃) + CF_3COO^- H_3N^+ R_2 R_3 monitored by NMR ESI-MS</p>		
entry	peptide	products
1	13a	6a-OCD₃ and 10a
2	13b	6a-OCD₃ and 10b
3	13c	6a-OCD₃ and 10c
4	13d	6a-OCD₃ and 10d
5	13e	6a-OCD₃ and 10e
6	13f	6a-OCD₃ and 10f
7	13g	6a-OCD₃ and 10g
8	13h	6a-OCD₃ and 10h
9	14	6b-OCD₃ and 10d
10	15	no change
11	16	no change
12	17	no change

3.2.4 Methanolysis studies of *Traeg*-aa peptides (**13a-h/14**) by NMR and ESI-MS:

The time dependent ^1H NMR experiment was performed with *Traeg* derived peptides and control peptides under the above optimized conditions to explore the mechanistic aspects of the hydrolysis/solvolysis of the *Traeg* derived amide bonds. Thus a series of ^1H NMR spectra of the peptides **13a-h/14**, including control peptides **15/16**, were recorded with 7.0 minutes time intervals for 1.0 h after and before the addition of TFA. After the completion of NMR experiments, the same samples were analyzed by ESI-MS. The spectral data, time dependent ^1H NMR and ESI-MS data are provided in the appendix. The extended region of the time dependent ^1H NMR spectra of dipeptide **13f** and mass spectra of **13f/13h** are depicted in **Figure 3.9/3.10**. Before analyzing the time dependent NMR spectra of peptides, we assigned all the proton signals of peptides **13e/f/g/h**, **14**, **15**, **16** by comparing with the NMR data of our previously discussed monomer **5a** and peptides **13a/b/c/d**.⁸

We here described the significant changes observed in the time dependent ^1H NMR spectra of **13f**. After the addition of TFA, changes in chemical shifts of $\alpha_1/\alpha_2\text{-CH}_2$ protons signals and their intensities were observed in ^1H NMR spectra of dipeptide **13f** with respect to time (**Figure 3.9a**). The ^1H NMR signals of $\alpha_1\text{-CH}_2$ (δ 4.2, d) was shifted to δ 4.4 (s) and $\alpha_2\text{-CH}_2$ (δ 4.46-4.41, q) to δ 4.06 (q). Importantly, the intensity of proton signal at δ 4.4 (s) increases with time. After one hour, the $\alpha_1\text{-CH}_2$ protons are completely deshielded (δ 4.4, s), while the $\alpha_2\text{-CH}_2$ protons are shielded (δ 4.06, q). These ^1H NMR changes clearly indicates the formation of new derivatives. The mass spectrum of the same NMR sample of **13f** exhibits the new mass peak at (m/z) 340.0, instead of dipeptide **13f** mass at (m/z) 394.0 ($\text{M}+\text{H}$)⁺. The mass peak at (m/z) 340.0 is equivalent to the calculated mass of the *BocNH-Traeg-OCD*₃ (**6a-OCD**₃, **Figure 3.10b**). This is only possible due to the methanolysis of *Traeg* derived amide bond of di-peptide **13f** in CD₃OD in presence of TFA (5.0%). Almost similar spectral changes were observed in ^1H NMR spectra of other *Traeg* derived peptides **13a-h** with respect to time after

the addition of TFA. Similarly, the mass peak at (m/z) 340.0 ($M+H$) is also constantly observed in the mass spectrum of the other *Traeg* derived peptides after the time dependent ^1H NMR experiments. Overall, the time dependent ^1H NMR experiments and ESI-MS studies strongly supports the regioselective methanolysis of *Traeg* derived amide bond.

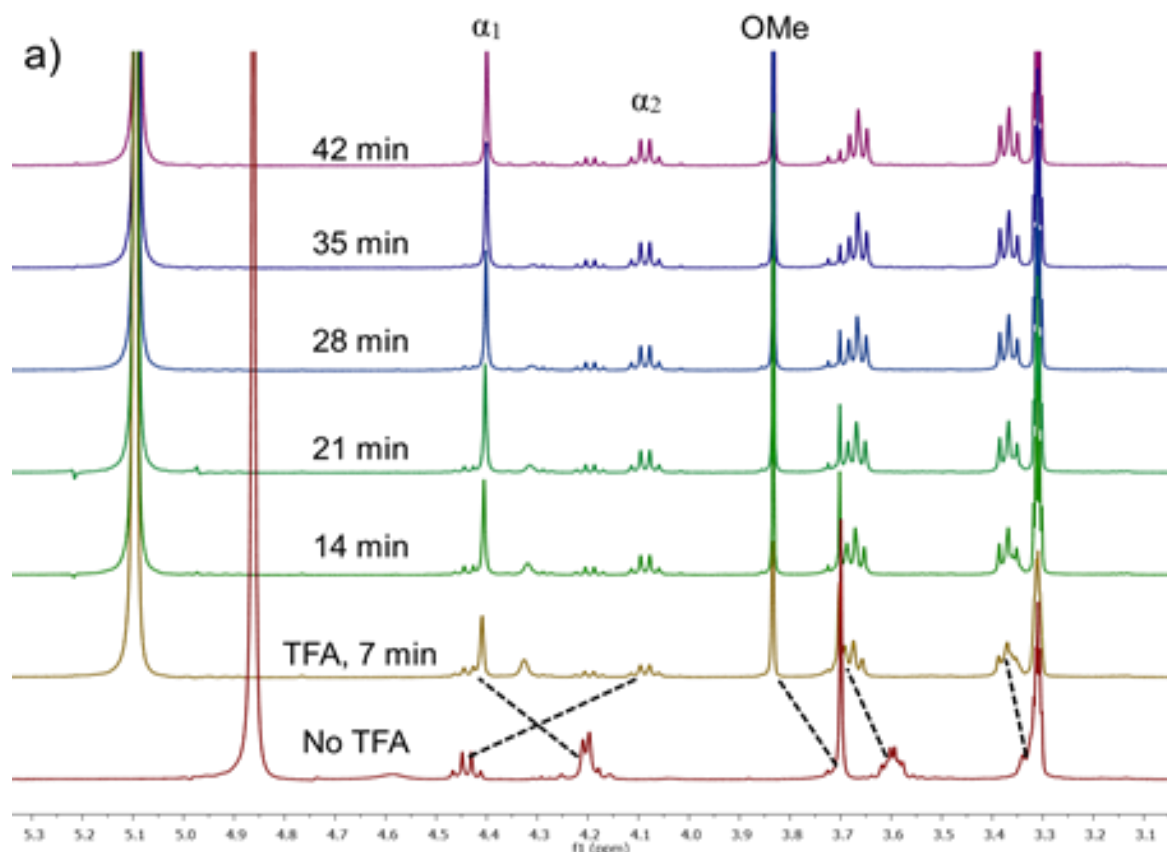


Figure 3.9 a) Time dependent ^1H -NMR spectra of *di*-peptide **6b**.

It is noteworthy to discuss about the ESI-MS spectrum of *tetra*-peptide **13h**. As expected, the mass spectrum exhibits two prominent mass peaks at (m/z) 340.0 and 390.0 after ^1H NMR experiment. These two mass peaks represent the formation of **6a-OCD₃** ($M+H$) and tripeptide **10h**, respectively (**Figure 3.10c**). These results reveal that the other amide bonds of *tri*-peptide **10h** are stable under the same acidic conditions. Similarly, the other *non-Traeg* amide bonds of *tri*-peptide **13d** and *N*-acylated-*di*-peptide **14** are also found stable. Further, Boc protecting group was stable under the same conditions. The mass analysis of **13d/h/14**

strongly supports the regioselective methanolysis of *Traeg* derived amide bond. We also calculated the rate constant ($k = 0.21423 \text{ min}^{-1}$) and half-life ($t_{1/2} = 3.23 \text{ min}$) of methanolysis of *di*-peptide **13f** by considering as pseudo first order reaction. The kinetic studies, plots and calculations are provided in the appendix.

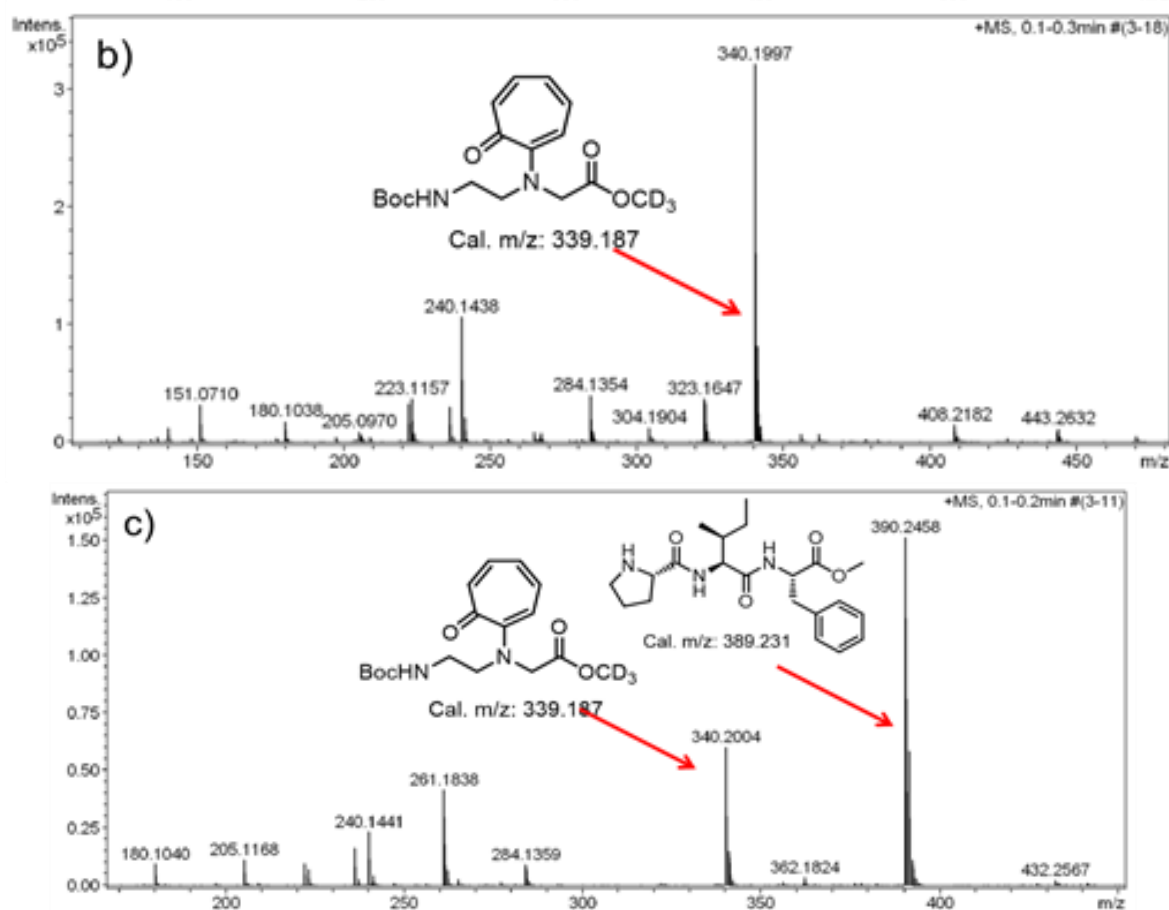


Figure 3.10 b) ESI-MS spectrum of dipeptide **13f** after time dependent NMR; c) ESI-MS spectrum of *tetra*-peptide **13h** after time dependent NMR.

3.2.5 Cleavage of *Traeg* amide into cationic troponyl lactone in acetonitrile

As presented above, in alcoholic solvents *Traeg* amide was cleaved into ester derivative. In contrast, in acetonitrile, *Traeg* amide was cleaved into cationic troponyl lactone (1,2-disubstituted tropylium cation (**24**), **Figure 3.11**). This is another interesting transformation of *Traeg* amide bond. In general, the conversion of amide into lactone is not known. Importantly, the obtained cationic troponyl lactone (tropylium cation) was stable under these conditions,

until there is a contamination of nucleophiles. However, the troponyl lactone was converted into ester in presence of excess alcoholic solvents and up on neutralization of the respective reaction mixture, a reversible amidation was observed. The stability of tropylium cation is due to its aromaticity and it is well-known in the literature. Tropylium cation has been known since 1891, infact it is one of the first prepared carbocations in the laboratory as hydrogen bromide salts by G. Merling.⁵⁹⁻⁶²

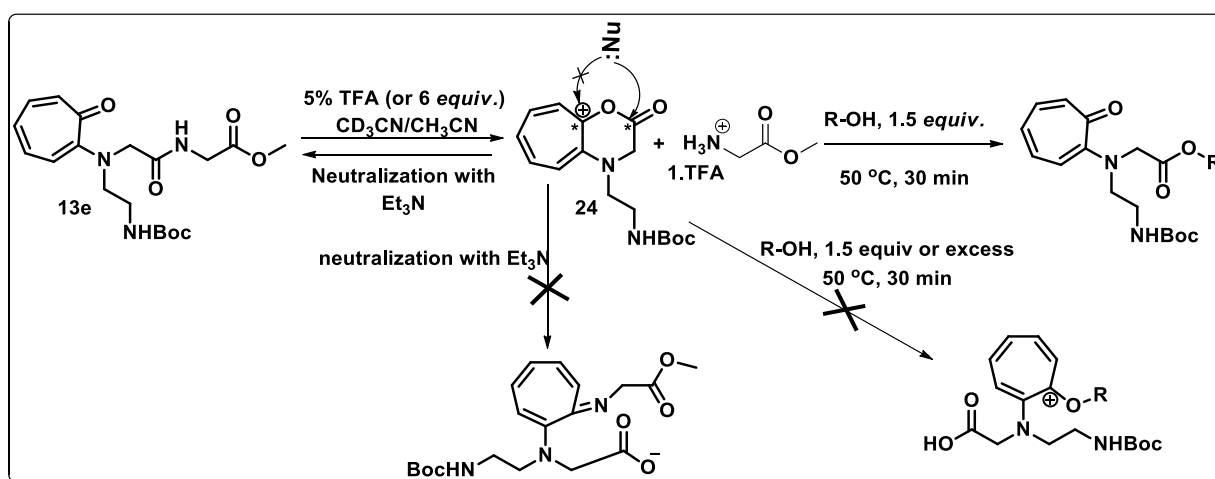
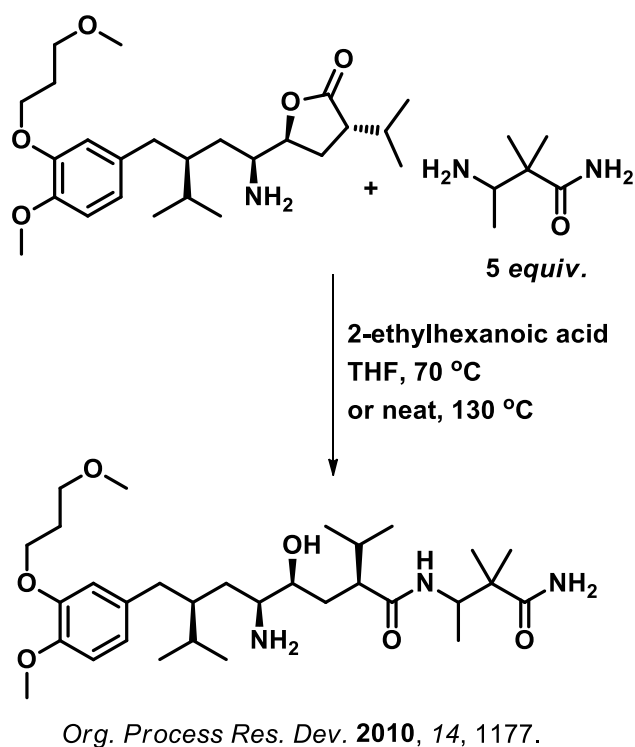


Figure 3.11 Representation of possible nucleophilic addition reactive centres in tropylium cation (*); nucleophile addition is represented with arrows.

After neutralization of the reaction mixture after amide cleavage with triethylamine, containing troponyl lactone and trifluoroacetate salt of amine respective amine, reversible amidation was occurred, the cationic troponyl lactone was instantly converted into starting material (amide). To best of our knowledge, so far, in the literature, there are no reports on such amide transformations, where cleavage of *Traeg* amide bond occurs in the presence of milder acidic conditions (5.0 % TFA/6.0 *equiv.*) in acetonitrile into troponyl lactone intermediate in one hour and instant reformation of amide bond just after neutralization of the same reaction mixture.

However, aminolytic cleavage of activated alkyl esters and lactones is known, which results in the formation of amide bond. And this aminolysis of activated esters and lactones

requires high temperatures (generally reflux conditions) and longer times. A reported example for lactone aminolysis is given in **Scheme 3.5**. Where, authors presented the syntheses of Aliskiren, an FDA approved drug for the treatment of hypertension, from respective lactone and free amine under given conditions.⁵⁸ The aminolysis of following lactone occurred in presence of 5.0 equiv. of amine and 2-ethylhexanoic acid catalyst at 130 °C.⁵⁸



Scheme 3.5 Reported conversion of lactone into amide

In contrary with reported aminolytic cleavage of lactones, the reactivity of troponyl lactone is distinctive. Hence, it is important to discuss the reactivity of troponyl lactone (**Figure 3.11**). In troponyl lactone presented above contains two reactive sites for nucleophile addition. As represented in **Figure 3.11**, there is a possibility of addition of nucleophile at both reactive centres (*), these are cationic center of troponyl carbonyl carbon and lactone ester carbonyl. But, practically, the nucleophile is attacking at the carbonyl carbon of lactone ester, instead of positively charged troponyl carbon (judging from NMR studies of reversible amidation, see

Figure 3.12). Both, alcoholic and amine nucleophiles are attacking selectively at lactone ester carbonyl irrespective of their nucleophilic strength. Though the syntheses of aminotroponimines from alkoxyamino tropylium cation followed by amination is reported (slower reaction, requires time based on the strength of nucleophile, in case of alky amines imination reaction requires 12 h and in case of aromatic amine requires 8 days).¹¹ But, in this case, the neutralization of the reaction mixture after formation of tropylium cation leads to the formation of starting material exclusively. This concludes that the reversible amidation is exclusive and faster than aminotroponimine formation.

On the other hand, the addition of 1.5 *equiv.* of hydroxyl nucleophile at room temperature leads to the formation of ester, the conversion was very less. But, the conversion was faster and high yielding, when the temperature of the reaction raised to 50 °C or with the addition of excess alkyl alcohol.

Interestingly, the synthesis of alkoxyamino tropylium cations from the aminotropones and triethyloxonium tetrafluoroborate is well-reported.⁴⁶⁻⁵⁰ In this reaction, the triethyloxonium tetrafluoroborate is an alkyl cation donor (electrophile), and troponyl carbonyl acts as nucleophile. Further, these substituted alkoxyamino tropylium cations were subjected to imination with desired amine to obtain aminotroponimines.⁴⁶⁻⁴⁹ But in case *Traeg* amide, the scenario is completely different, the amide is directly converting into cationic troponyl lactone (tropylium cation) in presence of 5.0% TFA (6 *equiv.*) in acetonitrile, where the amide carbonyl carbon is acting as electrophile. This is witnessed that, before forming the troponyl lactone, the *Traeg* amide must be converting into a strong electrophile after amide cleavage and that is further reacting with troponyl keto oxygen.

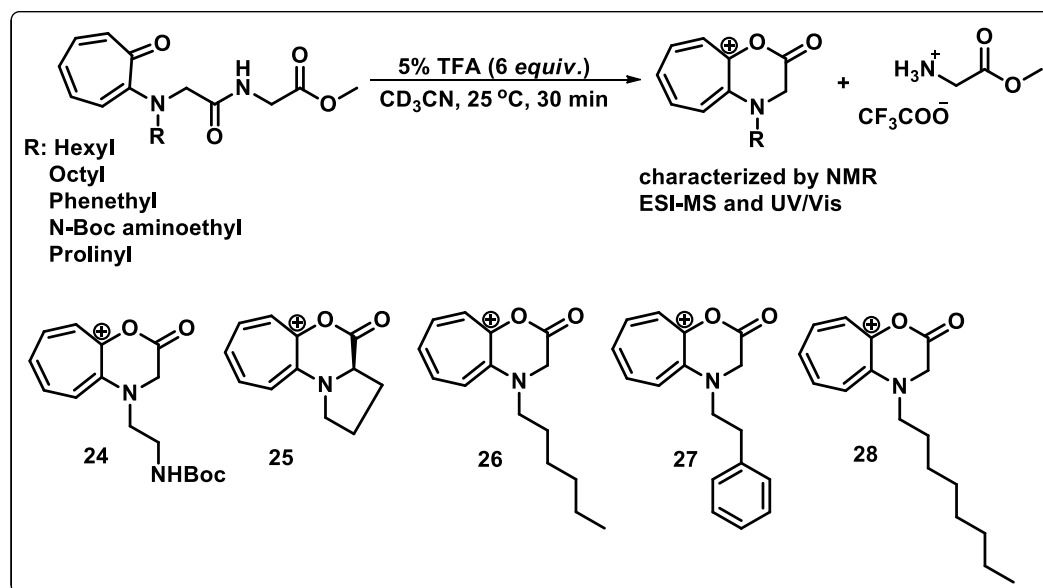
These interesting results led us to check the scope of the formation of *cationic troponyl lactone* (tropylium cation) with different substituents (acyclic and cyclic) at glycinate nitrogen

methyl ester hydrochloride and 2-tosyloxy tropone by following the reported literature procedure. The obtained monomers toponyl phenethyl glycine (*Trpeg*), toponyl hexylglycine (*Trhg*), toponyl octylglycine (*Trog*) and toponyl proline (*Trpro*) were hydrolysed to free carboxylic acid groups. These obtained free carboxylic acid monomers were coupled with glycine methyl ester under standard peptide coupling conditions (general procedures). The obtained peptides were characterized by NMR, ESI-MS and spectra are provided in appendix.

3.2.7 Synthesis and characterization of cationic troponyl lactones

Syntheses: After successful syntheses of various troponylglycinate peptides **19/21/23/9G/F**, all the troponylglycinate peptides were subjected to amide cleavage reaction in the presence of 6.0 *equiv.* of TFA (5.0%) in acetonitrile/acetonitrile- d_3 as solvent at 25 °C.

Scheme 3.7 Synthesis of cationic troponyl lactones from troponylglycinate peptides **19/21/23/9G/F**



In case of all the peptides (**13/19/21/23/9G/F**), formation of cationic troponyl lactones (**24-28**) were consistently observed. The respective amide cleaved into cationic troponyl lactone after treatment with TFA in CD₃CN very fast (~1.0 h) and observed conversion was almost >95.0%, (observed in ¹H & ¹³C NMR in CD₃CN, See **Figure 3.12**). Interestingly, *Trpro*-

Gly peptides (**9G/F**) also produced the troponyl lactone (**25**) irrespective of steric and electronic effects. The molecular ion peak of each synthesized lactone was observed in their respective mass spectra.

The formation of cationic troponyl lactone was characterized by NMR, ESI-MS and UV/Vis spectroscopy (See appendix two). These spectra results are explained below.

Characterization:

¹H and ¹³C NMR results:

¹H and ¹³C NMR spectra of *Trhg-Gly*-OMe peptide, its lactone (glycinate salt is also present) and after neutralization of same reaction mixture in CD₃CN is provided in **Figure 3.12**, which clearly demonstrates the reversible amidation reaction. To explain in few lines, ¹H and ¹³C NMR spectra of *Trhg-Gly*-OMe was changed completely after adding 6 *equiv.* of TFA in CD₃CN (**Figure 3.12**) within 50 minutes at 25 °C. Characteristic troponyl carbonyl carbon peak at δ 182.3 was completely disappeared and a new peaks at δ 152.81 & 154.51 were appeared. However, the detailed discussion on the characterization of cationic lactones is given below.

¹³C NMR results:

¹³C NMR chemical shifts of troponyl ring in peptides **19/23/9G**, after formation of troponyl lactones **25/26/28** are listed in **Table 3.4** and expanded region of respective ¹³C NMR spectra of lactones **25/26/28** in CD₃CN are provided in **Figure 3.12** (δ 126-156.0 ppm), and full spectra are provided in appendix two (the obtained spectra are calibrated to solvent residual peak of CD₃CN, δ 1.34 ppm). Troponyl ring carbon chemical shifts in troponyl lactones have shown very significant shifts over troponyl ring carbon chemical shifts in peptides. Here, it is worth to mention that the synthesized troponylglycinate peptides **19/21/23/9G** are dipeptides of glycine and respective troponylglycinate monomer.

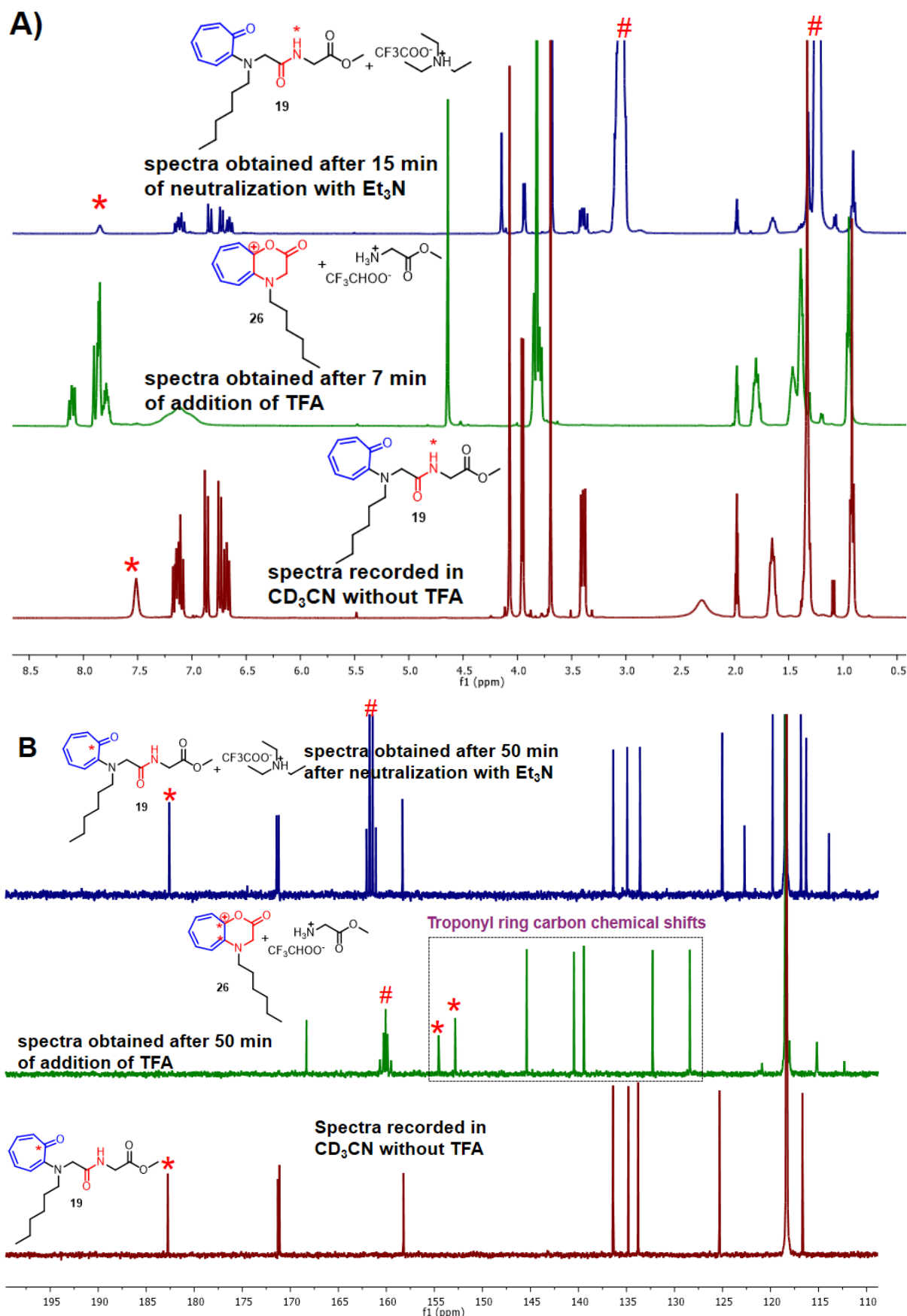


Figure 3.12 A & B) ¹H & ¹³C NMR of *Trhg*-Gly-OMe in CD₃CN, represents formation of troponium cation and the reverse amidation; A) # are triethyl amine peaks; B) # are Trifluoroacetate peaks.

The reason behind to synthesize all glycine dipeptides is to avoid the more number of peaks in the aromatic region (δ 126-156.0 ppm), where troponyl ring carbon signals appear. In ^{13}C NMR spectra of troponyl lactone **26** depicted in **Figure 3.12B**, after δ 100.0 ppm 9 signals are appearing other than trifluoroacetic acid peaks and CD_3CN solvent residual peak at δ 118.4 and 159-160 ppm, respectively. The two ester carbonyl carbons are resonating at δ 160.06 ppm (lactone carbonyl) and δ 168.30 ppm (glycine ester). Excluding these two peaks, rest of the seven peaks appearing in the region of δ 126-156.0 ppm are corresponds to troponyl ring carbons of troponyl lactone **26**. Hence, cationic carbon of troponyl ring in troponyl lactones

Table 3.4. ^{13}C NMR chemical shift values of troponyl ring in peptides (**19/23/9G**) and troponyl lactones (**25/26/28**)

troponylglycinate peptide for examination	^{13}C NMR chemical shifts of troponyl ring in peptides (δ in ppm)	^{13}C NMR chemical shifts of troponyl ring in lactone (δ in ppm)	^{13}C NMR chemical shifts of troponyl ring in peptides after reverse amidation (δ in ppm)
19	182.73, 158.20, 136.37, 134.79, 133.76, 125.30, 116.65	154.51, 152.81, 145.37, 140.46, 139.42, 132.26, 128.38	182.59, 158.31, 136.35, 134.90, 133.58, 125.01, 116.83
23	182.80, 158.23, 136.39, 134.79, 133.82, 125.34, 116.71	154.58, 152.84, 145.39, 140.50, 139.45, 132.30, 128.40	182.65, 158.33, 136.38, 134.90, 133.64, 125.08, 116.37
9G	181.03, 156.62, 136.35, 135.36, 132.74, 123.02, 113.74	153.89, 152.81, 144.76, 139.91, 138.73, 131.46, 129.31	181.06, 156.79, 136.53, 135.59, 132.68, 123.09, 113.94

must be resonating in this region. In HSQC spectrum of troponyl lactone **25**, the peaks at δ 153.89 and 152.81 ppm have not shown any cross peaks (**Figure A61&62**, Appendix two). Which revealed that these two peaks belongs to amine attached quaternary carbon and cationic quaternary carbon. However, we have recorded the ^{13}C NMR spectra of troponyl lactone **24** in CD_3CN in the range of δ 0-250.0 ppm to check whether the cationic carbon of troponyl ring is more deshielding than the carbonyl carbon peak (δ 182.0 ppm) of troponyl ring in the peptides.

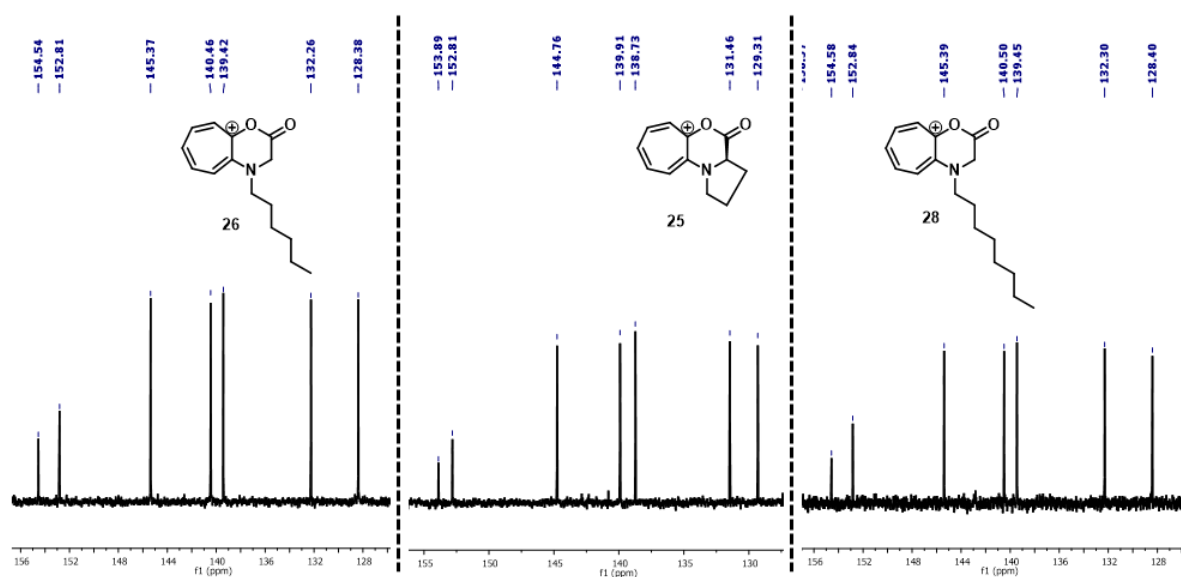


Figure 3.13 ^{13}C NMR chemical shifts of troponyl ring in synthesized lactones (**25/26/28**)

In the obtained ^{13}C NMR spectra, we found no peak after δ 170.0 ppm. Interestingly, in the literature, the appearance of cationic carbon signal of tropylium cation in the region of δ 150-160.0 ppm is well-reported.¹⁶ The ^{13}C NMR spectrum of tropylium ion tetrafluoroborate salt in CD_3CN has shown only one signal that corresponds to all carbons of tropylium cation ring at δ 156.87 ppm.¹⁶ This is due to chemical equivalent nature of tropylium cation carbons. Whereas the appearance of seven different peaks for cationic troponyl ring of lactones synthesized in present study is due to their chemical inequality. From the experimental results and literature reports, we conclude that the cationic carbon of troponyl ring is resonating in the region of 150-160.0 ppm, especially one of the peaks at δ 153.89 and 152.81 ppm and it is in good agreement with the literature reports.

Importantly, troponyl ring carbon chemical shifts are almost same for the all troponyl lactones (**24-28**) synthesized in present study with the variation of lesser or greater than δ 1.0 ppm. In **Figure 3.13**, an expanded spectral region of three different lactones (**25/26/28**) are depicted and labeled with their respective structures. All these three spectra have shown similar

peak pattern and chemical shift values. The chemical shift values of these lactones are given in **Table 3.4** (column 3).

Further, the cationic troponyl lactone formation was confirmed by ESI-MS. ESI-MS spectra of troponyl lactone **24** is depicted in **Figure 3.14**, where the molecular ion peak of troponyl lactone **24** and *tri*-peptide peaks **10h** was clearly observed. The formation of troponyl lactone **24** was examined with three *Traeg* peptides, in all cases troponyl lactone **24** molecular ion peak was consistently observed in their respective spectra (see appendix). Other cationic troponyl lactones **25-28** also have shown their mass peaks in their mass spectra. Interestingly, the formation of cationic troponyl lactone was further confirmed by UV/Vis spectroscopic studies. However, we tried to purify the cationic troponyl lactone through extraction and recrystallization methods. During extraction, the addition of water to the dichloromethane solution of crude product leads to instant formation of carboxylic acid derivative. On the other hand we were not able to crystalize the synthesized lactones.

Overall, the unusual cleavage of *Traeg* amides into cationic troponyl lactones in presence of 6 *equiv.* of TFA (5.0%) is established. The cationic lactones synthesized in this study are well-characterized by NMR, ESI-MS and UV/Vis studies.

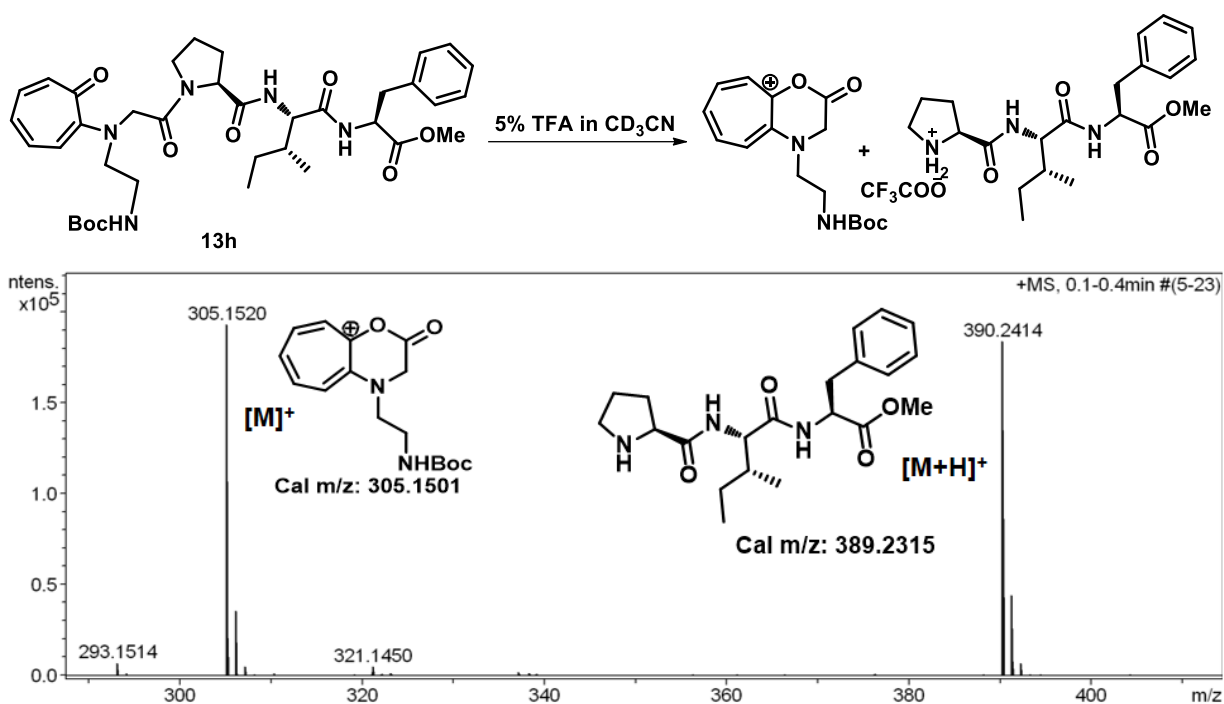
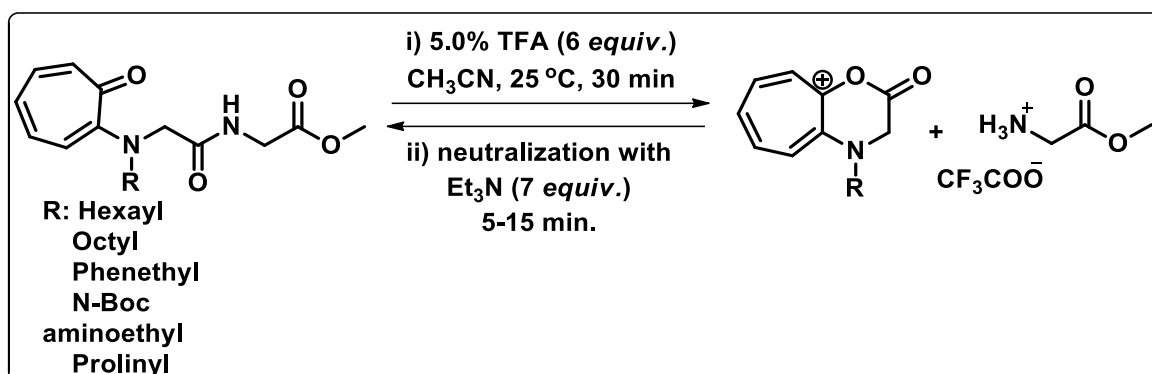


Figure 3.14 ESI-MS spectra of cationic troponyl lactone **24**.

3.2.8 Cationic troponyl lactone facilitated reversible amidation

The conversion of cationic troponyl lactone into ester with the addition of alcohol encouraged us to test the reactivity of amine nucleophile instead of hydroxyl nucleophile. We envisioned that a primary amine is a much stronger nucleophile than hydroxyl group, hence, it may be possible to obtain a mixture of products such as starting material and aminotroponimine



Scheme 3.8 Reversible amidation reaction.

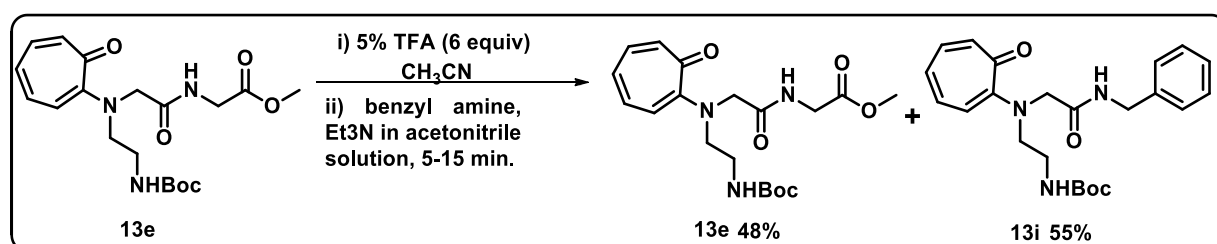
derivatives after neutralization of the reaction mixture with organic base, triethylamine. But as explained above, exclusively starting material was obtained (**Scheme 3.8**). The starting materials were obtained after reaction are in the range of 60 – 80% isolated yields (Table 3.5).

Table 3.5 Isolated yields of reverse amidation reaction

entry	compound	isolated yield (%) of starting materials after reverse amidation
1	13e	74
2	9G	69
3	19	79
4	21	66
5	23	71
6	13f	63
7	9F	60

3.2.9 Transamidation

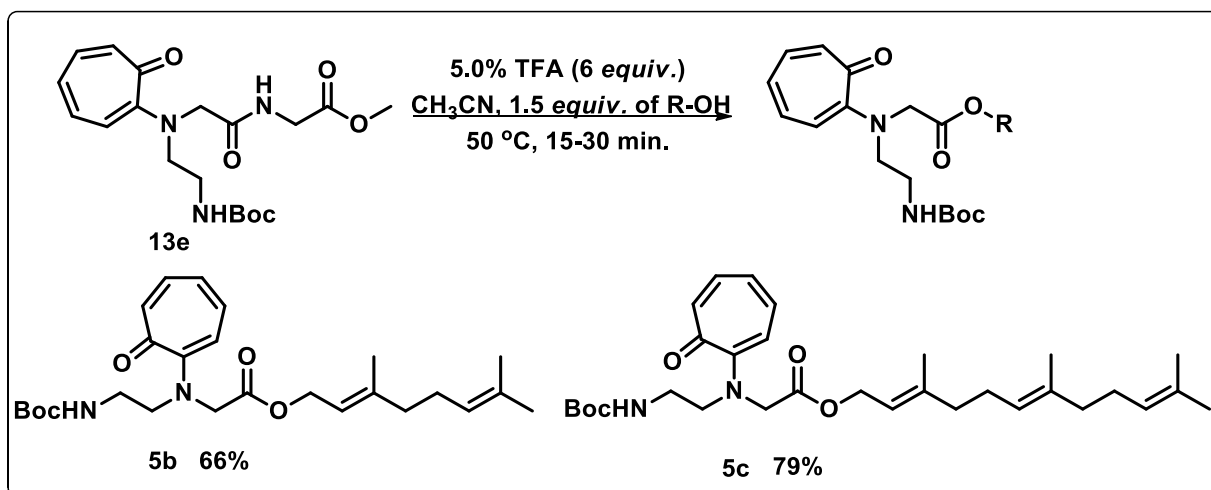
We also tried the transamidation reaction with cationic troponyl lactone reaction mixture, the reaction mixture was added to the acetonitrile solution of the other primary amine with 6 equiv of triethyl amine. We did not observe any exclusivity in reaction, obtained a mixture of products such as starting material and another peptide with newly added primary amine in equal ratio (**Scheme 3.9**).



Scheme 3.9 Transamidation reaction with benzyl amine.

3.2.10 Transesterification:

We demonstrated the use of *Traeg* as a protecting group for alcohols such as geraniol and farnesol under milder conditions (**Scheme 3.10**). The products were obtained in good yield without affecting ethylene groups.



Scheme 3.10 Transesterification with Geraniol and Farnesol.

3.2.11 UV-Visible studies

Tropolone and its derivatives are UV active. Therefore, we have attempted to study the formation of cationic troponyl lactone and its conversion into ester after addition of alcohol by UV/Vis spectroscopy. The *Traeg* monomer **5a** and *Traeg* peptides **13f/13g/13h** and control peptide **15** was considered for this study. The UV/Vis spectra of these compounds was recorded in non-nucleophilic solvent, anhydrous CH_3CN , before and after addition of TFA. Observed spectral parameters are provided in the **Table 3.6**. The absorption spectrum of peptide **13h** in CH_3CN has shown two absorption peaks at 352 and 410 nm and after addition of TFA (20 μL in 3.0 mL cuvette under given concentration) to the same sample these two absorption peaks disappeared and only one intense absorption peak was observed at $\lambda = 362$ nm (**Figure 3.15A**).

Table 3.6 Observed absorption peaks of *Traeg* peptides, *Traeb* peptide and monomers after addition of TFA and methanol.

entry	observed absorptions (nm) in ACN	observed absorptions (nm) in ACN+TFA (20 μL)	observed absorptions (nm) in ACN+TFA+MeOH (20 μL)
13f	348.0, 395.0	362.0	350.0, 391.0
13g	347.0, 397.0	362.0	352.0, 392.0
13h	352.5, 410.0	362.0	350.0, 391.0
5a	346.0, 402.0	348.0 386.0	348.0, 395.0
15	351.0, 407.0	311.0 386.0	313.0 388.0

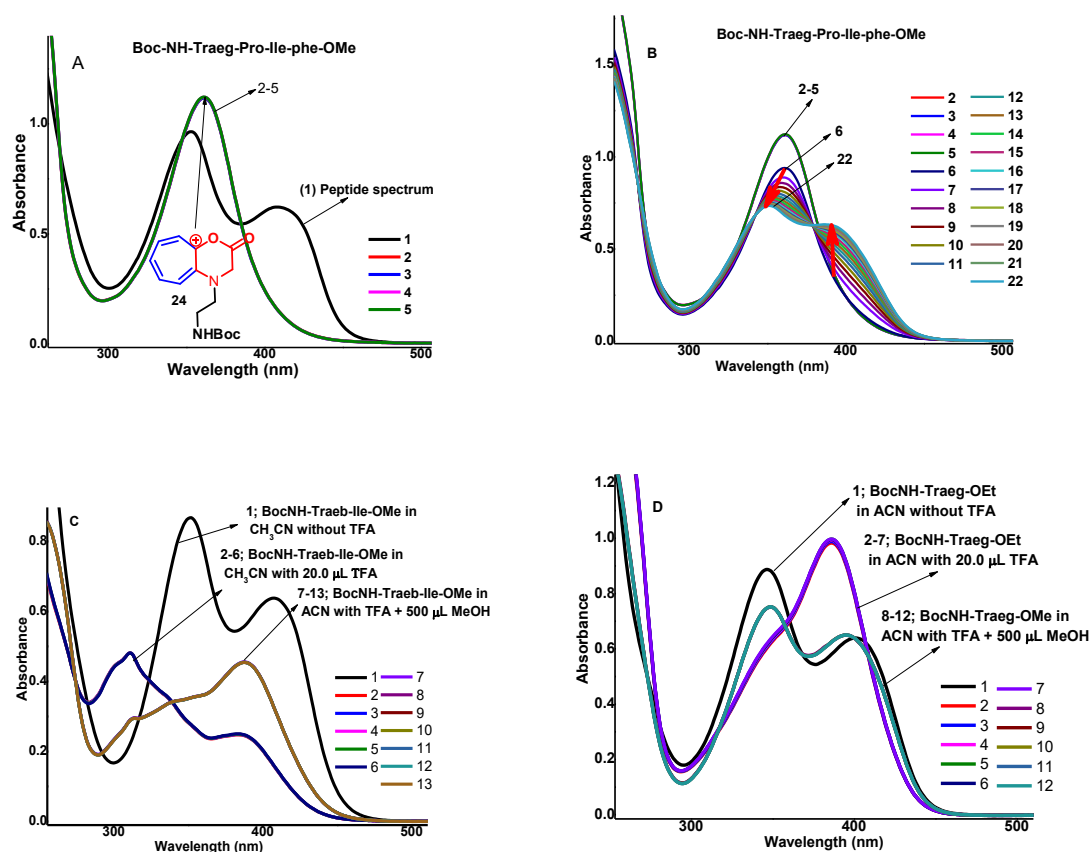


Figure 3.15 (A) Absorption spectra of BocNH-*Traeg*-Pro-Ile-Phe-OMe (**13h**, black) and lactone (**24**, green). (B) Conversion of troponyl lactone into methyl ester (7-22; each spectra recorded with two minutes time intervals). (C) Absorption studies of BocNH-*Traeb*-Ile-OMe (**15**). (d) Absorption studies of BocNH-*Traeg*-OEt (**5a**). All spectra were recorded with two minutes time intervals.

Before recording the absorption spectra after addition of TFA and the resultant solution was shaken well. And interestingly, the addition of excess methanol (500 μL) to the same sample leads to slow conversion of one absorption peak into two absorption peaks. The clear change in absorption spectra after addition of TFA to the peptide sample witnessed the formation of methyl ester of monomer. The similar absorption changes were observed with other *Traeg* derived peptides such as **13f/13g** in acetonitrile. In contrast, the control peptide **15** and monomer **5a** has not shown similar changes like *Traeg* peptides (See Figure 3.15). In case of control peptide and monomer, after addition of TFA a single and sharp absorption peak was

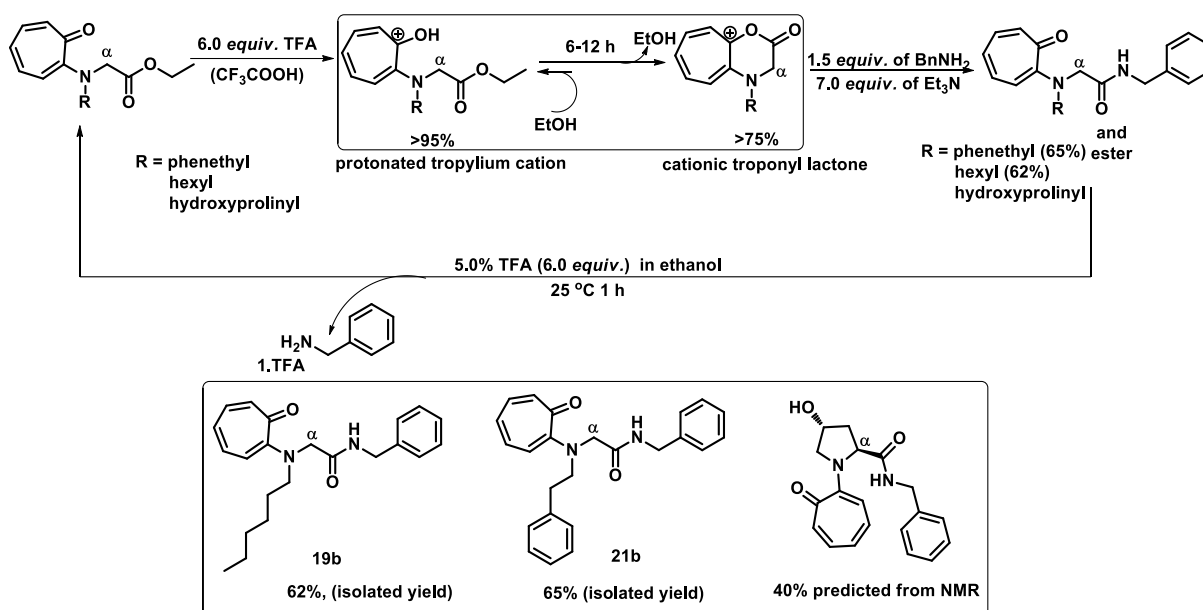
not observed, instead, the absorption peaks with shoulder peaks was observed (**Figure 3.15C&D**).

Overall, UV/Vis studies further strongly supported the formation of cationic troponyl lactone after cleavage of *Traeg* amide bond in acetonitrile in presence of TFA (here 20.0 μ L of TFA is added to the 3.0 mL peptide solution) and its further conversion into ester after addition of excess methanol.

3.2.12 Comparative control studies of lactone formation with monomers and peptides:

In fact, it is important to realize that the troponylglycinate esters are able to convert into cationic troponyl lactone or not, in contrast to troponylglycinate amides, in presence of 6.0 equiv. of TFA in CH_3CN . Hence, it is necessary to perform control studies with troponylglycinate esters under the same conditions to understand the relative reactivity of troponylglycinate amides and esters towards the formation of cationic troponyl lactone.

These control studies were carried out by performing the ^1H and ^{13}C NMR experiments. For that reason, the troponylglycinate esters **18/20** were treated with 6.0 *equiv.* of TFA in CD_3CN and recorded ^1H and ^{13}C NMR spectra. Changes in ^1H and ^{13}C NMR spectra were observed after addition of TFA like in case of troponylglycinate esters also (**Figure 3.12**). But the observed changes were fascinating in contrast to changes observed in the obtained ^1H and ^{13}C NMR spectra after troponylglycinate amide cleavage (**Figure 3.12 and 3.16/17**). The amide is cleaving into cationic troponyl lactone in less than 30.0 minutes in presence of 6.0 *equiv.* of TFA. Which means, the ^1H and ^{13}C NMR signals representing the peptide peaks are completely disappeared in their spectra after TFA treatment and obtained ^1H and ^{13}C NMR spectra contains peaks, only those represents cationic troponyl lactone and glycine ester (**Figure 3.12**).



Scheme 3.11 Conversion of troponylglycinate esters into cationic troponyl lactones *via* protonated esters, followed by base mediated amidation of cationic troponyl lactones.

In contrast, in case of troponylglycinate ester **18/20**, in addition to cationic troponyl lactone peaks, another set of peaks were observed (**Figure 16/17**). These peaks appearing most probably due to protonation of troponone carbonyl, which is more pronounced in acidic medium (**Scheme 3.11**). The formation of protonated troponyl cation is further witnessed by disappearance of troponyl carbonyl peak in ¹³C NMR spectra at $\sim \delta$ 180 ppm. However, appearance of ester carbonyl carbon peak at $\sim \delta$ 169.00 ppm and protonated cationic troponyl carbon at $\sim \delta$ 166.25 ppm reveals that the troponylglycinate esters are not converting into cationic troponyl lactone completely, even after 8-12 hours. (In case of amides, after treatment with TFA, amide carbonyl carbon peak in ¹³C NMR is completely disappeared). Relative to troponylglycinate amides, formation of cationic troponyl lactone from troponylglycinate esters is very slow.

These observations supports that, after addition of TFA, troponylglycinate esters and amides are first converting into protonated troponyl cationic form of esters and amides (**Scheme 3.11**). The protonated troponyl cation is further slowly converting into cationic

troponyl lactone with time. After six hours of addition of TFA, ~75.0% of protonated tropylium cationic ester is converted into cationic troponyl lactone. However, complete conversion of protonated form of tropylium cationic esters into lactone was not observed even after two days. This is happening due to reversible esterification (slow conversion of cationic troponyl lactone into protonated esters). While in case of amide cleavage, reversible reaction is not possible due to immediate protonation of cleaved free amine nucleophile as ammonium salt in TFA.

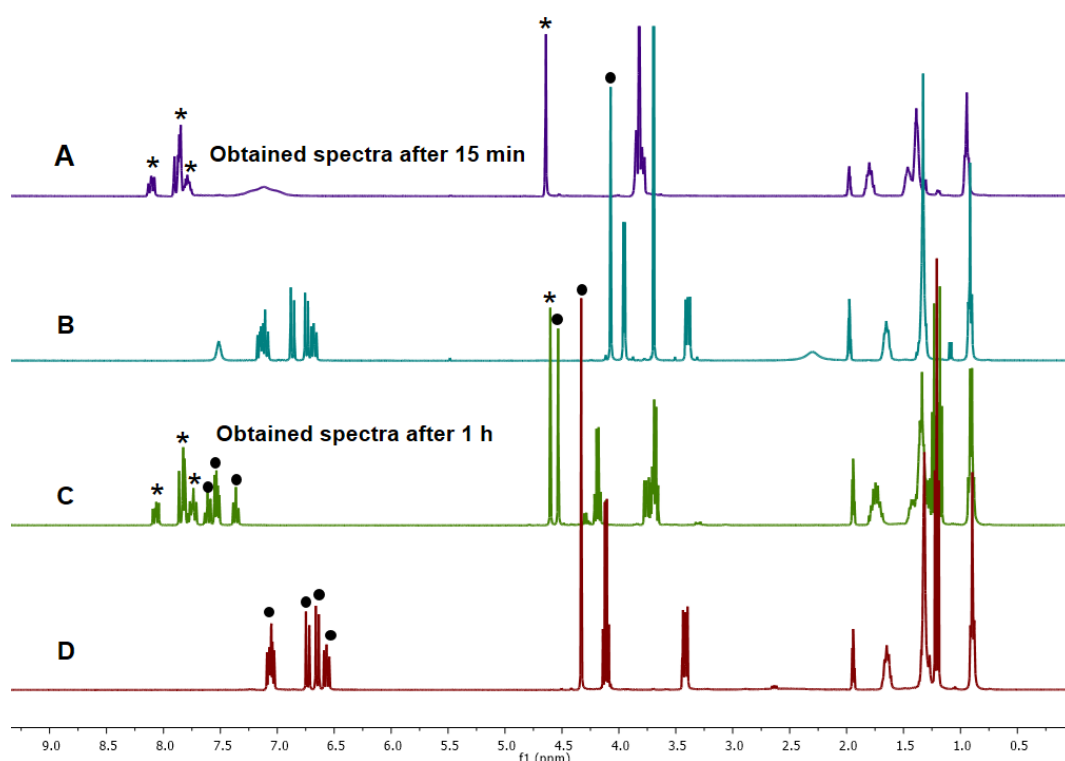


Figure 3.16 A) ¹H NMR of cationic troponyl lactone (**26**) obtained from peptide in CD₃CN. B) ¹H NMR of *Trhg-Gly* peptide (**19**) in CD₃CN. C) ¹H NMR of *Trhg* monomer **18** after addition of TFA (containing protonated form of monomer and cationic troponyl lactone) D) ¹H NMR of *Trhg* monomer **18** in CD₃CN. (*represent cationic troponyl lactone peaks, solid circles represents protonated monomer peaks).

More interestingly, the addition of 1.5 *equiv.* of amine and neutralization with sufficient amount of triethylamine (6.0-7.0 *equiv.*) results in instant formation of amide. Which transformation was established during reversible amidation. This results further strongly supports the conversion of troponylglycinate esters into cationic troponyl lactone.

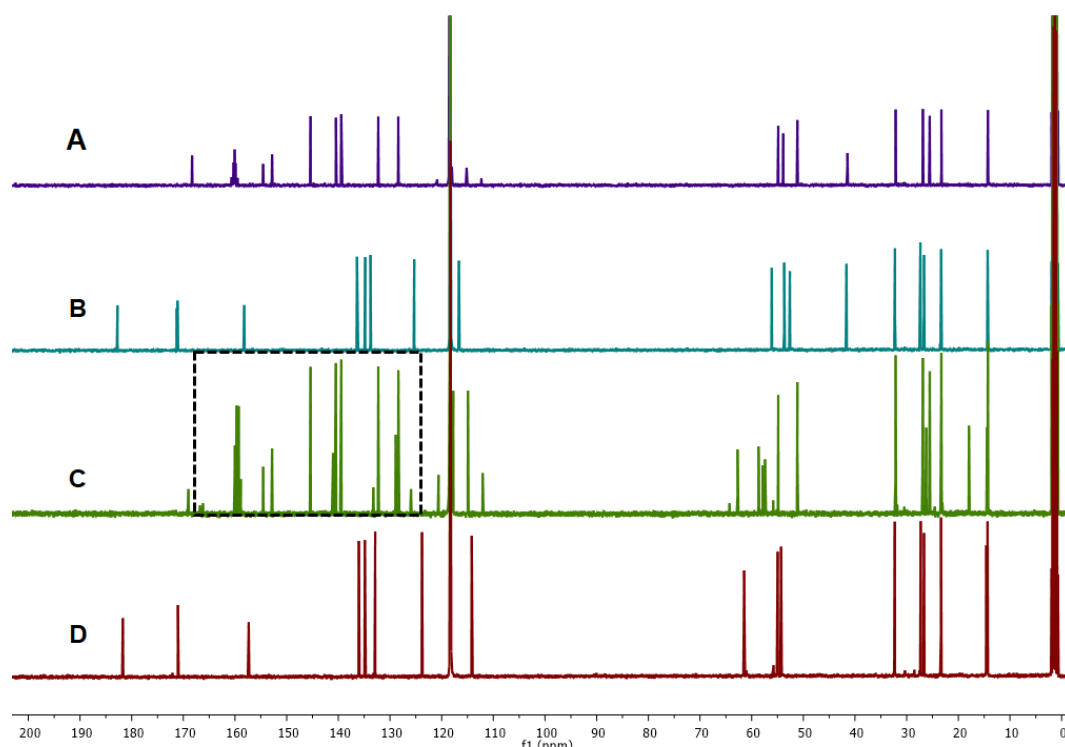


Figure 3.17 A) ^{13}C NMR of cationic troponyl lactone (**26**) obtained from peptide in CD_3CN . B) ^{13}C NMR of *Trhg-Gly* peptide (**19**) in CD_3CN . C) ^{13}C NMR of *Trhg* monomer **18** after addition of TFA (peaks represents protonated form of monomer and cationic troponyl lactone (**26**)). D) ^{13}C NMR of *Trhg* monomer **18** in CD_3CN .

The characteristic chemical shift values that differentiate protonated tropylium cation and cationic troponyl lactone are provided in **Figure 3.18**.

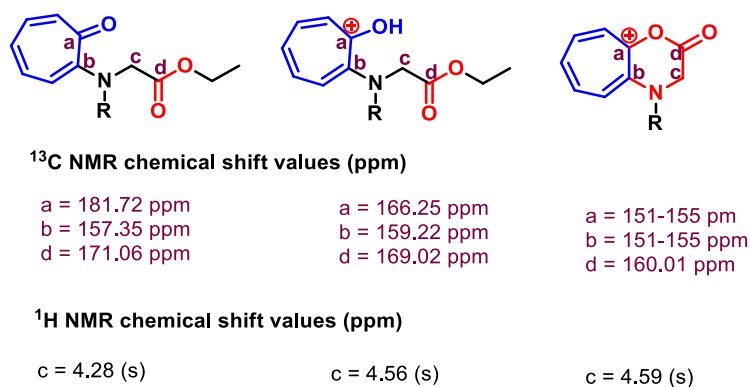


Figure 3.18 ^1H and ^{13}C NMR signals considered for comparative studies.

Overall, N-alkyl troponylglycinate esters are also converting into cationic troponyl lactone. However, the rate of conversion of troponylglycinate esters into cationic troponyl lactone is very slow when compare to troponylglycinate amides.

3.2.13 Control studies

Amide cleavage studies of BocNH-Traeb-Ile-OMe (15) and BocNH-Bnaeg-Phe-OMe (16): Further, we confirmed the regioselective amide cleavage of *Traeg* amide by performing the control experiments. For that reason, control dipeptides **15/16/17** were treated with 5.0% TFA in CD₃OD and recorded the time dependent ¹H NMR spectra. These control dipeptides **15/16/17** has shown only the downfield shift in their proton signals after the addition of TFA (Figure 3.19).

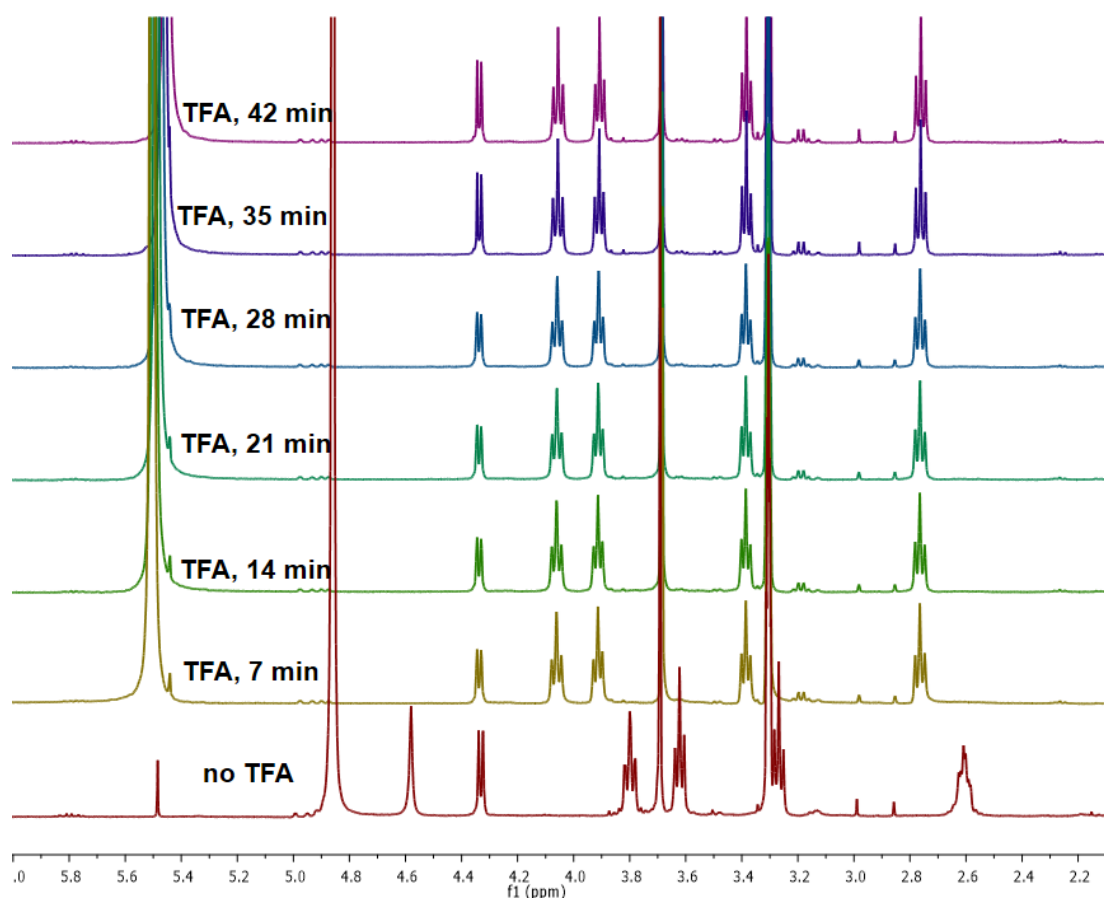


Figure 3.19 Time dependent ¹H NMR spectra of BocNH-Traeb-Ile-OMe in CD₃OD.

The mass spectra of control *di*-peptides **15/16** remained unchanged after one hour of TFA treatment. As expected, Boc deprotection was observed from the mass spectra of both control peptides **15/16** after leaving the same NMR samples for longer time, overnight under same conditions.

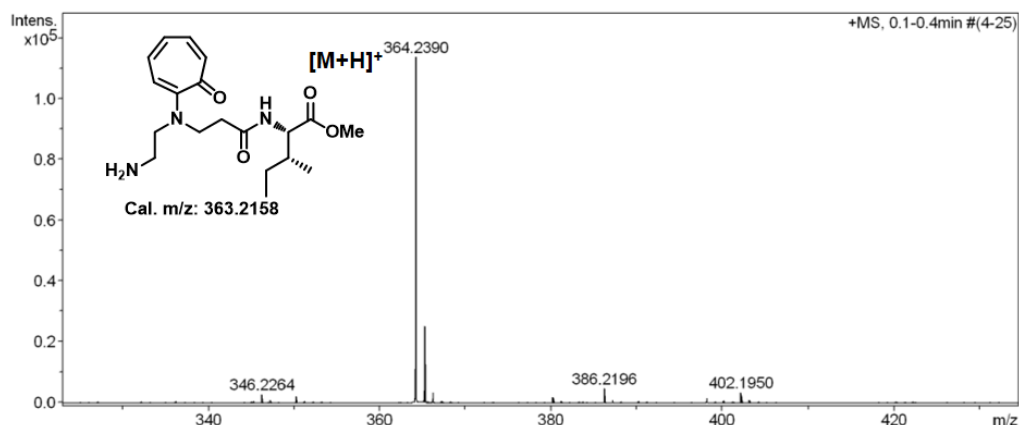
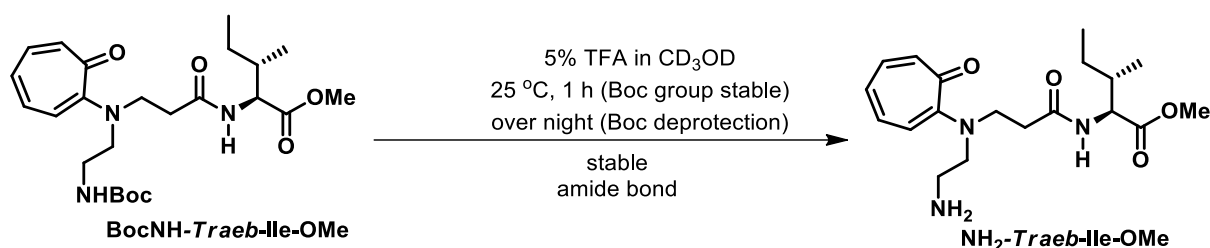


Figure 3.20 Scheme of Boc deprotection and ESI-MS spectrum of NH_2 -*Traeb*-Ile-OMe.

The mass spectra of Boc-deprotected *Traeb*-Ile-OMe is provided in **Figure 3.20**. These comparative studies revealed that only *Traeg* derived amide bonds are cleavable in the presence of 5% TFA.

Overall, these control studies revealed that troponyl moiety and glycinate α -methylene group are playing key role in the cleavage of *Traeg* and other troponylglycinate esters and amides.

3.2.14 Deuterium entrapment at α -methylene group:

Since the troponylglycinate esters and amides are behaving anomalously towards cleavage of acyl carbon and hetero atom bond in presence of 6.0 *equiv.* of TFA, it is important to find the cause for their unusual reactivity. Moreover, in the literature most of the ester and amide bonds are highly stable under these conditions.¹⁻⁷ More importantly, peptide nucleic acids, containing similar glycinate unit are also stable.^{42,43}

On the other hand, it is worth mention that the aminoethyl troponyl- β -alanate amide, a homologative derivative of troponylglycinates is also stable under the same conditions. Furthermore, aminoethyl benzylglycinate amide is also stable, where the troponyl ring is replaced by benzyl ring.

Hence, the troponylglycinate esters and amides are opting an alternative pathway for the cleavage of acyl carbon and heteroatom bond, other than conventional route. From the above control studies, it has been witnessed that the troponyl ring and glycinate α -methylene groups are must be playing a prominent role in the amide and ester cleavage of troponylglycinates. So far, NMR and UV/Vis studies revealed the role of troponyl ring in this unusual transformation. Especially, in case of ester conversion, the protonated tropylium cationic form of monomer was characterized by NMR in CD_3CN . Which revealed that the first step occurring in this process is protonation. After this step, the protonated form of monomer ester is slowly converting into cationic troponyl lactone. Hence, it is clear that the protonation of the troponyl carbonyl is key step in this process.

However, another clarity required in this process is, how the protonation of tropone carbonyl of monomer is driving it towards the cleavage of ester and amide bond. In the literature, we found that the conversion of carboxylic acid derivatives into *ketenes* containing electron withdrawing groups at α -carbon atom is well-established.⁵¹⁻⁵⁵ Moreover, solvolysis of amide bond via ketene intermediate is also well-known.⁵¹⁻⁵⁵

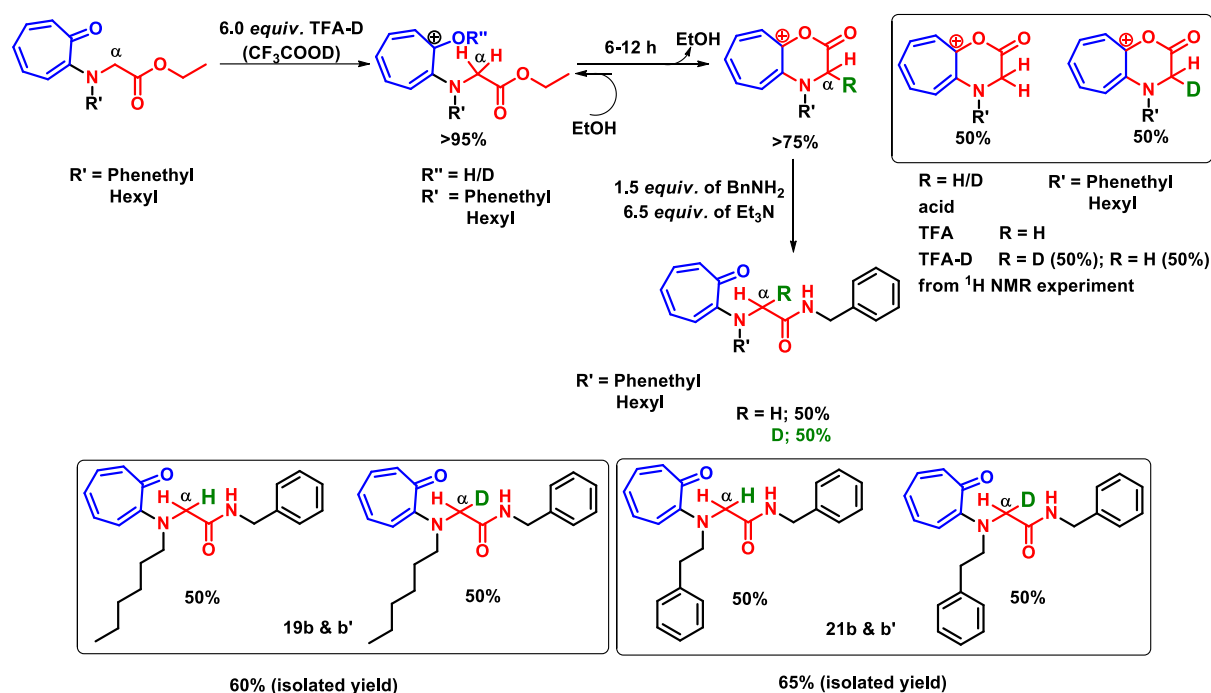
Hence, we assume that troponylglycinate amide and esters are also following the same pathway, what is reported. Because, the protonated tropylium cationic form of ester and amides must be acting as an electron withdrawing group. Moreover, the formation of cationic troponyl lactone in acetonitrile revealed that the amide and ester carbonyls are must be converting into highly reactive electrophiles for the addition of less nucleophilic troponyl carbonyl oxygen. Otherwise the addition of troponyl carbonyl oxygen at carbonyl carbon of amides and esters is

may not be possible owing to their stability. From these facts and literature, we realized that these esters and amides are converting into *ketene* intermediates, which formation is induced due to protonation of troponyl carbonyl and further reacting with troponyl carbonyl oxygen and alcohols. However, it is important to provide proper experimental results which supports our assumption.

If the troponylglycinate esters and amides are converting into cationic troponyl lactone through direct nucleophilic addition without the involvement of the glycinate α -methylene group, then ketene formation is ruled out in this transformation. If this transformation is occurring with the involvement of glycinate α -methylene group, then formation of ketene is more pronounced. Importantly, in the literature, the deprotonation of the α -methylene - $\text{CH}_2\text{C}=\text{O}$ facilitates the ketene formation $\alpha\text{-CH}=\text{C}=\text{O}$ and reprotonation of the ketene $\alpha\text{-CH}=\text{C}=\text{O}$ takes place after addition of nucleophile at carbonyl carbon. Overall, deprotonation and reprotonation of the α -methylene group plays an important role to proceed this transformation via *ketene* formation.

Hence, we take this advantage of reprotonation of *ketene*, and we assumed that, if we use the deuterated trifluoroacetic acid, instead of trifluoroacetic acid, if, the reaction is proceeding through ketene intermediate, during reprotonation of ketene, deuteration may occur instead of protonation, since the medium is rich with deuterium cation.

To confirm the above assumption, we performed the reaction with troponylglycinate monomers in presence of 6.0 *equiv.* of deuterated trifluoroacetic acid in CD_3CN , to convert monomers into cationic troponyl lactones.



Scheme 3.12 Conversion of troponylglycinate esters into cationic troponyl lactones via protonated esters, followed by base mediated amidation of cationic troponyl lactones.

After, 6 hours of addition of TFA-D, ^1H NMR of reaction mixture was recorded. Most surprisingly, we found the formation of a triplet peak in ^1H NMR at δ 4.54 ppm (**Figure 3.21**, represented in solid triangle). The ^1H NMR spectra obtained from the reaction performed with TFA-H does not contain any triplet at that particular position (**Figure 3.21**). We assume, the appearance of triplet is most probably due to deuteration at α -methylene group. Further, in ^{13}C NMR spectra two extra peaks were observed at δ 50-51.0 ppm, which is not found in the spectra obtained with TFA-H. The appearance of these peaks are due to splitting of CDH carbon in to triplet owing to nuclear spin of deuterium, which is one (**Figure 3.22**, one of the peaks of triplet is merged with its adjacent peak). Most importantly, in the ^{13}C DEPT135 NMR spectra of the same reaction mixture, clear triplet was observed in above, where CH_3 and CH will appear (**Figure 3.23**). This strongly supports the deuteration of glycinate α -methylene group during conversion of esters into cationic troponyl lactone in presence of deuterated trifluoacetic acid.

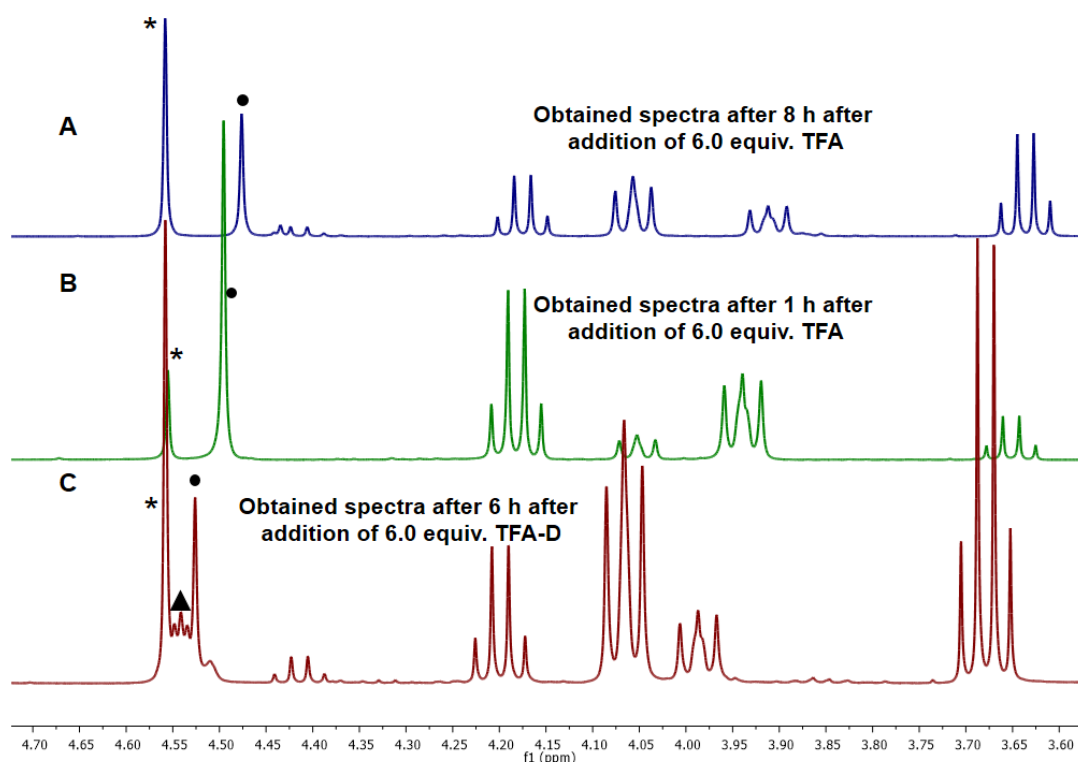


Figure 3.21 A) ^1H NMR spectra of Troponylglycinate 20 in CD_3CN after addition of TFA after 8 h. B) ^1H NMR spectra of Troponylglycinate 20 in CD_3CN after addition of TFA after 1 h. C) ^1H NMR spectra of Troponylglycinate 20 in CD_3CN after addition of TFA-D after 6 h. (* represents cationic troponyl lactone peaks; solid circles represents protonated monomer and solid triangle represents the CHD peak)

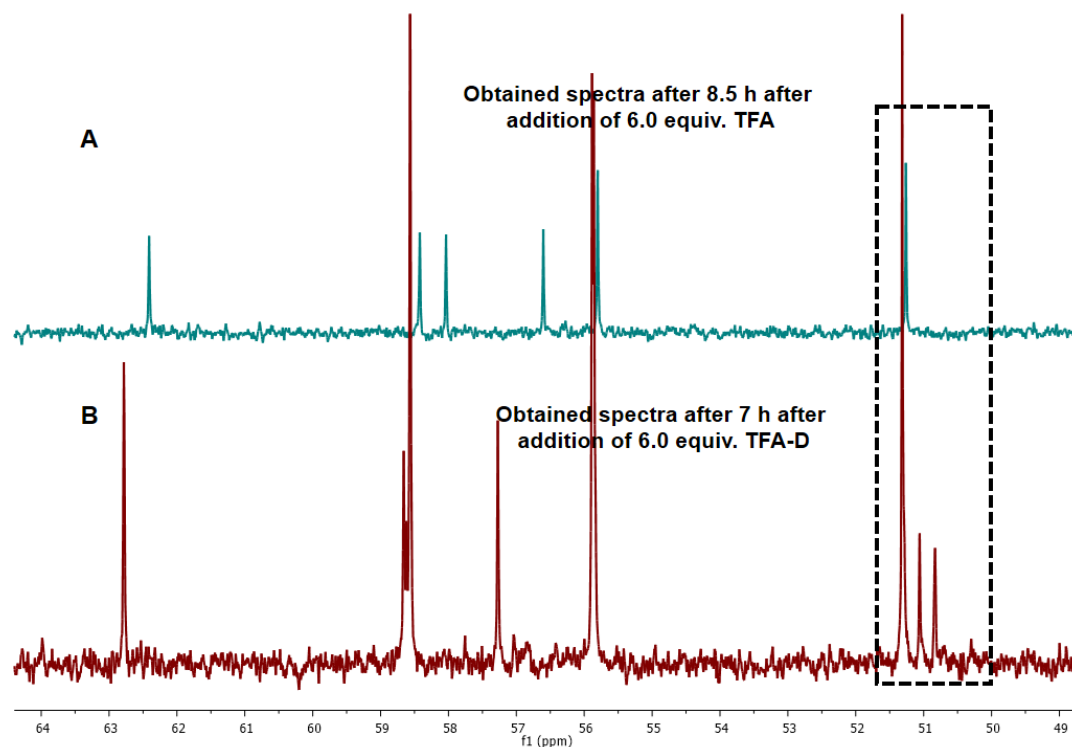


Figure 3.22 A) ^{13}C NMR spectra of *Trpeg* undeuterated lactone (obtained spectra after addition of TFA after 8 h). B) ^{13}C NMR spectra of *Trpeg* deuterated and undeuterated lactone. (obtained spectra after addition of TFA after 7 h)

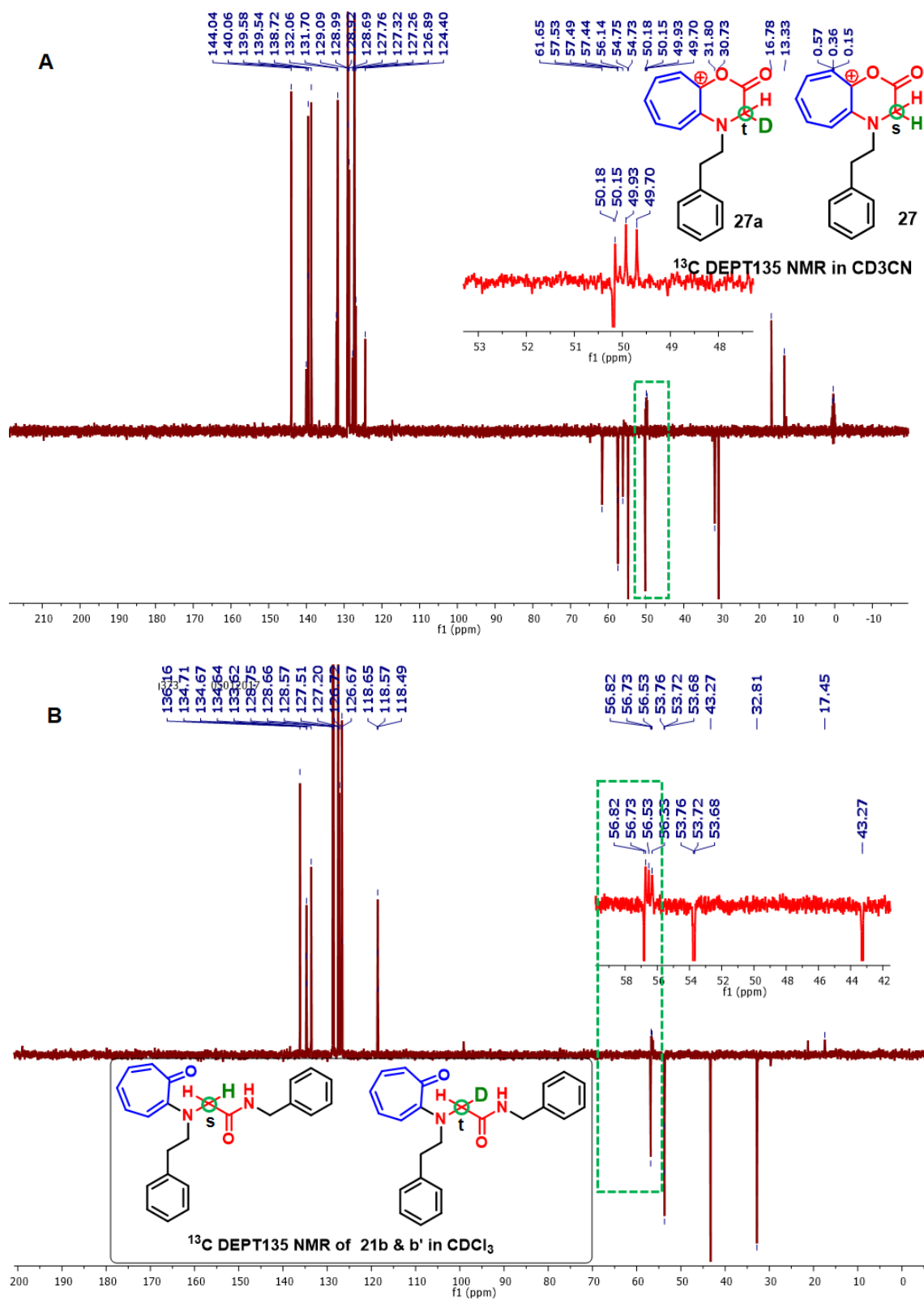


Figure 3.23 A) ^{13}C DEPT135 NMR spectra of deuterated and undeuterated *Trpeg* lactone in CD_3CN [green highlighted box represents triplet appeared due to CHD carbon]. B) ^{13}C DEPT135 NMR spectra of deuterated and undeuterated *Trpeg* and benzylamine dipeptide in CD_3CN [green highlighted box represents triplet appeared due to CHD carbon].

The same reaction mixture is allowed for amidation under optimized condition for reversible amidation (Scheme 3.8). The obtained cationic troponyl lactone is successfully converted into amide (Scheme 3.12). The ^{13}C DEPT NMR spectra of respective amide has also shown a triplet peak that represents deuterated $\underline{\text{CDH}}$ carbon atom (**Figure 3.23**). Further, the amide obtained from cationic troponyl lactone generated in presence of TFA-H has shown mass peak m/z at 395 $[\text{M}+\text{Na}]$ (**Figure 3.24A**) and the amide obtained from cationic troponyl lactone generated in presence of TFA-D has shown mass peak at m/z 396 $[\text{M}+\text{Na}]$ (**Figure 3.24B**). Only one unit difference was observed, this further strongly supported the deuteration at α -methylene group.

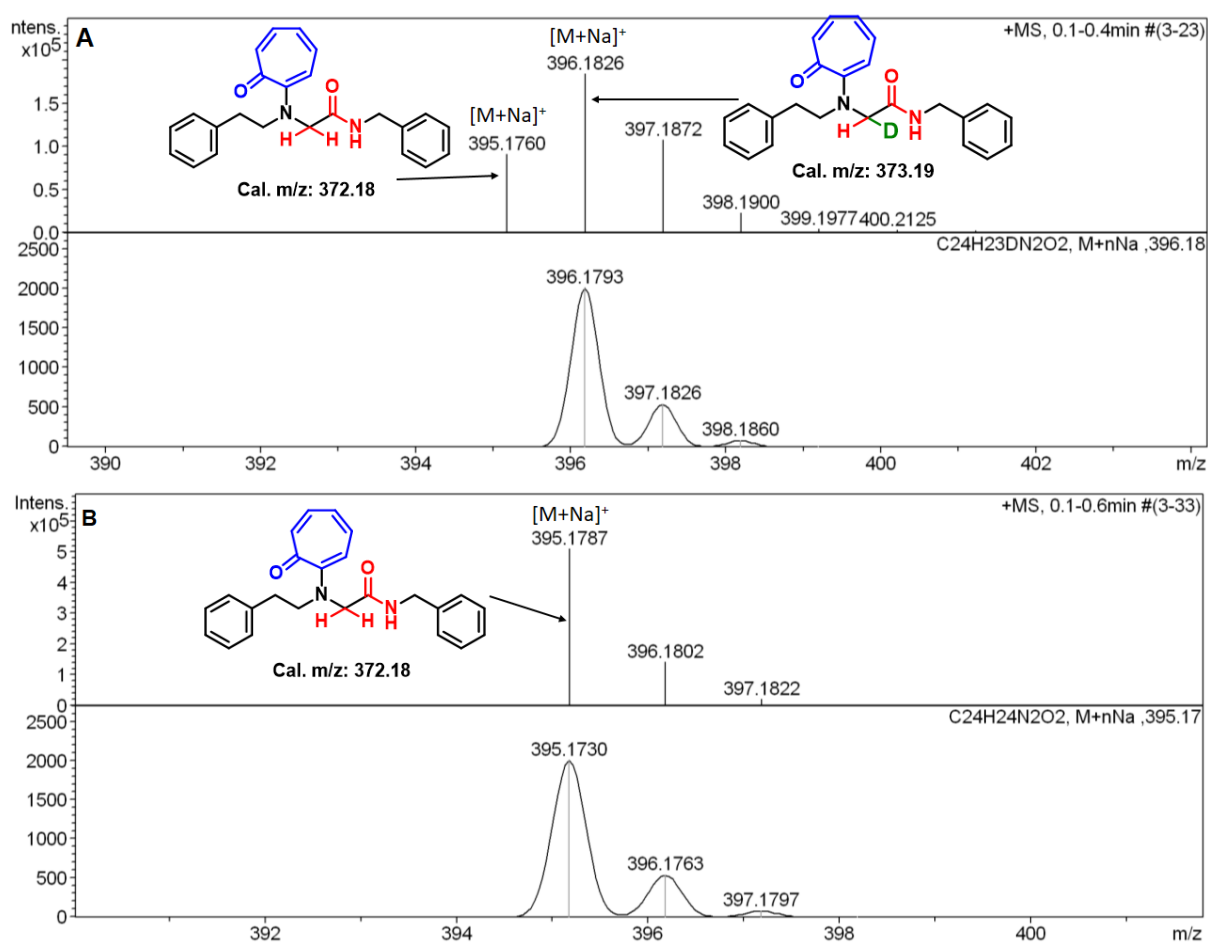


Figure 3.24 A) HRMS spectra of *Trpeg* and benzylamine deuterated peptide. B) HRMS spectra of *Trpeg* and benzylamine undeuterated peptide.

The deuteration at α -methylene group occurs only if the reaction proceeds through ketene intermediate. Because, simple enolization of ester or amide in presence of 6.0 *equiv.* of TFA is not known. However, α -deuteration of amino acids are reported in presence of ruthenium catalyst and D₂O as deuterium source at 135 °C and for very long time 36 h.⁶³ Hence, deuteration through simple enolization is not possible.

Overall, deuteration at α -methylene group is established in presence of deuterated trifluoroacetic acid. The deuteration at α -methylene group strongly supports that the conversion of troponylglycinate esters and amides into cationic troponyl lactone and esters is via reactive *ketene* intermediate.

3.2.15 Proposed *Traeg* amide cleavage reaction mechanism:

The regioselective cleavage of *Traeg* amide bond in presence of other *non-Traeg* amides encouraged us to propose a plausible reaction mechanism for *Traeg* amide cleavage.

Notable events in the *Traeg* amide cleavage are,

- (i) Only *Traeg* derived amide bonds (**13/19/21/23/9G/F**) are cleavable selectively and other *non-Traeg* amide bonds in the same molecule are stable.
- (ii) Reaction requires acidic conditions (5.0% TFA (6 *equiv.*) or 2.0 *equiv.* of PTSA or 1.0 N HCl).
- (iii) The amide bond derived from troponyl aminoethyl β -alanine (**15**), a homologative derivative of *Traeg* is stable under these conditions.
- (iv) The amide bond derived from benzyl aminoethylglycine (**16**), where Troponyl ring is replaced with benzyl group, is also stable.
- (v) In alcoholic solvents the *Traeg* amide was directly converted into ester after amide cleavage.

- (vi) Whereas in acetonitrile, the *Traeg* amide was cleaved into *cationic troponyl lactone* (**24-28**).
- (vii) The obtained troponyl lactone was further converted into ester in presence of excess alcohol.
- (viii) Most importantly, the cationic *troponyl lactone* was converted back to starting material instantly after neutralization of reaction mixture containing Troponyl lactone and respective free amine salt.

These events in the *Traeg* amide cleavage revealed that the reaction is not proceeding through the conventional mechanism of amide hydrolysis. The non-*Traeg* amides in the same molecule and control peptides **16/17** are stable under same conditions, which means that the troponyl moiety is playing a key role in this amide cleavage reaction. Further, the *Traeb* control amide (**15**) is stable under same conditions, hence, undoubtedly α -CH₂ of *Traeg* peptides is taking part in this amide cleavage reaction. Hence, troponyl moiety and α -CH₂ of *Traeg* peptides are playing key role in this acid mediated amide cleavage reaction.

The reaction is occurring in acidic medium and the protonation of troponyl carbonyl group is well-known in acidic medium which leads to the formation of stable tropylium cation.⁵⁶ Hence, the protonation of troponyl carbonyl in peptide **13** preferably occurs in TFA and leads to the formation tropylium cation, which is further stabilized by delocalization of charge via troponyl ring. And protonation of amide carbonyl in acidic medium is also well-reported. Therefore, the protonation of troponyl carbonyl and amide carbonyl may facilitates the *enolization* of α_1 -CH₂ protons. After enolization of amide carbonyl, since there will be no resonance between the carbonyl and nitrogen of amide, further the *protonation* of the amide N-atom may occurs in acidic medium. Consequently, the cleavage of the amide C-N bond is furnished by liberation of reactive *ketene* intermediate and respective amine derivative **10**.

The newly generated *ketene* intermediate proceeds towards nucleophilic addition to convert into stable ester/acid in presence of respective nucleophilic solvents alcohol/water. The hydrolysis of amide bond via the formation of *ketene* intermediate is illustrated in the literature.^{41,51-55}

Interestingly, in acetonitrile, *cationic troponyl lactone* was obtained, which means the ketone carbonyl of troponyl moiety is acting as nucleophile and reacting with electrophilic ketene intermediate. However, the direct attack of troponyl carbonyl at amide carbonyl carbon through nucleophilic addition is may not be possible. Because, as it is discussed already, the alkylation of troponyl ketone carbonyl requires a strong electrophilic donor triethyloxonium tetrafluoroborate. And particularly, the amide carbonyl is not such strong electrophile. Therefore, we assume that the direct attack of troponyl carbonyl at amide carbonyl and leading to formation of troponyl lactone is may not be possible.

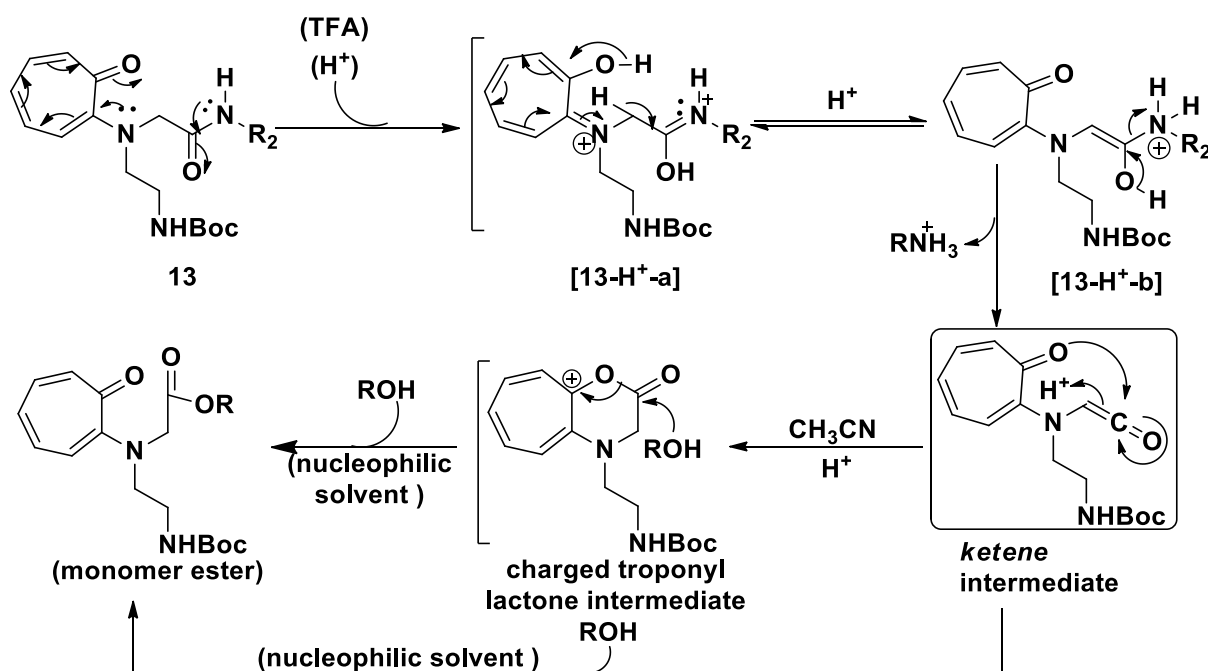


Figure 3.25 Possible mechanism of *Traeg* amide bond cleavage

Hence, most probably the *Traeg* amide cleavage reaction is occurring through the formation of *ketene* intermediate. We attempted to characterize the *ketene* intermediate in

anhydrous $\text{CH}_3\text{CN}:\text{TFA}$ (5.0%) but it is ended with *lactone* intermediate. However, the isolation of reactive *ketene* intermediate, having electron withdrawing group is difficult, especially at low pH in presence of nucleophilic solvents.⁵¹⁻⁵⁵ But in case of troponylglycinate esters, we have used TFA-D instead of TFA, to probe the role of $\alpha\text{-CH}_2$ group in this unusual cleavage of amide bond. Interestingly, deuteration at $\alpha\text{-CH}_2$ was observed and fully characterized by NMR and Mass. This further strongly supports the *Traeg* amide via *ketene* intermediate. Finally, the proposed mechanism for Traeg amide cleavage is provided in **Figure 3.17**.

More interesting part of this work is conversion of Troponylglycinate esters into cationic troponyl lactones and further to amides. This transformation also follows the similar mechanism as that of Troponylglycinate amide cleavage. However, the conversion of esters into cationic troponyl lactone was not complete and only 75-80% of ester was converted into lactone in 6-12 h and the amidation of cationic troponyl lactone results in formation of amide,

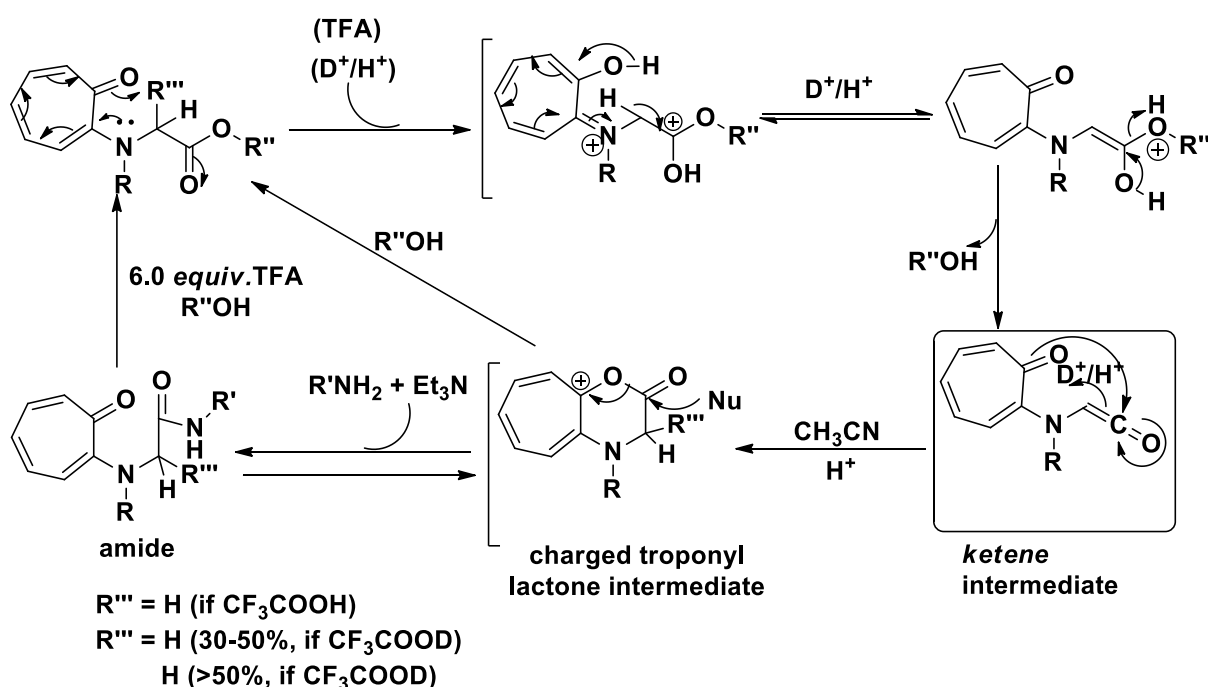


Figure 3.26 Possible mechanism of conversion of *Troponylglycinate* esters into cationic troponyl lactone and amide.

which are isolated in 60-66% yield. Overall, the conversion is slow, which is probably due reversible conversion of cationic troponyl lactone into ester and vice versa.

However, the reversible reaction rate is slow when compare to cationic forward reaction (cationic troponyl lactone). Further, monomer is less stable under these condition. Here, we have also successfully probed the role of α -CH₂ in troponylglycinate amide and ester cleavage by using the deuterated trifluoroacetic acid.

3.3 Conclusions

In summary, we have successfully established the regioselective cleavage of amide bond derived from *Traeg* in presence of 5.0% TFA (6 *equiv.*). The cleavage of *Traeg* amide into ester in alcoholic solvents and cationic troponyl lactone intermediate in acetonitrile was established. Initially, the *Traeg* amide solvolysis in deuterated methanol is demonstrated with nine *Traeg* peptides (*di/tri/tetra*-peptides, **13a-h**, **14**). During our mechanistical investigation, we found the unprecedented formation of cationic troponyl lactone in acetonitrile in presence of 6.0 *equiv.* of TFA. Further, to test the general scope of formation of cationic troponyl lactone, we have further synthesized the troponylglycinate dipeptides (**19/21/23/9G/F**) with different substituents at glycinate nitrogen atom in place of N-Boc aminoethyl substituent of *Traeg* monomer. Consistent conversion of all the synthesized dipeptides (**19/21/23/9G/F**) into cationic troponyl lactones (**24-28**) was characterized. Further, these cationic troponyl lactones were converted into ester with the addition of alcoholic solvents in excess or in stoichiometric ratio at 50 °C.

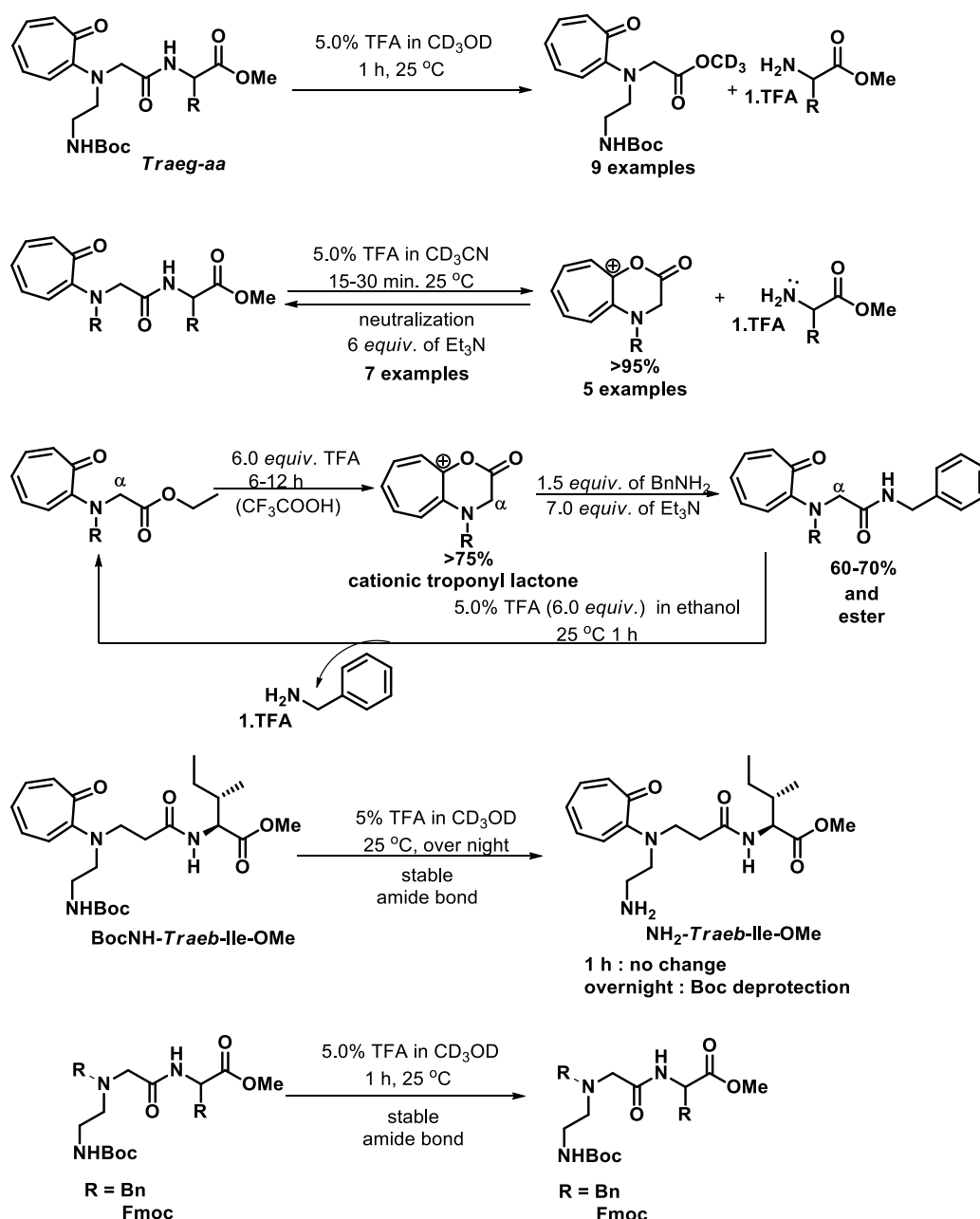


Figure 3.27 Schematic summary of this chapter.

Interestingly, the cationic troponyl lactones are converted back to respective peptides after neutralization of the reaction mixture with triethylamine and this reversible amidation was demonstrated with seven examples, all these reactions are monitored by NMR. Good yields of starting materials are isolated after reversible amidation reaction. Importantly, the breaking and reformation of *Traeg* amide is happening in two hours. To best of our knowledge, so far, there are no reports on such reversible amidation.

Further, conversion of troponylglycinate esters into cationic troponyl lactone and followed by base mediated amidation of cationic troponyl lactone is also demonstrated. Here, the troponylglycinate esters are converted into amides via cationic troponyl lactone without the use of peptide coupling reagents. This conversion witnessed the easy attachment of troponylglycinates to nitrogen via amide bond and they can be cleavable under mild condition. Hence, troponylglycinates can be used as protecting groups.

Suitable control experiments were performed to confirm the role of 2-aminotroponyl substituent in selective cleavage of *Traeg* derived amide bond. From the outcomes of all these studies a plausible reaction mechanism for *Traeg* amide cleavage is proposed and the role of troponyl moiety and α -CH₂ group were illustrated.

To end, such kind of conversions exhibited by the *N*-alkyltroponylglycinate amide and esters are not known in the literature. Hence, the outcomes of this work will provide enormous opportunities to employ *chromophoric Traeg* amino acid in caging/protection of free amine functionality of bioactive molecules. Hence the reactivity of those molecules may be regulated by UV-spectrophotometer in a temporal and spatial controlled manner.

3.4 Experimental section

Materials and instrumentation: All required materials were obtained from commercial suppliers and used without any further purification. Anhydrous dichloromethane was freshly prepared by distilling over Calcium hydride. Reactions were monitored by thin layer chromatography, visualized by UV and Ninhydrin. Column chromatography was performed in 230-400 and 100-200 mesh silica. Mass spectra were obtained from Bruker micrOTOF-Q II Spectrometer. NMR spectra were recorded on Bruker AV-400 at 298 K (¹H: 400 MHz, ¹³C: 100.6 MHz). ¹H and ¹³C{¹H} NMR chemical shifts were recorded in ppm downfield from

tetramethyl silane. Splitting patterns are abbreviated as: s, Singlet; d, doublet; dd, doublet of doublet; t, triplet; q, quartet; dq, doublet of quartet; m, multiplet.

General procedure for the synthesis of N-alkylglycinates (4 and related derivatives):

To the mixture of alkyl amine (1.0 *equiv.*) and triethylamine (3.0 *equiv.*) in acetonitrile, ethyl bromoacetate (1.2 *equiv.*) was added slowly at room temperature. The resultant reaction mixture is allowed to stir at room temperature until completion of the reaction, judged by TLC (12 h). After completion of the reaction, all volatiles were evaporated under vacuum to obtain crude product. The crude product was redissolved in dichloromethane and washed with saturated sodium bicarbonate solution. The combined organic layers were dried over sodium sulphate and concentrated under reduced pressure. The obtained crude product was purified through silica gel column chromatography and used for next step without any characterization.

Synthesis of N-Boc-aminoethylalanine (aala): N-Boc ethylene diamine and potassium carbonate was dissolved in acetonitrile, to this ethyl-2-bromo propanoate was added and allowed stirring at 50 °C for overnight. The completion of the reaction was judged by TLC. After completion, reaction mixture was filtered to remove potassium carbonate and filtrate was concentrated under reduced pressure. The crude residue was dissolved in saturated sodium bicarbonate and extracted with DCM. The combined organic layers were dried over sodium sulphate and evaporated to obtain crude product. The crude product was purified through silica gel column chromatography to obtain pure product.

Note: Same procedure was followed for the syntheses of N-Boc-amino ethylisobutyrate (*aaib*).

General procedure for the synthesis of monomers (5a, 6b-OEt, 7-OEt, 18, 20, 22): 2-tosyloxy tropone and N-alkyl glycinate backbone was dissolved in ethanol and refluxed for 48 h. Reaction completion was judged by TLC. After that all volatiles were evaporated under reduced pressure and crude product was extracted with water and brine solution. The combined

organic layers were dried over Na₂SO₄ and concentrated under reduced pressure. The obtained crude product was purified through silica gel column chromatography.

General procedure for the ester hydrolysis of monomers (6a, 6b, 7, 8): alkyl ester of the monomers were dissolved in ethanol and tetrahydrofuran (1:1) mixture. To this 2.0 *equiv.* of sodium hydroxide aqueous solution was added. Then reaction mixture is stirred for 30 min to 1 h. After completion of the reaction all volatiles were evaporated under reduced pressure. To the crude product 1N HCl was added and extracted with DCM or ethyl acetate. The combined organic layers were evaporated in *vacuo* and dried completely. The obtained product was used for the peptide synthesis without any further purification.

Note: In case of hydrolysis of troponyl proline (*Trpro*) monomer **9**, after completion of the reaction, all volatiles were evaporated. The crude residue was neutralized by using 1.0 N HCl to neutral pH (pH = 6.0 to 7.0). Then, water was evaporated. To the obtained crude product, methanol was added and filtered to remove NaCl salts. The filtrate was concentrated under *vacuum* and again redissolved in methanol and filtered. This process was done three times to remove NaCl salts. Then methanol filtrate was evaporated under reduced pressure, obtained product is allowed to dry and used for peptide syntheses.

General procedure for peptide synthesis (13, 14, 15, 16, 17, 19, 21, 23, 9G, 9F): Carboxylic acid monomer was dissolved in anhydrous DMF under nitrogen atmosphere and cooled to 0 °C. To this solution was added EDC.HCl or diisopropyl carbodiimide and allowed to stir for 10 minutes. Then L-amino acid methyl ester (1.5 *equiv.*) was neutralized with Et₃N (3.0 *equiv.*) and added to the cold reaction mixture. The reaction allowed to stir at 0 °C for 1 hour. Then stirred at room temperature or 48 °C (in cases of less conversion, reaction temperature was raised to 45-50 °C) for overnight. After completion of the reaction, the mixture was concentrated under reduced pressure. Concentrated reaction residue was re-dissolved in DCM (30 mL) and then washed with water thrice (3*30mL) followed by saturated sodium

bicarbonate (20.0 mL) by following extraction method. The washed organic layers were combined together, dried over Na₂SO₄. Then concentrated under reduced pressure, obtained crude product was purified through silica gel column. The obtained product was characterized by ¹H/¹³C NMR and Mass.

Note: In case of reactions, where diisopropyl carbodiimide was used as coupling reagent, diisopropyl urea was obtained as by product in the crude product residue after workup. The excess urea was removed by dissolving the crude product in ethyl acetate or ethyl acetate/hexane mixtures followed by crystallized urea filtration. This process was followed thrice to remove excess urea.

General procedure for the amide cleavage reaction: Traeg peptides was dissolved in solvent and added TFA (5.0% / 6.0 equiv). Reaction is allowed to stir at 25 °C for 30 min to 1 h. Reaction completion was judged by TLC. All volatiles were evaporated and washed with water. The organic layer was dried over Na₂SO₄ and concentrated under low pressure. The obtained crude product was purified through silica gel column chromatography.

Procedure for reversible amidation reaction: Troponylglycinate peptides (**13e/f/9G/F/19/21/23**) are dissolved in acetonitrile and to this 6.0 equiv. of TFA (5.0% in acetonitrile) was added. The resultant reaction mixture is allowed to stir at room temperature. Completion of the reaction was judged by TLC. After completion of the reaction, the reaction mixture was neutralized by adding enough triethylamine (7.0 equiv.). From the TLC we found that the reformation of troponylglycinate peptide.

Reversible amidation reaction monitoring by ¹H and ¹³C NMR experiments in CD₃CN: Troponylglycinate peptides (**13e/f/9G/F/19/21/23**) are dissolved in CD₃CN and recorded ¹H and ¹³C NMR. To the same sample 5.0%/6.0 equiv. of TFA is added and again recorded ¹H and ¹³C NMR. After addition of the TFA to the sample, as envisioned both ¹H and ¹³C NMR spectra

are completely changed. Importantly, characteristic tropone carbonyl peak at $\sim\delta$ 180-183.0 ppm was disappeared. Then, again to the same sample, 7 equiv. of triethylamine was added slowly at room temperature and recorded ^1H and ^{13}C NMR spectra. Both, ^1H and ^{13}C NMR spectra are reappeared. Interestingly, tropone carbonyl peak at $\sim\delta$ 180-183.0 ppm. After addition of TFA and triethylamine respective peaks of these materials were observed. Finally, the reaction mixture was evaporated under reduced pressure. The crude product was dissolved in dichloromethane/ethyl acetate and washed with water. The obtained organic layers were combined together, dried over sodium sulphate and concentrated under reduced pressure. The obtained crude product after extraction was purified through silica gel column chromatography and obtained yields are given in Table 3.5.

General procedure for esterification of Traeg peptides: Traeg peptides (1.0 equiv.) and alcohol (1.5 equiv.) (Farnesol or Geraniol) was taken in round bottom flask, to this mixture 6.0 equiv. of TFA was added and heated gently upto 50 °C in stirring, until completion of the reaction (15-30 min). The reaction was monitored by TLC. After completion of the reaction, volatiles were evaporated under reduced pressure at 50 °C in rota evaporator to obtain crude product. The obtained crude product was dissolved in dichloromethane and washed with water. Combined organic layers were dried over sodium sulphate and evaporated under vacuo. The obtained crude product was purified through silica gel column chromatography by using ethyl acetate and hexanes mixture as mobile phase. Obtained pure products are characterized by NMR and ESI-MS. The Complete conversion of tropolnyl lactone to ester was not observed in both cases.

Procedure for transamidation: To the Traeg peptide (**13e**) in acetonitrile, 6 equiv. of TFA was added and allowed to stir at room temperature to obtain the troponyl lactone. To the obtained troponyl lactone, benzyl amine in acetonitrile along with the 6-7.0 equiv. of triethylamine was added slowly. The resultant reaction mixture is allowed to stir at room

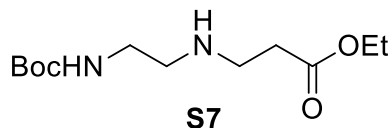
temperature until completion of the reaction, judged by TLC. After completion of the reaction all volatiles were evaporated under *vacuo*. The obtained crude product was dissolved in dichloromethane/ethyl acetate and washed with water. The combined organic layers were dried over sodium sulphate and concentrated under reduced pressure. The obtained crude product was purified through silicagel column chromatography and ethyl acetate : hexanes as mobile phase.

Procedure for time dependent NMR: Compound was dissolved in 450 μL of CD_3OD , recorded NMR. After that 5% TFA (with respect to volume of the solvent) was added to the same sample and recorded NMR with 7 min time intervals up to 1 h. All the spectra were recorded at 25 $^\circ\text{C}$ (298 K) and are given in stacked form.

General procedure for the conversion of troponylglycinate esters into cationic troponyl lactones followed by amidation and monitoring by NMR: *N*-alkyl troponylglycinate esters were dissolved in CD_3CN and to this solution 6.0 *equiv.* of trifluoroacetic acid (TFA-H) is added. After 6-12 h, ^1H and ^{13}C NMR spectra was recorded. Which reveals the formation of cationic troponyl lactone. Then, to the same solution 1.5 *equiv.* of benzylamine was added and after that 6-7.0 *equiv.* of triethylamine was added slowly. With is 5.0 minutes, cationic troponyl lactone was converted into amide. All volatiles were evaporated under reduced pressure and water was added to the crude product, and extracted with ethylacetate twice. The obtained organic layers were combined together, dried over sodium sulphate and evaporated to dryness to obtain crude product. The obtained crude product was purified through silica gel column chromatography by using ethylacetate:hexanes as mobile phase. All pure products are characterized by NMR and Mass.

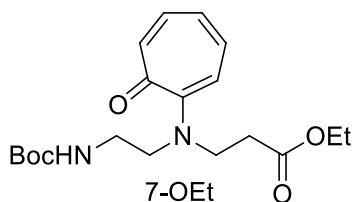
General procedure for the syntheses of deuterated cationic troponyl lactones and amides: Same procedure was followed and deuterated trifluoroacetic acid (TFA-D) was used instead of trifluoroacetic acid (TFA-H).

N-Boc-aminoethyl- β -alanate ester (**S7**)



2 gm (25 mmol) of *N*-Boc ethylenediamine (taken 2eq with respect to Ethyl 3-bromopropionate to decrease the formation of undesired dialkylated product) was dissolved in acetonitrile, to this 3.45 gm (25 mmol) of K_2CO_3 and 1.604 mL (12.5 mmol) Ethyl 3-bromopropionate was added. The reaction mixture is allowed to stirring at room temperature for 24 h. The reaction was monitored by TLC, 8% methanol in dichloromethane. After completion of the reaction, the reaction mixture was filtered and concentrated under low pressure. The crude product was purified by column chromatography 3-5% methanol in dichloromethane as mobile phase. 2.0 gm (61% yield) of pure product was obtained as colorless liquid and characterized by NMR and mass spectrometry. 1H NMR (400 MHz, $CDCl_3$) δ 5.01 (s, 1H), 4.14 (q, $J = 7.1$ Hz, 1H), 3.20 (dd, $J = 10.9, 5.3$ Hz, 1H), 2.87 (t, $J = 6.4$ Hz, 1H), 2.72 (t, $J = 5.8$ Hz, 1H), 2.48 (t, $J = 6.4$ Hz, 1H), 1.44 (d, $J = 10.5$ Hz, 5H), 1.25 (dd, $J = 9.3, 4.9$ Hz, 2H). ^{13}C NMR (101 MHz, $CDCl_3$) δ 172.67, 156.09, 79.12, 60.46, 48.69, 44.49, 40.01, 34.60, 28.36, 14.16. HRMS (ESI-TOF) m/z : $[M+H]^+$ calcd. for $C_{12}H_{24}N_2O_4$ 261.1809, found 261.1844.

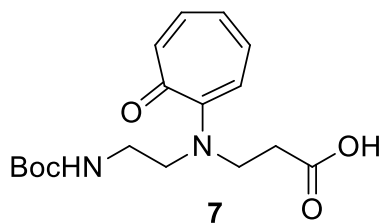
N-tropnyl-*N*-Boc-aminoethyl- β -alanate ester (**7-OEt**)



N-Boc-aminoethyl- β -alanate (3.84 mmol) was dissolved in ethanol and added 2-tosyloxy tropone (1.28 mmol), Et_3N (3.84 mmol). The reaction mixture was allowed to reflux for two days; the reaction was monitored by TLC with 40% ethylacetate in hexane. After completion of the reaction, the reaction mixture was filtered and concentrated under low pressure. The crude residue was redissolved in DCM and was washed with water, brine. The combined organic layers were dried over Na_2SO_4 and concentrated under reduced pressure to obtain crude

product. The crude product was purified by silica gel column chromatography (230-400 mesh) 23-25% ethylacetate in hexane as mobile phase. 300 mg (65% yield) of pure product was obtained as yellow viscous liquid and characterized by NMR and Mass spectrometric methods. ^1H NMR (400 MHz, CDCl_3) δ 7.02 (dt, $J = 21.6, 9.5$ Hz, 1H), 6.89 (d, $J = 11.8$ Hz, 1H), 6.59 (dd, $J = 17.9, 9.6$ Hz, 1H), 5.59 (s, 1H), 4.08 (q, $J = 7.1$ Hz, 1H), 3.70 (t, $J = 7.4$ Hz, 1H), 3.53 (t, $J = 6.1$ Hz, 1H), 3.33 (d, $J = 5.6$ Hz, 1H), 2.60 (t, $J = 7.3$ Hz, 1H), 1.37 (s, 5H), 1.20 (dd, $J = 10.1, 4.0$ Hz, 2H). ^{13}C NMR (101 MHz, CDCl_3) δ 181.97, 171.47, 156.95, 156.13, 135.42, 133.70, 133.00, 124.37, 115.46, 79.03, 60.65, 50.70, 46.78, 38.15, 31.83, 28.29, 14.03. HRMS (ESI-TOF) m/z : $[\text{M}+\text{H}]^+$ calcd. for $\text{C}_{19}\text{H}_{28}\text{N}_2\text{O}_5$ 365.2071, found 365.2087.

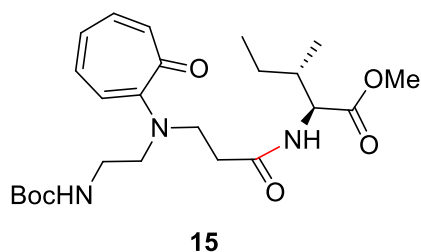
N-tropnyl-N-Boc-aminoethyl- β -alanate acid (7)



The compound was dissolved in EtOH and THF (1:1), to this 2 eq of NaOH was dissolved in little amount of water was added and allowed to stirring at room temperature. With progress in time, the solution turned into brick red color. The

reaction was monitored by TLC, after 10 minutes reaction was completed. The solvents were removed under reduced pressure at 50°C . Then, to the crude product 1N HCl was added and extracted thrice with DCM. The organic layers were combined together, dried over Na_2SO_4 and concentrated under low pressure to afford the pure product as yellow gelatinous liquid. The product was characterized by mass spectrometry.

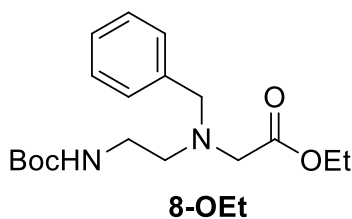
BocNH-Traeb-Ile-OMe (**15**):



The dipeptide was synthesized by following general procedure. 45 mg (41% yield) of pure product was obtained as yellow viscous liquid. ^1H NMR (400 MHz, CDCl_3) δ 7.08 (2 H, ddd, J 22.7, 11.4, 5.7), 6.93 (1 H, d, J 11.7), 6.78

(2 H, dd, J 17.9, 9.4), 6.69 – 6.54 (1 H, m), 5.55 (1 H, s), 4.52 (1 H, dd, J 8.4, 5.3), 3.81 – 3.72 (1 H, m), 3.71 (3 H, s), 3.68 (1 H, d, J 7.5), 3.64 – 3.45 (2 H, m), 3.45 – 3.27 (2 H, m), 2.59 (2 H, t, J 7.1), 2.03 – 1.92 (1 H, m), 1.93 – 1.77 (1 H, m), 1.52 – 1.32 (9 H, m), 1.29 – 1.20 (3 H, m), 0.89 (3 H, q, J 6.8). ^{13}C NMR (101 MHz, CDCl_3) δ 181.92, 172.44, 170.90, 157.14, 156.37, 135.65, 134.07, 133.00, 124.51, 115.79, 79.31, 56.65, 52.01, 50.90, 47.83, 38.15, 37.51, 34.52, 28.36, 25.22, 15.47, 11.49. HRMS (ESI-TOF) m/z : $[\text{M}+\text{H}]^+$ calcd. for $\text{C}_{24}\text{H}_{37}\text{N}_3\text{O}_6$ 464.2755, found 464.2731.

N-Benzyl-N-Boc-aminoethylglycine ester (*BocNH-Bnaeg-OEt*) (**8-OEt**)

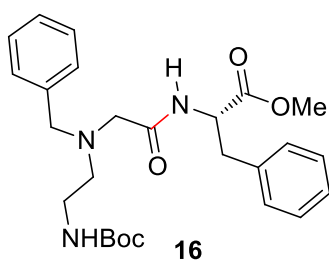


400 mg (1.62 mmol) of *aeg* backbone was dissolved in acetonitrile, to this 268 mg (1.94 mmol) of K_2CO_3 was added and allowed for stirring. To the stirring reaction mixture 234 μL (1.94 mmol) of benzyl bromide was added slowly. After

complete addition of benzyl bromide the reaction mixture allowed to stirring at room temperature for 4 hrs, then filtered and the filtrate was concentrated under reduced pressure to obtain crude product. The crude product was purified by column chromatography using appropriate mixture of ethyl acetate and hexane. 500 mg (92% yield) of the desired product was obtained as colorless liquid and characterized by NMR and mass spectrometric methods. ^1H NMR (400 MHz, CDCl_3) δ 7.37 – 7.30 (m, 4H), 7.30 – 7.23 (m, 1H), 5.23 (s, 1H), 4.16 (q, J = 7.1 Hz, 2H), 3.78 (s, 2H), 3.31 (s, 2H), 3.21 (d, J = 5.3 Hz, 2H), 2.86 – 2.70 (m, 2H), 1.55

– 1.37 (m, 9H), 1.27 (dd, $J = 9.0, 5.3$ Hz, 3H). ^{13}C NMR (101 MHz, CDCl_3) δ 171.47 (s), 156.10 (s), 138.49 (s), 128.86 (s), 128.37 (s), 127.26 (s), 78.94 (s), 60.45 (s), 58.21 (s), 54.41 (s), 53.28 (s), 28.41 (s), 14.18 (s). HRMS (ESI-TOF) m/z : $[\text{M}+\text{H}]^+$ calcd. for $\text{C}_{18}\text{H}_{28}\text{N}_2\text{O}_4$ 337.2122, found 337.2176.

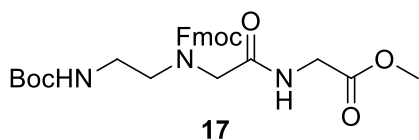
BocNH-Bnaeg-Phe-OMe (16):



The dipeptide was synthesized by following given general procedure. 400 mg (68% yield) of the pure product was obtained as colorless viscous liquid which turned into soft solid after long standing at -20°C . ^1H NMR (400 MHz, CDCl_3) δ 7.68 (d, $J = 8.6$

Hz, 1H), 7.34 – 7.20 (m, 6H), 7.17 (d, $J = 5.1$ Hz, 2H), 7.10 (d, $J = 6.0$ Hz, 2H), 5.09 (s, 1H), 4.85 (d, $J = 6.0$ Hz, 1H), 3.85 – 3.70 (m, 3H), 3.67 (s, 1H), 3.50 – 3.26 (m, 2H), 3.21 (dd, $J = 13.9, 5.4$ Hz, 1H), 3.16 – 3.02 (m, 3H), 2.94 (dd, $J = 22.6, 11.3$ Hz, 2H), 2.54 (dd, $J = 10.6, 5.3$ Hz, 2H), 1.57 – 1.35 (m, 9H). ^{13}C NMR (101 MHz, CDCl_3) δ 172.59, 170.87, 156.09, 137.64, 135.98, 129.25, 129.00, 128.69, 128.41, 127.35, 127.06, 79.18, 58.77, 57.62, 54.51, 52.64, 52.37, 38.22, 37.87, 28.40. HRMS (ESI-TOF) m/z : $[\text{M}+\text{H}]^+$ calcd. for $\text{C}_{26}\text{H}_{35}\text{N}_3\text{O}_5$ 470.2649, found 470.2833.

BocNH-Fmocaeg-Gly-OMe (17):



^1H NMR: (400 MHz, CDCl_3) δ 7.76 (d, $J = 7.0$ Hz, 2H), 7.57 (m, 2H), 7.40 (t, $J = 7.0$ Hz, 2H), 7.30 (d, $J = 18.4$ Hz, 2H), 6.72 (s, 1H), 5.24 (s, 1H), 4.52 (s, 2H), 4.21 (t, $J = 17.5$ Hz,

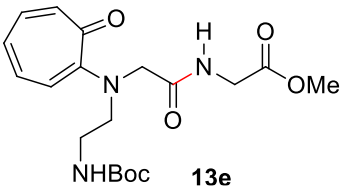
1H), 4.06 (s, $J = 30.2$ Hz, 1H), 3.91 (s, 2H), 3.76 (s, 1H), 3.73 (s, 3H), 3.44 (s, 1H), 3.30 (s, 2H), 3.00 (s, 1H), 1.40 (s, 9H). ^{13}C NMR (101 MHz, CDCl_3) δ 170.24, 170.06, 169.69, 169.23, 143.70, 141.24, 127.69, 127.10, 124.77, 119.89, 79.24, 67.61, 52.30, 47.13, 40.93, 28.28. HRMS (ESI-TOF) m/z : $[\text{M}+\text{H}]^+$ calcd. for $\text{C}_{27}\text{H}_{33}\text{N}_3\text{O}_7$ 512.2391, found 512.2451.

Analytical data of synthesized hybrid peptides:

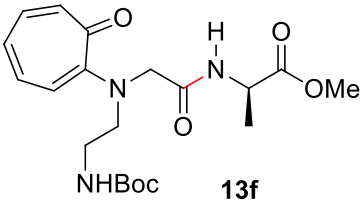
All the dipeptides were synthesized by following given general procedure.

(i) Analytical data (^1H & ^{13}C -NMR, HRMS) of some compounds are reported¹, those are *BocNH-Traeg-OEt* (**5a**), *Boc-Traeg-Ile-OMe* (**13c**), *Boc-Traeg-Phe-OMe* (**13a**), *Boc-Traeg-Pro-OMe* (**13b**), *Boc-Traeg-Gly-Phe-OMe* (**13d**). Remaining is listed below.

(ii) *BocNH-Traeg-Gly-OMe* (**13e**):

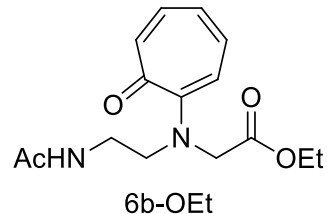
 120 mg (51% yield) of the pure product was obtained as yellow thick viscous liquid after isolation. ^1H NMR (400 MHz, CDCl_3) δ 8.19 (s, 1H), 7.26 – 6.96 (m, 3H), 6.89 (d, J = 9.8 Hz, 1H), 6.84 – 6.68 (m, 1H), 5.59 (s, 1H), 4.09 (d, J = 5.8 Hz, 2H), 3.90 (s, 2H), 3.81 – 3.66 (m, 3H), 3.49 (t, J = 5.6 Hz, 2H), 3.43 – 3.28 (m, 2H), 1.40 (d, J = 17.8 Hz, 9H). ^{13}C NMR (101 MHz, CDCl_3) δ 183.27, 170.53, 157.69, 156.17, 136.38, 135.07, 133.96, 127.31, 119.56, 79.23, 56.64, 52.26, 51.56, 40.96, 37.41, 28.28. HRMS (ESI-TOF) m/z : $[\text{M}+\text{H}]^+$ calcd. for $\text{C}_{19}\text{H}_{27}\text{N}_3\text{O}_6$ 394.1973, found 394.2010.

(iii) *BocNH-Traeg-Ala-OMe* (**13f**):

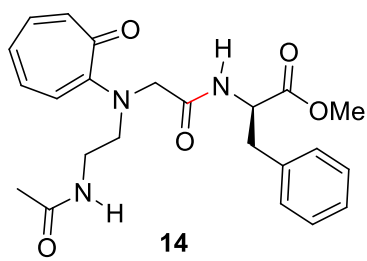
 110 mg (44% yield) of the pure product was obtained as yellow thick viscous liquid. ^1H NMR (400 MHz, CDCl_3) δ 8.05 (d, J = 6.9 Hz, 1H), 7.26– 6.98 (m, 3H), 6.95 – 6.79 (m, 1H), 6.81 – 6.70 (m, 1H), 5.65 (s, 1H), 4.74 – 4.49 (m, 1H), 4.01 (d, J = 16.3 Hz, 1H), 3.87 – 3.64 (m, 4H), 3.54 (m, 1H), 3.49 – 3.35 (m, 2H), 3.32 (dd, J = 16.3, 7.5 Hz, 1H), 1.48 – 1.40 (m, 3H), 1.41 – 1.33 (m, 9H). cis and trans isomers are existing around carbamate amide bond in 1:4, not predicted due to overlapping signals ^{13}C NMR (101 MHz, CDCl_3) δ 183.12, 173.30, 169.68, 157.59, 156.12, 136.40, 136.21, 134.80, 133.87,

132.72, 119.22, 113.10, 79.14, 64.83, 56.28, 52.27, 51.35, 127.56, 127.06, 47.88, 37.45, 28.23, 17.58. HRMS (ESI-TOF) m/z : $[M+H]^+$ calcd. for $C_{20}H_{29}N_3O_6$ 408.2129, found 408.2211.

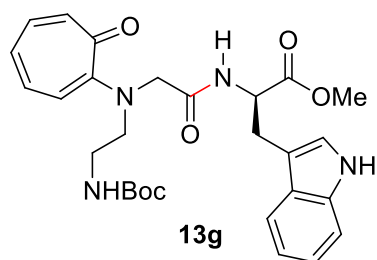
(iv) *AcNH-Traeg-OEt* (**6b-OEt**):

 300 mg (77% yield) of the pure product was obtained as yellow viscous liquid. 1H NMR (400 MHz, $CDCl_3$) δ 7.61 (1 H, s), 7.11 (1 H, dd, J 11.8, 8.3), 7.07 – 6.91 (2 H, m), 6.67 (2 H, dd, J 14.5, 7.9), 4.23 (2 H, tt, J 7.1, 3.6), 4.07 (2 H, d, J 22.9), 3.61 (2 H, t, J 5.6), 3.47 (2 H, dd, J 10.4, 5.1), 1.92 (3 H, d, J 5.7), 1.37 – 1.16 (3 H, m). ^{13}C NMR (101 MHz, $CDCl_3$) δ 182.19, 170.94, 170.77, 157.03, 136.06, 134.47, 134.44, 133.83, 126.02, 117.09, 61.34, 53.41, 51.12, 36.38, 22.97, 14.09. HRMS (ESI-TOF) m/z : $[M+Na]^+$ calcd. for $C_{15}H_{20}N_2O_4$ 315.1315, found 315.1374.

(v) *AcNH-Traeg-Phe-OMe* (**14**):

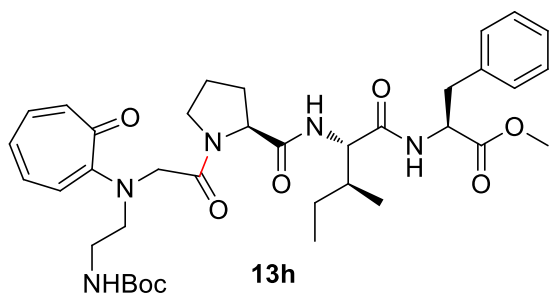
 90 mg (40% yield) of the obtained pure product was yellow thick liquid. 1H NMR (400 MHz, $CDCl_3$) 7.75 (1 H, d, J 7.9), 7.32 (1 H, d, J 4.7), 7.25 – 7.13 (4 H, m), 7.14 – 6.98 (4 H, m), 6.85 – 6.67 (2 H, m), 4.86 (1 H, dd, J 13.1, 7.5), 3.99 (1 H, d, J 16.7), 3.83 – 3.72 (1 H, m), 3.72 – 3.65 (3 H, m), 3.58 – 3.45 (1 H, m), 3.46 – 3.21 (3 H, m), 3.21 – 3.10 (1 H, m), 3.05 (1 H, dd, J 13.9, 7.3), 1.88 – 1.75 (3 H, m). ^{13}C NMR (101 MHz, $CDCl_3$) δ 182.94, 172.14, 171.16, 169.58, 157.76, 136.37, 135.73, 135.05, 133.94, 129.08, 128.49, 127.34, 127.02, 119.34, 55.57, 53.19, 52.36, 51.06, 37.71, 36.99, 22.79. HRMS (ESI-TOF) m/z : $[M+Na]^+$ calcd. for $C_{23}H_{27}N_3O_5$ 448.1843, found 448.1872.

(vi) *BocNH-Traeg-Trp-OMe* (**13g**):



125 mg (49% yield) of pure product was yellow viscous liquid. ^1H NMR (400 MHz, CDCl_3) δ 8.96 (1 H, s), 7.96 (1 H, s), 7.64 (1 H, d, J 6.4), 7.48 (1 H, d, J 7.6), 7.25 (1 H, dd, J 15.6, 7.5), 7.14 – 6.79 (6 H, m), 6.65 (2 H, t, J 10.3), 5.53 (1 H, s), 4.83 (1 H, d, J 5.5), 3.86 (2 H, q, J 16.8), 3.66 (3 H, t, J 11.1), 3.32 (2 H, d, J 10.3), 3.22 (2 H, dd, J 14.2, 7.6), 3.11 (2 H, s), 2.91 (1 H, d, J 3.3), 2.84 (1 H, d, J 2.6), 1.50 – 1.31 (9 H, m). cis and trans isomers are existing around carbamate amide bond in, not predicted due to overlapping signals ^{13}C NMR (101 MHz, CDCl_3) δ 182.39, 180.58, 173.69, 172.27, 169.53, 164.77, 162.59, 157.20, 156.10, 136.64, 136.07, 134.18, 133.90, 132.89, 127.77, 127.07, 126.47, 123.34, 121.68, 119.11, 118.32, 118.18, 113.30, 111.29, 109.25, 79.17, 64.84, 55.55, 52.68, 52.23, 51.14, 37.49, 28.24. HRMS (ESI-TOF) m/z : $[\text{M}+\text{H}]^+$ calcd. for $\text{C}_{28}\text{H}_{34}\text{N}_4\text{O}_6$ 523.2551, found 523.2777.

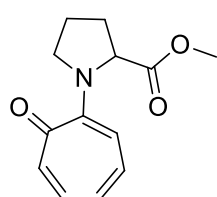
(vii) *BocNH-Traeg-Pro-Ile-Phe-OMe* (**13h**):



160 mg (38% yield) of pure product was obtained as semi solid, after long standing turned into solid. ^1H NMR (400 MHz, CDCl_3) δ 7.73 – 7.60 (m, 1H), 7.31 – 7.18 (m, 1H), 7.08 (dt, J = 13.4, 6.9 Hz, 6H), 6.94 (d, J = 6.6 Hz, 2H), 6.90 – 6.75 (m, 2H), 6.65 (dd, J = 19.8, 10.6 Hz, 1H), 5.92 – 5.61 (m, 1H), 4.65 – 4.43 (m, 2H), 4.43 – 4.25 (m, 1H), 3.90 (d, J = 16.5 Hz, 1H), 3.77 (d, J = 14.0 Hz, 1H), 3.75 – 3.62 (m, 3H), 3.56 (d, J = 11.2 Hz, 3H), 3.54 – 3.26 (m, 5H), 3.21 – 3.01 (m, 1H), 2.96 (dd, J = 13.6, 6.7 Hz, 1H), 2.72 (dd, J = 13.4, 7.8 Hz, 1H), 2.40 – 2.08 (m, 3H), 2.09 – 1.80 (m, 4H), 1.49 – 1.33 (m, 11H), 0.99 – 0.59 (m, 6H). cis and trans isomers are existing around carbamate amide bond, not predicted due to overlapping signals ^{13}C NMR (101 MHz, CDCl_3) δ 180.69, 171.75,

171.73, 171.67, 171.46, 171.10, 170.89, 170.71, 157.24, 156.22, 139.14, 136.79, 136.50, 136.19, 135.84, 134.79, 133.05, 132.82, 129.14, 129.04, 128.94, 128.42, 128.21, 128.11, 127.73, 126.90, 126.73, 126.44, 124.42, 124.02, 114.41, 113.96, 113.19, 79.32, 60.94, 60.55, 59.63, 59.26, 58.43, 57.99, 55.28, 54.44, 53.60, 52.99, 52.16, 51.90, 48.19, 46.81, 46.65, 37.93, 37.67, 36.96, 35.49, 28.28, 29.23, 24.62, 24.68, 14.01, 11.33. HRMS (ESI-TOF) m/z : $[M+H]^+$ calcd. for $C_{37}H_{51}N_5O_8$ 694.3810, found 694.3945.

(viii) *Trpro-OMe* (**9**):

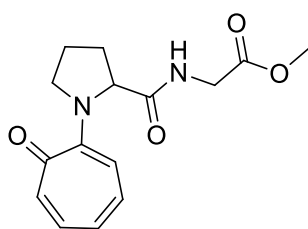


9

Proline methyl ester hydrochloride (2.0 *equiv.*) was dissolved in ethanol and neutralized with triethylamine (6.0 *equiv.*), to this 1.0 *equiv.* of 2-tosyloxy tropone was added and refluxed for overnight. After completion of the reaction all volatiles were evaporated and washed with water.

Combined organic layers were dried over sodium sulphate and concentrated to dryness. The obtained crude product was purified through silica gel column chromatography. 200 mg (50% yield) of pure product was obtained as dark yellow gelatinous liquid. 1H NMR (400 MHz, $CDCl_3$) δ 7.03 (q, J = 10.7 Hz, 2H), 6.86 (d, J = 11.7 Hz, 1H), 6.52 (t, J = 9.2 Hz, 1H), 6.42 (d, J = 10.5 Hz, 1H), 5.21 (d, J = 8.5 Hz, 1H), 3.72 (s, 3H), 3.65 – 3.53 (m, 1H), 3.45 (dd, J = 16.1, 7.3 Hz, 1H), 2.19 (dd, J = 17.9, 11.1 Hz, 1H), 2.12 – 1.90 (m, 4H). ^{13}C NMR (101 MHz, $CDCl_3$) δ 180.53, 173.29, 155.19, 136.06, 134.70, 132.43, 122.61, 113.11, 62.62, 51.94, 51.41, 31.10, 22.56.

(ix) *Trpro-Gly-OMe* (**9G**):



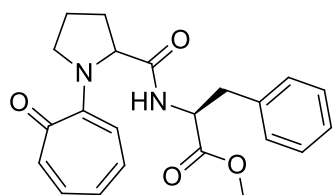
9G

Troponyl proline carboxylic acid derivative was dissolved in anhydrous DMF and resultant solution was cooled to 0 °C. To this diisopropyl carbodiimide was added and stirred at 0 °C for 5 minutes.

To the resultant mixture, glycine methyl ester neutralized with triethylamine was added at 0 °C. Then the reaction mixture stirred at 0 °C for 30-60 minutes

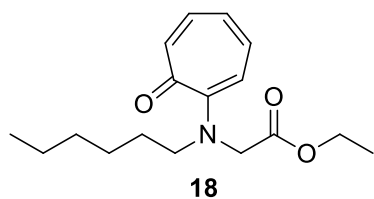
and reaction temperature raised to 50 °C. After reaction completion, DMF was evaporated and the resultant reaction mixture was washed with water and sodium bicarbonate solution. Combined organic layers were mixed and concentrated to dryness. The obtained crude product was purified through silica gel column chromatography. 110 mg (65% yield) of pure product was obtained as dark yellow gelatinous liquid. ^1H NMR (400 MHz, CDCl_3) δ 7.03 (dd, $J = 22.1, 11.3$ Hz, 3H), 6.86 (d, $J = 11.7$ Hz, 1H), 6.55 (t, $J = 9.2$ Hz, 1H), 6.45 (d, $J = 10.5$ Hz, 1H), 4.99 (s, 1H), 3.98 – 3.83 (m, 2H), 3.82 – 3.69 (m, 1H), 3.63 (s, 3H), 3.42 – 3.29 (m, 1H), 2.25 – 2.03 (m, 3H), 1.88 (dt, $J = 11.7, 5.7$ Hz, 1H). ^{13}C NMR (101 MHz, CDCl_3) δ 180.12, 174.13, 173.11, 170.09, 155.72, 136.08, 134.61, 132.13, 123.39, 114.32, 63.86, 51.94, 51.81, 40.83, 31.34, 23.08, 20.76. HRMS (ESI-TOF) m/z : $[\text{M}+\text{Na}]^+$ calcd. for $\text{C}_{15}\text{H}_{18}\text{N}_2\text{O}_4$ 313.1159, found 313.1164.

(x) *Trpro-Phe-OMe* (**9F**): ^1H NMR (400 MHz, CDCl_3) δ 7.32 – 7.19 (m, 3H), 7.17 (m,



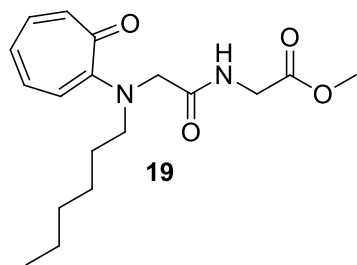
2H), 7.12 – 6.92 (m, 3H), 6.87 (app d, $J = 11.7$ Hz, 1H), 6.70 (d, $J = 7.1$ Hz, 1H), 6.62 – 6.51 (m, 1H), 6.40 (d, $J = 10.4$ Hz, 1H), 4.93 (app dd, $J = 7.9, 4.2$ Hz, 1H), 4.80 (app dd, $J = 13.6, 6.9$ Hz, 1H), 3.70 (dt, $J = 11.4, 5.6$ Hz, 1H), 3.62 (s, 3H), 3.40 – 3.26 (m, 1H), 3.14 (app dd, $J = 13.9, 5.8$ Hz, 1H), 3.03 (app dd, $J = 13.9, 6.9$ Hz, 1H), 2.22 – 2.07 (m, 1H), 2.01 (dd, $J = 11.5, 5.6$ Hz, 1H), 1.86 (app dd, $J = 12.4, 6.1$ Hz, 2H). ^{13}C NMR (101 MHz, CDCl_3) δ 180.29, 172.02, 171.58, 155.39, 136.00, 135.62, 134.17, 132.32, 129.05, 128.91, 128.30, 128.25, 126.76, 123.10, 113.64, 63.72, 52.93, 51.99, 51.51, 37.37, 31.01, 23.04. HRMS (ESI-TOF) m/z : $[\text{M}+\text{H}]^+$ calcd. for $\text{C}_{22}\text{H}_{24}\text{N}_2\text{O}_4$ 403.1628, found 403.1633.

(xi) *Trhg-OEt* (**18**):



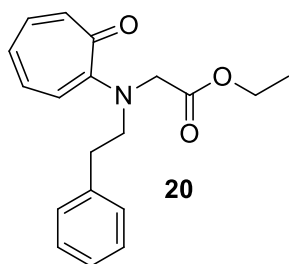
2 gm (85% yield) of pure product was isolated as yellow free liquid. ^1H NMR (400 MHz, CDCl_3) δ 7.04 – 6.91 (m, 2H), 6.83 (d, $J = 11.7$ Hz, 1H), 6.52 (dd, $J = 18.5, 9.9$ Hz, 2H), 4.31 (s, 2H), 4.18 – 4.04 (m, 2H), 3.42 – 3.27 (m, 2H), 1.71 – 1.52 (m, 2H), 1.34 – 1.23 (m, 6H), 1.23 – 1.15 (m, 4H), 0.83 (dd, $J = 9.6, 4.3$ Hz, 3H). ^{13}C NMR (101 MHz, CDCl_3) δ 181.35, 170.37, 156.76, 135.35, 133.82, 133.12, 123.81, 114.51, 60.83, 54.36, 53.29, 31.50, 26.67, 26.00, 22.55, 14.17, 13.96.

(xii) *Trhg-Gly-OMe* (**19**):



1.2 gm (65% yield) of pure product was obtained as yellow viscous liquid. ^1H NMR (400 MHz, CDCl_3) δ 8.12 (s, 1H), 7.21 – 7.11 (m, 1H), 7.05 (dd, $J = 22.8, 11.2$ Hz, 2H), 6.71 (t, $J = 9.7$ Hz, 2H), 4.09 (d, $J = 5.7$ Hz, 2H), 3.93 (s, 2H), 3.72 (s, 3H), 3.39 – 3.26 (m, 2H), 1.75 – 1.52 (m, 2H), 1.37 – 1.17 (m, 6H), 0.86 (t, $J = 6.6$ Hz, 3H). ^{13}C NMR (101 MHz, CDCl_3) δ 183.04, 170.63, 170.08, 157.98, 136.20, 134.18, 133.88, 126.13, 117.98, 56.02, 52.34, 52.17, 41.11, 31.43, 26.66, 25.73, 22.52, 13.92. HRMS (ESI-TOF) m/z : $[\text{M}+\text{Na}]^+$ calcd. for $\text{C}_{28}\text{H}_{26}\text{N}_2\text{O}_4$ 357.1785, found 357.1778.

(xiii) *Trpeg-OEt* (**20**):

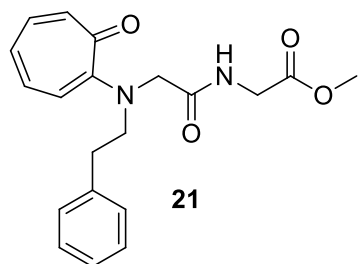


2.5 gm (80% yield) of pure product was obtained as yellow viscous liquid. ^1H NMR (400 MHz, CDCl_3) δ 7.33 (t, $J = 7.2$ Hz, 2H), 7.25 (d, $J = 7.0$ Hz, 3H), 7.15 – 7.02 (m, 2H), 6.98 (d, $J = 11.8$ Hz, 1H), 6.75 – 6.58 (m, 2H), 4.33 (s, 2H), 4.21

(q, $J = 7.0$ Hz, 2H), 3.78 – 3.64 (m, 2H), 3.03 (t, $J = 7.7$ Hz, 2H), 1.28 (t, $J = 7.0$ Hz, 3H).

^{13}C NMR (101 MHz, CDCl_3) δ 181.28, 170.09, 156.33, 138.39, 135.48, 133.72, 133.22, 128.53, 128.51, 126.42, 124.21, 114.67, 60.83, 55.62, 53.65, 32.64, 20.69, 14.01. HRMS (ESI-TOF) m/z : $[\text{M}+\text{Na}]^+$ calcd. for $\text{C}_{19}\text{H}_{21}\text{N}_2\text{O}_3$ 312.1594, found 312.1501.

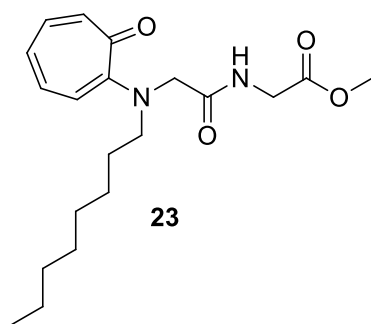
(xiv) *Trpeg-Gly-OMe* (**21**):



1.0 gm (60% yield) of pure product was isolated as yellow thick liquid. ^1H NMR (400 MHz, CDCl_3) δ 7.89 (s, 1H), 7.26 (t, $J = 7.2$ Hz, 2H), 7.16 (dt, $J = 23.2, 8.0$ Hz, 4H), 7.10 – 7.00 (m, 2H), 6.77 (t, $J = 10.8$ Hz, 2H), 3.96 (d, $J = 5.5$ Hz,

2H), 3.91 (s, 2H), 3.70 (s, 3H), 3.61 (t, $J = 7.5$ Hz, 2H), 2.91 (t, $J = 7.5$ Hz, 2H), 2.06 (s, 2H). ^{13}C NMR (101 MHz, CDCl_3) δ 183.06, 170.47, 169.92, 157.55, 138.44, 136.34, 134.72, 133.74, 128.77, 128.53, 126.88, 126.51, 119.04, 56.40, 53.72, 52.13, 41.06, 32.50, 20.71. HRMS (ESI-TOF) m/z : $[\text{M}+\text{Na}]^+$ calcd. for $\text{C}_{20}\text{H}_{22}\text{N}_2\text{O}_4$ 377.1472, found 377.1464.

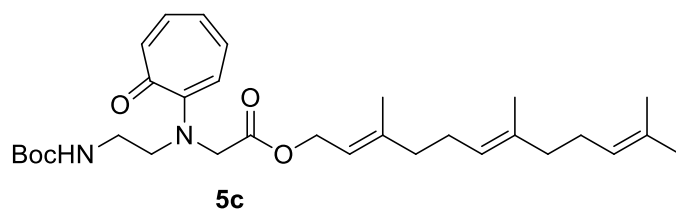
(xv) *Trog-Gly* (**23**):



600 mg (65% yield) of pure product was obtained as yellow viscous liquid. ^1H NMR (400 MHz, CDCl_3) δ 8.12 (s, 1H), 7.13 (dd, $J = 11.9, 8.3$ Hz, 1H), 7.04 (dd, $J = 23.8, 11.1$ Hz, 2H), 6.70 (t, $J = 10.0$ Hz, 2H), 4.08 (d, $J = 5.7$ Hz, 2H), 3.92 (s, 2H), 3.71 (s, 3H), 3.38 – 3.24

(m, 2H), 1.70 – 1.53 (m, 2H), 1.26 (d, $J = 15.0$ Hz, 11H), 1.12 (d, $J = 6.5$ Hz, 1H), 0.85 (t, $J = 6.8$ Hz, 3H). ^{13}C NMR (101 MHz, CDCl_3) δ 183.06, 170.57, 170.06, 157.96, 136.13, 134.19, 133.83, 126.07, 117.89, 56.00, 52.27, 52.15, 41.08, 31.68, 26.92, 26.98, 25.72, 23.41, 22.56, 14.02. HRMS (ESI-TOF) m/z : $[\text{M}+\text{Na}]^+$ calcd. for $\text{C}_{20}\text{H}_{30}\text{N}_2\text{O}_4$ 385.2098, found 385.2087.

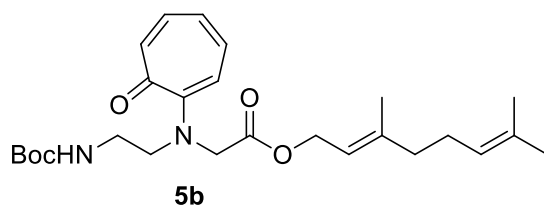
(xvi) *Trpeg-farnesol (5c)*:



50 mg (79% yield) of pure product was obtained as light yellow viscous liquid.

^1H NMR (400 MHz, CDCl_3) δ 7.35 – 7.27 (m, 2H), 7.27 – 7.18 (m, 3H), 7.13 – 6.98 (m, 2H), 6.94 (d, J = 11.8 Hz, 1H), 6.70 – 6.56 (m, 2H), 5.34 (dd, J = 7.1, 6.0 Hz, 1H), 5.09 (t, J = 6.6 Hz, 2H), 4.65 (t, J = 7.2 Hz, 2H), 4.32 (d, J = 4.5 Hz, 2H), 3.78 – 3.63 (m, 2H), 3.10 – 2.93 (m, 2H), 2.17 – 1.93 (m, 9H), 1.76 (s, 1H), 1.68 (s, 7H), 1.60 (d, J = 3.4 Hz, 5H). ^{13}C NMR (101 MHz, CDCl_3) δ 181.52, 170.24, 170.20, 156.45, 142.83, 142.65, 142.57, 138.60, 135.75, 135.54, 135.41, 135.38, 133.65, 133.54, 131.52, 131.31, 131.27, 128.67, 128.63, 126.54, 124.35, 124.27, 124.22, 123.57, 13.34, 118.84, 117.94, 117.92, 114.74, 61.85, 61.58, 55.66, 53.69, 39.76, 39.63, 39.47, 32.88, 29.64, 26.66, 26.18, 25.65, 23.32, 17.64, 17.60, 16.49, 16.47, 15.96, 14.07.

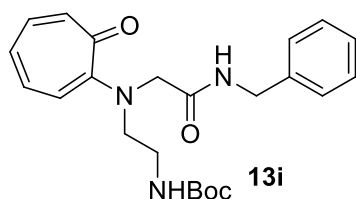
(xvii) *Trpeg-Geraniol (5b)*:



40 mg (66% yield) of pure product was obtained as light yellow viscous liquid.

^1H NMR (400 MHz, CDCl_3) δ 7.35 – 7.27 (m, 2H), 7.28 – 7.19 (m, 3H), 7.14 – 6.98 (m, 2H), 6.94 (d, J = 11.7 Hz, 1H), 6.63 (dd, J = 21.0, 9.9 Hz, 2H), 5.33 (td, J = 7.1, 1.2 Hz, 1H), 5.07 (ddd, J = 6.8, 4.0, 1.2 Hz, 1H), 4.66 (d, J = 7.1 Hz, 2H), 4.32 (s, 2H), 3.77 – 3.62 (m, 2H), 3.07 – 2.93 (m, 2H), 2.14 – 1.97 (m, 4H), 1.68 (s, 6H), 1.59 (s, 3H). ^{13}C NMR (101 MHz, CDCl_3) δ 181.55, 170.27, 156.48, 142.62, 138.62, 135.42, 133.69, 133.56, 131.81, 128.69, 128.66, 126.57, 124.31, 123.69, 117.94, 114.79, 61.89, 55.68, 53.72, 39.49, 32.90, 29.66, 26.26, 25.65, 17.66, 16.49.

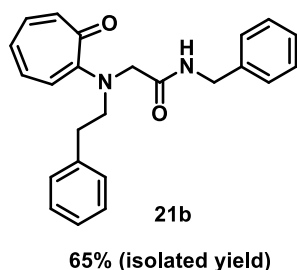
(xviii) *Traeg-NHCH₂Ph* (**13i**):



20 mg (49% yield) of pure product was obtained as yellow viscous liquid. ¹H NMR (400 MHz, CDCl₃) δ 7.75 (t, *J* = 5.7 Hz, 1H), 7.37 – 7.18

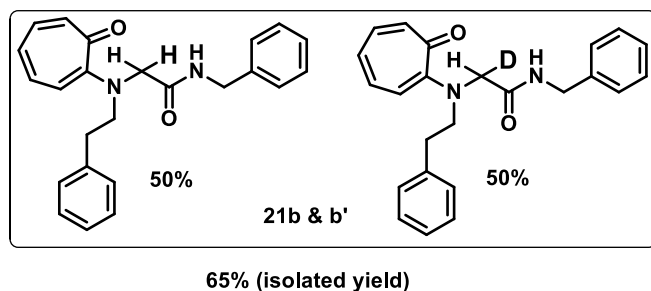
(m, 5H), 7.14 (ddd, *J* = 11.9, 8.2, 1.0 Hz, 1H), 7.10 – 6.94 (m, 2H), 6.86 (d, *J* = 10.0 Hz, 1H), 6.80 – 6.67 (m, 1H), 5.41 (s, 1H), 4.44 (t, *J* = 8.1 Hz, 2H), 3.99 (s, 2H), 3.50 (t, *J* = 6.2 Hz, 2H), 3.32 (d, *J* = 5.6 Hz, 2H), 1.53 – 1.31 (m, 9H). ¹³C NMR (101 MHz, CDCl₃) δ 182.85, 169.42, 157.49, 156.13, 138.14, 136.18, 134.58, 133.94, 128.53, 127.37, 127.20, 126.75, 118.51, 56.06, 51.46, 43.21, 37.84, 29.62, 28.30.

(xix) *Trpeg-NHCH₂Ph* (**21b**):



15 mg (65%) of pure product was isolated as yellow viscous liquid. ¹H NMR (400 MHz, CDCl₃) δ 7.72 (s, 1H), 7.33 – 7.14 (m, 10H), 7.14 – 7.06 (m, 3H), 7.06 – 6.97 (m, 2H), 6.74 (t, *J* = 9.9 Hz, 2H), 4.40 (d, *J* = 6.1 Hz, 2H), 3.92 (s, 2H), 3.65 – 3.55 (m, 2H), 2.94 – 2.80 (m, 2H). ¹³C NMR (101 MHz, CDCl₃) δ 183.14, 169.67, 157.52, 138.39, 138.36, 136.14, 134.72, 133.59, 128.75, 128.65, 128.57, 127.51, 127.20, 126.71, 126.66, 118.63, 56.84, 53.74, 43.28, 32.83. HRMS (ESI-TOF) *m/z*: [M+Na]⁺ calcd. for C₂₄H₂₄N₂O₂ 395.1730, found 395.1742.

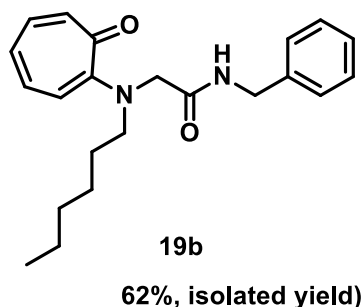
(xx) *Trpeg-NHCH₂Ph* (**21b & b'**):



27 mg (65%) of pure product was isolated as yellow viscous liquid. ¹H NMR (400 MHz, CDCl₃) δ 7.74 (s,

1H), 7.35 – 7.13 (m, 10H), 7.10 (dd, *J* = 13.4, 6.3 Hz, 3H), 7.02 (t, *J* = 10.3 Hz, 2H), 6.73 (t, *J* = 9.5 Hz, 2H), 4.40 (d, *J* = 6.1 Hz, 2H), **3.90 (d, *J* = 6.8 Hz, 1H)**, 3.68 – 3.54 (m, 2H), 2.94 – 2.78 (m, 2H). ¹³C NMR (101 MHz, CDCl₃) δ 183.03, 169.63, 157.43, 138.32, 138.28, 136.08, 134.63, 134.60, 133.55, 128.68, 128.58, 128.50, 127.44, 127.13, 126.64, 126.59, 118.58, 118.50, 118.42, 56.82 (CH₂), **56.73, 56.53, 56.33 (t, CHD)**, 53.68, 53.65, 43.20. HRMS (ESI-TOF) *m/z*: [M+H]⁺ calcd. for C₂₄H₂₃DN₂O₂ 396.1793, found 396.1800.

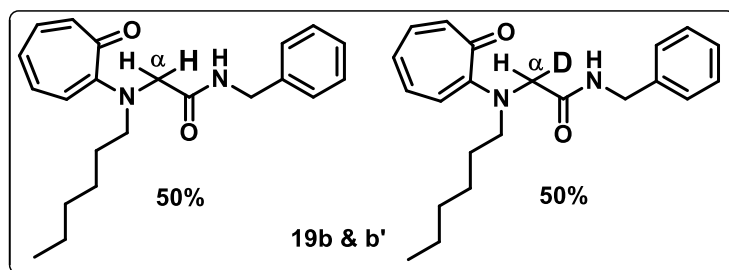
(xxi) *Trhg-NHCH₂Ph* (**19b**):



25 mg (62%) of pure product was isolated as yellow viscous liquid. ¹H NMR (400 MHz, CDCl₃) δ 7.99 (s, 1H), 7.33 – 7.25 (m, 4H), 7.25 – 7.18 (m, 1H), 7.13 (ddd, *J* = 11.9, 8.3, 1.3 Hz, 1H), 7.02 (ddd, *J* = 17.0, 13.3, 6.3 Hz, 2H), 6.68 (dd, *J* = 20.7, 9.8 Hz, 2H), 4.50 (d, *J* = 6.0 Hz, 2H), 3.92 (s,

2H), 3.36 – 3.23 (m, 2H), 1.65 – 1.46 (m, 2H), 1.35 – 1.15 (m, 8H), 0.86 (dd, *J* = 9.4, 4.1 Hz, 4H). ¹³C NMR (101 MHz, CDCl₃) δ 183.09, 170.06, 157.96, 138.42, 136.13, 134.15, 133.80, 128.57, 127.58, 127.21, 126.09, 117.89, 56.57, 52.36, 43.33, 31.47, 26.72, 26.02, 22.54, 13.99. HRMS (ESI-TOF) *m/z*: [M+H]⁺ calcd. for C₂₂H₂₈N₂O₂ 375.2043, found 375.2017.

(xxii) *Trhg-NHCH₂Ph* (**19b**):



70% (isolated yield)

35 mg (60%) of pure product was isolated as yellow viscous liquid. ¹H NMR (400 MHz, CDCl₃) δ 8.01 (s, 1H), 7.35 – 7.27 (m, 2H), 7.24 (dq,

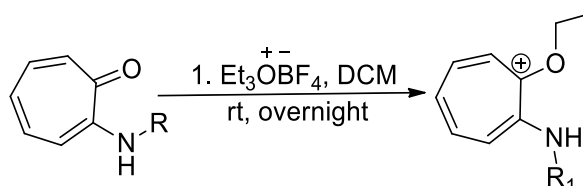
J = 6.1, 4.0 Hz, 1H), 7.14 (ddd, *J* = 11.9, 8.3, 1.2 Hz, 1H), 7.10 – 6.94 (m, 1H), 6.69 (dd, *J* = 20.7, 9.9 Hz, 1H), 4.51 (d, *J* = 6.0 Hz, 1H), 3.93 (d, *J* = 6.8 Hz, 1H), 3.38 – 3.23 (m, 1H), 1.36 – 1.18 (m, 4H), 0.88 (dd, *J* = 9.3, 4.2 Hz, 2H). ¹³C NMR (101 MHz, CDCl₃) δ 183.00, 182.98, 182.95, 169.96, 157.86, 138.35, 136.07, 134.03, 134.00, 133.76, 128.50, 127.51, 127.14, 126.03, 125.98, 125.94, 117.83, 117.75, 117.67, 56.49, 56.40, 56.20, 55.98, 52.31, 52.26, 52.22, 43.25, 31.40, 26.64, 25.95, 22.47, 20.98, 13.92. HRMS (ESI-TOF) *m/z*: [M+H]⁺ calcd. for C₂₂H₂₇DN₂O₂ 376.2106, found 376.2080.

3.5 References and notes

1. Branden, C.; Tooze, J. *Introduction to Protein Structure*; Garland: New York, NY, **1991**.
2. Aubé, J. *Angew. Chem., Int. Ed.* **2012**, *51*, 3063.
3. Pattabiraman, V. R.; Bode, J. W. *Nature*, **2011**, *480*, 471.
4. Shen, B.; Makley, D. M.; Johnston, J. N. *Nature*, **2010**, *465*, 1027.
5. Radzicka, A.; Wolfenden, R. *J. Am. Chem. Soc.* **1996**, *118*, 6105.
6. Szostak, M.; and Aubé, J. *Chem. Rev.* **2013**, *113*, 5701–5765.
7. Jonathan Clayden, Nick Greeves, and Stuart Warren. *Organic Chemistry*, 2012, 2nd Edition.
8. Clayden, J.; Moran, W. J. *Angew. Chem., Int. Ed.* **2006**, *45*, 7118.
9. Szostak, M.; Aube, J. *Org. Biomol. Chem.* **2011**, *9*, 27.
10. Clayden, J. *Nature*. **2012**, *481*, 274.
11. Tani, K.; Stoltz, B. M. *Nature*. **2006**, *441*, 731.
12. Blackburn, G. M.; Plackett, J. D. *J. Chem. Soc. Perkin Trans. 2.* **1972**, 1366.
13. Kirby, A. J.; Komarov, I. V.; Wothers, P. D.; Feeder, N. *Angew. Chem., Int. Ed.* **1998**, *37*, 785.
14. Aaron, J. B.; Subhajyoti, C.; Brandon Q. M.; Victor S. B.; Robert H. C. *New. J. Chem.* **2016**, *40*, 1974.
15. Szostak, M.; Lei, Y.; Victor W. D.; Douglas R. P.; and Aube, J. *J. Am. Chem. Soc.*, **2010**, *132*, 8836.;
16. Szostak, R.; Aube, J.; Szostak, M. *Chem. Commun.*, **2015**, *51*, 6395.
17. Igor V. K.; Yanik, S.; Ishchenko, A. Y.; Davies, J. E.; Goodman, J. M.; Kirby, A. J. *J. Am. Chem. Soc.* **2015**, *137*, 926–930.
18. Hu, F.; Lalancette, R.; Szostak, M. *Angew. Chem. Int. Ed.* **2016**, *55*, 5062 –5066.

19. Bythell, B. J.; Suhai, S.; Somogyi, Á.; Paizs, B. *J. Am. Chem. Soc.* **2009**, *131*, 14057.
20. Fernandes, N. M.; Fache, F.; Rosen, M.; Nguyen, P.-L.; Hansen, D. E. *J. Org. Chem.* **2008**, *73*, 6413.
21. Hutchby, M.; Houlden, C. E.; Ford, J. G.; Tyler, S. N. G.; Gagné, M. R.; Lloyd-Jones, G. C.; Booker-Milburn, K. I. *Angew. Chem., Int. Ed.* **2009**, *48*, 8721.
22. Mujika, J. I.; Mercero, J. M.; Lopez, X. *J. Am. Chem. Soc.* **2005**, *127*, 4445.
23. Shimizu, Y.; Noshita, M.; Mukai, Y.; Morimoto, H.; Ohshima, T. *Chem. Commun.* **2014**, *50*, 12623.
24. Gomez-Reyes, B.; Yatsimirsky, A. K. *Org. Biomol. Chem.* **2003**, *1*, 866.
25. Kita, Y.; Nishii, Y.; Higuchi, T.; Mashima, K. *Angew. Chem., Int. Ed.* **2012**, *51*, 5723.
26. Milović, N. M.; Kostić, N. M. *J. Am. Chem. Soc.* **2003**, *125*, 781.
27. Stephenson, N. A.; Zhu, J.; Gellman, S. H.; Stahl, S. S. *J. Am. Chem. Soc.* **2009**, *131*, 10003.
28. Vikki, E.; Mary, F. M.; Ruth, L. W. *Tetrahedron* **2014**, *70*, 7593.
29. Hie, L.; Noah F.; Nathel, F.; Shah, T. K.; Baker, E. L.; Hong, X.; Yang, Y-F.; Liu, P.; Houk, K. N.; Garg, N. K. *Nature*, **2015**, *524*, 79.
30. Simmons, B. J.; Weires, N. A.; Dander, J. E.; Garg N. K. *ACS Catal.* **2016**, *6*, 3176.
31. Weires, N. A.; Baker, E. L.; Garg, N. K. *Nat. Chem.*, **2016**, *8*, 75.
32. Baker, E. L.; Yamano, M. M.; Zhou, Y.; Anthony S. M.; Garg, N. K., *Nat. Commun.*, DOI: 10.1038/ncomms11554.
33. Ruider S. A.; Maulide, N. *Angew. Chem. Int. Ed.* **2015**, *54*, 13856 – 13858.
34. Liu, C.; Achtenhagen, M.; Szostak, M. *Org. Lett.* **2016**, *18*, 2375–2378.
35. Meng, G.; Szostak, M. *Org. Lett.* **2015**, *17*, 4364–4367.
36. Meng, G.; Szostak, M. *Org. Lett.* **2016**, *18*, 796–799.
37. Meng, G.; Szostak, M. *Angew. Chem. Int., Ed.* **2015**, *54*, 14518-14522.

38. Meng, G.; Szostak, M. *Org. Biomol. Chem.* **2016**, *14*, DOI: 10.1039/c6ob00084c.
39. Shi, S.; Meng, G.; Szostak, M. *Angew. Chem. Int., Ed.*, **2016**, *55*, DOI: 10.1002/anie.201601914.
40. Liu, Y.; Meng, G.; Liu, R.; Szostak, M. *Chem. Commun.*, **2016**, *52*, DOI: 10.1039/c6cc02324j.
41. Hutchby, M.; Houlden, C. E.; Haddow, M. F.; Tyler, S. N. G.; Lloyd-Jones, G. C.; Booker-Milburn, K. I. *Angew. Chem., Int. Ed.* **2012**, *51*, 548.
42. Nielsen, P. E.; Egholm, M.; Berg, R. H.; Buchardt, O. *Science*. **1991**, *254*, 1497.
43. Sharma, N. K.; Ganesh, K. N. *Chem. Commun.* **2005**, 4330.
44. Balachandra, C.; Sharma, N. K. *Tetrahedron*. **2014**, *70*, 7464.
45. Balachandra, C.; Sharma, N. K. *Org. Lett.* **2015**, *17*, 3948.
46. Dochnahl, M.; Löhnwitz, K.; Pissarek, J.-W.; Biyikal, M.; Schulz, S. R.; Schön, S.; Meyer, N.; Roesky, P. W.; Blechert, S. *Chem. - Eur. J.* **2007**, *13*, 6654.
47. Zulys, A.; Dochnahl, M.; Hollmann, D.; Löhnwitz, K.; Herrmann, J.-S.; Roesky, P. W.; Blechert, S., *Angew. Chem., Int. Ed.* **2005**, *44*, 7794.;
48. Dochnahl, M.; Pissarek, J.-W.; Blechert, S.; Lohnwitz, K.; Roesky, P. W., *Chem. Commun.* **2006**, 3405.;
49. Davis, W. M.; Roberts, M. M.; Zask, A.; Nakanishi, K.; Nozoe, T.; Lippard, S. J., *J. Am. Chem. Soc.* **1985**, *107*, 3864.;
50. Reported conventional synthesis of alkyloxy amino tropylium cation.



51. Tidwell, T. T. *Angew. Chem. In. Ed.* **2005**, *44*, 5778.
52. Brady, W. T.; Liddell, H. G.; Vaughn, W. L. *J. Org. Chem.* **1966**, *31*, 626.

53. Cho, B. R.; Jeong, H. C.; Seung, Y. J.; Pyun, S. Y. *J. Org. Chem.* **2002**, *67*, 5232.
54. Allen, A. D.; Tidwell, T. T. *J. Am. Chem. Soc.* **1987**, *109*, 2774.
55. Allen, A. D.; Tidwell, T. T. *Chem. Rev.* **2013**, *113*, 7287.
56. Pauson, P. L. *Chem. Rev.* **1955**, *55*, 9-136.
57. Wang, T. C.; Qiao, J. X. *Tetrahedron Lett.* **2016**, *57*, 1941.
58. Foley, M. A.; Jamison, T. F. *Org. Process Res. Dev.* **2010**, *14*, 1177.
59. Merling, G. *Chem. Ber.* **1891**, *24*, 3108.
60. Doering, W. V. E.; Knox, L. H. *J. Am. Chem. Soc.* **1954**, *76*, 3203.
61. Dauben, H. J.; Gadeckt, F. A.; Harmon, K. M.; Pearson, D. L. *J. Am. Chem. Soc.* **1957**, *79*, 4557.
62. <http://cssp.chemspider.com/article.aspx?id=481> (tropylium cation synthesis and spectra).
63. Chatterjee, B.; Krishnakumar, V.; Gunanathan, C. *Org. Lett.* **2016**, *18*, 5892.

3.6 Appendix-3

Table of Contents

1. Characterization data, Time dependent NMR and Mass spectrum after time dependent NMR of <i>BocNH-Traeg-Phe-OMe</i> (13a).....	170
2. Characterization data, time dependent NMR and Mass spectrum after time dependent NMR of <i>BocNH-Traeg-Ile-OMe</i> (13c)	172
3. Characterization data ($^1\text{H}/^{13}\text{C}$ NMR and HRMS), Time dependent NMR and Mass spectrum after time dependent NMR of <i>BocNH-Traeg-Gly-Phe-OMe</i> (13d).....	176
4. Characterization data ($^1\text{H}/^{13}\text{C}$ -NMR and HRMS), Time dependent NMR and Mass spectrum after time dependent NMR of <i>BocNH-Traeg-Gly-OMe</i> (13e)	178
5. Characterization data ($^1\text{H}/^{13}\text{C}$ -NMR and HRMS), Time dependent NMR and Mass spectrum after time dependent NMR of <i>BocNH-Traeg-Ala-OMe</i> (13f).....	182
6. Characterization data ($^1\text{H}/^{13}\text{C}$ NMR and HRMS) of 6b-OEt	186
7. Characterization data ($^1\text{H}/^{13}\text{C}$ NMR and HRMS), Time dependent NMR and Mass spectrum after time dependent NMR of <i>AcNH-Traeg-Phe-OMe</i> (14)	188
8. Characterization data ($^1\text{H}/^{13}\text{C}$ NMR and HRMS), Time dependent NMR and Mass spectrum after time dependent NMR of <i>BocNH-Traeg-Trp-OMe</i> (13g)	192
9. Characterization data ($^1\text{H}/^{13}\text{C}$ NMR and HRMS), Time dependent NMR and Mass spectrum after time dependent NMR of <i>BocNH-Traeg-Pro-Ile-Phe-OMe</i> (13h)	196
10. Characterization data ($^1\text{H}/^{13}\text{C}$ NMR and HRMS) <i>Trpro</i> (9):.....	200
11. Characterization data ($^1\text{H}/^{13}\text{C}$ NMR and HRMS) <i>Trpro-Gly</i> (9G):.....	202
12. Characterization data ($^1\text{H}/^{13}\text{C}$ NMR and HRMS) <i>TrPro-Phe-OMe</i> (9F):.....	204
13. Characterization data ($^1\text{H}/^{13}\text{C}$ NMR and HRMS) <i>Trhg</i> (18):	206
14. Characterization data ($^1\text{H}/^{13}\text{C}$ NMR and HRMS) <i>Trhg-Gly</i> (19).....	207
15. Characterization data ($^1\text{H}/^{13}\text{C}$ NMR and HRMS) <i>Trpeg</i> (20):	209
16. Characterization data ($^1\text{H}/^{13}\text{C}$ NMR and HRMS) <i>Trpeg-Gly</i> (21):.....	211
17. Characterization data ($^1\text{H}/^{13}\text{C}$ NMR and HRMS) <i>Trog-Gly</i> (23):	213
18. Characterization data ($^1\text{H}/^{13}\text{C}$ NMR and HRMS) <i>Trpro lactone</i> (25):.....	215
19. HSQC spectra of <i>Trpro lactone</i> (25):.....	216
20. Monitoring of reversible amidation by $^1\text{H}/^{13}\text{C}$ NMR of <i>Trpro-Gly</i> (9G):.....	219
21. Characterization data ($^1\text{H}/^{13}\text{C}$ NMR and HRMS) <i>Trpeg lactone</i> (27):	220
22. Monitoring of reversible amidation by $^1\text{H}/^{13}\text{C}$ NMR of <i>Trpeg-Gly</i> (21).....	222
23. Characterization data ($^1\text{H}/^{13}\text{C}$ NMR and HRMS) <i>Trhg lactone</i> (26):.....	223
24. Monitoring of reversible amidation by $^1\text{H}/^{13}\text{C}$ NMR of <i>Trhg-Gly</i> (19)	225
25. Characterization data ($^1\text{H}/^{13}\text{C}$ NMR and HRMS) <i>Trog lactone</i> (28):.....	226

26.	Monitoring of reversible amidation by $^1\text{H}/^{13}\text{C}$ NMR of <i>Trog-Gly</i> (23):	228
27.	Characterization data ($^1\text{H}/^{13}\text{C}$ NMR and HRMS) <i>Trpeg-Farnesol</i> (5c):	229
28.	Characterization data ($^1\text{H}/^{13}\text{C}$ NMR and HRMS) <i>Trpeg-Geraniol</i> (5b):	230
29.	Characterization data ($^1\text{H}/^{13}\text{C}$ NMR and HRMS) <i>Traeg-Benzyl amine</i> (13i):.....	231
30.	NMR ($^1\text{H}/^{13}\text{C}$) and HRMS spectra of control monomer 8-OEt :	232
31.	Characterization data ($^1\text{H}/^{13}\text{C}$ NMR and HRMS), Time dependent NMR and Mass spectrum after time dependent NMR of <i>BocNH-Bnaeg-Phe-OMe</i> (16):.....	234
32.	Characterization data ($^1\text{H}/^{13}\text{C}$ NMR and HRMS), Time dependent NMR and Mass spectrum after time dependent NMR of <i>BocNH-Fmocaeg-Gly-OMe</i> (17):.....	240
33.	$^1\text{H}/^{13}\text{C}$ NMR spectra of <i>Trhg-OEt</i> and <i>Trhg</i> lactone in CD_3CN after addition of TFA.....	244
34.	$^1\text{H}/^{13}\text{C}/\text{DEPT}135$ NMR spectra of <i>Trhg-OEt</i> and $\alpha\text{-CH}_2$ deuterated <i>Trhg</i> lactone in CD_3CN after addition of TFA-D	245
35.	$^1\text{H}/^{13}\text{C}/\text{DEPT}135$ NMR and HRMS spectra of <i>Trhg-NHCH}_2\text{Ph}</i> in CDCl_3	247
36.	$^1\text{H}/^{13}\text{C}/\text{DEPT}135$ NMR and HRMS spectra of <i>Trhg-NHCH}_2\text{Ph}</i> and α -methylene deuterated ($\alpha\text{-CHD}$) <i>Trhg-NHCH}_2\text{Ph}</i> in CDCl_3	250
37.	$^1\text{H}/^{13}\text{C}$ NMR spectra of <i>Trpeg-OEt</i> and <i>Trpeg</i> lactone in CD_3CN after addition of TFA.....	253
38.	$^1\text{H}/^{13}\text{C}$ NMR spectra of <i>Trpeg-OEt</i> and $\alpha\text{-CH}_2$ mono deuterated <i>Trpeg</i> lactone in CD_3CN after addition of TFA-D	254
39.	$^1\text{H}/^{13}\text{C}/\text{DEPT}135$ NMR and HRMS spectra of <i>Trpeg-NHCH}_2\text{Ph}</i> in CDCl_3	256
40.	$^1\text{H}/^{13}\text{C}/\text{DEPT}135$ NMR and HRMS spectra of <i>Trpeg-NHCH}_2\text{Ph}</i> and α -methylene deuterated ($\alpha\text{-CHD}$) <i>Trpeg-NHCH}_2\text{Ph}</i> in CDCl_3	259
41.	NMR ($^1\text{H}/^{13}\text{C}$) and HRMS spectra of Ethyl N-Boc aminoethyl β -alanate (S7):	262
42.	NMR ($^1\text{H}/^{13}\text{C}$) and HRMS spectra of <i>Troponyl aminoethyl β-alanate</i> (7-OEt):.....	264
43.	Mass spectrum of <i>Troponyl aminoethyl β-alanine</i> (7):	266
44.	Characterization data ($^1\text{H}/^{13}\text{C}$ NMR and HRMS), Time dependent NMR and Mass spectrum after time dependent NMR <i>BocNH-Traeb-Ile-OMe</i> (15):.....	267
45.	Characterization data ($^1\text{H}/^{13}\text{C}$ NMR and HRMS) of <i>BocNH-AAIB-OEt</i> :.....	272
46.	Rate constant determination of amide solvolysis (CD_3OD) in peptide 13f :.....	275
39.	UV-Vis Spectroscopic studies of lactone formation:	279
47.	$^1\text{H}/^{13}\text{C}$ -NMR of <i>BocNH-Traeg-Gly-OMe</i> (13e) in CD_3CN before and after addition of TFA: 288	
49.	LC-MS spectrum of <i>Boc-Traeg- Ile-OMe</i> :.....	292

1. Characterization data, Time dependent NMR and Mass spectrum after time dependent NMR of *BocNH-Traeg-Phe-OMe* (**13a**).

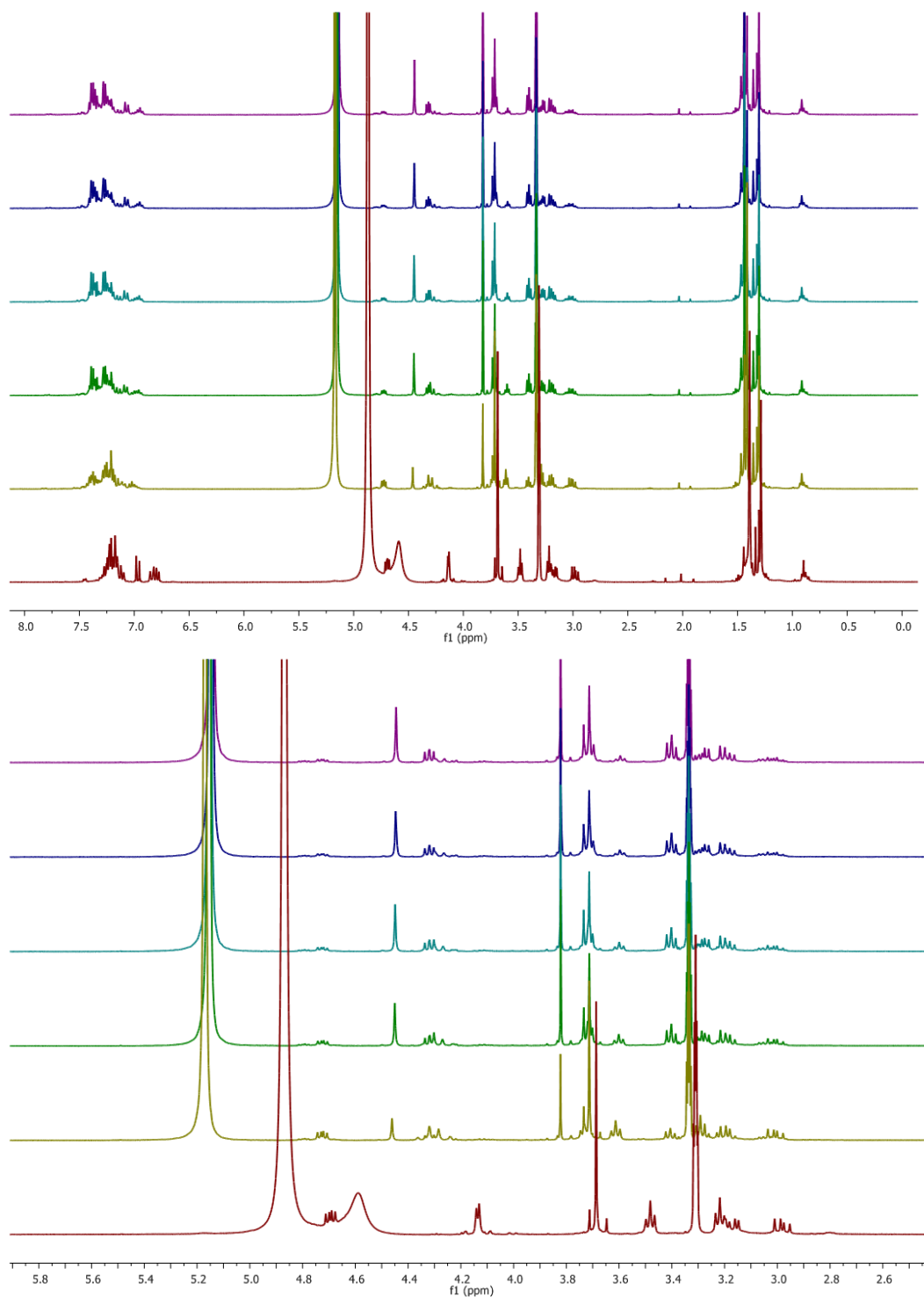


Figure A1. Time dependent NMR of *BocNH-Traeg-Phe-OMe* (**13a**) in CD₃OD and 5.0% TFA

Display Report

Analysis Info

Analysis Name D:\Data\NOV-2013\NKS\22112013NKSBC_915TFA100.d
 Method Pos_tune_low.m
 Sample Name 23112013_NKS_GC_TETRAAMINE
 Comment

Acquisition Date 11/24/2013 10:26:44 AM

Operator Amit
 Instrument micrOTOF-Q II 10337

Acquisition Parameter

Source Type	ESI	Ion Polarity	Positive	Set Nebulizer	0.4 Bar
Focus	Not active	Set Capillary	4500 V	Set Dry Heater	180 °C
Scan Begin	50 m/z	Set End Plate Offset	-500 V	Set Dry Gas	4.0 l/min
Scan End	3000 m/z	Set Collision Cell RF	130.0 Vpp	Set Divert Valve	Waste

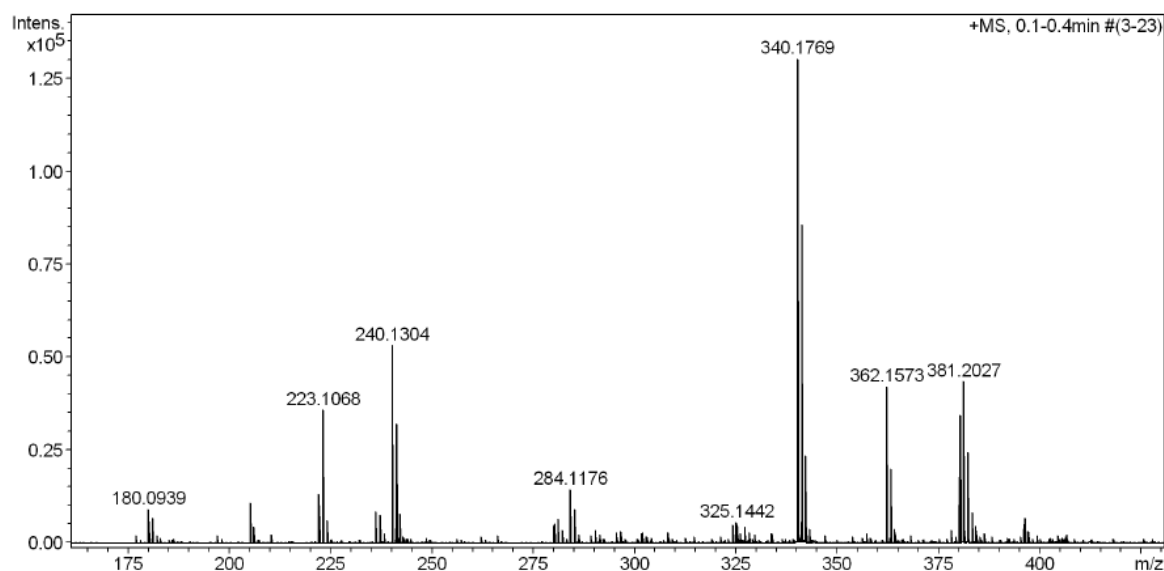
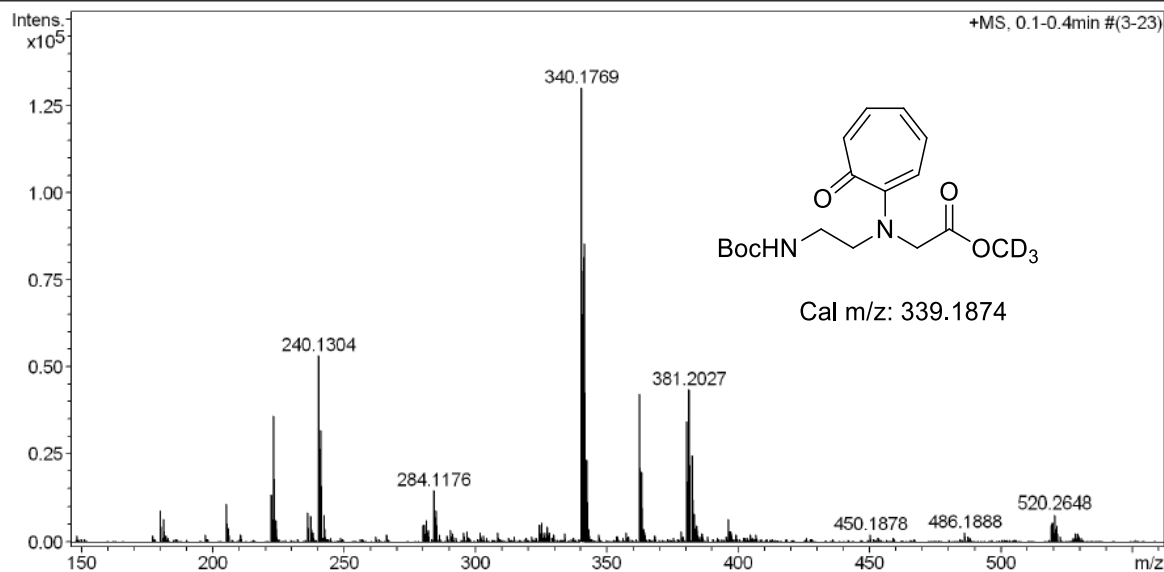


Figure A2. Time Dependent NMR of *BocNH-Traeg-Phe-OMe* (**13a**) in 5.0% TFA in CD₃OD

2. Characterization data, time dependent NMR and Mass spectrum after time dependent NMR of *BocNH-Traeg-Ile-OMe* (**13c**)

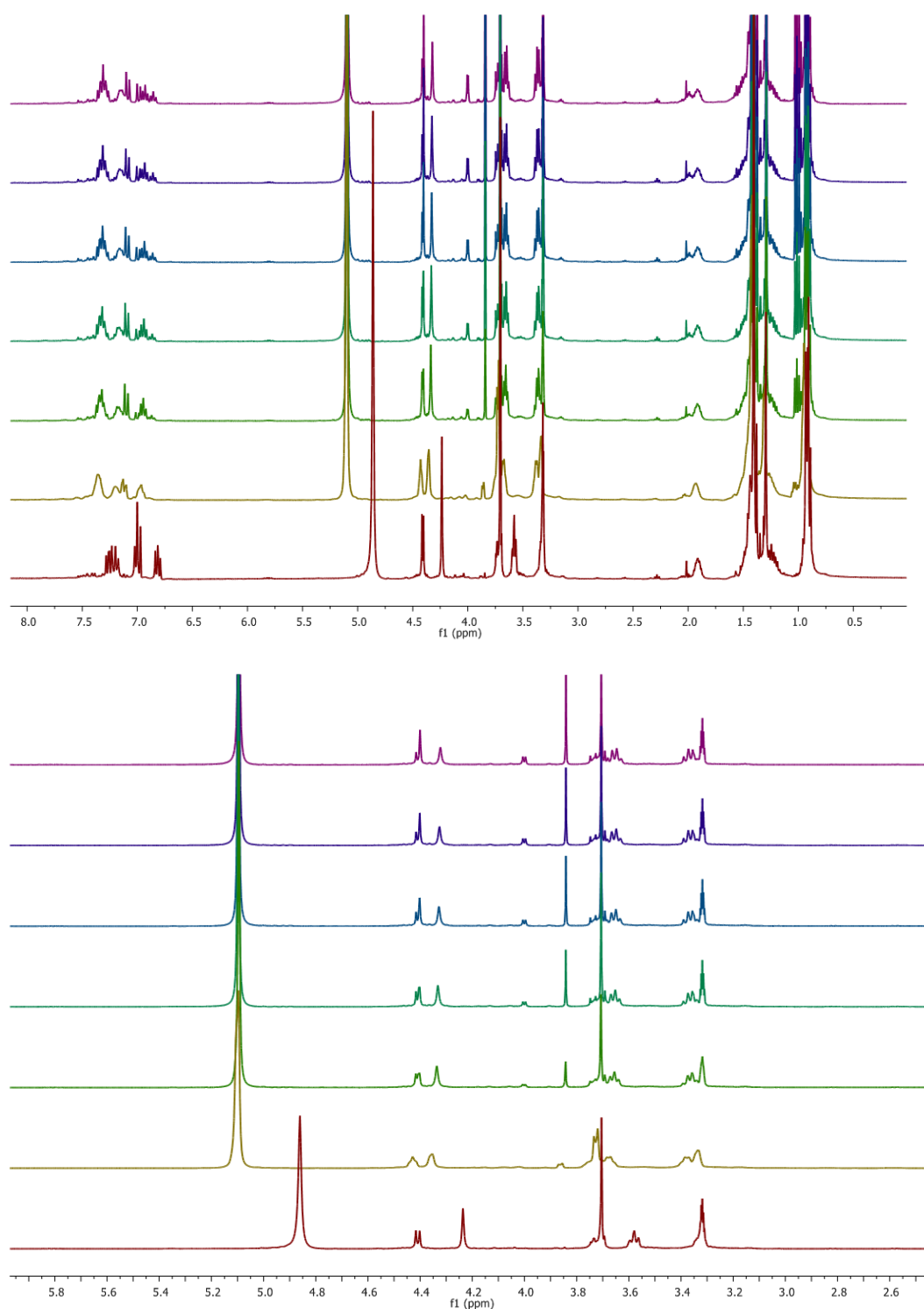


Figure A3. Time dependent NMR of *BocNH-Traeg-Ile-OMe* (**13c**) in CD₃OD and 5.0% TFA at interval of 7.0 minutes

Generic Display Report

Analysis Info

Analysis Name D:\Data\AUG-2014\NKS\20082014_NKS_CB_450D.d
 Method Pos_tune_low.m
 Sample Name LCMS-NISER
 Comment

Acquisition Date 8/20/2014 2:54:14 PM

Operator A.S.Sahu
 Instrument micrOTOF-Q II

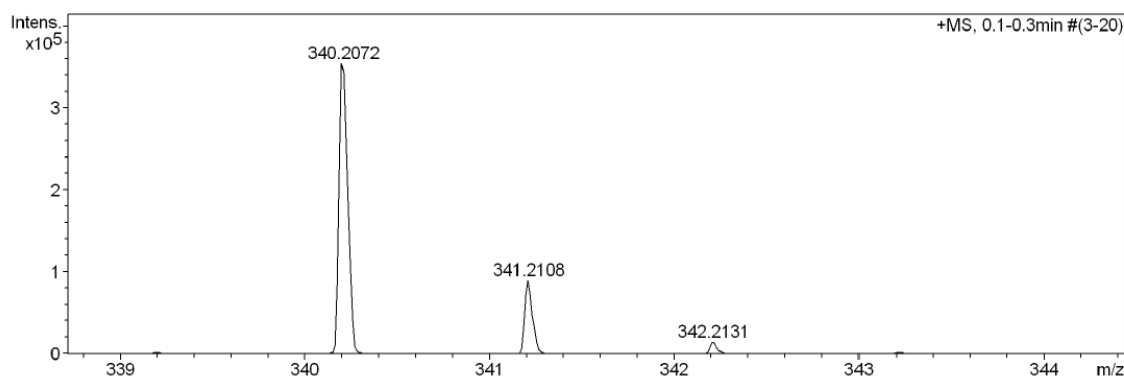
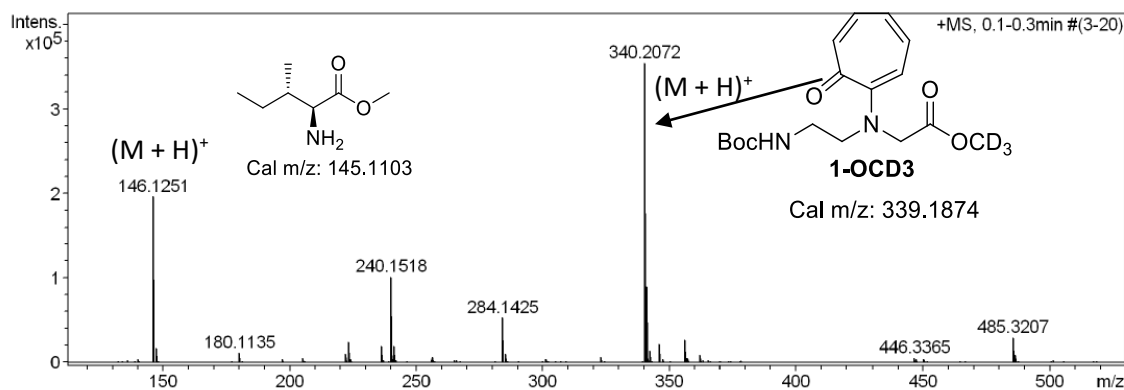
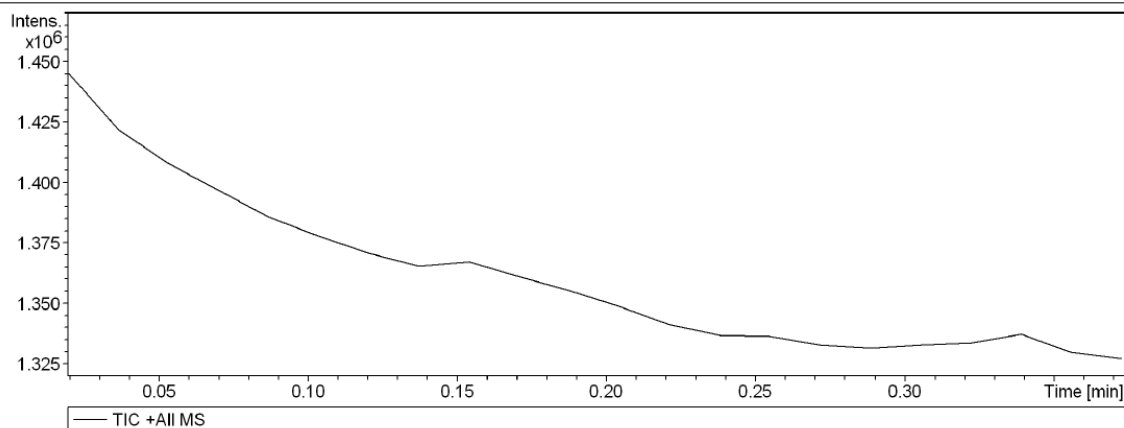


Figure A4. Mass spectrum of *BocNH-Traeg-Ile-OMe* (**13c**) after time dependent NMR experiment in CD₃OD.

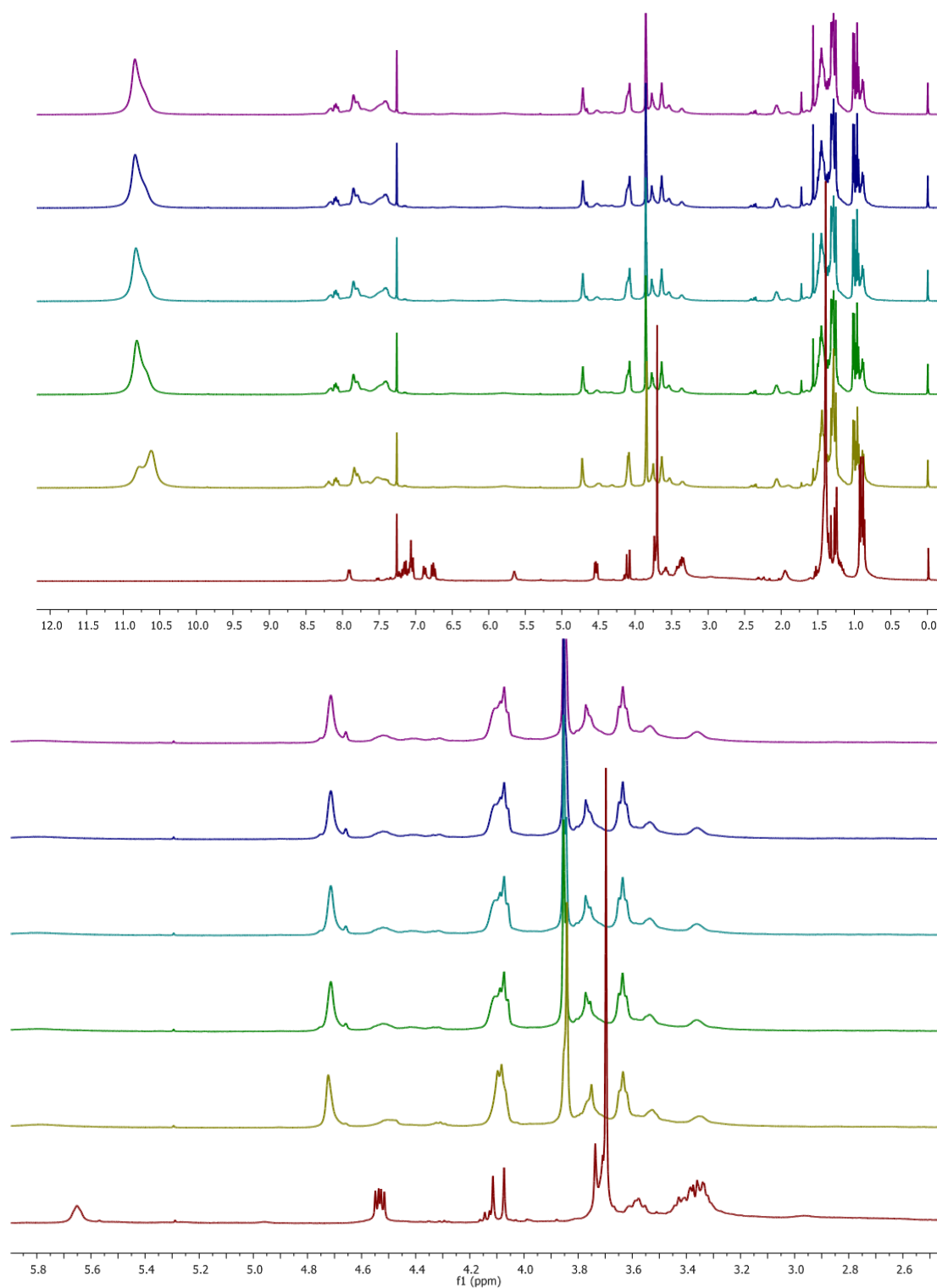


Figure A5. Time dependent NMR of *BocNH-Traeg-Ile-OMe* (**13c**) in CDCl_3 and 5% TFA at interval of 7.0 minutes.

Display Report

Analysis Info

Analysis Name D:\Data\MARCH-2014\NKS\12032014_NKS_CB_TRIAL.d
 Method Pos_tune_low.m
 Sample Name ACN
 Comment

Acquisition Date 3/12/2014 3:34:55 PM

Operator RAJKUMAR
 Instrument micrOTOF-Q II 10337

Acquisition Parameter

Source Type	ESI	Ion Polarity	Positive	Set Nebulizer	0.4 Bar
Focus	Not active	Set Capillary	4500 V	Set Dry Heater	180 °C
Scan Begin	50 m/z	Set End Plate Offset	-500 V	Set Dry Gas	4.0 l/min
Scan End	3000 m/z	Set Collision Cell RF	130.0 Vpp	Set Divert Valve	Waste

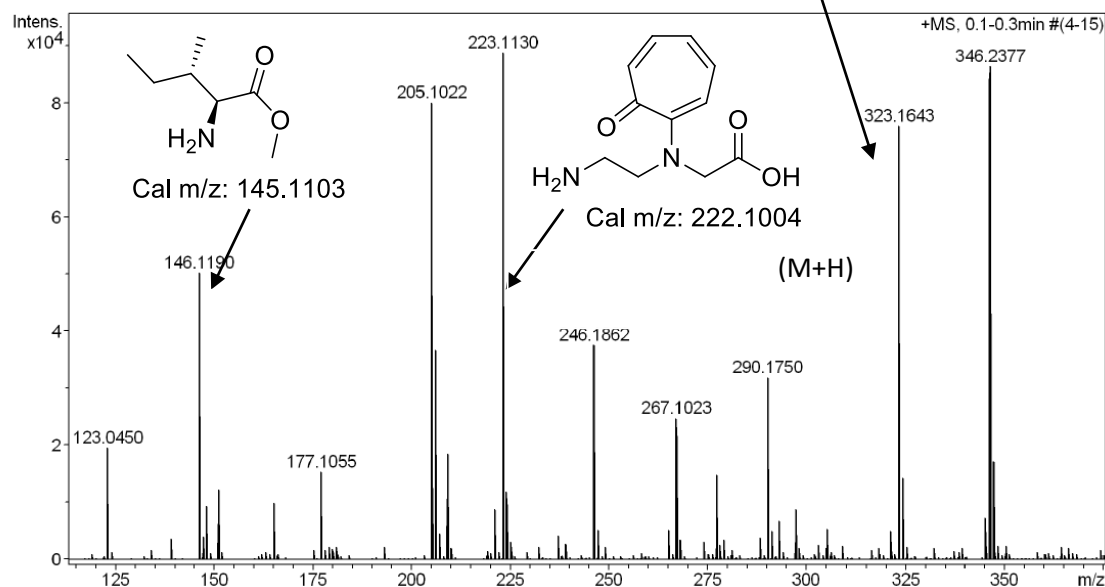
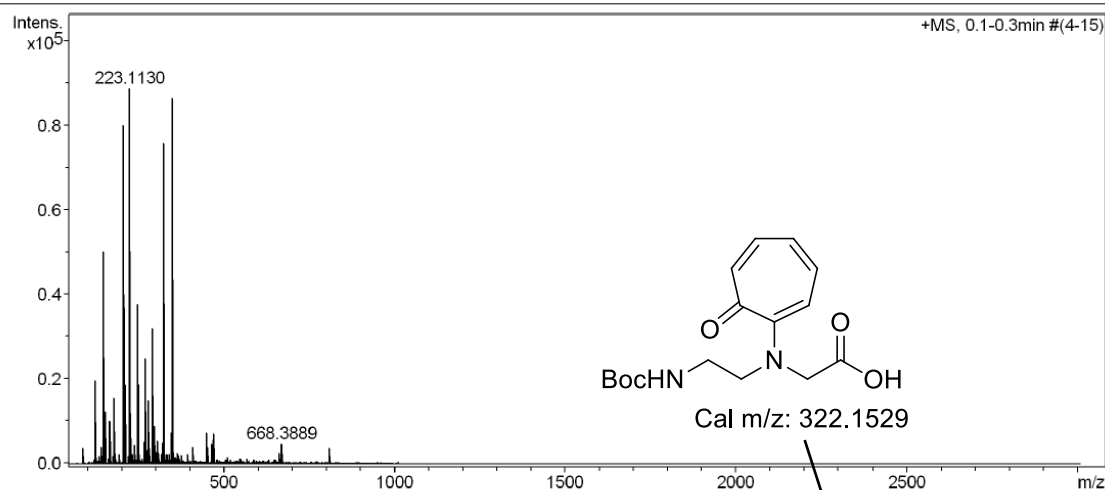


Figure A6. Mass spectrum of BocNH-Traeg-Ile-OMe (13c) after time dependent NMR experiment in CDCl₃

3. Characterization data ($^1\text{H}/^{13}\text{C}$ NMR and HRMS), Time dependent NMR and Mass spectrum after time dependent NMR of *BocNH-Traeg-Gly-Phe-OMe* (**13d**)

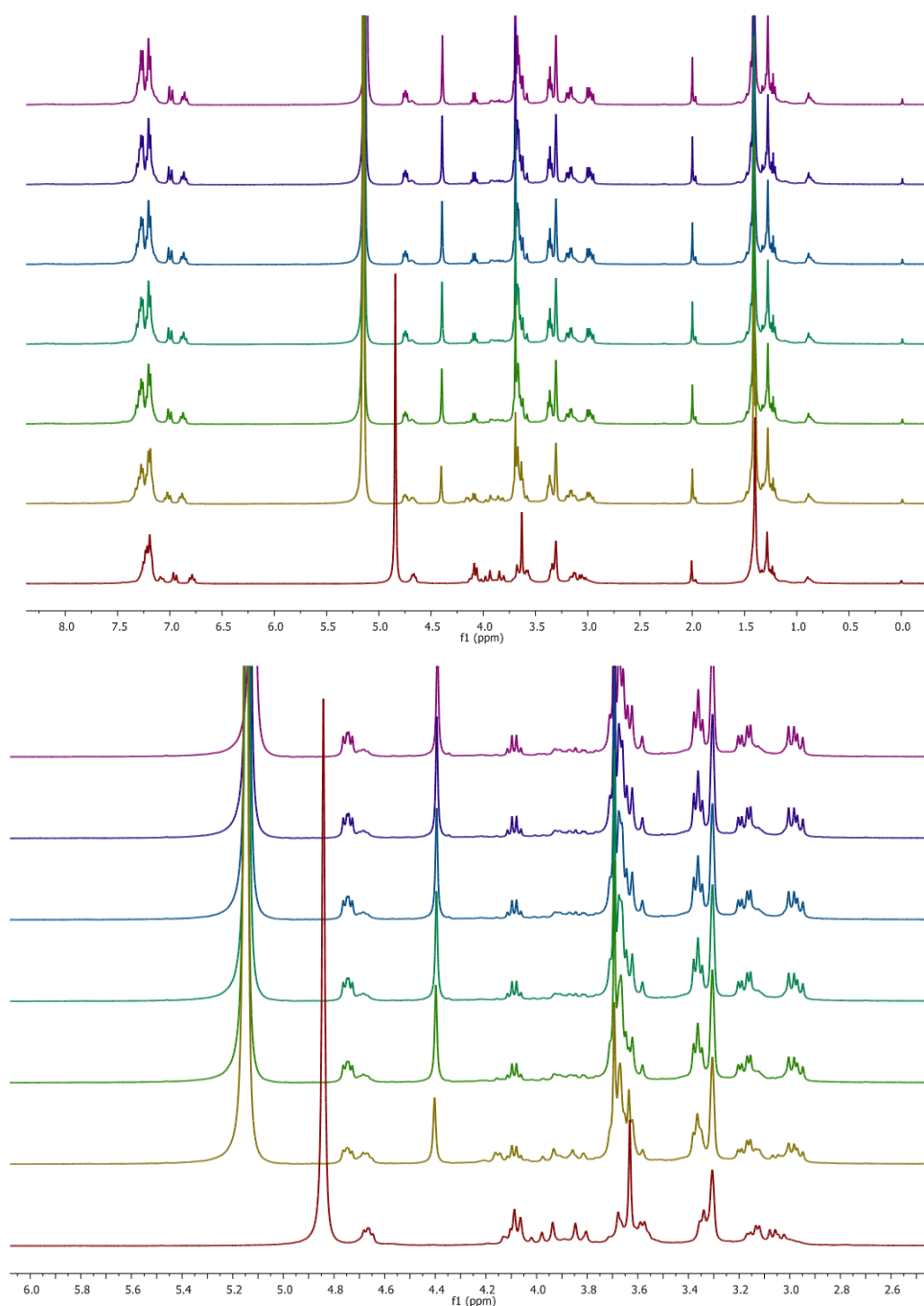


Figure A7. Time dependent NMR of *BocNH-Traeg-Gly-Phe-OMe* (**13d**) in CD_3OD and 5% TFA

Display Report

Analysis Info

Analysis Name D:\Data\JAN-2014\INKS\24012014_NKS_CB_TRTPCLE.d
 Method Pos_tune_low.m
 Sample Name ACN
 Comment

Acquisition Date 1/24/2014 7:11:50 PM

Operator A.S.Sahu
 Instrument micrOTOF-Q II 10337

Acquisition Parameter

Source Type	ESI	Ion Polarity	Positive	Set Nebulizer	0.4 Bar
Focus	Not active	Set Capillary	4500 V	Set Dry Heater	180 °C
Scan Begin	50 m/z	Set End Plate Offset	-500 V	Set Dry Gas	4.0 l/min
Scan End	3000 m/z	Set Collision Cell RF	130.0 Vpp	Set Divert Valve	Waste

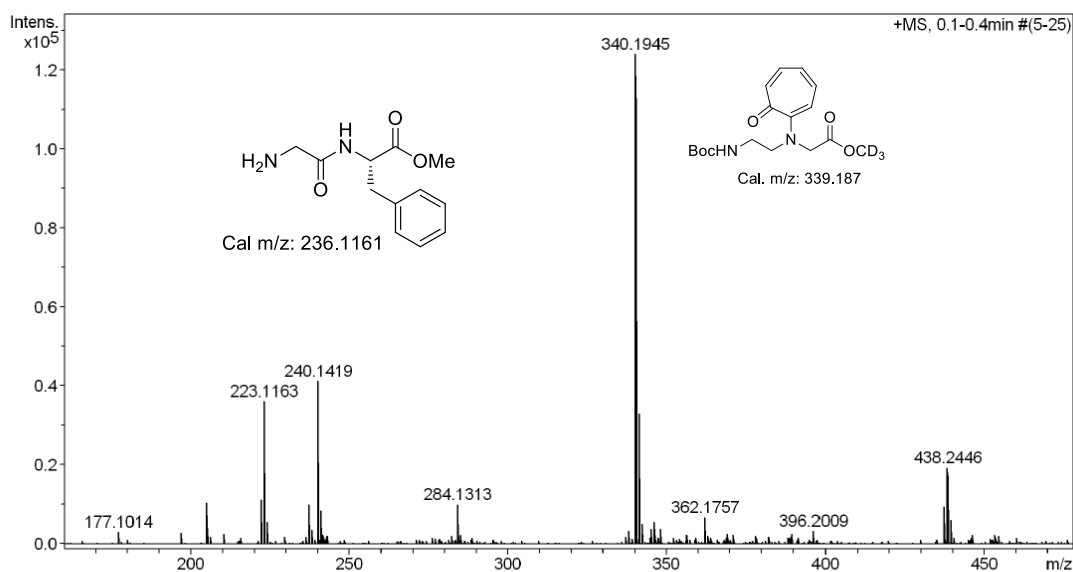
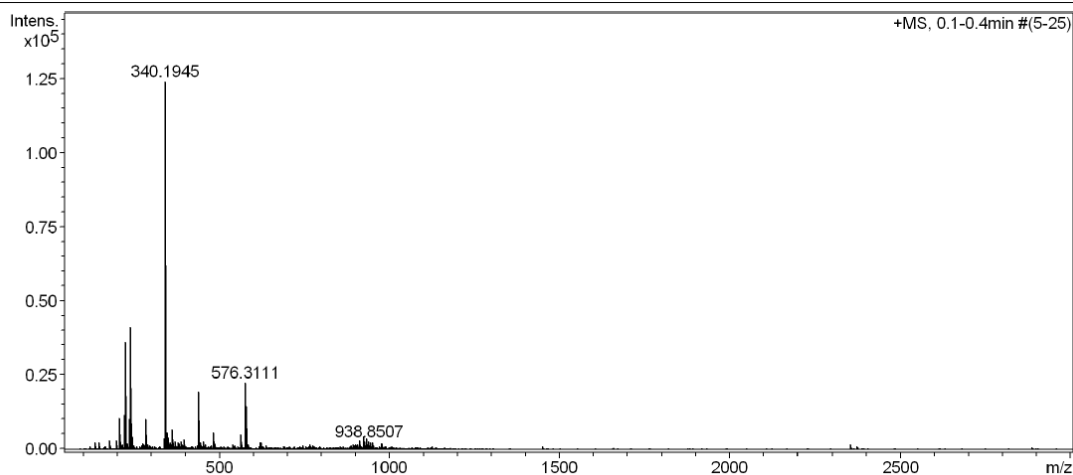


Figure A8. Mass spectrum of *BocNH-Traeg-Gly-Phe-OMe* (**13d**) after time dependent NMR experiment in CD₃OD.

4. Characterization data ($^1\text{H}/^{13}\text{C}$ -NMR and HRMS), Time dependent NMR and Mass spectrum after time dependent NMR of *BocNH-Traeg-Gly-OMe* (**13e**)

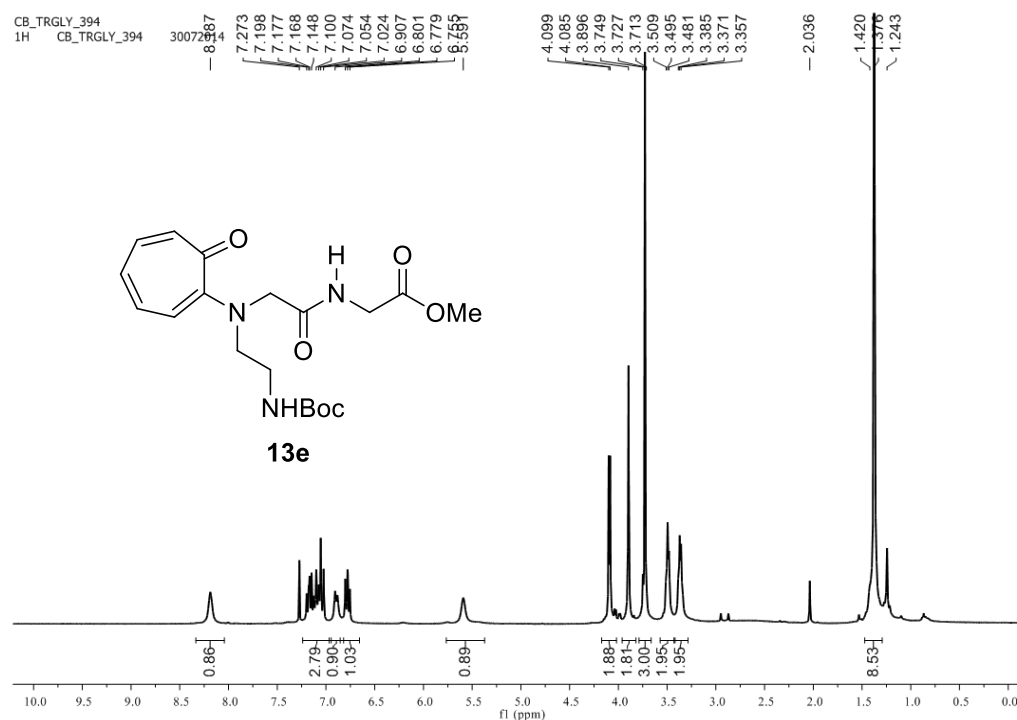


Figure A9. ^1H -NMR spectrum of *BocNH-Traeg-Gly-OMe* (**13e**) in CDCl_3

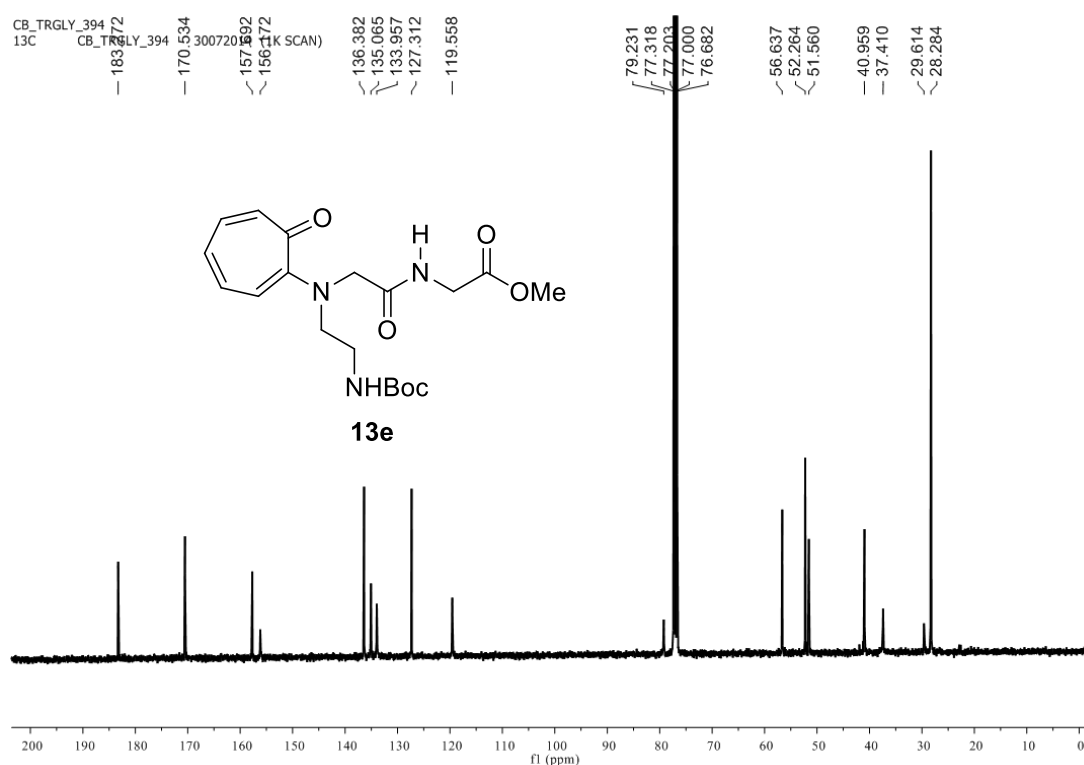


Figure A10. ^{13}C -NMR spectrum of *Boc-Traeg-Gly-OMe* (**13e**) in CDCl_3 .

Generic Display Report

Analysis Info

Analysis Name D:\Data\AUG-2014\NKS\14082014_NKS_CB_786.d
Method Pos_tune_low.m
Sample Name
Comment

Acquisition Date 8/14/2014 4:47:34 PM

Operator A.S.Sahu
Instrument micrOTOF-Q II

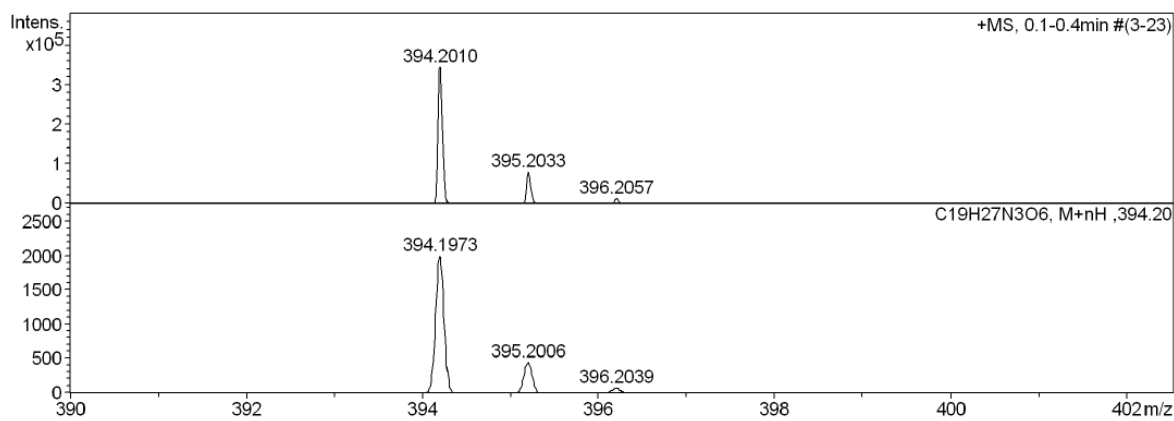
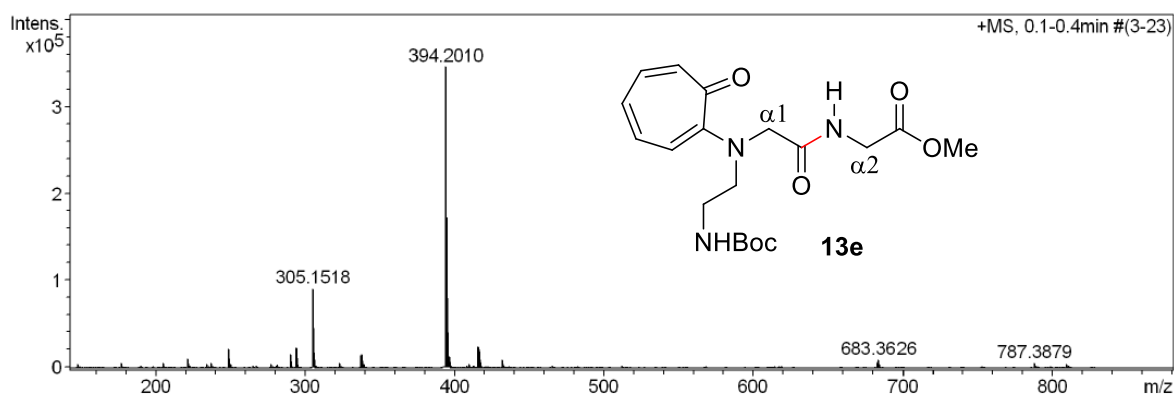
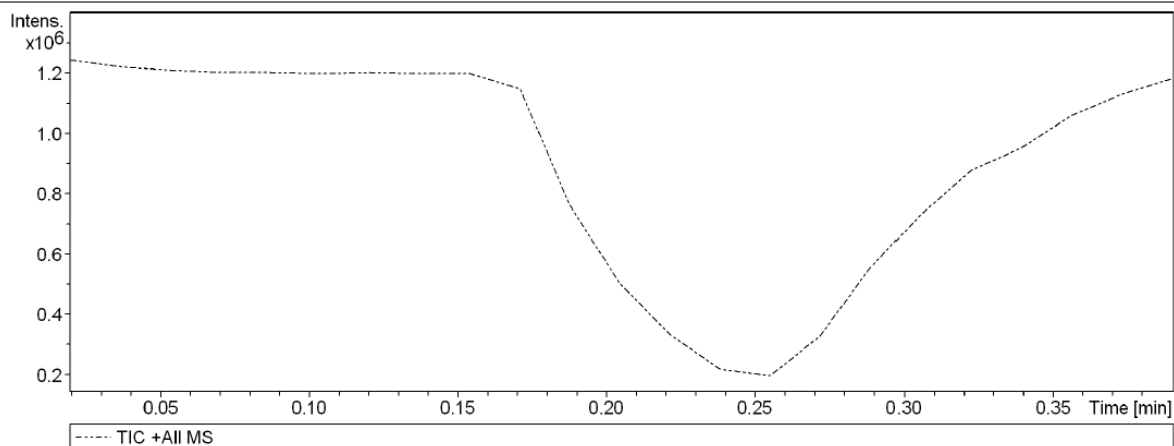


Figure A11. Mass spectrum of *BocNH-Traeg-Gly-OMe* (**13e**)

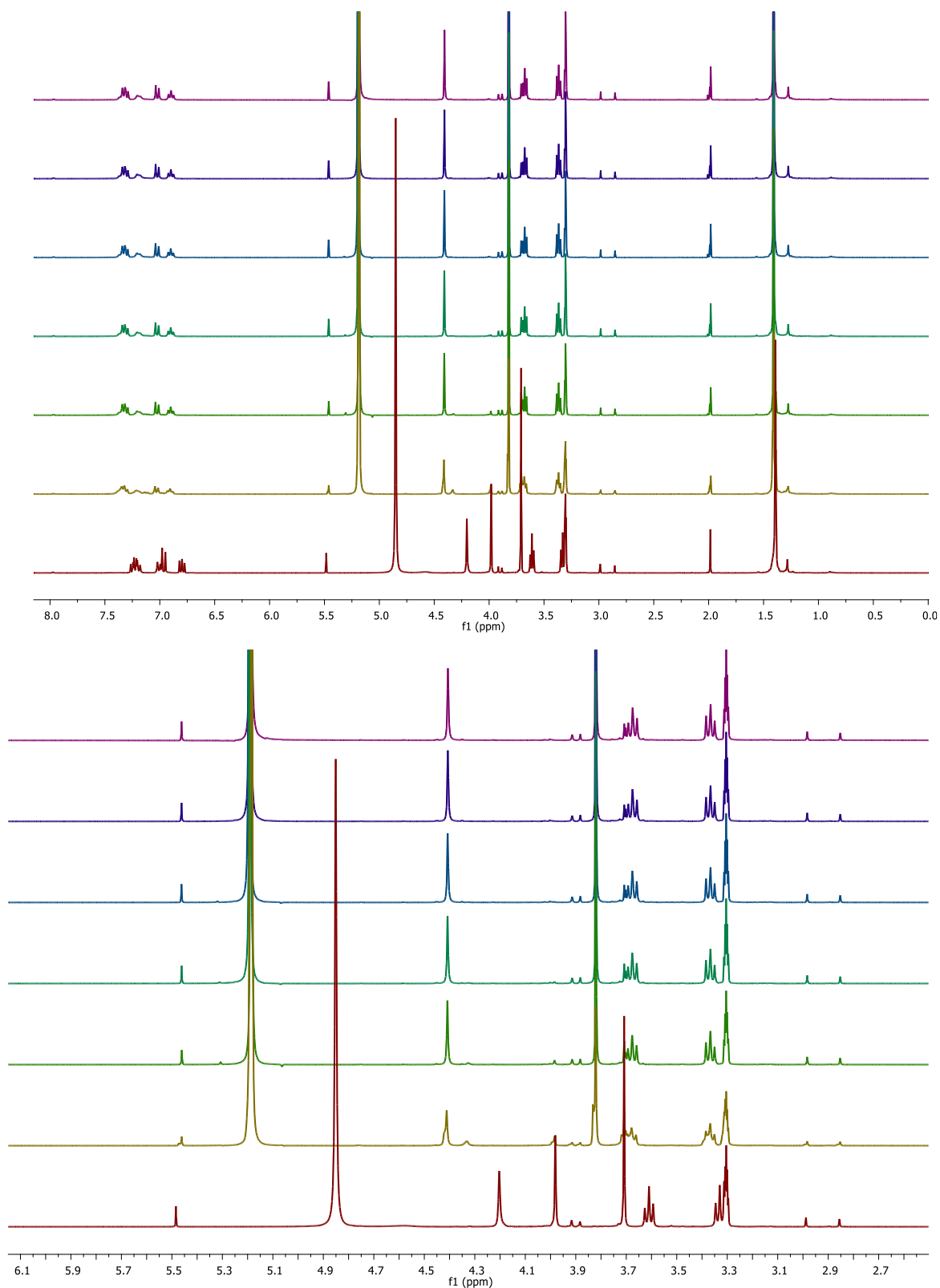


Figure A12. Time dependent NMR of *BocNH-Traeg-Gly-OMe* (13e) in CD_3OD and 5% TFA at interval of 7.0 minutes

Generic Display Report

Analysis Info

Analysis Name D:\Data\AUG-2014\INKS\20082014_NKS_CB_786D.d
Method Pos_tune_low.m
Sample Name LCMS-NISER
Comment

Acquisition Date 8/20/2014 3:23:46 PM

Operator A.S.Sahu
Instrument micrOTOF-Q II

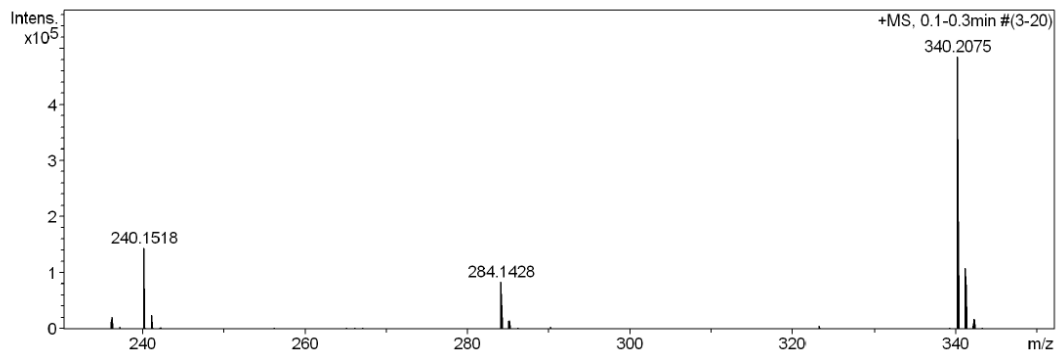
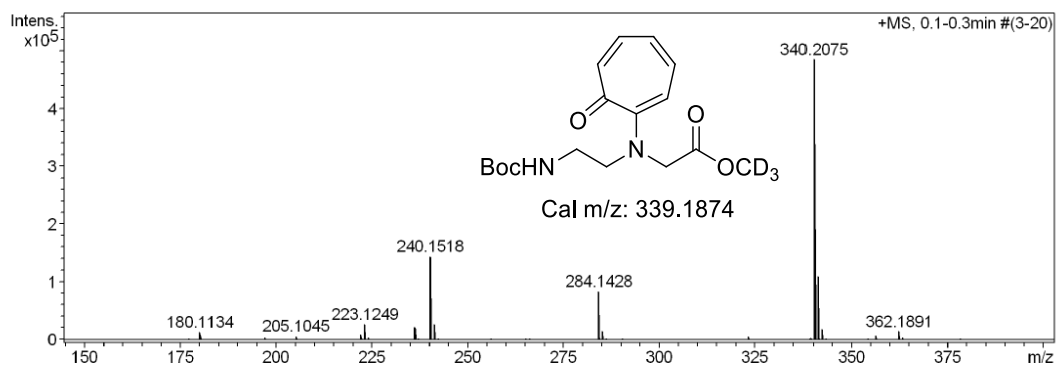
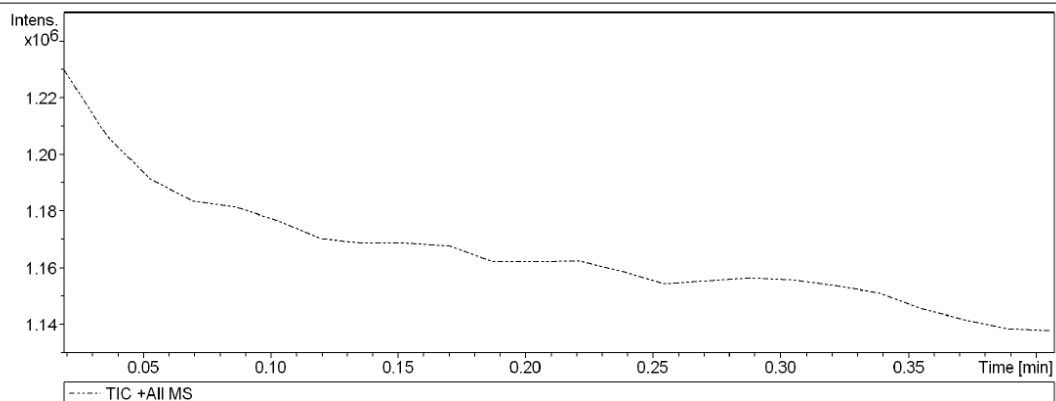


Figure A13. Mass spectrum of *BocNH-Traeg-Gly-OMe* (**13e**) after time dependent NMR experiment in CD₃OD

5. Characterization data ($^1\text{H}/^{13}\text{C}$ -NMR and HRMS), Time dependent NMR and Mass spectrum after time dependent NMR of *BocNH-Traeg-Ala-OMe* (**13f**)

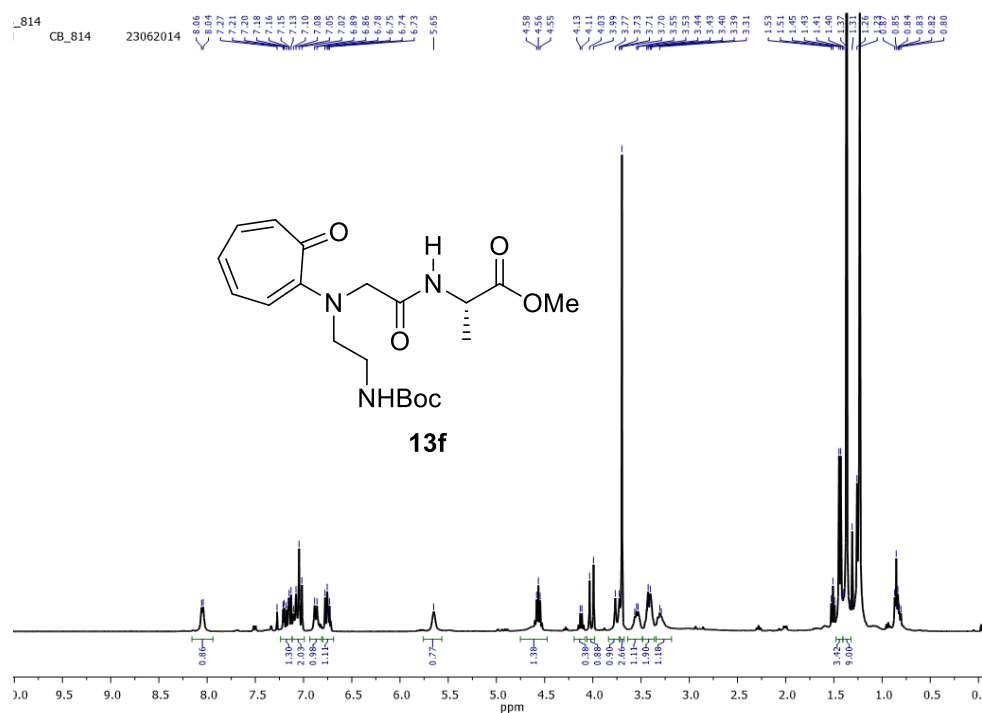


Figure A14. ^1H -NMR spectrum of *BocNH-Traeg-Ala-OMe* (**13f**)

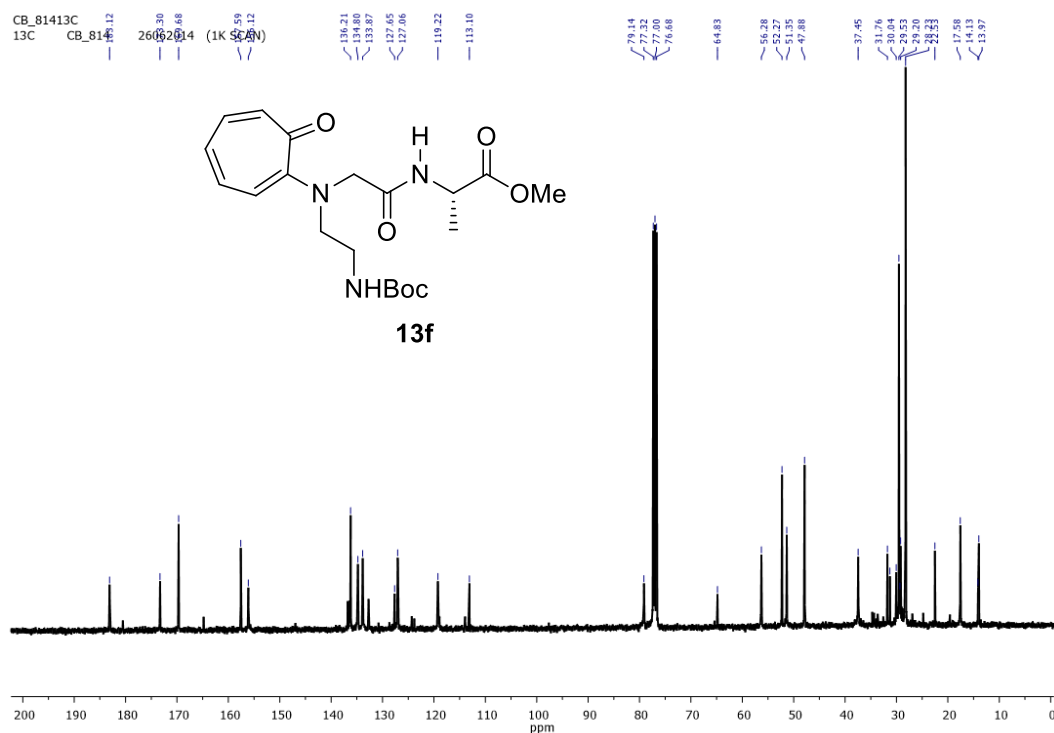


Figure A15. ^{13}C -NMR spectrum of *BocNH-Traeg-Ala-OMe* (**13f**)

Generic Display Report

Analysis Info

Analysis Name D:\Data\AUG-2014\NKS\14082014_NKS_CB_814_RE.d
 Method Pos_tune_low.m
 Sample Name
 Comment

Acquisition Date 8/14/2014 11:22:33 AM

Operator A.S.Sahu
 Instrument micrOTOF-Q II

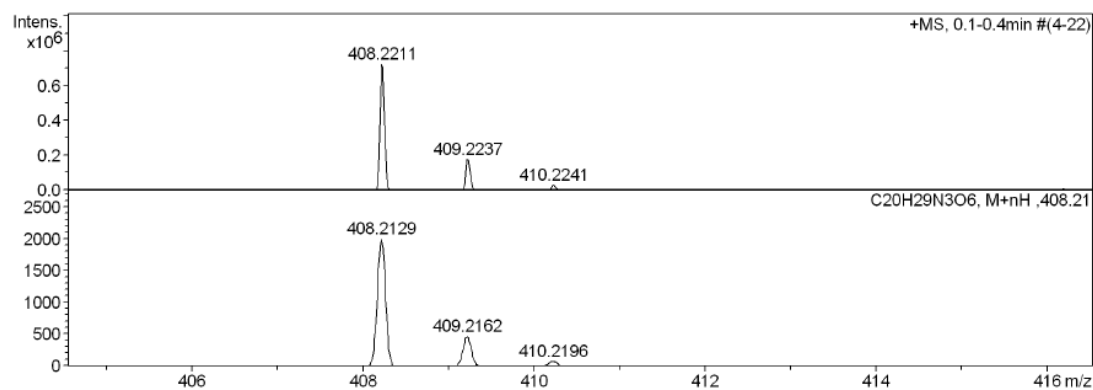
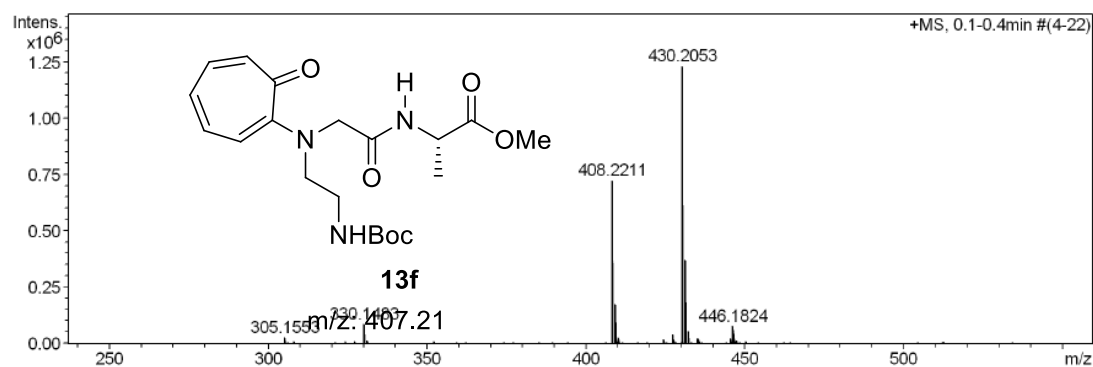
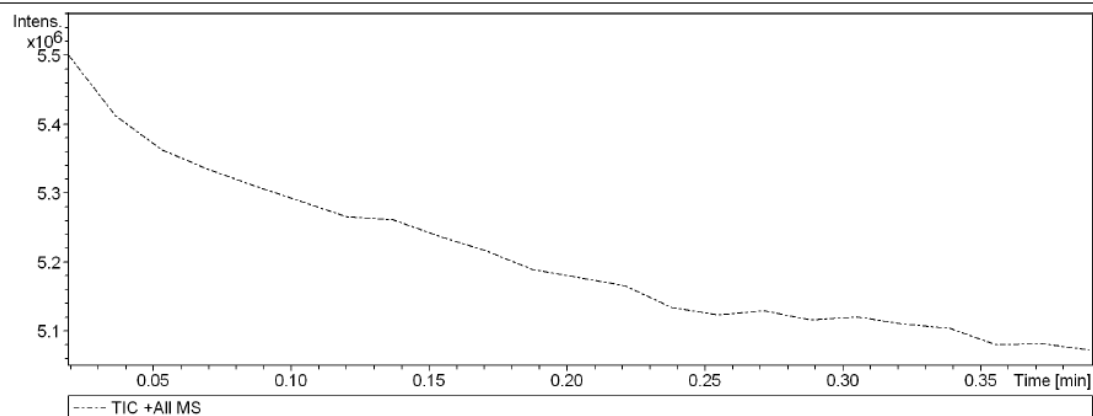


Figure A16. Mass spectrum of *BocNH-Traeg-Ala-OMe* (**13f**)

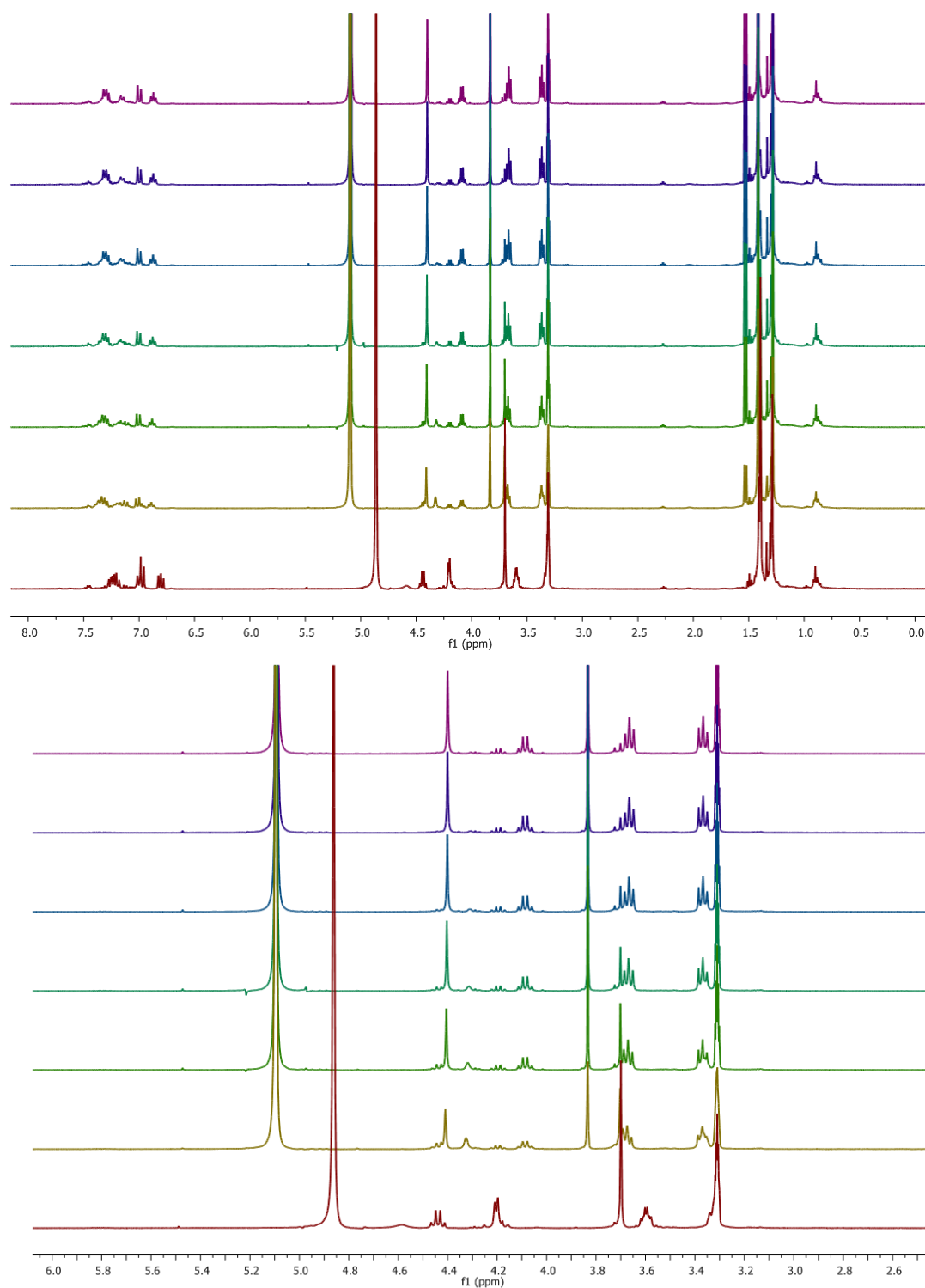


Figure A17. Time dependent NMR of *BocNH-Traeg-Ala-OMe* (**13f**) in CD_3OD and 5% TFA in interval of 7.0 minutes

Generic Display Report

Analysis Info

Analysis Name D:\Data\AUG2014\NKS\18082014_NKS_CB_814D.d
Method Pos_tune_low.m
Sample Name
Comment

Acquisition Date 8/18/2014 10:07:06 AM

Operator RAJKUMAR
Instrument micrOTOF-Q II

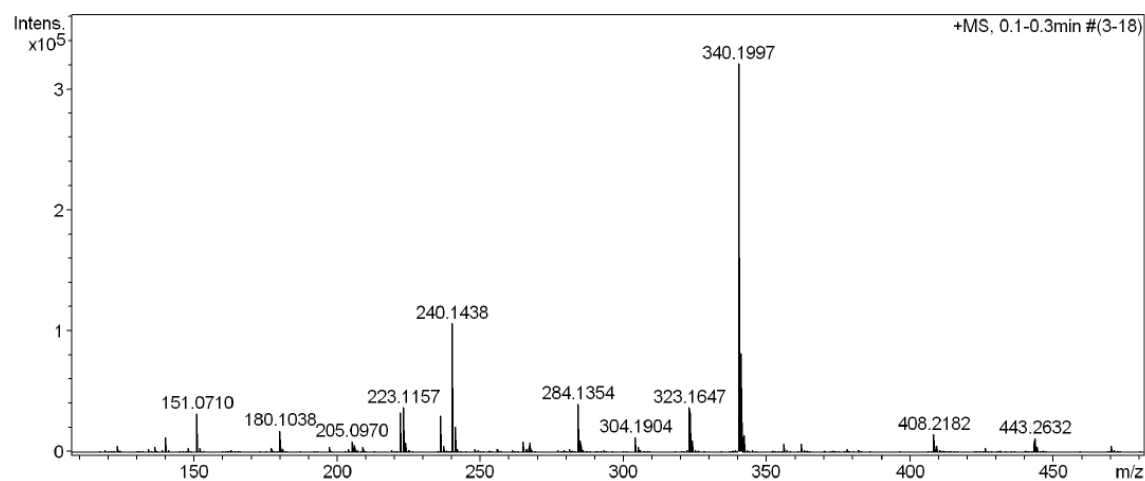
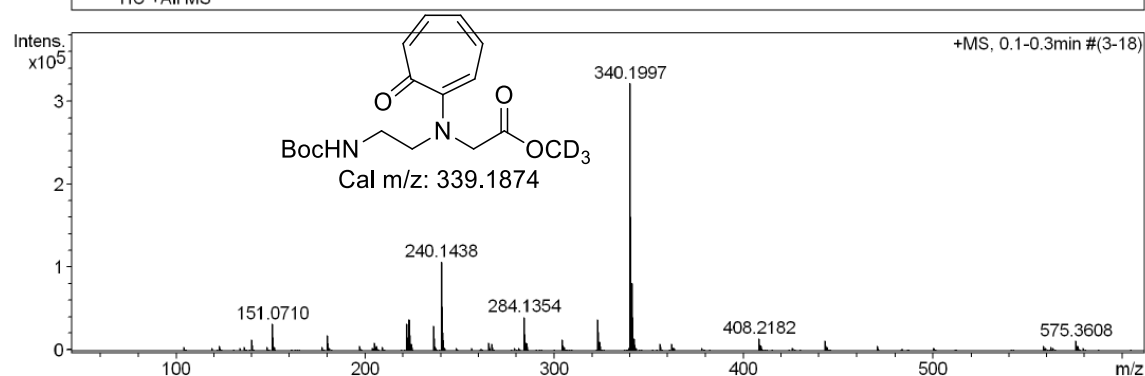
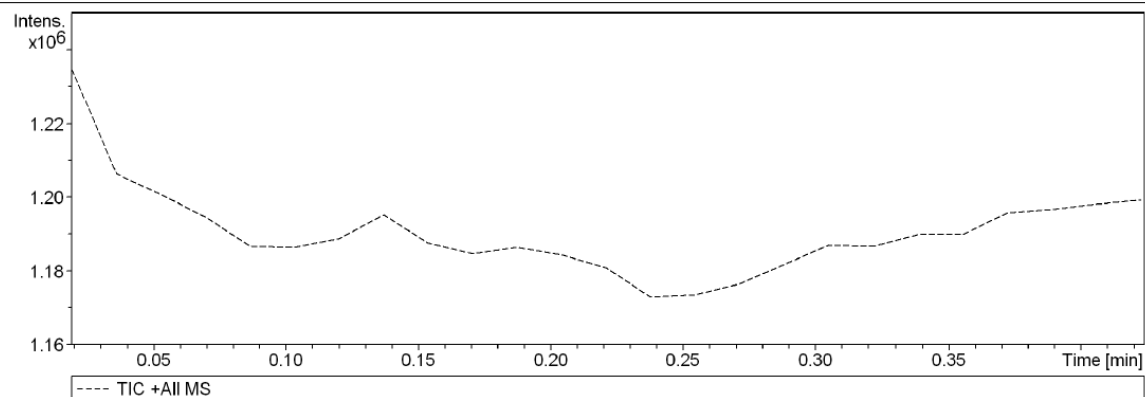


Figure A18. Mass spectrum of *BocNH-Traeg-Ala-OMe* (**13f**) after time dependent NMR experiment in CD₃OD

6. Characterization data ($^1\text{H}/^{13}\text{C}$ NMR and HRMS) of **6b-OEt**

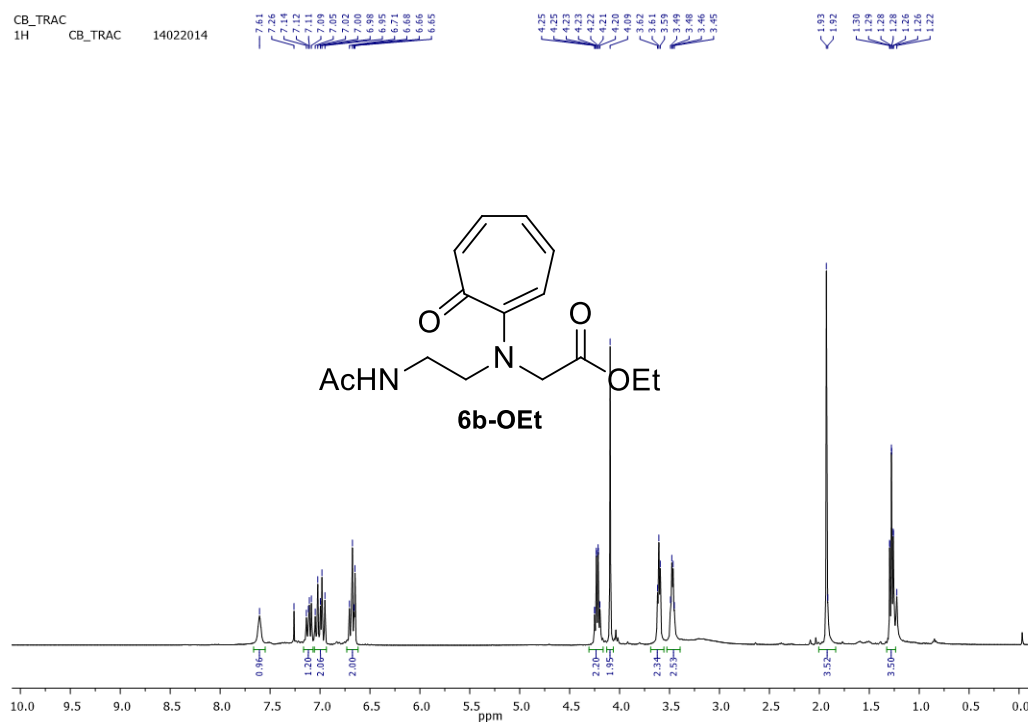


Figure A19. ^1H NMR spectrum of AcNH-Traeg-OEt (**6b-OEt**) in CDCl_3

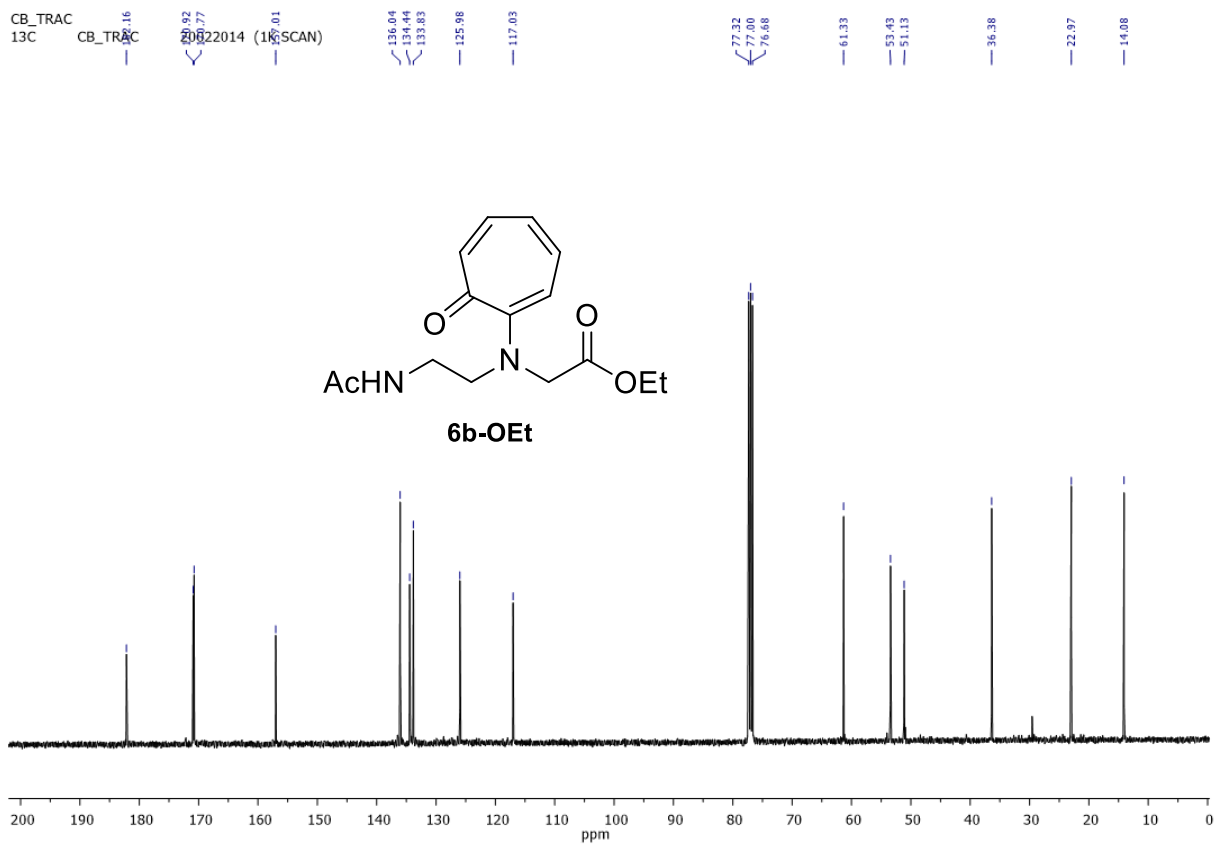


Figure A20. ^{13}C NMR spectrum of AcNH-Traeg-OEt (**6b-OEt**) in CDCl_3

Display Report

Analysis Info

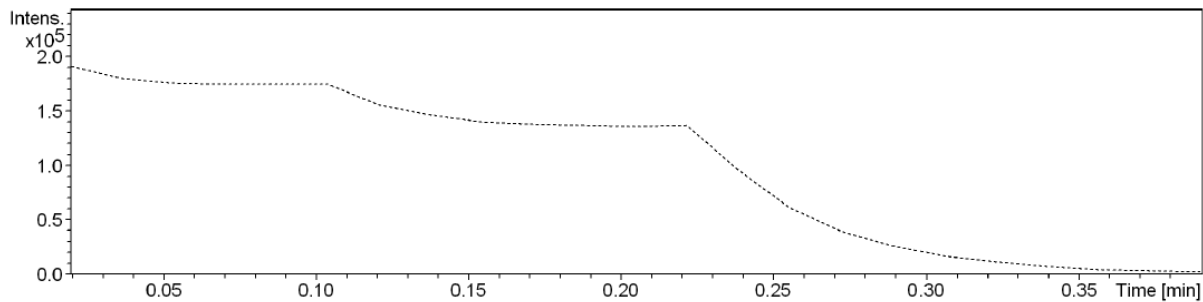
Analysis Name D:\Data\FEB-2014\NKS\27022014_NKS_CB_TRAC.d
Method Pos_tune_low.m
Sample Name ACN
Comment

Acquisition Date 2/27/2014 10:24:03 AM

Operator A.S.Sahu
Instrument micrOTOF-Q II 10337

Acquisition Parameter

Source Type	ESI	Ion Polarity	Positive	Set Nebulizer	0.4 Bar
Focus	Not active	Set Capillary	4500 V	Set Dry Heater	180 °C
Scan Begin	50 m/z	Set End Plate Offset	-500 V	Set Dry Gas	4.0 l/min
Scan End	3000 m/z	Set Collision Cell RF	130.0 Vpp	Set Divert Valve	Waste



----- TIC +All MS

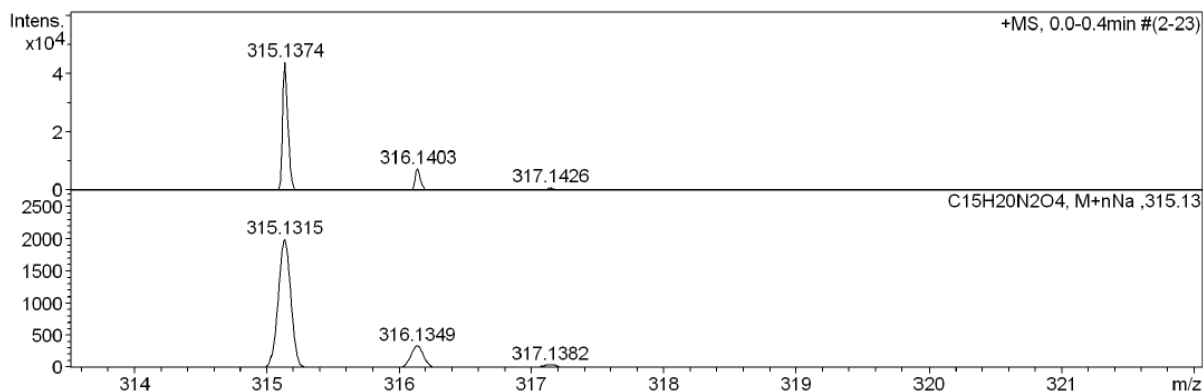
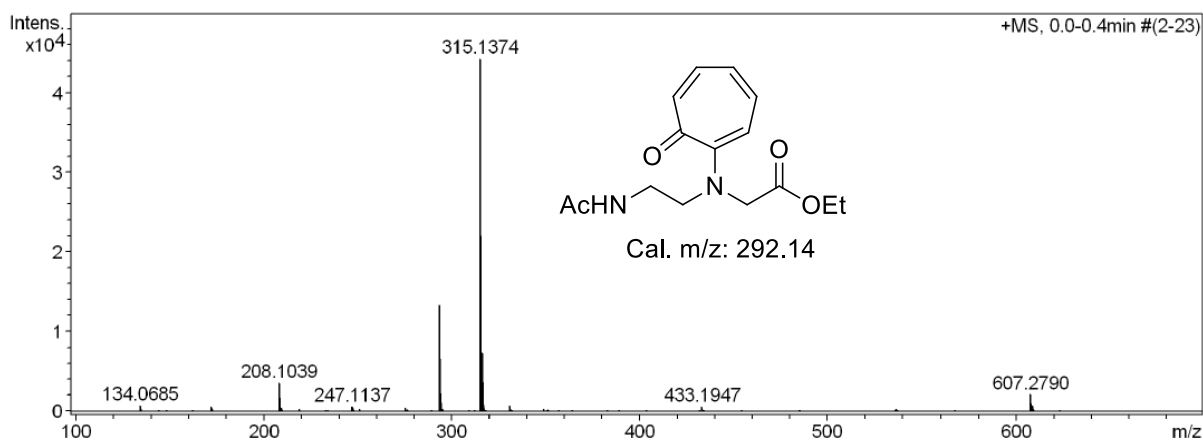


Figure A21. HRMS Mass spectrum of *AcNH-Traeg-OEt* (**6b-OEt**)

7. Characterization data ($^1\text{H}/^{13}\text{C}$ NMR and HRMS), Time dependent NMR and Mass spectrum after time dependent NMR of *AcNH-Traeg-Phe-OMe* (**14**)

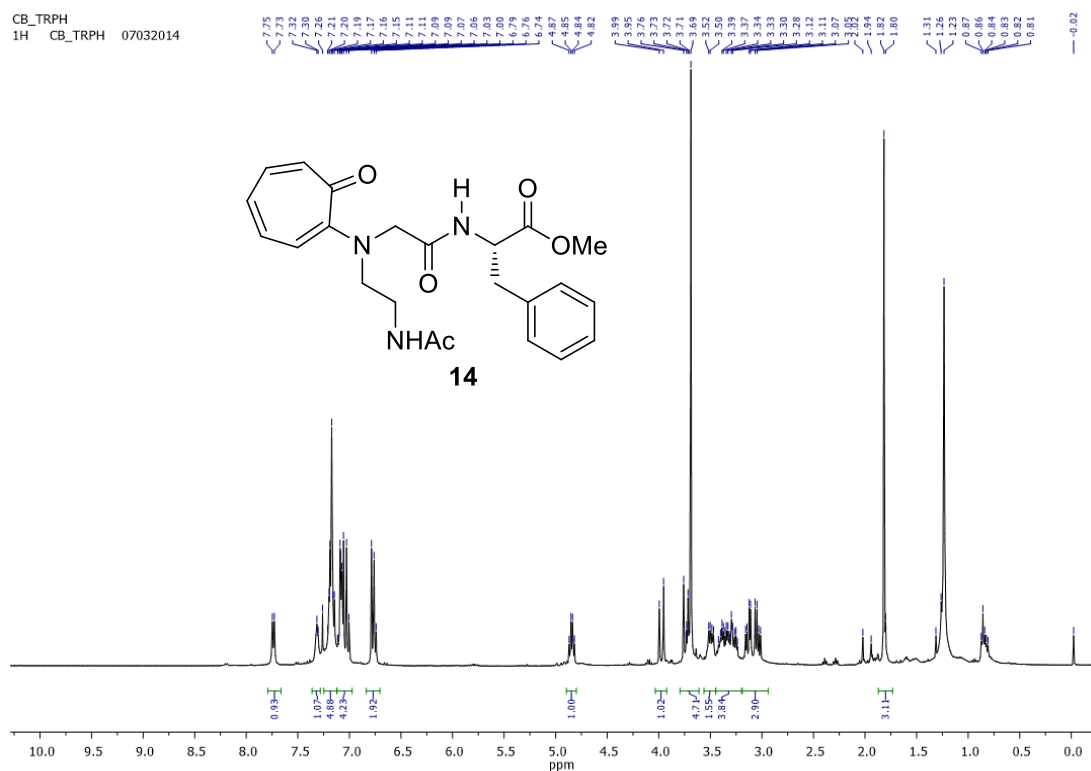


Figure A22. ^1H NMR of *AcNH-Traeg-Phe-OMe* (**14**) in CDCl_3

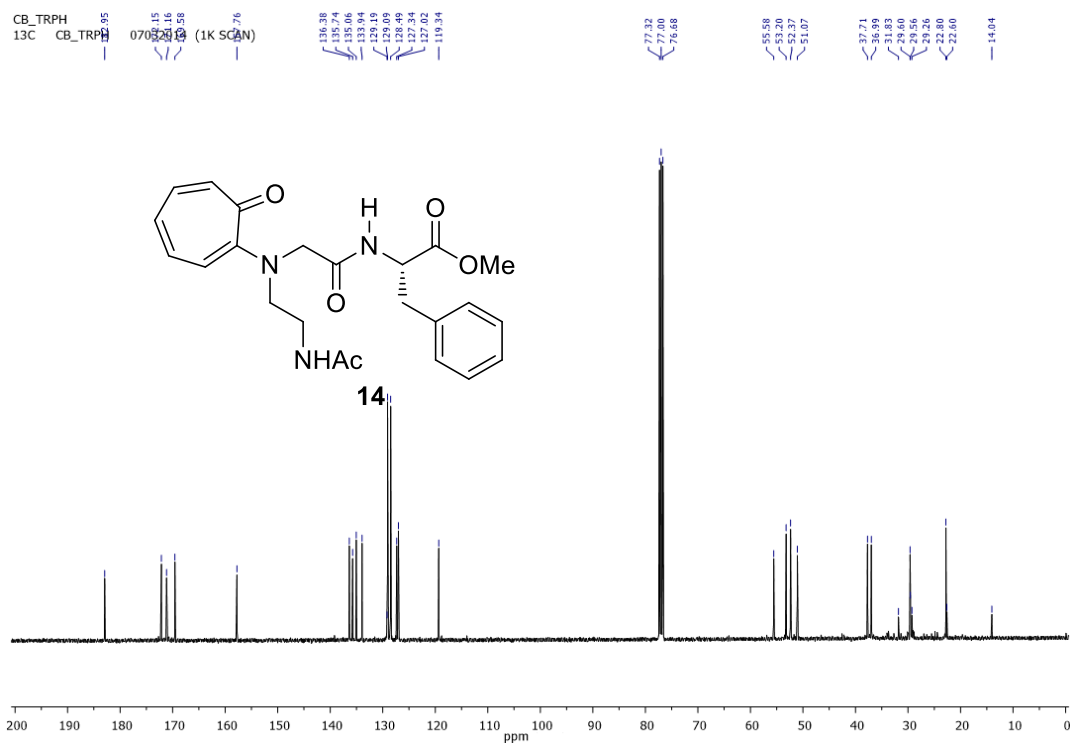


Figure A23. ^{13}C NMR of *AcNH-Traeg-Phe-OMe* (**14**) in CDCl_3

Display Report

Analysis Info

Analysis Name D:\Data\MARCH-2014\NKS\08032014_NKS_CB_TRPH.d
Method Pos_tune_low.m
Sample Name ACN
Comment

Acquisition Date 3/8/2014 11:29:25 AM

Operator A.S.Sahu
Instrument micrOTOF-Q II 10337

Acquisition Parameter

Source Type	ESI	Ion Polarity	Positive	Set Nebulizer	0.4 Bar
Focus	Not active	Set Capillary	4500 V	Set Dry Heater	180 °C
Scan Begin	50 m/z	Set End Plate Offset	-500 V	Set Dry Gas	4.0 l/min
Scan End	3000 m/z	Set Collision Cell RF	130.0 Vpp	Set Divert Valve	Waste

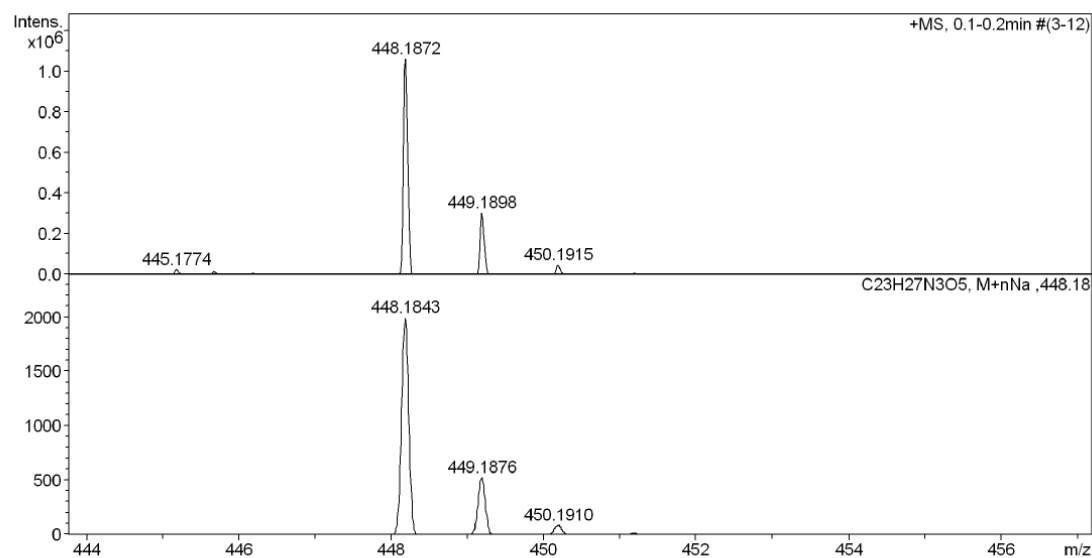
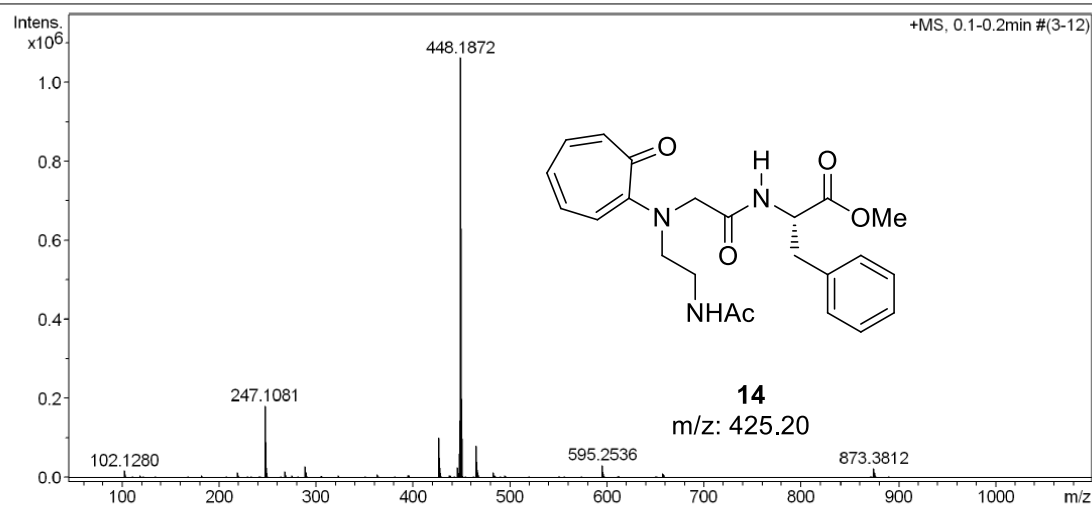


Figure A24. HRMS mass spectrum of *AcNH-Traeg-Phe-OMe* (**14**)

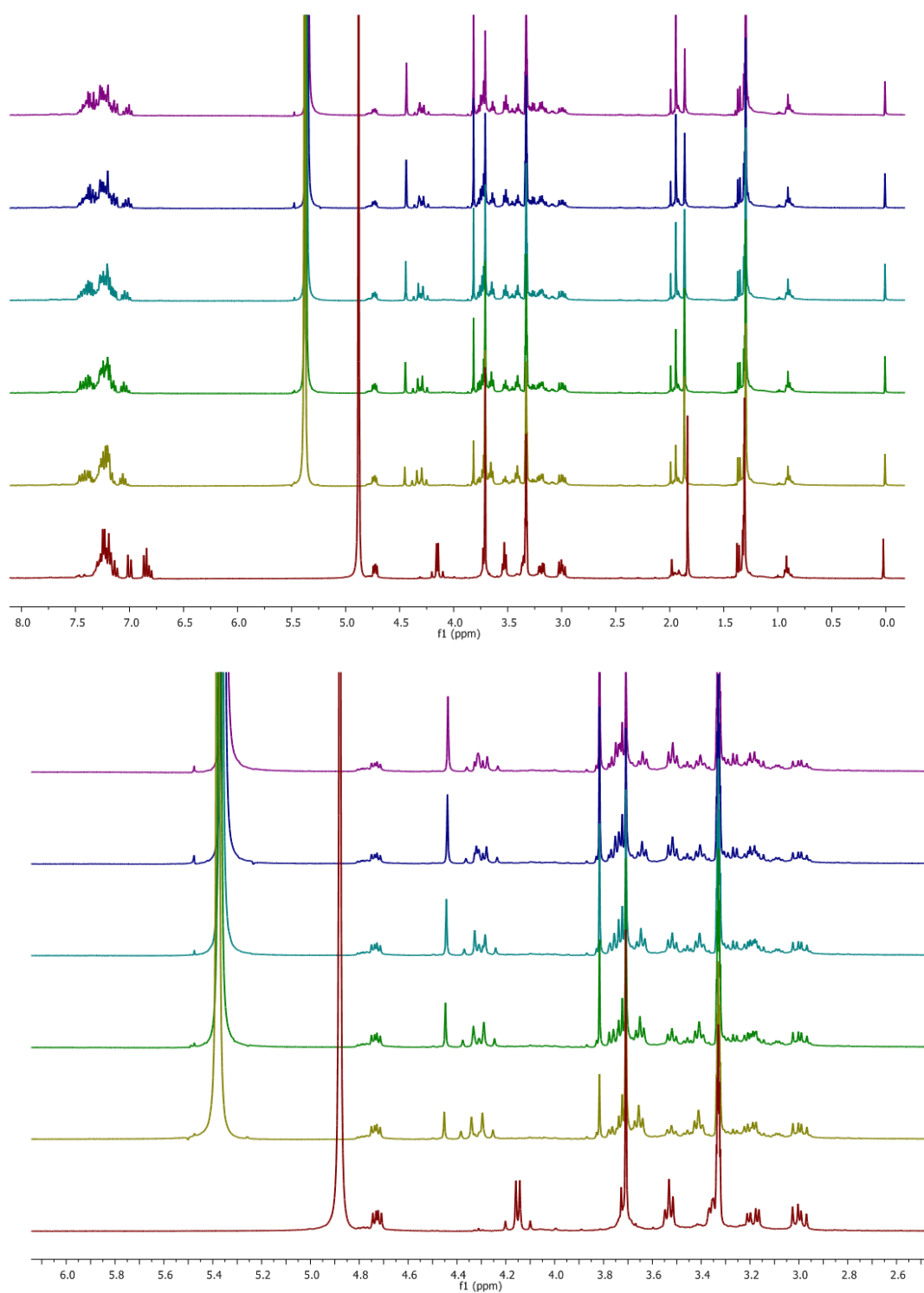


Figure A25. Time dependent NMR of *Ac-Traeg-Phe-OMe* (**14**) in CD₃OD and 5% TFA

Display Report

Analysis Info

Analysis Name	D:\Data\APRIL-2014\NKS_CB_ACTRPHTF1H\24042014_NKS_VIN_EXPT_2.d	Acquisition Date	4/24/2014 7:00:09 PM
Method	Pos_tune_low.m	Operator	A.S.Sahu
Sample Name		Instrument	micrOTOF-Q II 10337
Comment			

Acquisition Parameter

Source Type	ESI	Ion Polarity	Positive	Set Nebulizer	0.4 Bar
Focus	Not active	Set Capillary	4500 V	Set Dry Heater	180 °C
Scan Begin	50 m/z	Set End Plate Offset	-500 V	Set Dry Gas	4.0 l/min
Scan End	3000 m/z	Set Collision Cell RF	130.0 Vpp	Set Divert Valve	Waste

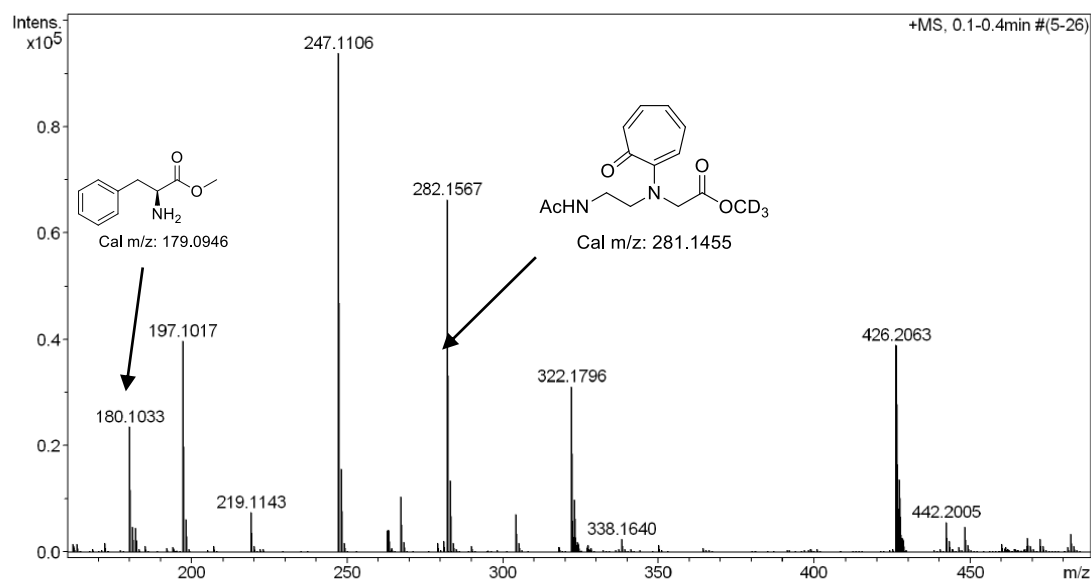
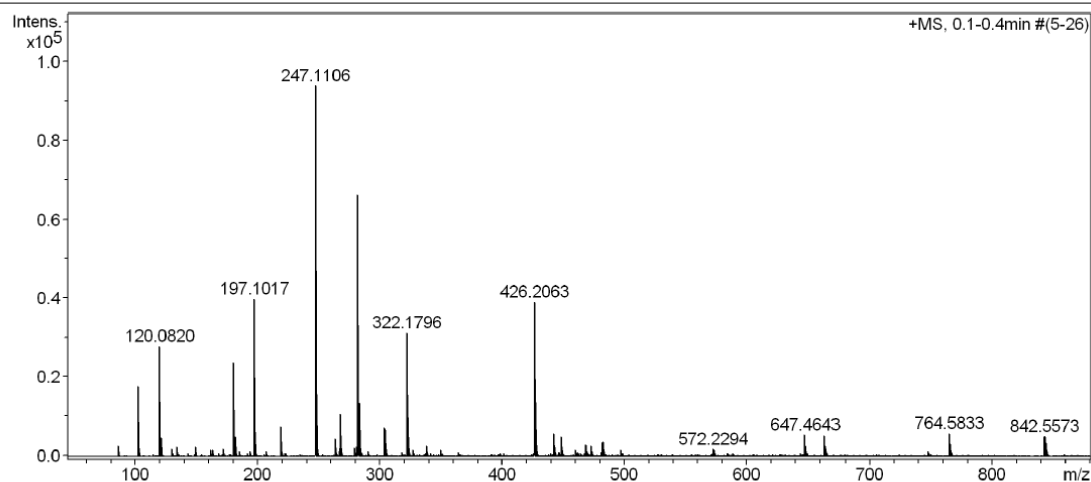


Figure A26. Mass spectrum of *Ac-Traeg-Phe-OMe* (**14**) after time dependent NMR Experiment in CD₃OD

8. Characterization data ($^1\text{H}/^{13}\text{C}$ NMR and HRMS), Time dependent NMR and Mass spectrum after time dependent NMR of *BocNH-Traeg-Trp-OMe* (**13g**)

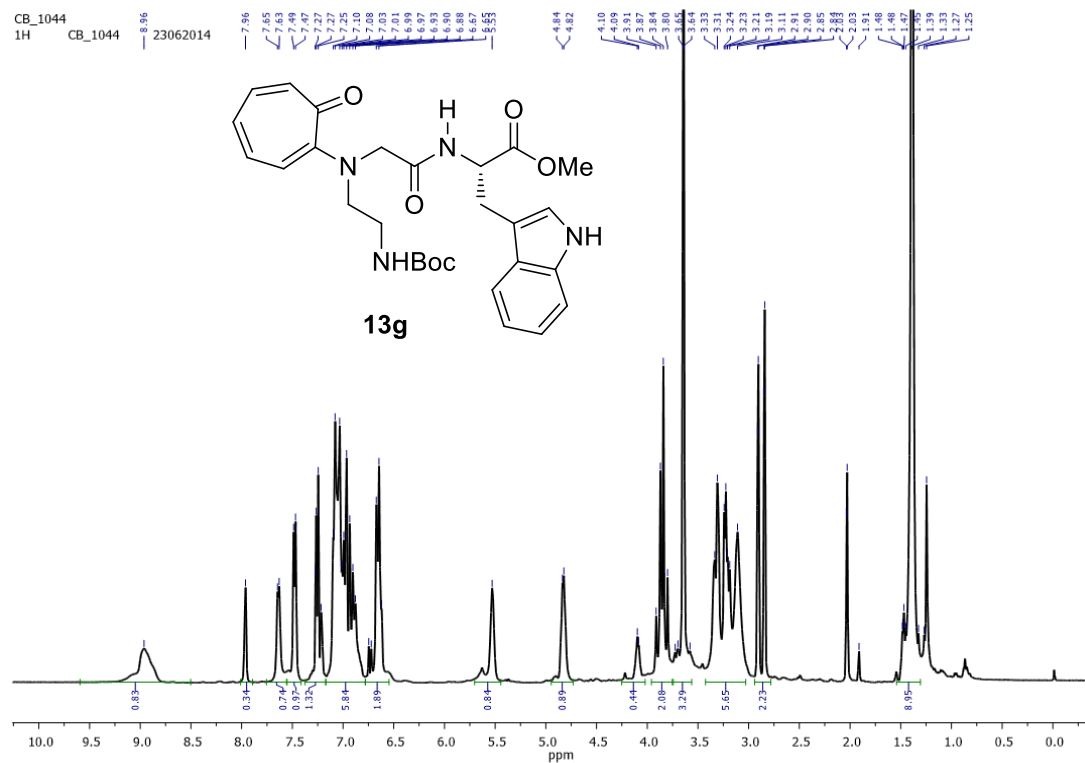


Figure A27. ^1H NMR spectrum of *BocNH-Traeg-Trp-OMe* (**13g**) in CDCl_3

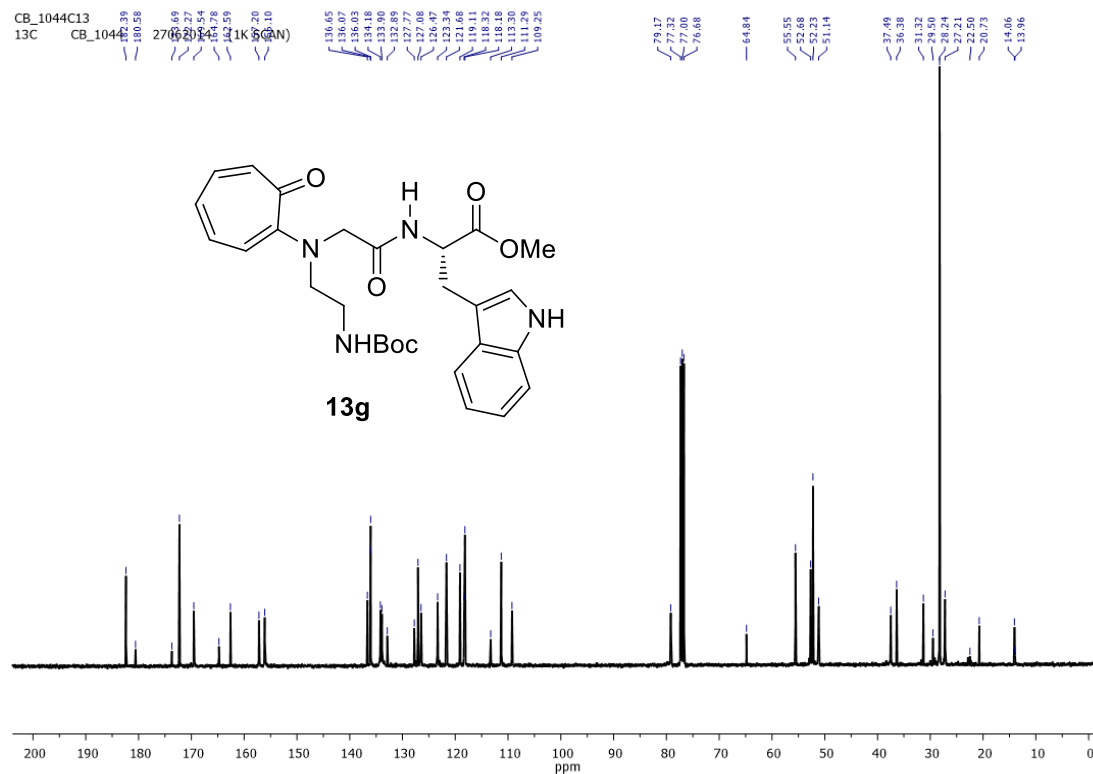


Figure A28. ^{13}C NMR spectrum of *BocNH-Traeg-Trp-OMe* (**13g**) in CDCl_3

Generic Display Report

Analysis Info

Analysis Name D:\Data\AUG2014\NKS\14082014_NKS_CB_1044_RE.d
Method Pos_tune_low.m
Sample Name
Comment

Acquisition Date 8/14/2014 11:37:39 AM

Operator A.S.Sahu
Instrument micrOTOF-Q II

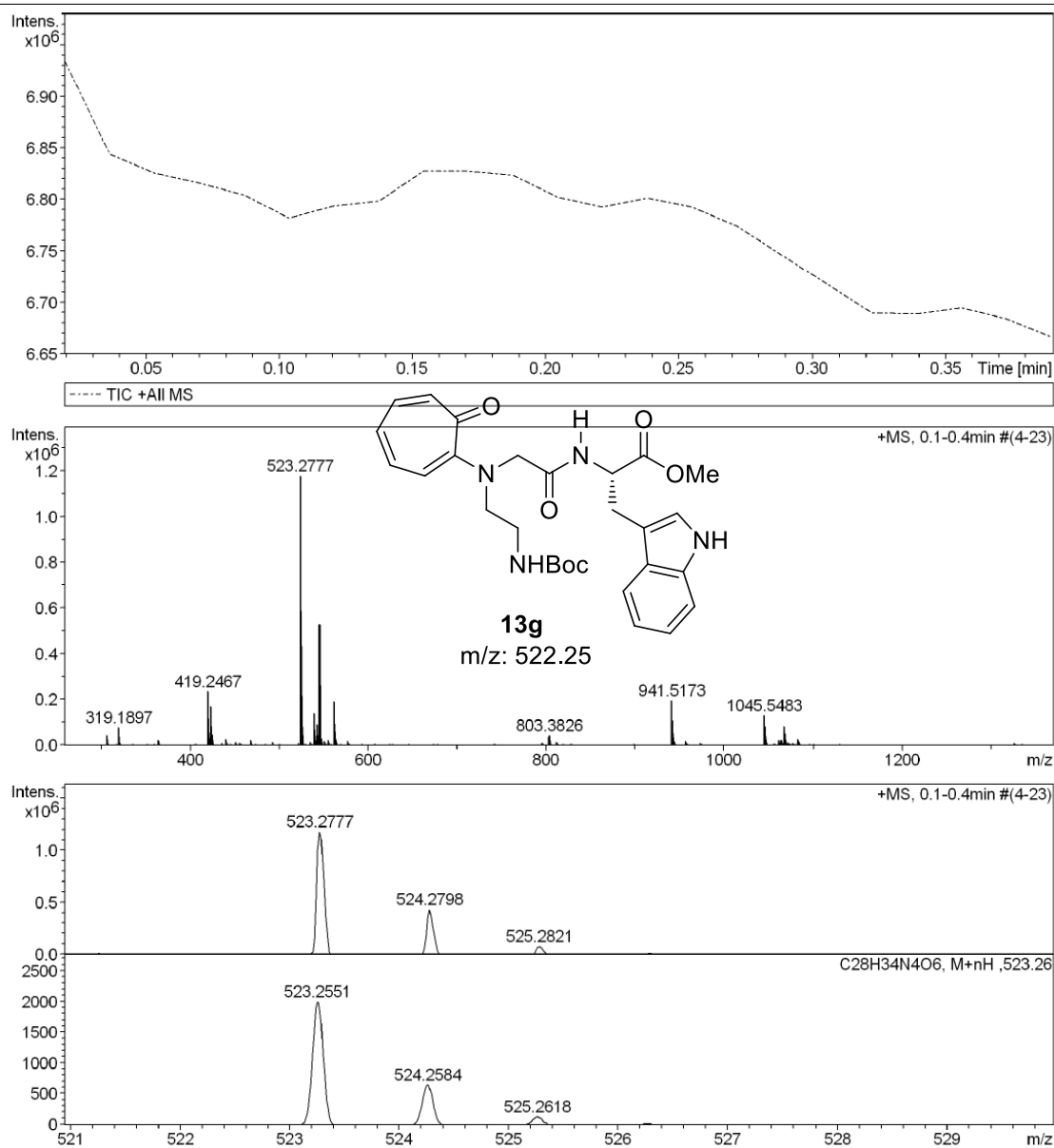


Figure A29. Mass spectrum of *BocNH-Traeg-Trp-OMe* (**13g**)

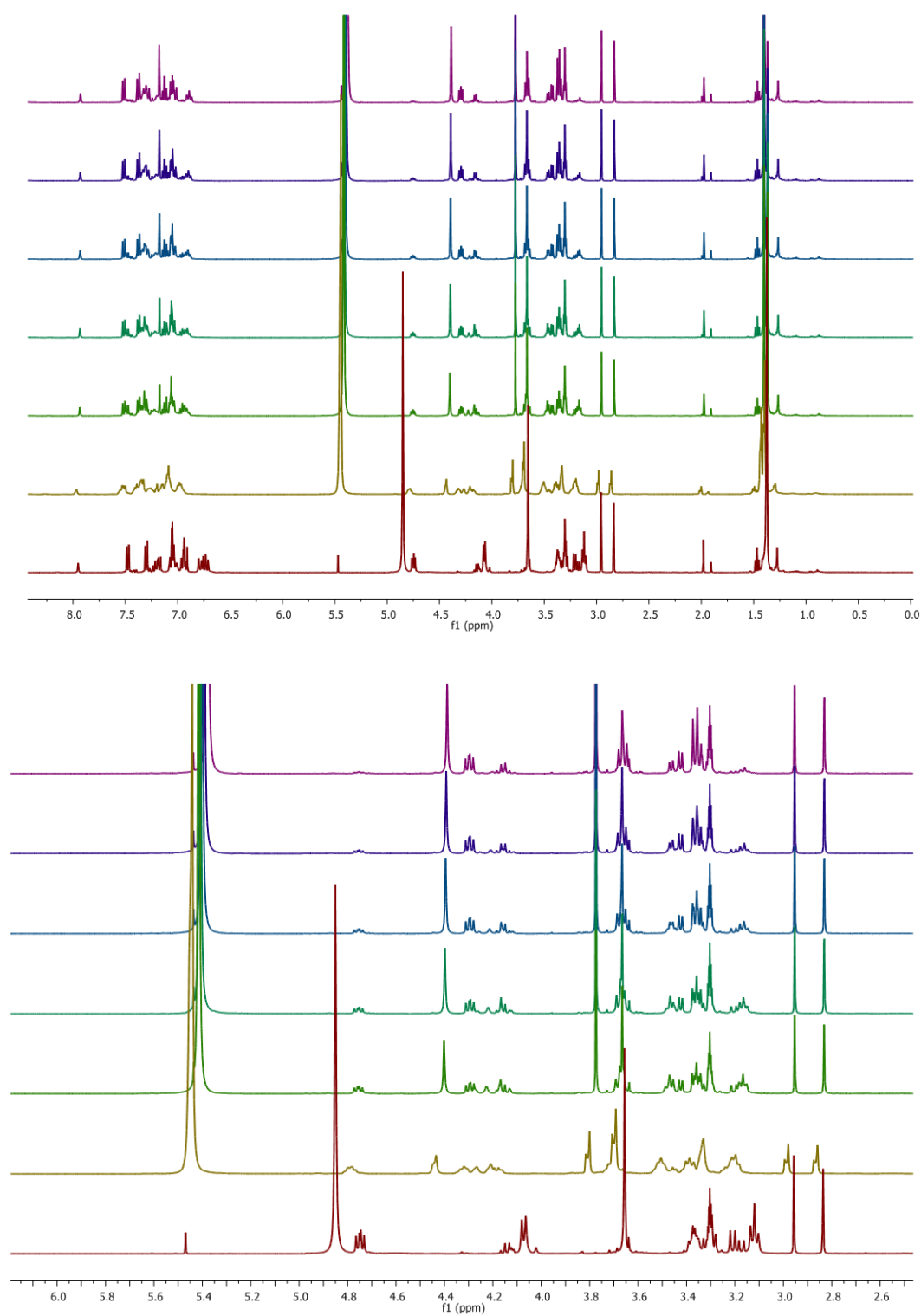


Figure A30. Time dependent NMR of *Boc-Traeg-Trp-OMe* (**13g**) in CD_3OD and 5% TFA

Generic Display Report

Analysis Info

Analysis Name D:\Data\AUG2014\NKS\18082014_NKS_CB_1044D.d
 Method Pos_tune_low.m
 Sample Name
 Comment

Acquisition Date 8/18/2014 10:27:32 AM

Operator RAJKUMAR
 Instrument micrOTOF-Q II

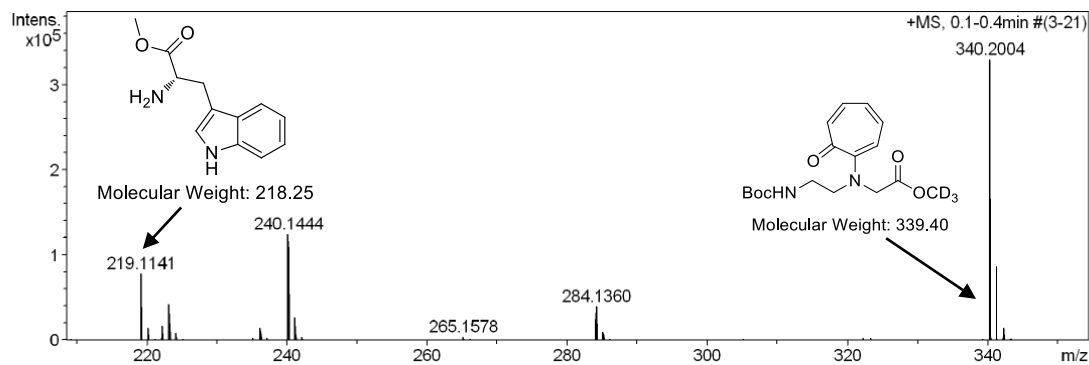
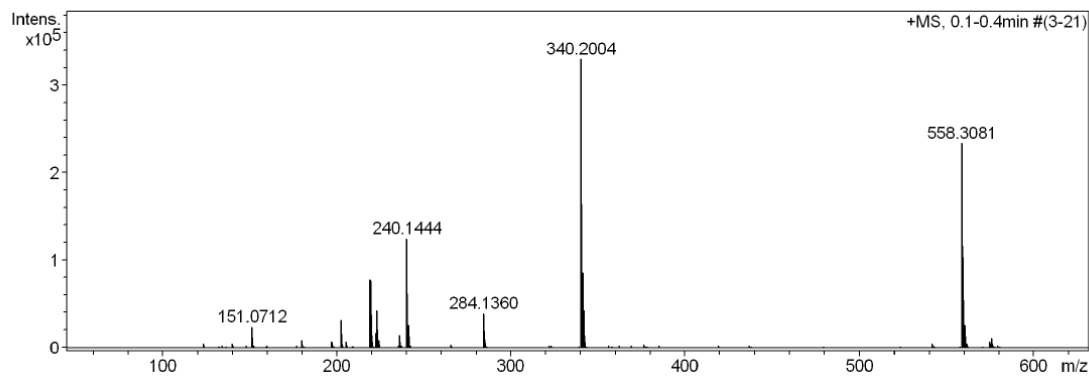
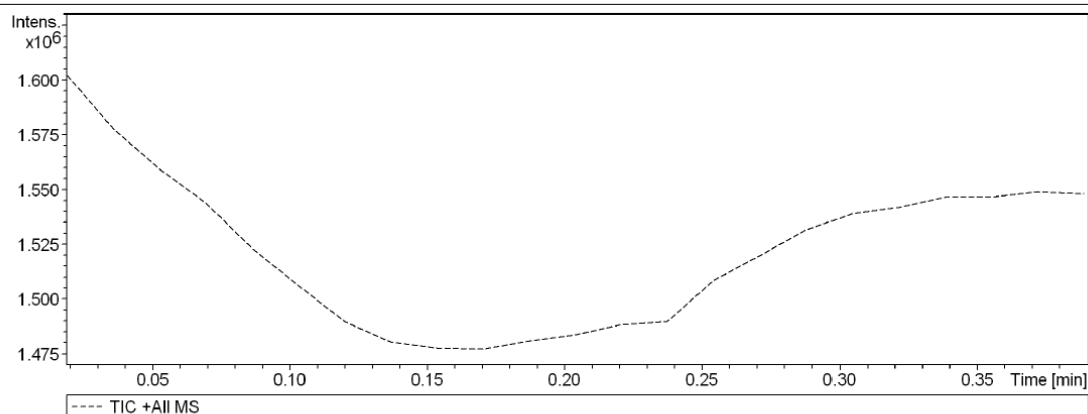


Figure A31. Mass spectrum of *BocNH-Traeg-Trp-OMe* (**13g**) after time dependent NMR experiment in CD₃OD

9. Characterization data ($^1\text{H}/^{13}\text{C}$ NMR and HRMS), Time dependent NMR and Mass spectrum after time dependent NMR of *BocNH-Traeg-Pro-Ile-Phe-OMe* (**13h**)

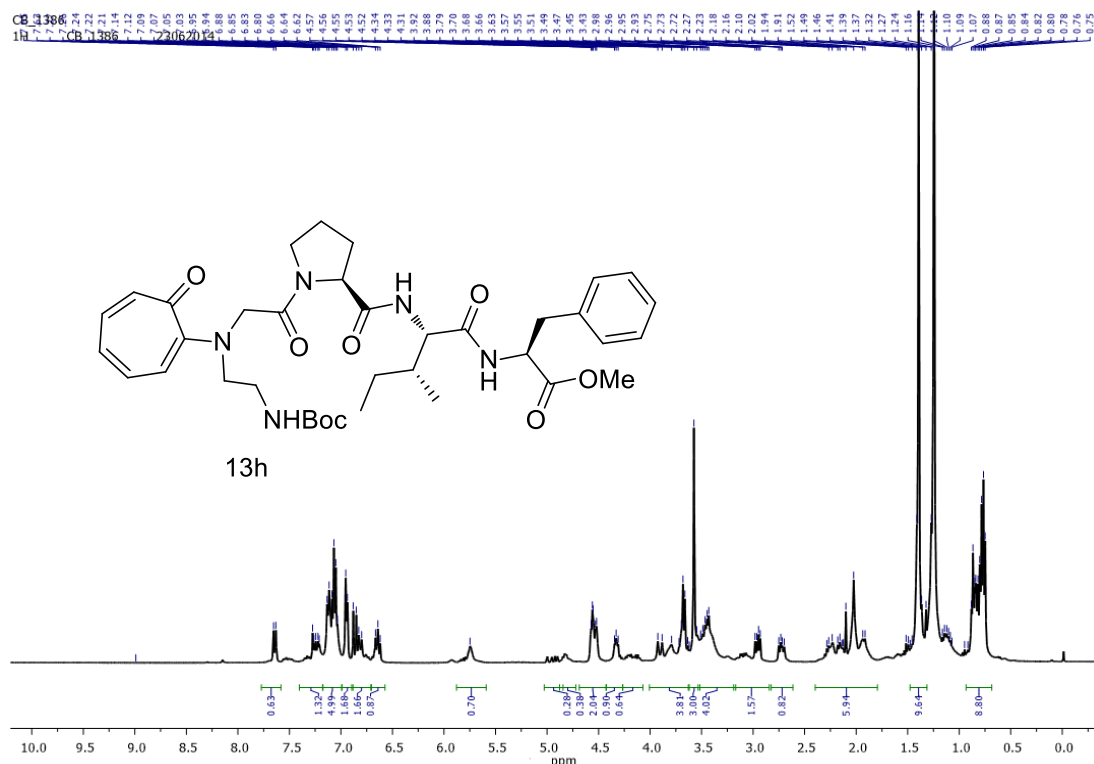


Figure A32. ^1H NMR spectrum of *BocNH-Traeg-Pro-Ile-Phe-OMe* (**13h**) in CDCl_3

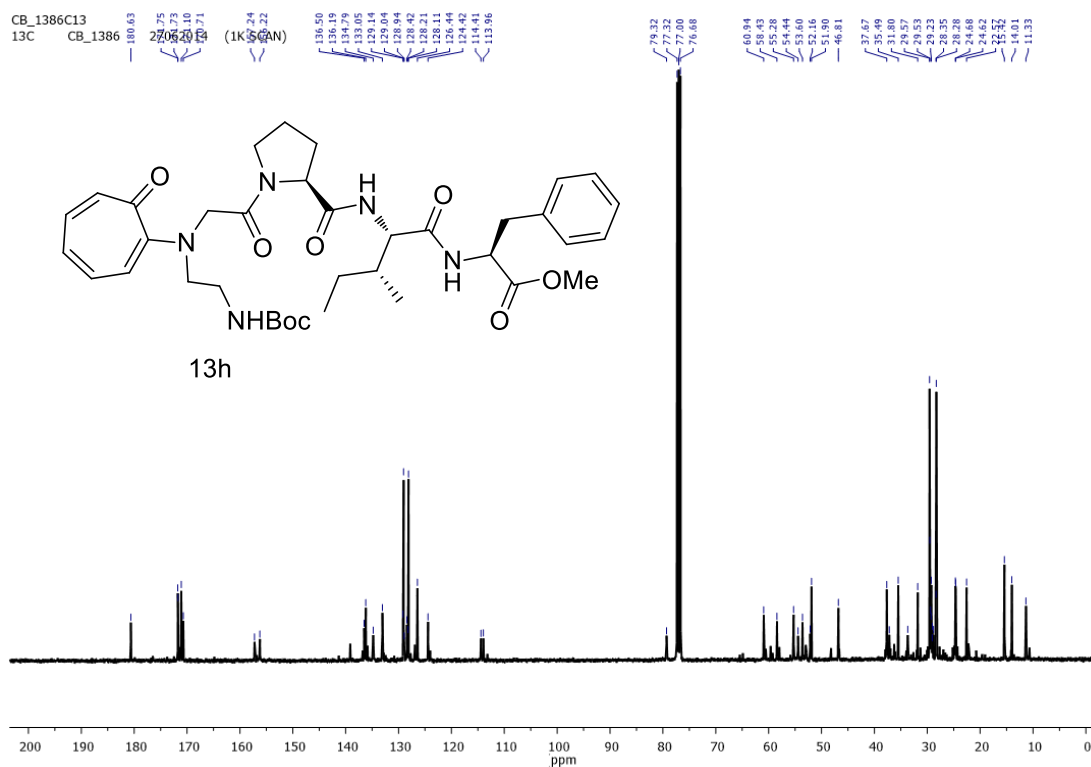


Figure A33. ^{13}C NMR spectrum of *BocNH-Traeg-Pro-Ile-Phe-OMe* (**13h**) in CDCl_3

Generic Display Report

Analysis Info

Analysis Name D:\Data\AUG-2014\NKS\14082014_NKS_CB_1386.d
 Method Pso_tune_wide.m
 Sample Name
 Comment

Acquisition Date 8/14/2014 11:08:52 AM

Operator A.S.Sahu
 Instrument micrOTOF-Q II

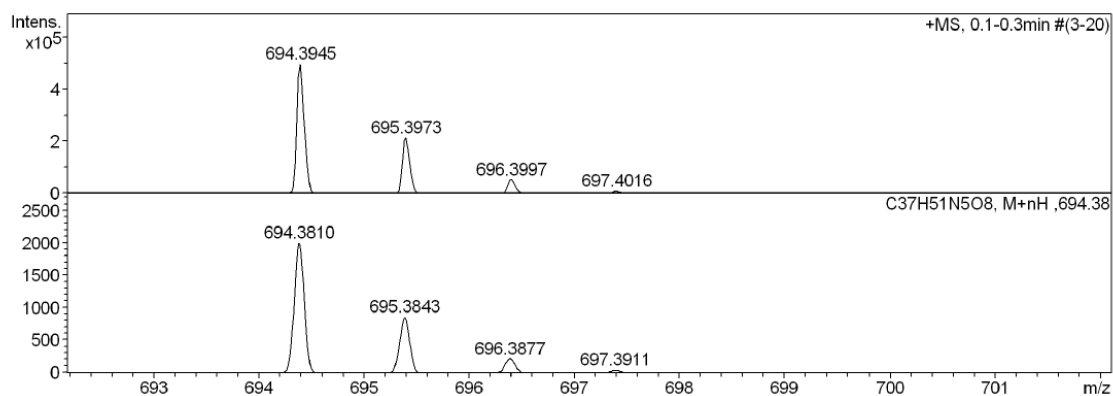
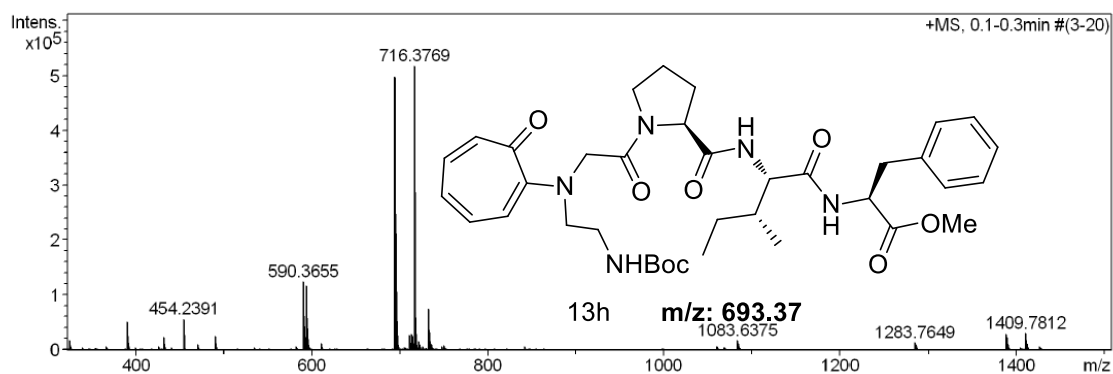
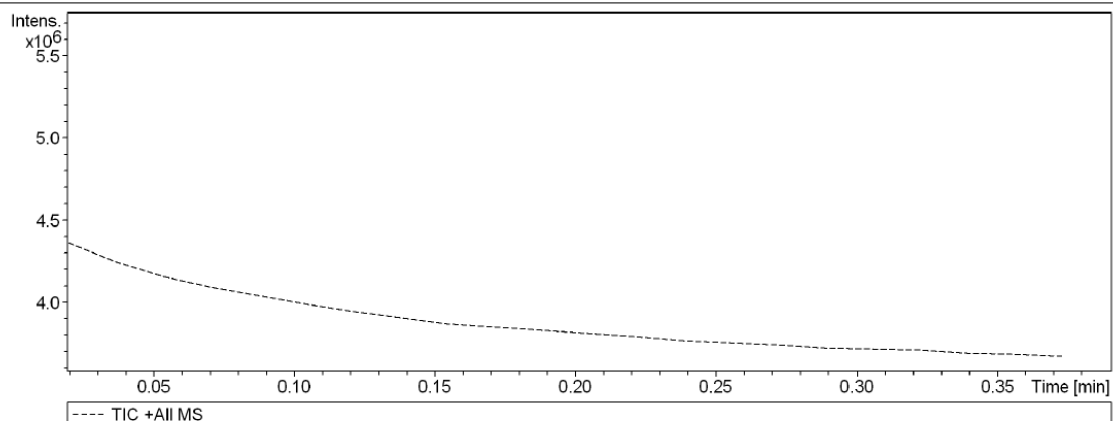


Figure A34. HRMS mass spectrum of *BocNH-Traeg-Pro-Ile-Phe-OMe* (**13h**)

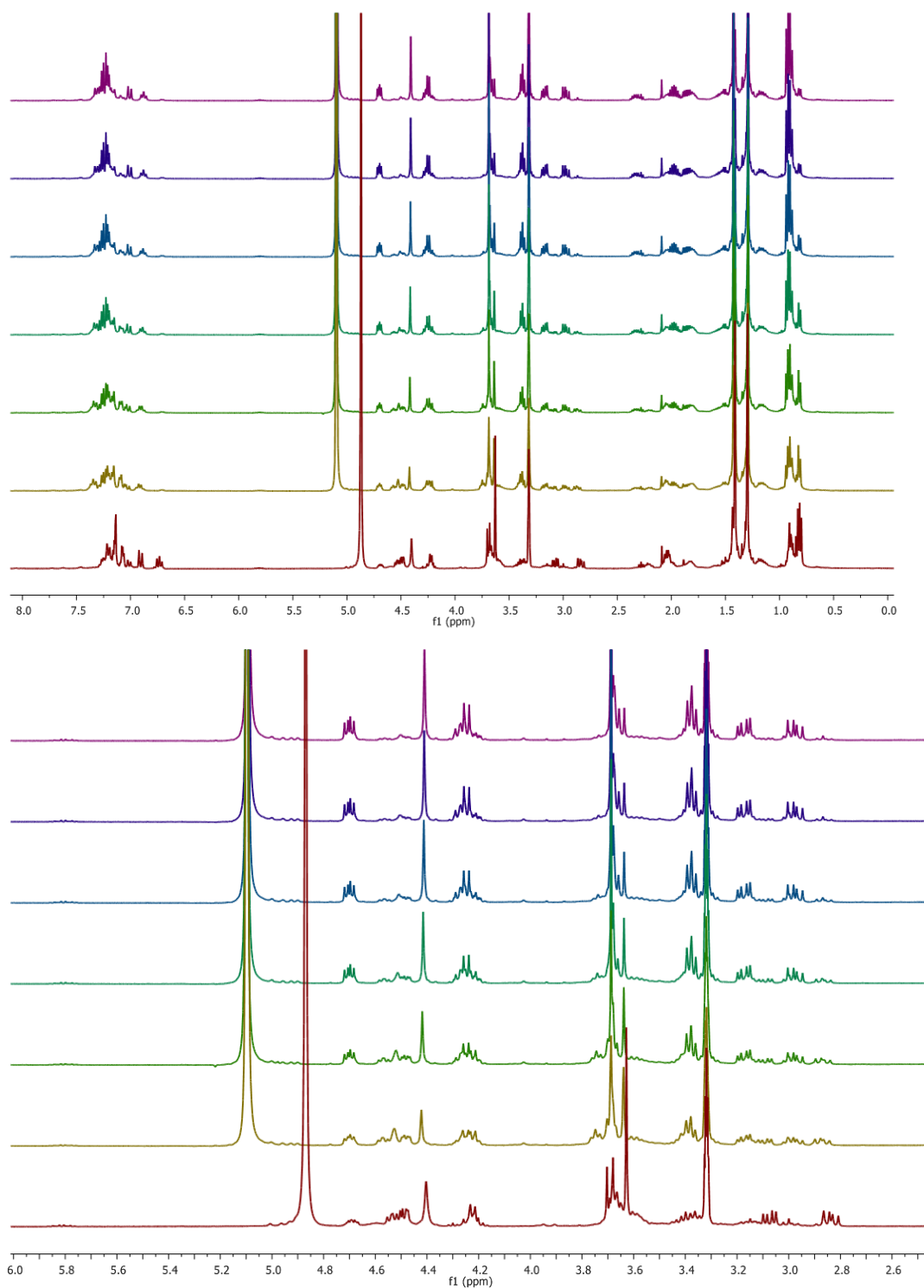


Figure A35. Time dependent NMR of BocNH-Traeg-Pro-Ile-Phe-OMe (**13h**) in CD₃OD and 5% TFA

Generic Display Report

Analysis Info

Analysis Name D:\Data\AUG2014\NKS\14082014_NKS_CB_1386D.d
 Method Pos_tune_low.m
 Sample Name
 Comment

Acquisition Date 8/14/2014 8:11:31 PM

Operator A.S.Sahu
 Instrument micrOTOF-Q II

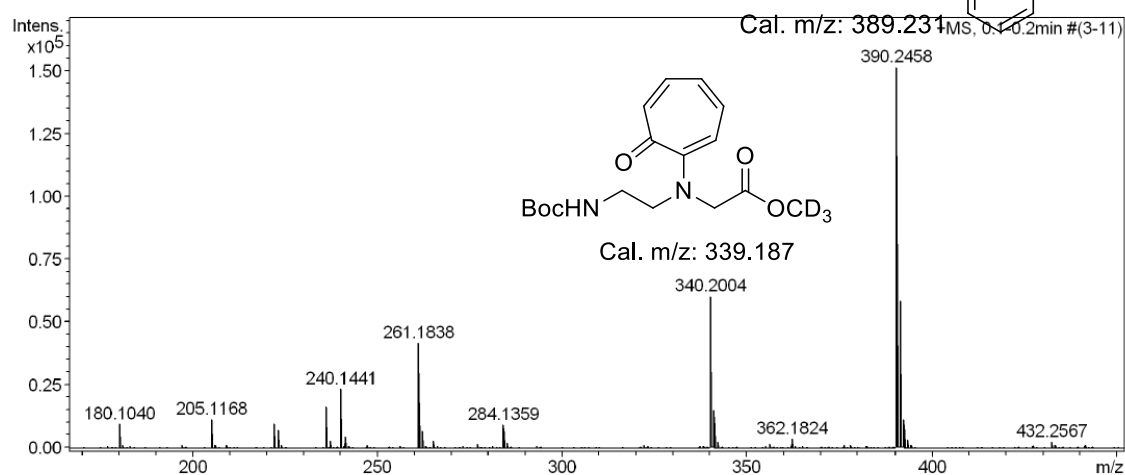
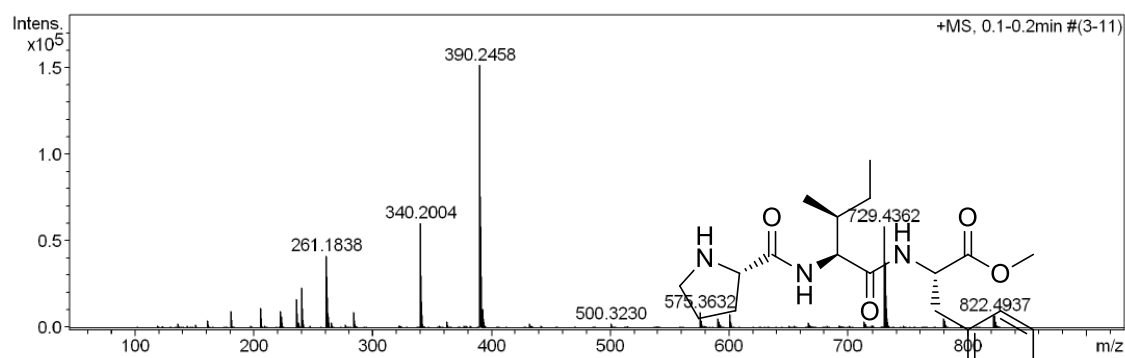
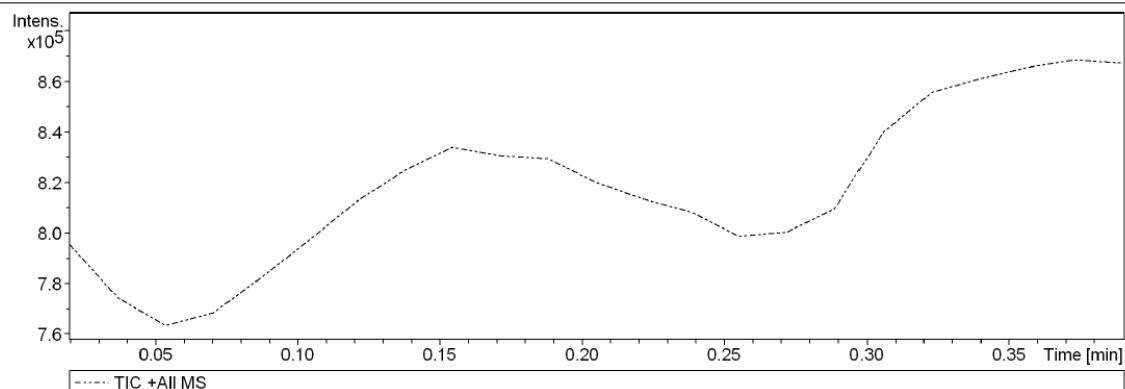


Figure A36. Mass spectrum of *BocNH-Traeg-Pro-Ile-Phe-OMe* (**13h**) after time dependent NMR experiment in CD₃OD.

10. Characterization data ($^1\text{H}/^{13}\text{C}$ NMR and HRMS) *Trpro* (**9**):

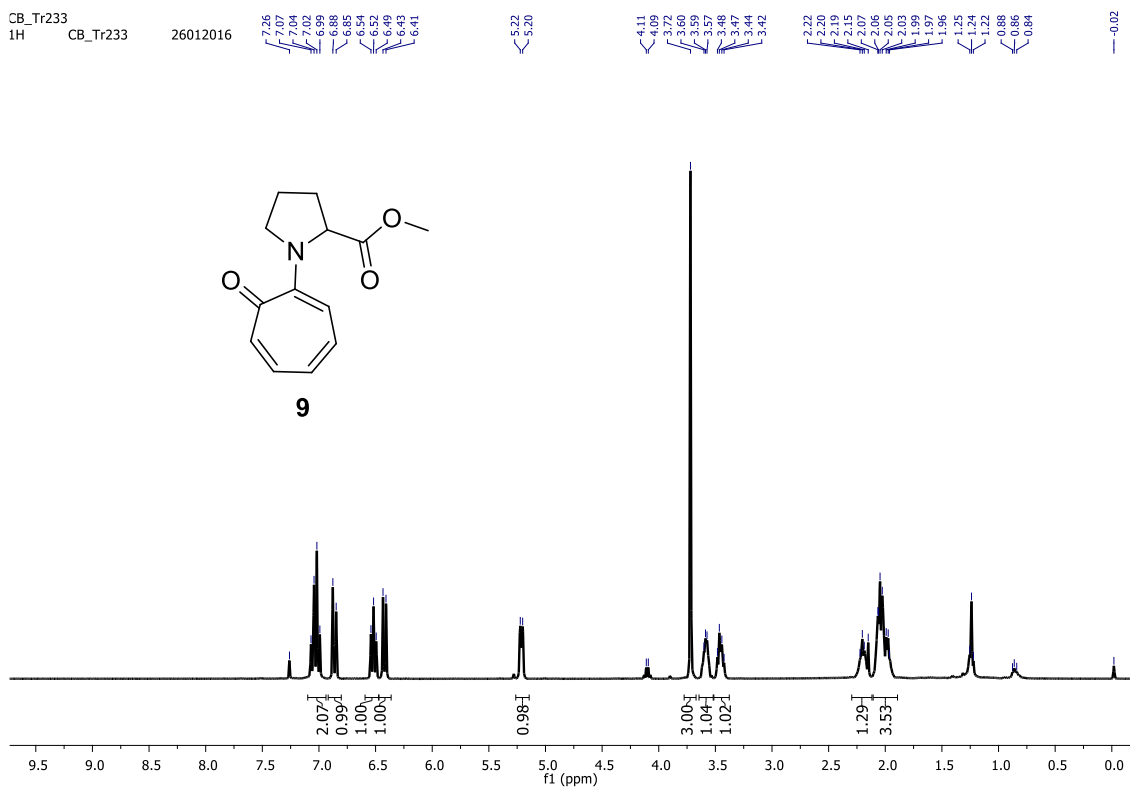


Figure A37. ^1H NMR of *Trpro* in CDCl_3

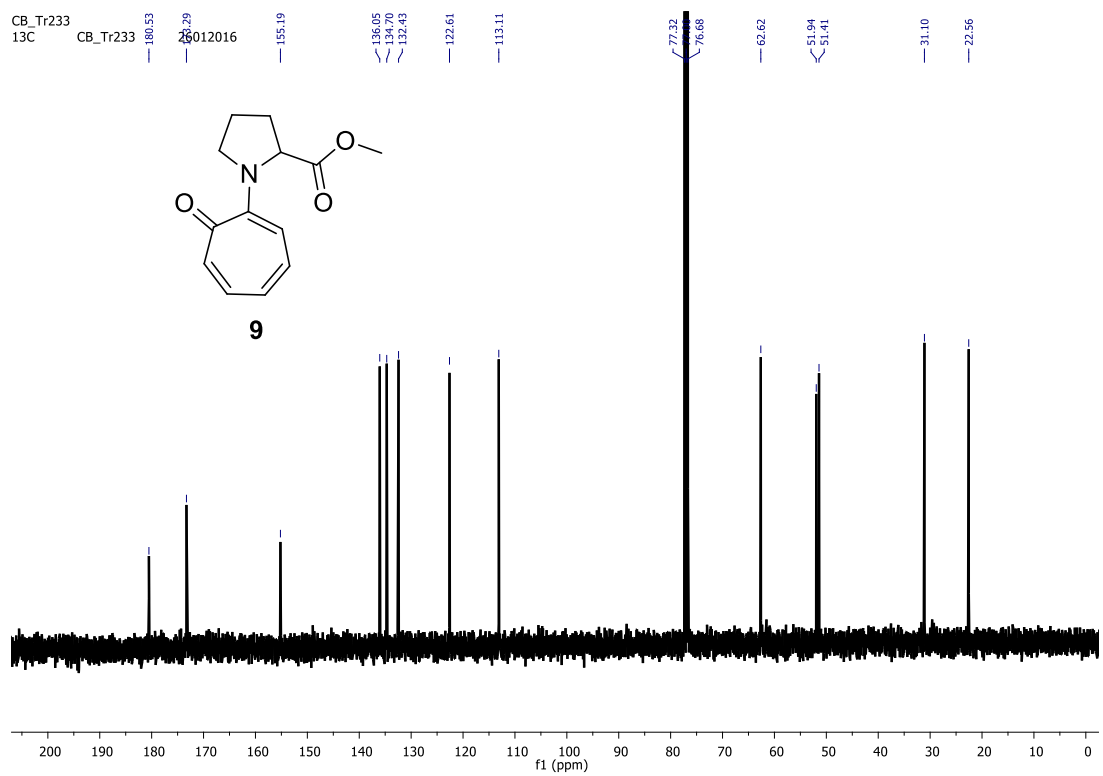


Figure A38. ^{13}C NMR of *Trpro* in CDCl_3 .

Display Report

Analysis Info

Analysis Name D:\Data\JAN-2016\NKS\25012016_NKS_CB_233.d
Method Pos_tune_low.m
Sample Name Bruker micro TOF -Q II
Comment

Acquisition Date 1/25/2016 11:08:20 PM

Operator Amit S.Sahu
Instrument microTOF-Q II 10337

Acquisition Parameter

Source Type	ESI	Ion Polarity	Positive	Set Nebulizer	0.4 Bar
Focus	Not active	Set Capillary	4000 V	Set Dry Heater	180 °C
Scan Begin	50 m/z	Set End Plate Offset	-500 V	Set Dry Gas	4.0 l/min
Scan End	3000 m/z	Set Collision Cell RF	130.0 Vpp	Set Divert Valve	Waste

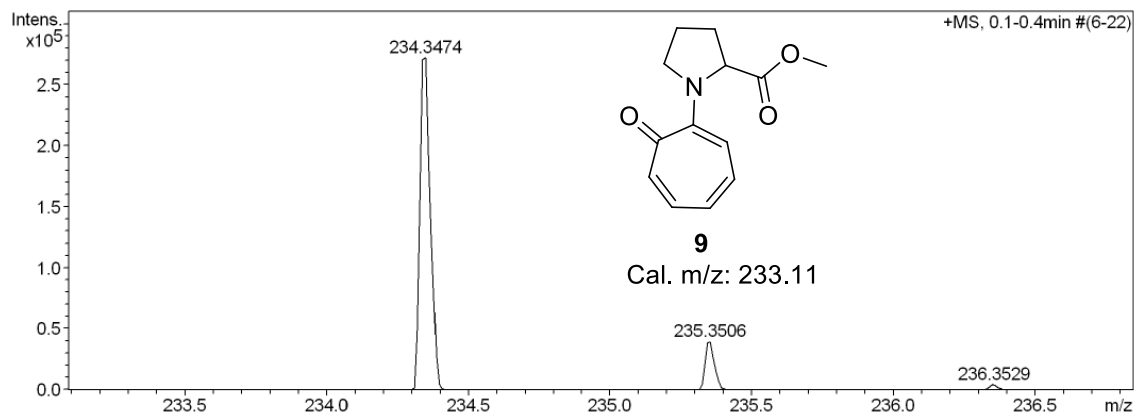
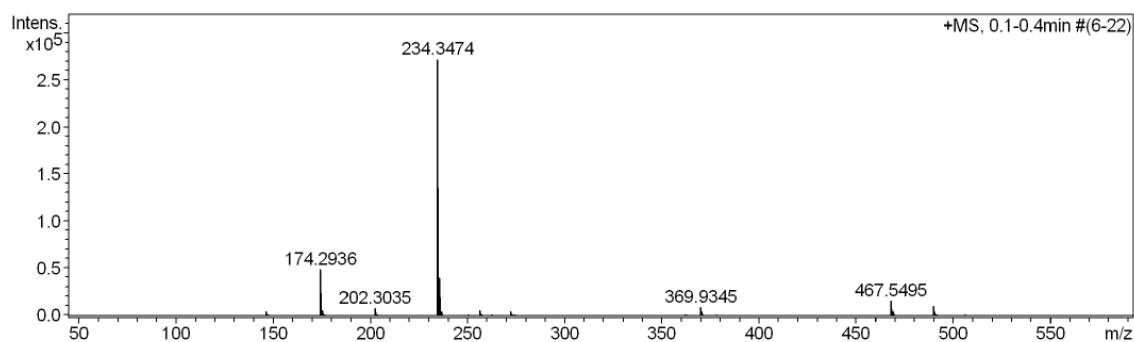
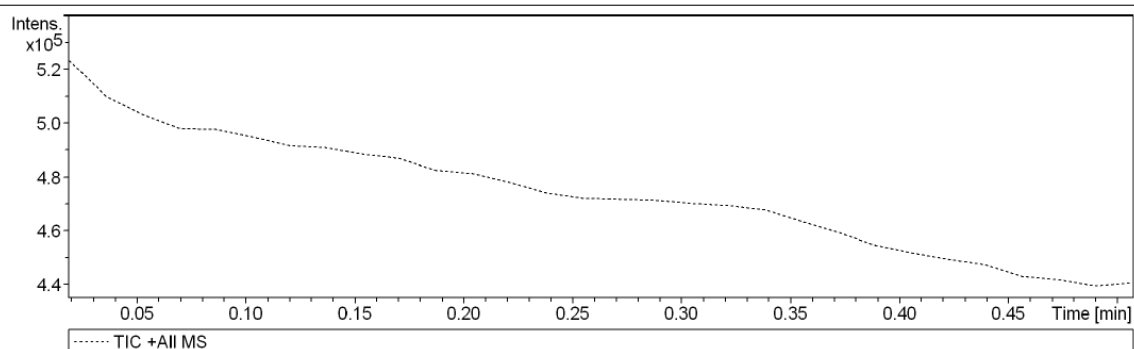


Figure A39. MS mass spectrum of *Trpro* (9).

11. Characterization data ($^1\text{H}/^{13}\text{C}$ NMR and HRMS) *Trpro-Gly* (**9G**):

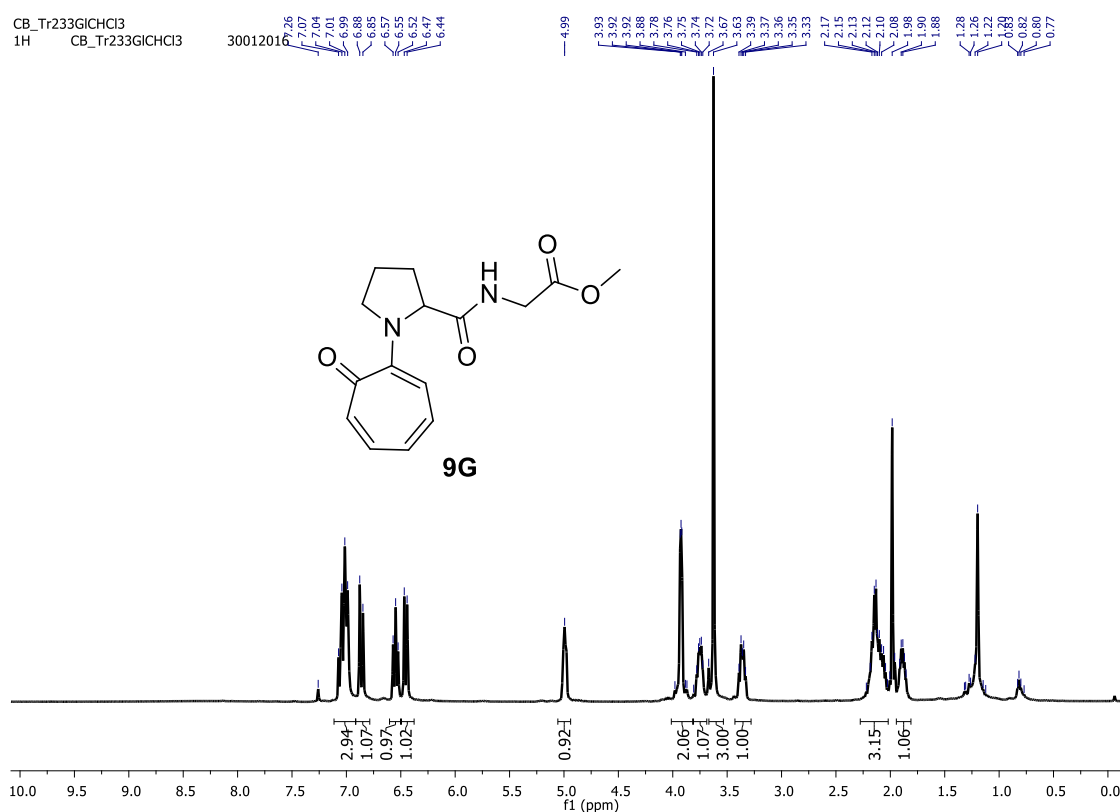


Figure A40. ^1H NMR of *Trpro-Gly* (**9G**) in CDCl_3

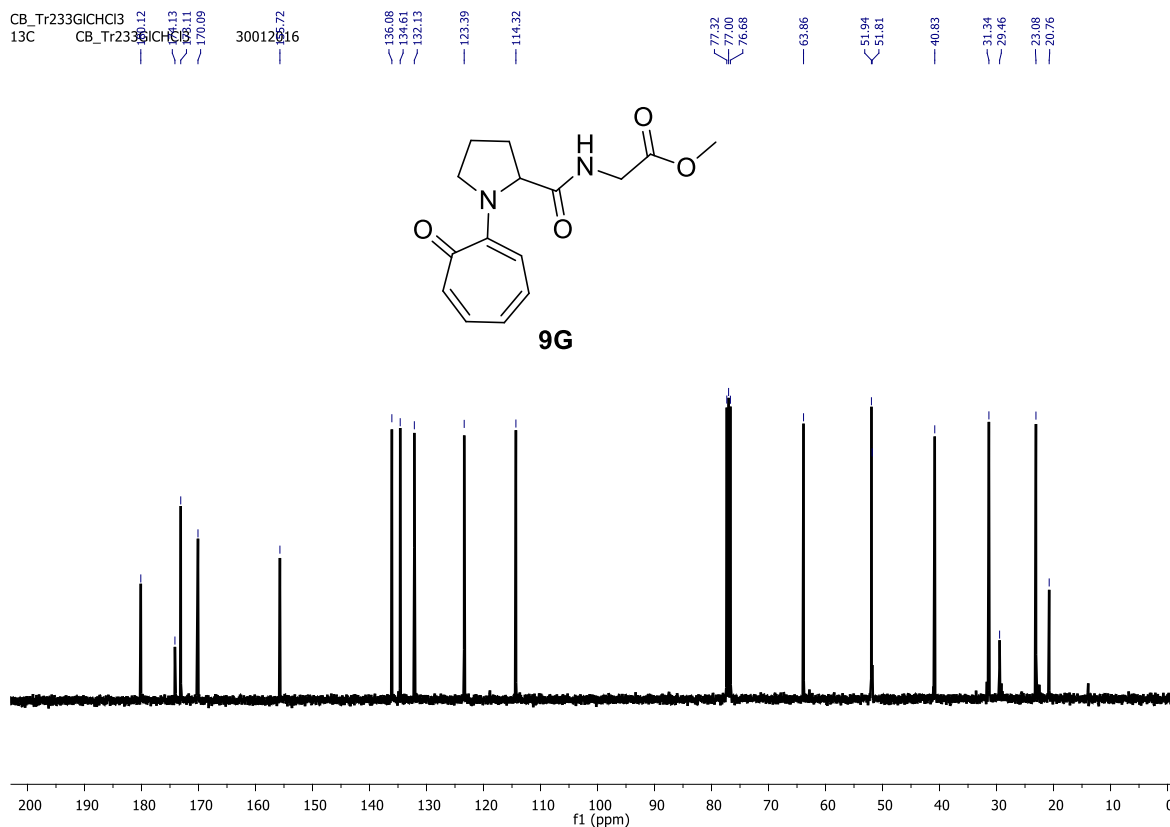


Figure A41. ^{13}C NMR of *Trpro-Gly* (**9G**) in CDCl_3

Generic Display Report

Analysis Info

Analysis Name D:\Data\AUG-2016\NKS\10082016_NKS_CB_TRPRO_GLY.d
Method Pos_tune_low_nks_LOW.m
Sample Name Bruker micro TOF -Q II
Comment

Acquisition Date 8/10/2016 6:35:33 PM

Operator Amit S.Sahu
Instrument micrOTOF-Q II

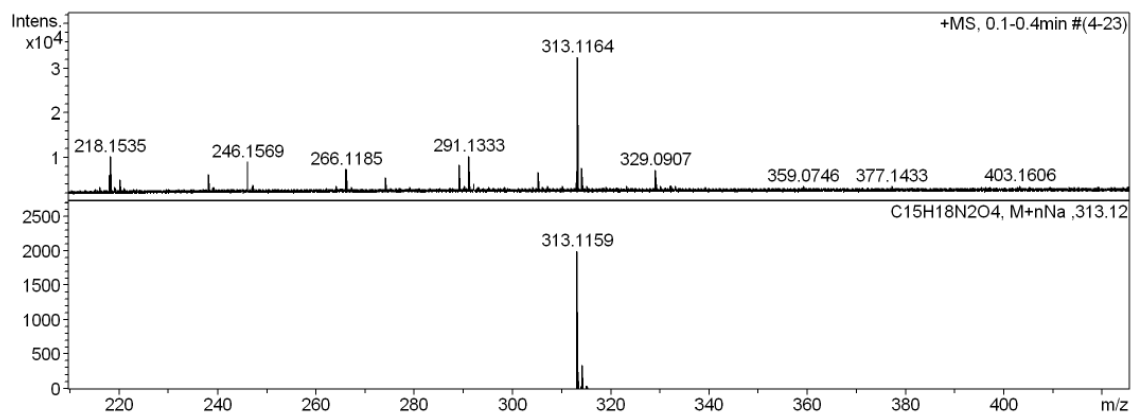
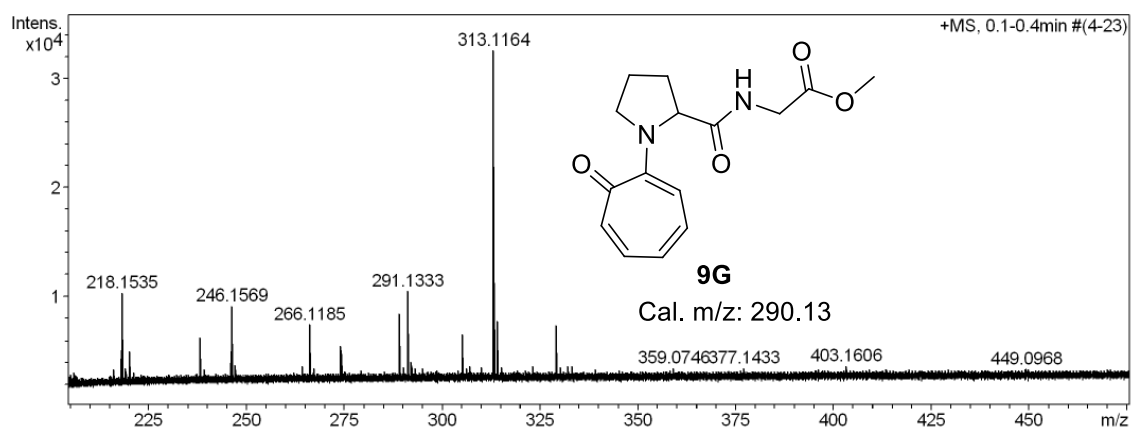
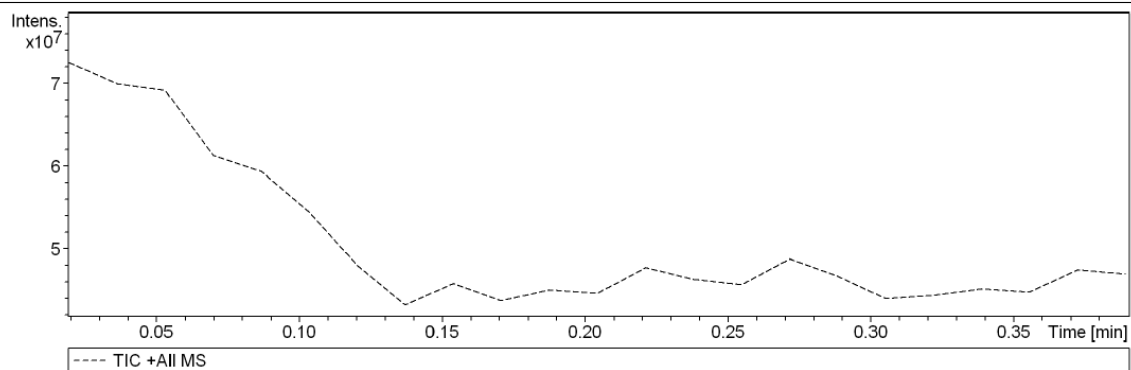


Figure A42. HRMS mass spectrum of *Trpro-Gly* (**9G**)

12. Characterization data ($^1\text{H}/^{13}\text{C}$ NMR and HRMS) *TrPro-Phe-OMe* (**9F**):

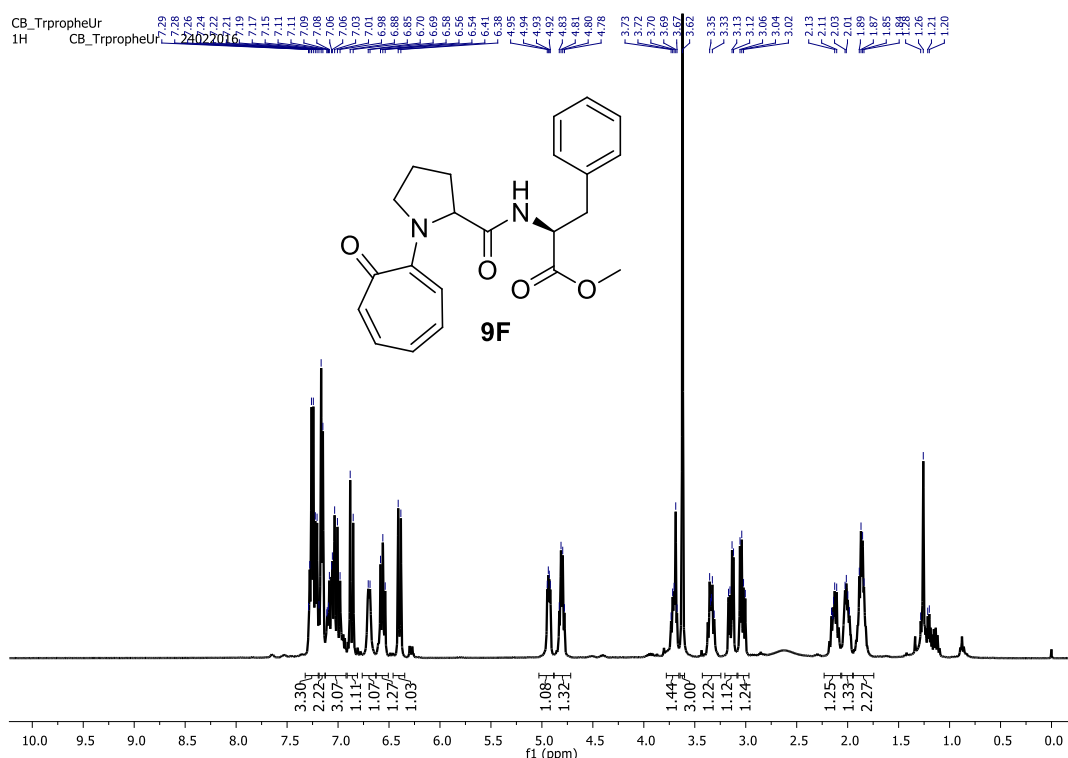


Figure A43. ^1H NMR of *Trpro-Phe* (**9F**) in CDCl_3

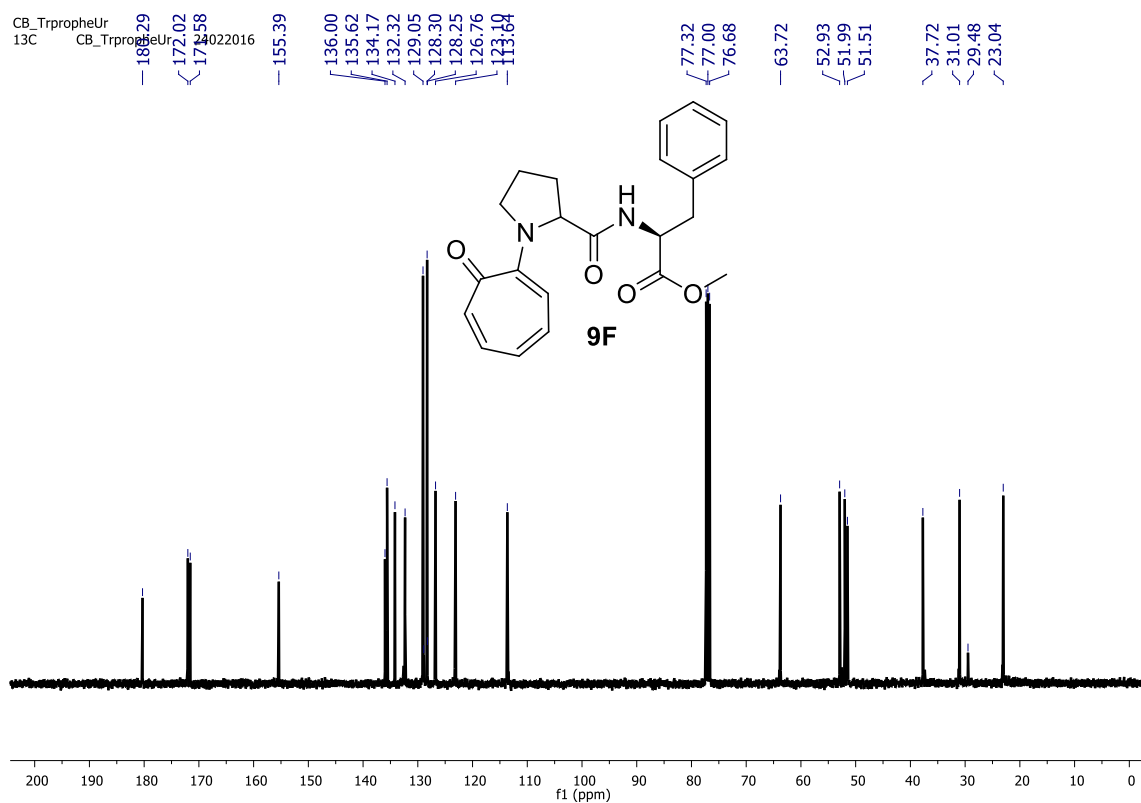


Figure A44. ^{13}C NMR of *Trpro-Phe* (**9F**) in CDCl_3

Generic Display Report

Analysis Info

Analysis Name D:\Data\AUG-2016\NKS\10082016_NKS_CB_TRPROPHE.d
Method Pso_tune_wide.m
Sample Name Bruker micro TOF -Q II
Comment

Acquisition Date 8/10/2016 6:18:06 PM

Operator Amit S.Sahu
Instrument microTOF-Q II

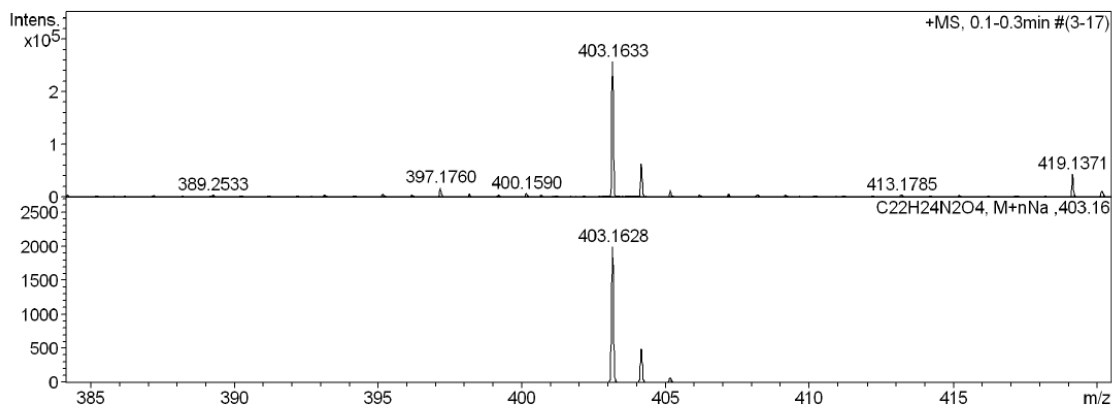
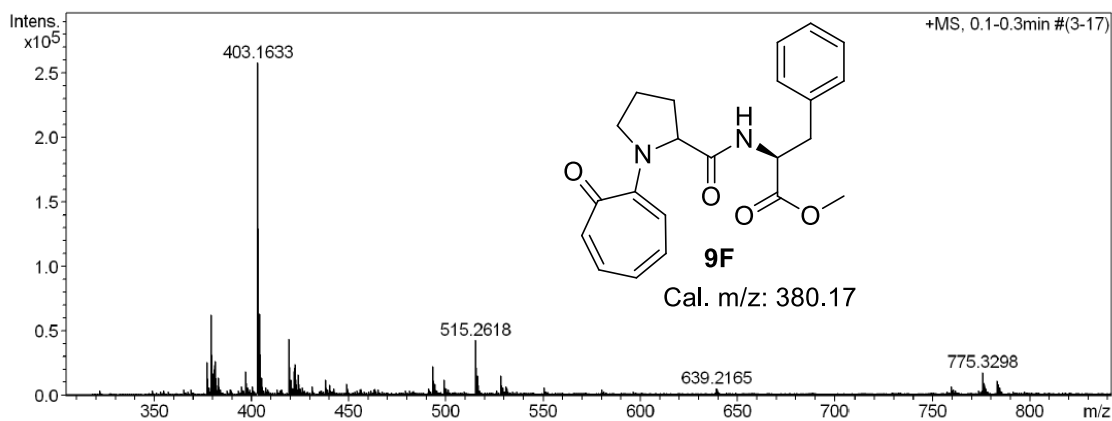
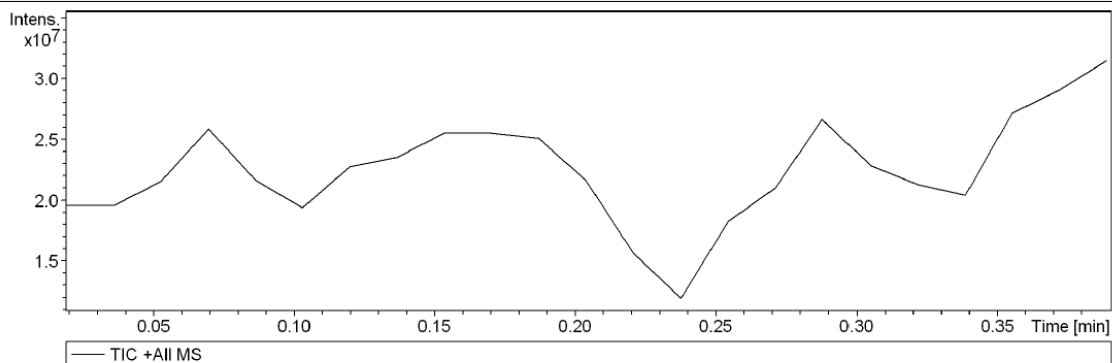


Figure A45. HRMS mass spectrum of *Trpro*-Phe (**9F**)

13. Characterization data ($^1\text{H}/^{13}\text{C}$ NMR and HRMS) *Trhg* (**18**):

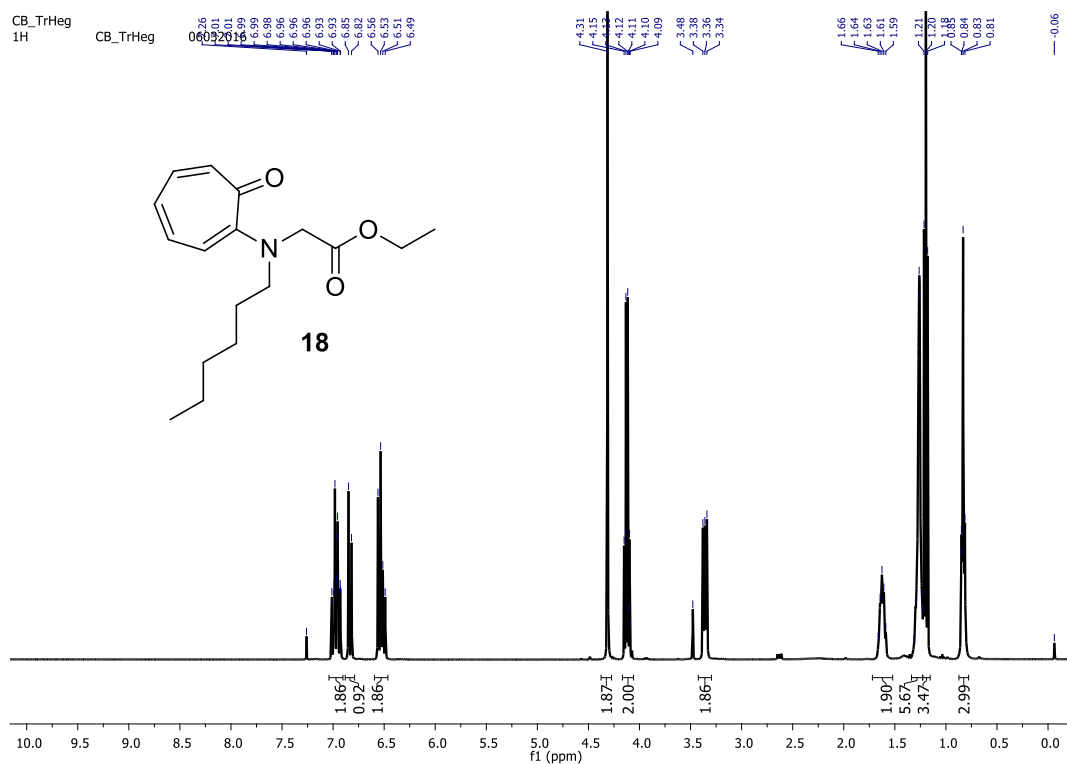


Figure A46. ^1H NMR of *Trhg* (**18**) in CDCl_3

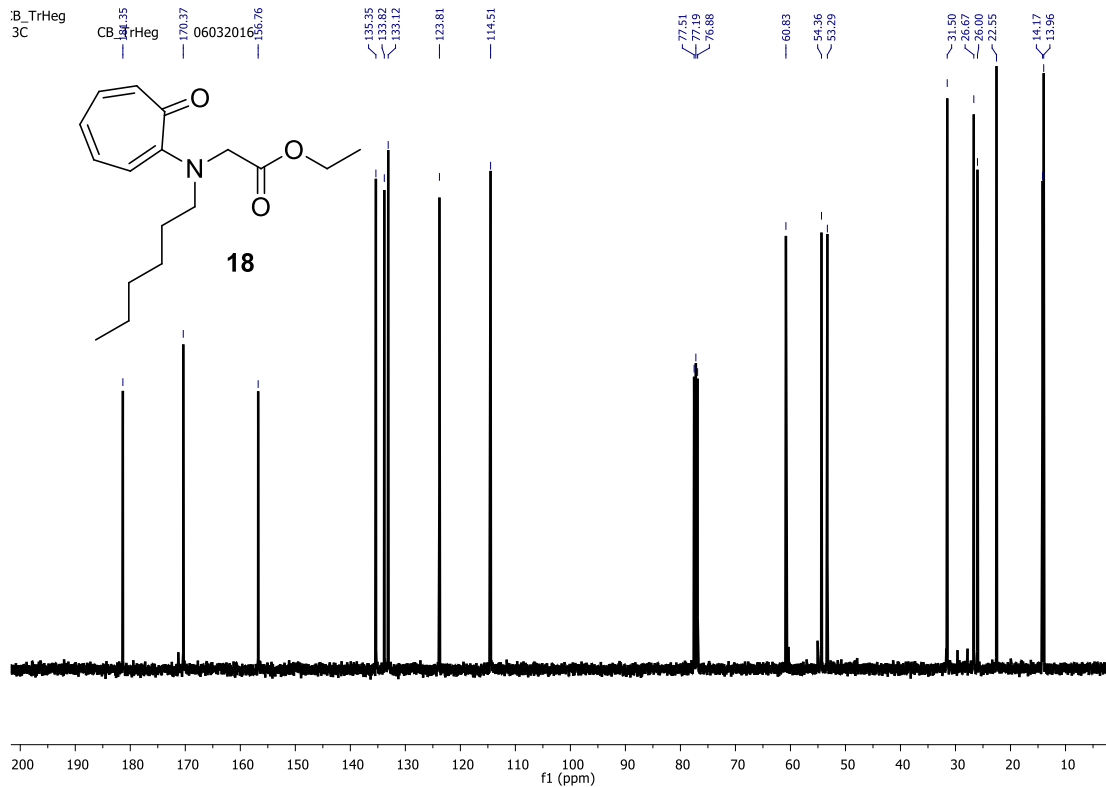


Figure A47. ^{13}C NMR of *Trhg* (**18**) in CDCl_3

14. Characterization data ($^1\text{H}/^{13}\text{C}$ NMR and HRMS) *Trhg-Gly* (**19**)

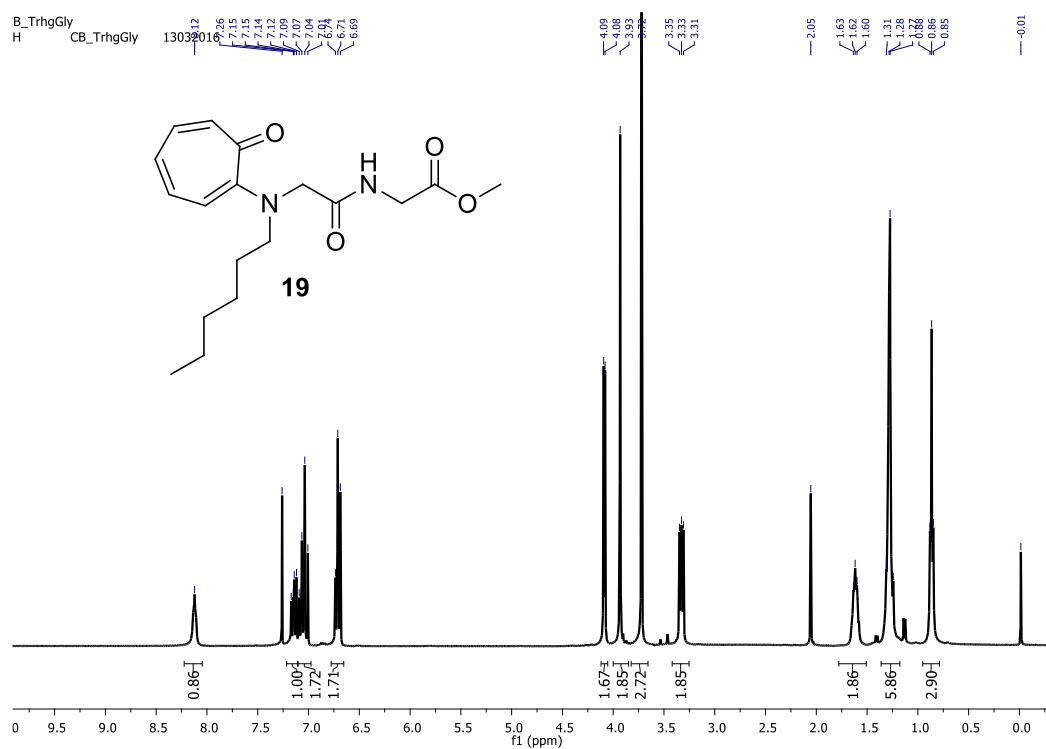


Figure A48. ^1H NMR of *Trhg-Gly* (**19**) in CDCl_3

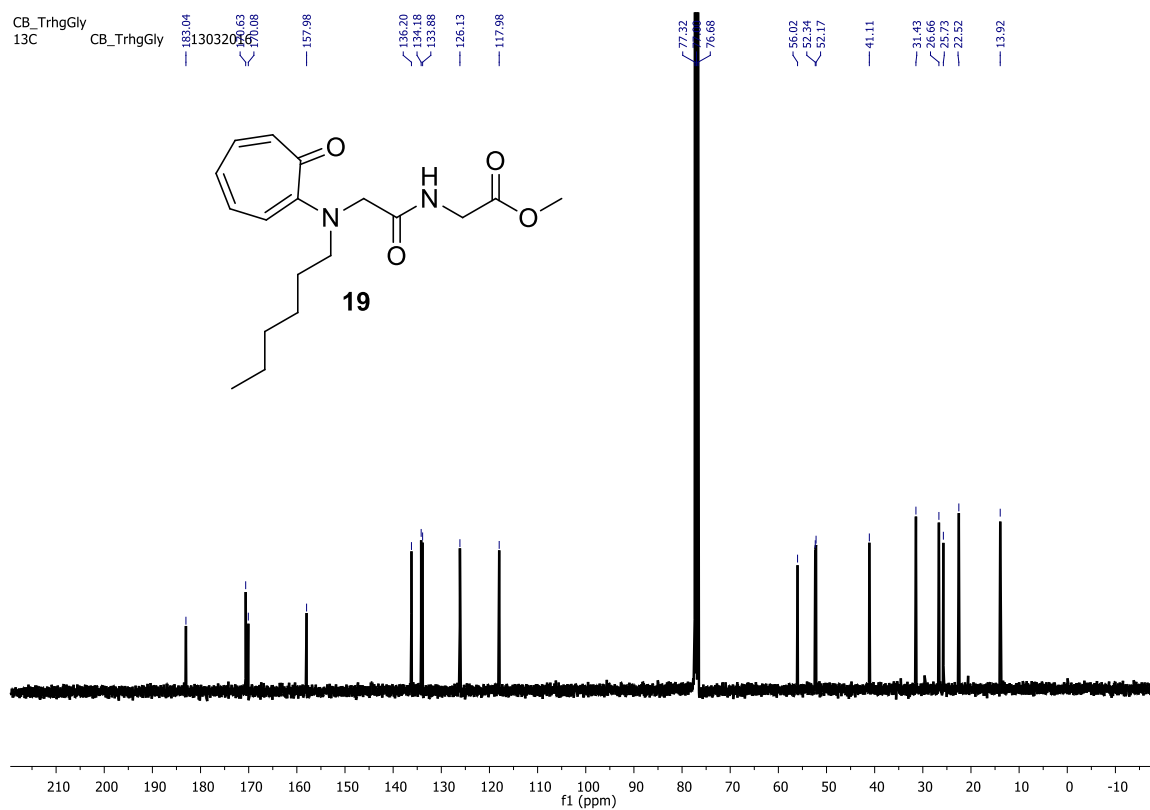


Figure A49. ^{13}C NMR of *Trhg-Gly* (**19**) in CDCl_3

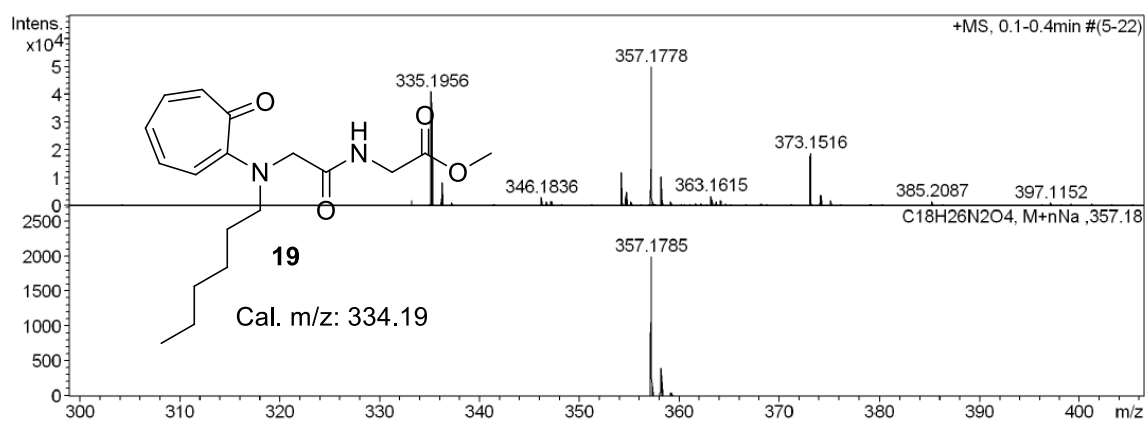
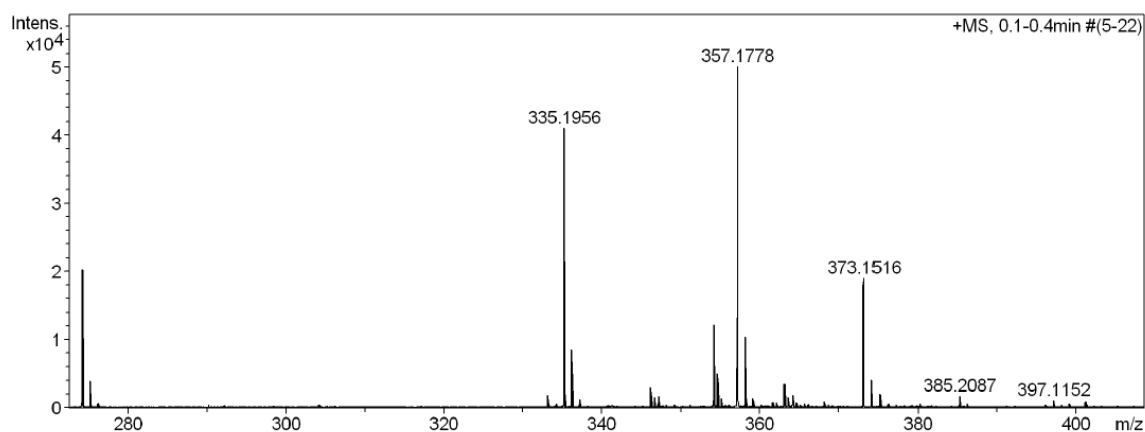
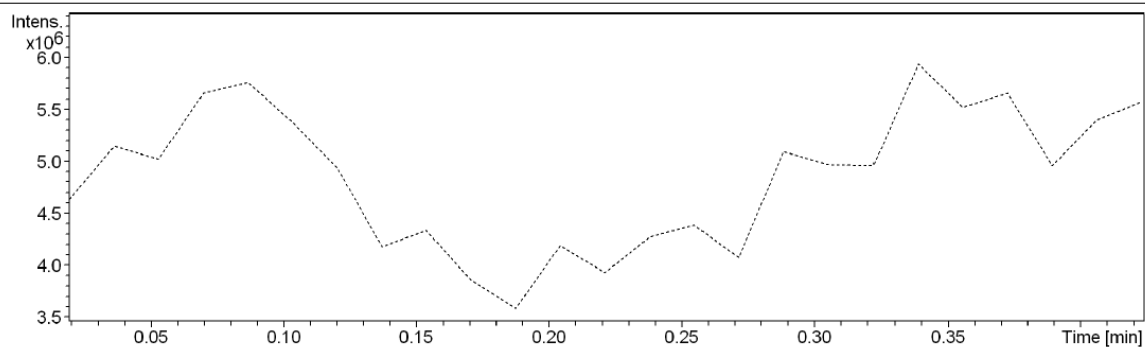
Generic Display Report

Analysis Info

Analysis Name D:\Data\AUG-2016\NKS\10082016_NKS_CB_TRHGGLY.d
Method Pos_tune_low_nks_LOW.m
Sample Name Bruker micro TOF -Q II
Comment

Acquisition Date 8/10/2016 5:29:09 PM

Operator Amit S.Sahu
Instrument microTOF-Q II



15. Characterization data ($^1\text{H}/^{13}\text{C}$ NMR and HRMS) *Trpeg* (**20**):

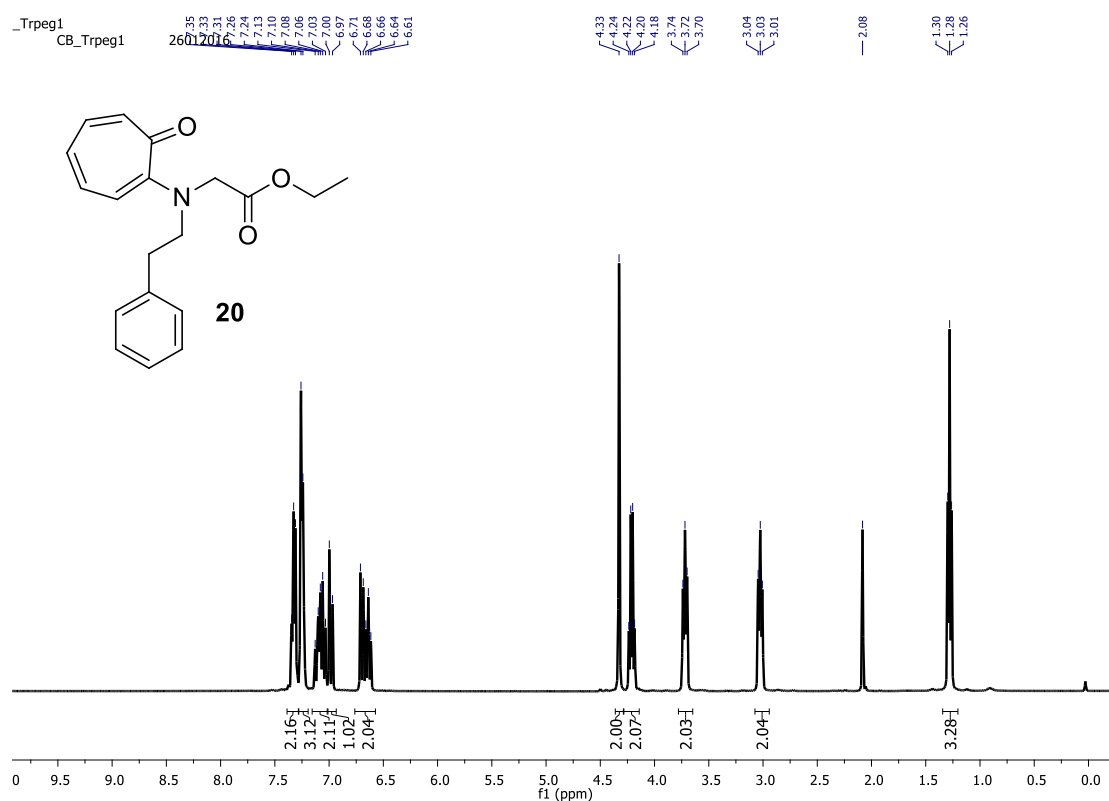


Figure A50. ^1H NMR of *Trpeg* (**20**) in CDCl_3

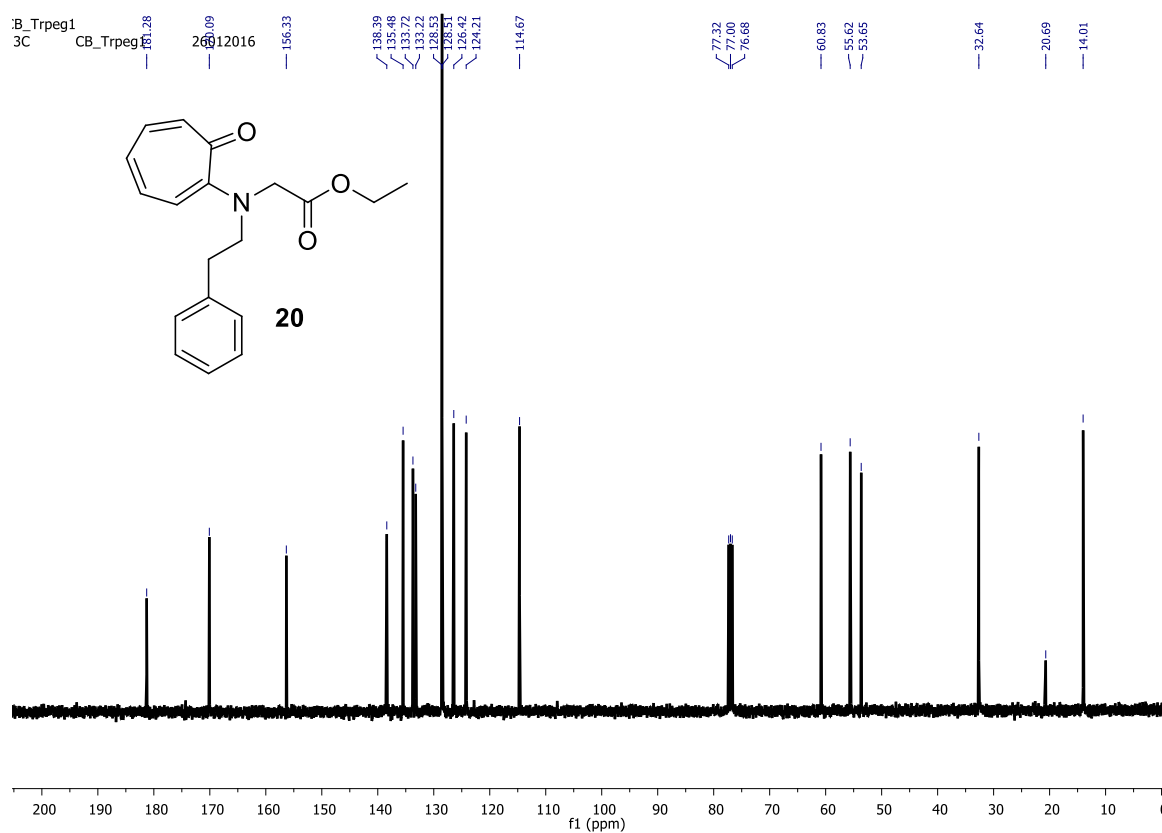


Figure A51. ^{13}C NMR of *Trpeg* (**20**) in CDCl_3

Generic Display Report

Analysis Info

Analysis Name D:\Data\AUG-2016\NKS\11082016_NKS_CB_TRPEGMONO.d
Method Pos_tune_low_nks_LOW.m
Sample Name Bruker micro TOF -Q II
Comment

Acquisition Date 8/11/2016 5:45:07 PM

Operator Amit S.Sahu
Instrument micrOTOF-Q II

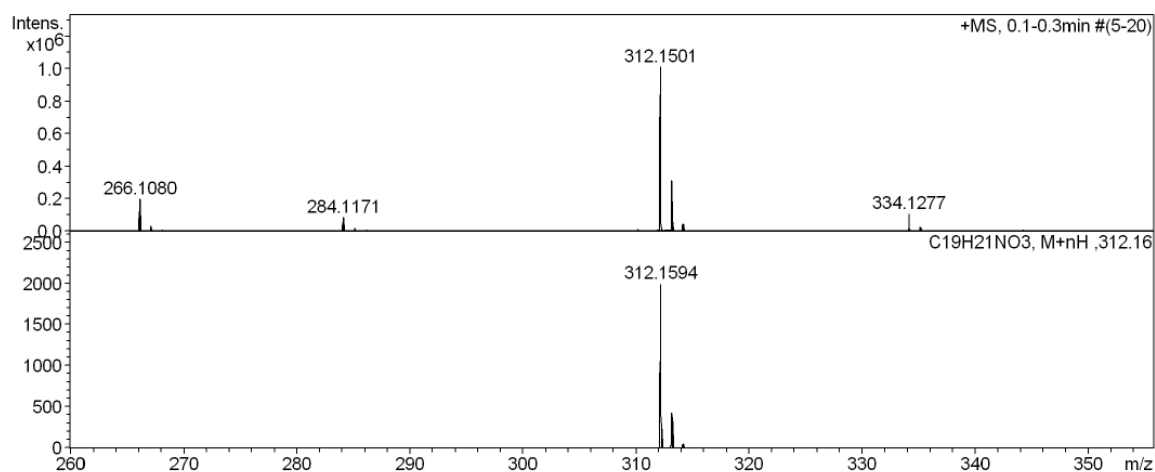
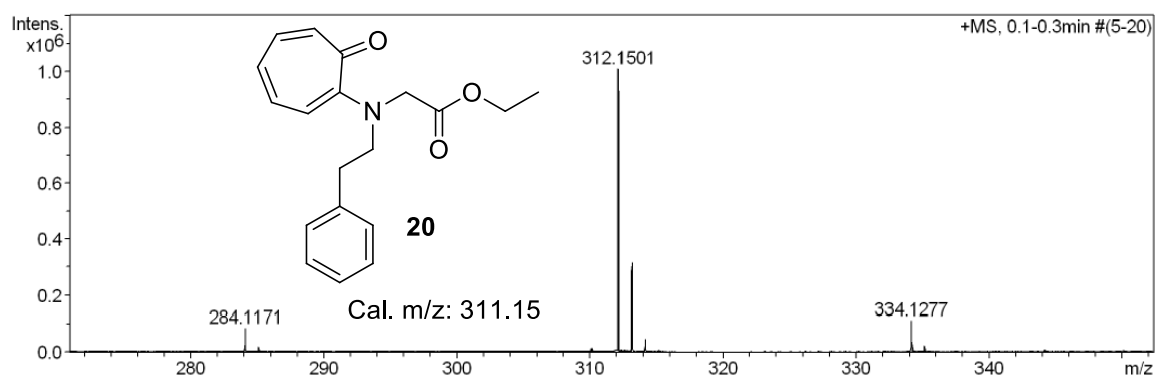
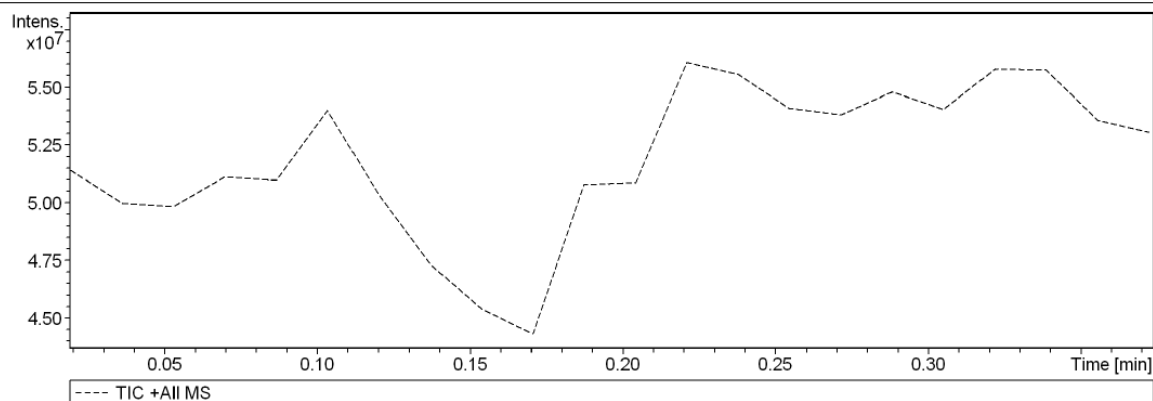


Figure A52. HRMS mass spectrum of *Trpeg* (**20**)

16. Characterization data ($^1\text{H}/^{13}\text{C}$ NMR and HRMS) *Trpeg-Gly* (**21**):

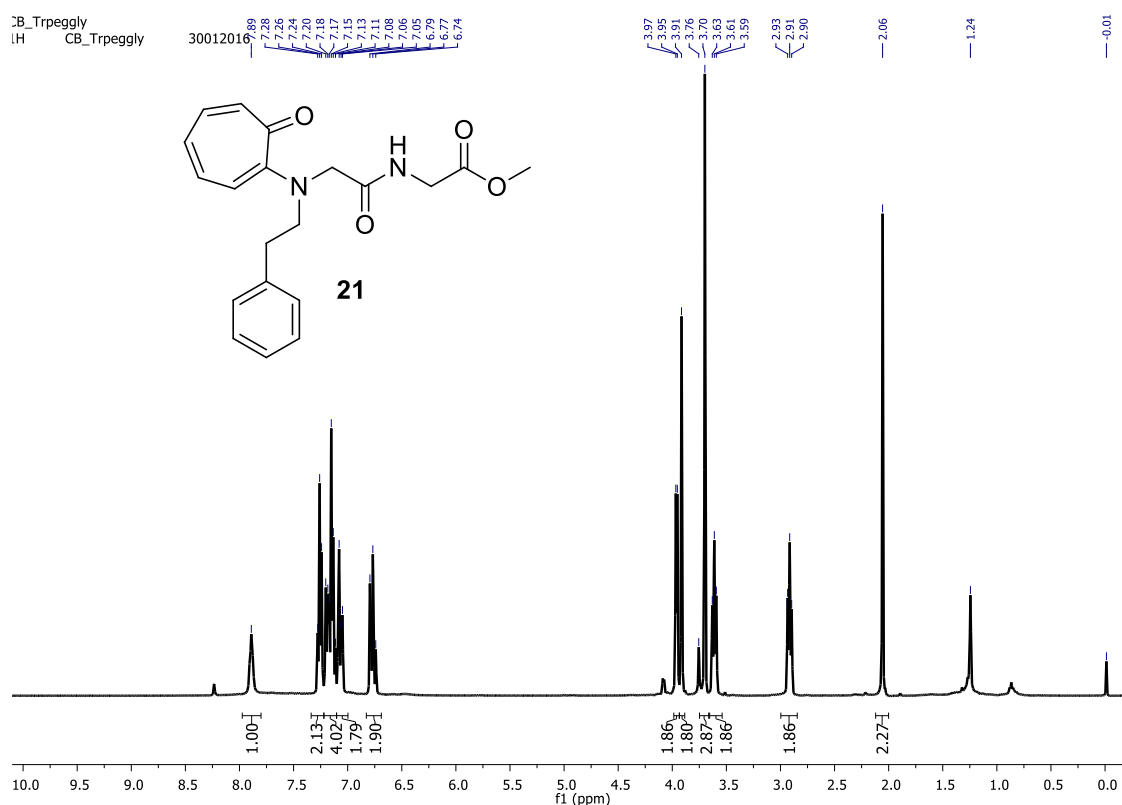


Figure A53. ^1H NMR of *Trpeg-Gly* (**21**) in CDCl_3

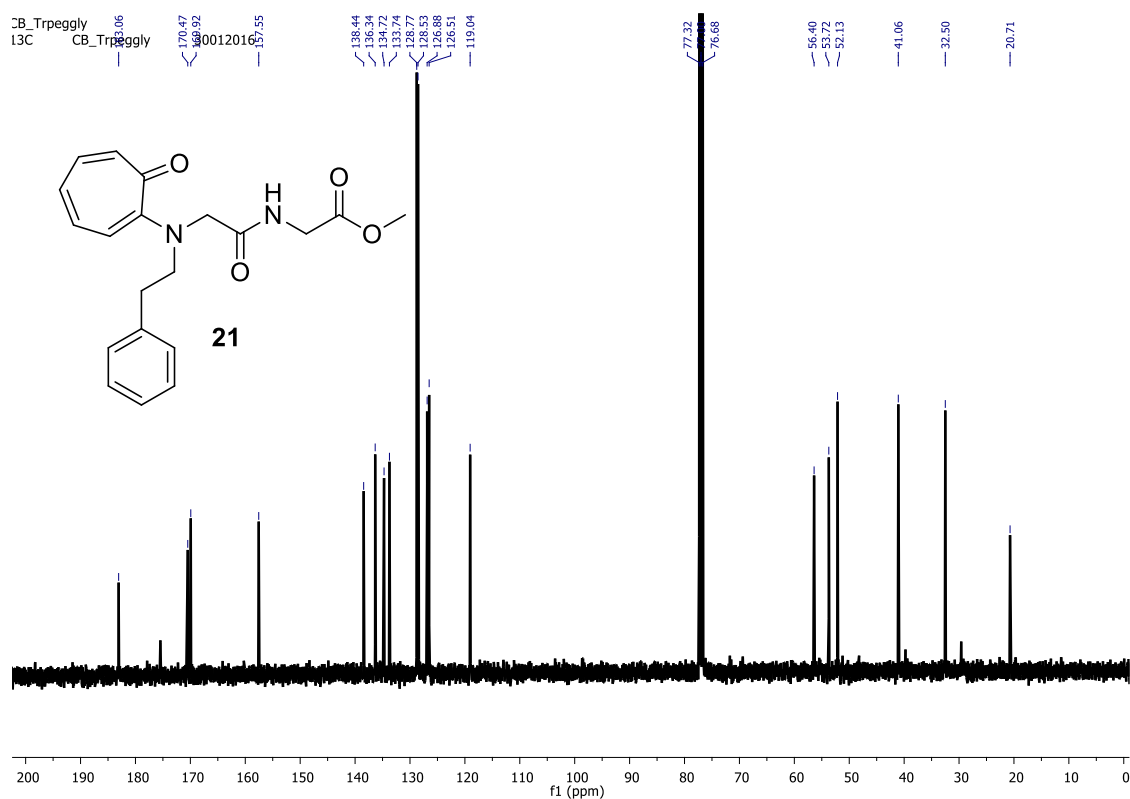


Figure A54. ^{13}C NMR of *Trpeg-Gly* (**21**) in CDCl_3

Generic Display Report

Analysis Info

Analysis Name D:\Data\AUG-2016\NKS\10082016_NKS_CB_TRPEGGLY1.d
Method Pos_tune_low_nks_LOW.m
Sample Name Bruker micro TOF -Q II
Comment

Acquisition Date 8/10/2016 6:05:40 PM

Operator Amit S.Sahu
Instrument microTOF-Q II

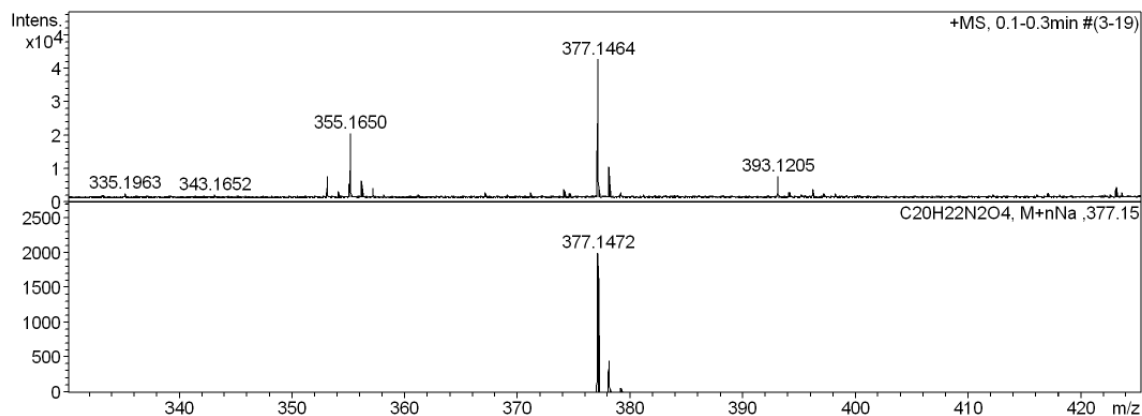
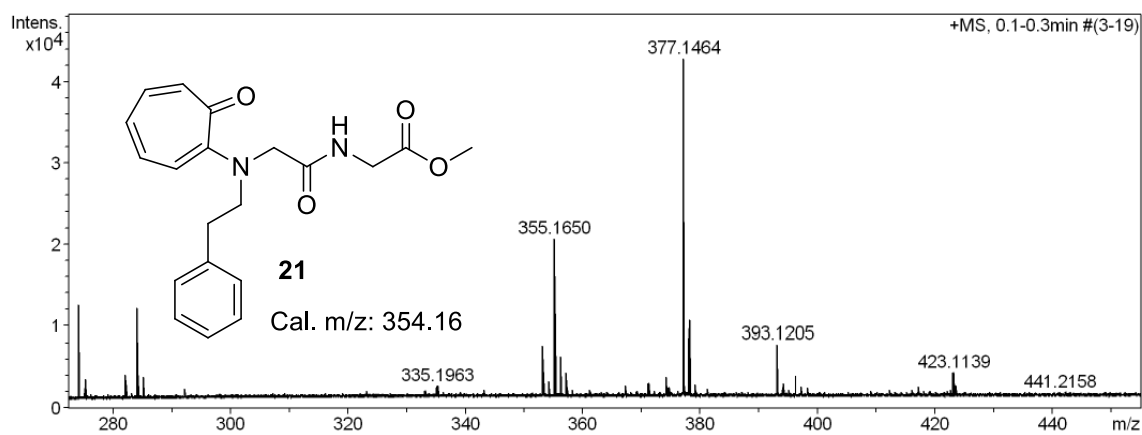
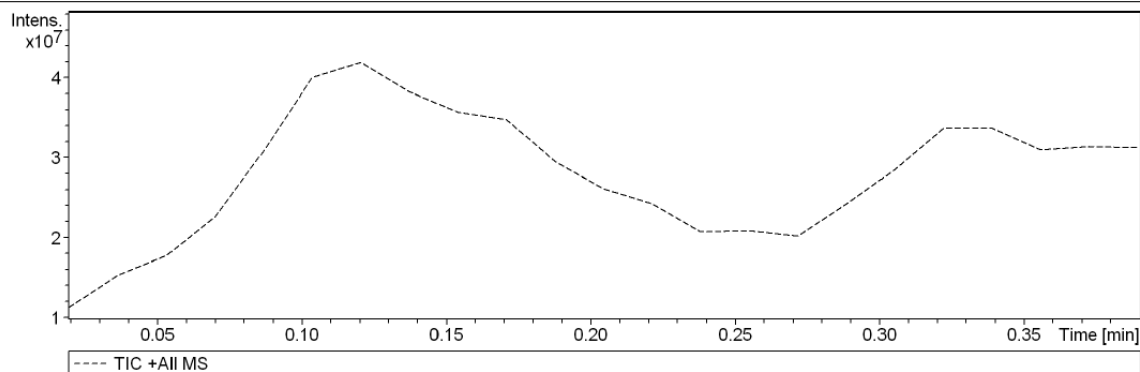


Figure A55. HRMS mass spectrum of *Trpeg-Gly* (**21**)

17. Characterization data ($^1\text{H}/^{13}\text{C}$ NMR and HRMS) *Trog-Gly* (**23**):

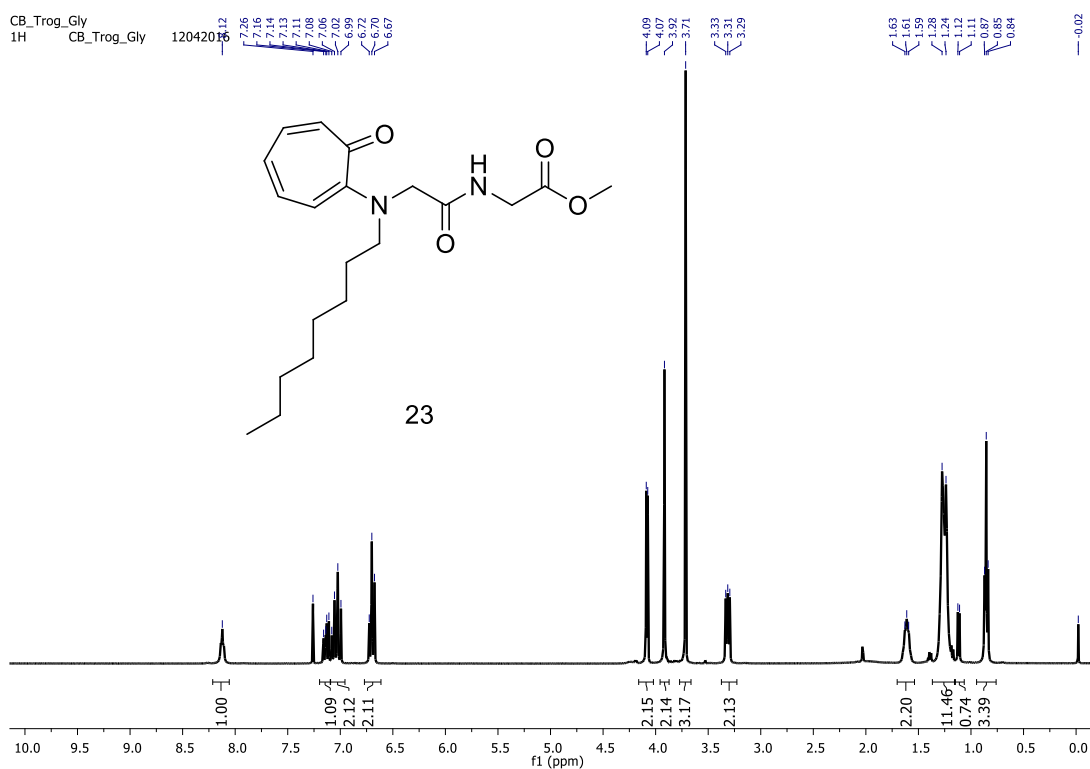


Figure A56. ^1H NMR of *Trog-Gly* (**23**) in CDCl_3

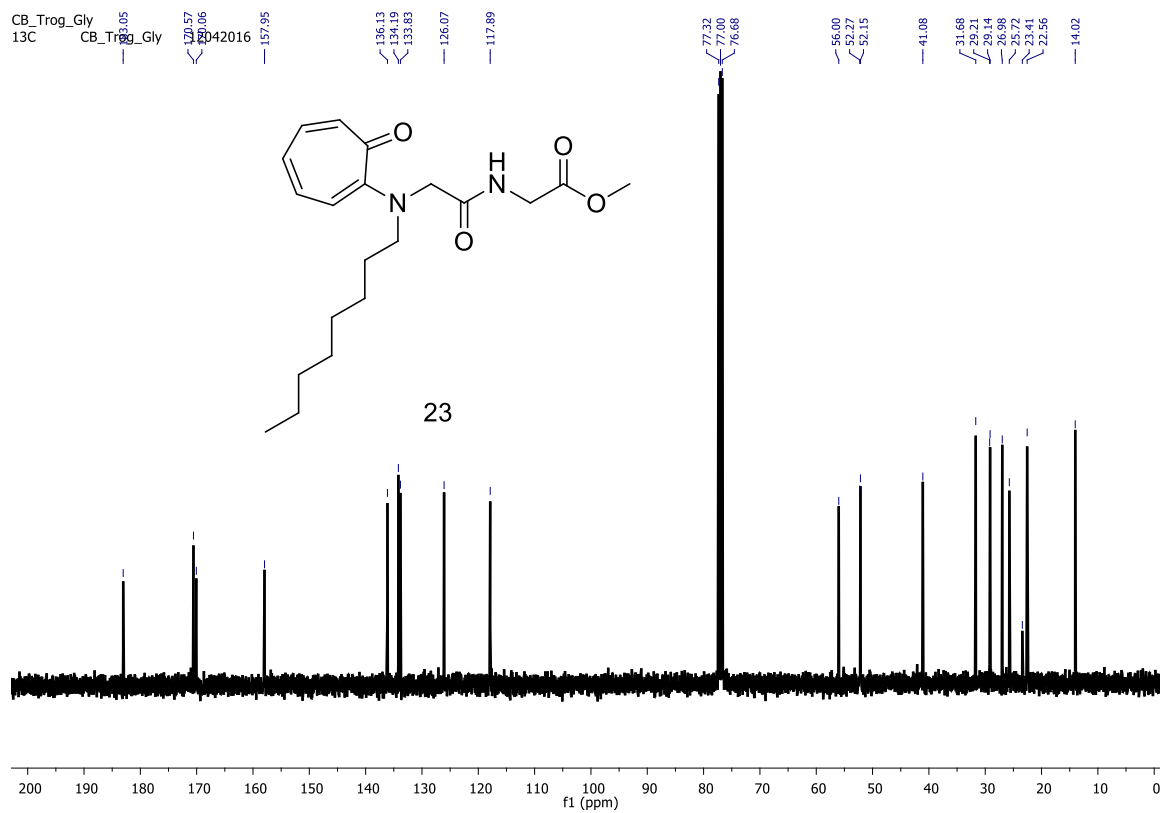


Figure A57. ^{13}C NMR of *Trog-Gly* (**23**) in CDCl_3

Generic Display Report

Analysis Info

Analysis Name D:\Data\AUG-2016\NKS\10082016_NKS_CB_TROGGLY.d
Method Pos_tune_low_nks_LOW.m
Sample Name Bruker micro TOF -Q II
Comment

Acquisition Date 8/10/2016 5:06:26 PM

Operator Amit S.Sahu
Instrument micrOTOF-Q II

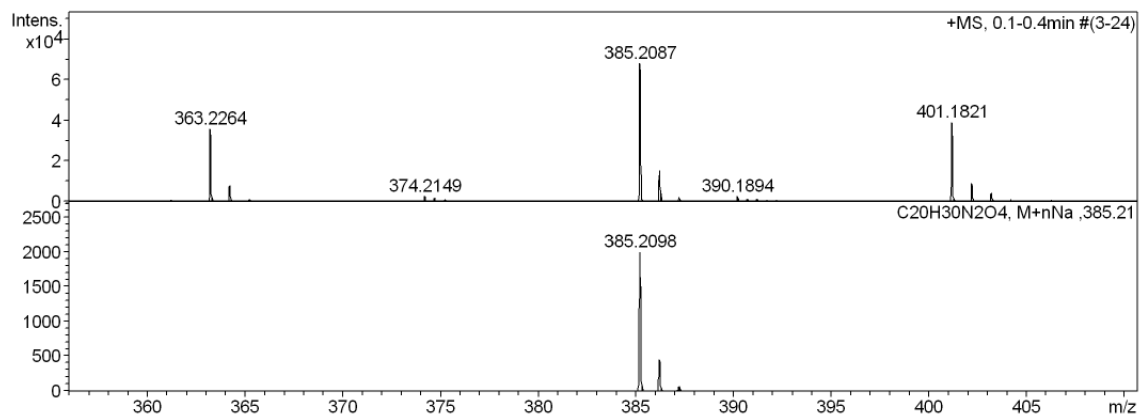
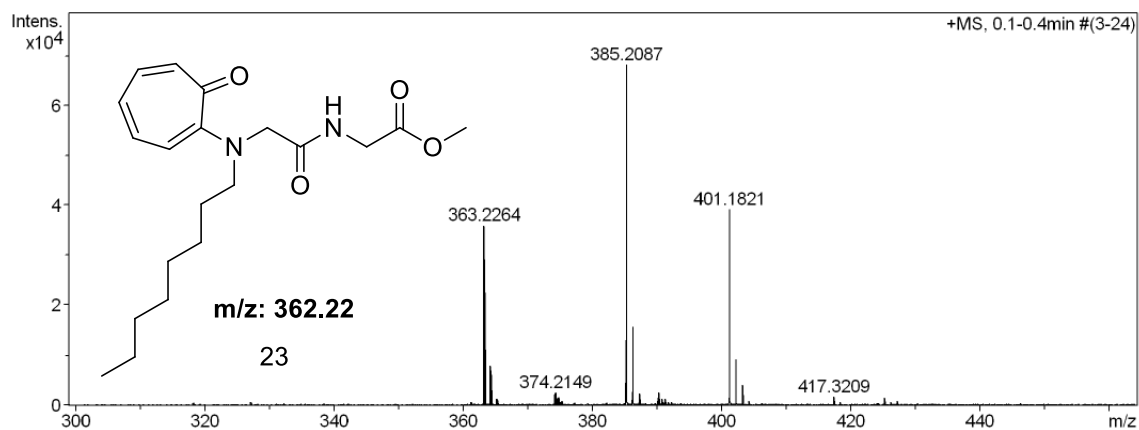
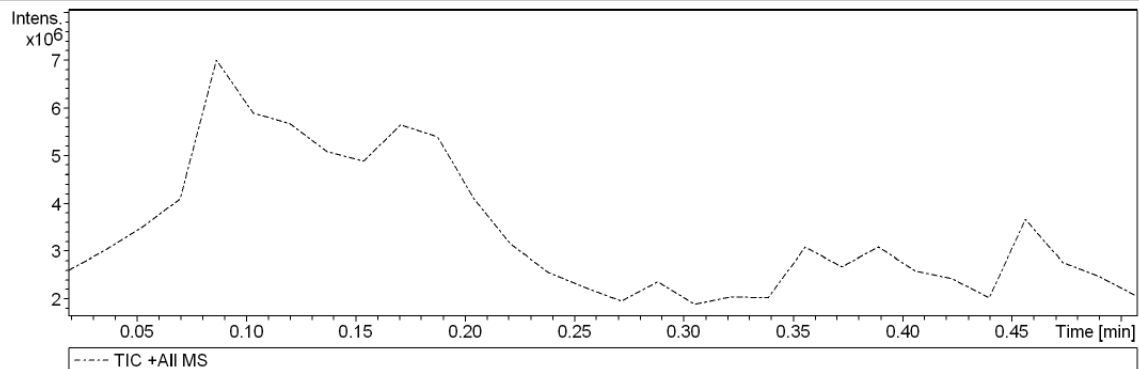
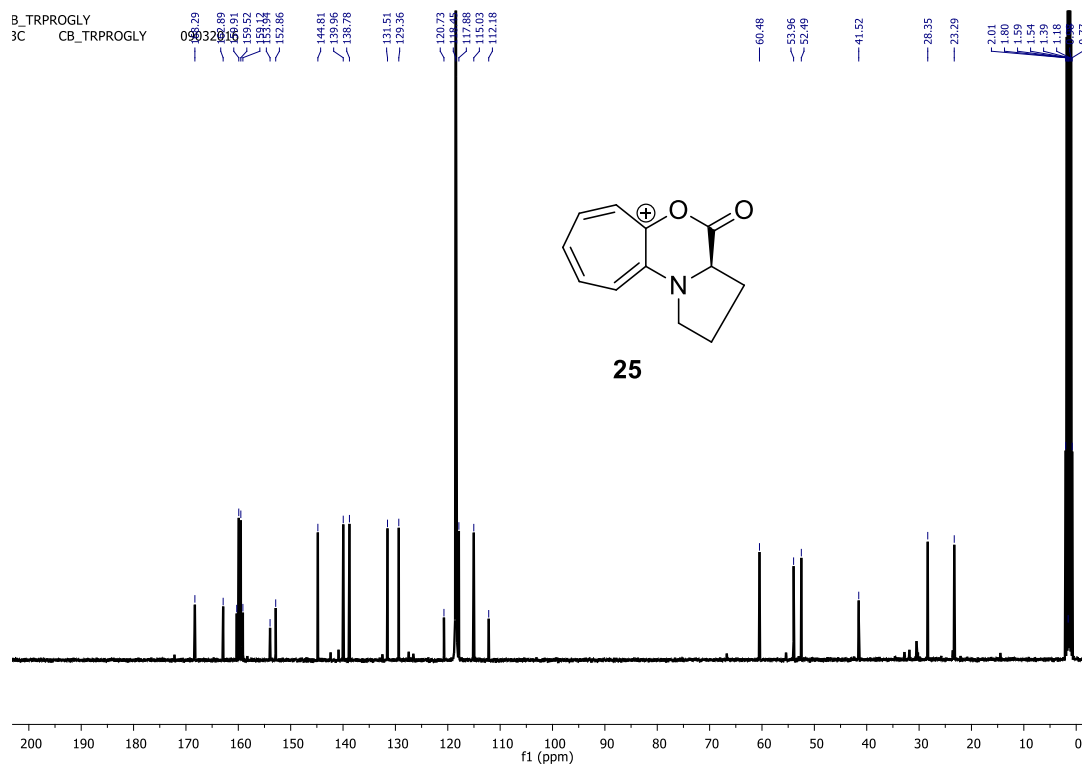
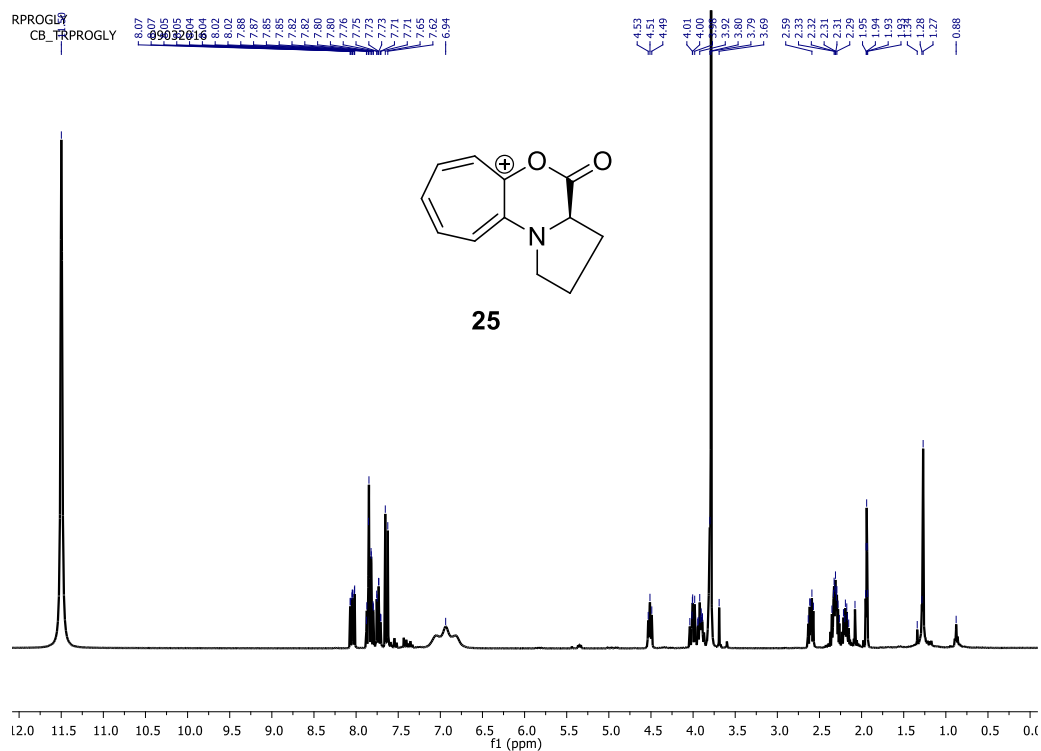


Figure A58. HRMS mass spectrum of *Trog-Gly* (**23**).

18. Characterization data ($^1\text{H}/^{13}\text{C}$ NMR and HRMS) *Trpro* lactone (**25**):



19. HSQC spectra of *Trpro lactone* (**25**):

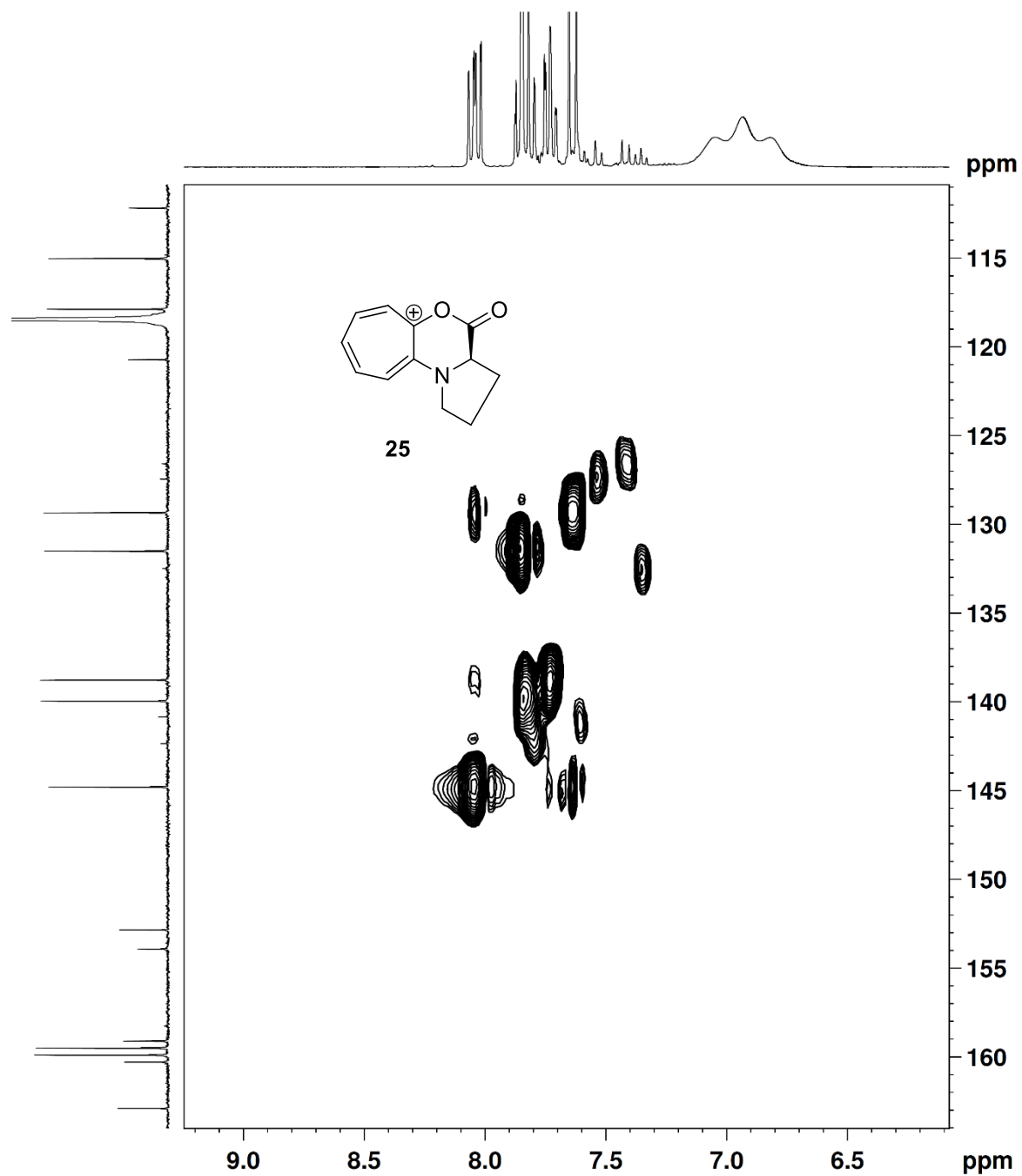


Figure A61. HSQC of *Trpro lactone* (**25**) and Glycine ester in CD_3CN

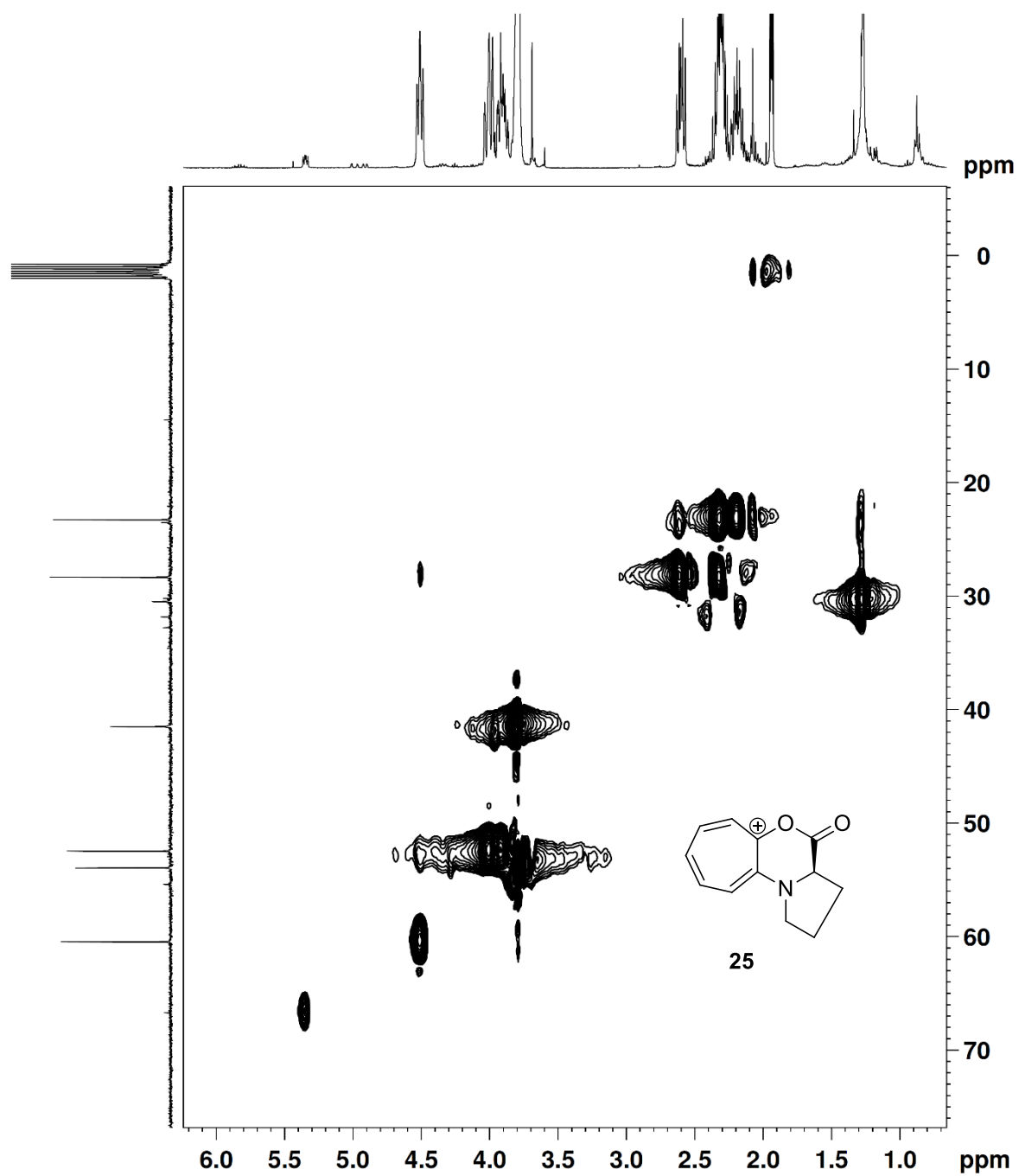


Figure A62. HSQC of *Trpro* lactone (25) and Glycine ester in CD_3CN

Generic Display Report

Analysis Info

Analysis Name D:\Data\AUG-2016\NKS\10082016_NKS_CB_TRPRO_LAC1.d
Method Pos_tune_low_nks_LOW.m
Sample Name Bruker micro TOF -Q II
Comment

Acquisition Date 8/10/2016 7:17:14 PM

Operator Amit S.Sahu
Instrument microTOF-Q II

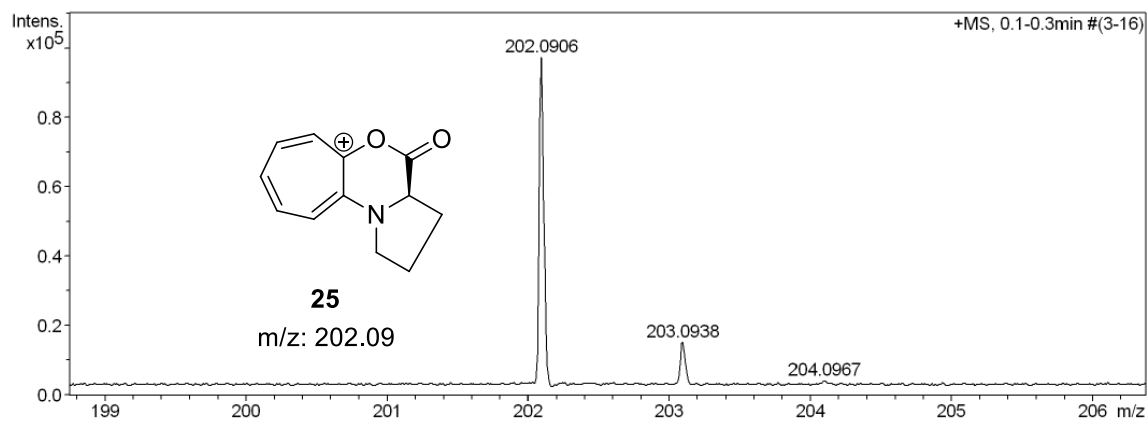
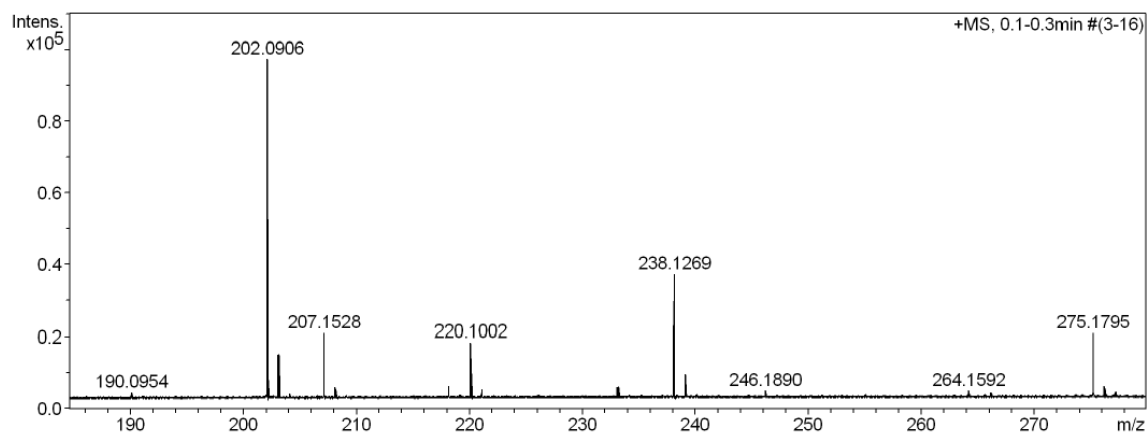
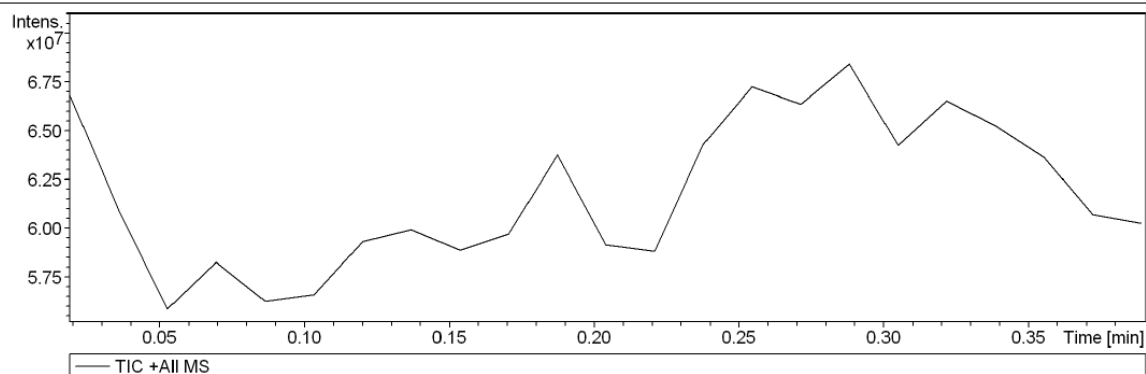


Figure A63. HRMS mass spectrum of *Trpro lactone* (**25**)

20. Monitoring of reversible amidation by $^1\text{H}/^{13}\text{C}$ NMR of *Trpro-Gly* (**9G**):

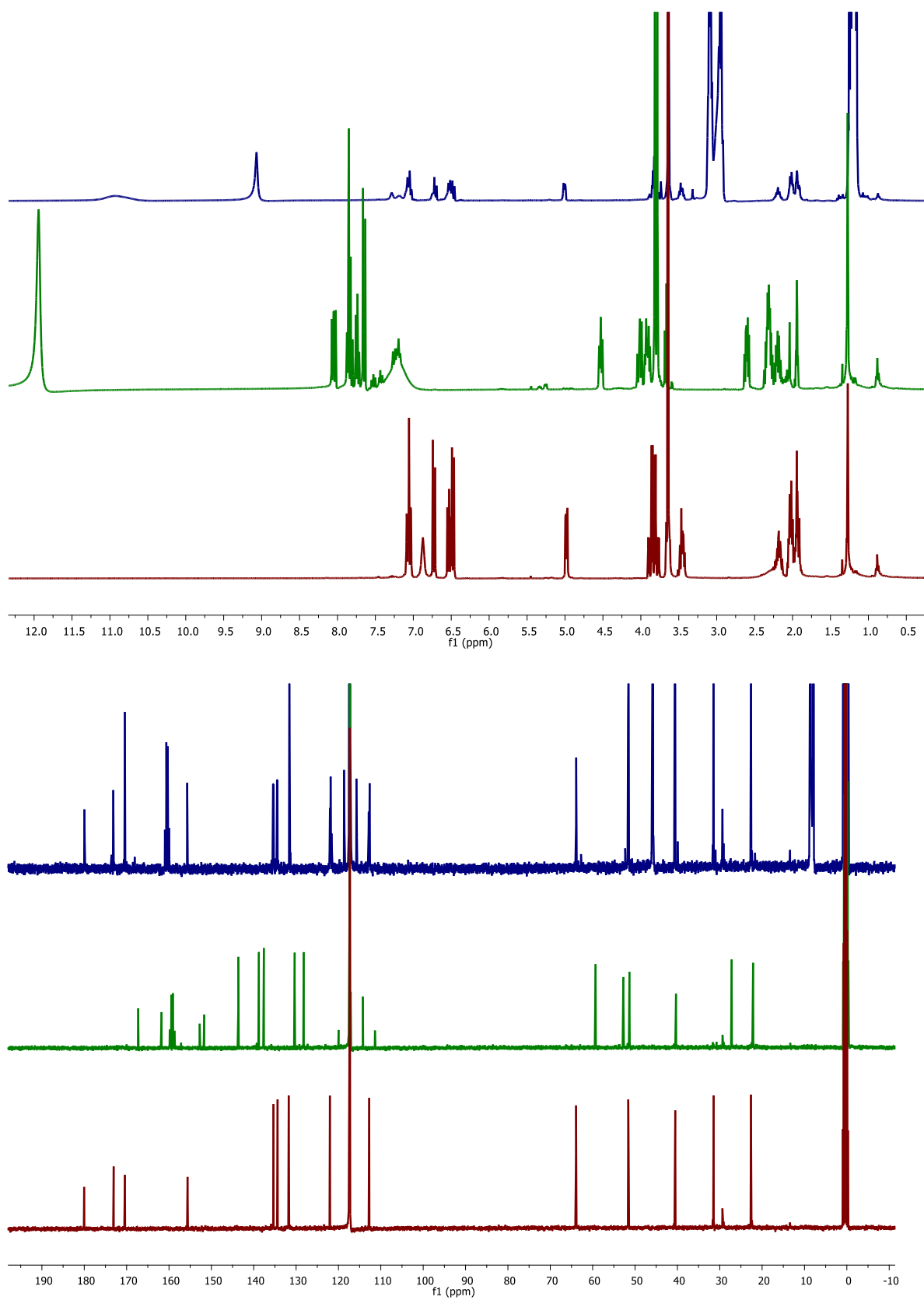


Figure A64. Time dependent NMR $^1\text{H}/^{13}\text{C}$ of *Trpro-Gly* (**9G**) in CD_3CN

21. Characterization data ($^1\text{H}/^{13}\text{C}$ NMR and HRMS) *Trpeg lactone* (**27**):

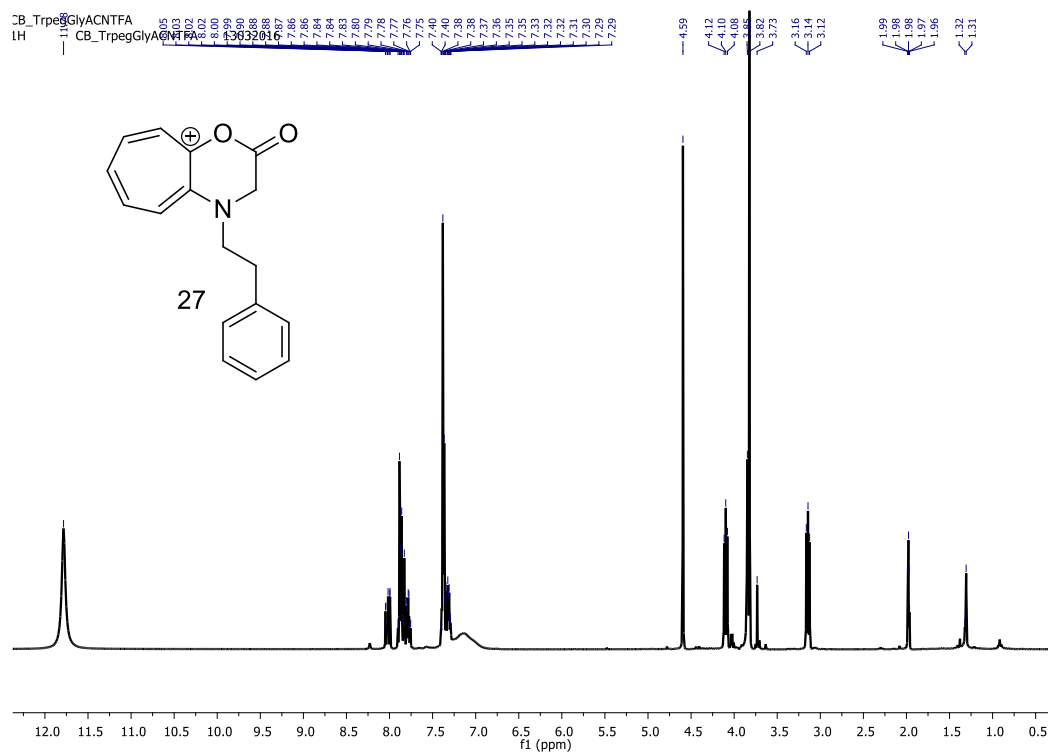


Figure A65. ^1H NMR of *Trpeg lactone* (**27**) and Glycine ester in CD_3CN

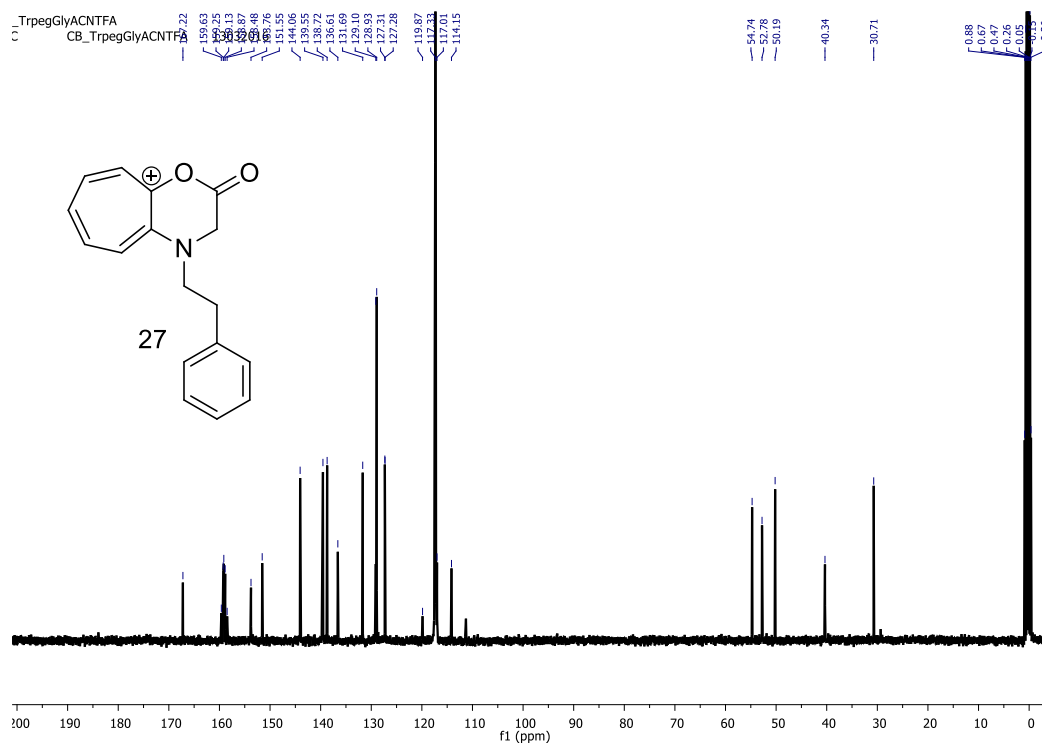


Figure A66. ^{13}C NMR of *Trpeg lactone* (**27**) and Glycine ester in CD_3CN

Generic Display Report

Analysis Info

Analysis Name D:\Data\AUG-2016\NKS\10082016_NKS_CB_TRPEG_LAC.d
Method Pos_tune_low_nks_LOW.m
Sample Name Bruker micro TOF -Q II
Comment

Acquisition Date 8/10/2016 6:57:31 PM

Operator Amit S.Sahu
Instrument microTOF-Q II

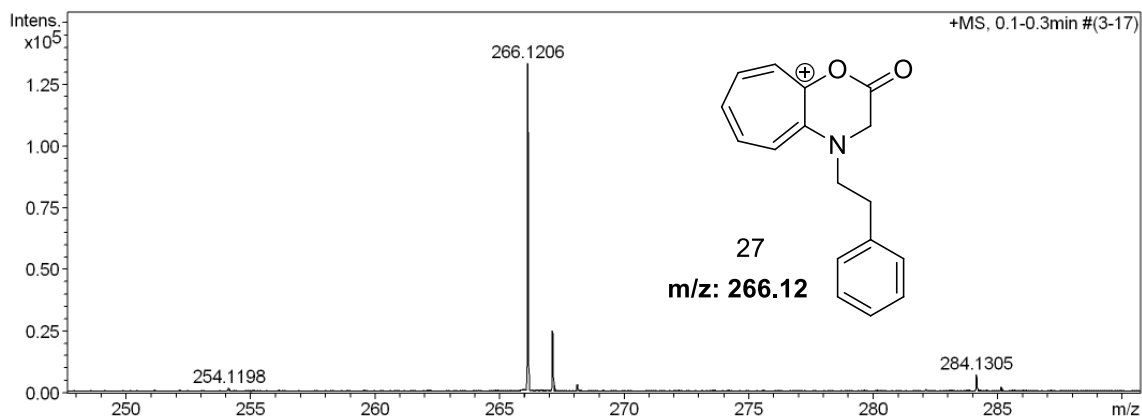
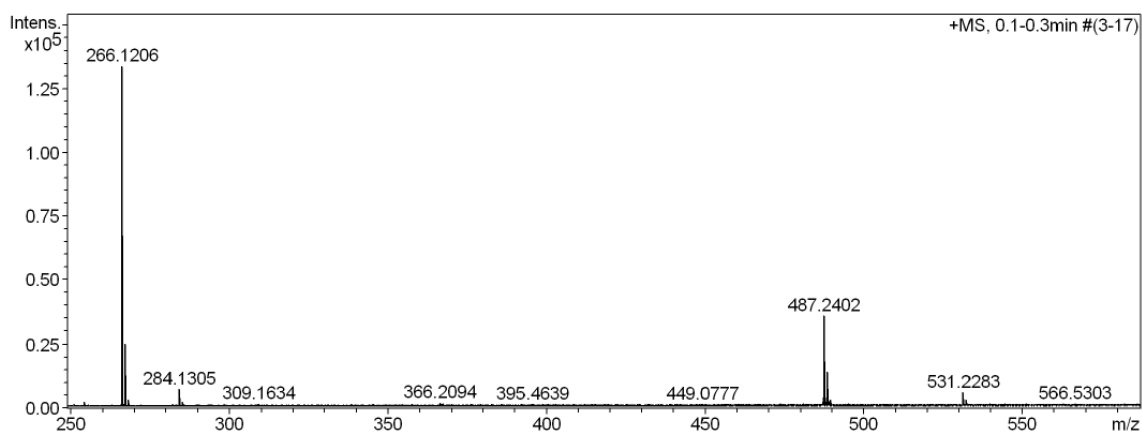
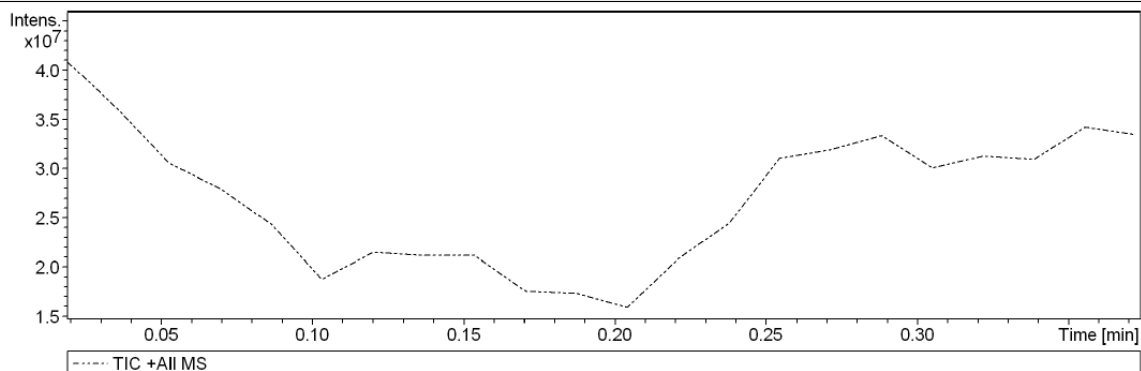


Figure A67. HRMS mass spectrum of *Trpeg lactone* (**27**).

22. Monitoring of reversible amidation by $^1\text{H}/^{13}\text{C}$ NMR of *Trpeg-Gly* (**21**)

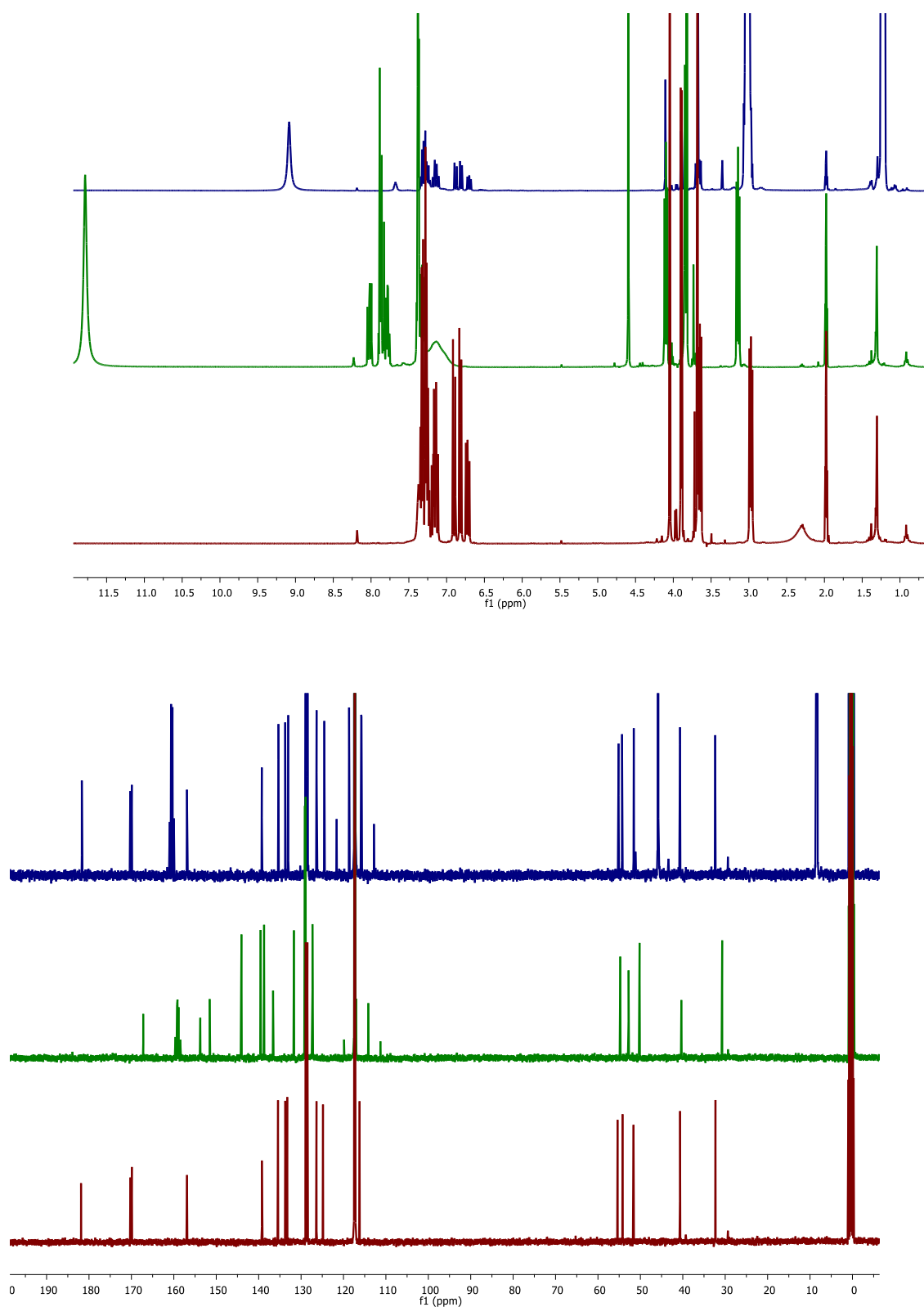


Figure A68. Time dependent NMR $^1\text{H}/^{13}\text{C}$ of *Trpeg-Gly* (**21**) in CD_3CN

23. Characterization data ($^1\text{H}/^{13}\text{C}$ NMR and HRMS) *Trhg lactone* (**26**):

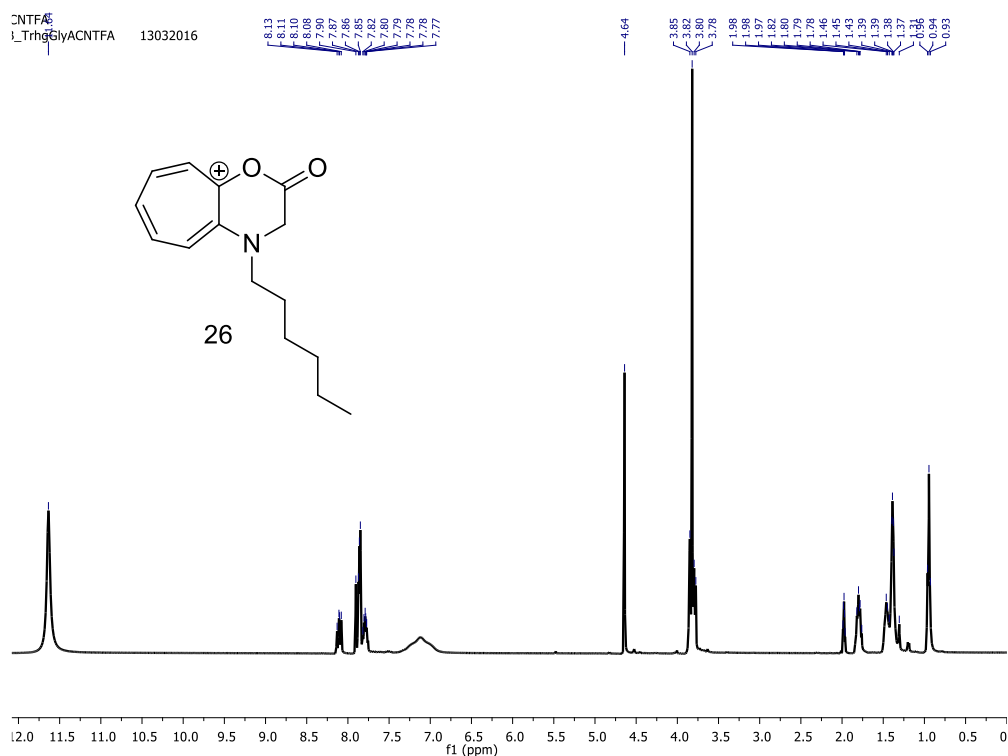


Figure A69. ^1H NMR of *Trhg lactone* (**26**) and Glycine ester in CD₃CN

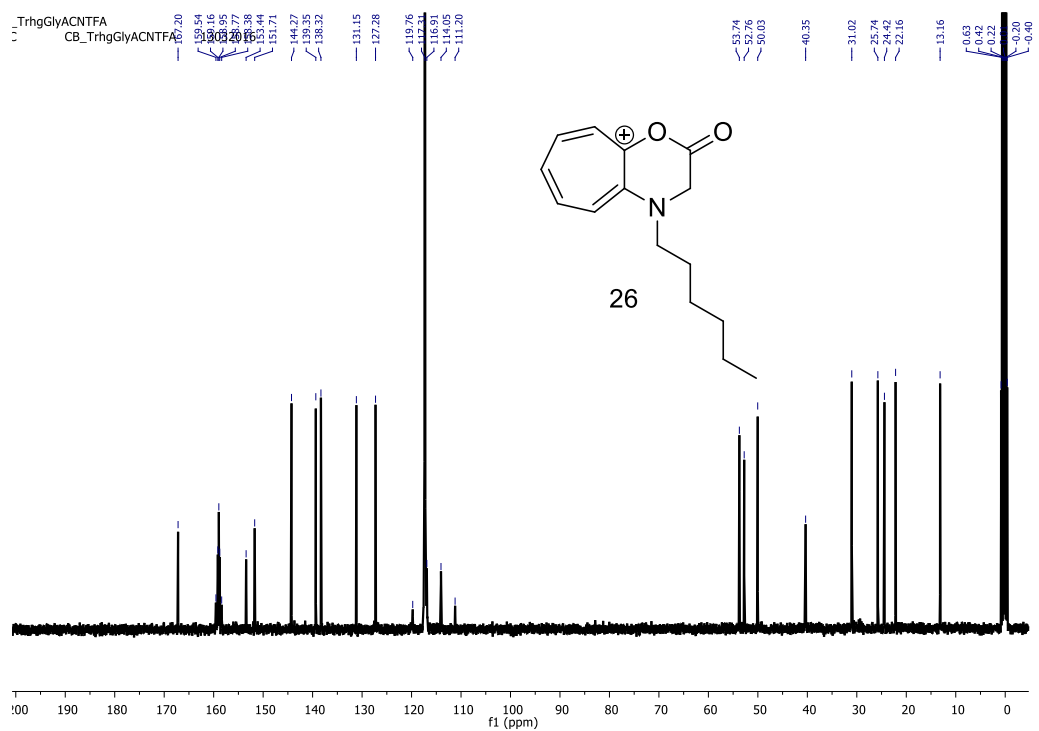


Figure A70. ^{13}C NMR of *Trhg lactone* (**26**) and Glycine ester in CD₃CN

Generic Display Report

Analysis Info

Analysis Name D:\Data\AUG-2016\NKS\10082016_NKS_CB_TRHG_LAC1.d
Method Pos_tune_low_nks_LOW.m
Sample Name Bruker micro TOF -Q II
Comment

Acquisition Date 8/10/2016 7:33:09 PM

Operator Amit S.Sahu
Instrument micrOTOF-Q II

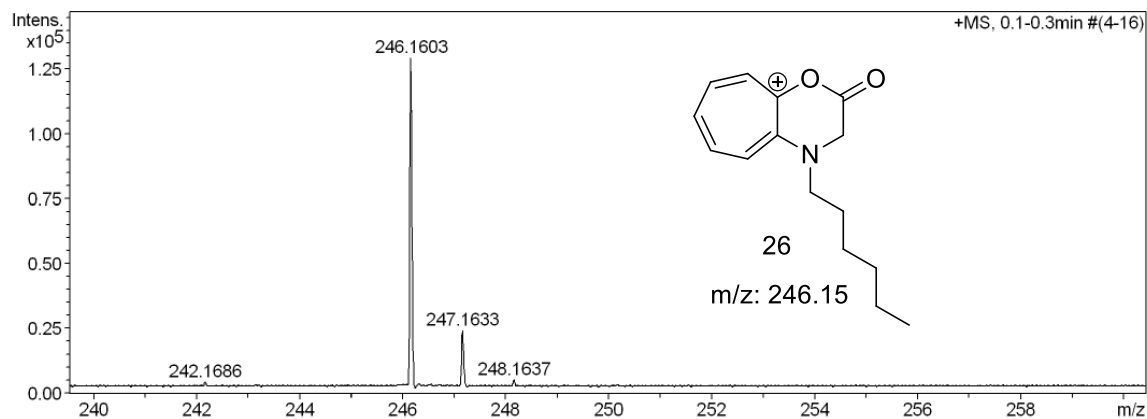
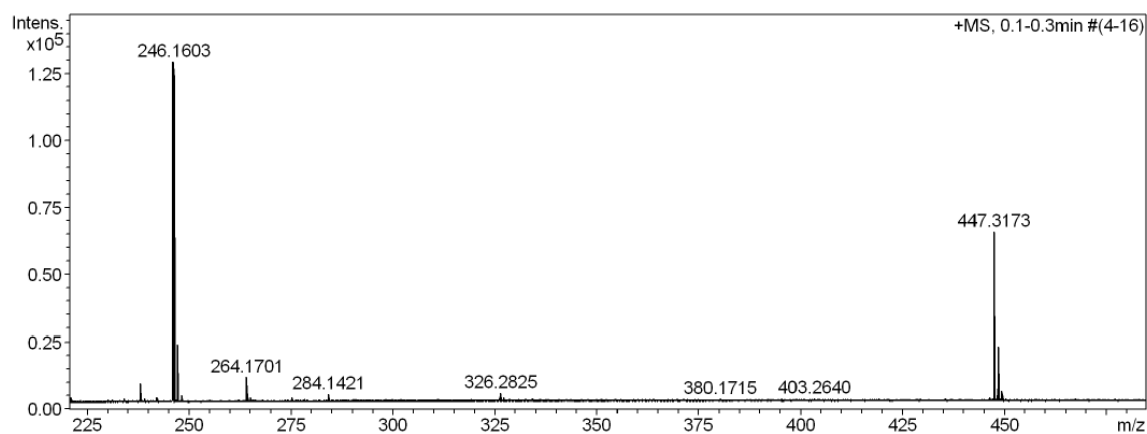
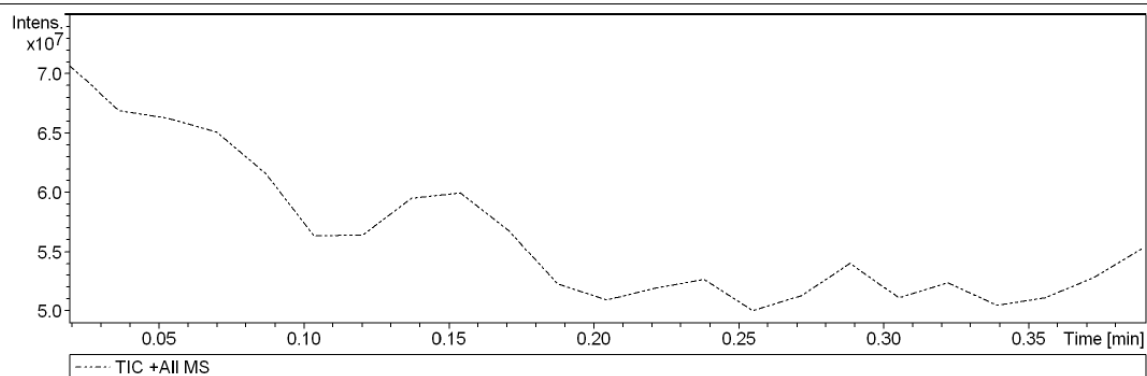


Figure A71. HRMS mass spectrum of *Trhg* lactone (**26**).

24. Monitoring of reversible amidation by $^1\text{H}/^{13}\text{C}$ NMR of *Trhg-Gly* (**19**)

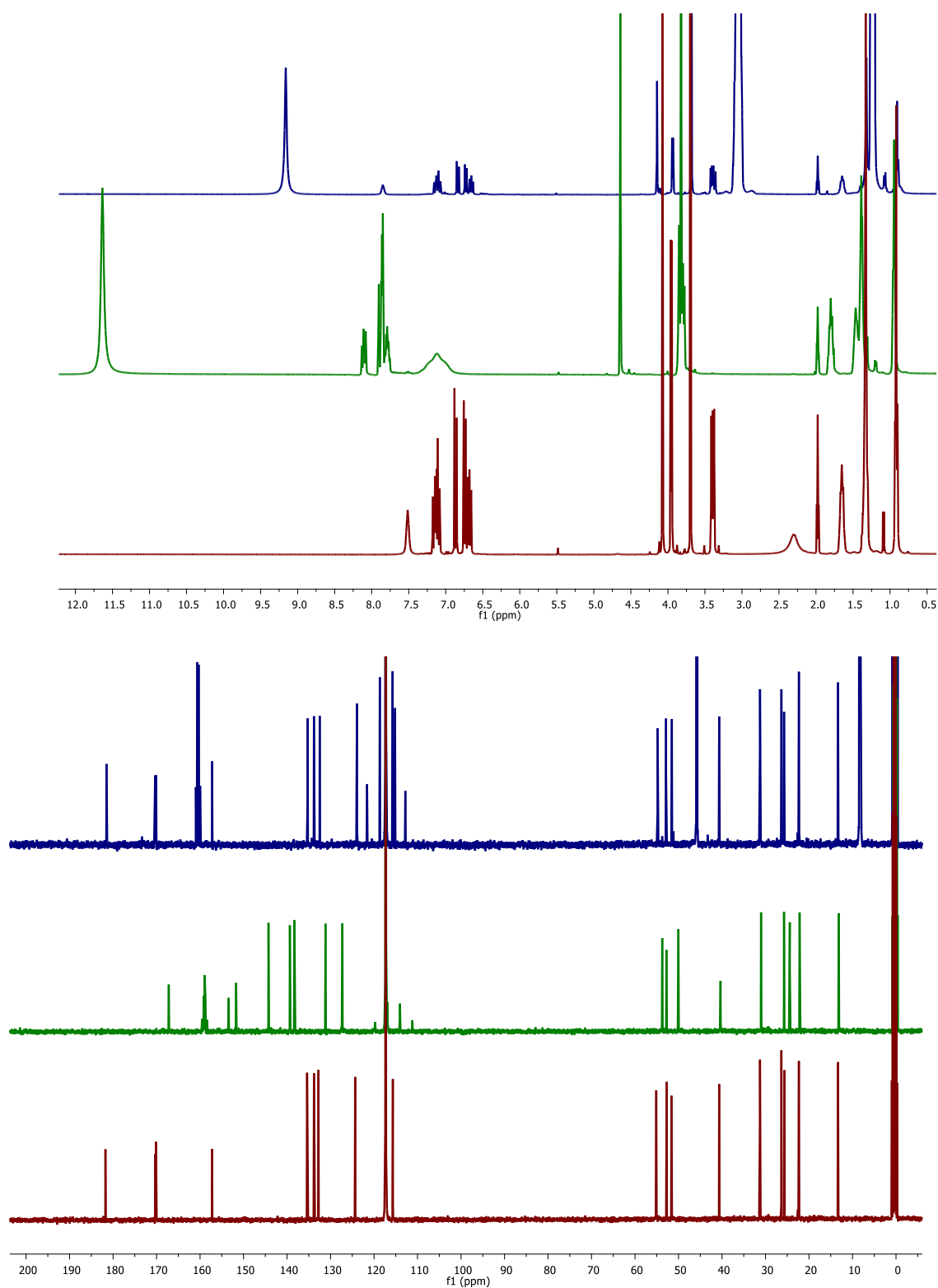


Figure A72. Time dependent NMR $^1\text{H}/^{13}\text{C}$ of *Trhg-Gly* (**19**) in CD_3CN

25. Characterization data ($^1\text{H}/^{13}\text{C}$ NMR and HRMS) *Trog lactone* (**28**):

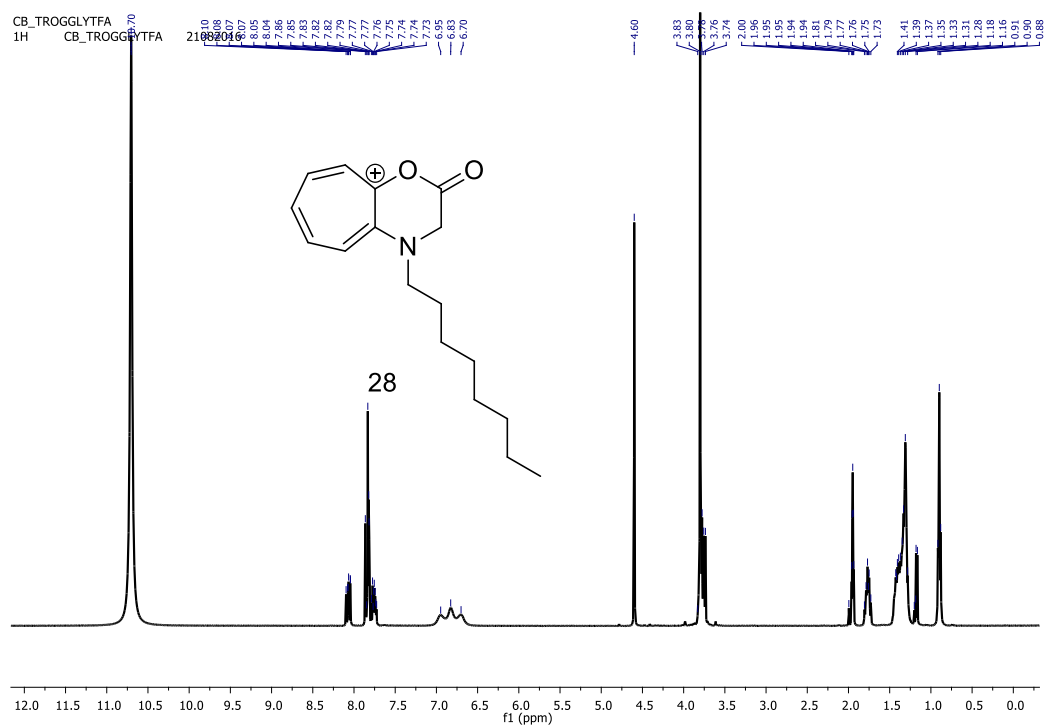


Figure A73. ^1H NMR of *Trog lactone* (**28**) and Glycine ester in CD_3CN

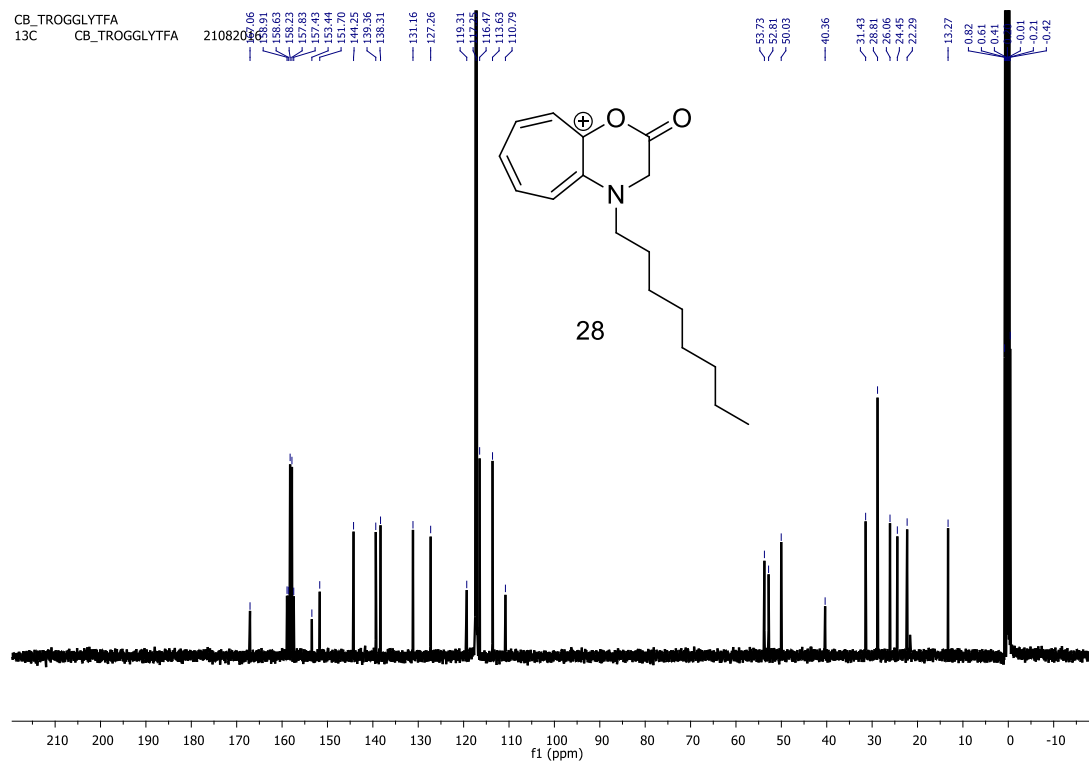


Figure A74. ^{13}C NMR of *Trog* lactone (**28**) and Glycine ester in CD_3CN

Generic Display Report

Analysis Info

Analysis Name D:\Data\AUG-2016\NKS\10082016_NKS_CB_TROG_LAC1.d
Method Pos_tune_low_nks_LOW.m
Sample Name Bruker micro TOF -Q II
Comment

Acquisition Date 8/10/2016 7:48:32 PM

Operator Amit S.Sahu
Instrument micrOTOF-Q II

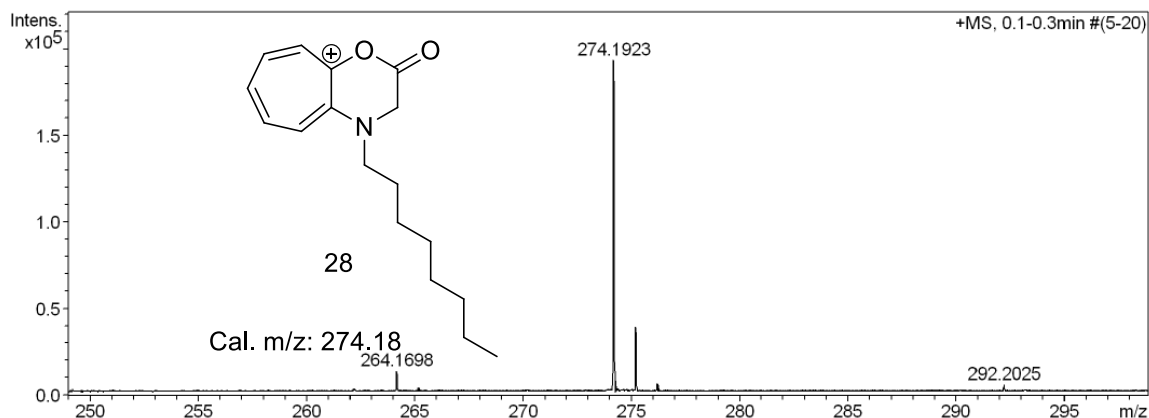
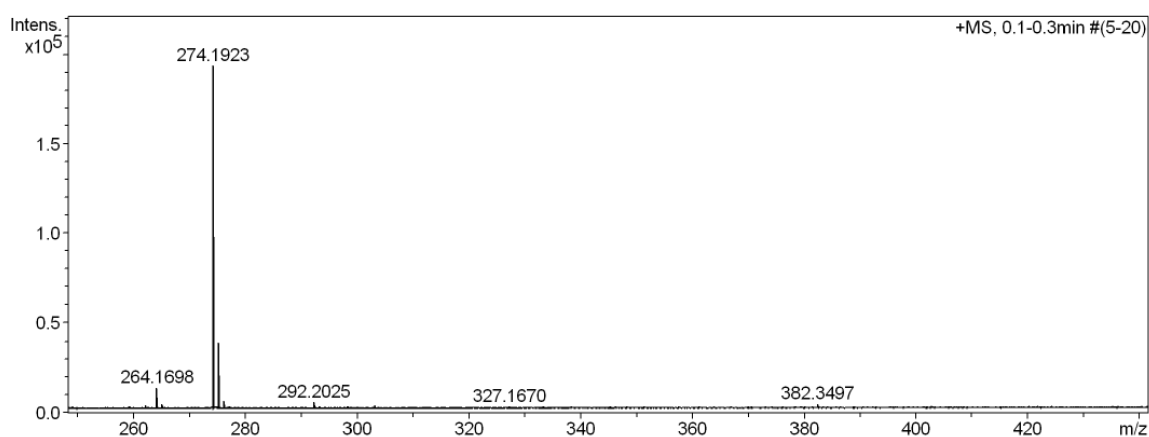
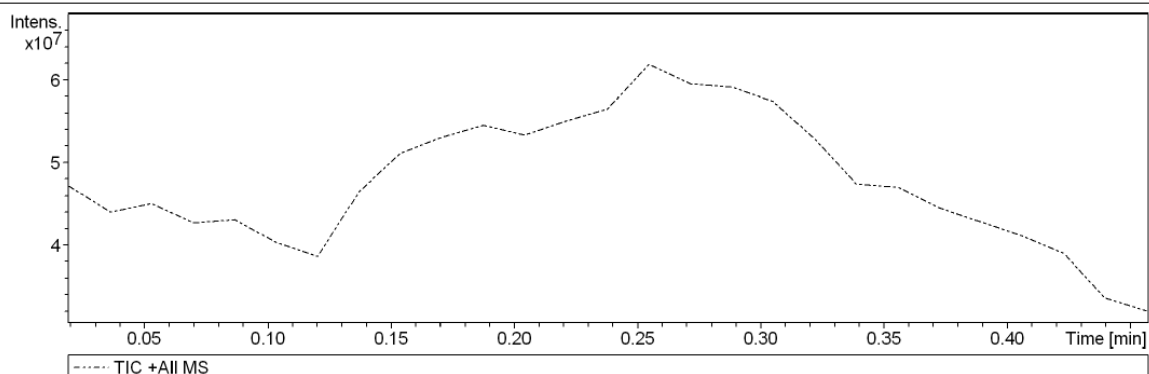


Figure A75. HRMS mass spectrum of *Trog lactone (28)*

26. Monitoring of reversible amidation by $^1\text{H}/^{13}\text{C}$ NMR of Trog-Gly (23):

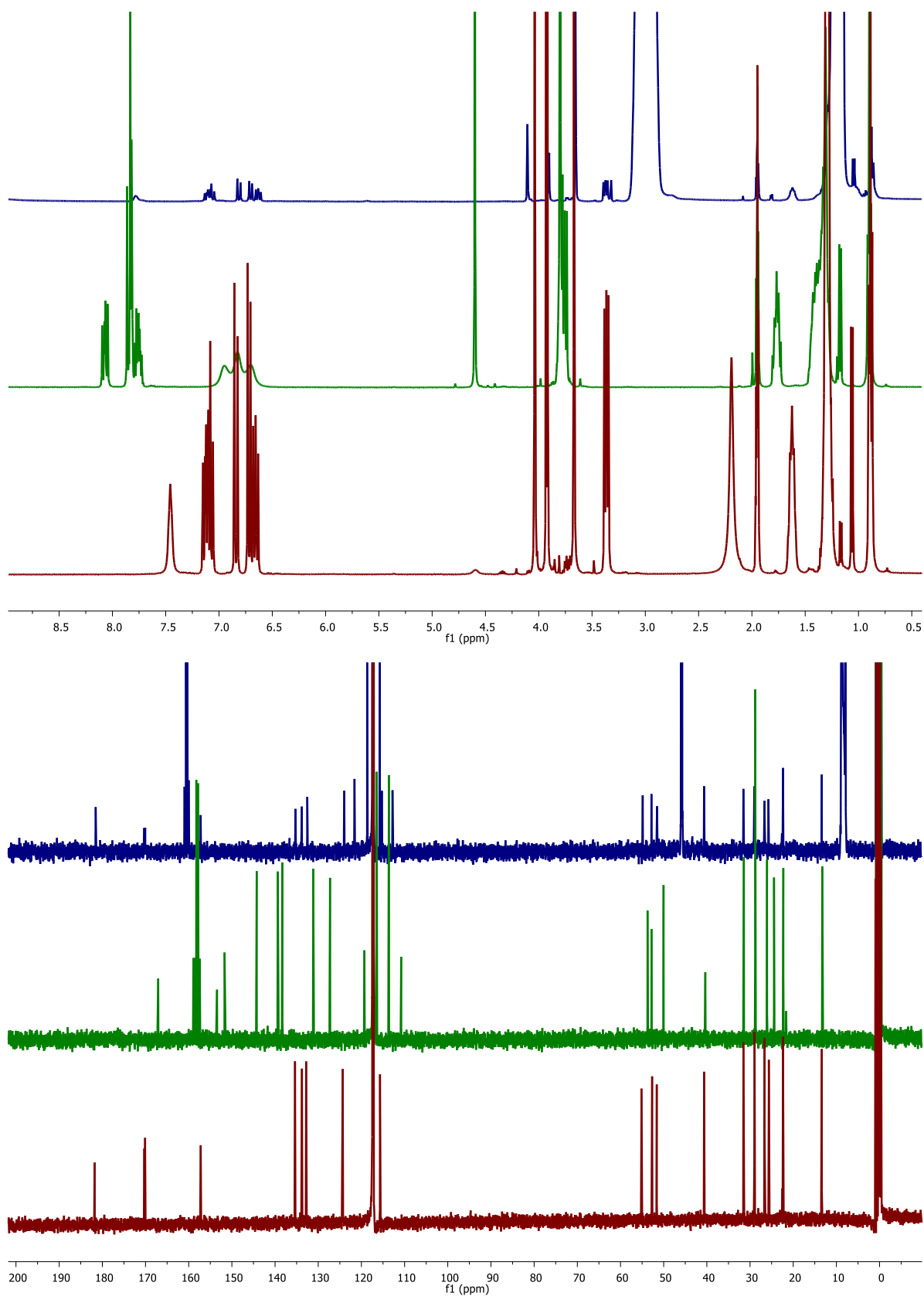


Figure A76. Time dependent NMR $^1\text{H}/^{13}\text{C}$ of Trog-Gly (23) in CD_3CN

27. Characterization data ($^1\text{H}/^{13}\text{C}$ NMR and HRMS) *Trpeg-Farnesol* (**5c**):

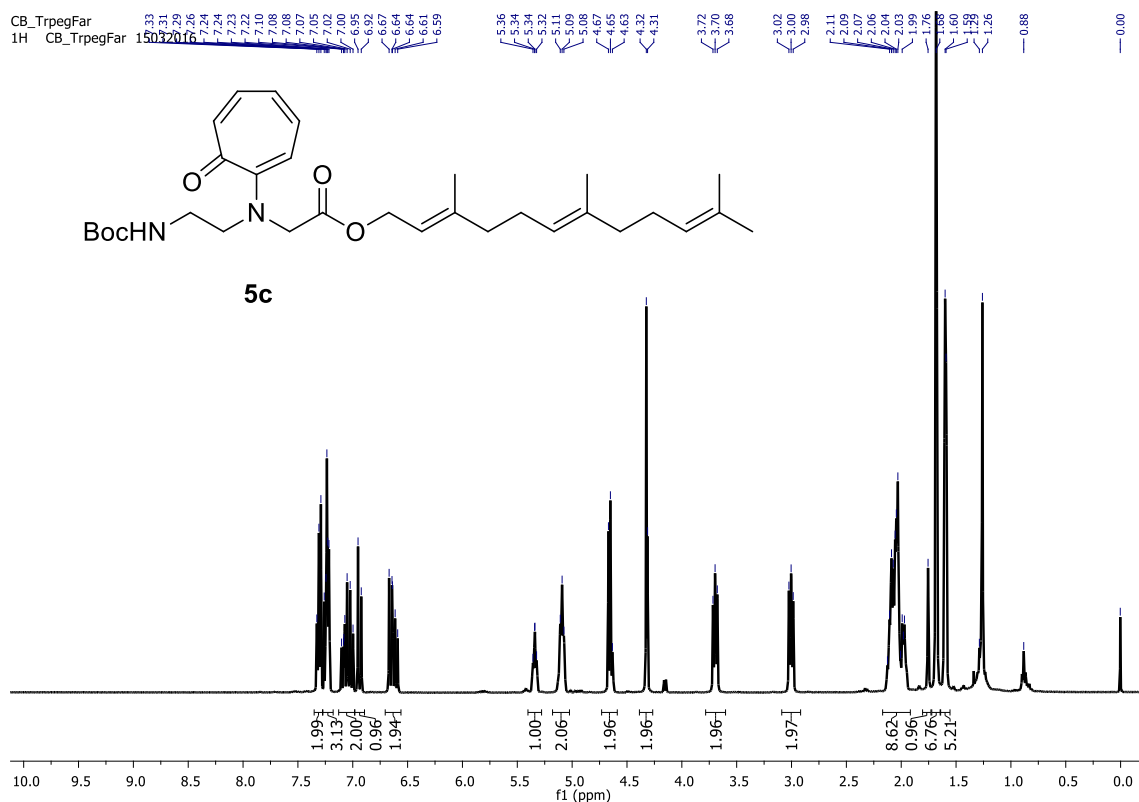


Figure A77. ^1H NMR of *Trpeg-Farnesol* (**5c**) in CDCl_3

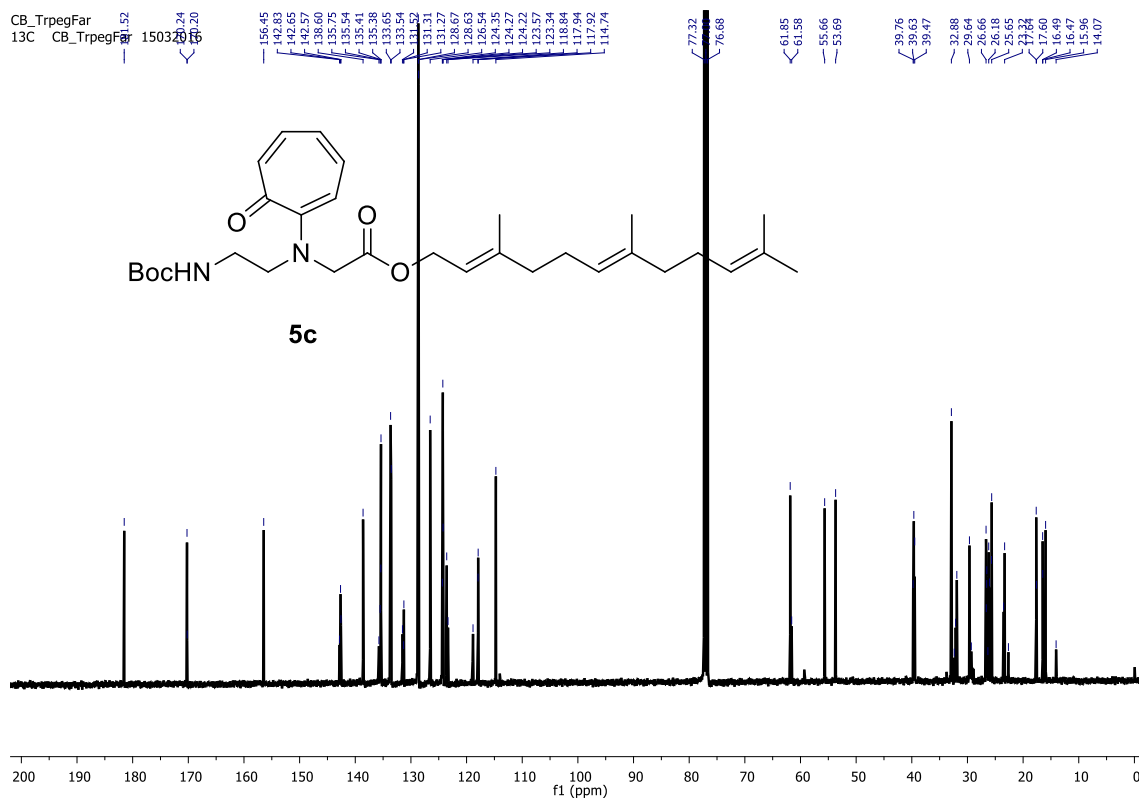


Figure A78. ^{13}C NMR of *Trpeg-Farnesol* (**5c**) in CDCl_3

28. Characterization data ($^1\text{H}/^{13}\text{C}$ NMR and HRMS) *Trpeg-Geraniol* (**5b**):

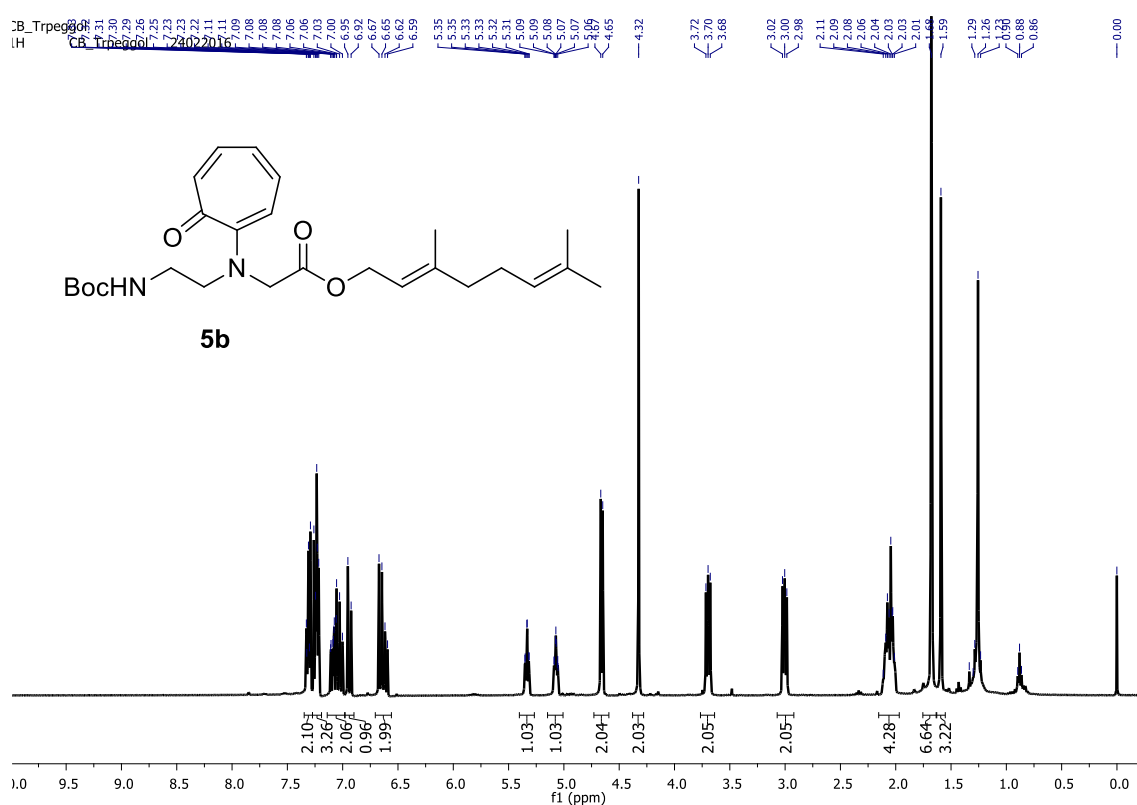


Figure A79. ^1H NMR of *Trpeg-Geraniol* (**5b**) in CDCl_3

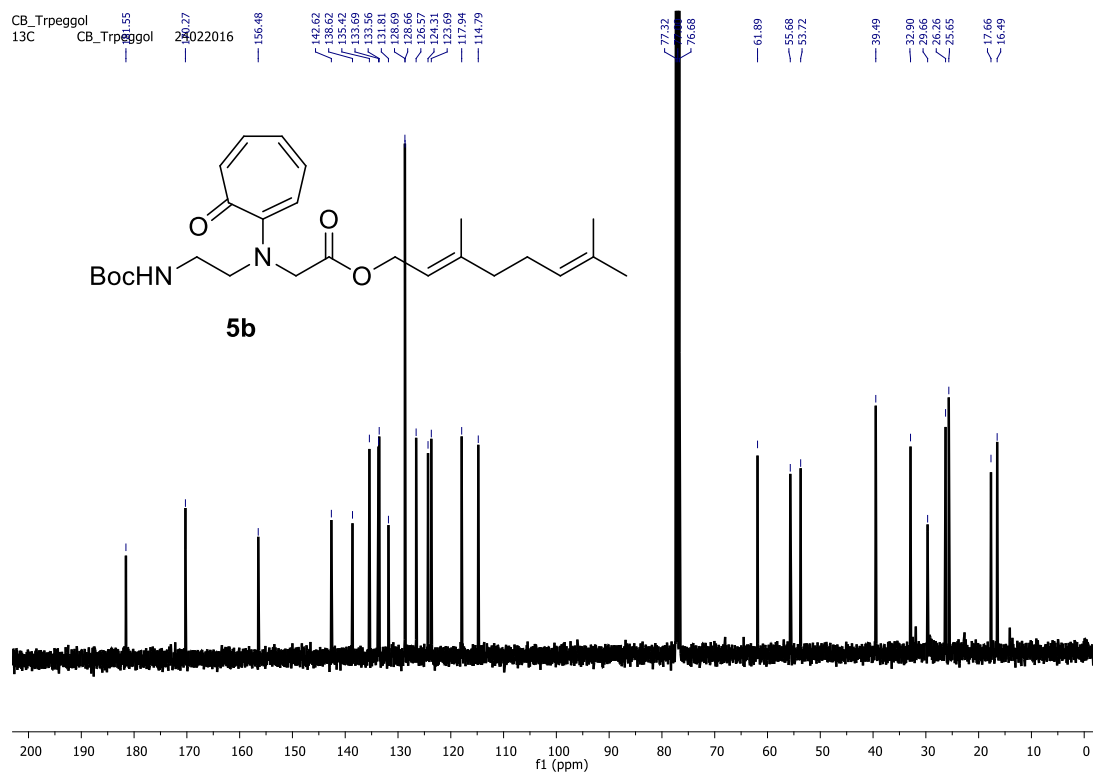


Figure A80. ^{13}C NMR of *Trpeg-Geraniol* (**5b**) in CDCl_3

29. Characterization data ($^1\text{H}/^{13}\text{C}$ NMR and HRMS) *Traeg-Benzyl amine* (**13i**):

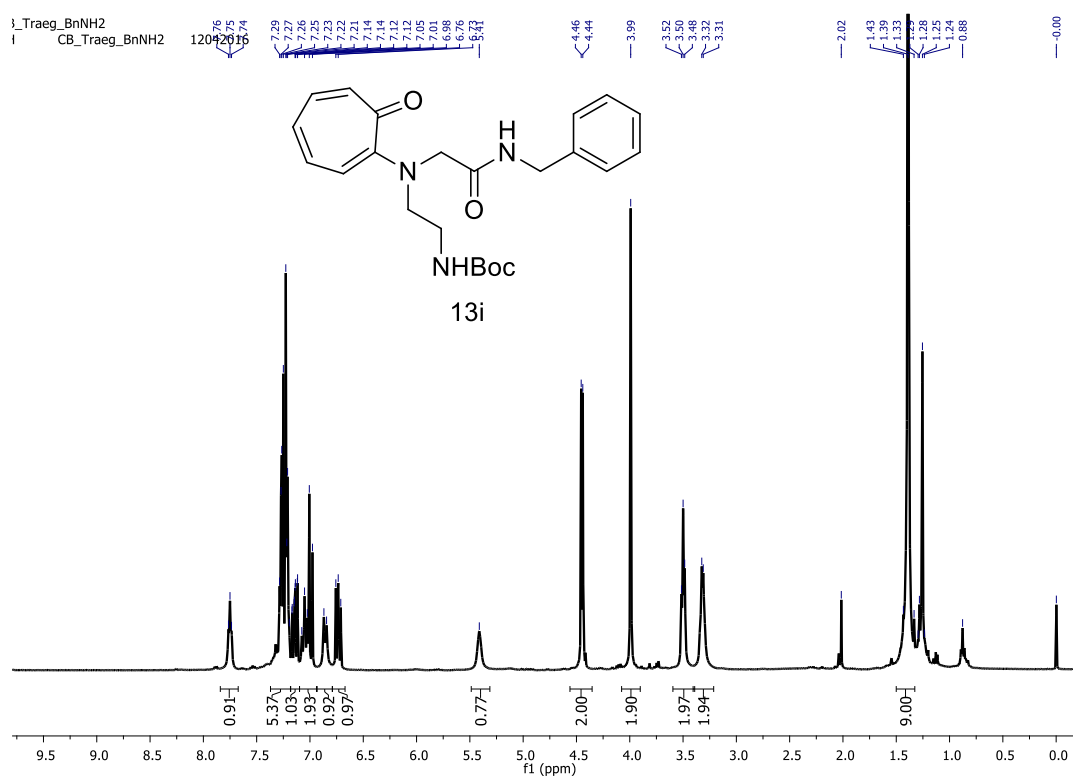


Figure A81. ^1H NMR of *Traeg-Benzyl amine* (**13i**) in CDCl_3

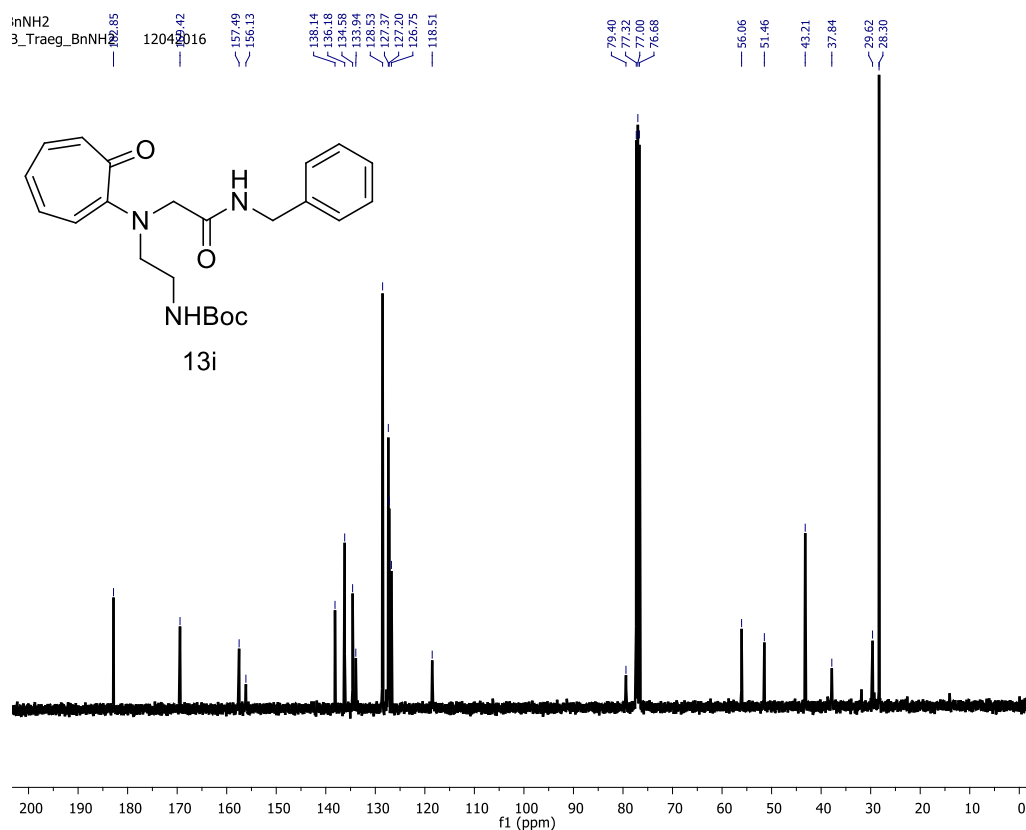


Figure A82. ^{13}C NMR of *Traeg-Benzyl amine* (**13i**) in CDCl_3

30. NMR ($^1\text{H}/^{13}\text{C}$) and HRMS spectra of control monomer **8-OEt**:

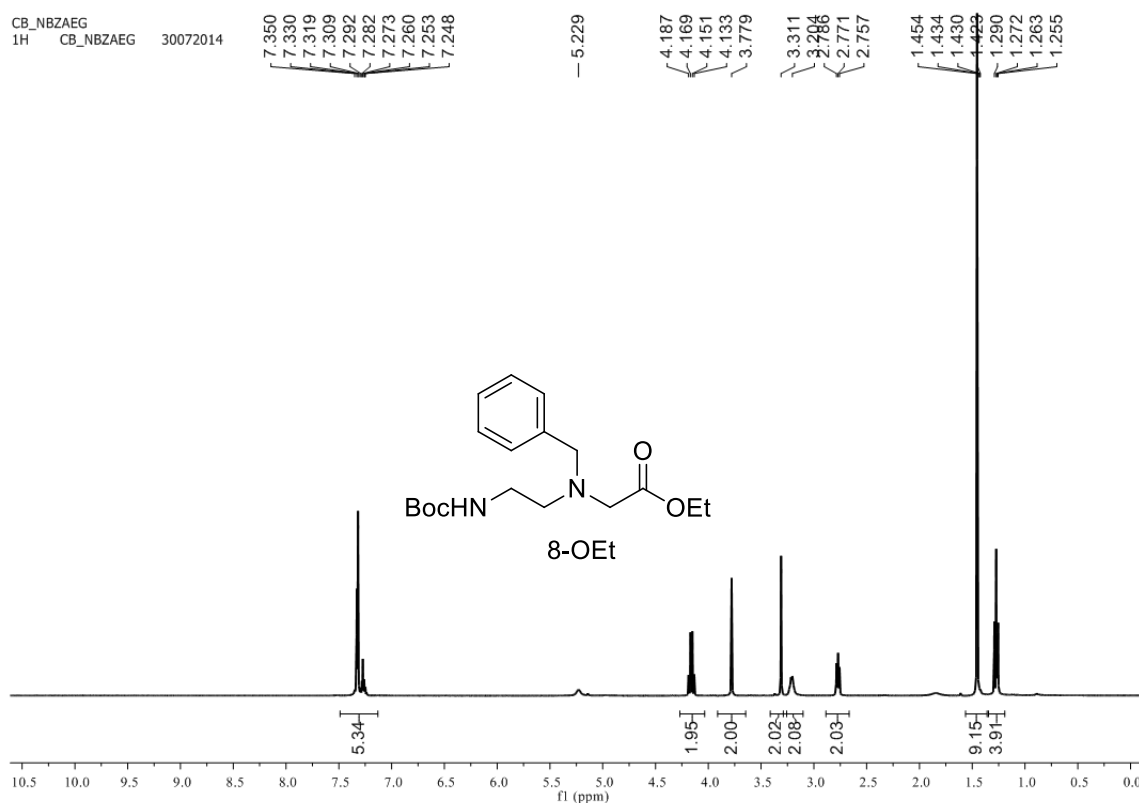


Figure A83. ^1H NMR spectrum of *BocNH-Bnaeg-OEt* (**8-OEt**) in CDCl_3

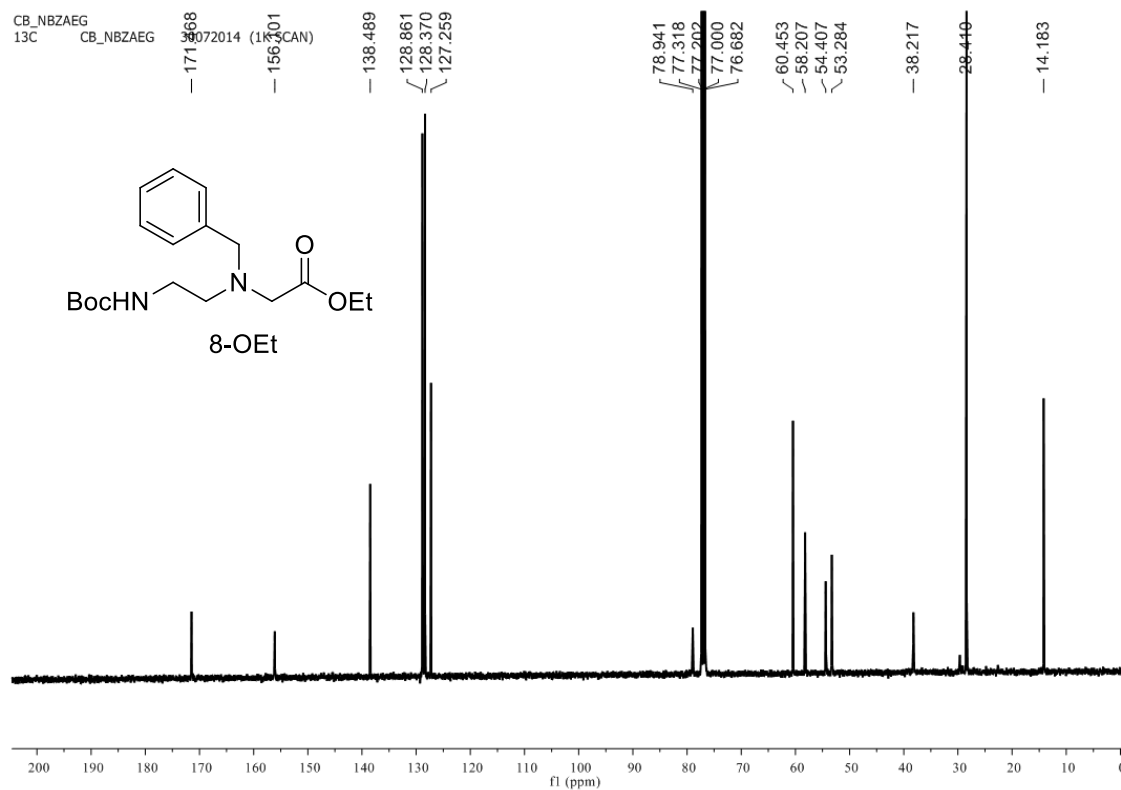


Figure A84. ^{13}C NMR spectrum of *BocNH-Bnaeg-OEt* (**8-OEt**) in CDCl_3

Generic Display Report

Analysis Info

Analysis Name D:\Data\AUG-2014\NKS\14082014_NKS_CB_NB_ZAEG.d
Method Pos_tune_low.m
Sample Name
Comment

Acquisition Date 8/14/2014 4:56:28 PM

Operator A.S.Sahu
Instrument micrOTOF-Q II

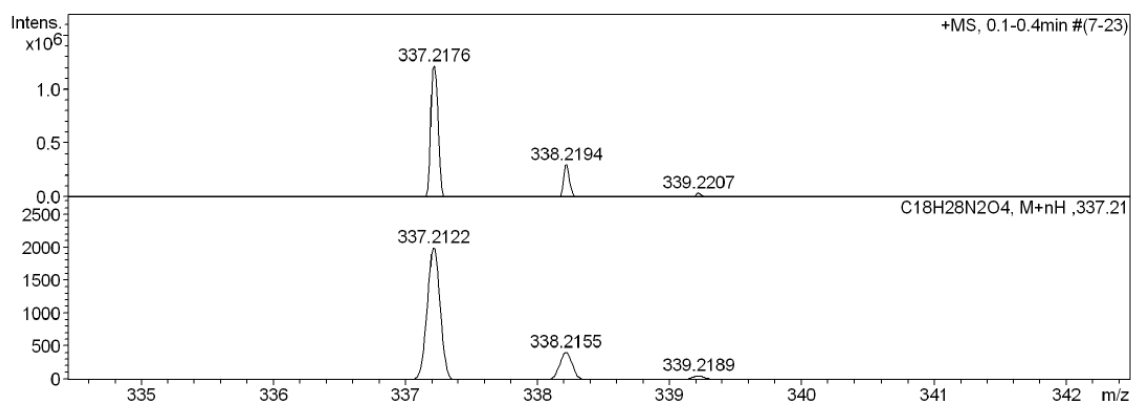
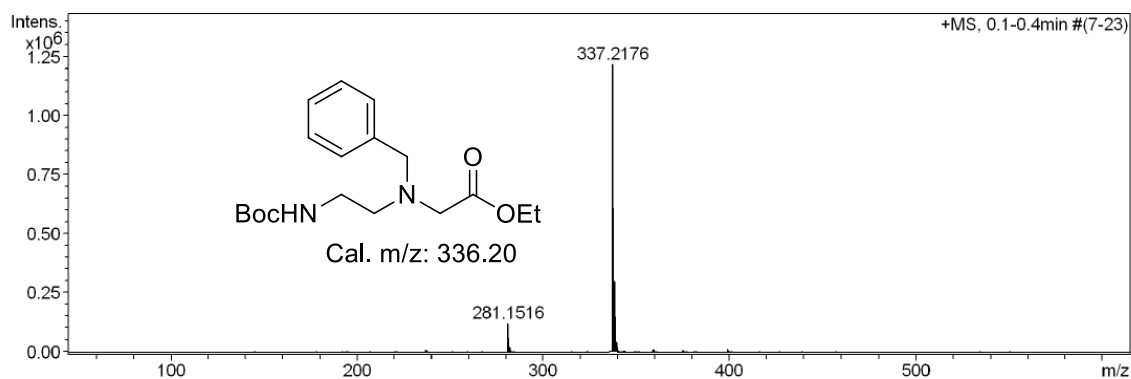
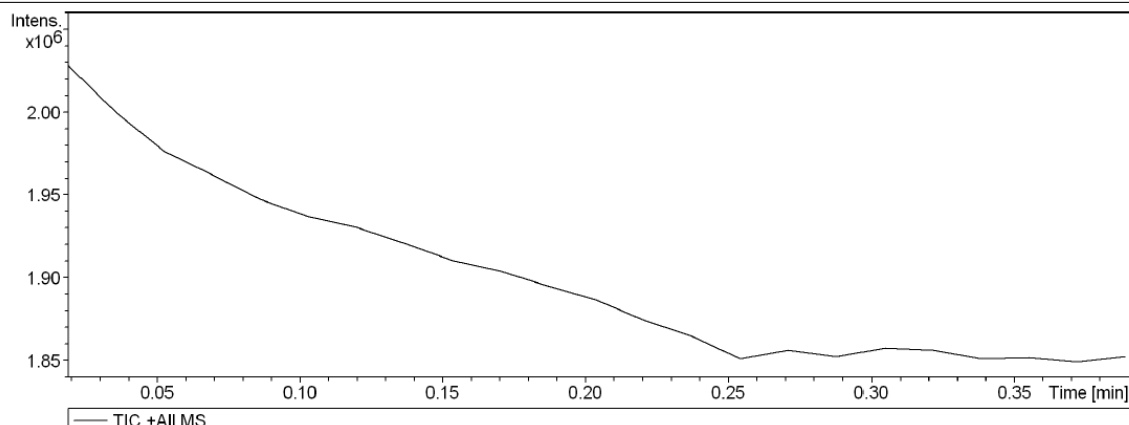


Figure A85. HRMS mass spectrum of *BocNH-Bnaeg-OEt* **8-OEt**

31. Characterization data ($^1\text{H}/^{13}\text{C}$ NMR and HRMS), Time dependent NMR and Mass spectrum after time dependent NMR of *BocNH-Bnaeg-Phe-OMe* (**16**)

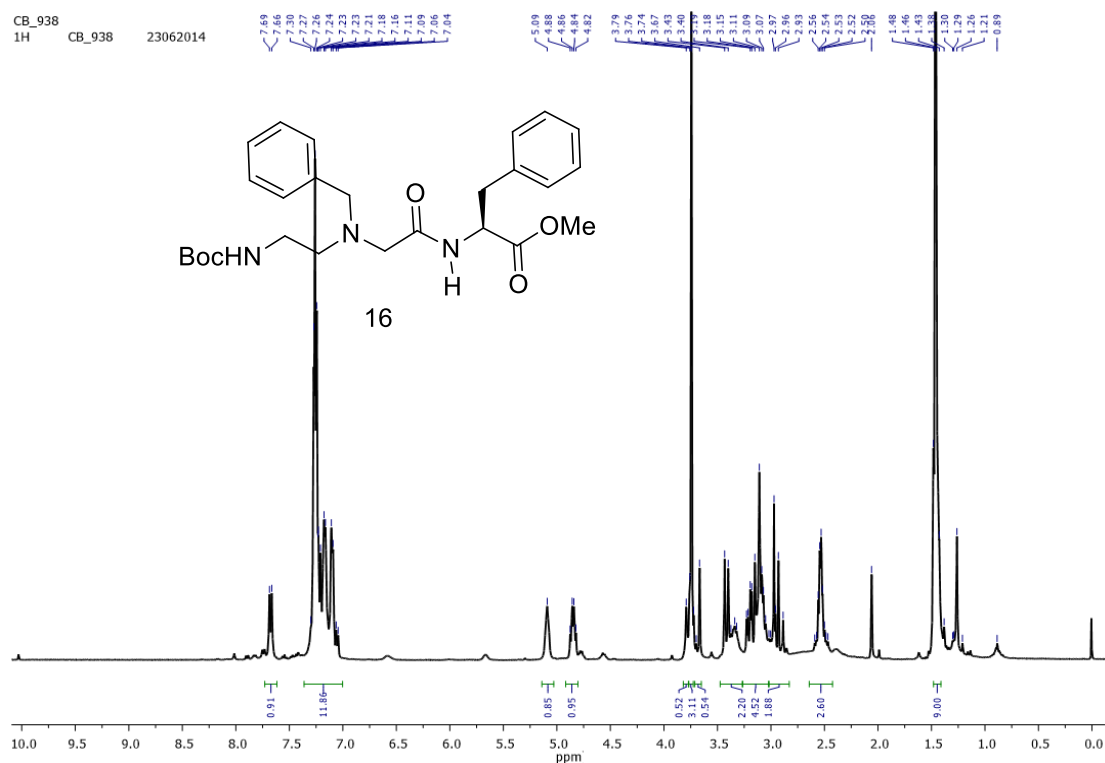


Figure A86. ^1H NMR spectrum of *BocNH-Bnaeg-Phe-OMe* (**16**) in CDCl₃

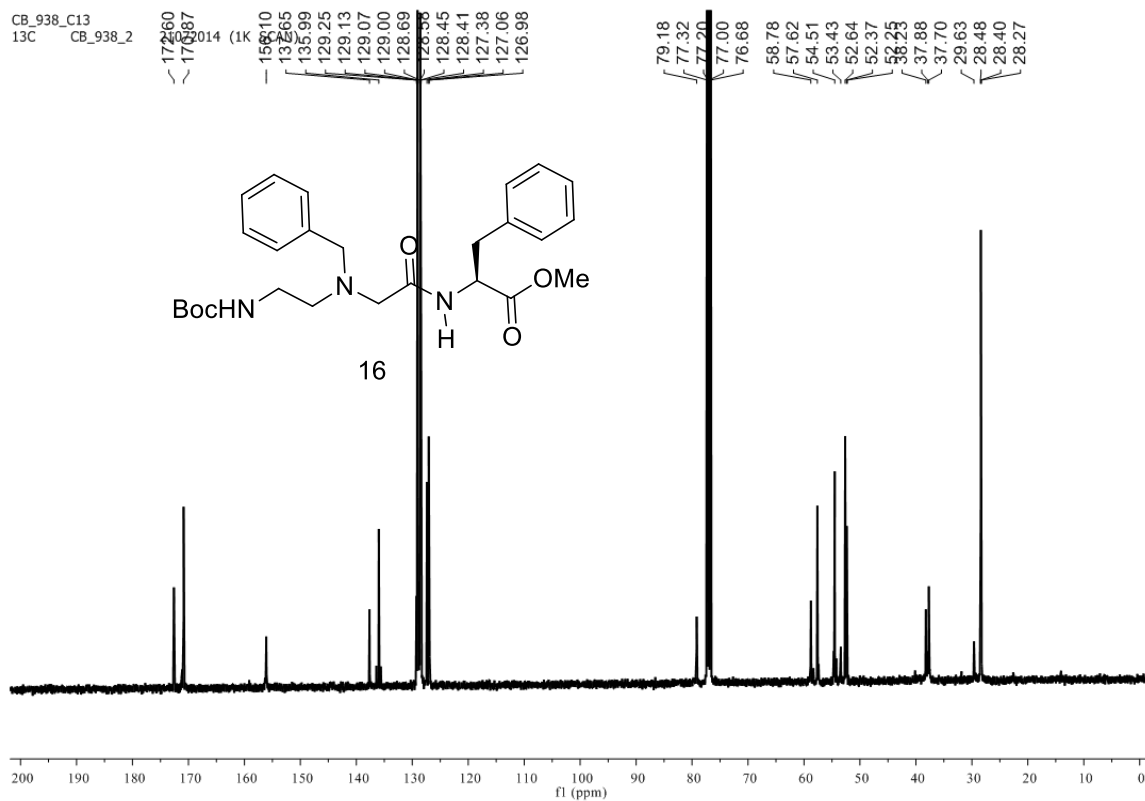


Figure A87. ^{13}C NMR spectrum of *BocNH-Bnaeg-Phe-OMe* (**16**) in CDCl₃

Generic Display Report

Analysis Info

Analysis Name D:\Data\AUG2014\NKS\14082014_NKS_CB_938.d
Method Pos_tune_low.m
Sample Name
Comment

Acquisition Date 8/14/2014 11:47:53 AM

Operator A.S.Sahu
Instrument micrOTOF-Q II

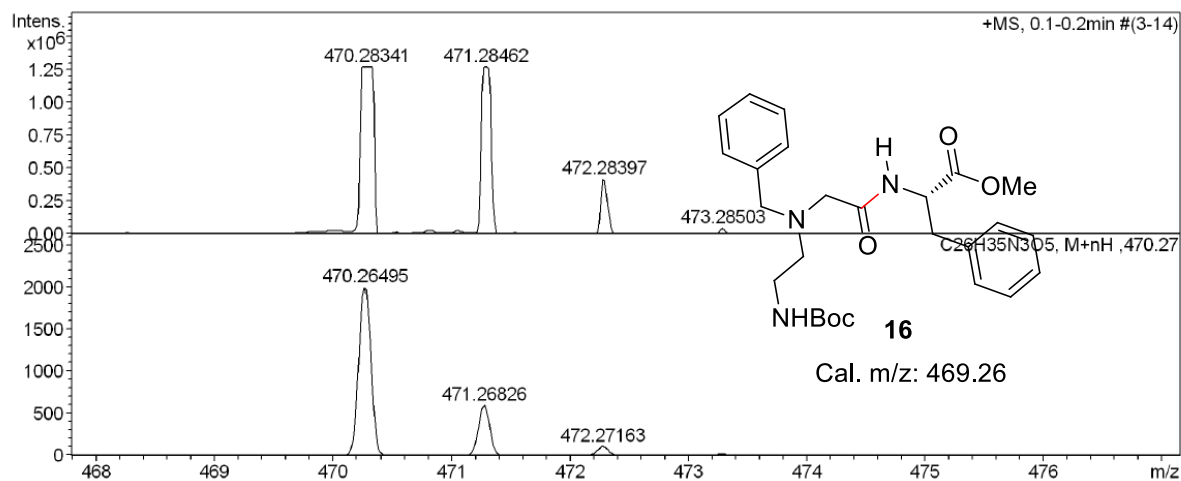
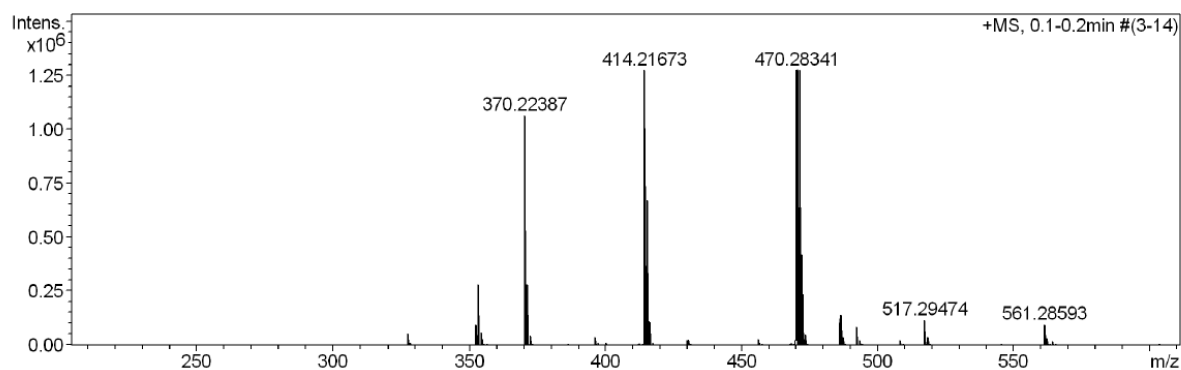
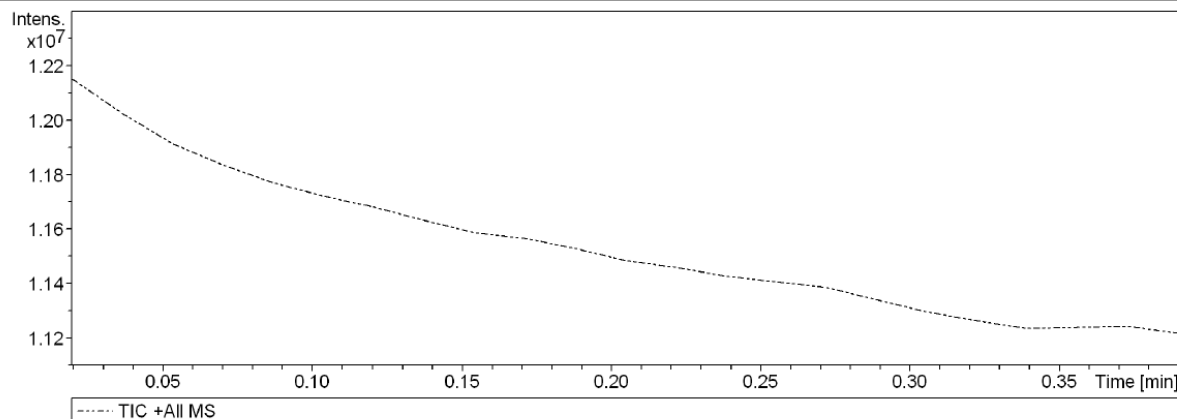


Figure A88. HRMS mass spectrum of *BocNH-Bnaeg-Phe-OEt* (**16**)

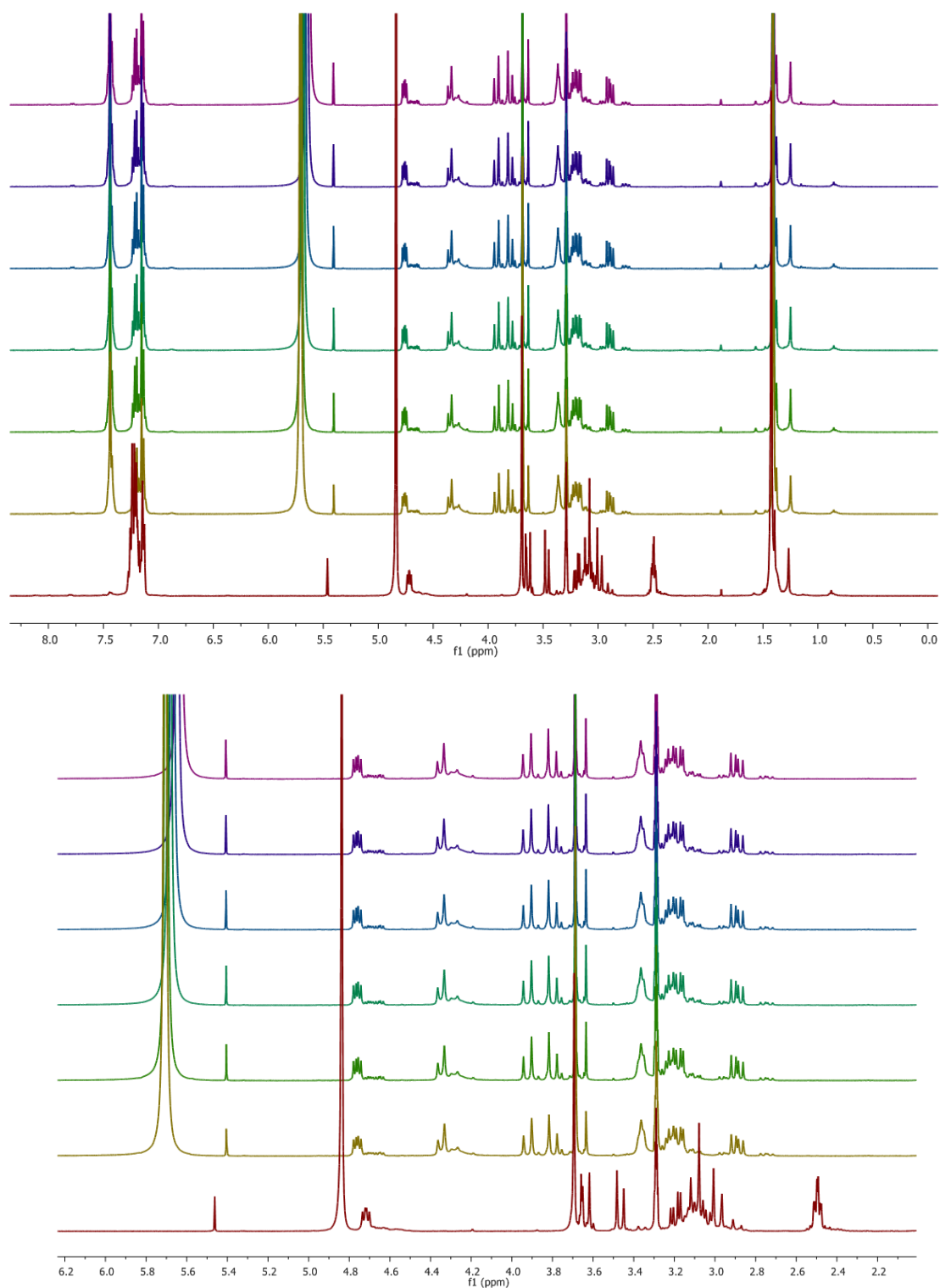


Figure A89. Time dependent NMR of *BocNH-Bnaeg-Phe-OMe* (**16**) in CD₃OD and 5% TFA

Generic Display Report

Analysis Info

Analysis Name D:\Data\AUG-2014\NKS\31082014_NKS_CB_938TFA.d
Method Pos_tune_low.m
Sample Name LCMS-NISER
Comment

Acquisition Date 8/31/2014 4:51:30 PM

Operator G.CH.S.REDDY.
Instrument microTOF-Q II

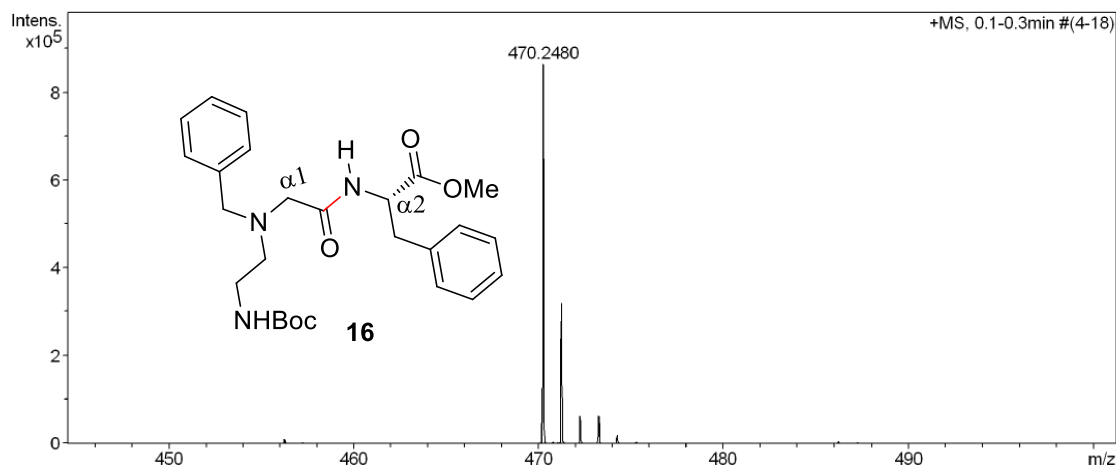
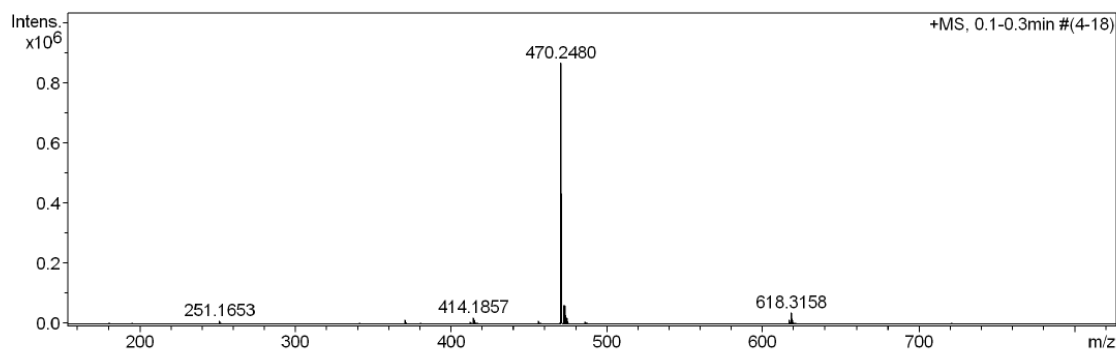
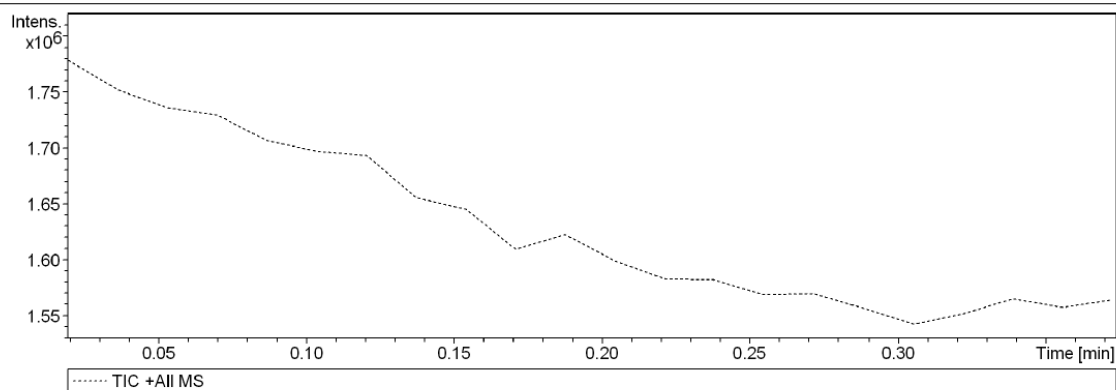


Figure A90. Mass spectrum of *BocNH-Bnaeg-Phe-OMe* (**16**) after time dependent NMR experiment in CD₃OD

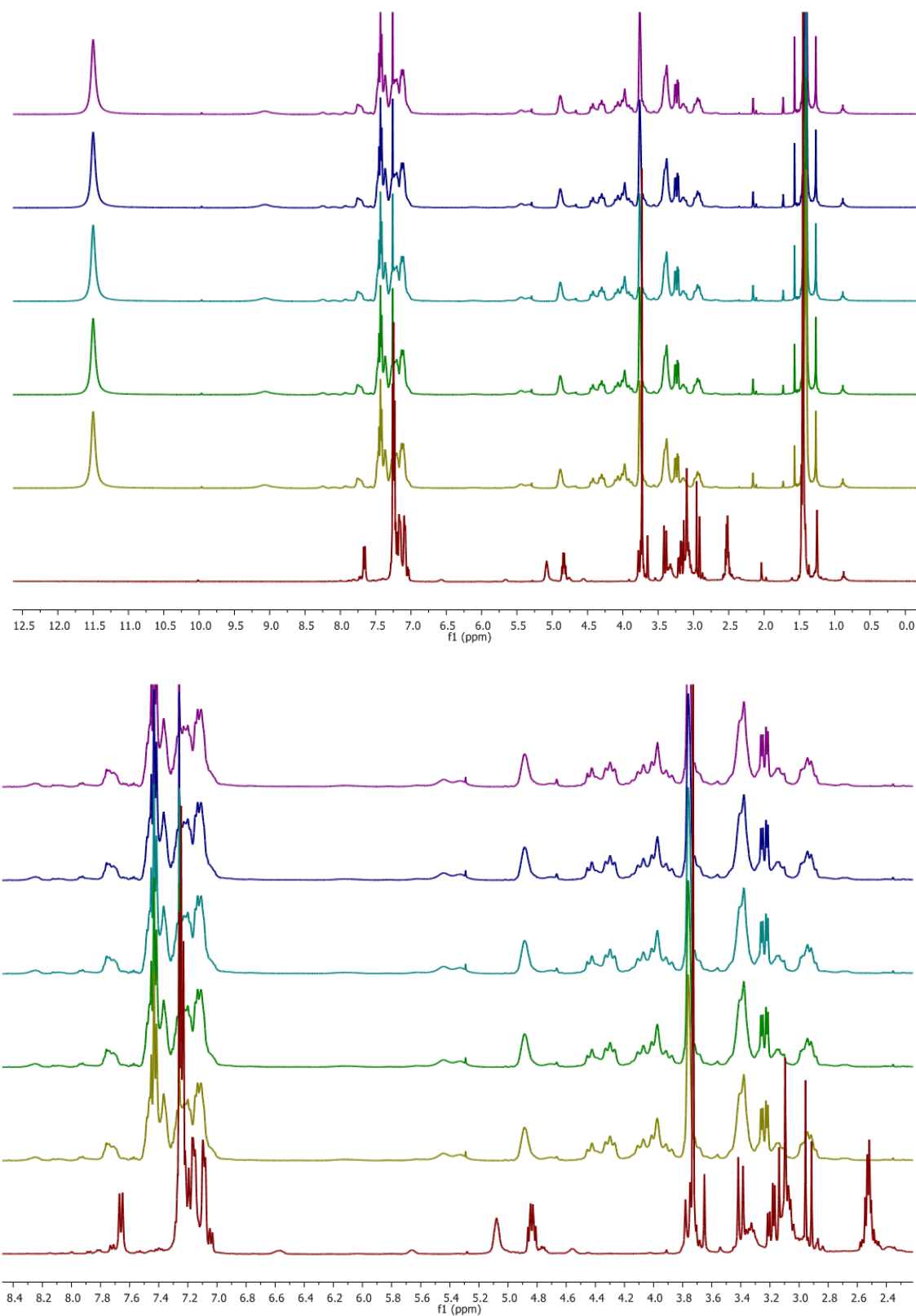


Figure A91. Time dependent NMR of BocNH-Bnaeg-Phe-OMe (**16**) in CDCl₃ and 5% TFA

Generic Display Report

Analysis Info

Analysis Name D:\Data\AUG-2014\NKS\31082014_NKS_CB_938CDCl3TFA.d
Method Pos_tune_low.m
Sample Name LCMS-NISER
Comment

Acquisition Date 8/31/2014 5:42:01 PM

Operator G.CH.S.REDDY.
Instrument micrOTOF-Q II

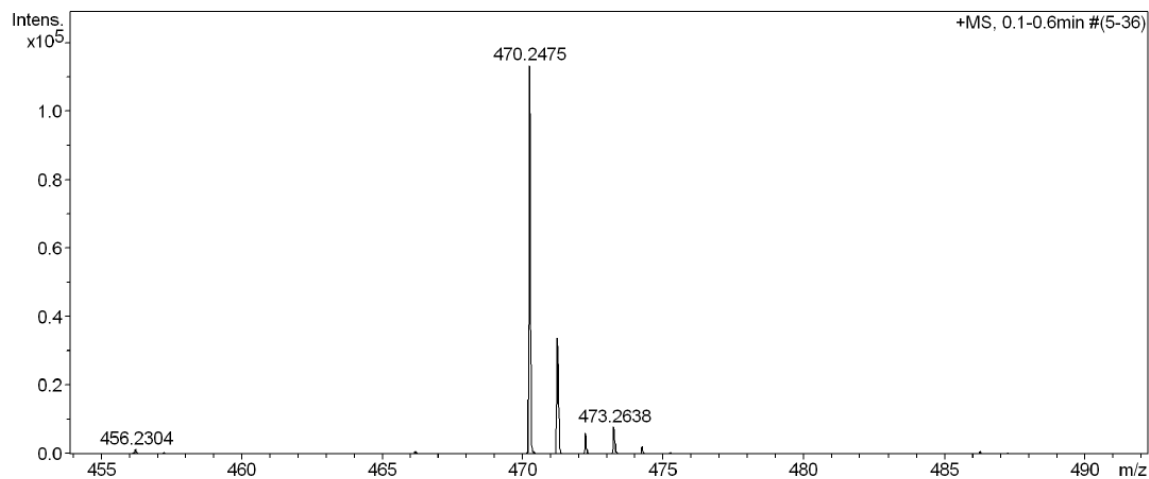
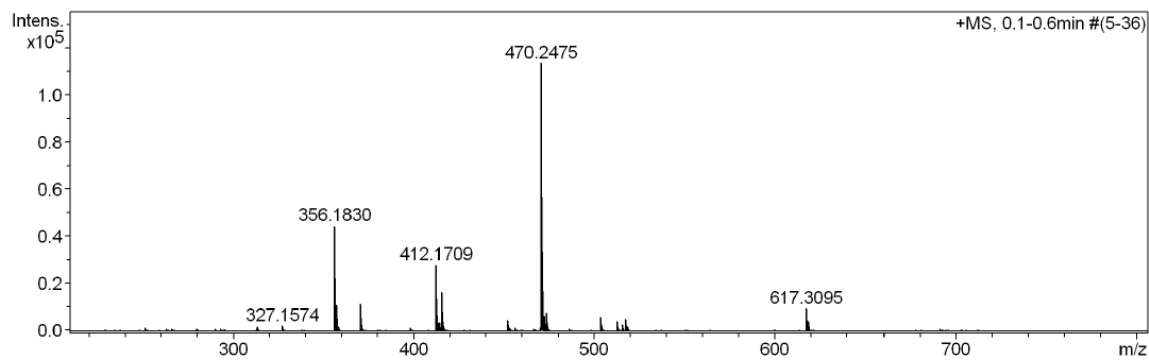
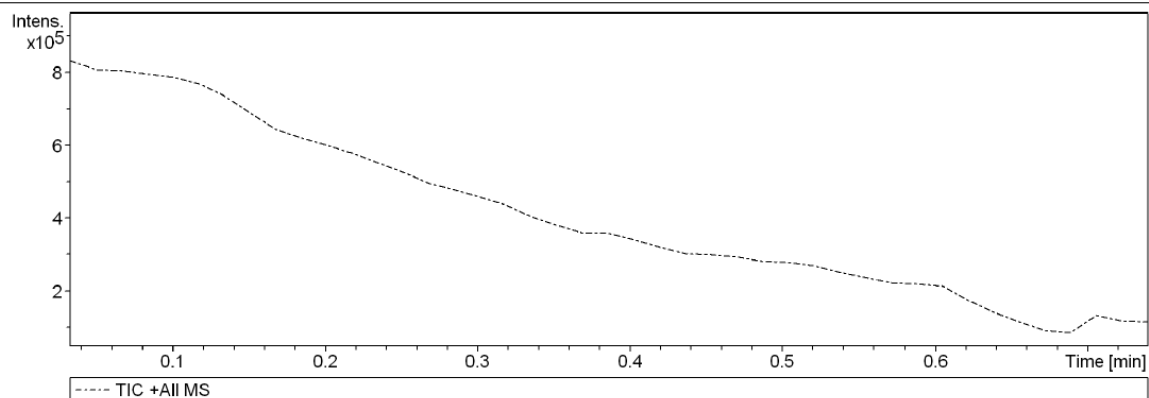


Figure A92. Mass spectrum of *BocNH-Bnaeg-Phe-OMe* (**16**) after time dependent NMR experiment in CDCl₃.

32. Characterization data ($^1\text{H}/^{13}\text{C}$ NMR and HRMS), Time dependent NMR and Mass spectrum after time dependent NMR of *BocNH-Fmocag-Gly-OMe* (**17**)

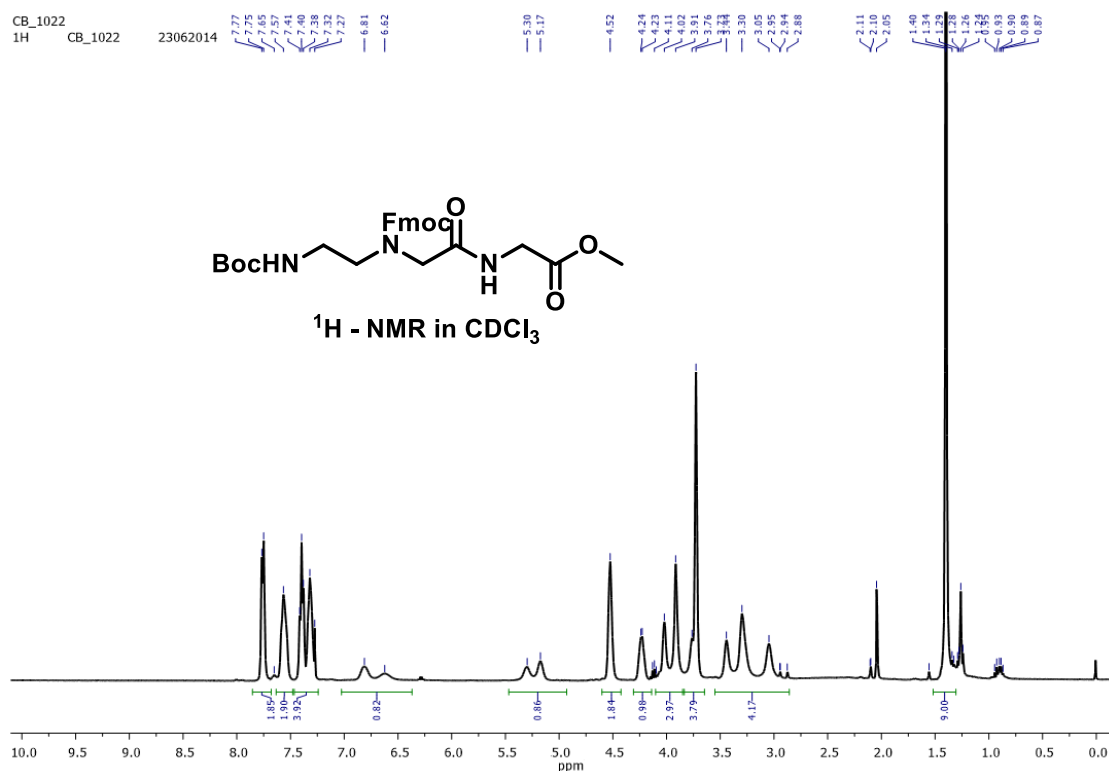


Figure A93. ^1H NMR spectrum of *BocNH-Fmocag-Gly-OMe* (**17**) in CDCl_3

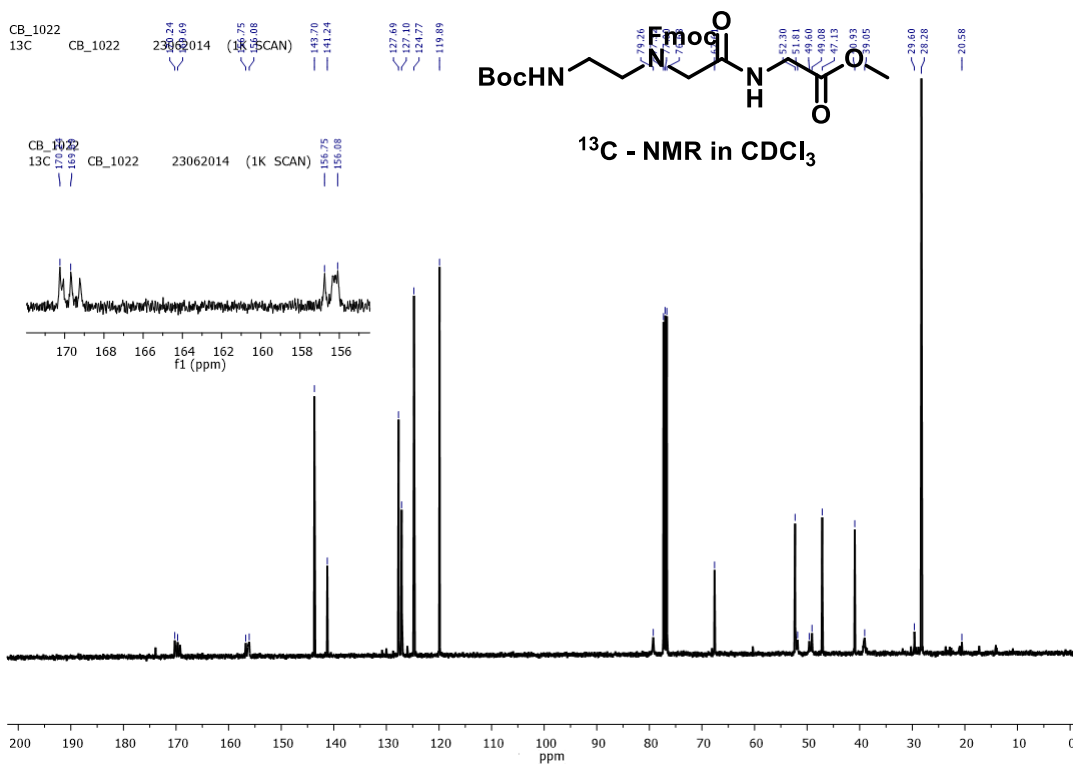


Figure A94. ^{13}C NMR spectrum of *BocNH-Fmocag-Gly-OMe* (**17**) in CDCl_3

Generic Display Report

Analysis Info

Analysis Name D:\Data\AUG-2014\NKS\14082014_NKS_CB_1022.d
 Method Pso_tune_wide.m
 Sample Name
 Comment

Acquisition Date 8/14/2014 4:30:53 PM

Operator A.S.Sahu
 Instrument micrOTOF-Q II

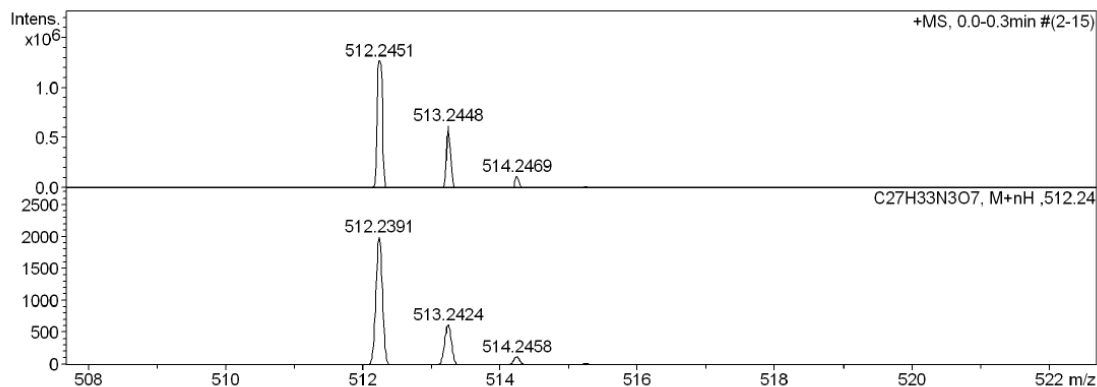
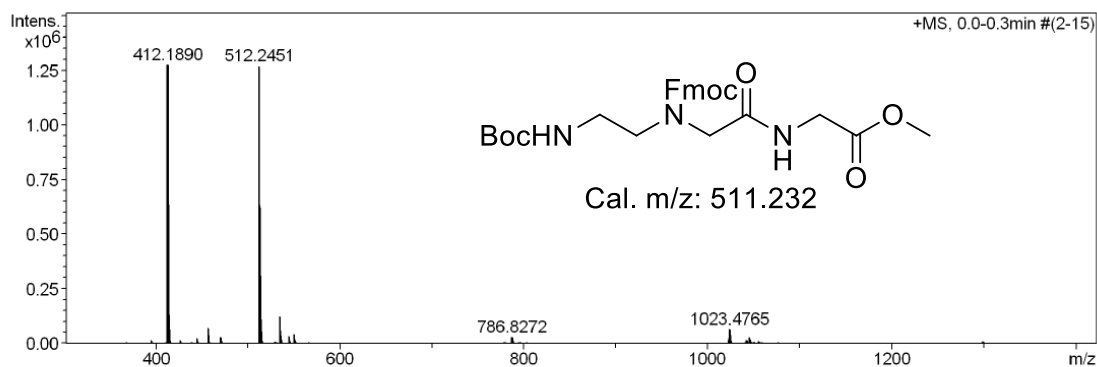
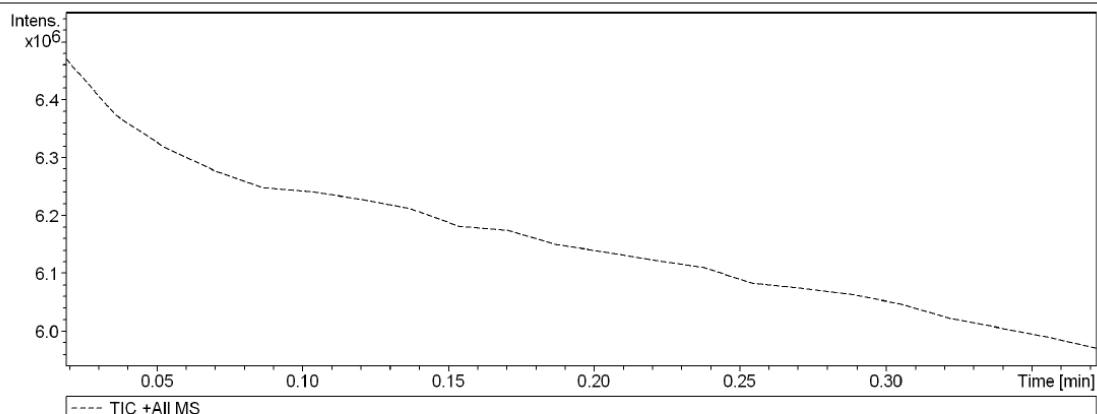


Figure A95. HRMS mass spectrum of *BocNH-Fmocagg-Gly-OEt* (**16**)

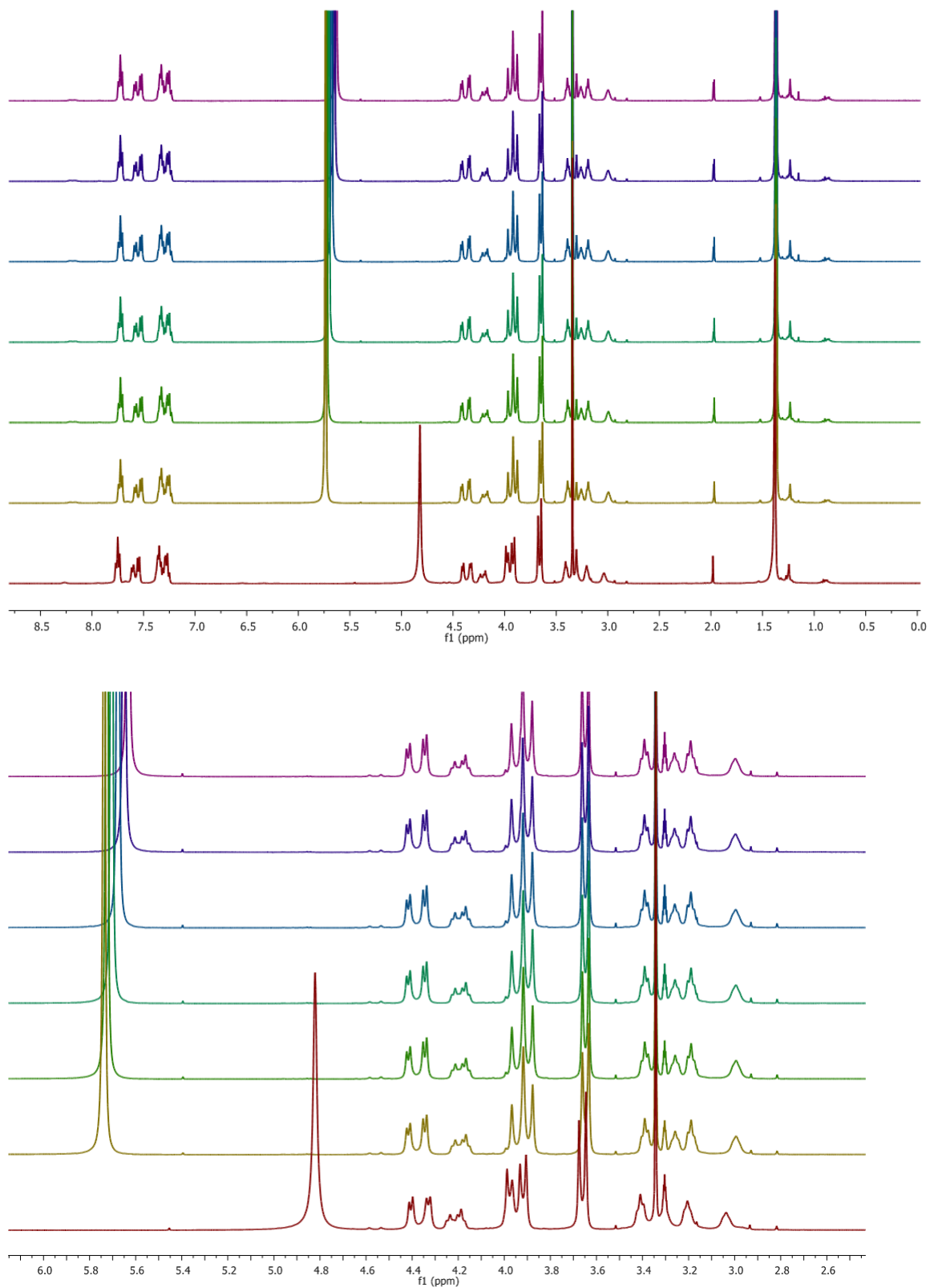


Figure A96. Time dependent NMR of *BocNH-Fmoc-aeg-Gly-OMe* (**17**) in CDCl_3 and 5% TFA

Generic Display Report

Analysis Info

Analysis Name D:\Data\AUG-2014\CSP\31082014_1022 TFA.d
Method Pos_tune_low.m
Sample Name LCMS-NISER
Comment

Acquisition Date 8/31/2014 4:38:15 PM

Operator G.CH.S.REDDY.
Instrument micrOTOF-Q II

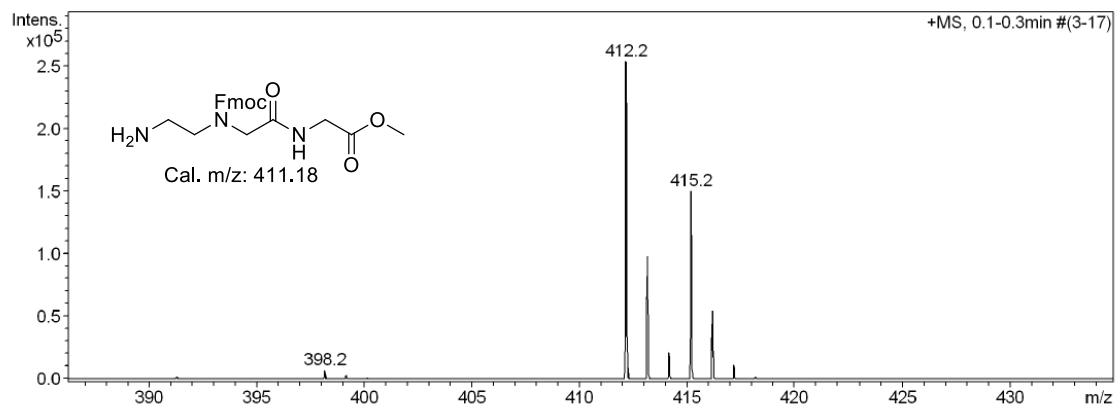
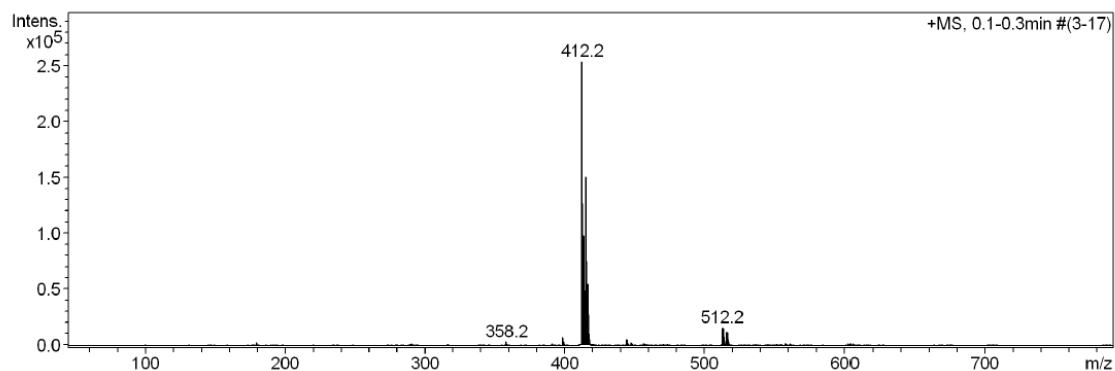
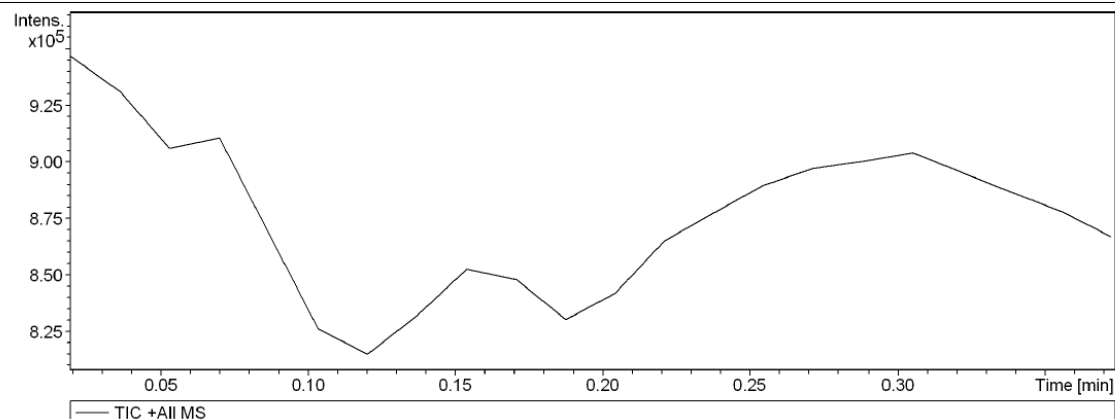


Figure A97. Mass spectrum of *BocNH-Fmocag-Gly-OMe* (**17**) after time dependent NMR experiment in CD₃OD, overnight.

33. $^1\text{H}/^{13}\text{C}$ NMR spectra of *Trhg*-OEt and *Trhg* lactone in CD_3CN after addition of TFA

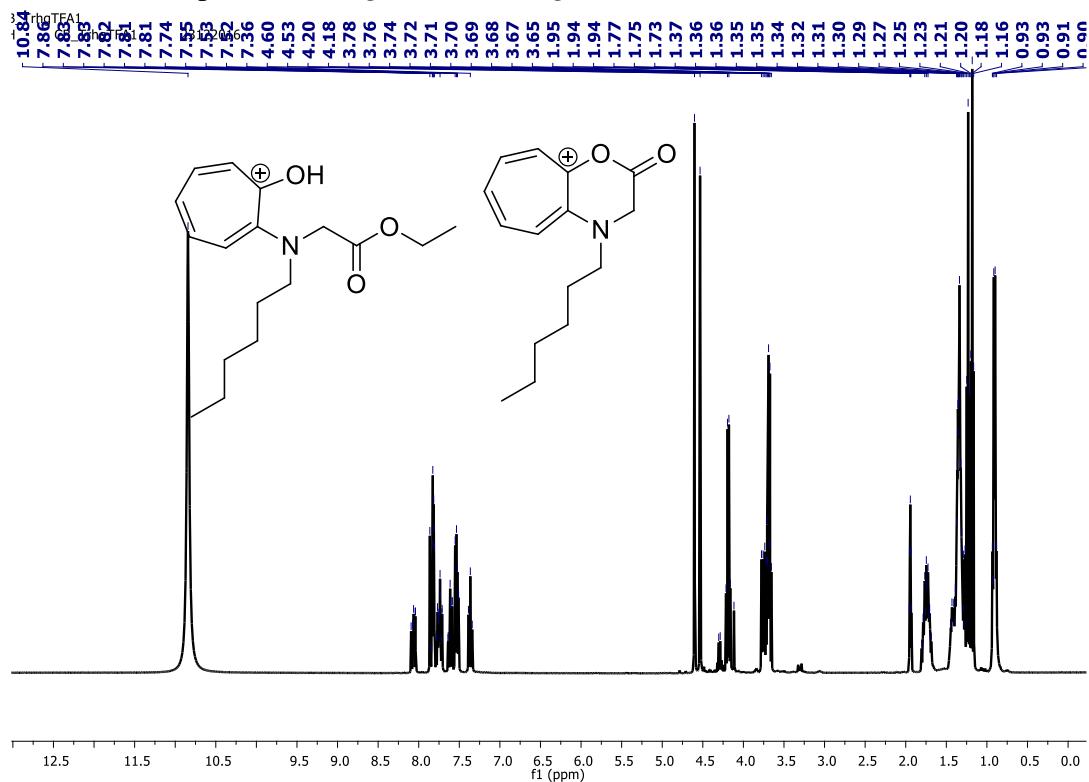


Figure A98. ^1H NMR spectrum of *Trhg*-OEt (18) and *Trhg* lactone (26) in CD_3CN .

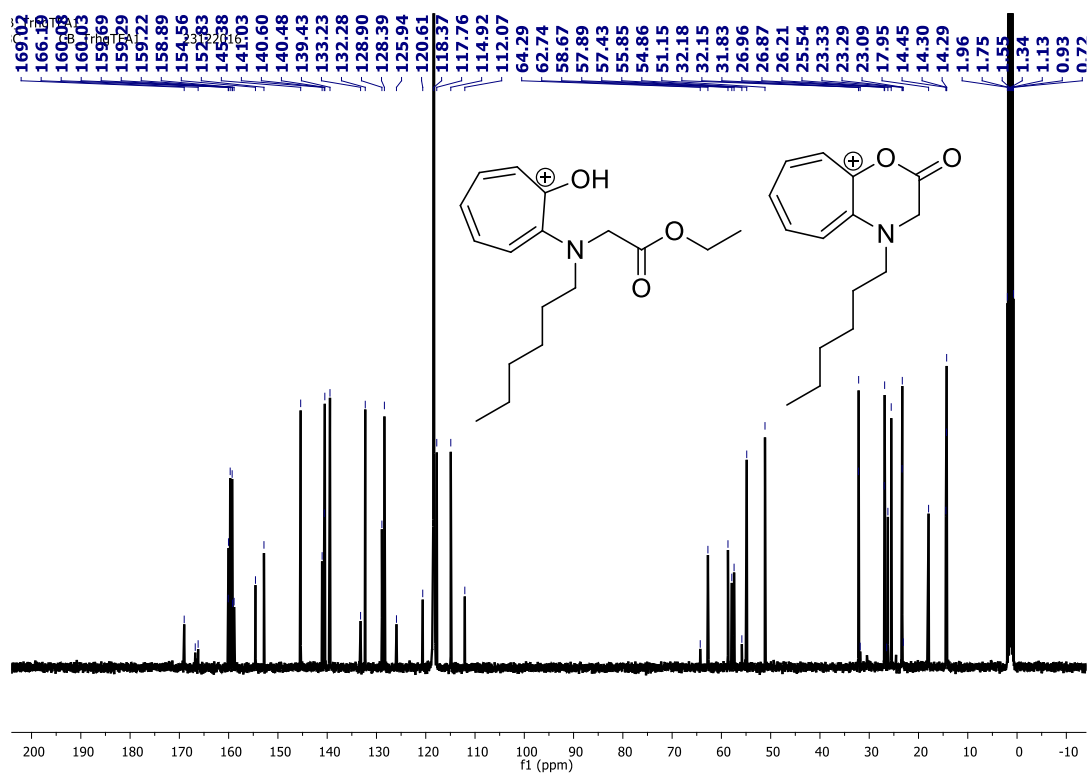


Figure A99. ^{13}C NMR spectrum of *Trhg*-OEt (18) and *Trhg* lactone (26) in CD_3CN

34. $^1\text{H}/^{13}\text{C}/\text{DEPT}135$ NMR spectra of *Trhg*-OEt and $\alpha\text{-CH}_2$ deuterated *Trhg* lactone in CD_3CN after addition of TFA-D

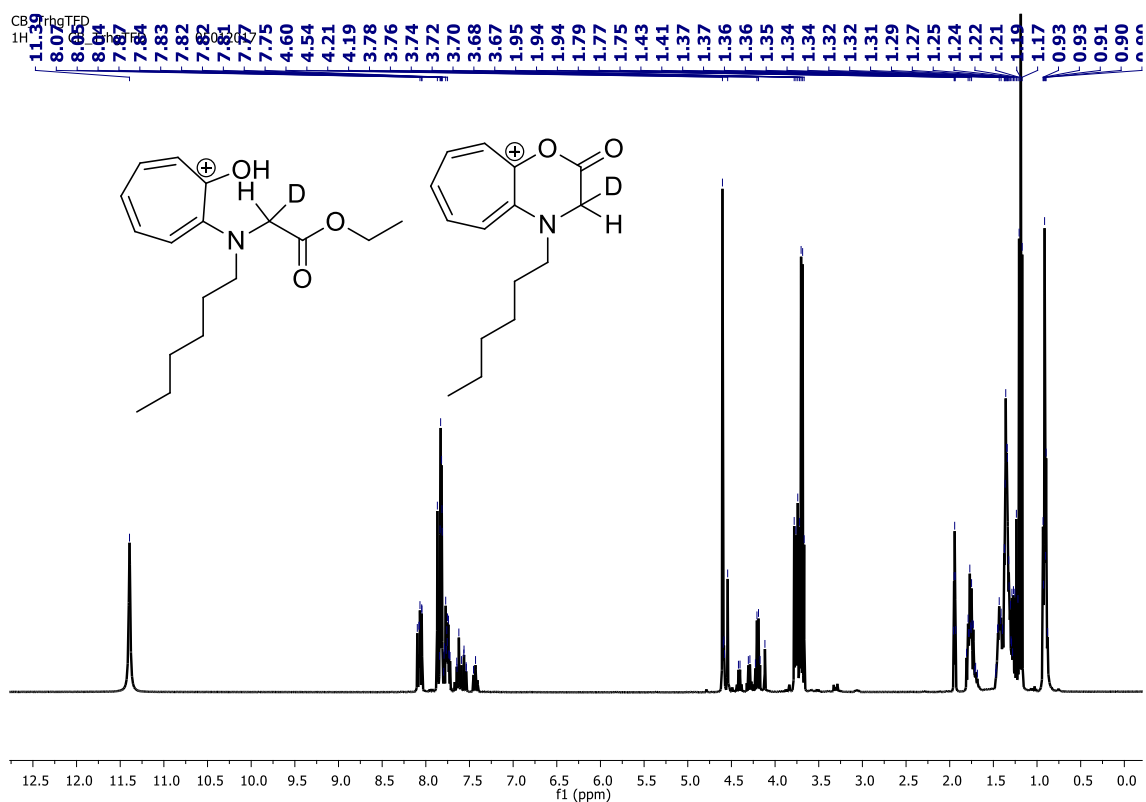


Figure A100. ^1H NMR spectrum of *Trhg*-OEt (18) and deuterated *Trhg* lactone (26).

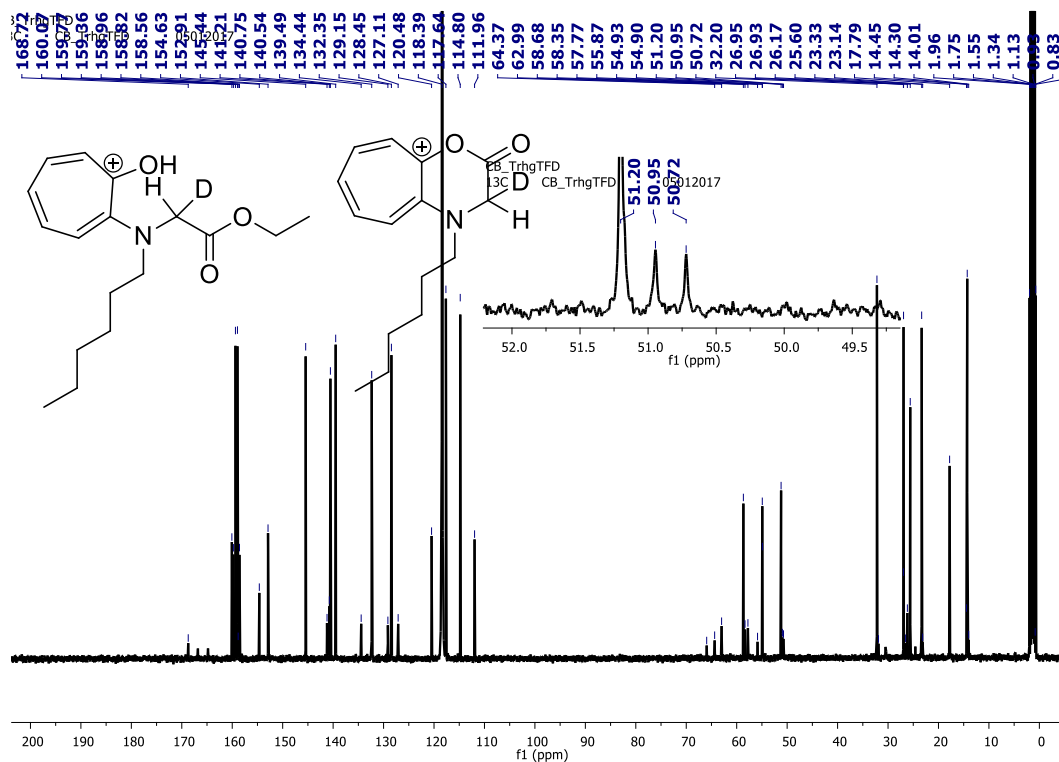


Figure A101. ^{13}C NMR spectrum of *Trhg*-OEt (18) and deuterated *Trhg* lactone (26).

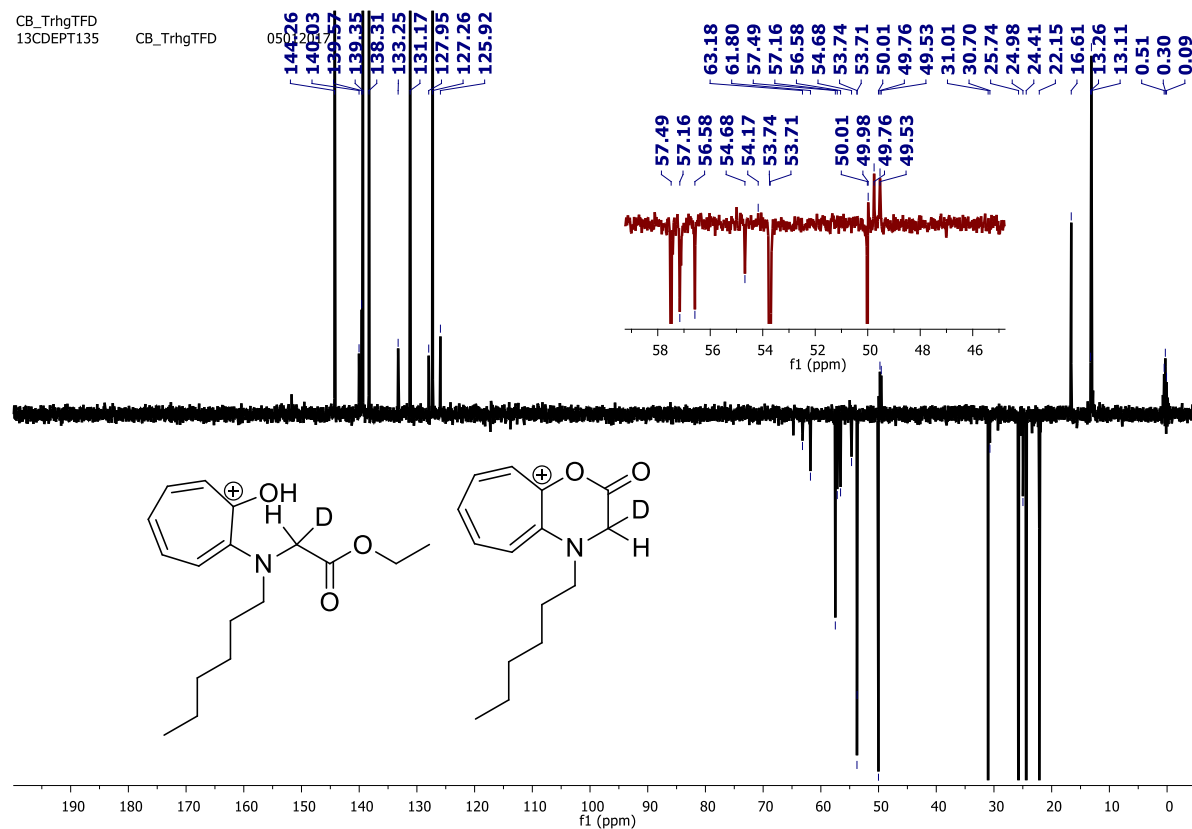


Figure A102. $^{13}\text{CDEPT135}$ NMR spectrum of *Trhg*-OEt (18) and deuterated *Trhg* lactone (26) in CD_3CN .

35. $^1\text{H}/^{13}\text{C}/\text{DEPT}135$ NMR and HRMS spectra of *Trhg*- NHCH_2Ph in CDCl_3

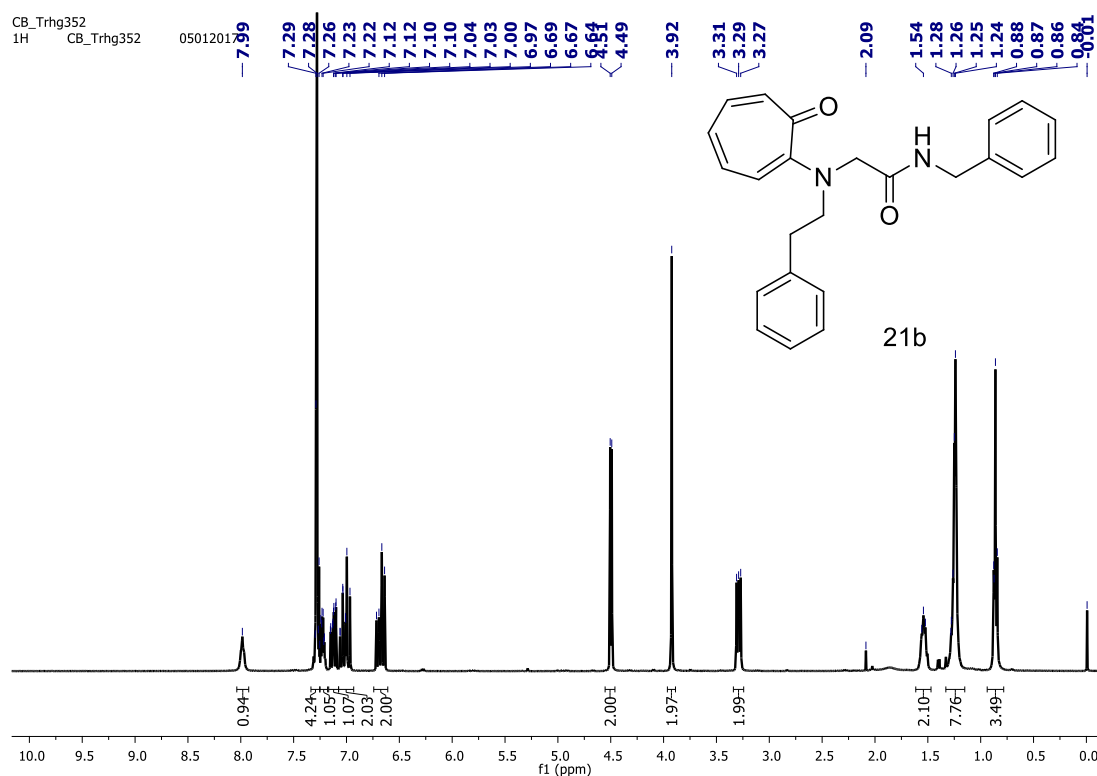


Figure A103. ^1H NMR spectrum of *Trhg*- NHCH_2Ph (19b) in CDCl_3 .

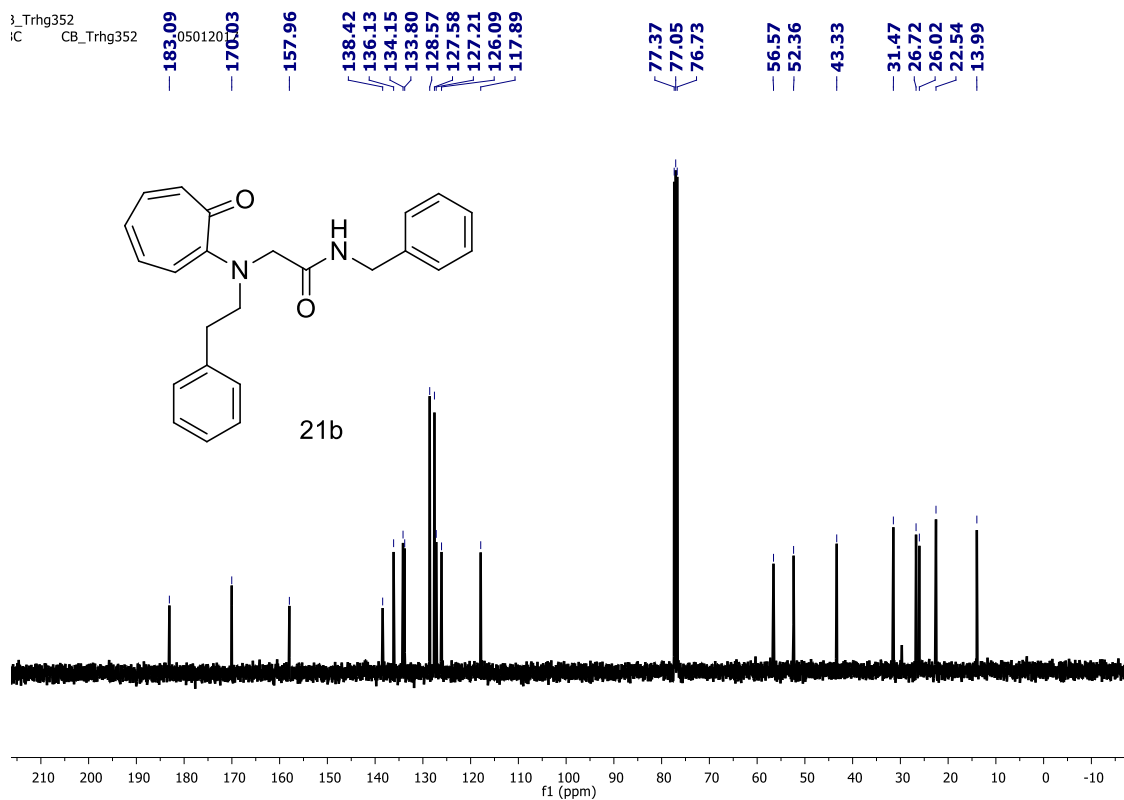


Figure A104. ^{13}C NMR spectrum of *Trhg*- NHCH_2Ph (19b) in CDCl_3

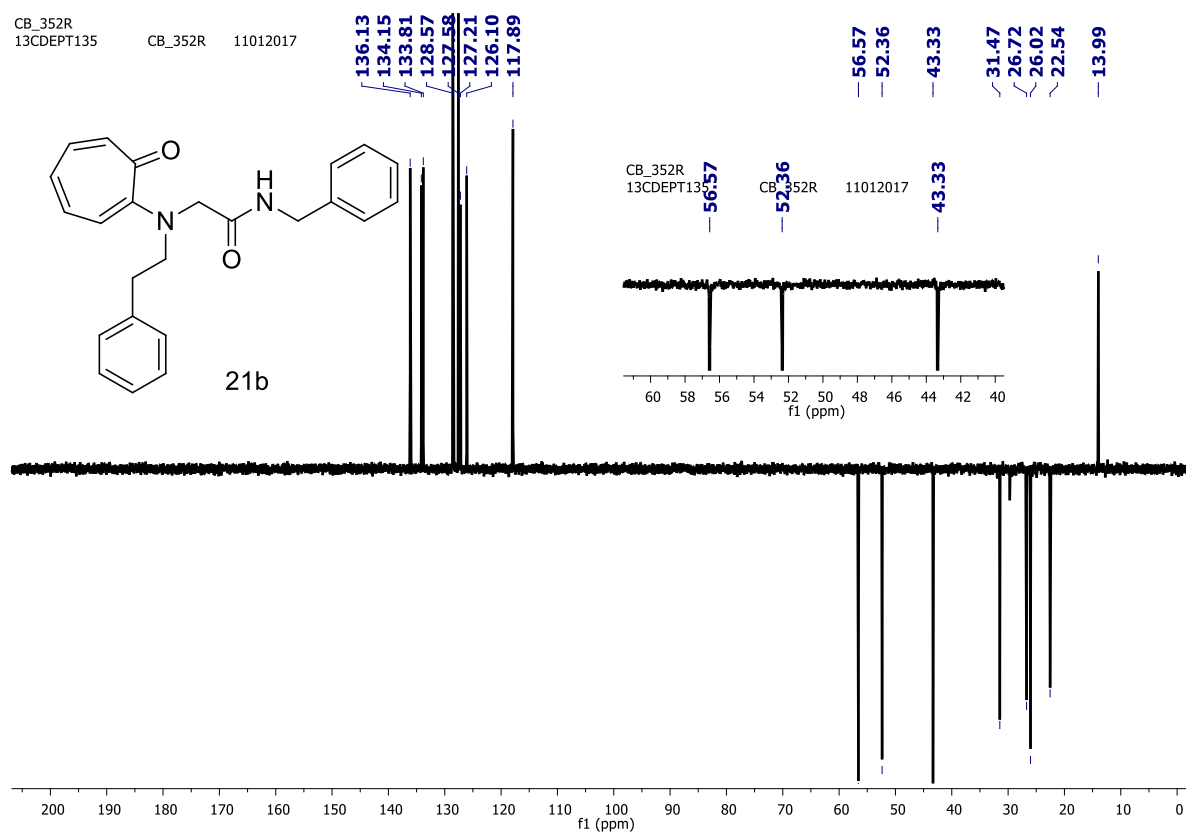


Figure A105. ¹³CDEPT135 NMR spectrum of *Trhg-NHCH₂Ph* (**19b**) in CDCl₃

Generic Display Report

Analysis Info

Analysis Name D:\Data\JAN-2017\NKS\06012017_NKS_CB_352.d
 Method Pos_tune_low.m
 Sample Name Bruker micro TOF -Q II
 Comment

Acquisition Date 1/6/2017 2:53:29 PM

Operator Amit S.Sahu
 Instrument micrOTOF-Q II

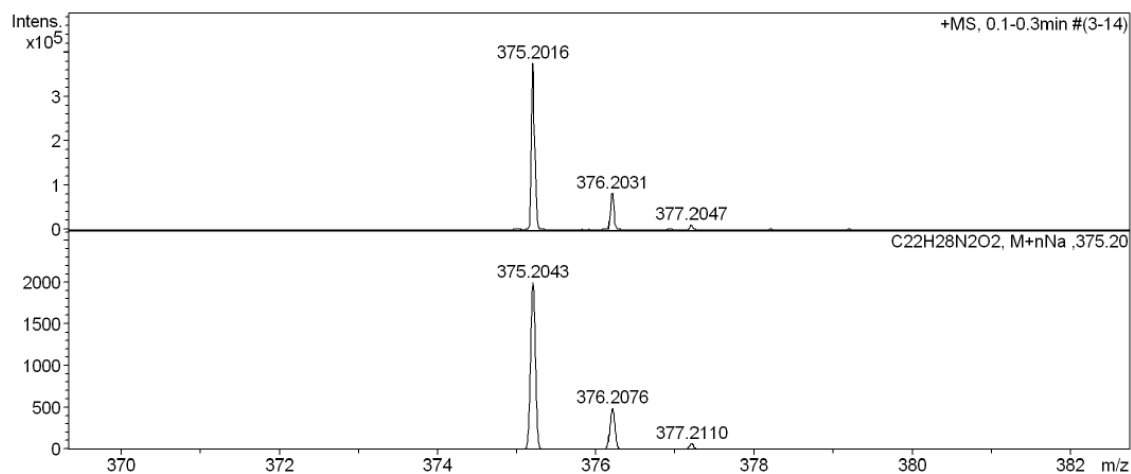
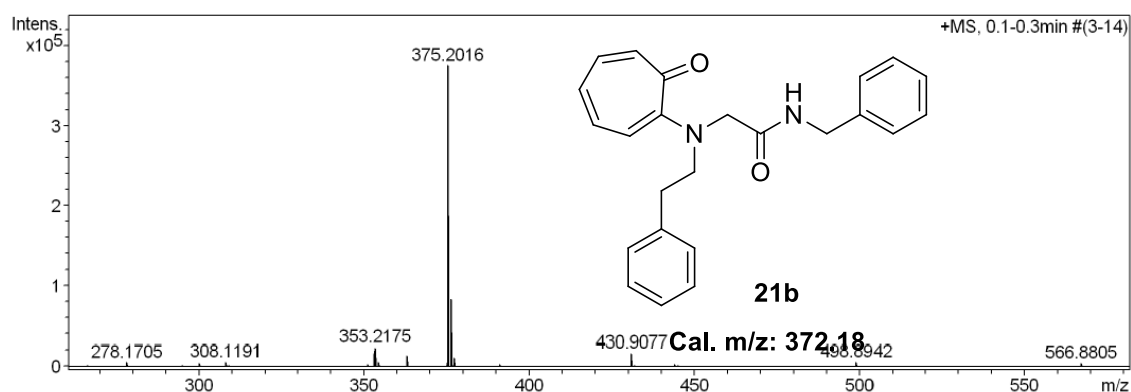
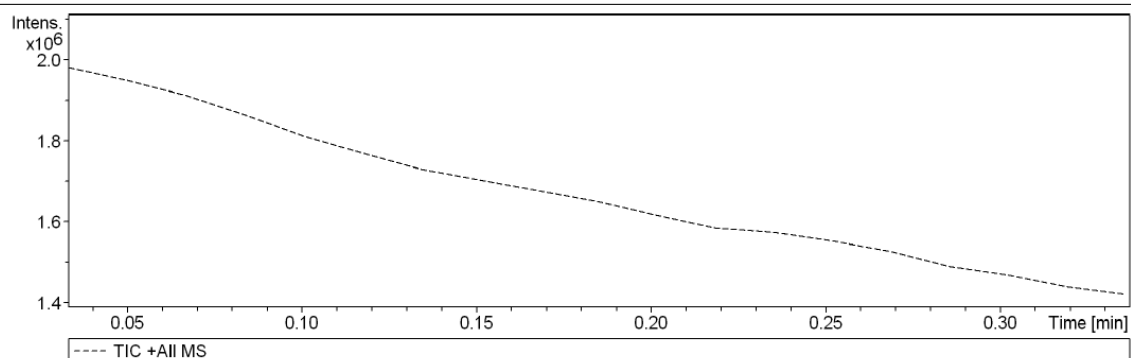


Figure A106. HRMS spectrum of *Trhg*-NHCH₂Ph (**19b**).

36. $^1\text{H}/^{13}\text{C}/\text{DEPT}135$ NMR and HRMS spectra of *Trhg*-NHCH₂Ph and α -methylene deuterated (α -CHD) *Trhg*-NHCH₂Ph in CDCl₃

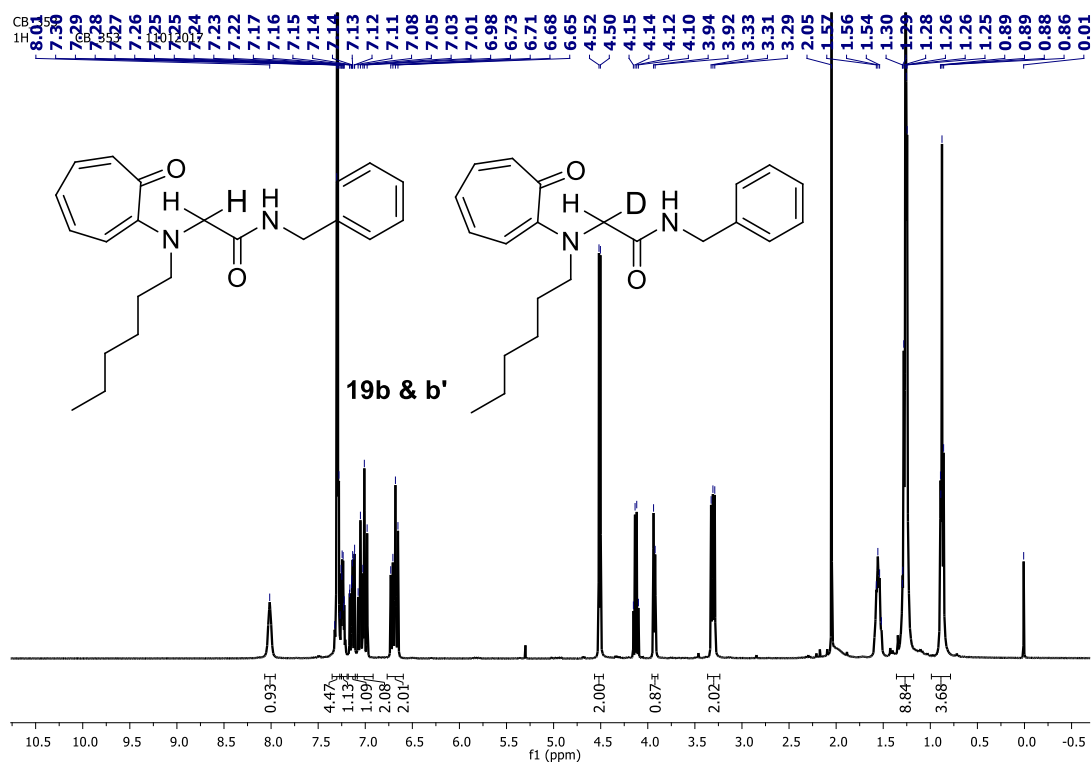


Figure A107. ^1H NMR spectrum of **19b** and **19b'** in CDCl₃

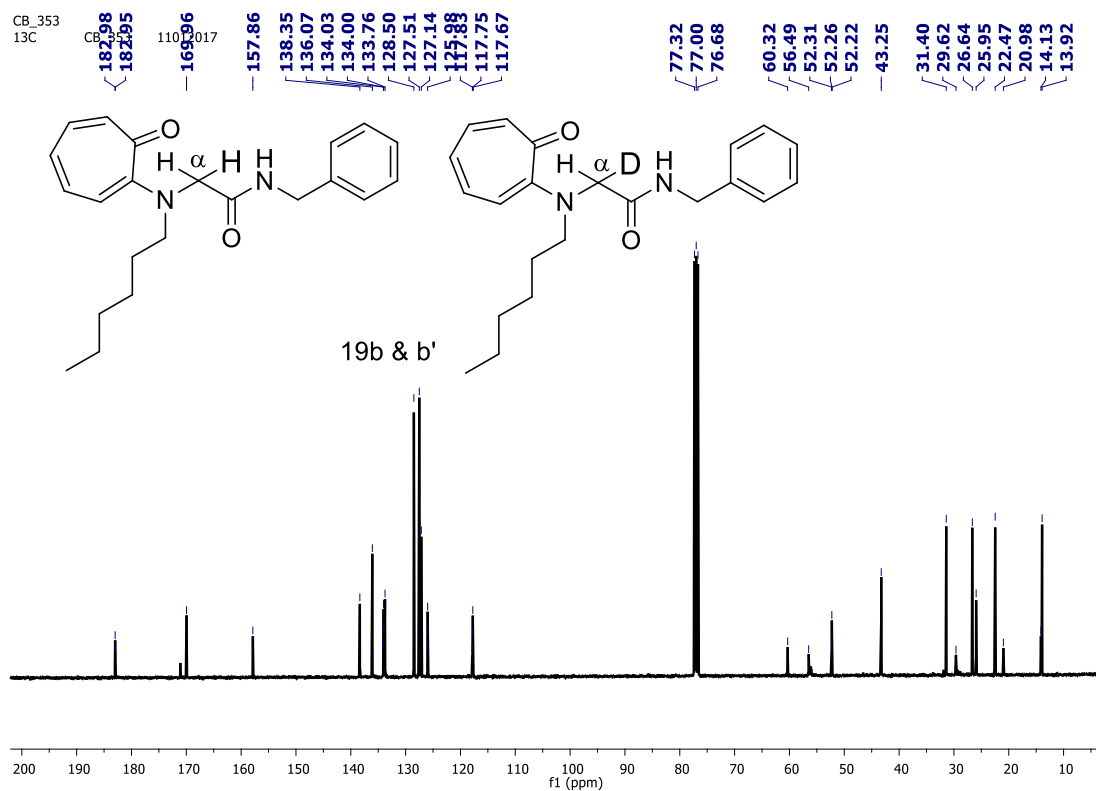


Figure A108. ^{13}C NMR spectrum of **19b** and **19b'** in CDCl₃

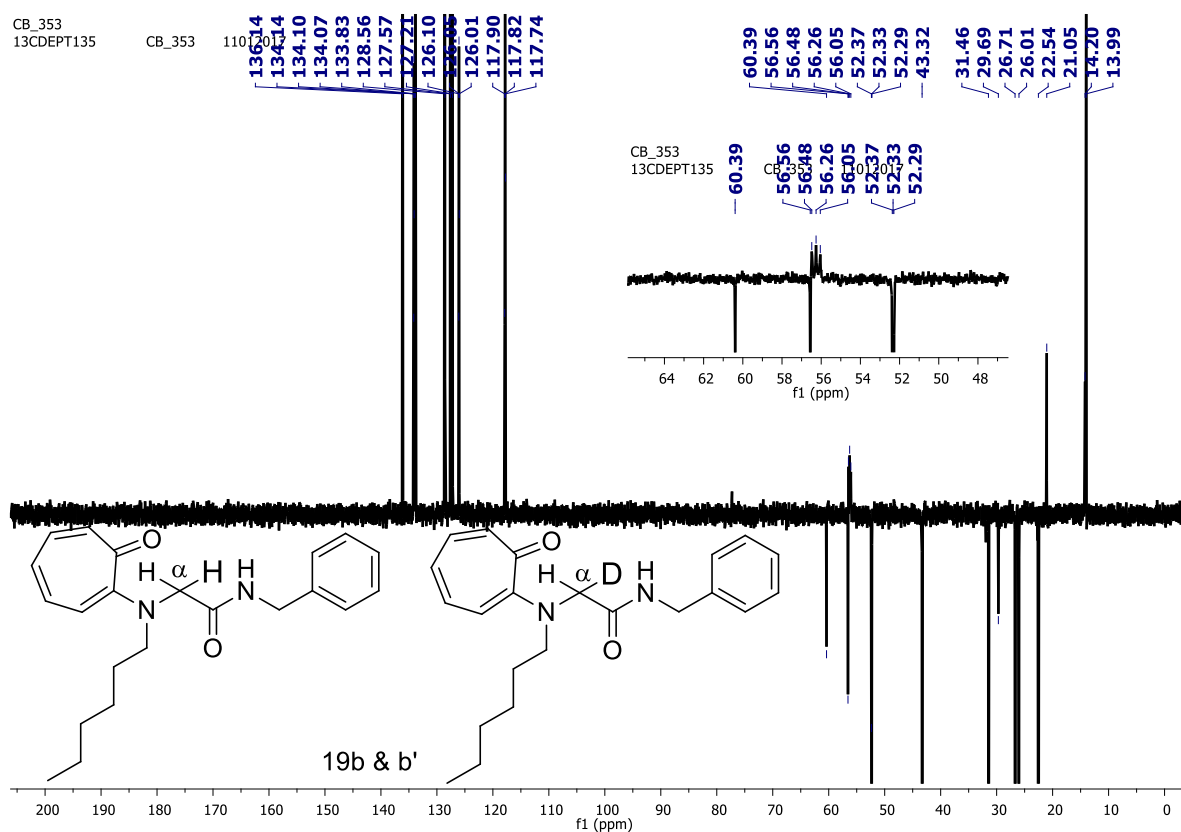


Figure A109. $^{13}\text{CDEPT135}$ NMR spectrum of **19b** and **19b'** in CDCl_3

Generic Display Report

Analysis Info

Analysis Name D:\Data\JAN-2017\NKS\10012017_NKS_CB_353_R.d
Method Pso_tune_wide.m
Sample Name Bruker micro TOF -Q II
Comment

Acquisition Date 1/10/2017 5:23:37 PM

Operator Amit S.Sahu
Instrument micrOTOF-Q II

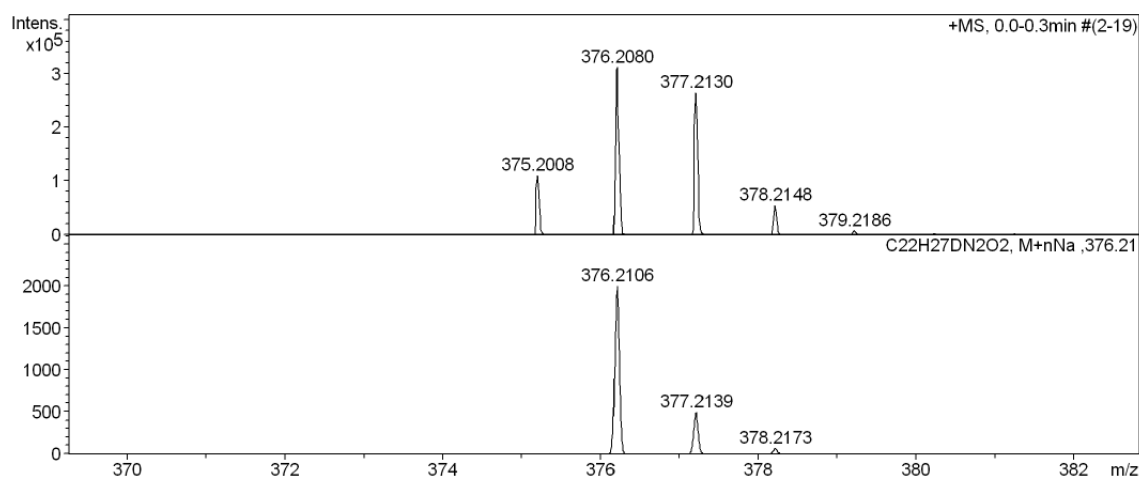
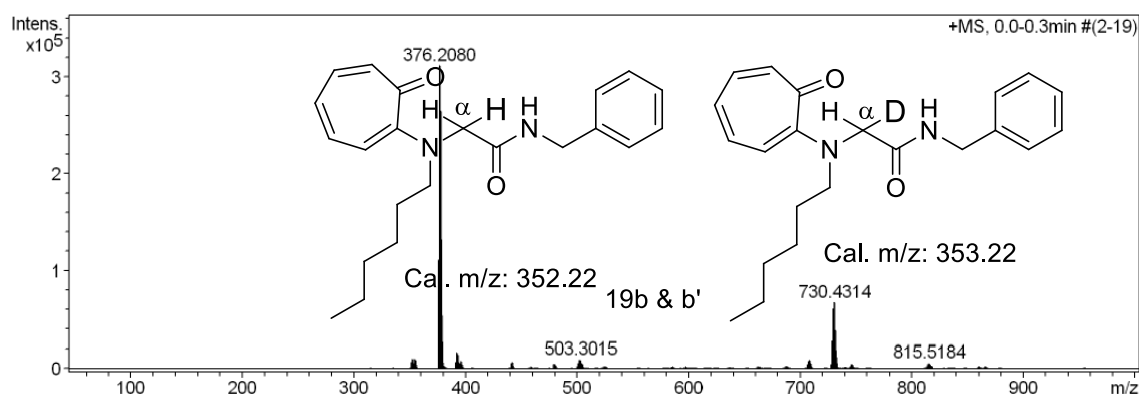
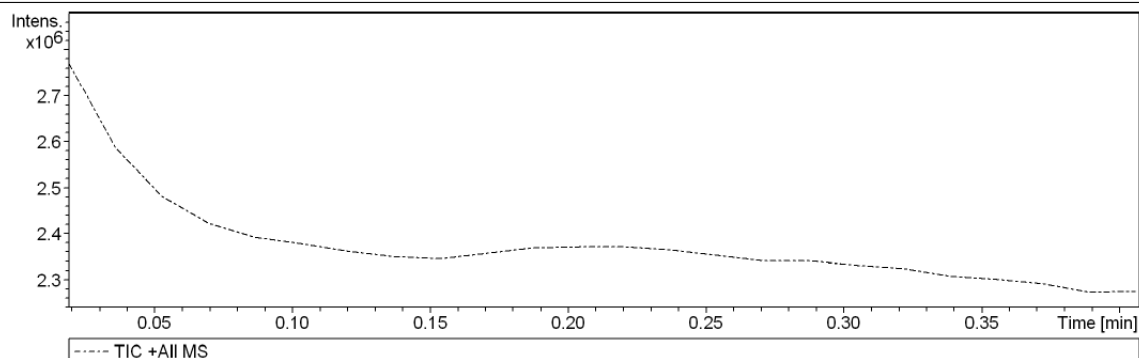


Figure A110. HRMS spectrum of **19b** and **19b'**

37. $^1\text{H}/^{13}\text{C}$ NMR spectra of *Trpeg*-OEt and *Trpeg* lactone in CD_3CN after addition of TFA

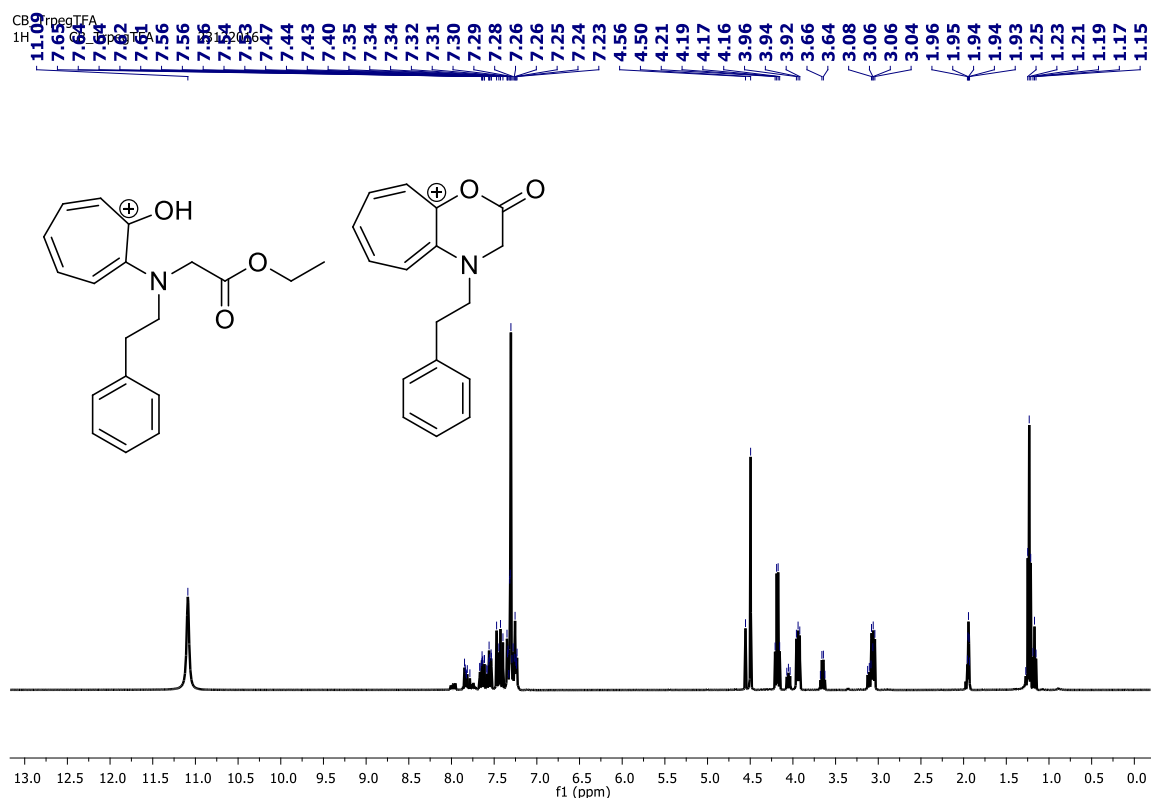


Figure A111. ^1H NMR spectrum of *Trpeg*-OEt (19) and *Trpeg* lactone (27) in CD_3CN

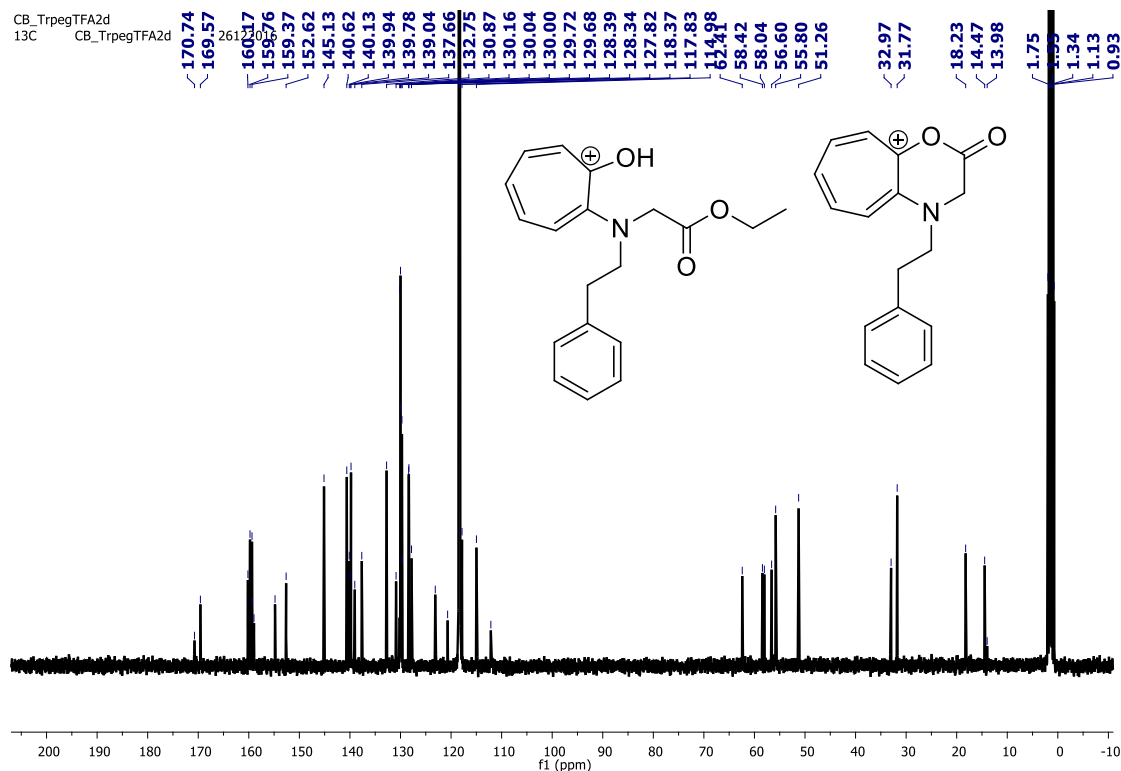


Figure A112. ^{13}C NMR spectrum of *Trpeg*-OEt (19) and *Trpeg* lactone (27) in CD_3CN

38. $^1\text{H}/^{13}\text{C}$ NMR spectra of *Trpeg*-OEt and α - CH_2 mono deuterated *Trpeg* lactone in CD_3CN after addition of TFA-D

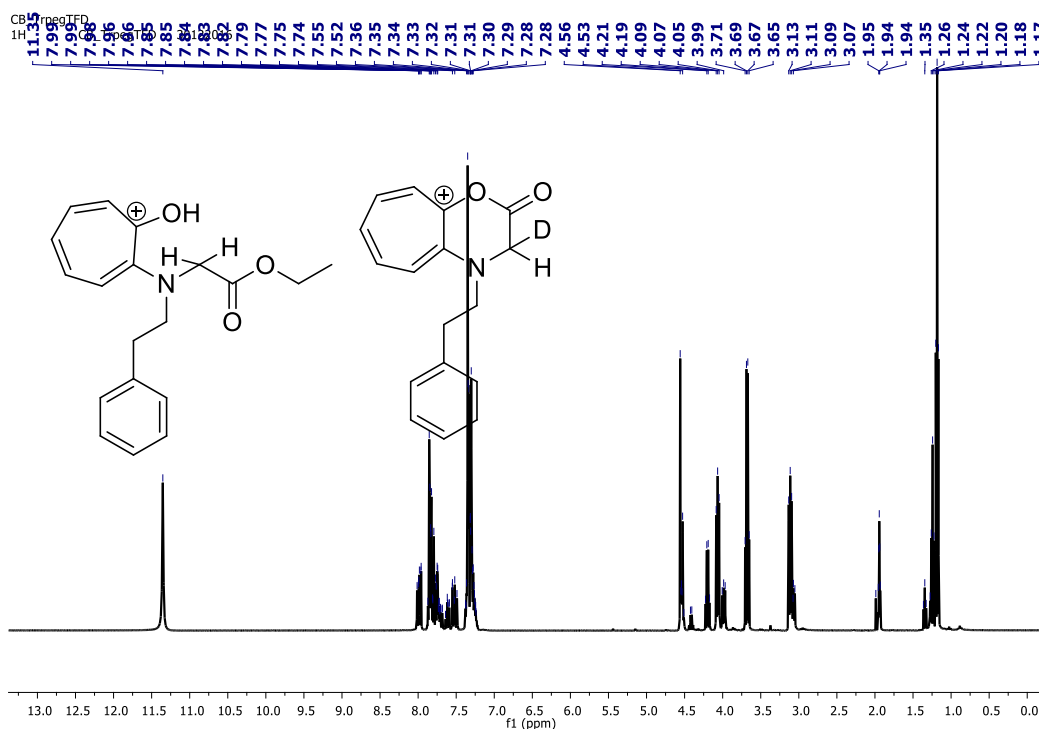


Figure A113. ^1H NMR spectrum of *Trpeg*-OEt (19) and deuterated *Trpeg* lactone (27).

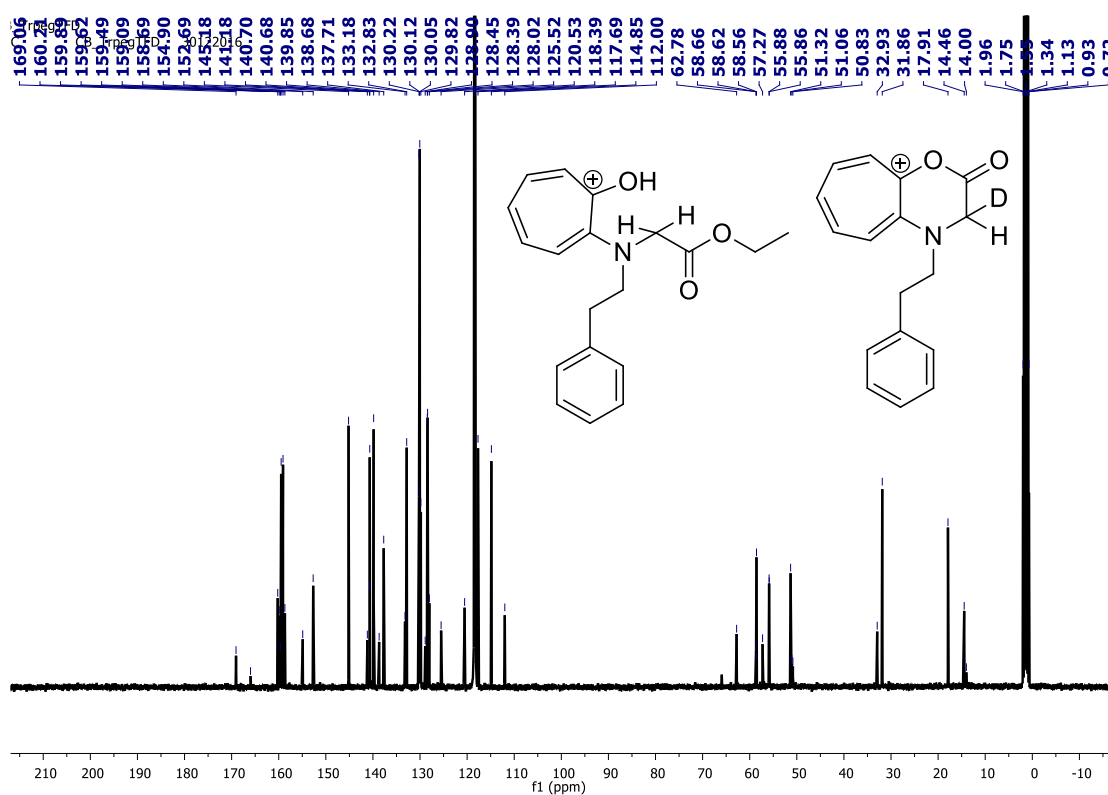


Figure A114. ^{13}C NMR spectrum of *Trpeg*-OEt (19) and deuterated *Trpeg* lactone (27).

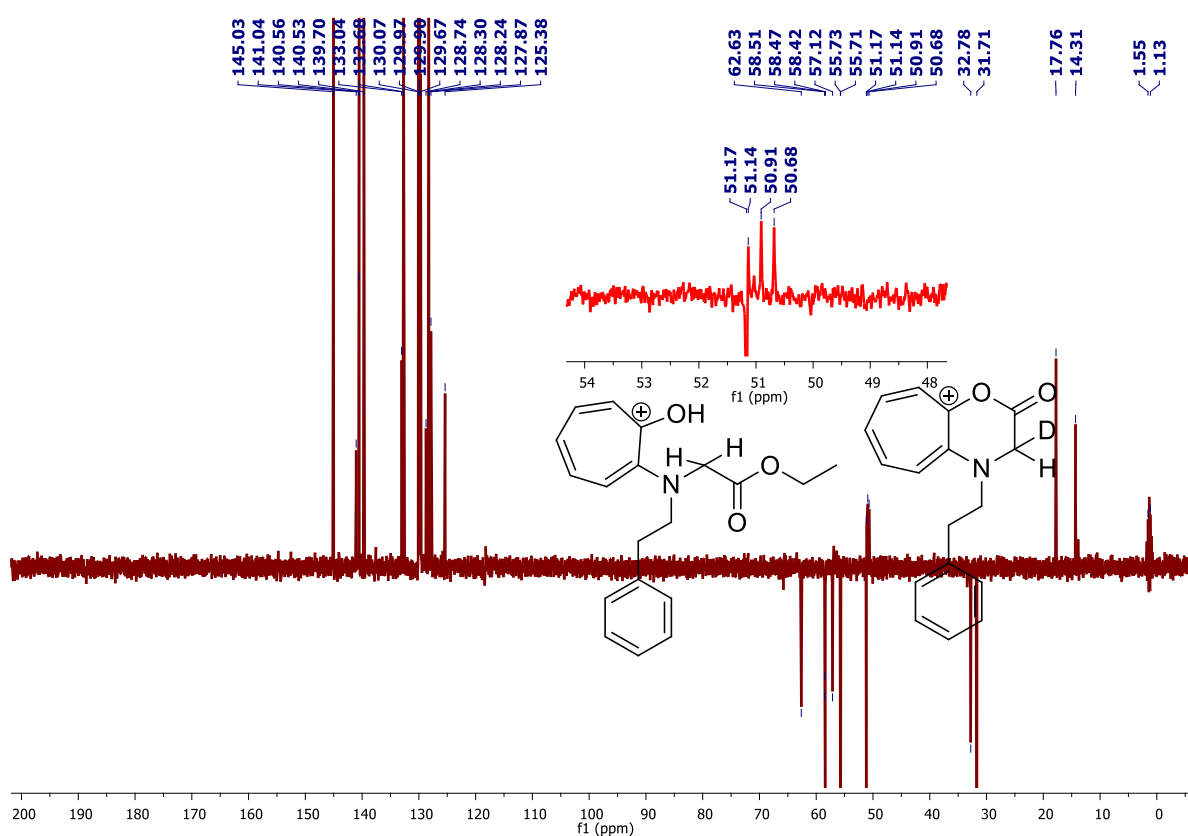


Figure A115. $^{13}\text{CDEPT135}$ NMR spectrum of *Trpeg*-OEt (19) and deuterated *Trpeg* lactone (27).

39. $^1\text{H}/^{13}\text{C}/\text{DEPT}135$ NMR and HRMS spectra of *Trpeg-NHCH₂Ph* in CDCl_3

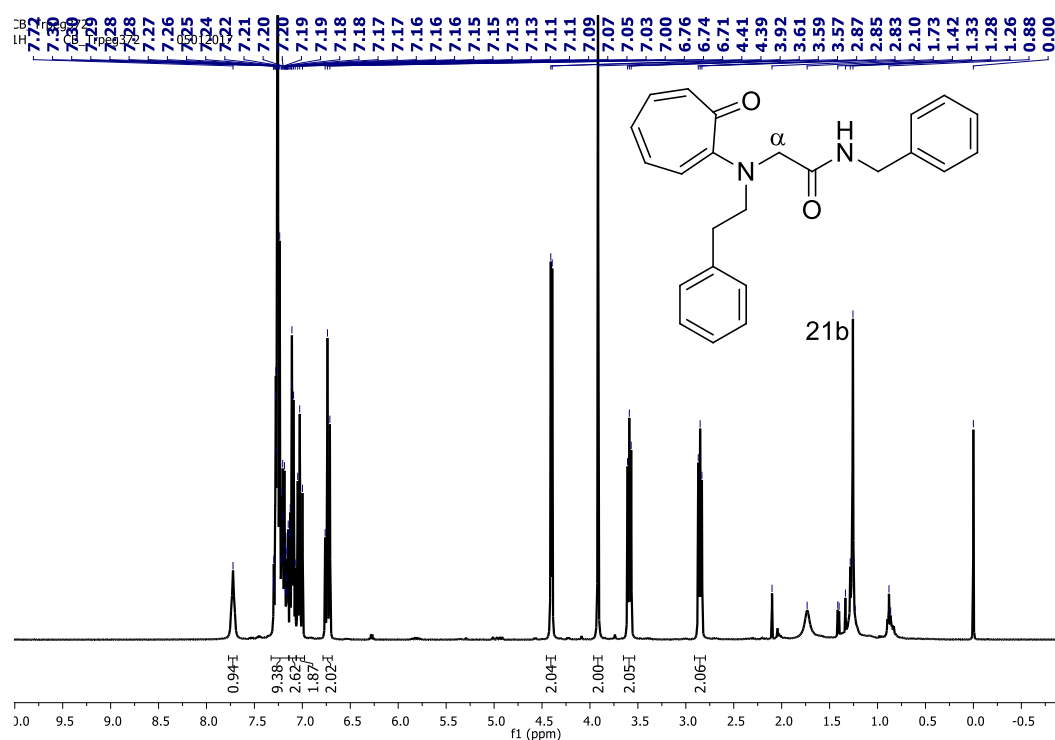


Figure A116. ^1H NMR spectrum of *Trpeg-NHCH₂Ph* (21) in CDCl_3

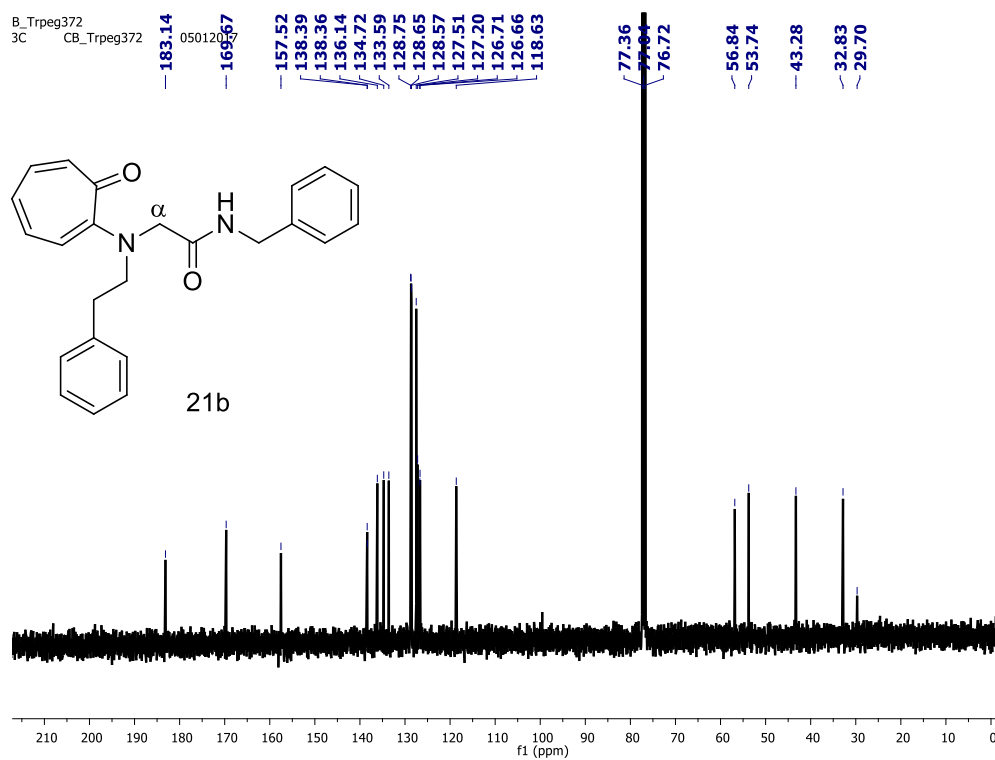


Figure A117. ^{13}C NMR spectrum of *Trpeg-NHCH₂Ph* (21) in CDCl_3

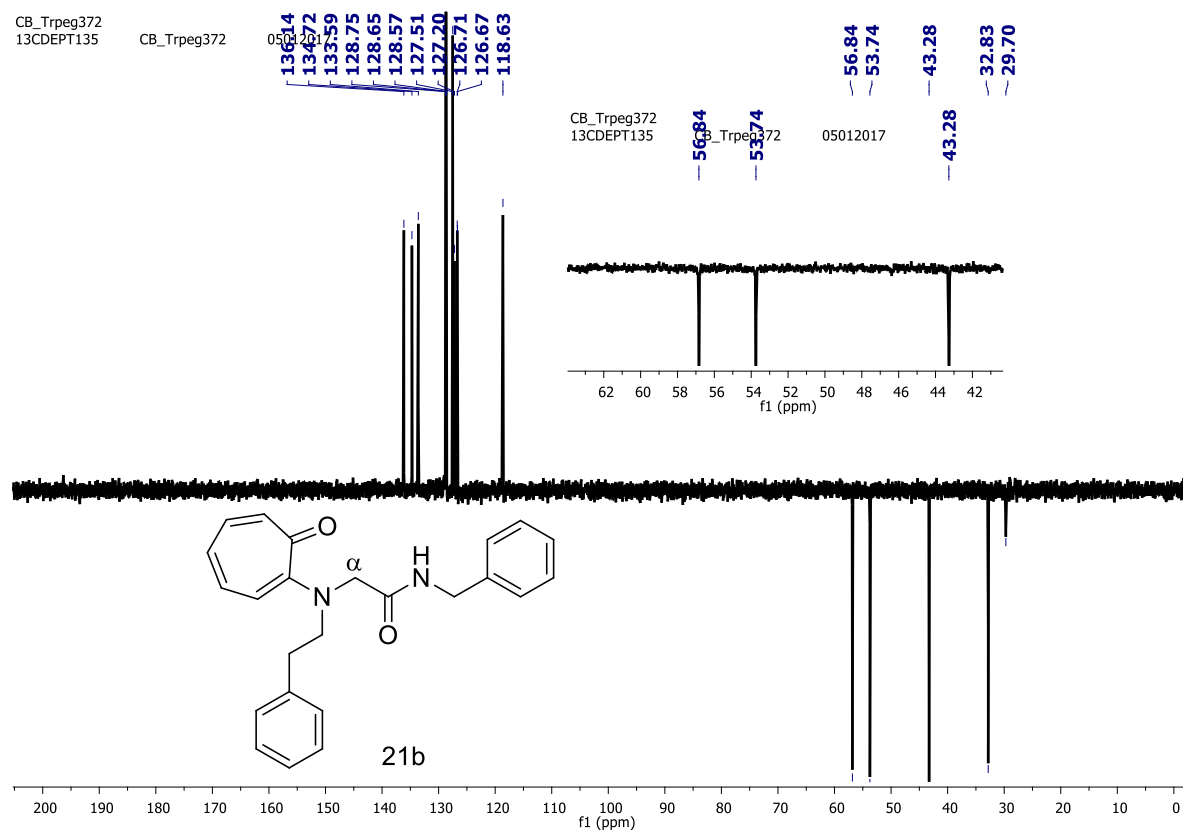


Figure A118. $^{13}\text{CDEPT135}$ NMR spectrum of *Trpeg-NHCH₂Ph* (**21**) in CDCl_3

Generic Display Report

Analysis Info

Analysis Name D:\Data\JAN-2017\NKS\10012017_NKS_CB_372_R.d
 Method Pos_tune_low.m
 Sample Name Bruker micro TOF -Q II
 Comment

Acquisition Date 1/10/2017 3:46:55 PM

Operator Amit S.Sahu
 Instrument micrOTOF-Q II

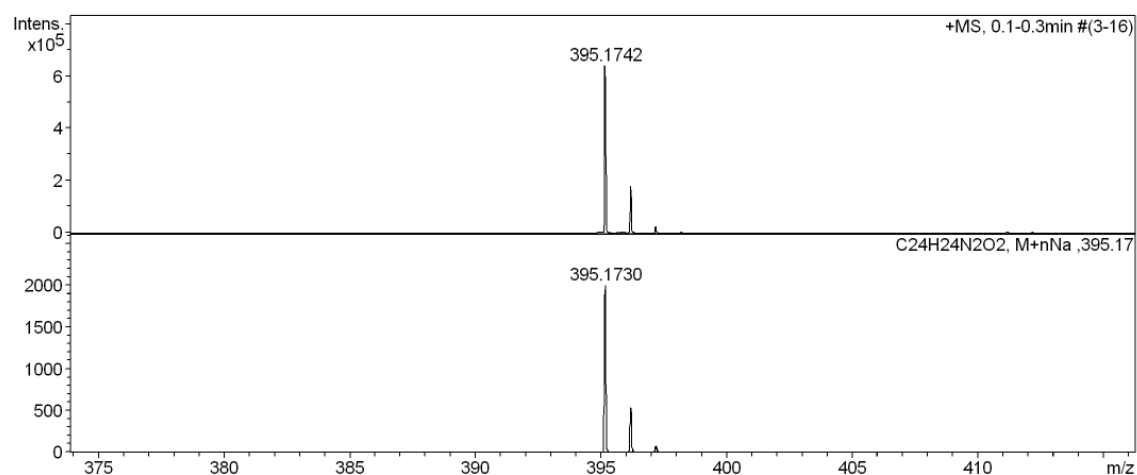
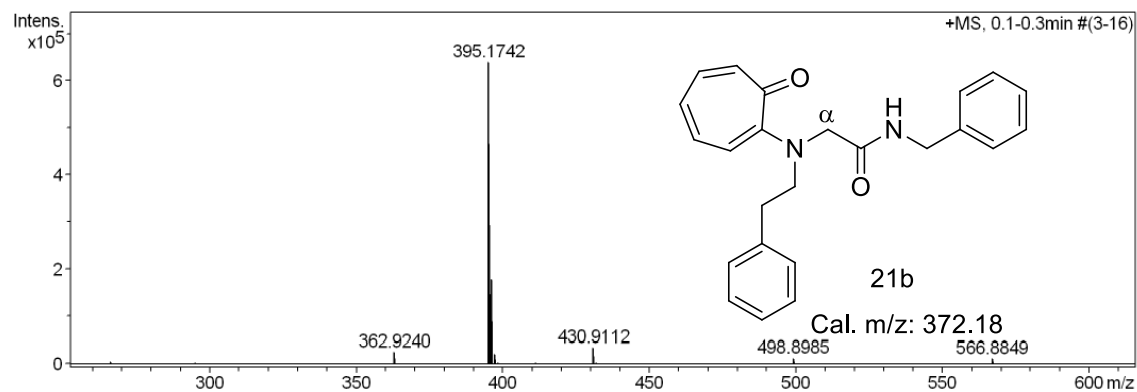
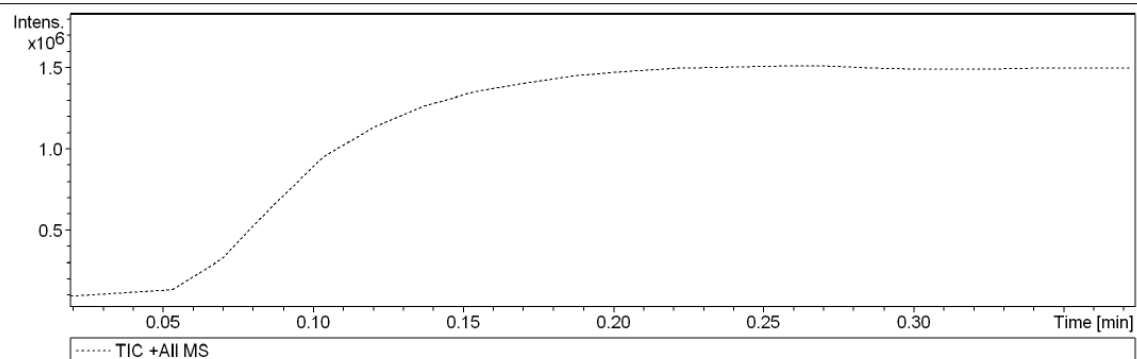


Figure A119. HRMS spectra of *Trpeg-NHCH₂Ph* (**21**) in CDCl₃

40. $^1\text{H}/^{13}\text{C}/\text{DEPT}135$ NMR and HRMS spectra of *Trpeg*-NHCH₂Ph and α -methylene deuterated (α -CHD) *Trpeg*-NHCH₂Ph in CDCl₃

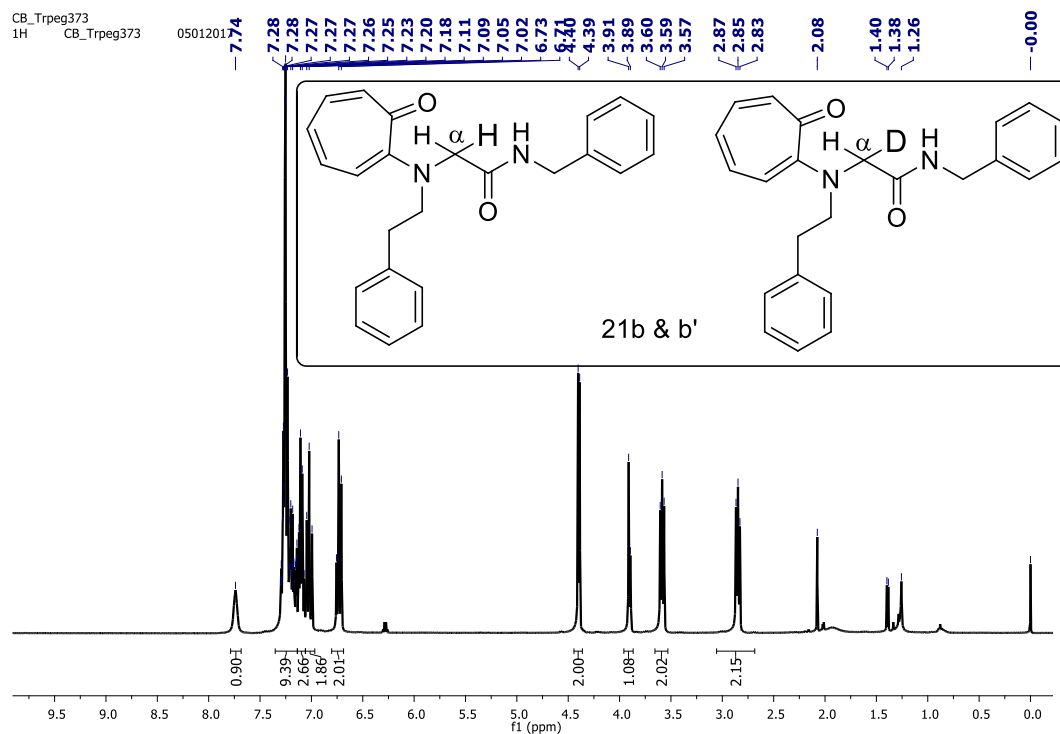


Figure A120. ^1H NMR spectrum of **21** and **21'** in CDCl₃

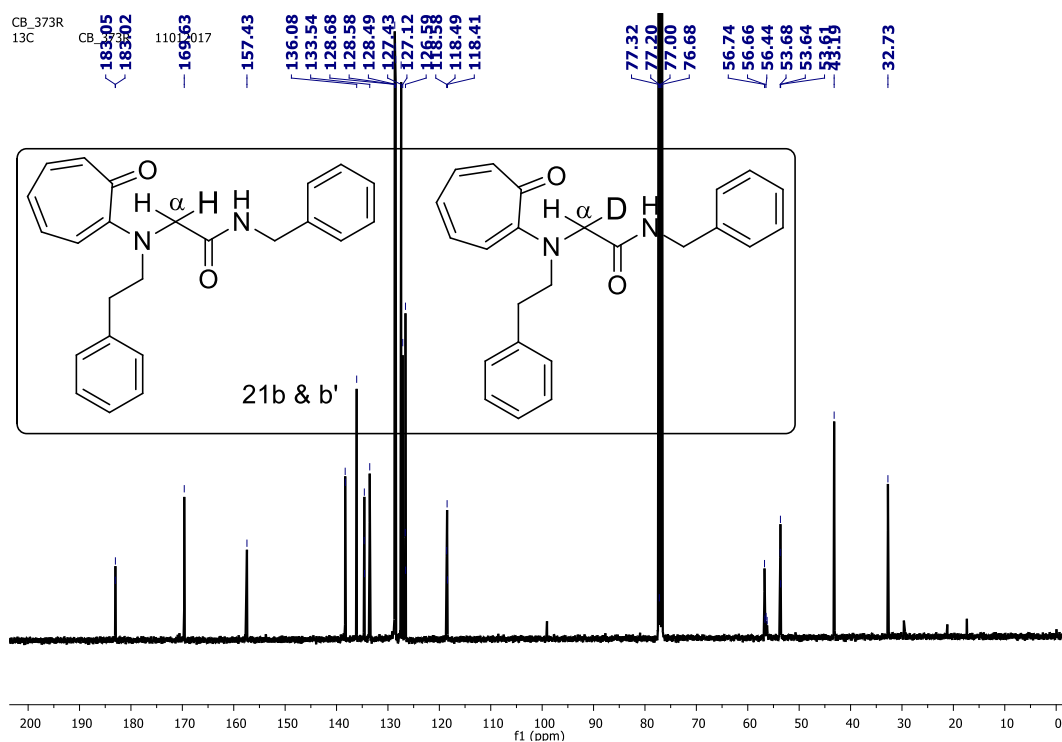


Figure A121. ^{13}C NMR spectrum of **21** and **21'** in CDCl₃

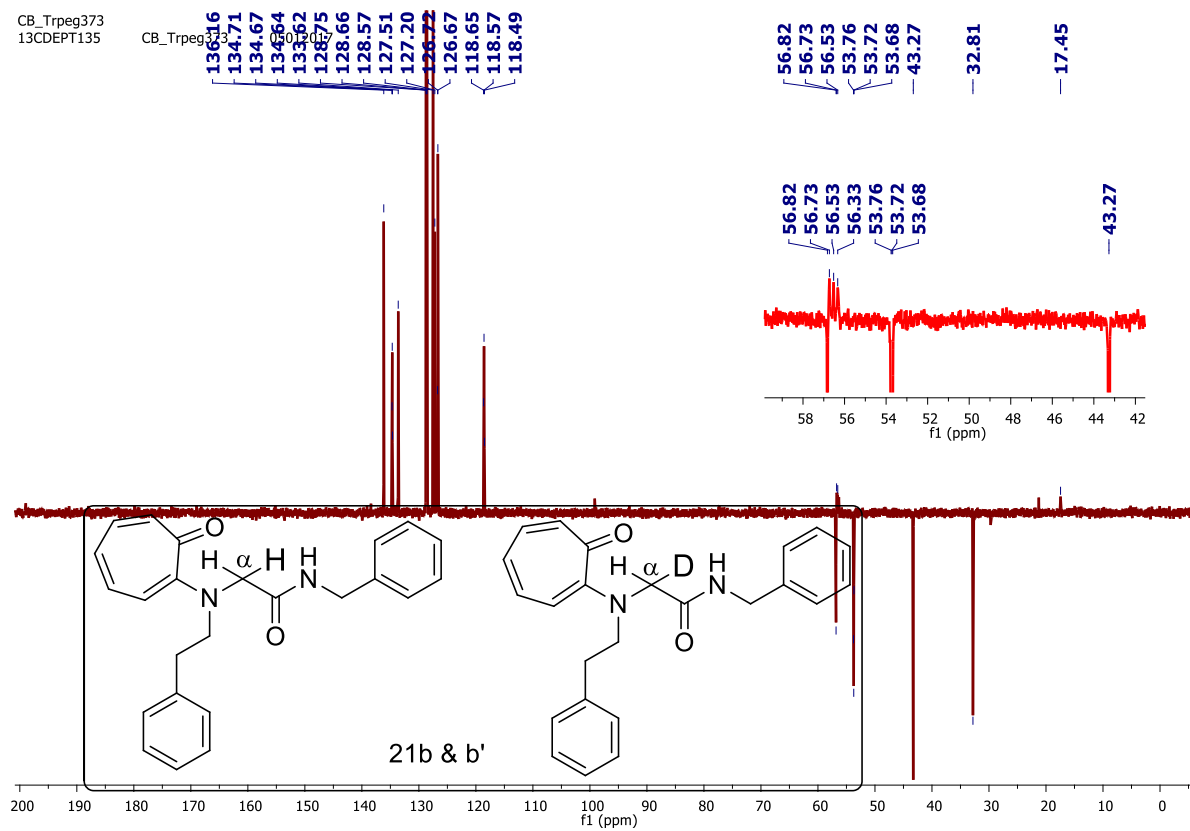


Figure A122. $^{13}\text{CDEPT135}$ NMR spectrum of **21** and **21'** in CDCl_3

Generic Display Report

Analysis Info

Analysis Name D:\Data\JAN-2017\NKS\10012017_NKS_CB_373R.d
 Method Pos_tune_low.m
 Sample Name Bruker micro TOF -Q II
 Comment

Acquisition Date 1/10/2017 3:56:21 PM

Operator Amit S.Sahu
 Instrument microTOF-Q II

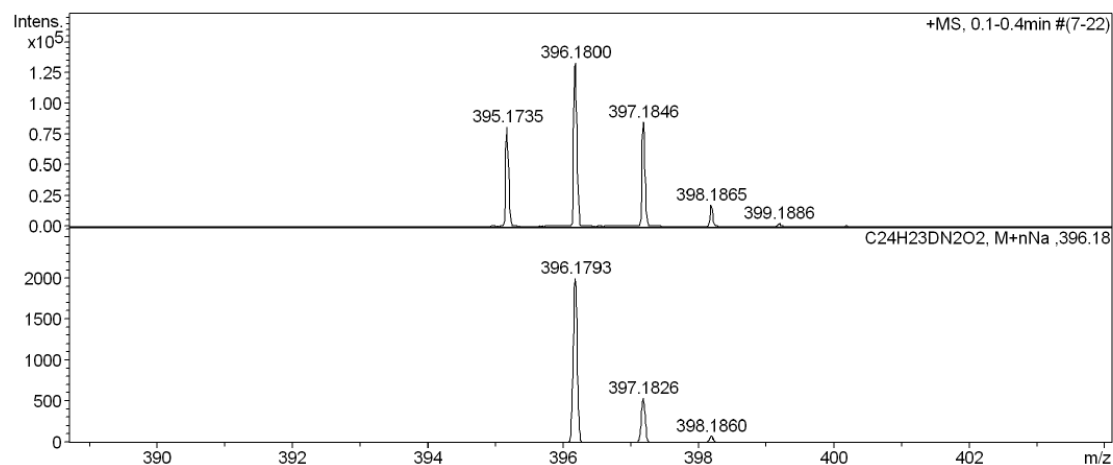
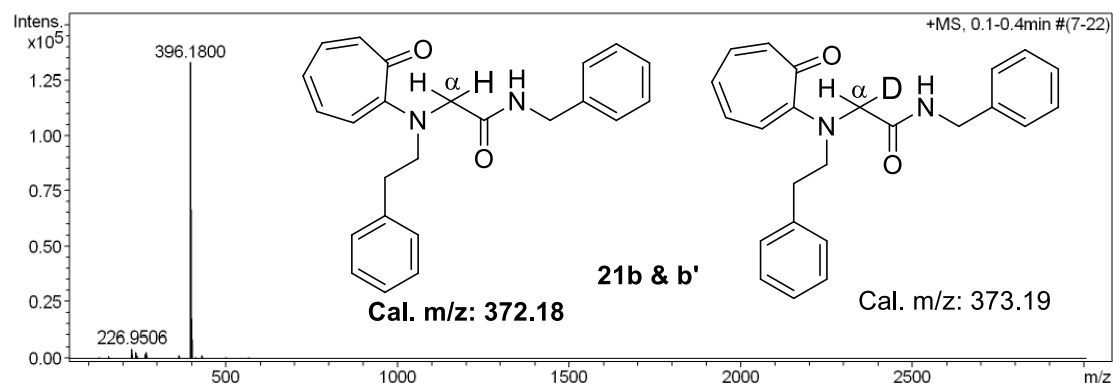
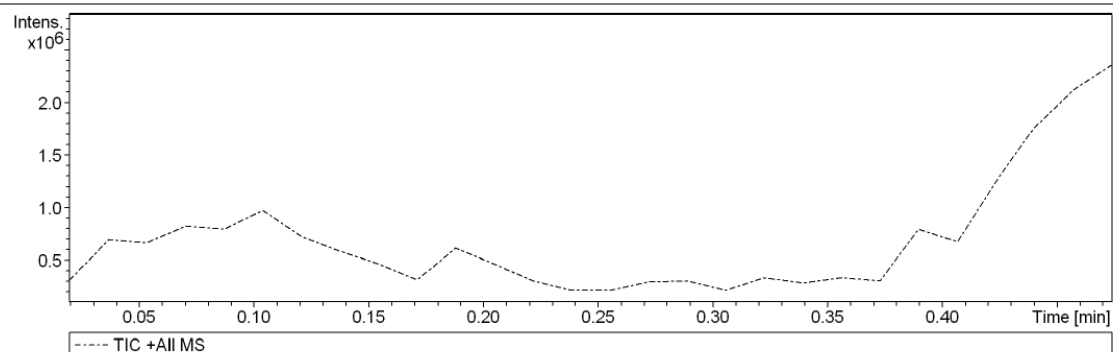


Figure A123. HRMS spectrum of **21** and **21'**

41. NMR ($^1\text{H}/^{13}\text{C}$) and HRMS spectra of Ethyl *N*-Boc aminoethyl β -alanate (**S7**):

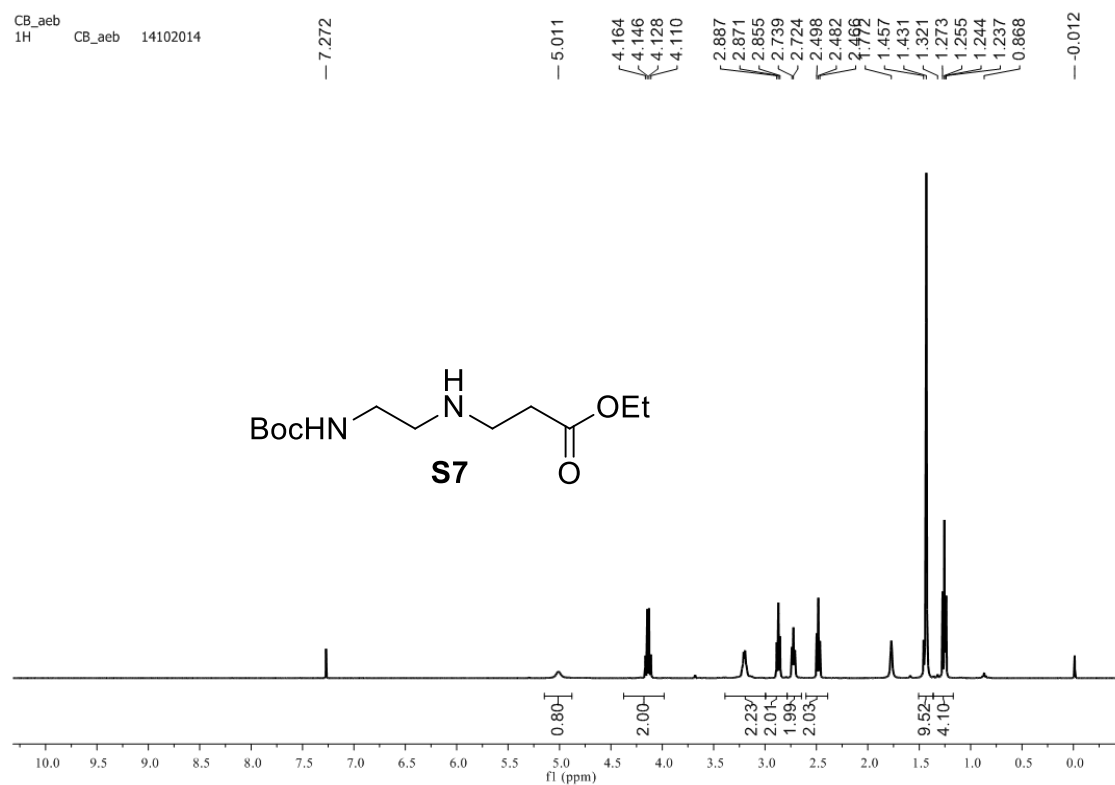


Figure A124. ^1H NMR spectrum of *Boc-aeb-OEt* (**S7**) in CDCl_3

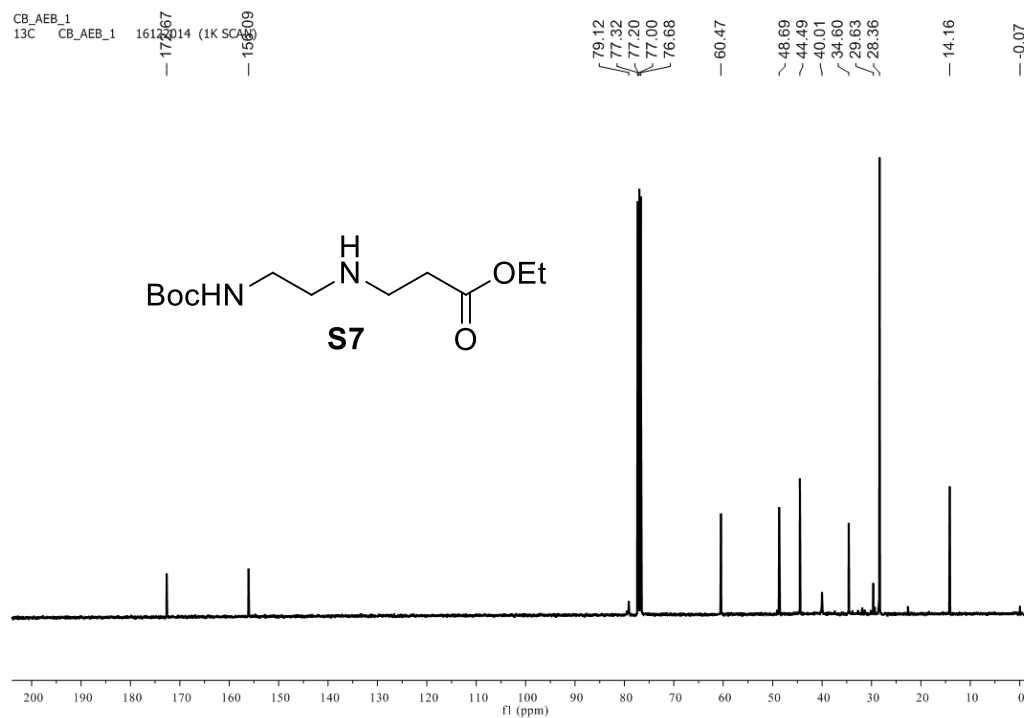


Figure A125. ^{13}C NMR spectrum of *Boc-aeb-OEt* (**S7**) in CDCl_3

Generic Display Report

Analysis Info

Analysis Name D:\Data\OCT-2014\NKS\28102014_NKS_CB_aeb.d
Method Pos_tune_low.m
Sample Name LC-MS NISER
Comment

Acquisition Date 10/28/2014 12:19:17 PM

Operator NISER
Instrument micrOTOF-Q II

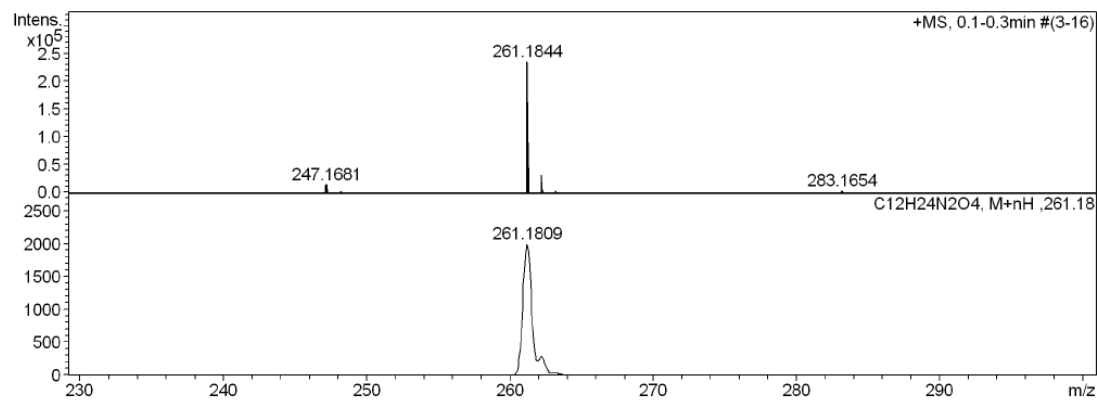
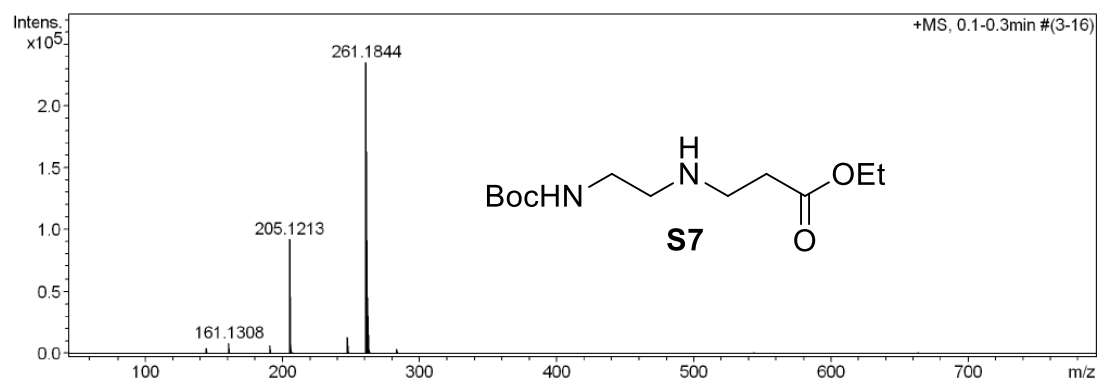
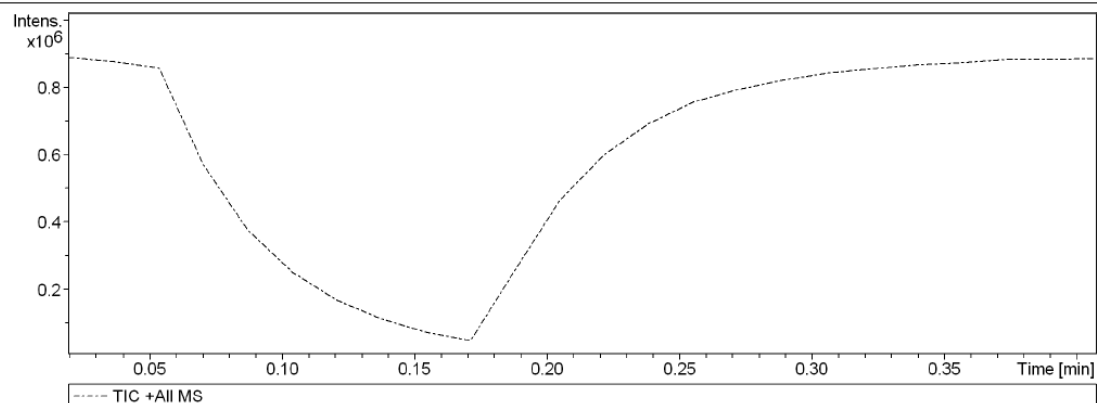


Figure A126. HRMS mass spectrum of *Boc-aeb-OEt* (S7)

42. NMR ($^1\text{H}/^{13}\text{C}$) and HRMS spectra of *Troponyl aminoethyl β -alanate (7-OEt)*:

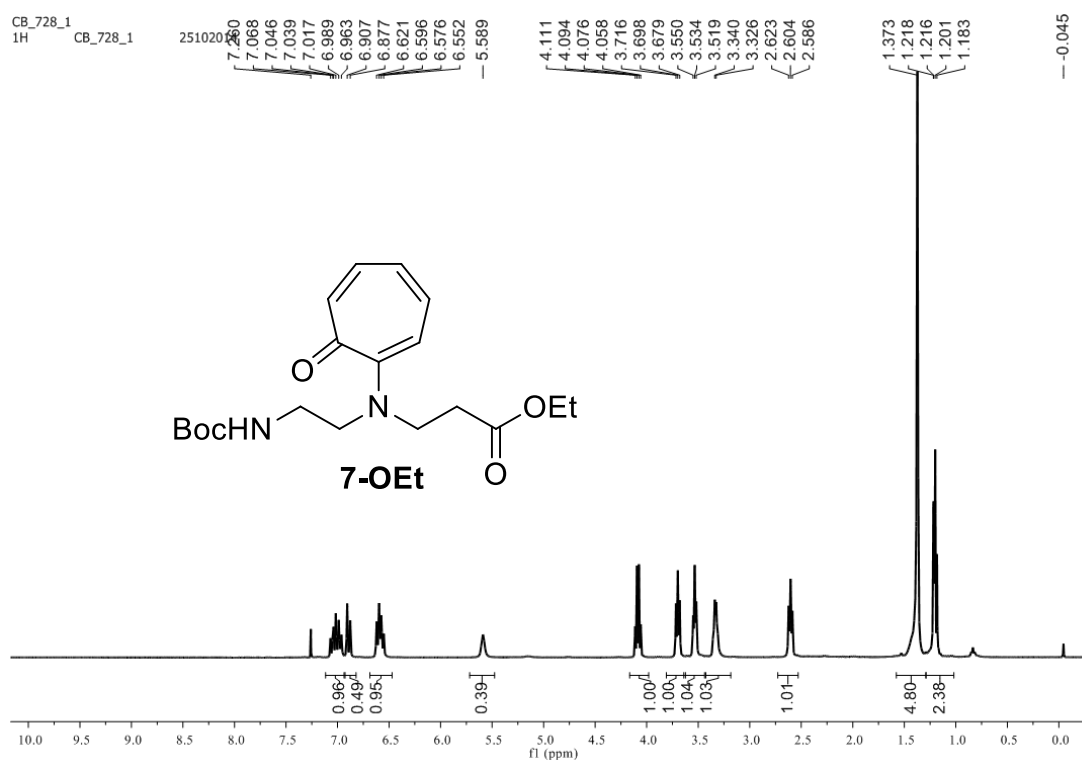


Figure A127. ^1H NMR spectrum of *Boc-NH-Traeb-OEt (7-OEt)* in CDCl₃

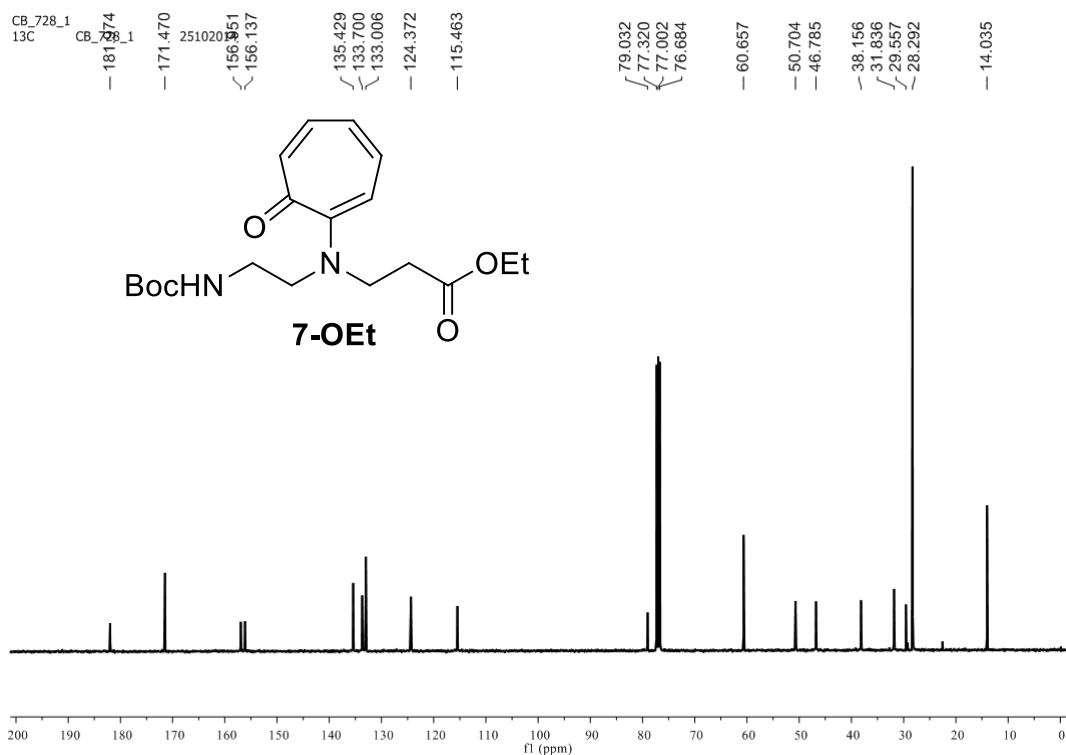


Figure A128. ^{13}C NMR spectrum of *Boc-NH-Traeb-OEt (7-OEt)* in CDCl₃

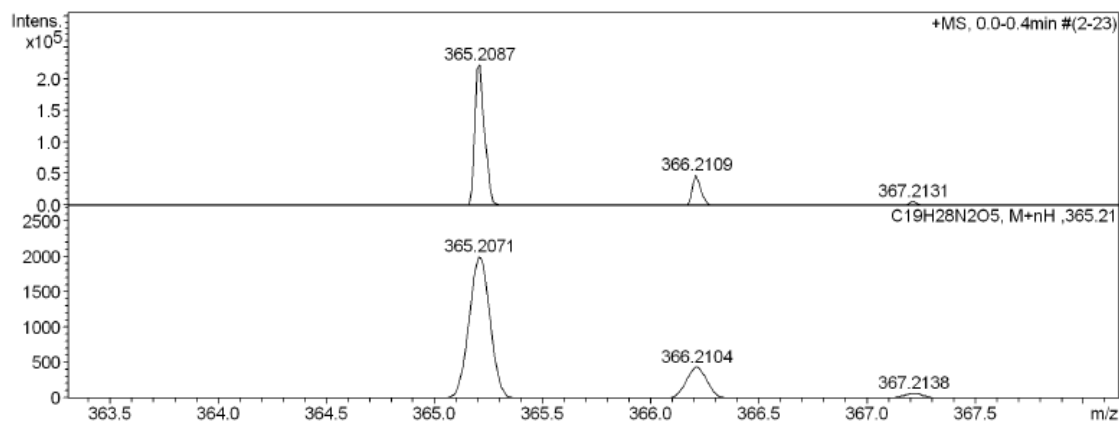
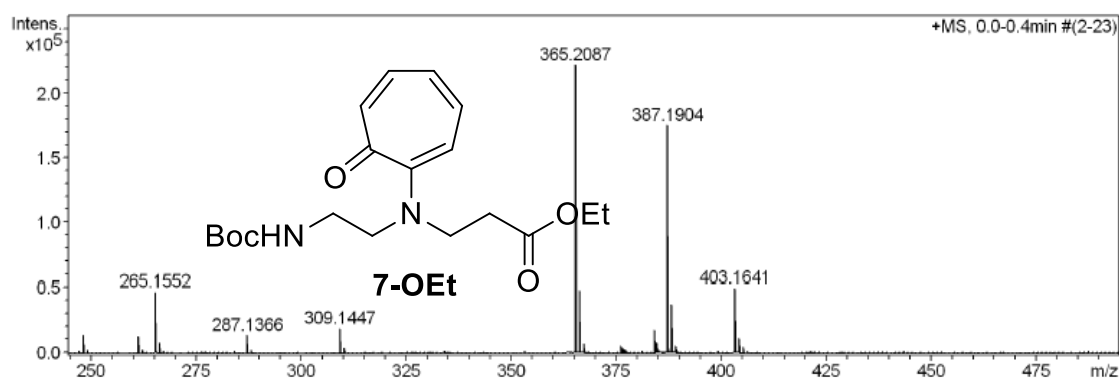
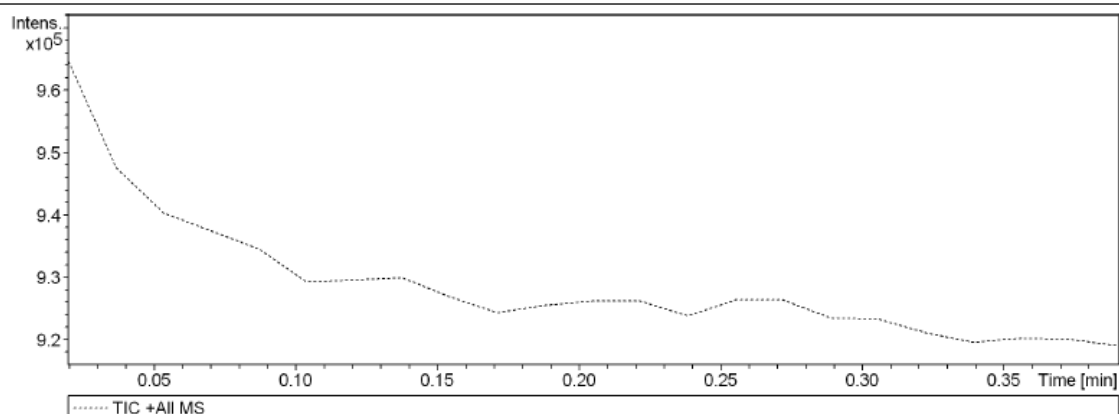
Generic Display Report

Analysis Info

Analysis Name D:\Data\OCT-2014\NKS\28102014_NKS_CB_aebtr.d
 Method Pos_tune_low.m
 Sample Name LC-MS NISER
 Comment

Acquisition Date 10/28/2014 2:14:30 PM

Operator NISER
 Instrument micrOTOF-Q II



Bruker Compass DataAnalysis 4.0

printed: 12/22/2014 3:41:18 PM

Page 1 of 1

Figure A129. HRMS mass spectrum of *BocNH-Traeb-OEt* (7-OEt)

43. Mass spectrum of *Troponyl aminoethyl β-alanine* (**7**):

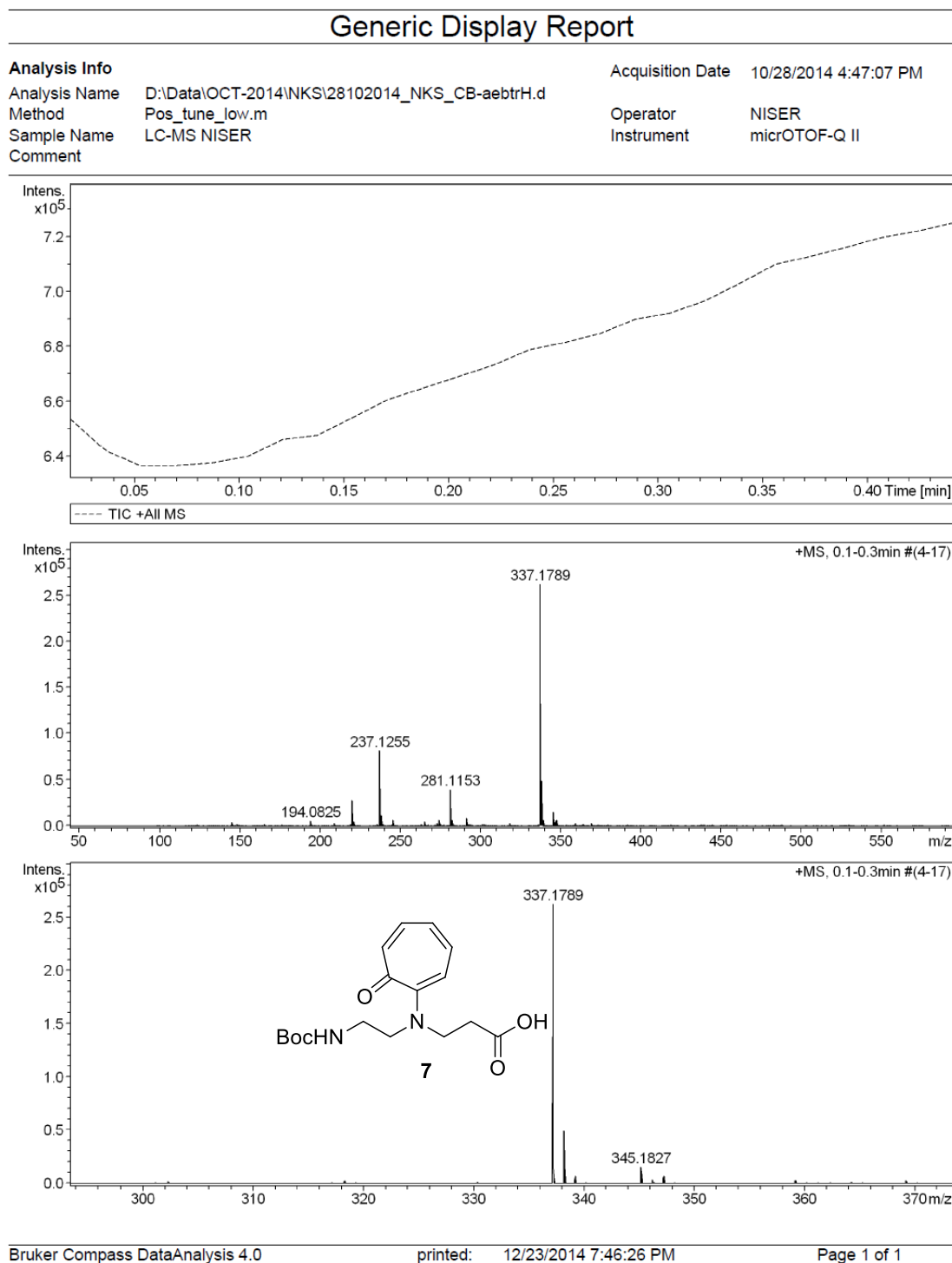


Figure A130. Mass spectrum of *BocNH-Traeb-OH* (**7**).

44. Characterization data ($^1\text{H}/^{13}\text{C}$ NMR and HRMS), Time dependent NMR and Mass spectrum after time dependent NMR *BocNH-Traeb-Ile-OMe* (**15**):

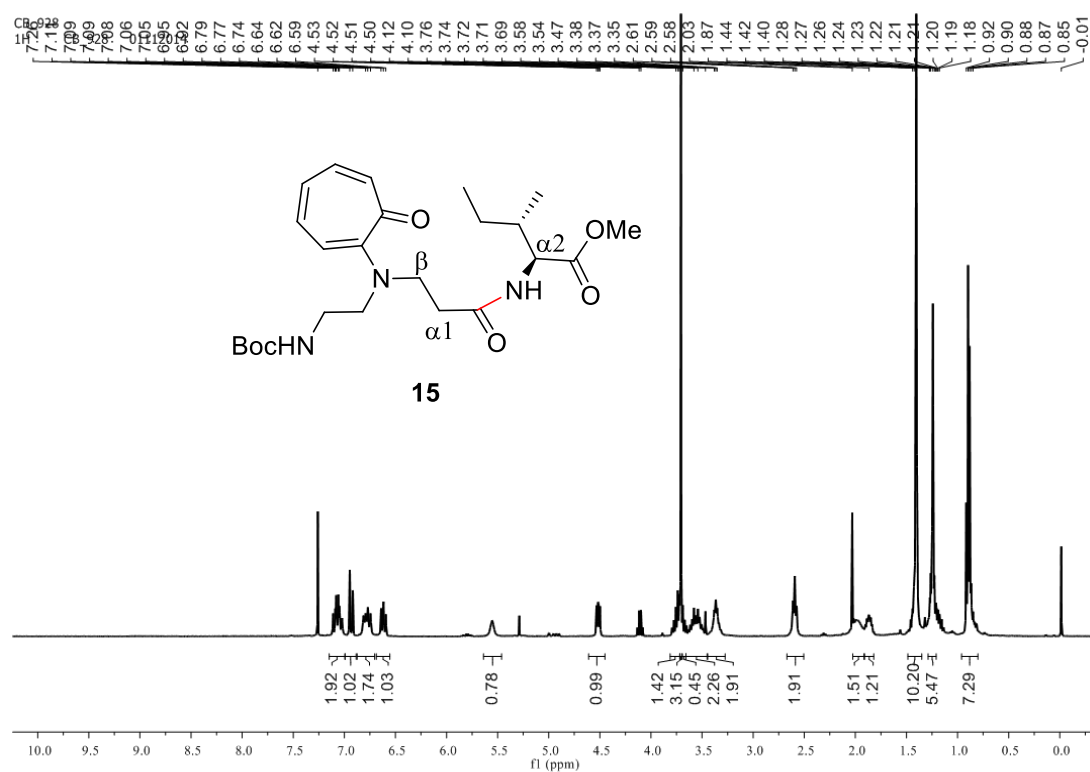


Figure A131. ^1H NMR spectrum of *BocNH-Traeb-Ile-OMe* (**15**) in CDCl_3

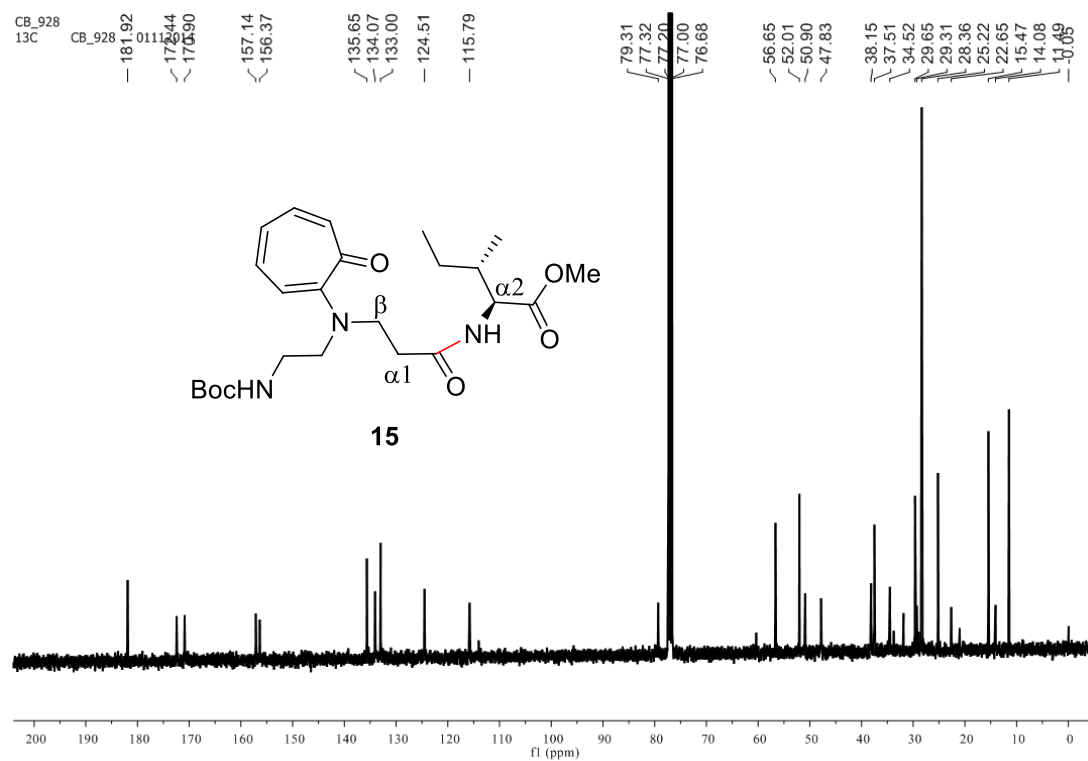


Figure A132. ^{13}C -NMR spectrum of *BocNH-Traeb-Ile-OMe* (**15**) in CDCl_3

Generic Display Report

Analysis Info

Analysis Name D:\Data\NOV-2014\NKS\1112014_NKS_CB_AEBTRILE4PU1.d

Method Pos_tune_low.m

Sample Name LC-MS NISER

Comment

Acquisition Date 11/1/2014 2:33:43 PM

Operator NISER

Instrument micrOTOF-Q II

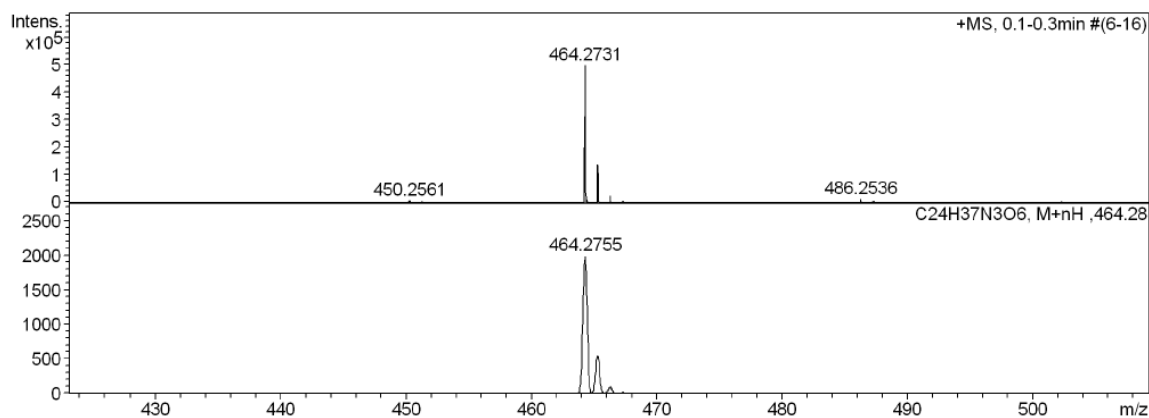
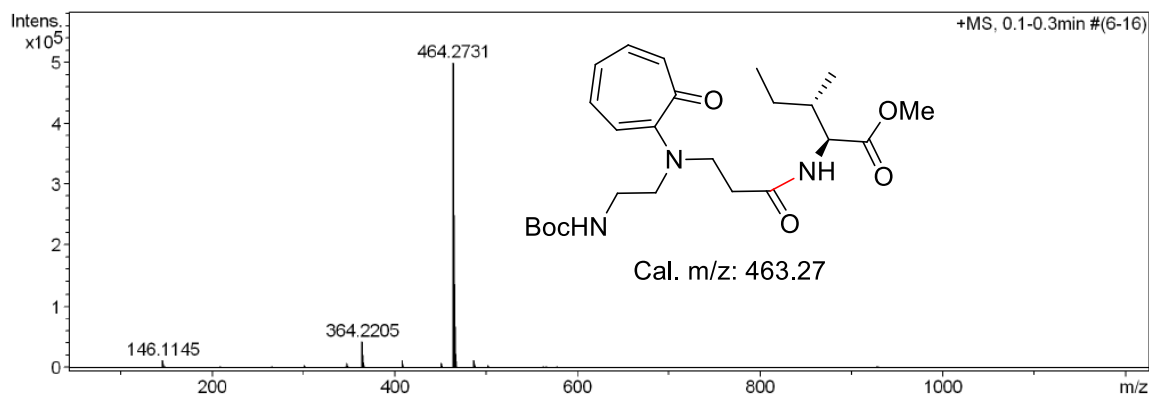
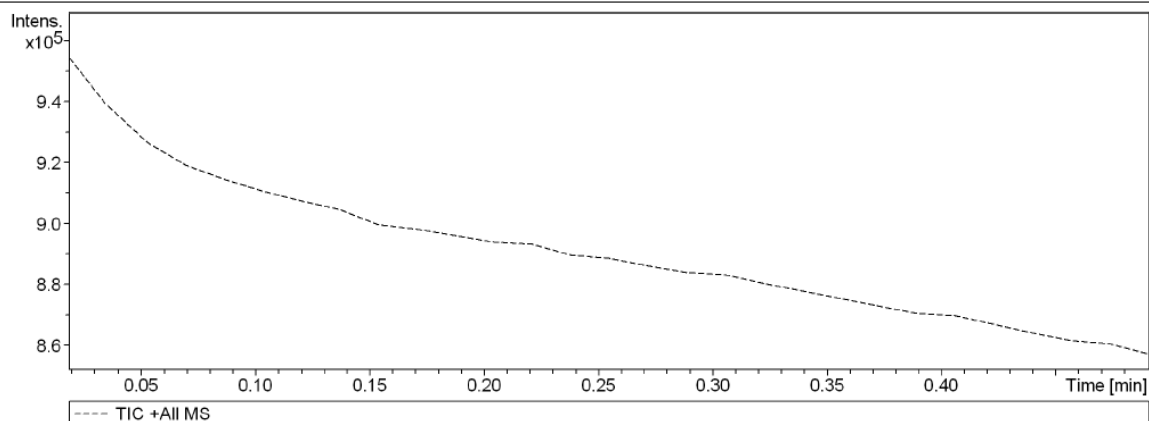


Figure A133. HRMS mass spectrum of *BocNH-Traeb-Ile-OMe* (15)

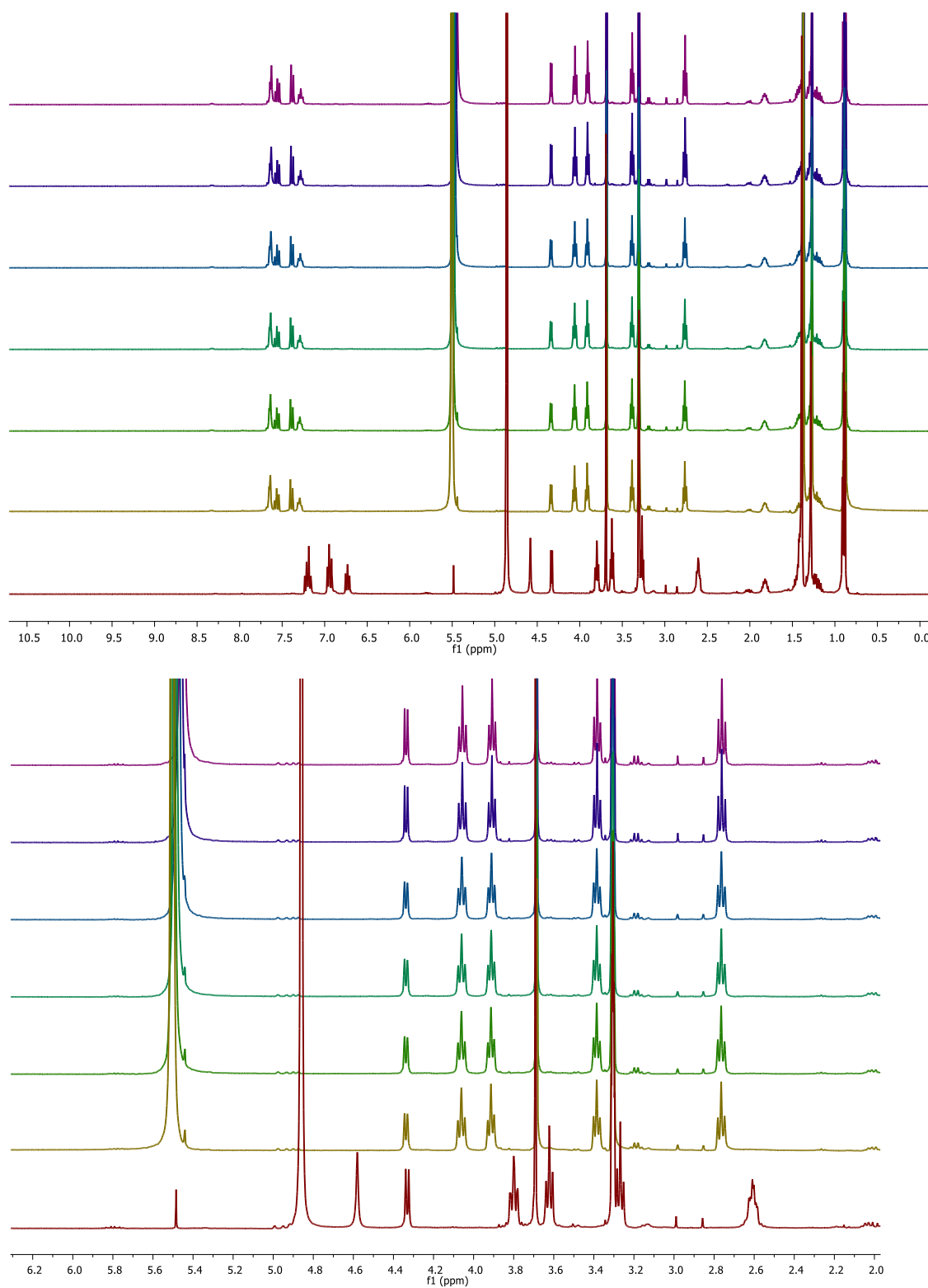


Figure A134. Time dependent NMR of *BocNH-Traeb-Ile-OMe* (**15**) in CD₃OD and 5% TFA.

Generic Display Report

Analysis Info

Analysis Name D:\Data\NOV-2014\NKS\08112014_NKS_CB_928TFACD30D2H.d
Method Pos_tune_low.m
Sample Name 07112014NKSGC_196_24HPTTP+KLEN
Comment

Acquisition Date 11/8/2014 9:12:38 PM

Operator NISER

Instrument micrOTOF-Q II

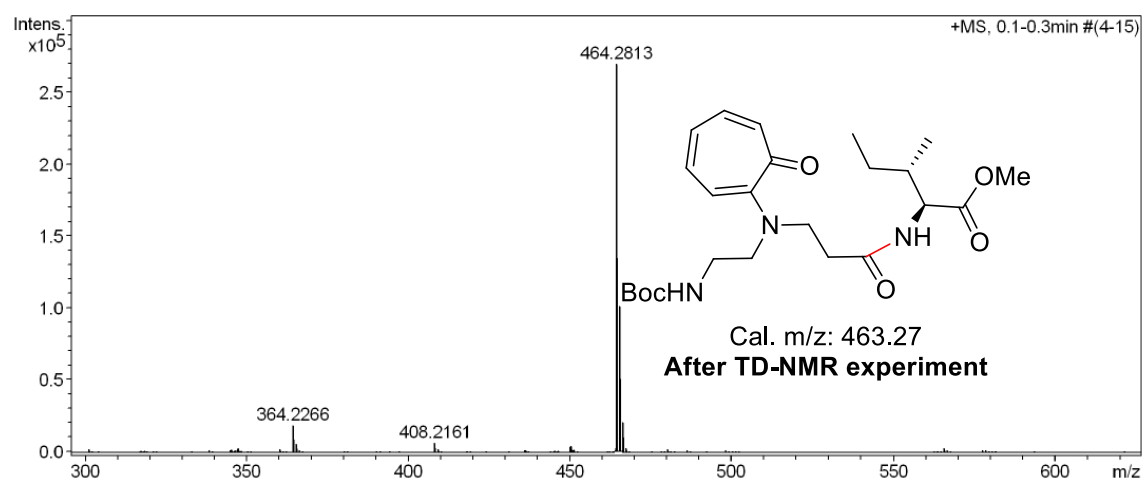
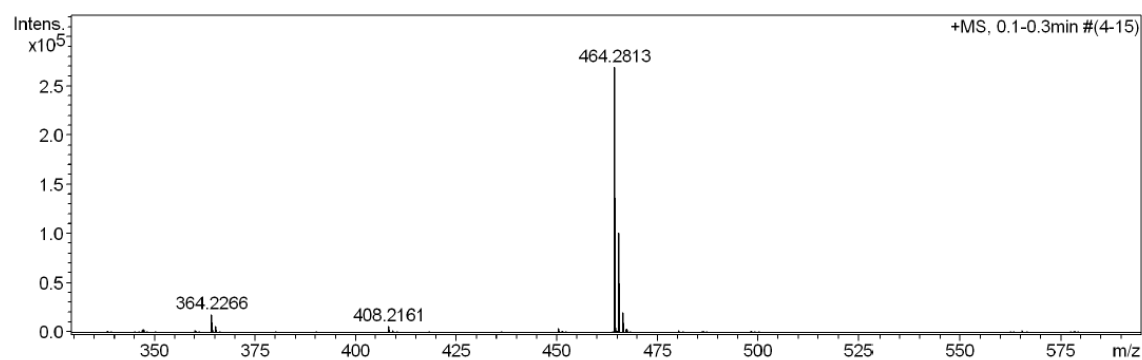
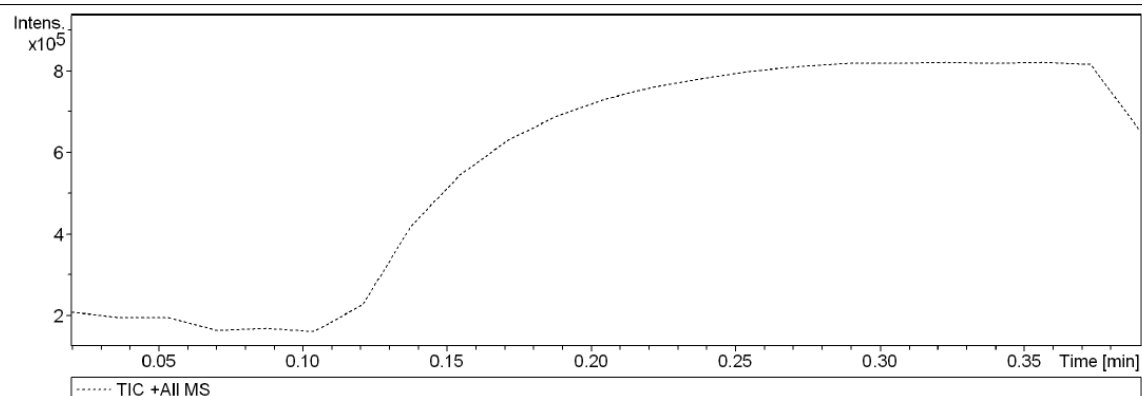


Figure A135. Mass spectrum of *BocNH-Traeb-Ile-OMe* (**15**) after time dependent NMR experiment in CD₃OD.

Generic Display Report

Analysis Info

Analysis Name D:\Data\NOV-2014\NKS\01112014_NKS_CB_928TFAOVERNIGHT.d
Method Pos_tune_low.m
Sample Name LC-MS NISER
Comment

Acquisition Date 11/2/2014 11:12:14 AM
Operator NISER
Instrument micrOTOF-Q II

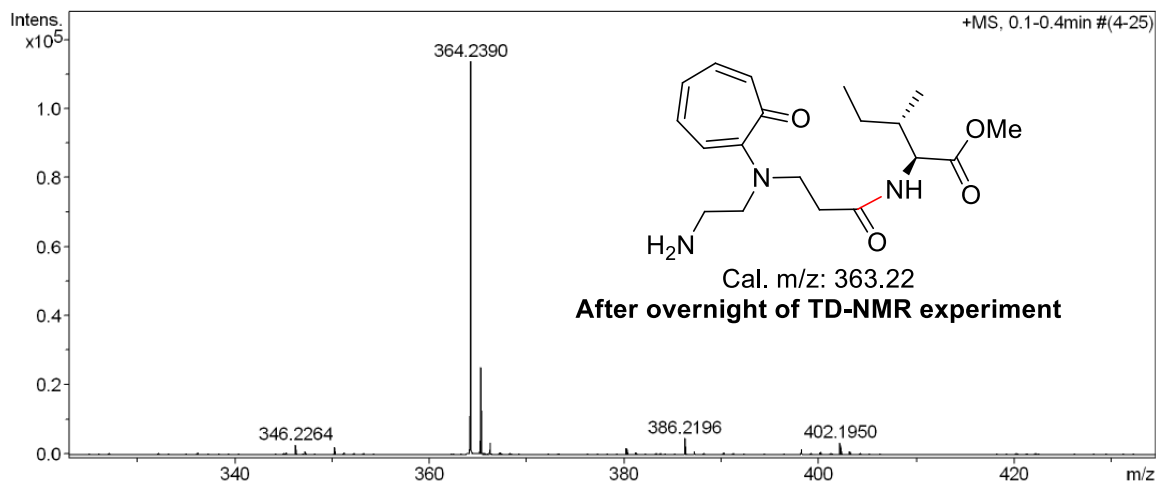
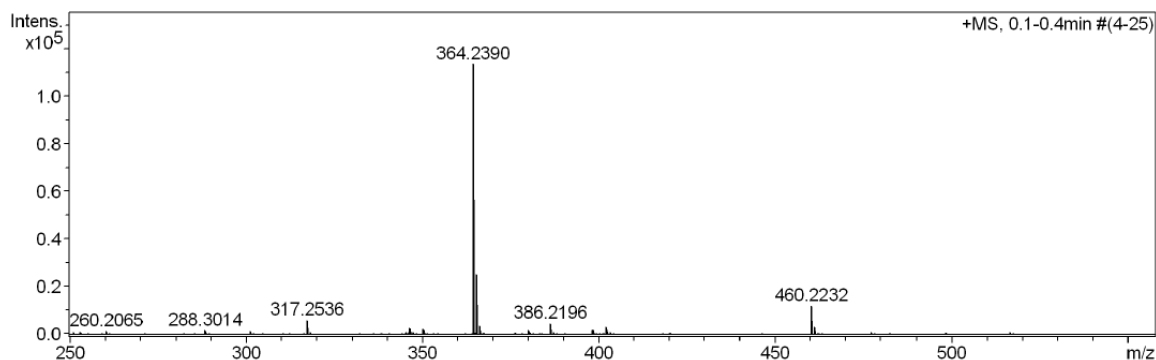
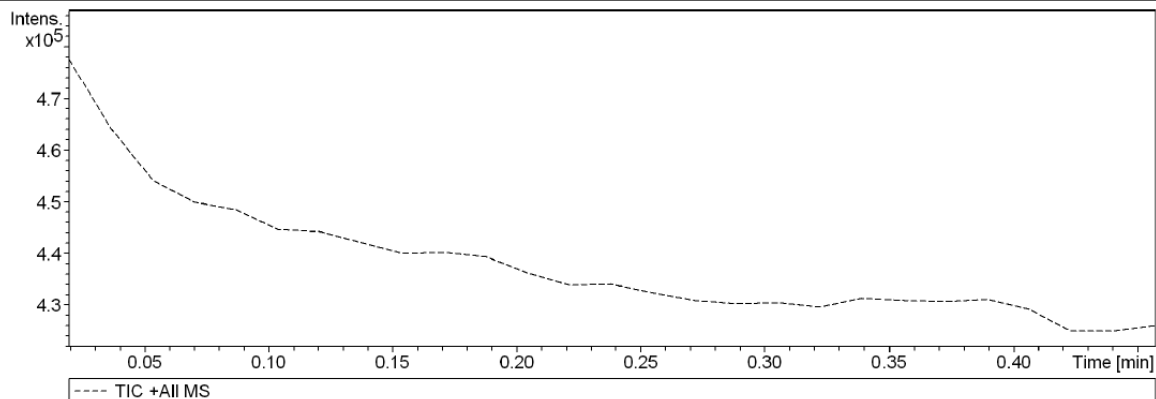


Figure A136. Mass spectrum of BocNH-Traeb-Ile-OMe (**15**) after time dependent NMR experiment in CD₃OD after overnight.

45. Characterization data ($^1\text{H}/^{13}\text{C}$ NMR and HRMS) of *BocNH-AAIB-OEt*:

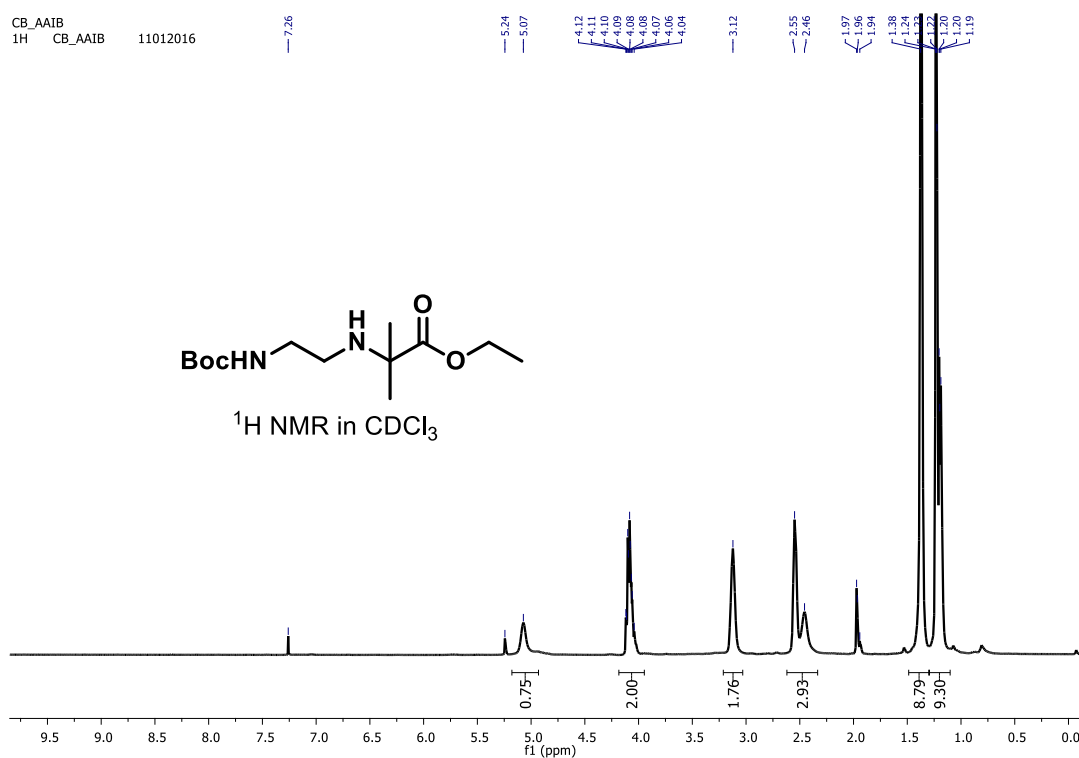


Figure A137. ^1H NMR spectrum of *BocNH-AAIB-OEt* in CDCl_3

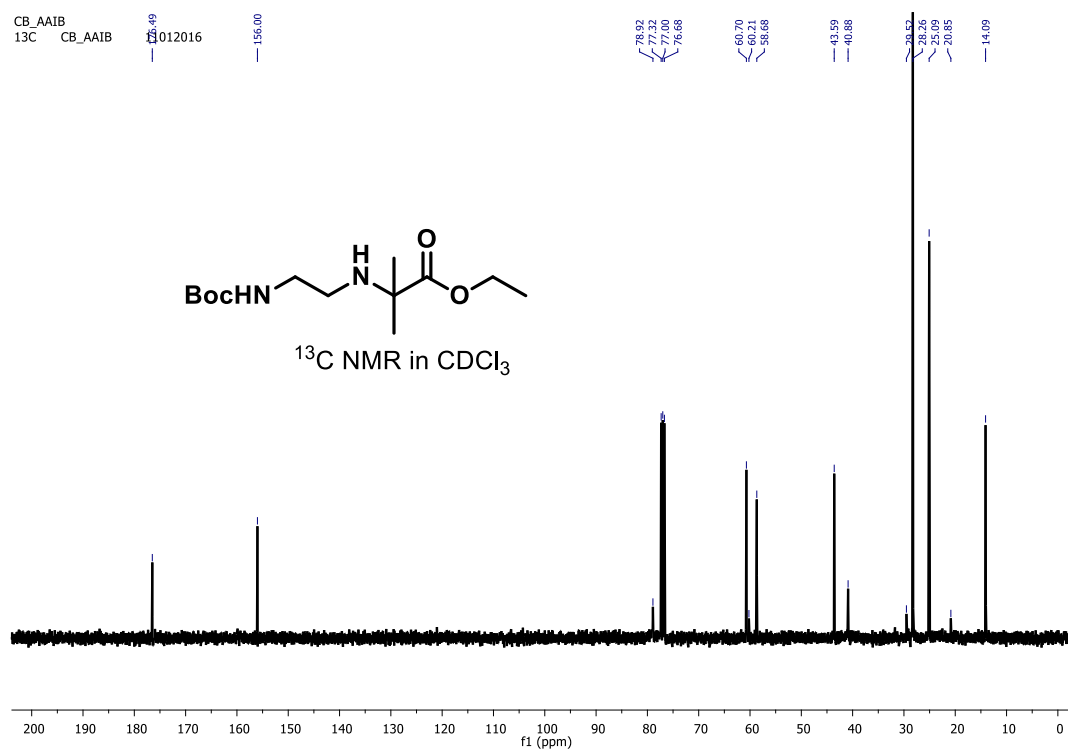


Figure A138. ^{13}C NMR spectrum of *BocNH-AAIB-OEt* in CDCl_3

Display Report

Analysis Info

Analysis Name D:\Data\JAN-2016\NKS\05012016_NKS_CB_AAIB.d
 Method Pos_tune_low.m
 Sample Name Bruker micro TOF -Q II
 Comment

Acquisition Date 1/5/2016 3:30:33 PM

Operator A.S.SAHU
 Instrument micrOTOF-Q II 10337

Acquisition Parameter

Source Type	ESI	Ion Polarity	Positive	Set Nebulizer	0.4 Bar
Focus	Not active	Set Capillary	4000 V	Set Dry Heater	180 °C
Scan Begin	50 m/z	Set End Plate Offset	-500 V	Set Dry Gas	4.0 l/min
Scan End	3000 m/z	Set Collision Cell RF	130.0 Vpp	Set Divert Valve	Waste

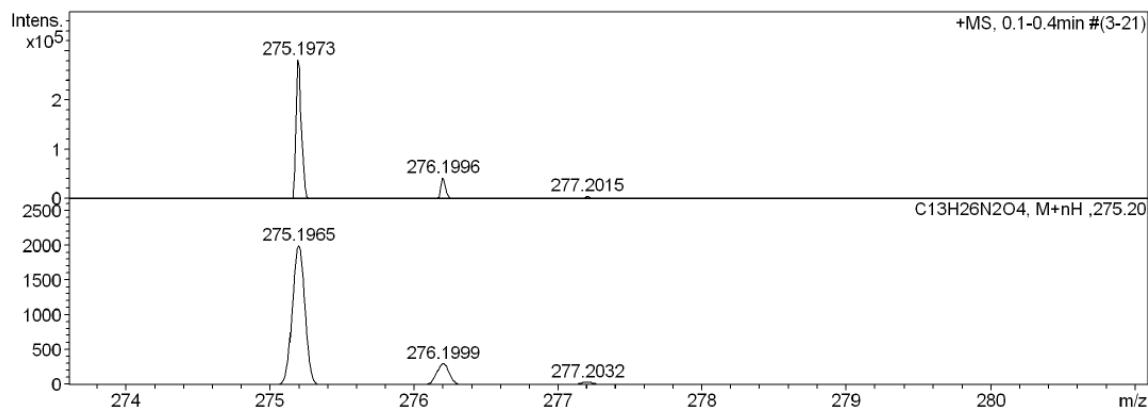
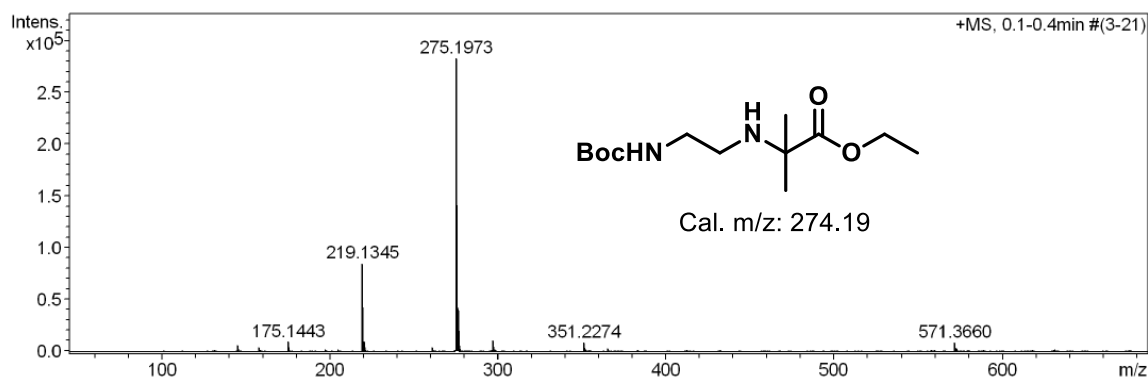
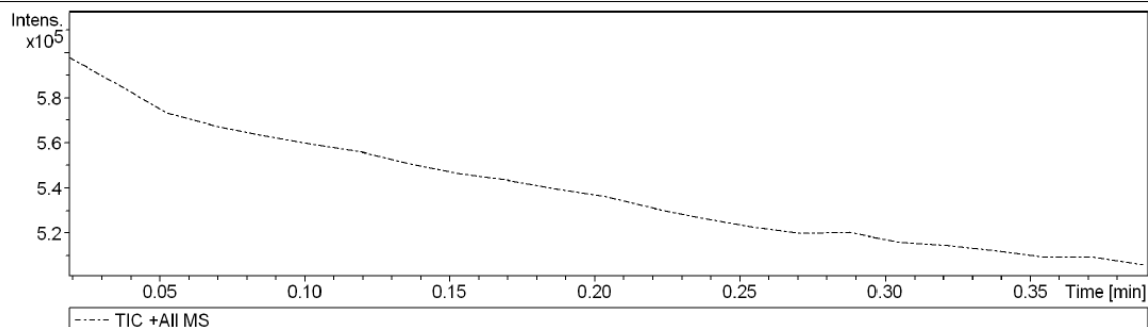


Figure A139. HRMS spectrum of *BocNH-AAIB-OEt*

Display Report

Analysis Info

Analysis Name D:\Data\JAN-2016\NKS\05012016_NKS_CB_AALA.d
 Method Pos_tune_low.m
 Sample Name Bruker micro TOF -Q II
 Comment

Acquisition Date 1/5/2016 3:13:40 PM
 Operator A.S.SAHU
 Instrument microOTOF-Q II 10337

Acquisition Parameter

Source Type	ESI	Ion Polarity	Positive	Set Nebulizer	0.4 Bar
Focus	Not active	Set Capillary	4000 V	Set Dry Heater	180 °C
Scan Begin	50 m/z	Set End Plate Offset	-500 V	Set Dry Gas	4.0 l/min
Scan End	3000 m/z	Set Collision Cell RF	130.0 Vpp	Set Divert Valve	Waste

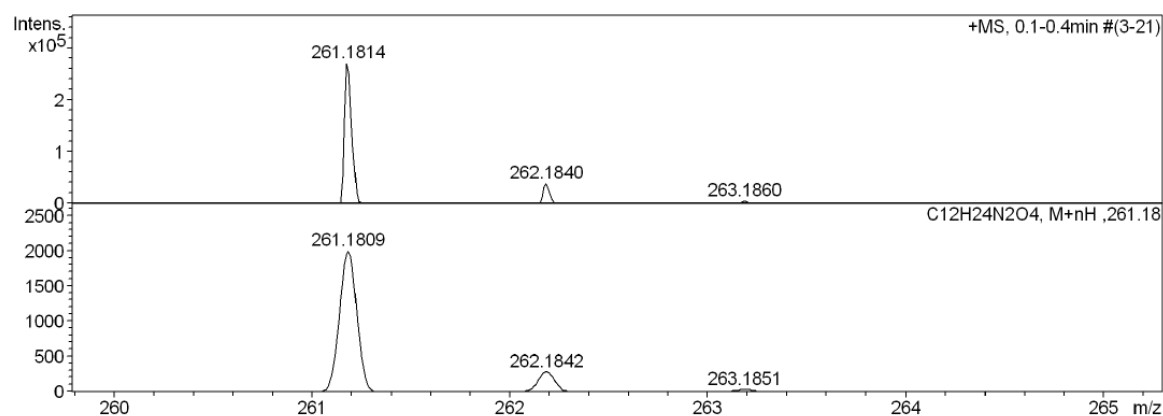
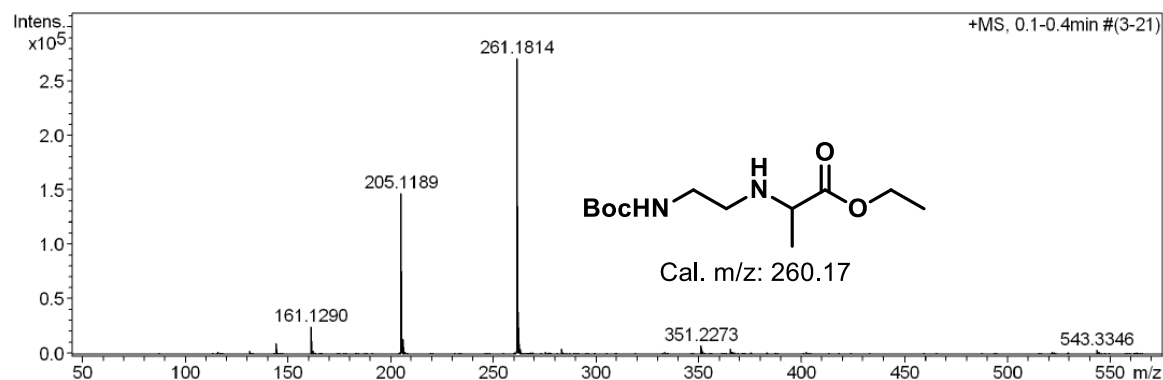
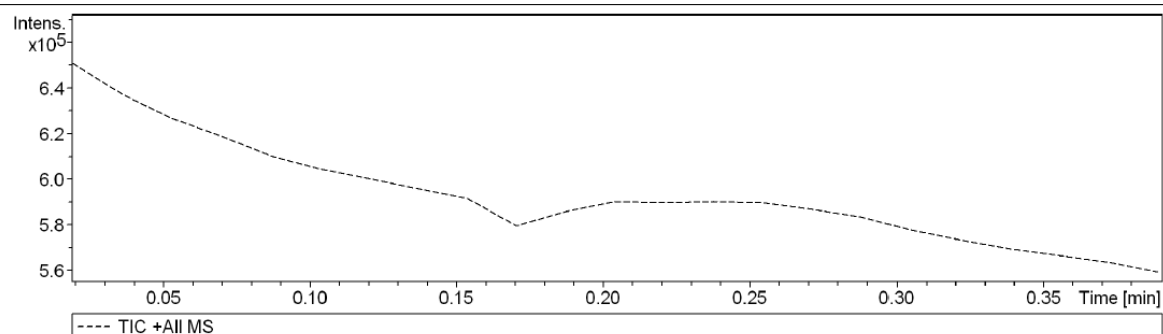
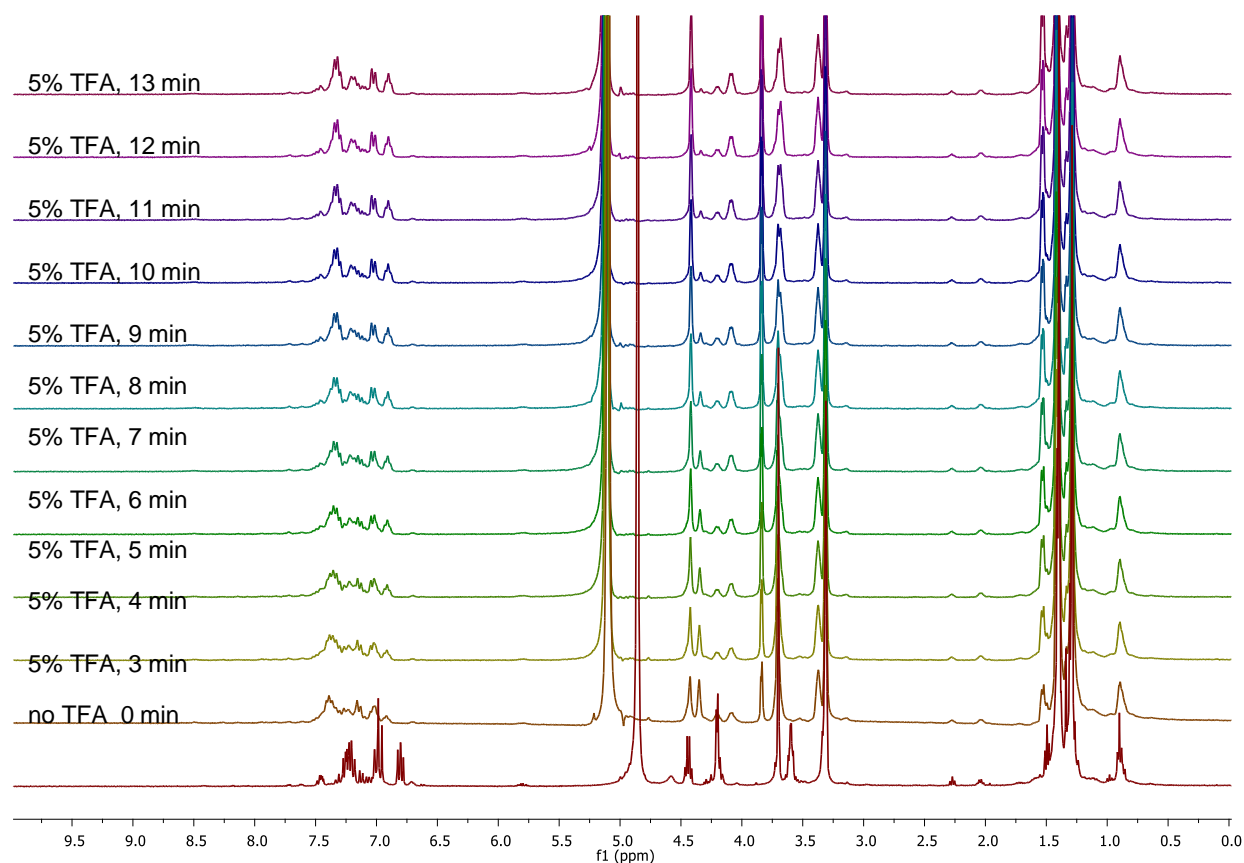


Figure A140. HRMS spectrum of *BocNH-AAIa-OEt*

46. Rate constant determination of amide solvolysis (CD_3OD) in peptide **13f**:

NMR experiment: 6.0 mg of peptide (**13f**) was dissolved in 450.0 μL of CD_3OD and recorded NMR. Then 23.0 μL of TFA was added to the sample, obtained the first ^1H NMR spectra after 3.0 minutes and remaining are with 1.0 minute time interval. In order to maintain time, the spectrum was generated with 5 scans

a) Full range spectra



b) Expanded spectra (2.0-6.0 ppm)

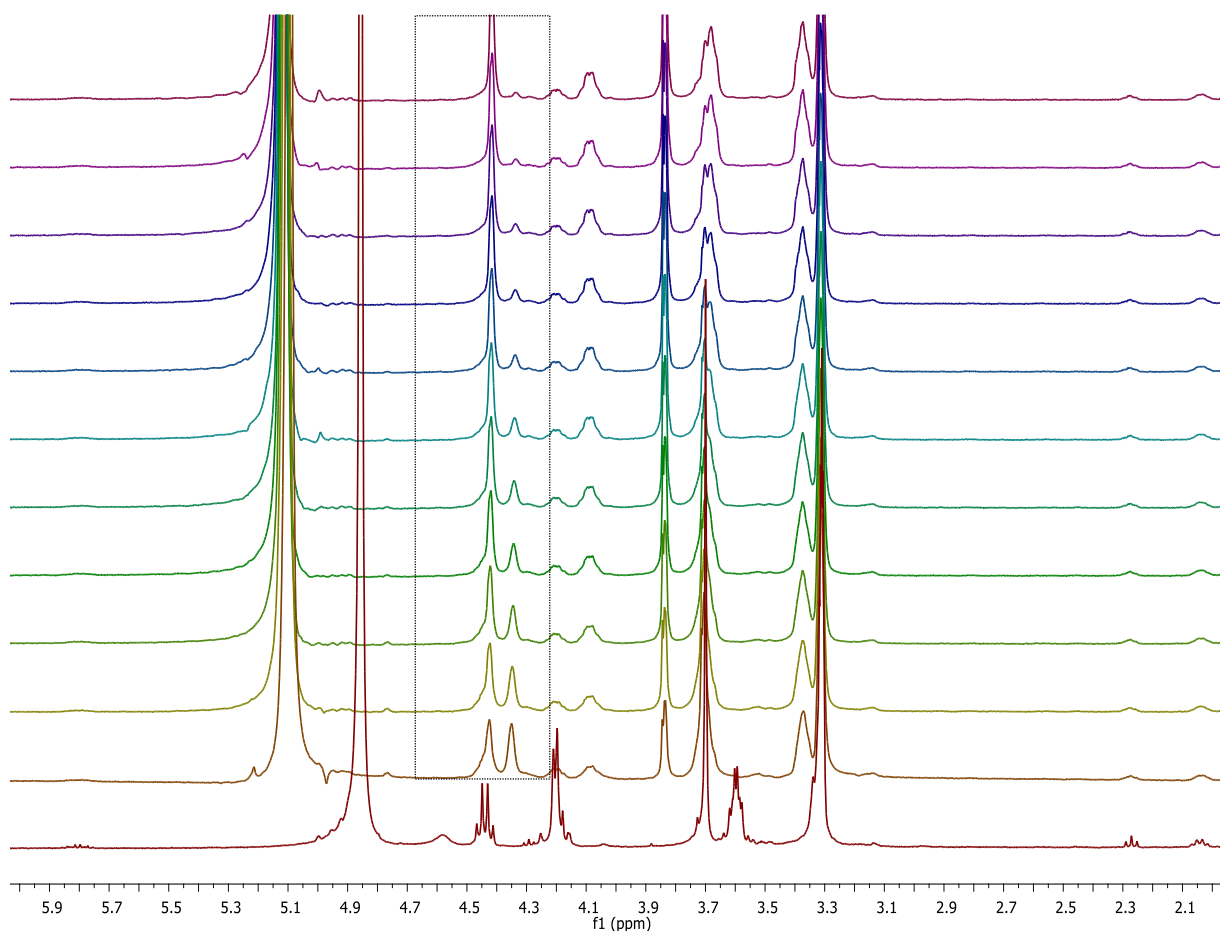


Figure A141. Time dependent NMR of *BocNH-Traeg-ala-OMe* (**13f**) in CD₃OD and 5% TFA. A) full range and b) expanded range (2.0-6.0 ppm). The spectra were obtained with 1 minute time interval and 5 scans.

Procedure for rate constant determination:

Peptide (**13f**) was taken in 450 μ L of 5% CD₃OD solution and studied with NMR. From integrated NMR spectra, the mole fraction of the peptide α -CH₂ with time was calculated by following literature procedure.¹ We considered the pseudo first order kinetics with respect to concentration of peptide **13f**.

Rate constant of peptide 6b by NMR

Since Pseudo 1st order reaction



Pseudo 1st order kinetic equation:

$$A_t = A_0 \cdot \exp(-kt); \text{ equation in Integrated form: } \ln(A_t/A_0) = -kt$$

A₀: Initial of concentration of starting material (A) at time Zero

A_t: concentration of starting material at time t

t: Time; k: rate constant of reaction; Half-life of reaction (T_{1/2}): $\ln(2)/k$

Herein we calculated the rate constant of hydrolysis of peptide **13f** with 5.0% TFA by Time dependent ¹H-NMR studies. We have extracted integration of α-CH₂ proton (δ 4.35 ppm) at different interval of time by considering the CH₃ proton of methyl ester of **13f** as reference with Integration 3.0.

Total Integration before adding TFA	0	2		
Time (min)	Integration α1-CH ₂ at δ-4.45	Integration α1- CH ₂ at δ-4.35	I _t /I ₀	ln(I _t /I ₀)
3	1.25	1.5	0.75	-0.28768
4	1.36	0.87	0.435	-0.83241
5	1.38	0.71	0.355	-1.03564
6	1.42	0.61	0.305	-1.18744
7	1.49	0.49	0.245	-1.4065
8	1.5	0.42	0.21	-1.56065
9	1.65	0.34	0.17	-1.77196
10	1.66	0.29	0.145	-1.93102

We have modified the equation as following:

$A_0 = I_0$ and $A_t = I_t$, where I is ¹H NMR integration of α-CH₂ proton (δ 4.35 ppm)

I_0 : 2, Integration of α-CH₂ proton before adding TFA

I_t : Integration of α-CH₂ proton at time t (min) after adding TFA

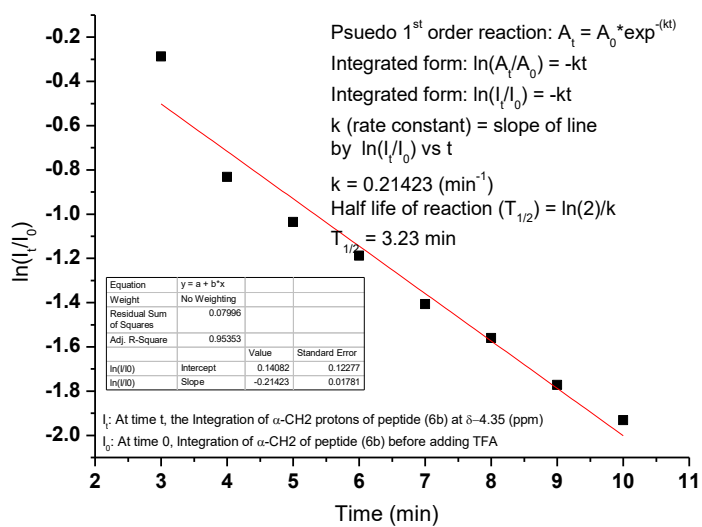
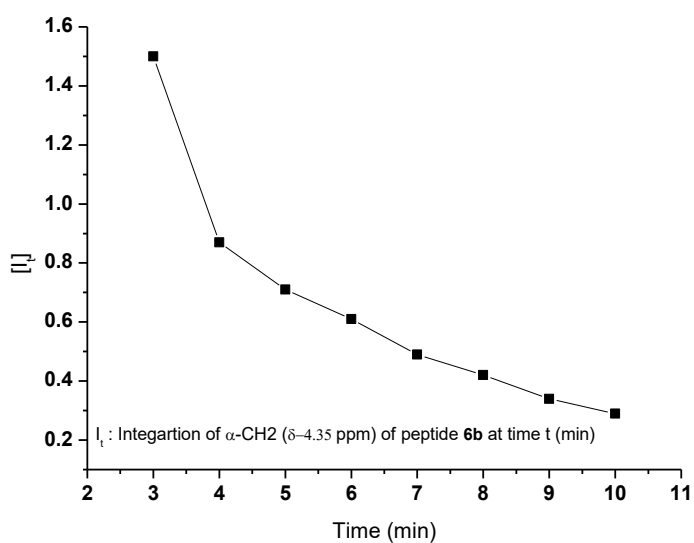
Integrated form: $\ln(I_t/I_0) = -kt$

k (rate constant) = slope of line with $\ln(I_t/I_0)$ vs t plot

k = 0.21423 (min⁻¹);

Half-life of reaction ($T_{1/2}$) = $\ln(2)/k$;

$T_{1/2} = 3.23$ min.



References:

1. Koudriavtsev, A. B.; Linert, W., *Journal of Chemical Education*. **2009**, 86, 1234.

39. UV-Vis Spectroscopic studies of lactone formation:

UV-measurements:

Instrument:

Absorption spectra were obtained using Perkin-Elmer λ -750, at room temperature and under same parameters. All measurements were carried out in 3 mL cuvette.

The peptide was dissolved in anhydrous CH_3CN (3 mL), recorded the absorption. After that, to the same sample, was added 20 μL TFA and recorded absorption. Again to the same sample 500 μL MeOH was added and recorded the absorption with two minutes time interval. The observed absorptions and shift in absorption maximum after TFA addition followed by MeOH addition was tabulated in table. All the measurements were carried out with two minutes time interval at room temperature and under same instrumental parameters.

Initial concentration of samples:

13f: 180 μM

13g: 120 μM

13h: 198 μM

15: 280 μM

5a: 141 μM

entry	observed absorptions (nm) in ACN λ_{max}	observed absorptions (nm) in ACN+TFA λ_{max}	observed absorptions (nm) in ACN+TFA+MeOH λ_{max}
13f	348.0, 395.0	362.0	350.0, 391.0
13g	347.0, 397.0	362.0	352.0, 392.0
13h	352.5, 410.0	362.0	350.0, 391.0
5a	346.0, 402.0	386.0	348.0, 395.0
15	351.0, 407.0	311.0	388.0

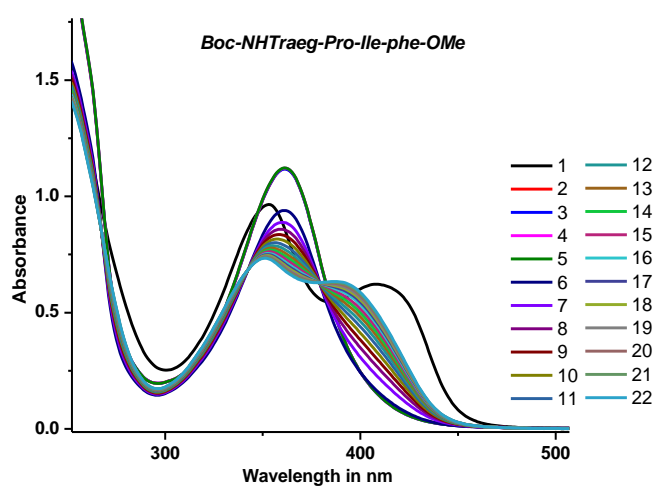


Figure A142. UV absorption studies of peptide **13h** cleavage; 1 absorption spectra of tetra peptide **13h** in CH_3CN (black); 2-5 absorption spectra after adding 20 μL TFA in same sample; 6-22 absorption spectra after adding 500 μL MeOH in same sample.

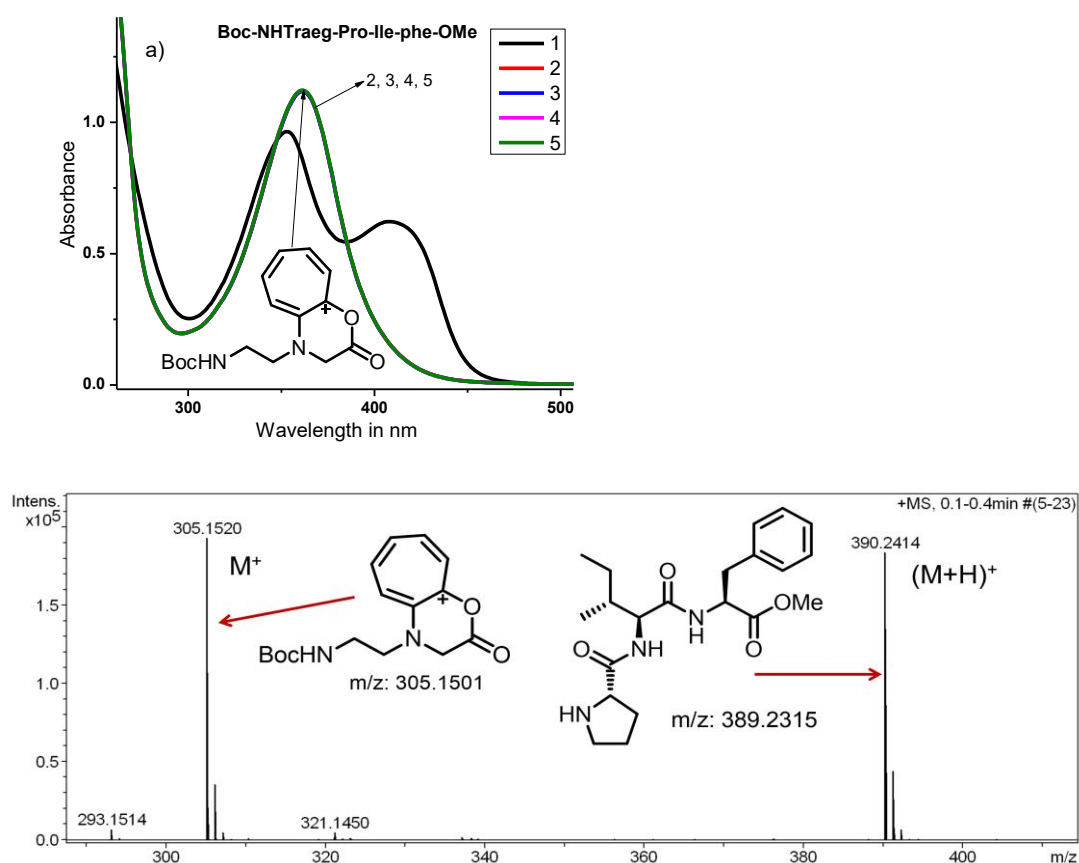


Figure A143. a) 1 absorption spectra of tetra peptide **13h** in CH_3CN (black); 2-5 absorption spectra after adding 20 μL TFA in same sample (all four spectra overlaid); b) Mass spectra in CH_3CN after adding TFA.

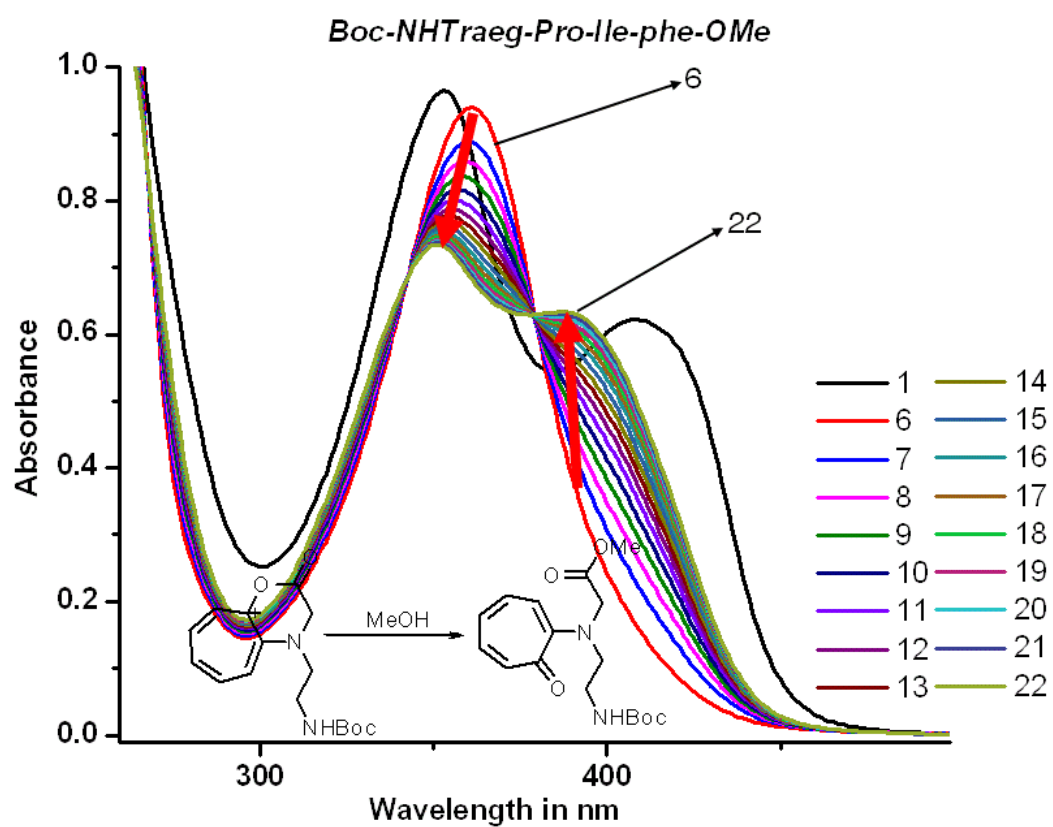


Figure A144: 1 absorption spectra of tetra peptide **13h** in CH_3CN (black); 6-22 monitoring of lactone conversion into methyl ester after adding MeOH (reaction monitoring); **6** is generated after one minute of methanol addition, **22** is generated after 34 minutes.

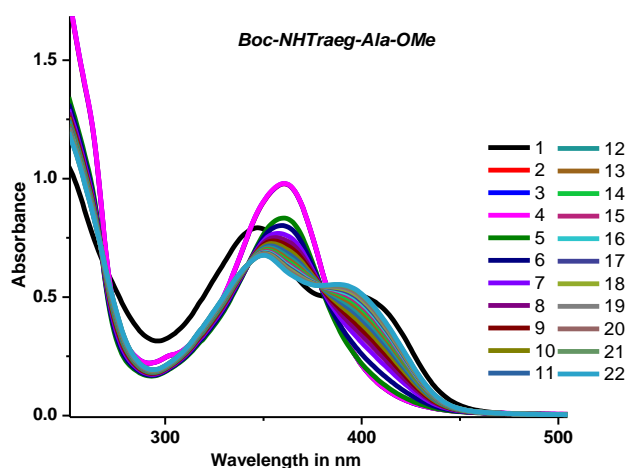


Figure A145. UV absorption studies of peptide **13f** cleavage; 1 absorption spectra of dipeptide **13f** in CH_3CN (black); 2-5 absorption spectra after adding 20 μL TFA in same sample; 5-22 absorption spectra after adding 500 μL MeOH in same sample.

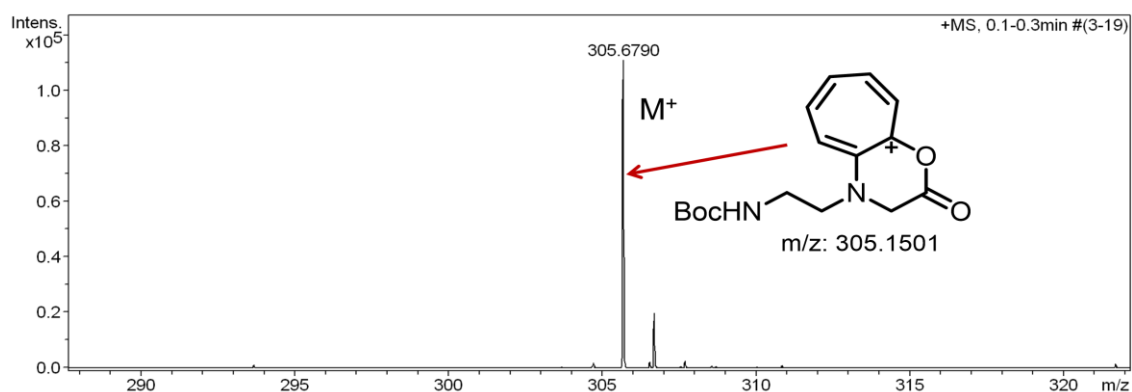
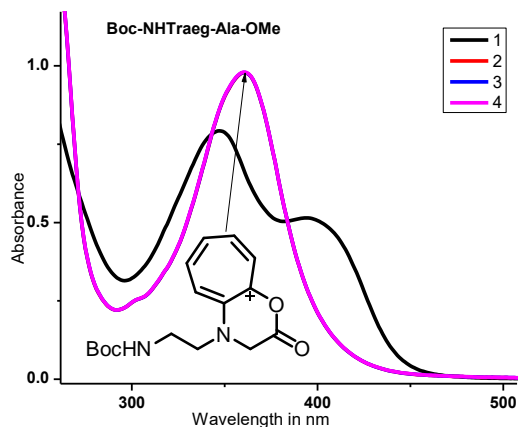


Figure A146. a) 1 absorption spectra of dipeptide **13f** in CH_3CN (black); 2-4 absorption spectra after adding 20 μL TFA in same sample (all four spectra over lied); b) Mass spectra in CH_3CN after adding TFA.

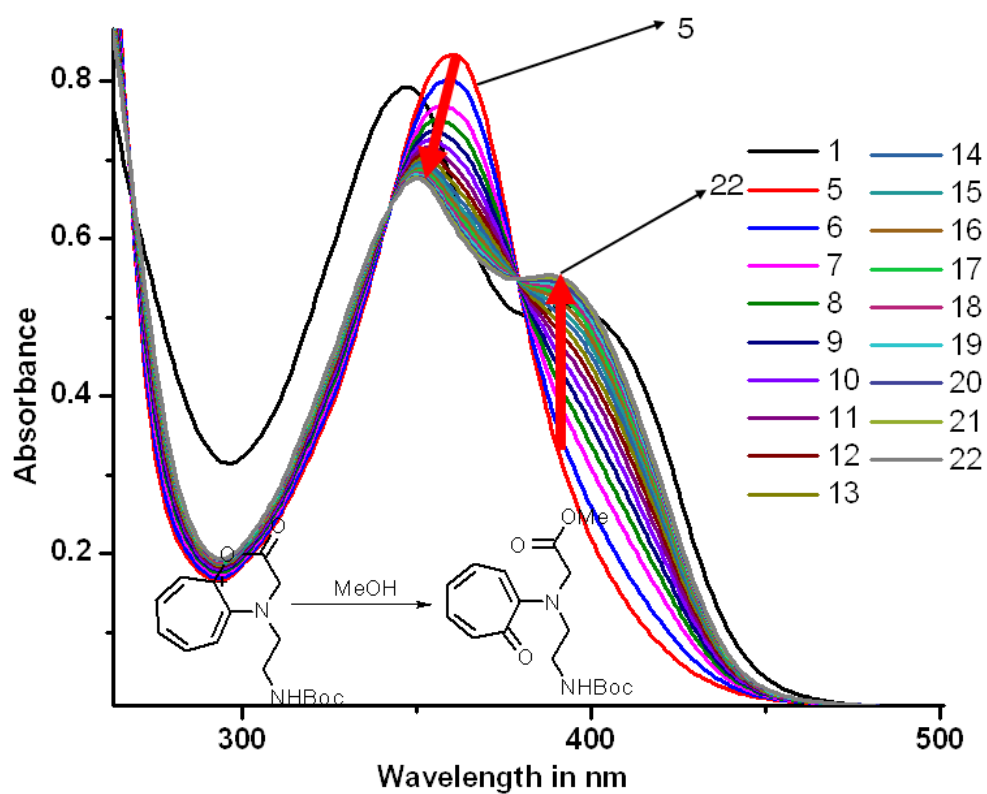


Figure A147. 1 absorption spectra of dipeptide **13f** in CH_3CN (black); 5-22 monitoring of lactone conversion into methyl ester after adding MeOH (reaction monitoring); **5** is generated after 1 minute of methanol addition, **22** is generated after 34 minutes.

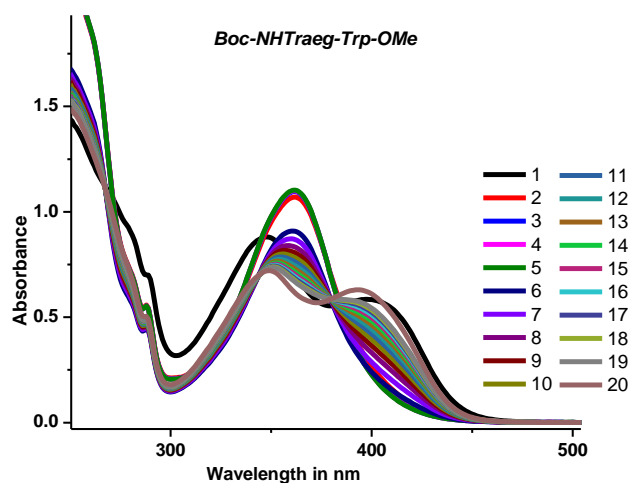


Figure A148. UV absorption studies of peptide 6e cleavage in CH_3CN ; 1 absorption spectra of tetra peptide **13g** in CH_3CN (black); 2-5 absorption spectra after adding 20 μL TFA in same sample; 6-19 absorption spectra after adding 500 μL MeOH in same sample.

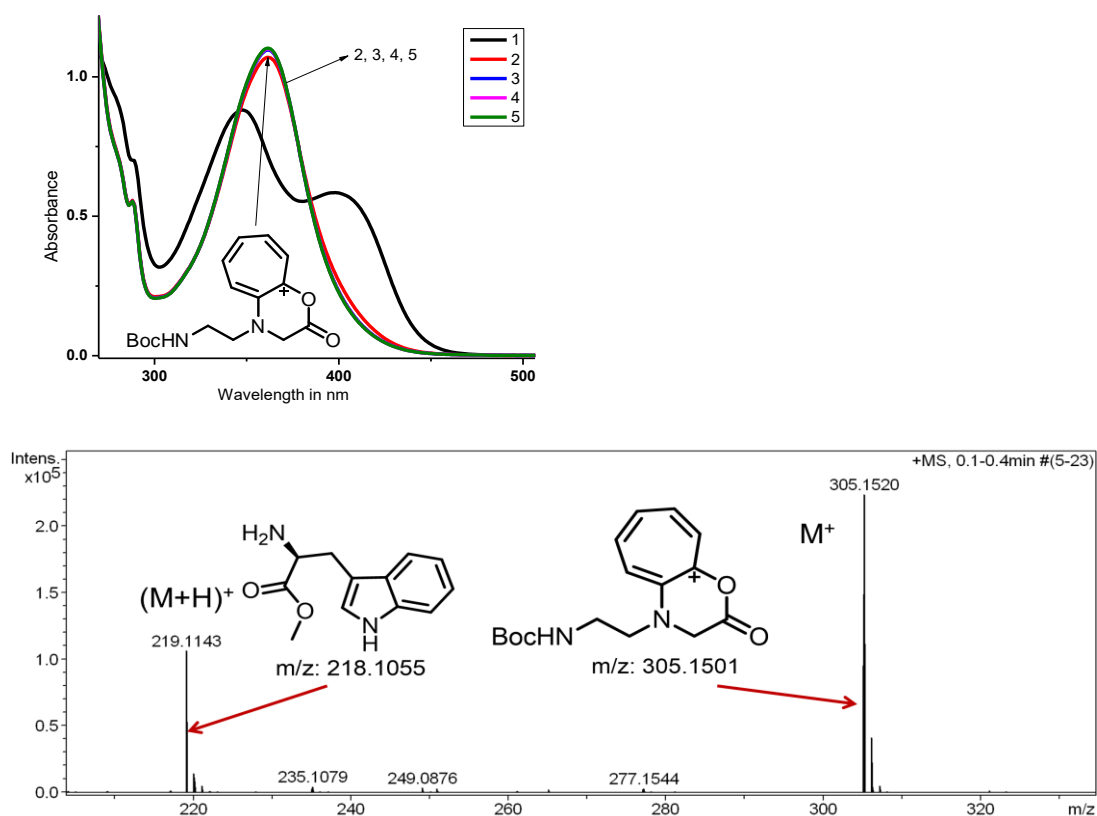


Figure A149. a) 1 absorption spectra of dipeptide **13g** in CH_3CN (black); 2-5 absorption spectra after adding 20 μL TFA in same sample (all four spectra overlaid); b) Mass spectra in CH_3CN after adding TFA.

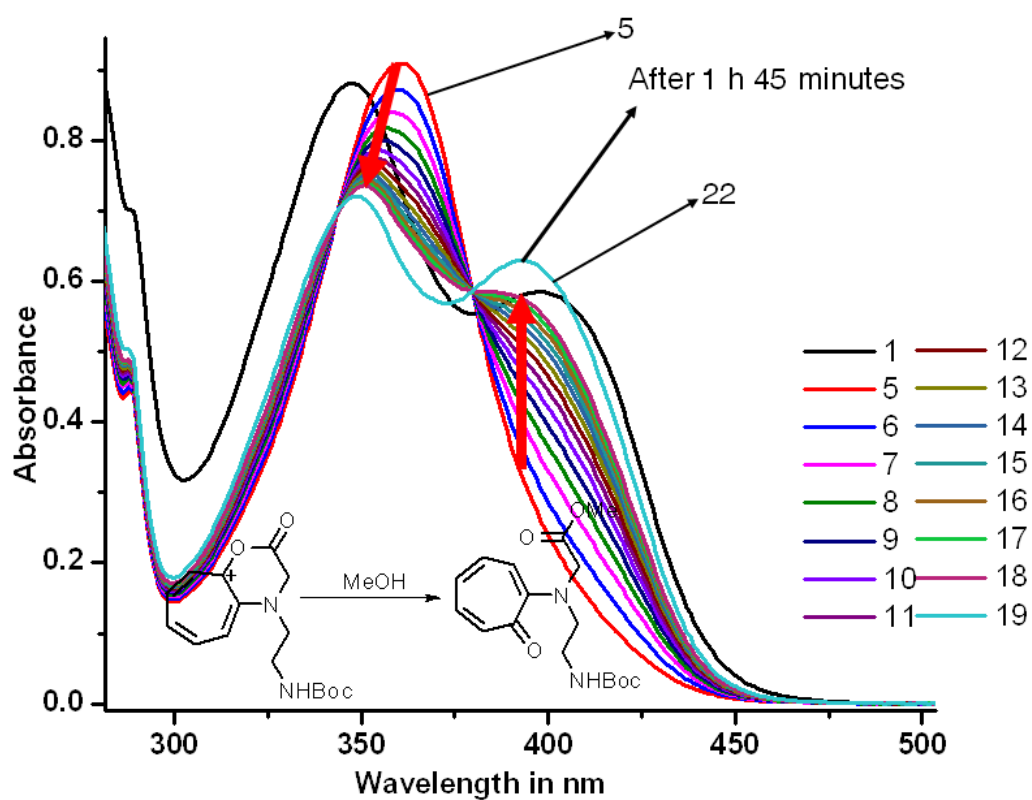


Figure A150. 1 absorption spectra of dipeptide **13g** in CH_3CN (black); 5-19 monitoring of lactone conversion into methyl ester after adding MeOH (reaction monitoring); 5 is generated after 1 minute of methanol addition, 18 is generated after 26 minutes.

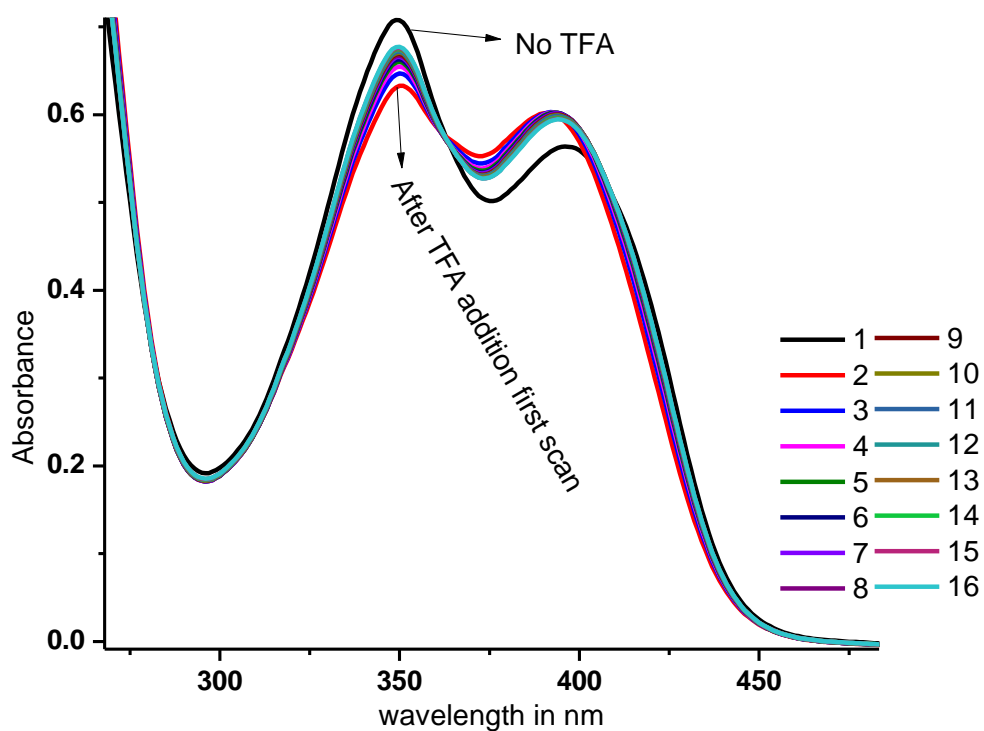


Figure A151. Amide cleavage studies of dipeptide **13f** by UV-Vis spectroscopy in methanol; 1 absorption spectra of dipeptide **13f** in methanol; 2-16 absorption spectra generated after adding TFA with two minutes time interval.

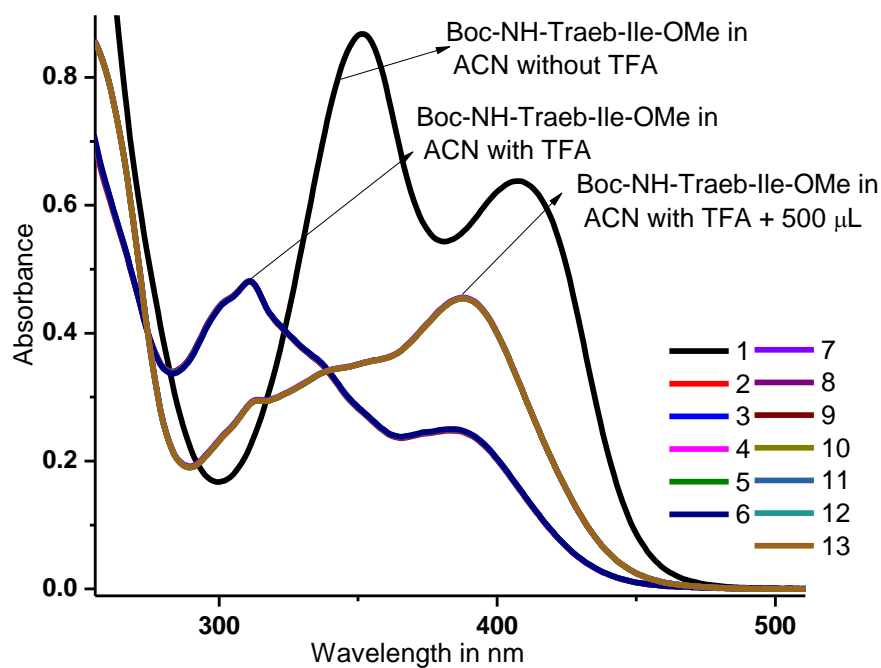


Figure A152. UV absorption studies of control peptide **15** in CH₃CN; 1 absorption spectra of peptide **15** in CH₃CN (black); 2-6 absorption spectra after adding 20 μ L TFA in same sample; 7-13 absorption spectra after adding 500 μ L MeOH in same sample.

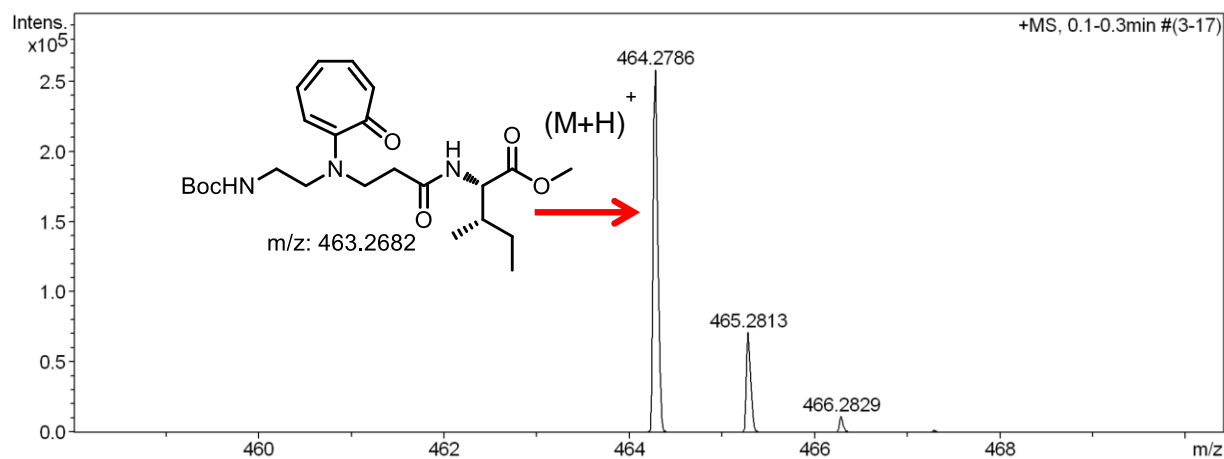


Figure A153. Mass spectra of control dipeptide *BocNH-Traeb-Ile-OMe* (**15**) in CH₃CN and 5% TFA.

47. $^1\text{H}/^{13}\text{C}$ -NMR of *BocNH-Traeg-Gly-OMe* (**13e**) in CD_3CN

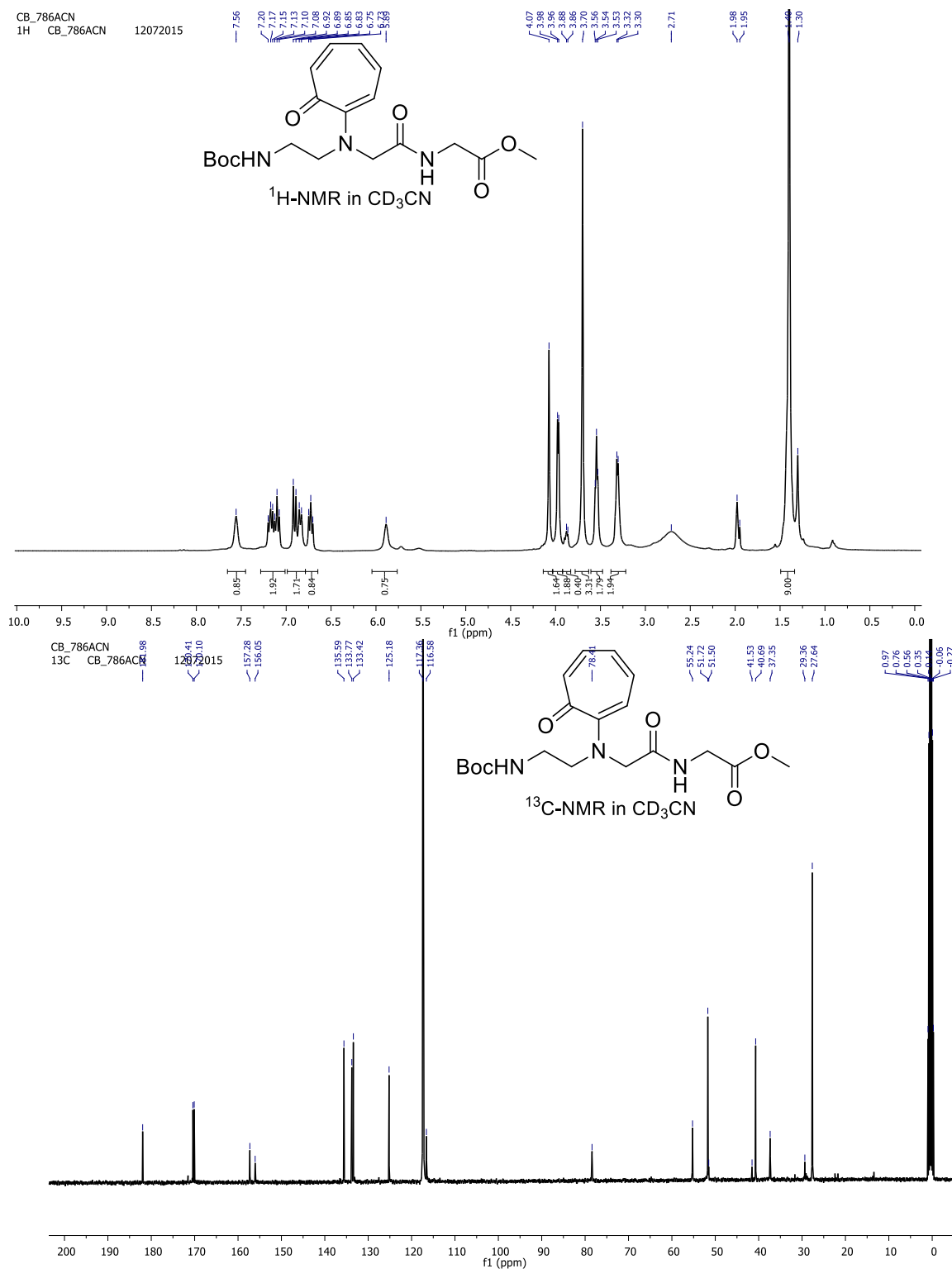


Figure A154. ^1H & ^{13}C -NMR spectrum of *BocNH-Traeg-Gly-OMe* (**13e**)

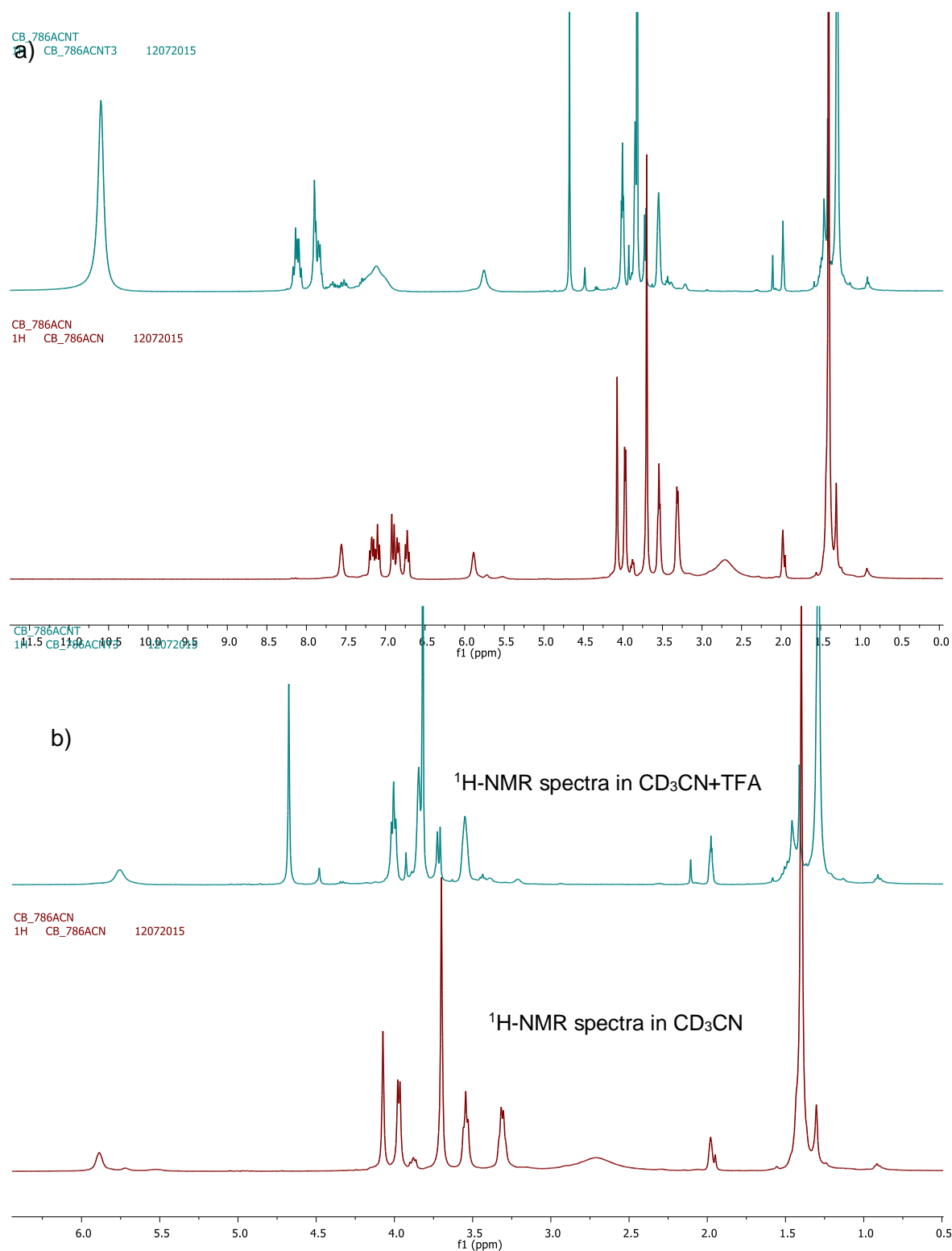


Figure A155. ¹H-NMR spectrum of *BocNH-Traeg-Gly-OMe* (**6a**) after and before addition of TFA in CD₃CN; a) Full range spectra; b) Expanded region.

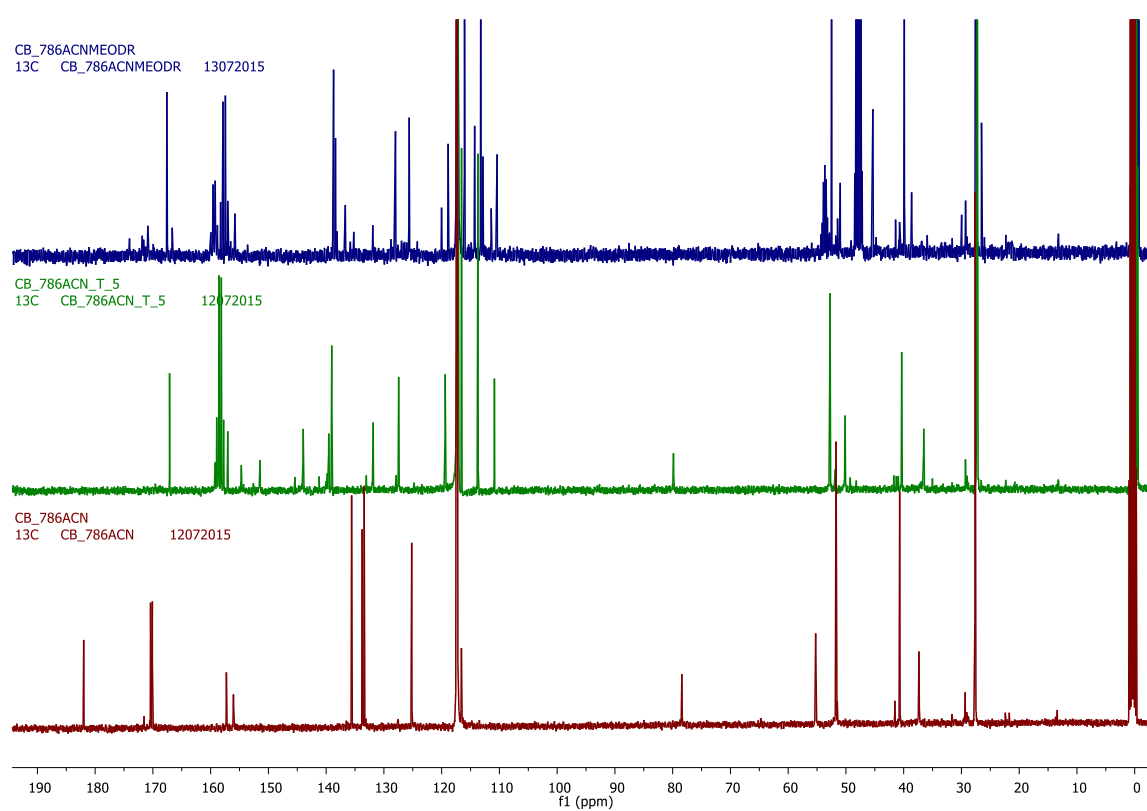


Figure A156. a) ^{13}C -NMR spectrum of *BocNH-Traeg-Gly-OMe* (**13e**) in CD_3CN ; b) ^{13}C -NMR spectrum of *BocNH-Traeg-Gly-OMe* (**6a**) in CD_3CN after TFA addition (5%); c) ^{13}C -NMR spectrum of *BocNH-Traeg-Gly-OMe* (**6a**) in CD_3CN + 100 μL CD_3OD after 24 h of TFA addition.

48. ^{13}C -NMR spectrum of *Ac-NHTraeg-Phe-OMe* (**7**) after addition of TFA in CD_3OD :

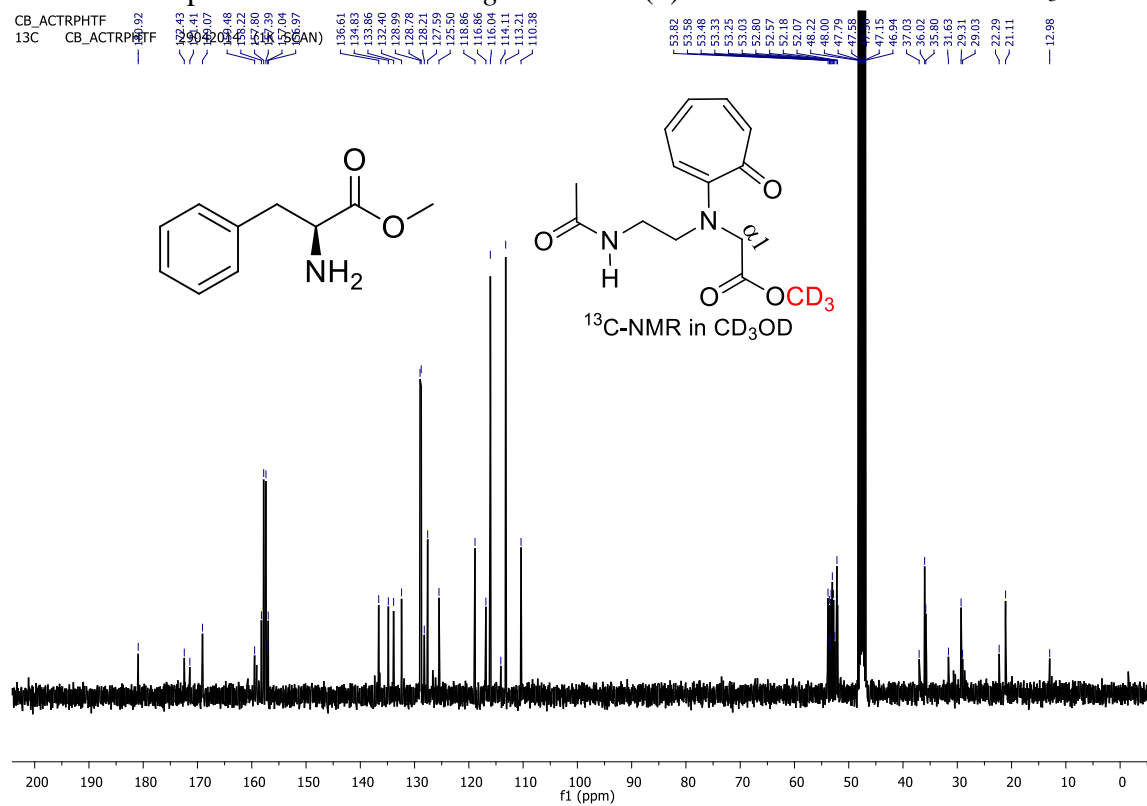


Figure A157. ^{13}C -NMR spectrum of *Ac-NHTraeg-Phe-OMe* (**14**) after addition of TFA in CD_3OD (after cleavage of amide bond).

49. LC-MS spectrum of Boc-*Traeg*- Ile-OMe:

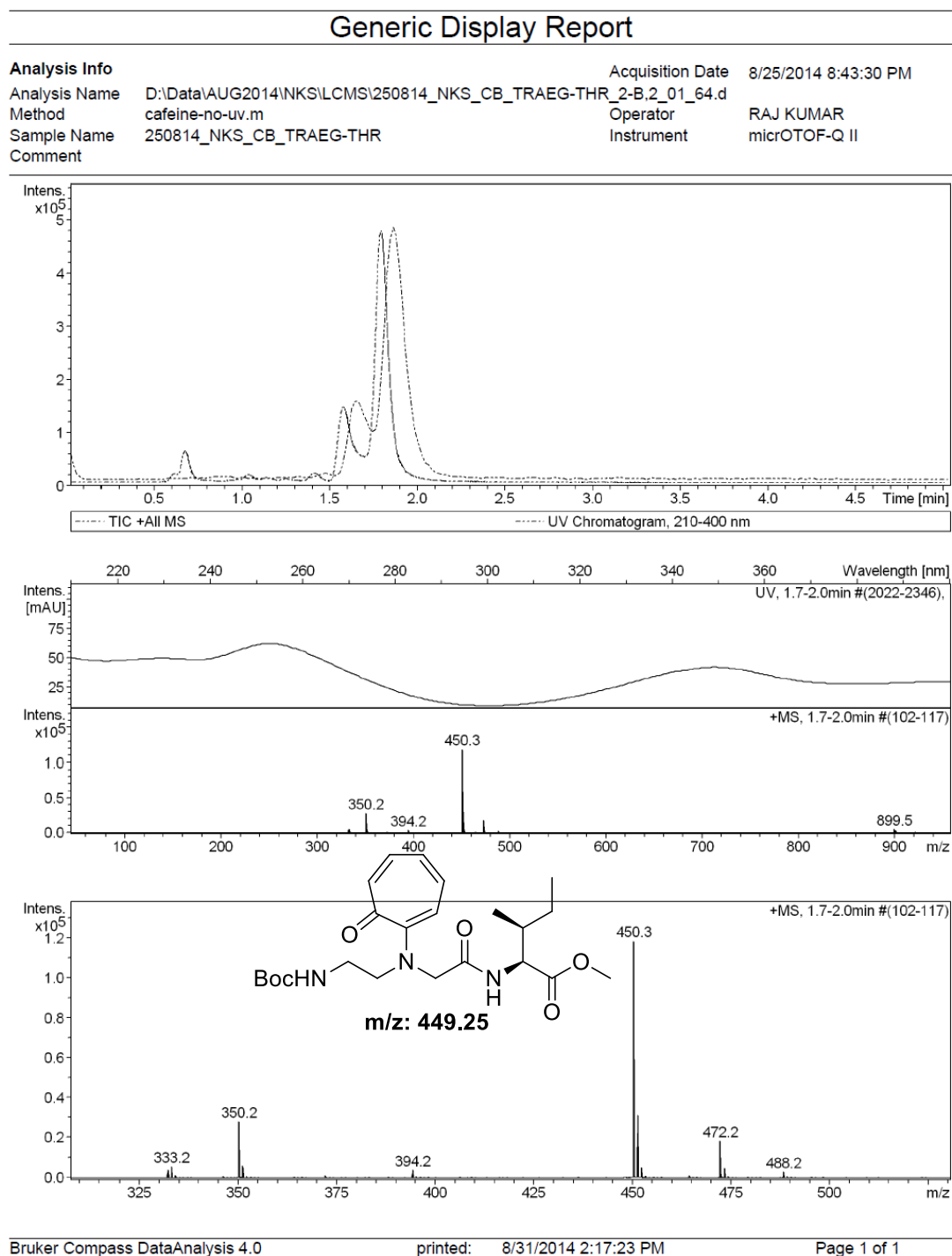


Figure A158. LC-MS spectrum of BocNH-*Traeg*- Ile-OMe.

Generic Display Report

Analysis Info

Analysis Name	D:\Data\AUG2014\NKS\LCMS\250814_NKS_CB_TRAEG-THR_CTL_2-B,3_01_65.d
Method	cafeine-no-uv.m
Sample Name	250814_NKS_CB_TRAEG-THR_CTL
Comment	

Acquisition Date 8/25/2014 8:49:42 PM

Operator RAJ KUMAR

Instrument micrOTOF-Q II

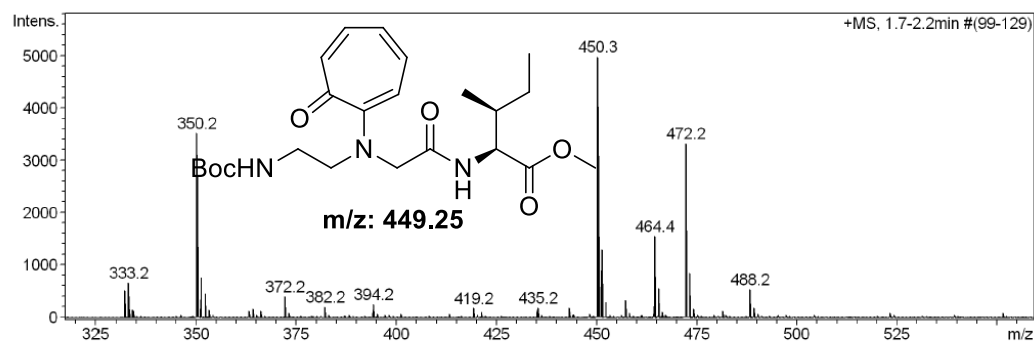
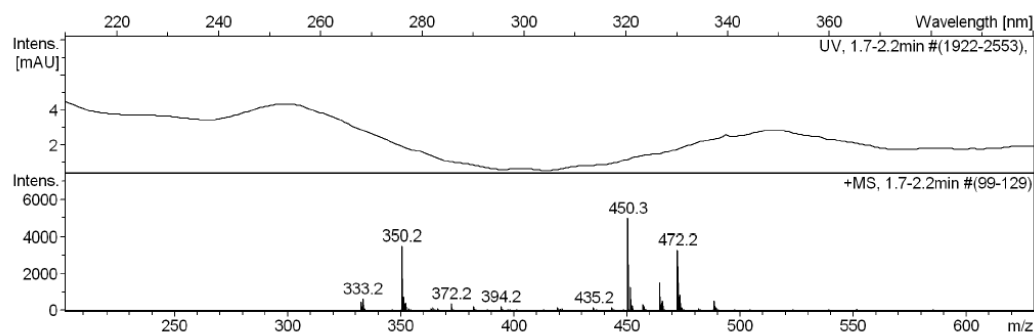
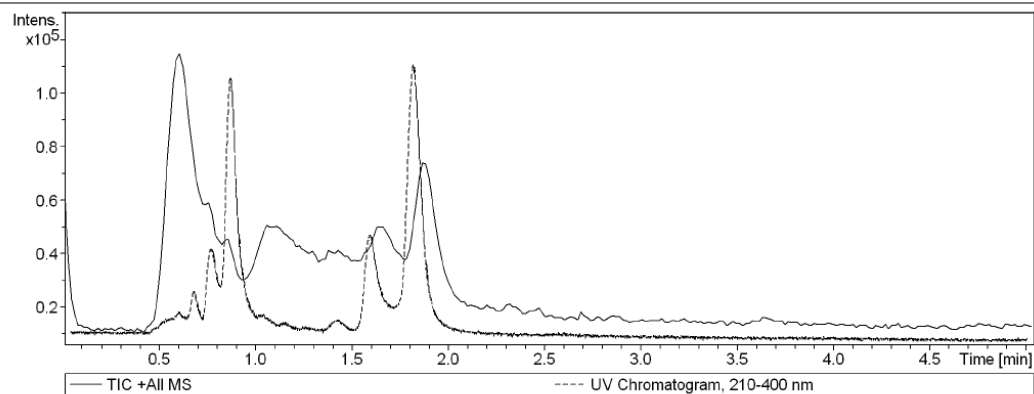


Figure A159. LC-MS spectrum of BocNH-*Traeg*-Ile-OMe and N-Boc-L-Threonine Methyl ester

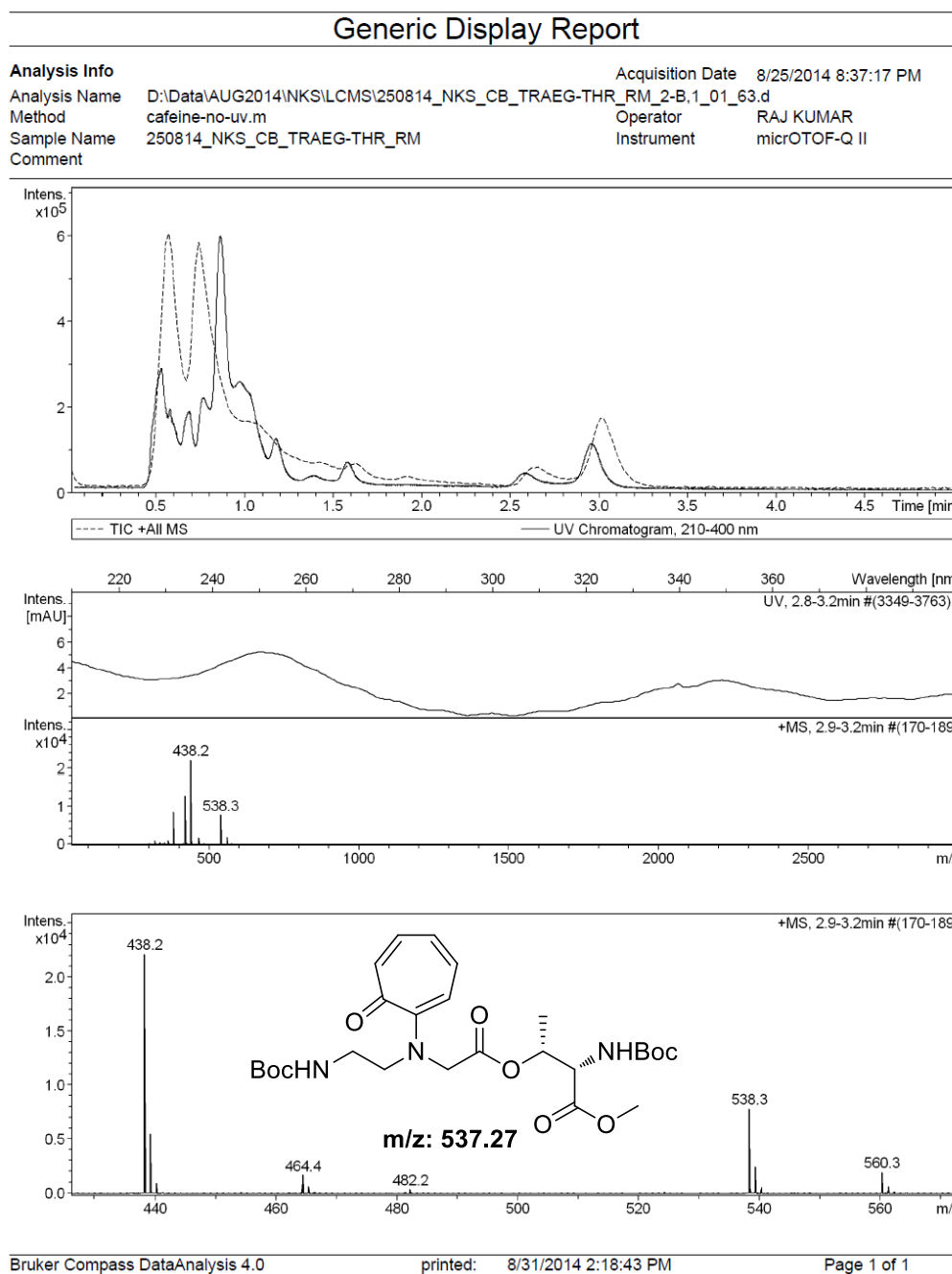


Figure A160. LC-MS spectrum of Boc-*Traeg*- Ile-OMe and N-Boc-L-Threonine Methyl ester after addition of 5.0% TFA

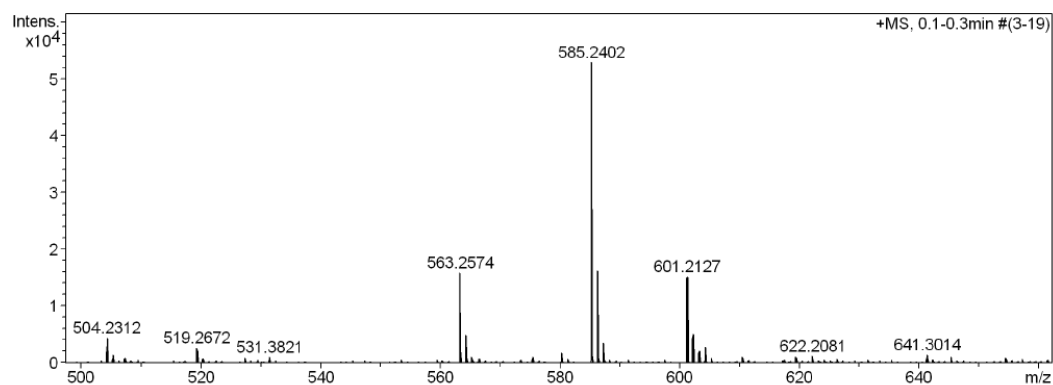
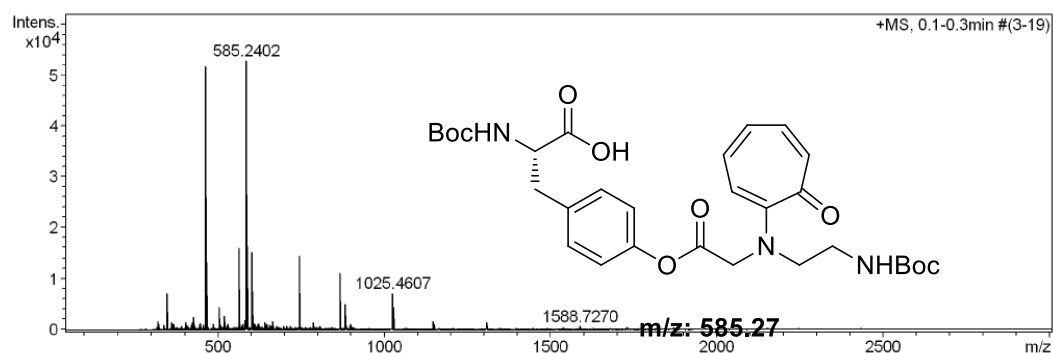
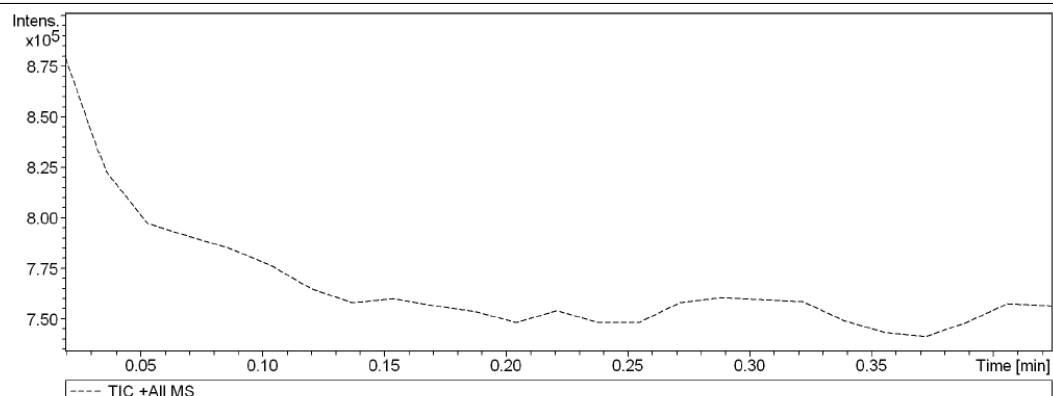
Generic Display Report

Analysis Info

Analysis Name D:\Data\AUG-2014\NKS\260814_NKS_CB_TrTyrTF_W.d
 Method Pso_tune_wide.m
 Sample Name LCMS-NISER
 Comment

Acquisition Date 8/26/2014 3:12:54 PM

Operator RAJ KUMAR
 Instrument microTOF-Q II



Bruker Compass DataAnalysis 4.0

printed: 8/31/2014 2:08:16 PM

Page 1 of 1

Figure A161. Mass spectrum of Boc-*Traeg*-Ile-OMe and Boc-tyrosine reaction mixture after addition of 5.0% TFA in acetonitrile.

Generic Display Report

Analysis Info

Analysis Name D:\Data\AUG-2014\NKS\260814_NKS_CB_TrSerTF_W.d
 Method Pso_tune_wide.m
 Sample Name LCMS-NISER
 Comment

Acquisition Date 8/26/2014 3:24:24 PM

Operator RAJ KUMAR
 Instrument microTOF-Q II

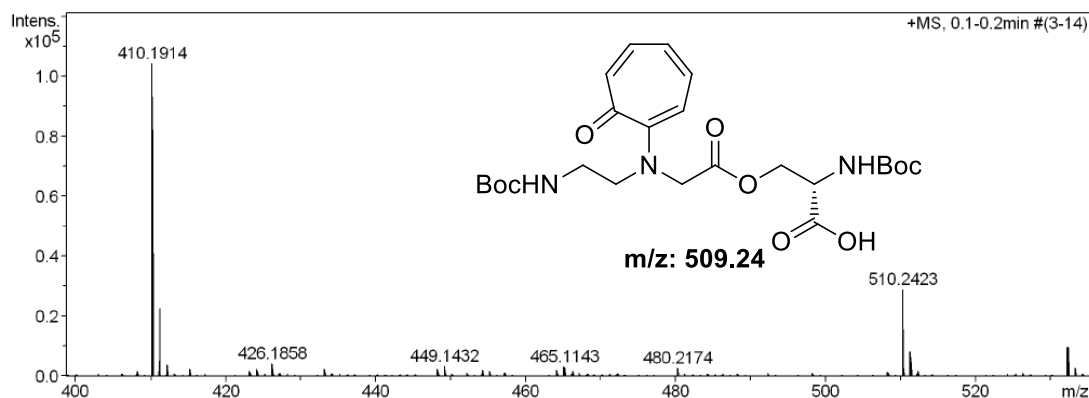
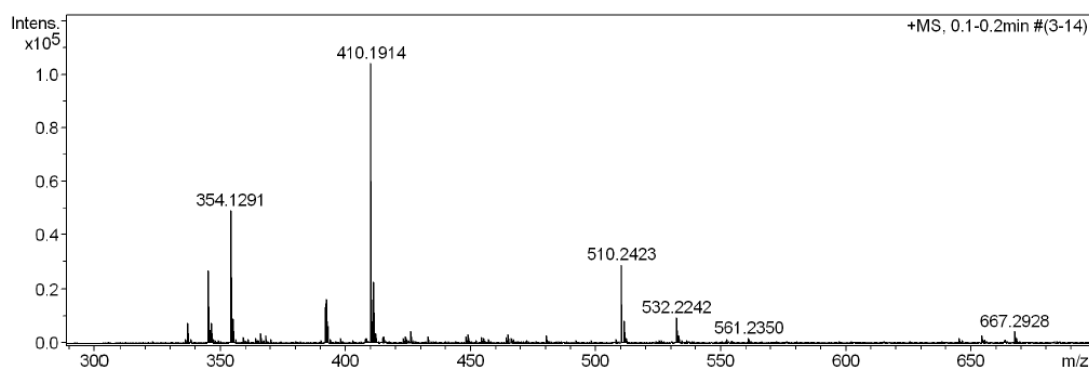
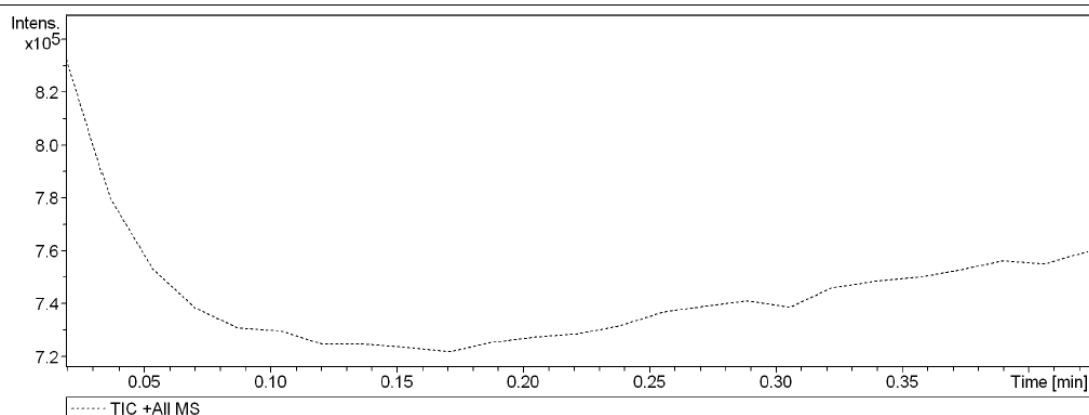


Figure A162. Mass spectrum of Boc-Traeg-Ile-OMe and Boc-Serine reaction mixture after addition of 5% TFA in CAN

CHAPTER FOUR

Synthesis of Novel Fluorescent Molecules from Aminotroponimines

Chapter 4: Synthesis of Novel Fluorescent Molecules from Aminotroponimine

4.1 Introduction

Tropolone and tropone chemical moieties are unique seven-membered ring non-benzenoid aromatic system present in many biologically active natural products (described in chapter one).¹⁻³ The electronic structure of the tropolonoids is distinctive from the benzenoid aromatic compounds and have characteristic photophysical properties (absorption and emission).⁴⁻¹⁵ Though chemical and electronic structures of tropolone and tropolonoid natural products are established in early years of its discovery, but fluorescence of the tropolonoid skeleton came into limelight when Aria and Okuyama reported the fluorescence of colchicine upon binding with the tubulin protein.⁵⁻⁹ Colchicine contains a methoxytropone moiety (**Figure 1B, C ring**) and a therapeutic drug used to treat the gout-arthritis.^{2,3}

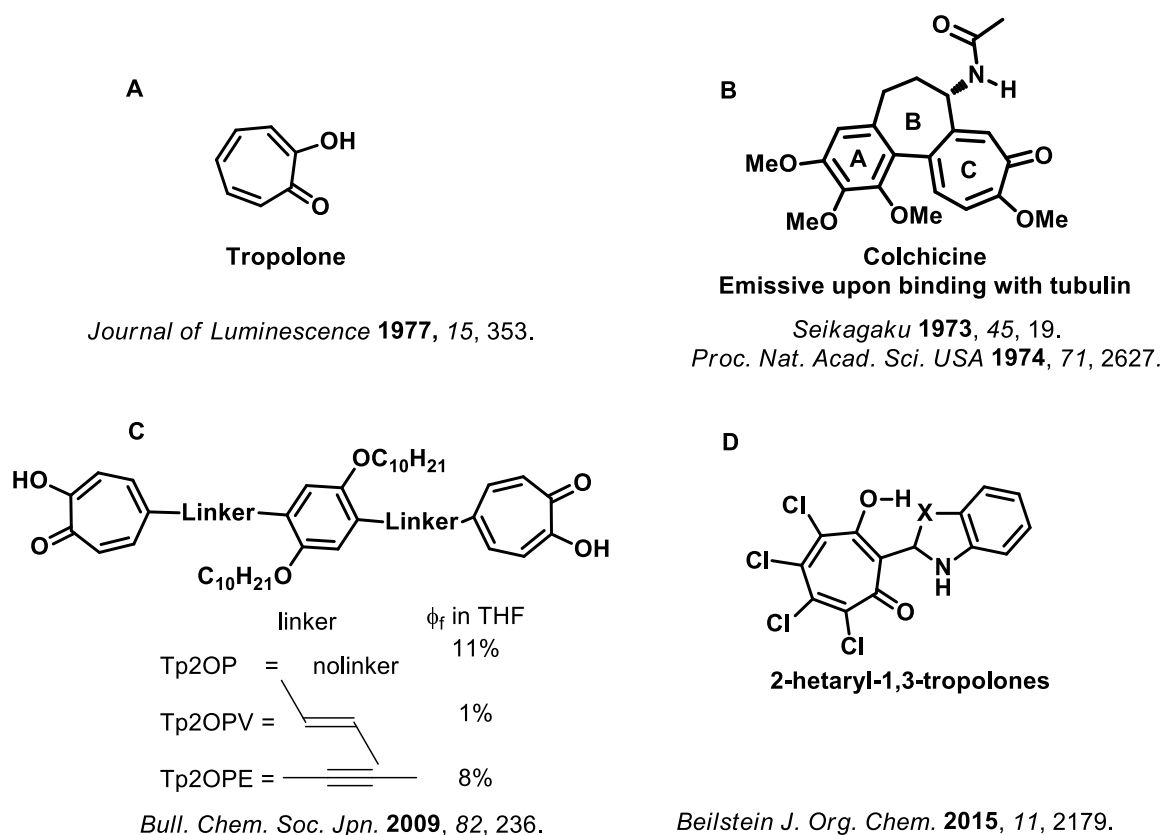


Figure 4.1 Chemical structures of A) tropolone. B) Colchicine C) 2-hetaryl-1,3-tropolones

Colchicine has shown negligible fluorescence in aqueous media, however, the fluorescence increased dramatically with quantum yield 0.03 after binding with the tubulin protein.^{6,7}

Later, fluorescent properties of tropolone were also explored, quantum yields of both tropolone and colchicine are very low at room temperature.¹¹⁻¹⁵ Interestingly, tropolone and colchicine have shown reportedly greater quantum yields at low temperature (77.0 K).^{11,12} Moreover, substituted tropolone derivatives (2-hetaryl-1,3-tropolones, **Figure 4.1D**) have shown fluorescence with enhanced quantum yields.¹¹⁻²¹ The fluorescence properties of dimeric tropolone derivatives linked by phenyl group and suitable connecting linkers have been also explored (**Figure 4.1C**). In the literature, absorption properties of 5-nitrosotropolone and 5-tropolonediazonium salts have also been reported recently.^{20,21}

On the other hand, aminotroponimines are synthesized from tropolone as its structural analogues, where hydroxyl and carbonyl functional groups are replaced with nitrogen as amine and imine functional groups, which are called as ‘aminotroponimines’. They are synthetic aza-derivatives of tropolone and bidentate nitrogen chelating ligands (**Figure 4.2A**).²¹⁻²⁷ The aminotroponimine metal complexes are synthesized extensively with almost all the metals and a few have been used as catalysts in selective organic transformation reactions.^{22-24, 42-45} In addition to aminotroponimines, the synthesis of tropocoronands and their metal complexes has also been elaborated (**Figure 4.2B**), which are derived from macrocyclic aminotroponimines and metals.²⁵⁻²⁷

However, the synthesis and hydrolytic stability of a few 2-bora-1,3-diazaazulene complexes have been reported in early 1962 but the fluorescent properties of these molecules are not explored yet.²⁸ On the other hand, boron-dipyrromethene (BODIPY, **Figure 4.3A**) fluorescent dyes are widely explored.³⁵⁻⁴¹ Importantly, organic fluorescent dyes are enormously useful in different fields for many applications such as labeling agents,²⁹ chemical sensors,^{30,31} cell imaging agents³² and energy related cassette entities.^{33,34} Overall, fluorescent molecules

consisting of tropolonoid core structure are yet to be fully explored. Hence, it is important to develop the fluorescent molecules containing tropolonoid aromatic system.

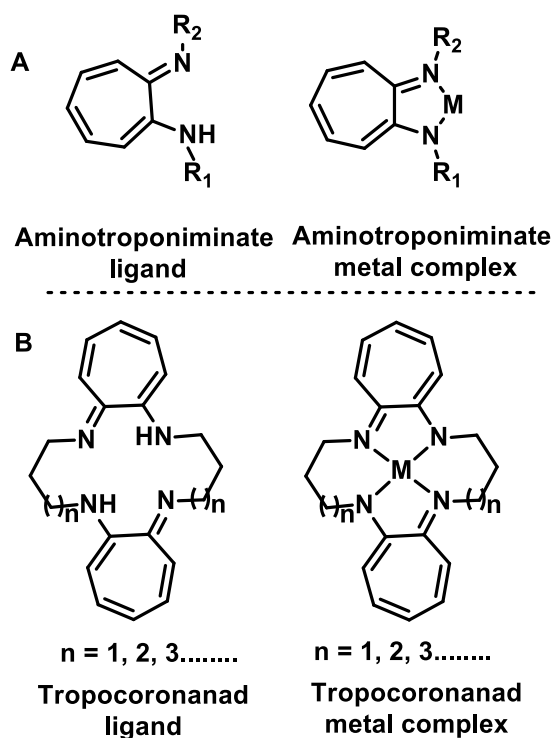


Figure 4.2 Chemical structures of A) aminotroponimine ligand and metal complexes B) tropocoronands and its metal complexes.

4.1.1 Present work

During our attempts to synthesize the homologous peptides from troponyl aminoethyl glycine (chapter I), the free amine salt of troponyl aminoethylglycinate ($\text{NH}_2\text{-Traeg-COOEt}$) cyclized into aminotroponimine derivative (**Figure 4.3B**) after neutralization with triethylamine. In the literature, the fluorescence properties of tropolone in different mediums are reported such as acidic and basic water, and cyclohexane. As mentioned above, tropolone and colchicine have shown fluorescence with low quantum yields. However, this encouraged us to examine the fluorescence of cyclic aminotroponimines.

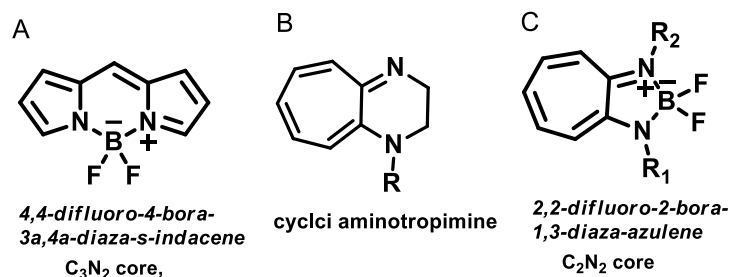


Figure. 4.3 Chemical structures of A) boron-dipyrromethene core. C&D) cyclic aminotroponimine and boron-aminotroponimine core (this work).

To our delight, we found that the obtained cyclic aminotroponimines are exhibiting green fluorescence in acidic water and in methanol. Interestingly, they are stable in acidic and basic mediums. Further, the fluorescent properties of these derivatives were studied in different environments.

The fluorescent properties of cyclic aminotroponimines and a few reported tropolonoids, and boron-dipyrromethene complexes inspired us to design a set of novel organic fluorescent molecules, boron-aminotroponimines (2,2-difluoro-2-bora-1,3-diaza-azulene, **Figure 4.3C**). These molecules are synthesized from aminotroponimine ligand, containing tropolonoid aromatic system, in place of dipyrromethene ligand of BODIPY complexes. However, boron-aminotroponimine core structure is a bicyclic core structure with the seven membered troponyl ring and a five membered ring, which is distinctive from BODIPY core structure.

This chapter explains the unprecedented syntheses of cyclic aminotroponimines and their photophysical properties (absorption, emission, pH and solvent dependent fluorescence properties). On the other hand, the syntheses and characterization of boron-aminotroponimines as BODIPY analogues are demonstrated. We have examined their photophysical properties. Our initial efforts to explore the synthesis and photophysical studies of the boron-aminotroponimine complexes may provide opportunities to synthesize the novel fluorescent

molecules via fine derivatization of aminotroponimine ligands and followed by complexation with Boron.

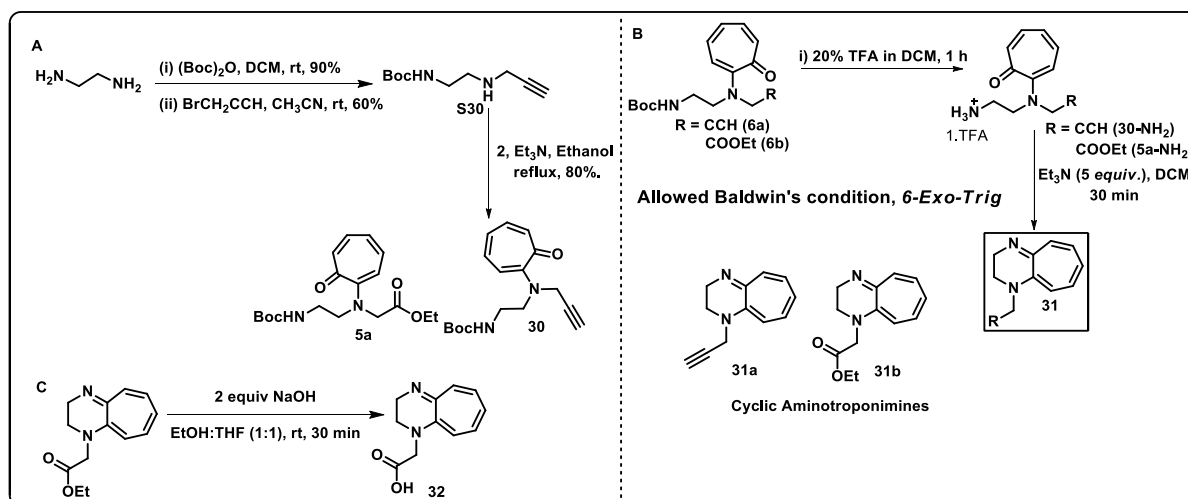
4.2 Results and Discussion

4.2A Cyclic aminotroponimines: Synthesis and photophysical studies

4.2A.1 Syntheses

N-Boc-aminoethyl propergylamine backbone is synthesized by following general procedure presented in experimental section. Troponylation of *aeg* and *N*-Boc-aminoethyl propergyl amine backbones carried out by following the previously presented procedures. Synthesis of monomer **30** (*N*-Boc aminoethyl *N*-troponyl propergylamine) is shown in **Scheme 4.1A** and was characterized by single crystal X-ray analysis. The ORTEP diagram and its molecular packing diagram are depicted in **Figure 4.4**.

Scheme 4.1 (A) Synthesis of monomer **S30**. (B) Synthesis of cyclic aminotroponimines **31a/b**; (C) hydrolysis of cyclic aminotroponimine ester.



After synthesis of monomers, Boc group was deprotected by using 20.0% TFA in DCM. The obtained free amine salts (**30/5a-NH₂**) after evaporation of TFA and solvent, were neutralized with excess triethylamine (5-7 equiv.). The neutralization of free amine salts (**30/5a-NH₂**) led to the cyclization, and formation of cyclic aminotroponimines was

characterized (**Scheme 4.1B**). The formation of the cyclic aminotroponimines is an unprecedented pathway. Usually, the synthesis of acyclic aminotroponimines (see in synthetic Scheme of boron-aminotroponimines, **Scheme 4.2**) from aminotropones requires to convert aminotropones into 2-aminoethoxy tropylium cation by reacting aminotroponimines with strong electrophile donor, triethyloxonium tetrafluoroborate (**Scheme 4.2**), followed by imination reaction with desired amine. But in this case, a simple neutralization of free amine trifluoroacetate salts of aminotropones leads to the formation of cyclic aminotroponimines in an unprecedented manner. Obtained cyclic aminotroponimines were characterized by NMR and ESI-MS. It is noteworthy to mention that the obtained cyclic aminotroponimines are stable in acidic and basic mediums.

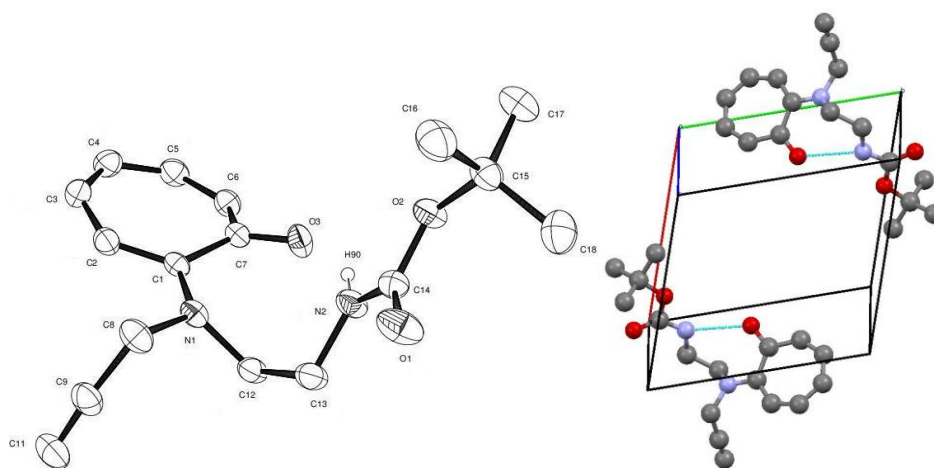


Figure 4.4 (A) ORTEP diagram of monomer **30**. (B) Molecular packing diagram of **30**.

4.2A.2 Photophysical studies of cyclic aminotroponimines

After synthesis of cyclic aminotroponimines (**31a/b**), their photophysical properties were studied. Absorption and emission of aminotropones (**5a/30b**) and cyclic aminotroponimines (**31a/b**) were measured in methanol. Their absorption and fluorescence spectra are provided in **Figure 4.4**. For control studies, absorption of tropolone (**1**) was also recorded. Photophysical parameters are given in **Table 4.1**

Table 4.1 photophysical parameters of compound **31a** and **b**

entry	compound ($\epsilon^* \text{ M}^{-1}\text{cm}^{-1}$)	λ_{abs} (nm)	λ_{em} (nm)	$\phi_f(\%)$
1	1	320, 402		-
2	5a	349, 399	no emission	-
	30	349, 408	no emission	-
3	31a ($\epsilon^* 3.15 \times 10^3$)	362, 449	486	5.2
4	31b ($\epsilon^* 3.15 \times 10^3$)	362, 449	487	4.6

Tropolone exhibits absorption maxima ($\lambda_{\text{max,abs}}$) at 320 nm, with two absorption peaks at 320 and 402 nm. The appearance of two absorption peaks for tropolone is due to two different electronic transitions.¹¹⁻¹⁵ The UV/vis spectra of aminotropone **5a** exhibits two absorption peaks at 399 nm and 349 nm. These two absorption peaks are separated by 3591 cm^{-1} . Similarly aminotropone **30** also exhibits two absorption peaks at 348 nm and 408 nm (Table 4.1, Entry 2&3). The higher wavelength absorption peak in case of aminotropone **30** is redshifted over **5a**. The appearance of two absorptions peaks is possibly due to electronic transitions to two different electronically excited states. However, redshift in absorption peaks is observed with aminotropones, when compare to absorption pattern of tropolone in methanol. This redshift is possibly due to replacing the hydroxyl group of tropolone with amine group. On the other hand, the absorption spectra of **31a/b** also shows two absorption peaks at 362 nm (λ_{max}) and 449 nm (Table 4.1, Entry 3 & 4) and further redshifted was observed over tropolone and aminotropones. Interestingly, broad absorption band was observed in case of cyclic aminotroponimines and the second absorption peak at 449 nm is appeared as shoulder peak. Tropolone, aminotropone, cyclic aminotroponimine have shown two absorption peaks and these are due to two different electronic transitions. A redshift was observed from tropolone to cyclic aminotroponimines. The further redshift in absorption maxima of cyclic aminotroponimines is due to replacing both the oxygen atoms with the nitrogen atoms.

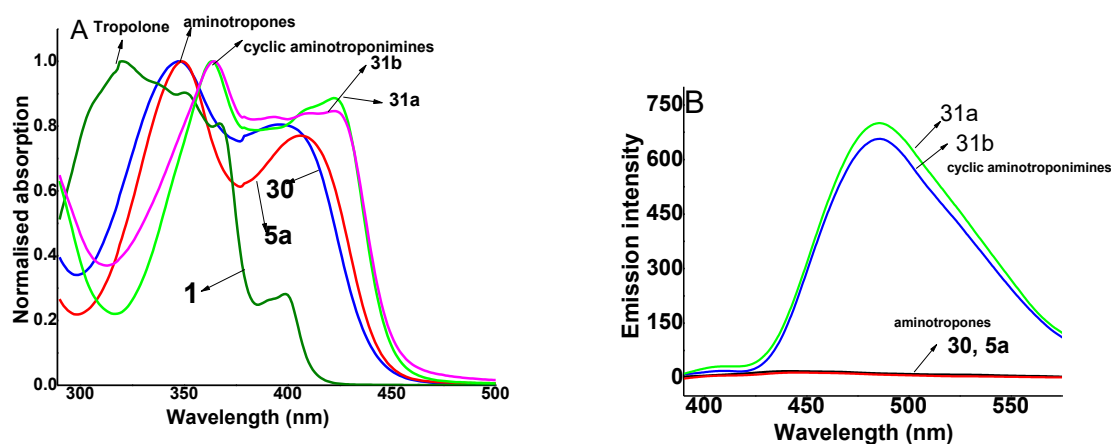


Figure 4.5 A) Normalized absorption spectra of tropolone, **5a/30** and **31a/b** in methanol. B) Emission spectra of **5a/30** and **31a/b** in methanol at λ_{ex} 362 nm (concentration is given **5a** = 90 μ M, **30** = 150 μ M, **31a** = 60 μ M, **31b** = 70 μ M).

Then, emission properties of aminotropones and cyclic aminotroponimines were recorded. First the emission spectra of aminotropones **5a/30** was recorded in methanol as control experiments and from these experiments it has been learnt that the aminotropones (**5a/30**) are non-fluorescent molecules (**Figure 4.5B**). The emission spectra of cyclic aminotroponimines **31a/b** are recorded in methanol at excitation wavelength 362 nm and spectra are given in **Figure 4.5B**. These emission experiments revealed that only cyclic aminotroponimines **31a/b** are fluorescent molecules with significant fluorescence intensity, at emission maxima (λ_{em}) 486 nm. It is worth mention that the cyclicaminotroponimines are exhibiting green fluorescence with 8 π -electrons. These initial studies of cyclic aminotroponimines encouraged us to design novel fluorophores with tropolonoid aromatic system.

Thereafter, quantum yields (ϕ_f) of **31a/b** were calculated by following established comparative protocol. Quinine sulphate in 0.1 M H_2SO_4 was used as reference standard to calculate quantum yield of **31a/b**. After systematic analysis and calculations, quantum yield

(ϕ_f) of **31a** (Table 1, Entry 3) and **31b** (Table 1, Entry 4) were obtained with values 5.2% for **31a** and 4.6% for **31b**.

As mentioned above fluorescent properties of tropolone are reported.¹¹ In the literature, the absorption and emission maxima of tropolone varies with the nature of the medium.¹¹ Tropolone has shown weak fluorescence in cyclohexane ($\lambda_{\text{abs}} = 323$ (max), 356, 374; $\lambda_{\text{em}} = 405$ nm), which was decreased in acidic medium ($\lambda_{\text{abs}} = 315$ (max), 350; $\lambda_{\text{em}} = 390$ nm) by two fold and in basic medium ($\lambda_{\text{abs}} = 330$ (max), 390; $\lambda_{\text{em}} = 425$ nm) further decreased.¹¹ Importantly, enhancement in quantum efficiency of tropolone and colchicine is reported at low temperature (77 K) and their values are 0.18 and 0.25 respectively.^{11,12}

Hence, we attempted to test the fluorescence properties of cyclic aminotroponimines in different mediums. In contrast to tropolone, amine and imine functional groups of cyclic aminotroponimines are more basic in nature, as a result the sensitivity of the molecule may possibly enhance towards the nature of the medium. Hence, absorption and emission studies of cyclic aminotroponimines **31a/b** was performed in MeOH, H₂O, 1.0 N HCl, 1.0 N NaOH, CHCl₃ to understand the effect of nature of the medium. The obtained spectra are depicted in **Figure 4.6**. UV-absorption spectra of **31a** clearly exhibits two absorption peaks in water and 1.0 N HCl, these are probably due to electronic and charge transfer transitions, the absorption pattern is similar as in methanol. In contrast, only one absorbance peak at λ_{abs} 362 nm was observed in basic pH (aq. 1N NaOH), it may be due to electronic transition. The other absorption peak at λ_{abs} 449 nm due to charge transfer transition is depleted significantly. In aprotic polar solvent, CHCl₃, **31a** exhibits only one major absorption peak at 362 nm (λ_{abs}), while absorption peak at 449 nm are also marginally suppressed. It may be due to non-existence of polarized tropylium cation in basic medium and CHCl₃. The similar results are obtained from **31b** (**Figure. 4.6C&D**).

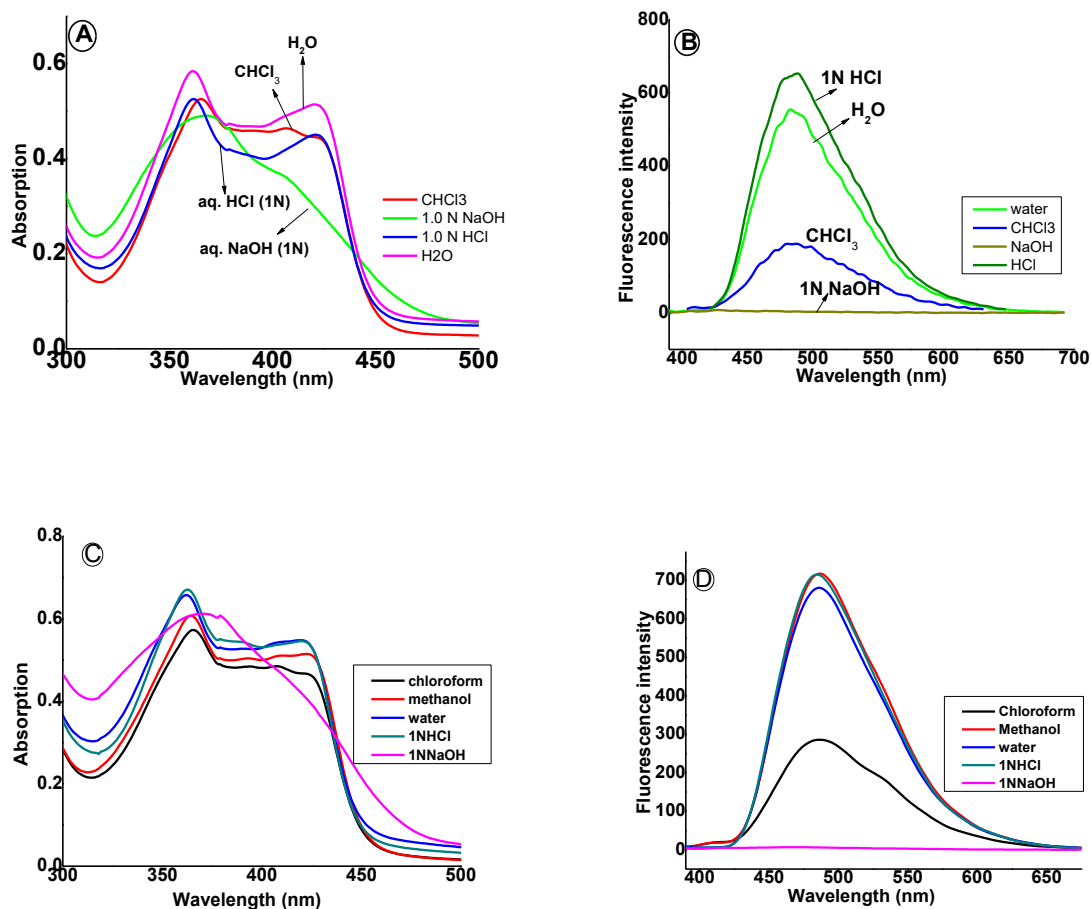


Figure 4.6 A) Absorption spectra **31a** (160.0 μM) in different mediums. B) Emission spectra **31a** (60.0 μM) in different mediums. C) Absorption spectra **31b** (160.0 μM) in different mediums. D) Emission spectra **31b** (60.0 μM) in different mediums.

Emission studies are also performed in MeOH, H_2O , 1.0 N HCl, 1.0 N NaOH and CHCl_3 . The obtained emission spectra are depicted in **Figure 4.6B&D**. Maximum fluorescence intensity was observed in acidic medium. The fluorescence intensity was decreased significantly in chloroform and a quenching of fluorescence was observed in basic medium (1.0 N NaOH). The decrease in fluorescence intensity of cyclic aminotroponimines in aprotic solvents is due to less possibility of protonation of imine functional group. As a result, formation of charged tropylium cation does not occur. This is also supported by the quenching of fluorescence in basic medium. Overall, these studies suggest that the formation of tropylium cation is important to exhibit the significant fluorescence by the cyclic aminotroponimines.

4.2A.3 pH and solvent effects on fluorescence properties

Next, pH dependent fluorescence studies were performed. Fluorescence spectra of 33 μ M aqueous solution of **31a/b** at different pH conditions were recorded. The pH dependent fluorescence spectra of aminotroponimine derivative of **31a/b** are given in **Figure 4.7A/B**. Fluorophores (**31a/b**) were dissolved in water to obtain 54.0 mM stock solution and the samples were diluted with buffer to 36 μ M to maintain constant ionic strength. Sodium acetate and sodium chloride buffer was used. Changes in pH of the samples were obtained by adding 3.0-1.0 N NaOH or 3.0-1.0 N HCl, where dilution effects were negligible. After preparing samples emission was recorded from low pH to high pH. Obtained spectra are depicted in **Figure 4.7**.

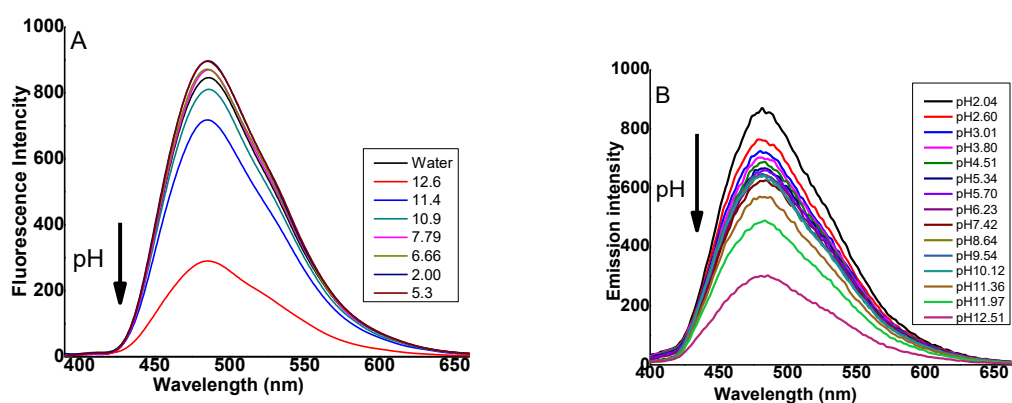


Figure 4.7 (A) pH dependent fluorescence measurements of **31a** (A), **31b** (B).

Cyclic aminotroponimines (**31a/b**) have shown higher fluorescence intensity in acidic medium and the fluorescence intensity is decreased in basic medium. The pH dependent fluorescence studies further supports the protonation of imine group of **31a/b** in acidic environments is playing key role in exhibiting fluorescence.

Overall, these studies revealed that the fluorescence properties are governed by the nature of the medium and existence of polarized imine group.

Solvent dependent fluorescence studies were also performed with both analogues **31a/b**. Emission spectra were recorded in different solvent systems. The obtained spectra are depicted in **Figure 4.8**. Protic polar solvents are water, 1.0 N HCl, propanol, ethanol, methanol and aprotic polar solvents are acetonitrile, dimethyl sulphoxide, chloroform, dichloroethane, dichloromethane, tetrahydrofuran. The fluorescence intensity order for **31a** in solvent systems are perceived as $\text{CH}_3\text{CN} > \text{H}_2\text{O} > \text{MeOH} > \text{EtOH} > \text{DCE} > \text{PrOH} > \text{DMSO} \sim \text{CHCl}_3 \sim \text{DCM} > \text{THF}$. The similar pattern for **31b** in similar solvent systems are observed as $\text{CH}_3\text{CN} > \text{H}_2\text{O} \sim \text{MeOH} > \text{EtOH} > \text{DCE} \sim \text{DMSO} > \text{PrOH} > \text{DCM} \sim \text{CHCl}_3 > \text{THF}$. Surprisingly, these results revealed that the fluorescent intensities of **31a/b** are exhibited maximum in acetonitrile, even more than protic solvents and minimum in THF.

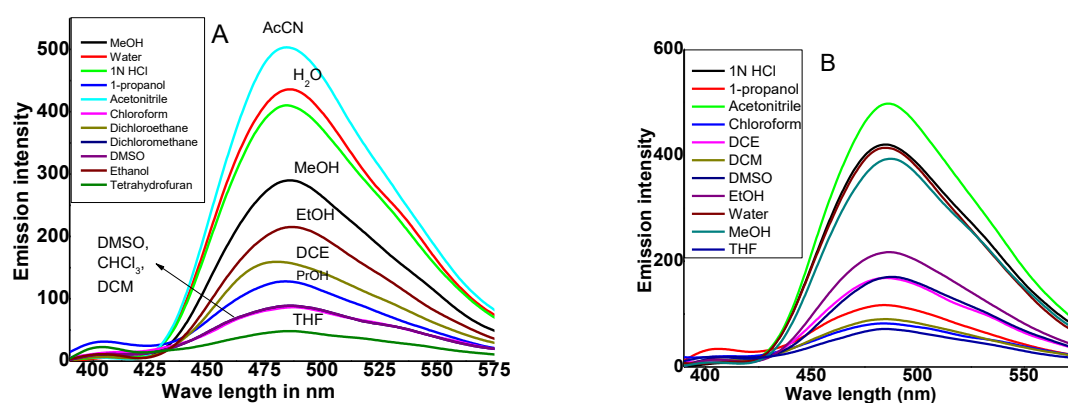


Figure 4.8 (A) Emission of **31a** with concentration (10.6 μM); (B) Emission spectra of **31b** with concentration of (7.5 μM) in in different solvents systems using same instrument parameters.

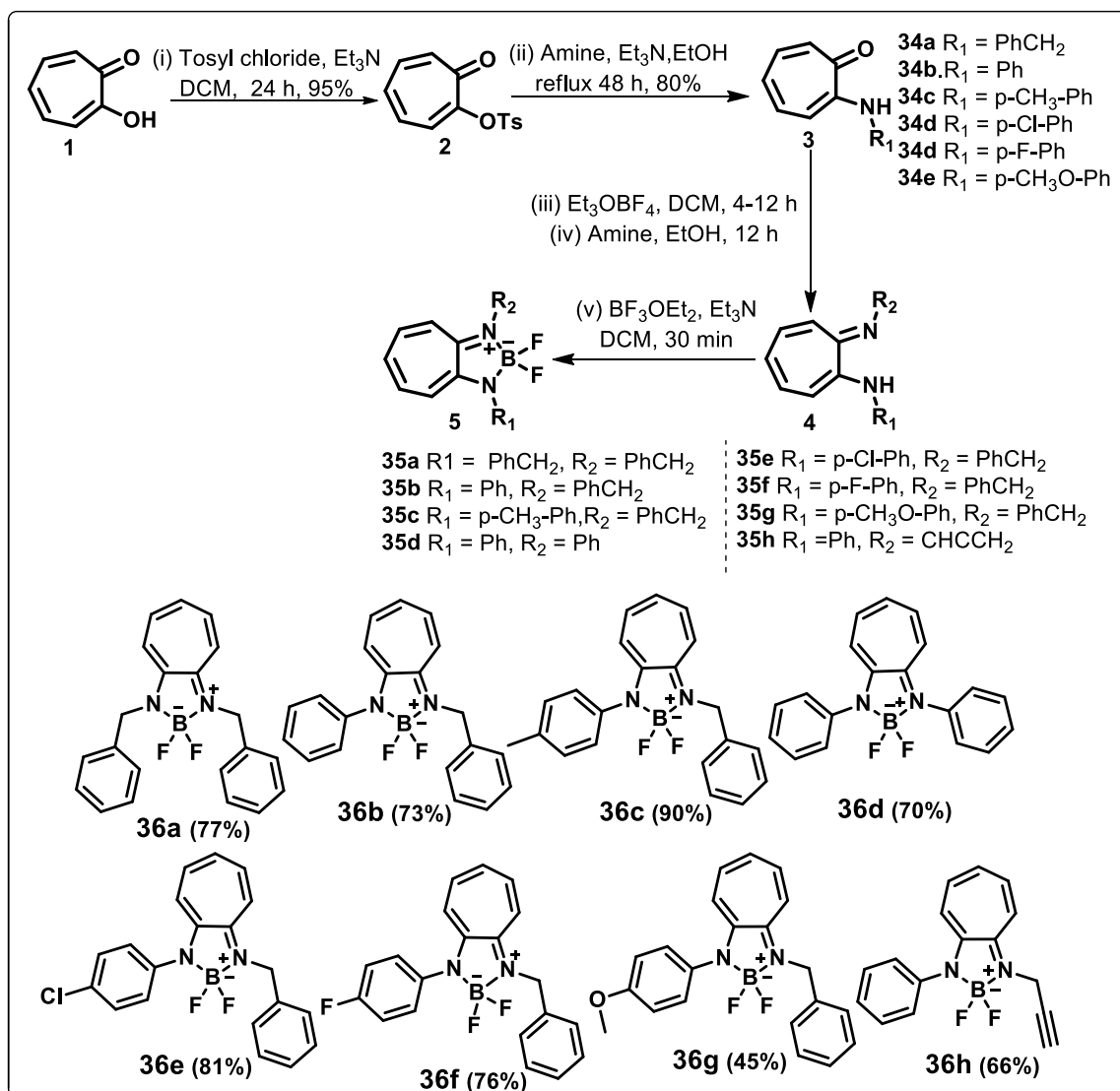
We have also carried out the Click reaction with **31b** and synthetic 4-azidoproline ester to test the stability of cyclic aminotroponimine. The reaction worked without affecting other functional groups. ESI-MS spectra are provided in appendix.

4.2B Boron-Aminotroponimine complexes: Syntheses and photophysical studies

4.2B.1 Syntheses and characterization

We began the syntheses of boron-aminotroponimine complexes from commercially available tropolone by following the previously reported procedures.⁴⁶⁻⁴⁸

Scheme 4.2 Synthesis of boron-aminotroponimine complexes

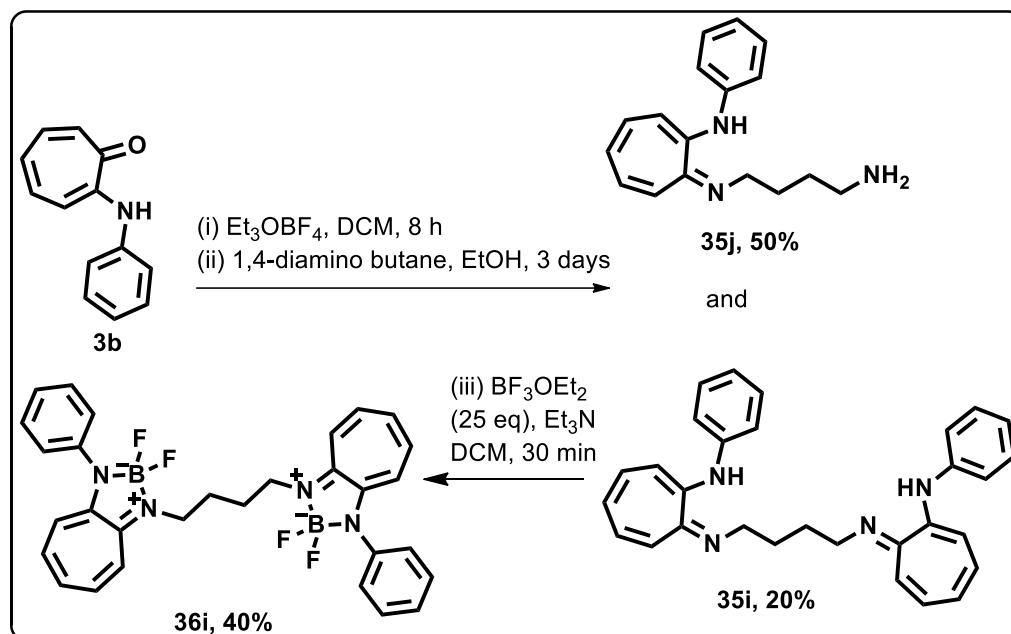


In scheme 4.2, tropolone was converted into 2-tosyloxypolone and then treated with different amines (ca. 3.0 *equiv.*) which produced *N*-substituted aminotroponone derivatives (**34**) in good yield. These aminotropones (**34**) were further converted into aminotroponimines (**35**) by treating sequentially with triethyloxonium tetrafluoroborate and an amine.^{11a}

Importantly, the reaction was fast with alkyl amines (benzyl/propargyl) as compared to aryl amines. The reported conversion of *N*-phenyl aminotroponone (**34b**) into *N*-(Phenyl)-2-(phenylamino)troponimine (**35d**) was extremely slow (ca. 8.0 days) and yield was approx. 45.0%.⁴⁶ Further, these aminotroponimines were converted into boron-aminotroponimines by treating with an excess of boron trifluoride diethyl etherate (10 equiv.) and triethylamine (10 equiv.) at room temperature within 30.0 minutes. Exceptionally, the synthesis of *N,N'*-diaryl substituted boron complex (**36d**) required 20 equivalents of boron trifluoride diethyl etherate and triethylamine.

Further, we designed a dimeric complex **36i** that contain two monomeric units of **34b** connected by a butyl chain. This dimeric complex (**36i**) was synthesized from the *N*-phenyl aminotroponone (**34b**) and 1,4-diaminobutane (**Scheme 4.3**).

Scheme 4.3 Synthesis of dimeric aminotroponimine **35i** and its boron complex **36i**.



First *N*-phenyl aminotroponone (**34b**) was treated with triethyloxonium tetrafluoroborate followed by the treatment with 1,4-diaminobutane results in formation of *N,N'*-(diphenyl)-2-(1,4-diaminobutyl) ditroponimine with moderate yield (20.0%). To avoid the formation of monomeric ligand (**35j**), only 1.0 equivalent of 1,4-diaminobutane was added portionwise, but

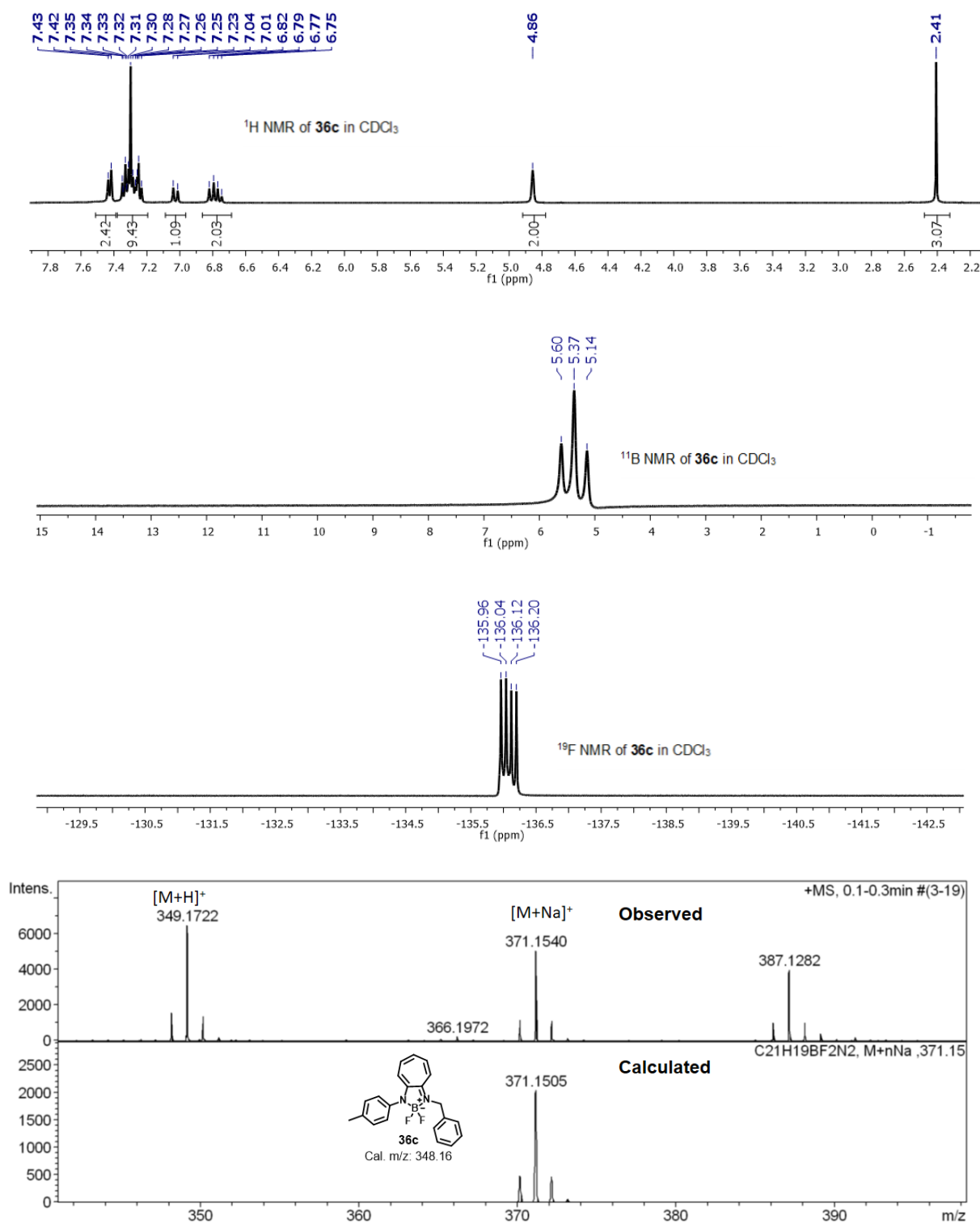


Figure 4.9 ¹H NMR (first), ¹¹B NMR (second), ¹⁹F NMR (third) of **36c** in CDCl₃. HRMS spectrum of **36c** (last).

still we were unable to control the formation of the monomeric ligand (**35j**). Next, this dimeric ligand was subjected to BF₂-complexation under the above optimized conditions, which

produced the desired complex (**36i**) with good yield (40.0%). The synthesized boron-aminotroponimine complexes are stable at room temperature/in the open air and were characterized by ^1H , ^{13}C , ^{11}B , ^{19}F NMR and HRMS (ESI-MS). ^{11}B NMR of all boron-complexes has shown a triplet peak for all boron-complexes in the range of δ 4.9-5.5 ppm. The appearance of triplet peak is due to coupling of ^{11}B with two neighbor ^{19}F atoms (nuclear spin is $1/2$). ^{19}F NMR of boron-complexes has shown a quartet peak in the range of δ -130.0 to -140.0 ppm. The appearance of quartet peak is due to coupling of ^{19}F atoms with neighbor one ^{11}B atom (nuclear spin is $3/2$). ^1H , ^{11}B , ^{19}F NMR and HRMS spectra of boron-complex **36c** is depicted in **Figure 4.9**. Their spectral data are provided in the appendix.

Finally, the chemical structure of one of the boron complexes **36c**, was established by the single crystal X-ray analysis and its ORTEP diagram is depicted in **Figure 4.10A**. The X-ray analytical data as cif file is also deposited in Cambridge Crystallographic Data Center (CCDC) with CCDC number 1400815. The asymmetric unit of complex **36c** is depicted in **Figure 4.10B**, which shows well-ordered molecular packing in its unit cell. The crystal structure analysis revealed that the boron center exists in distorted tetrahedral geometry and both the seven and five membered rings of boron-aminotroponimine core structure are tilted in 7.19° . $\text{N}_2\text{-B}$ bond is a typical N-B single bond, with the bond length 1.542 Å. The bond length of $\text{N}_1\text{-B}$ is 1.528 Å, which is lesser than $\text{N}_2\text{-B}$ bond length.⁵⁴ Selected bond lengths and bond angles are given in Table 4.2. The crystals of the boron complex **36c** were grown in chloroform by slow evaporation method for single crystal X-ray diffraction studies. Though, we attempted to crystallize the other solid boron complexes like **36a**, **36d** but our trials ended with needle like structures, from which we could not collect good X-ray diffraction data.

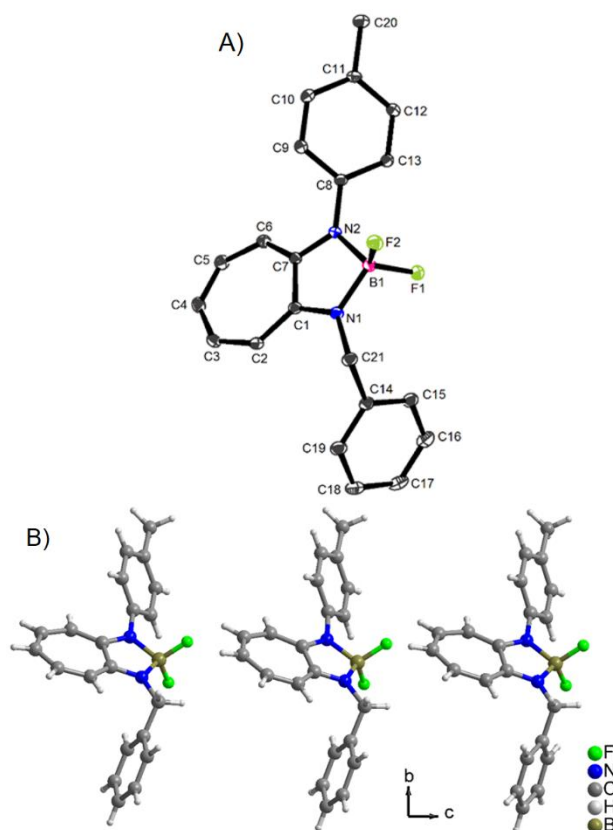


Figure. 4.10 A) ORTEP diagram of **36c** with 25% probability of ellipsoids, hydrogen atoms are deleted for clarity; B) Asymmetric unit of **36c**.

Table 4.2 Selected bond lengths and bond angles of boron complex **36c** in solid state.

selected bond lengths	selected bond angles	selected bond angles
$C_1-C_7 = 1.463 \text{ \AA}$	$N_1-B-N_2 = 98.10^\circ$	$F_1-B-N_2 = 113.90^\circ$
$C_1-N_1 = 1.334 \text{ \AA}$	$F_2-B-N_2 = 112.26^\circ$	$C_1-N_1-B = 112.87^\circ$
$C_7-N_2 = 1.350 \text{ \AA}$	$F_1-B-F_2 = 107.72^\circ$	$C_7-N_2-B = 111.64^\circ$
$N_1-B = 1.528 \text{ \AA}$	$F_2-B-N_1 = 113.44^\circ$	$N_2-C_7-C_1 = 108.45^\circ$
$N_2-B = 1.542 \text{ \AA}$	$F_1-B-N_1 = 111.36^\circ$	$N_1-C_1-C_7 = 108.61^\circ$

4.2B.2 Photophysical studies of aminotroponimines and boron-aminotroponimines

Absorption properties of aminotroponimine ligands: After synthesis, we performed the photophysical studies with the boron-aminotroponimine complexes (**36a-i**). First, the absorption and emission of aminotroponimine ligands (**35a-g**) were recorded in cyclohexane as control experiments. The absorption spectra of ligands (**35a-g**) in cyclohexane and acetonitrile are depicted in **Figure 4.11A&C**, respectively. Their absorption parameters are tabulated in **Table 4.3**. The UV-Vis spectrum of aminotroponimine ligand **35a** exhibits three

peaks at 416 nm, 359 nm and 345 nm in cyclohexane. The absorption peaks at 359 and 345 nm has shown partial splitting and separated by 1130 cm^{-1} . While a clear separation was observed between the absorption peaks at 416 and 359 nm and separated by 3817.0 cm^{-1} . The absorption peak at 416 nm is a broad absorption peak. The appearance of two major absorption peaks are due to transition to two different electronically excited states. The partial splitting between the two peaks at 359 nm and 345 nm is possibly due to the vibronic progression of the electronic transition to the same electronically excited state. In literature, similar kind of absorption patterns is reported for tropolone in cyclohexane.¹¹⁻¹⁴ But, a redshift in absorption peaks and changes in their intensities are observed with aminotroponimine ligand **35a** when compared to

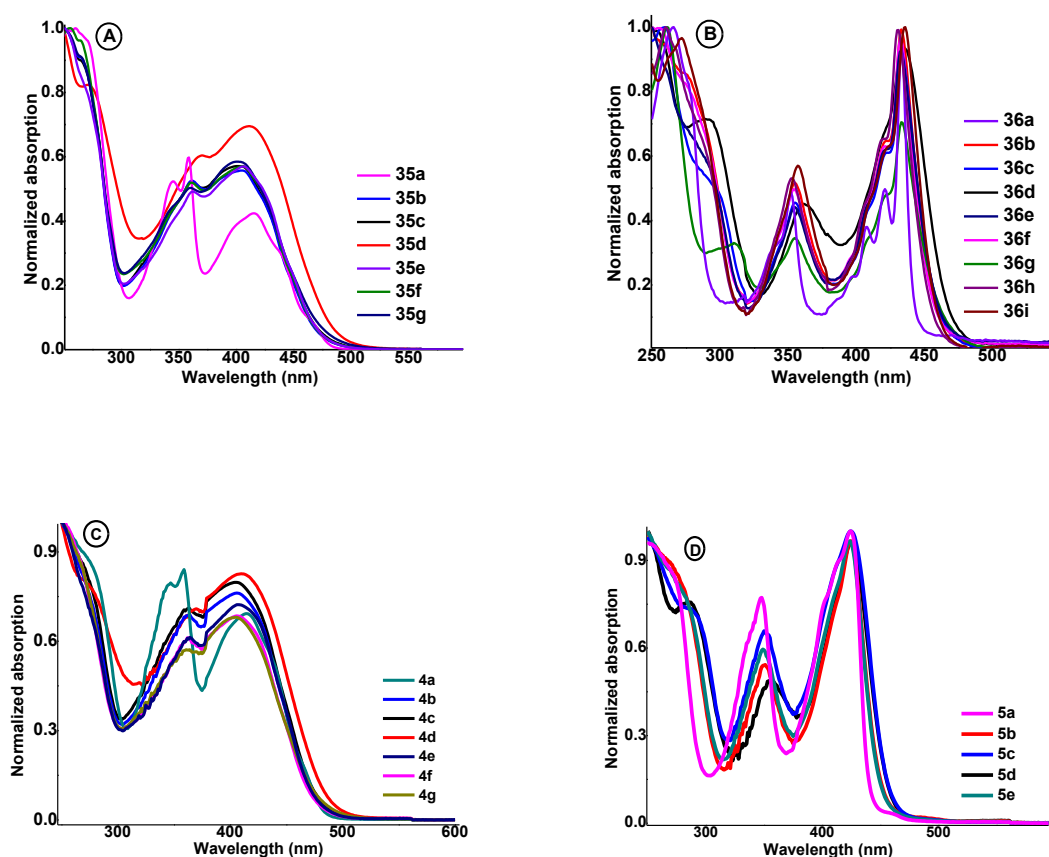


Figure 4.11 A) Absorption spectra of aminotroponimate ligands (**35a-g**) in cyclohexane. B) Normalized absorption spectra of boron-complexes (**36a-i**) in cyclohexane. C) Normalized absorption spectra of aminotroponimine ligands (**35a-g**) in acetonitrile. D) Normalized absorption spectra of boron-aminotroponimines in acetonitrile (**36a-e**).

tropolone absorption spectrum in cyclohexane. The absorption spectra of the remaining aminotroponimine ligands **35b-g** exhibits a broad absorption peak with the absorption maxima at ca. 402 (for **35d**, λ_{max} =412 nm) and a shoulder peak at 362 nm (**Figure. 4.11A**).

Table 4.3 Absorption parameters of aminotroponimine ligands

entry	Absorption maxima in cyclohexane (nm)	Other absorptions in cyclohexane (nm)	Absorption maxima in CH ₃ CN (nm)	Other absorption peaks in CH ₃ CN (nm)
4a	345, 359	416	358, 346	415
4b	402	362	406	363
4c	402	362	405	363
4d	412	362	410	363
4e	402	362	407	363
4f	402	362	405	363
4g	402	362	405	363

We also found a blueshift in absorption maxima for aminotroponimine ligands **35b/c/e/f/g** (λ_{max} =402 nm) over **35a** (λ_{max} =416 nm). This blueshift of ligands **35b/c/e/f/g** is due to replacing the benzyl substituent at amine nitrogen atom of the ligand with phenyl and substituted phenyl substituents. The presence of phenyl ring at *N*-atom of aminotroponimine decreases the basicity of nitrogen, and subsequently the delocalization of nitrogen lone pair decreases towards the troponyl ring. [14b,c] However, the substituents on the phenyl ring does not have any effect on the absorption maxima of ligands **35b/c/e/f/g**. For example, **35b/c/e/f/g** have shown similar absorption pattern though ligand **35e/f** contains 4-chlorophenyl/4-fluorophenyl substituents and ligands **35b/c/g** contains phenyl/4-methylphenyl/4-methoxyphenyl substituents on nitrogen atoms. In contrast, the absorption maxima of aminotroponimine ligand **35d** is redshifted over **35b/c/e/f/g** to ca. 412 nm with a shoulder peak at 362 nm. This is possibly occurring due to replacement of two benzyl substituents with the phenyl substituents, as a result extension of conjugation towards phenyl ring occurs through the imine *N*-atom of aminotroponimines.

All aminotroponimine ligands, other than **35a**, have shown broad absorption peak with absorption maxima at 402 nm and 412 nm (**35d**) and a shoulder peak at 362

nm. The absorption spectra of aminotroponimine ligands (**35b-g**) in acetonitrile has shown more separation between 363 nm and 405-410 nm absorption peaks (**Figure 4.11C**), unlike absorption spectra in cyclohexane. Interestingly, in case of ligand **35a**, partial merging of absorption peaks at 346 and 358 nm was observed in acetonitrile. These studies supports that the appearance of shoulder peak at ~362 nm is most probably due to another electronic transition.⁴⁹⁻⁵²

Overall, two electronic transitions were observed for all aminotroponimine ligands in cyclohexane and acetonitrile, and substituents on the nitrogen atoms of ligands have significant effect on their absorption properties. However, the emission spectra of these ligands (**35a-g**) did not exhibit any significant emission peaks. These studies supports the feature that the ligands are non-fluorescent molecules in cyclohexane solvent.

Absorption properties of boron-aminotroponimines: Then, the absorption spectra of boron-aminotroponimine complexes (**36a-i**) were recorded in cyclohexane and acetonitrile. Their spectra are provided in **Figure. 4.11B&D**. The absorption spectra of these boron-aminotroponimine complexes exhibits only two major absorption bands at ~350 nm and 430 nm, with absorption maxima at ~430 nm (approx.) in cyclohexane. The occurrence of two absorption peaks are due to two different electronic transitions. The separation between the two absorption peaks are more or less similar for all boron complexes. Significant redshift in the absorption maxima is observed from aminotroponimines to boron-aminotroponimines. The summary of UV-vis absorption data of boron-aminotroponimines (**36a-i**) are provided in **Table 4.4** (column 2). The extinction coefficients (ϵ) of **36a-i** are determined at $\lambda_{abs,max}$ 430 nm from the respective absorption spectra and their values are described in **Table 4.3** (column 3). Unlike

aminotroponimine ligands, absorption maxima for all boron complexes **36a-i** are observed at ~430 nm (**Figure 4.11B**, **Table 4.4**). Importantly, sharp absorption peaks were observed in case of boron-aminotroponimines in cyclohexane, ethanol and acetonitrile. The appearance of sharp absorption peaks indicates the rigidification of the structure after BF₂-complexation. The absorption spectra of boron complex **36a** in cyclohexane has shown sharp absorption peaks at 433, 421, and 408 nm and in case of other complexes (**36b-i**) these peaks were appeared as shoulder peaks. The appearance of these peaks are due to vibronic transition to the same electronically excited state. This was further supported by the absorption spectra in ethanol and acetonitrile, where these peaks are merged and single absorption peak was observed at ~425 nm (**Figure 4.11C**). From the literature, it has been learnt that the occurrence of vibronics are indication of less conformational disorder.^{14a} In case of boron complex **36a**, the occurrence of well-resolved vibronic peaks are possibly due to less conformational disorder. Whereas, in boron complex **36d** the vibronic peaks are merged and single absorption peak was observed, this is probably due to more conformational disorder.

Emission properties of boron-aminotroponimines: The emission spectra of boron complexes (**36a-i**) were then recorded at excitation wavelength 350 nm in cyclohexane. These spectra are depicted in **Figure. 4.12** and emission maxima ($\lambda_{em.}$), Stokes shifts and quantum yields are summarized in **Table 4.4**. Boron-aminotroponimines have shown remarkable fluorescence character. The photograph taken under handheld UV lamp is depicted in **Figure 4.13** in solid and solution states. It is important to discuss the emission properties of these complexes. First of all, unlike absorption, tremendous variations in the

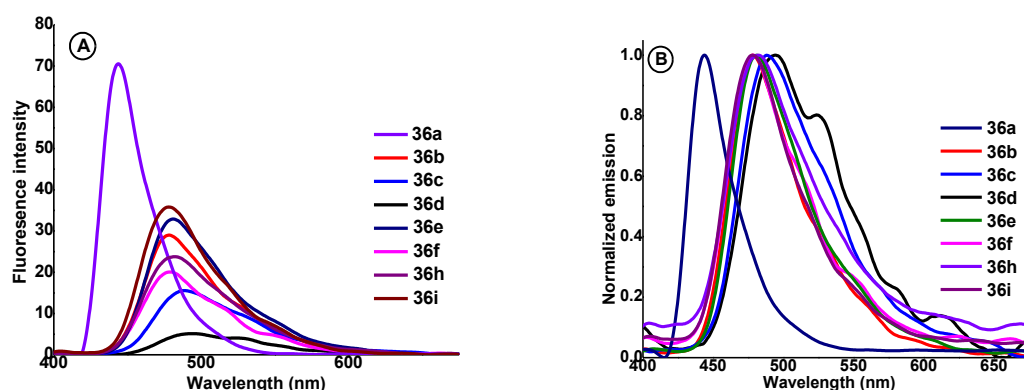


Figure 4.12 A) Emission spectra of boron-aminotroponimine complexes (**36a-i**) in cyclohexane at 20.0 μM concentration. B) Normalized emission spectra of boron complexes (**36a-i**) in cyclohexane.

Table 4.4 Photophysical parameters of *boron-aminotroponimines*

entry	λ_{abs}^a (nm)	ϵ^a ($\text{M}^{-1} \text{cm}^{-1}$)	λ_{em}^{ac} (nm)	Φ_f^b	Stokes shift (nm)	Stokes shift (cm^{-1})
36a	433, 421, 408, 352	36881	445	0.17	12	622
36b	434, 421, 355	16709	478	0.17	44	2120
36c	434, 421, 355	24651	487	0.07	53	2508
36d	435, 362	18342	494	0.05	59	2746
36e	432, 421, 355	12789	482	0.17	50	2402
36f	432, 421, 355	11571	479	0.15	47	2272
36g^d	433, 355	15155	nd	nd	nd	nd
36h	431, 419, 354	16670	478	0.15	47	2281
36i	435, 421, 357	18042	478	0.28	43	2068

^aAll measurements were carried out in cyclohexane, ^bQuantum yields were determined by considering quinine sulfate in 0.1 M H_2SO_4 as standard reference. ^c $\lambda_{\text{ex}} = 350$ nm.
^dboron complex **36g** has shown negligible fluorescence in cyclohexane.

emission properties of boron-aminotroponimines were observed. Nature of the substituents on the nitrogen atoms of the boron-aminotroponimines have dramatic effect on emission properties such as emission maxima and quantum yield. Boron complex **36a** exhibits strong emission at 445 nm (blue fluorescence) with 12 nm Stokes shift. Whereas the boron complexes **36b/h**, containing one *N*-phenyl substituent at nitrogen atom, have shown emission maxima (λ_{em}) at 478 nm (green fluorescence) with larger Stokes shift (44 nm). Interestingly, complex **36d**, containing *N,N'*-diphenyl substituents on nitrogen atoms, emits at wavelength 487 nm

(λ_{em}) with further enhancement in Stokes shift (59 nm). Thus, *N*-phenyl substituted boron complexes shows noticeable redshift in their emission maxima with a corresponding increase in the Stokes shift. The emission maxima of boron complexes **36e/f** is more redshifted when compare to **36b** and their Stokes shifts are 50 and 47 nm, respectively (chlorophenyl/fluorophenyl substituents). Moreover, boron complexes **36c** has shown further redshift in emission maxima when compare to **36b/e/f**. Overall, presence phenyl and substituted phenyl substituents on nitrogen atoms of boron complexes leads to larger Stokes shifts. Furthermore, the electron donating groups containing phenyl substituents on nitrogen atom of boron complexes causes more redshift. Here, we also attempted to investigate the effect of excitation wavelength on emission maxima. The boron complexes **36a/b/c/e/f** were excited at a wavelength 433 nm in cyclohexane. Their emission spectra are given in Supplementary Data. These results indicate that the emission wavelength is independent of excitation wavelength.

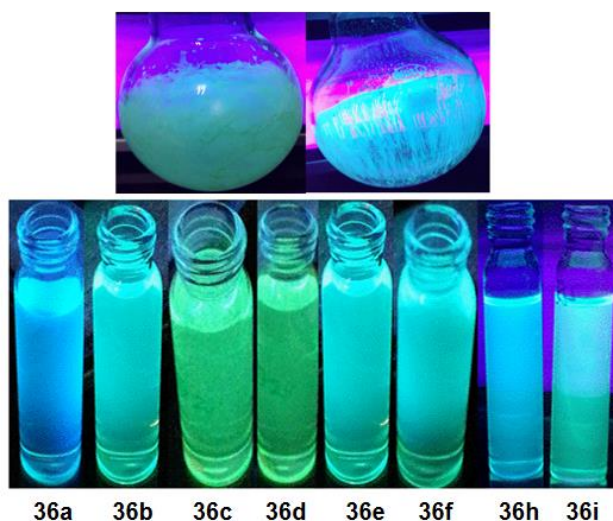


Figure 4.12 (A) Photographs of solid boron complexes. (B) Photograph of boron complexes in cyclohexane under hand hold UV lamp illumination.

Further, the quantum yields of boron-aminotroponimines (**36a-i**) were determined in cyclohexane by following the well-known relative method.¹⁶ Quinine sulfate in H₂SO₄ (0.1 M)

was used as reference standard. All the measurements were carried out under same instrumental parameters ($\lambda_{\text{ex}} = 350 \text{ nm}$, for reference and samples to be analyzed) and at 20°C . The obtained emission spectra are depicted in **Figure. 4.12** and their quantum yields are given in **Table 4.4**. As mentioned above, nature of the substituents on nitrogen atoms have significant effect on the quantum yield of boron-aminotroponimines **36a-i**. The maximum quantum yield achieved with the monomeric boron-aminotroponimines **36a/b/e/f/h** is 0.15-0.17 (Φ_f). The quantum yield of remaining monomeric boron-aminotroponimines such as **36c/d** is 0.07 and 0.05, respectively. However, as envisioned, the quantum yield of the dimeric boron complex **36i** was remarkably increased, almost twofold ($\Phi_f=0.28$). Interestingly, the calculated quantum yield for boron complexes **36a** and **36b** was same irrespective of their substituents. In case of other complexes, we found that the presence of electron donating groups on *N*-atoms of their ligands such as 4-methylphenyl (**36c**, $\Phi_f=0.07$), 4-methoxyphenyl (**36g**, negligible fluorescence) leads to dramatic decrease in the quantum yield, while presence of electron withdrawing substituents such as 4-chlorophenyl (**36e**, $\Phi_f=0.17$) and 4-fluorophenyl (**36f**, $\Phi_f=0.15$) does not lead to significant changes in quantum yield of respective boron complexes when compared to **36b** ($\Phi_f=0.17$). Overall, substituents at the nitrogen atoms of the boron-aminotroponimines have significant effect on emission maxima and quantum yield, unlike absorption.

We also recorded the absorption and emission spectra of boron-aminotroponimines (**36a-i**) in ethanol. Their spectra are provided in Supplementary Data. Unlike in cyclohexane, only two absorption peaks at ~ 425 and 350 nm are observed with all boron-aminotroponimines. However, the blue shifts (5-10 nm) in absorption and emission maxima was observed in ethanol and the larger Stokes shifts were also observed in ethanol. Except for **36a**, their quantum yields were significantly diminished in ethanol. Overall, our spectroscopic studies strongly suggest that boron-aminotroponimine complexes are fluorescent molecules like BODIPY analogue, but aminotroponimine precursors are non-fluorescent molecules.

4.3 Conclusions

In summary, the designed Boron-aminotroponimine complexes as BODIPY analogues are successfully synthesized and studied their photophysical characters with spectroscopic methods. The structure of one of boron complex (**36c**) is also established by single crystal X-ray analysis. The photophysical properties of those complexes are here found tunable in non-polar solvent by altering the nature of N-substituents of their ligands. The quantum yield of monomeric boron complexes are enhanced, almost by two folds, in non-polar solvent just by converting into dimeric form. The effect of environment polarity in quantum yield of those boron-complexes are also addressed which reveals that polar solvent significantly decreases their quantum yields. Hence, these results provide enormous opportunities to construct novel fluorophores from aminotroponimate ligand and Boron derivatives. Our further works are under progress to construct ligands and their Boron complexes to further improve the quantum yield.

4.4 Experimental Section

Materials, instrumentation and methods: All required materials and solvents were purchased from commercial suppliers and used without any further purification unless noted. Anhydrous dichloromethane was freshly prepared by distilling over Calcium hydride. Reactions were monitored by thin layer chromatography, visualized by UV and Ninhydrin. Column chromatography was performed in 230-400 and 100-200 mesh silica. Mass spectra were obtained from Bruker micrOTOF-Q II Spectrometer and the samples were prepared in acetonitrile and injected in acetonitrile and water mixture. NMR spectra were recorded on Bruker AV-400 at room temperature (^1H : 400 MHz, ^{13}C : 100.6 MHz). ^1H and ^{13}C NMR chemical shifts were recorded in ppm, downfield from tetramethyl silane. Splitting patterns are abbreviated as: s, Singlet; d, doublet; dd, doublet of doublet; t, triplet; q, quartet; dq, doublet

of quartet; m, multiplet. Absorption spectra were obtained using Perkin-Elmer λ -750. Fluorescence spectra were obtained from Perkin-Elmer LS-55 using Xenon lamp. All spectroscopic measurements were carried out with spectroscopic grade, non-degassed solvents and at 20°C.

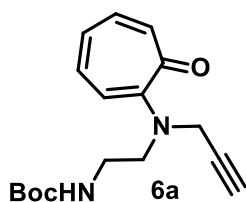
Relative fluorescence quantum yields were determined by comparing with quinine sulfate quantum yield in 0.1 M H₂SO₄ (0.54). The obtained values were substituted in the equation given below.

$$\Phi_x = \Phi_r \times \frac{F_x}{F_r} \times \frac{1 - 10^{-A_r}}{1 - 10^{-A_x}} \times \frac{\eta_x^2}{\eta_r^2}$$

The subscripts x and r refers sample to be measured and reference. F denotes the area under curve of the integrated fluorescence spectra, A stands for optical density at excited wavelength, η represents refractive index of the solvent used.

1. *tert*-butyl(2-(prop-2-yn-1-ylamino)ethyl)carbamate (**5a**): N-Boc ethylenediamine (7.5 mmol, 1.2 gm) was dissolved in 20 mL of acetonitrile and added K₂CO₃ (1.03 gm, 7.5 mmol). Propargyl bromide (5.0-6.0 M in toluene (7.5 mmol, 0.769 mL) was added to the above mixture slowly and allowed to stirring at room temperature. After 4 h the reaction mixture was filtered to remove K₂CO₃ and the filtrate was concentrated to get crude product. Later the crude product was purified through silica gel column hexanes and ethyl acetate as eluents to get desired product in 37% yield (550 mg) and used in further steps without any characterization.

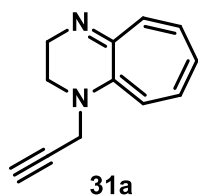
2. *tert*-butyl (2-((7-oxocyclohepta-1,3,5-trien-1-yl)(prop-2-yn-1-yl)amino)ethyl)carbamate



(**30**): 550 mg (2.77 mmol) of N-Boc aminoethyl propargyl amine was dissolved in ethanol. To this Et₃N (3.33 mmol, 465 μ L) and 2-tosyloxy tropone (**2**, 3.33 mmol, 920 mg) was added. The suspension was allowed to reflux for 30 hrs, after completion of the reaction, all volatiles were

removed under low pressure to get the crude product. The crude product was purified through silica gel column with 20% ethylacetate in hexane. The collected fractions were evaporated at 45⁰C under reduced pressure to get the desired product (**30**) in 44% yield (370 mg) and the obtained product was stored at -20⁰C. ¹H NMR (400 MHz, CDCl₃) δ 7.18 – 6.91 (m, 4H), 6.76 – 6.61 (t, 1H), 5.97 (s, 1H), 4.09 (d, *J* = 2.2 Hz, 2H), 3.52 (t, *J* = 6.0 Hz, 2H), 3.39 (dd, *J* = 11.2, 5.6 Hz, 2H), 2.28 (t, *J* = 2.2 Hz, 1H), 1.41 (d, *J* = 15.1 Hz, 9H). ¹³C NMR (101 MHz, CDCl₃) δ 182.61, 157.95, 156.38, 135.83, 135.19, 133.85, 126.56, 118.85, 79.00, 78.24, 73.52, 48.64, 39.92, 38.01, 28.43. HRMS (ESI-TOF) *m/z*: [M+Na]⁺ calcd. for C₁₇H₂₂N₂O₃ 325.1523, found 325.1518.

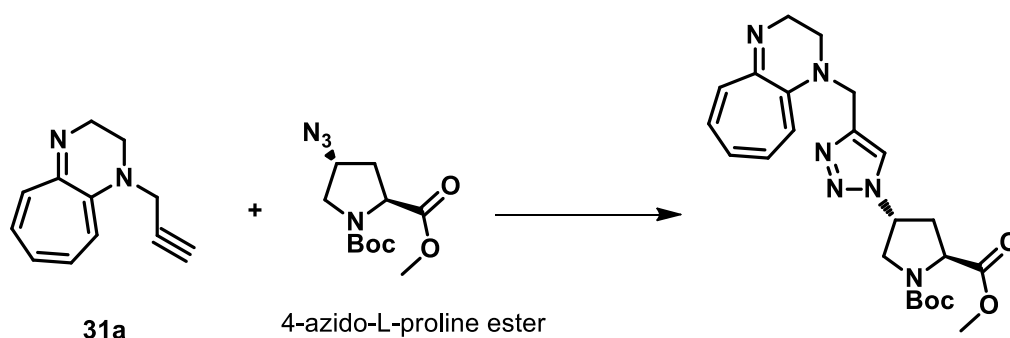
3. *1-(prop-2-yn-1-yl)-2,3-dihydro-1H-cyclohepta[b]pyrazine (31a)*:



64 mg (0.21 mmol) of compound **6a** was taken in round bottom flask, to this 20% TFA in DCM (4 mL) was added and allowed to stirring at room temperature. The reaction was monitored by TLC, after completion of the reaction all volatiles were evaporated to get desired product and used in next step. The obtained product was dissolved in 5mL of DCM and 7 eq of Et₃N was added, the reaction mixture was allowed to stirring at room temperature. Reaction was monitored by TLC, visualized by fluorescence lamp and finally in order to confirm it was characterized by Mass spectrometer. After completion of the reaction all solvents were removed under reduced pressure to get desired product. To remove excess ET₃N, to the obtained product tert-butyl methyl ether was added, shaken well and decanted gently. This process was repeated for three times and obtained product (90%, 35 mg) was characterized as desired product with NMR and Mass Spectrometry techniques. ¹H NMR (400 MHz, CDCl₃) δ 7.73 (d, *J* = 11.6 Hz, 1H), 7.45 (dd, *J* = 19.1, 9.2 Hz, 2H), 7.13 (d, *J* = 10.9 Hz, 1H), 7.05 (t, *J* = 9.4 Hz, 1H), 4.35 (d, *J* = 2.3 Hz, 2H), 3.87 (s, 2H), 3.70 (t, *J* = 5.0 Hz, 2H), 2.44 (dd, *J* = 4.8, 2.4 Hz, 1H). ¹³C NMR (101 MHz, CDCl₃) δ 155.07, 146.37, 139.92, 137.10, 129.24, 126.07, 119.83, 75.14, 74.67, 46.53, 43.04, 40.74,

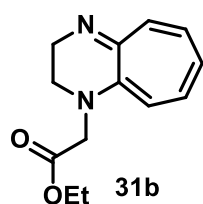
(45.68, 8.41, Et₃N peaks). HRMS (ESI-TOF) m/z: [M+H]⁺ calcd. for C₁₂H₁₂N₂ 185.1073, found 185.1078.

4. *Click reaction*: To the mixture of DIPEA, acetic acid and CuI, was added a mixture of 4-azido-L-proline methyl ester and **7** in dichloromethane. The reaction mixture is allowed to stir at room temperature for 3 hrs. After completion of the reaction, the reaction mixture was filtered through filter paper and the filtrate was concentrated to get desired product and characterized by Mass spectrometry. HRMS (ESI-TOF) m/z: [M+H]⁺ calcd. for C₂₃H₃₀N₆O₄ 455.2401, found 455.2422.



Ligation of fluorophore **31a** with amino acids *via* Click reaction.

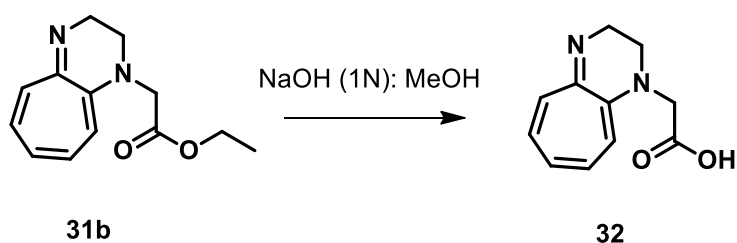
6. Ethyl 2-(2,3-dihydro-1H-cyclohepta[b]pyrazin-1-yl) acetate (**31b**):



Ethyl-(2-N-Boc-aminoethyl)troponylglycinate(**6b**) 50 mg was taken, to this 20% TFA in DCM was added and allowed to stirring at room temperature.

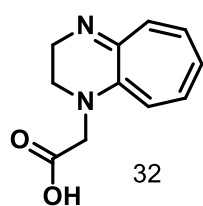
The reaction was monitored by thin layer chromatography and after completion of the reaction, TFA and DCM was evaporated to obtain 2-amino ethyl troponyl glycinate (**5a**) as TFA salt. To this 7 equiv. of Et₃N was added. The reaction mixture is allowed to stirring for 1 hrs. The reaction was monitored by TLC, visualized by fluorescence lamp and finally in order to confirm, it was characterized by Mass spectrometer. After completion of the reaction all volatiles were removed under reduced pressure and to the crude product, *tert*-butyl methyl ether was added, shaken well and decanted gently to remove excess of Et₃N. This

process was repeated for three times and obtained product (90%, 35 mg) was characterized as desired product with NMR and Mass Spectrometry. ^1H NMR (400 MHz, CDCl_3) δ 7.74 (t, J = 17.5 Hz, 1H), 7.47 (d, J = 28.5 Hz, 1H), 7.32 (dd, J = 12.5, 5.8 Hz, 1H), 7.18 – 6.89 (m, 1H), 6.76 (d, J = 10.3 Hz, 1H), 4.37 (s, 2H), 4.32 – 4.21 (q, 2H), 3.92 (d, J = 31.0 Hz, 2H), 3.71 (s, 2H), 1.33 – 1.26 (t, 3H). ^{13}C NMR (101 MHz, CDCl_3) δ 166.98, 154.88, 147.03, 139.85, 136.72, 128.92, 126.00, 118.27, 62.45, 54.77, 48.42, 40.90, 14.07. HRMS (ESI-TOF) m/z : $[\text{M}+\text{H}]^+$ calcd. for $\text{C}_{13}\text{H}_{16}\text{N}_2\text{O}_2$ 233.1285, found 233.1253.



Scheme S2. Hydrolysis of **31b** ester

7. 2-(2,3-dihydro-1H-cyclohepta[b]pyrazin-1-yl) acetic acid (**32**):

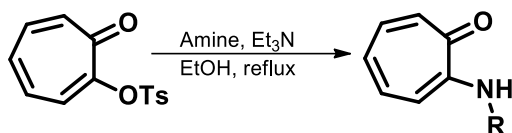


2-amino ethyl troponyl glycinate was taken in water and to this 5 eq of NaOH was added. The reaction mixture is allowed to stirring for 1 hrs, the reaction was monitored by TLC and also a drop of reaction mixture was taken in glass vial, added 1N HCl, this was visualized by fluorescence lamp, where green fluorescence was observed. Finally in order to confirm the reaction mixture was analyzed by mass spectrometry. After completion of the reaction, the basic solution was neutralized to pH 7 with 1N HCl under careful monitoring. Then all volatiles were removed under reduced pressure. To the crude product methanol was added, shaken well, and filtered through filter paper. The filtrate was concentrated to get desired product. To this again methanol was added and filtered, the filtrate was concentrated. This process was repeated for three times to remove excess sodium salts.

The product was characterized with NMR and Mass spectrometry. HRMS (ESI-TOF) m/z :

$[M+H]^+$ calcd. for $C_{11}H_{12}N_2O_2$ 205.0972, found 205.0949.

General procedure for the synthesis of aminotropones:



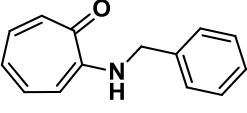
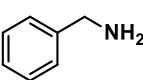
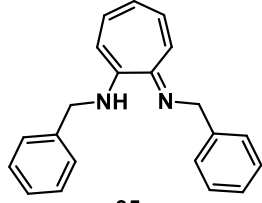
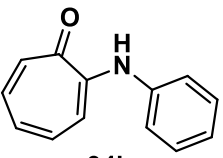
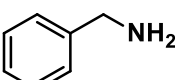
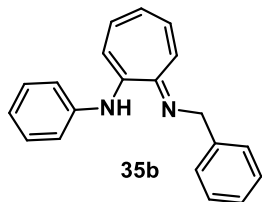
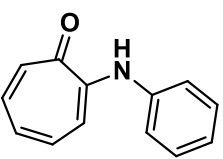
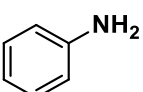
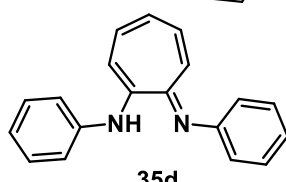
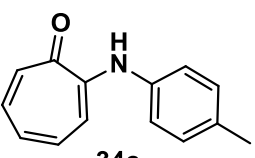
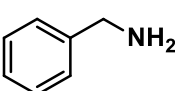
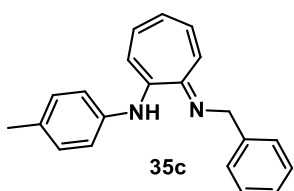
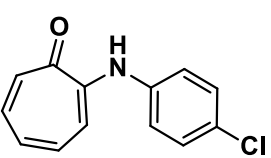
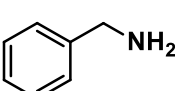
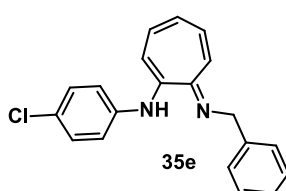
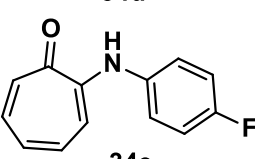
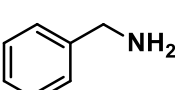
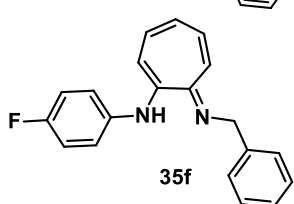
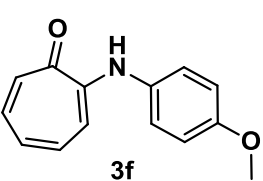
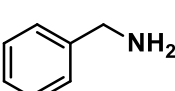
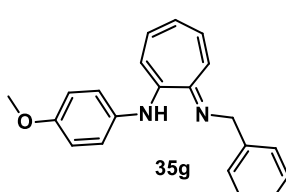
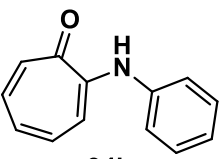
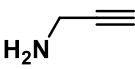
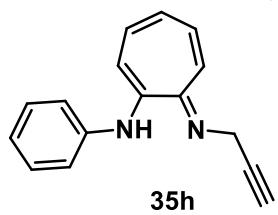
entry	amine	product	yield
1.		 34a	90%
2.		 34b	85%
3.		 34c	92%
4.		 34d	78%
5.		 34e	80%
6.		 34f	85%

2-

tosyloxypone and anilines (2-3 equiv) were dissolved in ethanol, to this Et₃N was added. The reaction mixture was allowed to reflux and monitored by TLC. The general reaction time for all the reactions is 16-24 h. All volatiles were evaporated under reduced pressure after reaction completion which was judged by TLC. To the crude product 1N HCl was added and extracted with dichloromethane (thrice), the combined organic layers were dried over Na₂SO₄ and evaporated under reduced pressure. The obtained crude product was purified by silica gel column chromatography by using ethyl acetate and hexane mixture as mobile phase.

General procedure for synthesis of aminotroponimines: Triethyloxonium tetrafluoroborate (1.2 equiv) was dissolved in anhydrous dichloromethane, to the resultant solution aminotropone solution in anhydrous dichloromethane was added slowly. The reaction mixture was allowed to stir for overnight at room temperature and all volatiles were evaporated under reduced pressure. The crude residue was taken up in anhydrous ethanol and alkyl/aryl amine was added slowly at room temperature. The resultant mixture was allowed to stir at room temperature for 10 h. The completion of the reaction was judged by TLC and volatiles were evaporated under vacuo to obtain the crude product. To the crude product, 1.0 M NaOH was added and extracted with dichloromethane (thrice). The organic layers were combined together, dried over Na₂SO₄ and concentrated under vacuo. The crude product was purified through silica gel column chromatography by using 5-10% EtOAc and hexanes as mobile phase.



entry	aminotropone	amine	aminotroponimine	yield
1.	 34a	 	 35a	82%
2.	 34b	 	 35b	68%
3.	 34b	 	 35d	46%
4.	 34c	 	 35c	78%
5.	 34d	 	 35e	57%
6.	 34e	 	 35f	56%
7.	 34f	 	 35g	87%
8.	 34b	 	 35h	74%

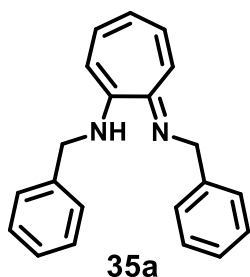
Procedure for the synthesis of N,N'-(diphenyl)-2-(1,4-diaminobutyl)ditroponimine:

Triethyloxonium tetrafluoroborate was dissolved in DCM to this N-phenyl aminotropone solution in DCM was added slowly. The reaction mixture left for stirring at room temperature for overnight. Then all the volatiles were evaporated under reduced pressure. Obtained residue was redissolved in ethanol and to this 1.0 equiv 1, 4-diaminobutane was added in two portions. The reaction mixture was allowed for stirring for 2 days. All the volatiles were evaporated under reduced pressure and to the obtained crude residue 1 NaOH was added and extracted thrice with DCM. Combined organic layers were dried over sodium sulphate and concentrated under vacuo. The obtained crude product was purified through silica gel chromatography.

General procedure for synthesis of boron-aminotroponimines: Aminotroponimine was dissolved in anhydrous dichloromethane and to this 10 equivalents of anhydrous triethylamine was added under nitrogen atmosphere. To the resultant reaction mixture 10 equivalents of $\text{BF}_3 \cdot \text{OEt}_2$ was added drop wise and left to stirring at room temperature until reaction completion, as judged by TLC, all reactions were completed within half an hour (For the synthesis of **36d**, 20 equivalents of triethylamine and $\text{BF}_3 \cdot \text{OEt}_2$ was used, whereas for the synthesis of **36i**, 25 equivalents of triethylamine and $\text{BF}_3 \cdot \text{OEt}_2$ was used). All volatiles were evaporated under reduced pressure and to the crude residue, water was added to quench the unreacted $\text{BF}_3 \cdot \text{OEt}_2$ and extracted with ethyl acetate (thrice). The combined organic layers were dried over sodium sulfate and concentrated. The crude product was purified through silica gel column chromatography by using 100% DCM as mobile phase.

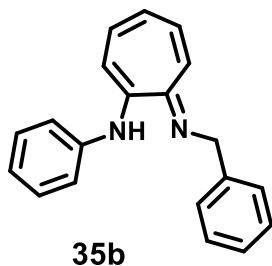
Analytical data:

N-(benzyl)-2-(benzylamino)troponimine (**35a**):



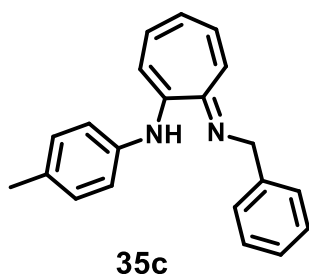
The pure product was obtained as bright yellow solid. ¹ (350 mg, isolated yield = 82%, mp = 82-84 °C). ¹H NMR (400 MHz, CDCl₃) δ 7.46 – 7.33 (m, 8H), 7.33 – 7.25 (m, 2H), 6.81 (t, *J* = 10.1, 2H), 6.42 (app d, *J* = 10.9, 2H), 6.23 (t, *J* = 9.2, 1H), 4.64 (s, 4H). ¹³C NMR (101 MHz, CDCl₃) δ 153.32, 139.68, 133.34, 128.47, 127.29, 126.80, 118.54, 111.08, 50.21. HRMS (ESI-TOF) *m/z*: [M+H]⁺ calcd. for C₂₀H₂₁N₂ 301.1699, found 301.1731.

N-(phenyl)-2-(benzylamino)troponimine (**35b**):



The pure product was obtained as yellow solid. (400 mg, isolated yield = 68%, mp = 112-114 °C). FT-IR (KBr plate) *v* = 3264, 3060, 3027, 2922, 1589, 1527, 1512, 1467, 1452, 1414, 1387, 1356, 1298, 1275, 1232, 1166, 1019, 846, 746, 696. ¹H NMR (400 MHz, CDCl₃) δ 7.47 – 7.30 (m, 7 H), 7.09 (t, *J* = 7.3, 1H), 6.91 (d, *J* = 7.8, 2H), 6.88 – 6.75 (m, 2H), 6.72 – 6.67 (m, 1H), 6.38 – 6.15 (m, 2H), 4.62 (s, 2H). ¹³C NMR (101 MHz, CDCl₃) δ 155.07, 151.25, 150.86, 137.38, 133.88, 133.22, 129.44, 128.76, 127.46, 127.27, 122.64, 120.98, 120.93, 120.03, 105.67, 47.29. HRMS (ESI-TOF) *m/z*: [M+H]⁺ calcd. for C₂₀H₁₈N₂ 287.1543, found 287.1575.

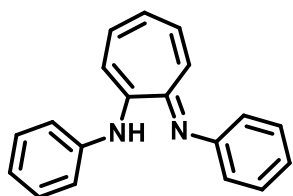
N-(4-methyl phenyl)-2-(benzylamino)troponimine (**35c**):



The pure product is obtained as yellow solid. ¹ (390 mg, isolated yield = 78%, mp = 115-117 °C) ¹H NMR (400 MHz, CDCl₃) δ 7.99 (s, 1H), 7.46 – 7.36 (m, 4H), 7.35 – 7.28 (m, 1H), 7.19 (d, *J* = 7.7, 2H), 6.88 – 6.74 (m, 4H), 6.69 – 6.64 (m, 1H), 6.25 (t, *J* = 9.3, 1H), 6.18 (app d, *J* = 9.9, 1H), 4.60 (s, 2H), 2.37 (s, 3H). ¹³C NMR (101 MHz, CDCl₃) δ 155.15, 150.85, 148.49, 137.45, 133.73, 132.98, 131.95, 130.00, 128.72, 127.39, 127.22, 120.94,

120.75, 119.90, 105.44, 47.25, 20.85. HRMS (ESI-TOF) m/z : $[M+H]^+$ calcd. for $C_{21}H_{20}N_2$ 301.1699, found 301.1717.

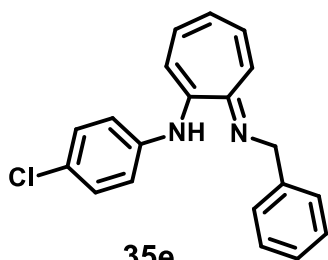
N-(Phenyl)-2-(phenylamino)troponimine (**35d**):



35d

Bright red viscous liquid turned into soft solid after long standing at room temperature.¹ (240 mg, isolated yield = 46%) 1H NMR (400 MHz, $CDCl_3$) δ 7.46 (app dd, $J=10.2, 5.4$, 4H), 7.21 (t, $J=6.6$, 6H), 6.92 (d, $J=11.1$, 2H), 6.83 – 6.73 (m, 2H), 6.39 (t, $J=9.2$, 1H). ^{13}C NMR (101 MHz, $CDCl_3$) δ 151.75, 145.05, 133.36, 129.39, 123.84, 122.47, 122.04, 114.82. HRMS (ESI-TOF) m/z : $[M+H]^+$ calcd. for $C_{19}H_{16}N_2$ 273.1386, found 273.1328.

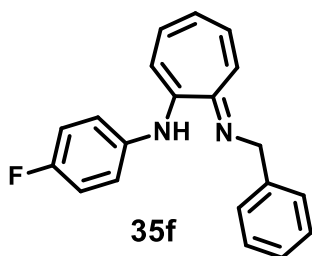
N-(4-chloro phenyl)-2-(benzylamino)troponimine (**35e**):



35e

The pure product was obtained as light yellow solid. (190 mg, isolated yield = 57%, mp = 145-147 °C). FT-IR (KBr plate) ν = 3265, 3062, 3028, 2959, 2922, 2851, 1589, 1512, 1467, 1452, 1415, 1388, 1356, 1276, 1234, 1087, 1022, 1008, 850, 839, 737, 708, 696. 1H NMR (400 MHz, $CDCl_3$) δ 7.38 (d, $J=5.8$ Hz, 4H), 7.32 (d, $J=8.4$ Hz, 3H), 6.87 – 6.80 (m, 3H), 6.72 (s, 2H), 6.29 (d, $J=4.5$ Hz, 1H), 6.22 (app d, $J=9.9$ Hz, 1H), 4.60 (s, 2H). ^{13}C NMR (101 MHz, $CDCl_3$) δ 155.42, 150.90, 149.88, 137.24, 134.17, 133.61, 129.46, 128.80, 127.62, 127.53, 127.26, 122.41, 120.73, 120.26, 106.07, 47.28. HRMS (ESI-TOF) m/z : $[M+H]^+$ calcd. for $C_{20}H_{17}ClN_2$ 321.1153, found 321.1160.

N-(4-fluoro phenyl)-2-(benzylamino)troponimine (**35f**):

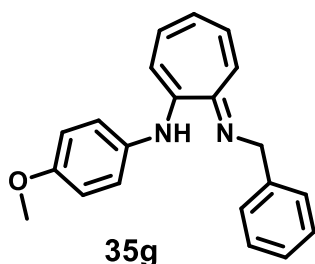


35f

The pure compound was obtained as off red solid. (400 mg, isolated yield = 56%, mp = 105-108 °C) FT-IR (KBr plate) ν = 3263, 3031, 2922, 1590, 1526, 1494, 1467, 1452, 1415, 1387, 1356, 1275, 1213, 1195, 860, 842, 785, 738, 696. 1H NMR (400 MHz, $CDCl_3$) δ 7.38

(t, $J = 6.6$ Hz, 4H), 7.35 – 7.28 (m, 1H), 7.08 – 7.03 (m, 2H), 6.89 – 6.78 (m, 3H), 6.78 – 6.64 (m, 2H), 6.27 (t, $J = 8.7$ Hz, 1H), 6.21 (app d, $J = 9.7$ Hz, 1H), 4.60 (s, 2H). ^{13}C NMR (101 MHz, CDCl_3) δ 160.13, 157.74, 155.62, 150.87, 147.18, 137.31, 134.05, 133.40, 128.78, 127.50, 127.27, 122.15, 122.08, 120.71, 120.11, 116.17, 115.95, 105.83, 47.28. HRMS (ESI-TOF) m/z : $[\text{M}+\text{H}]^+$ calcd. for $\text{C}_{20}\text{H}_{17}\text{FN}_2$ 305.1499, found 305.1462.

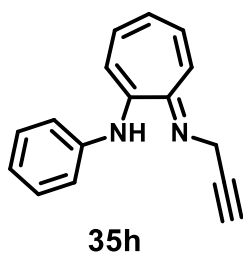
N-(4-methoxy phenyl)-2-(benzylamino)troponimine (**35g**):



The pure product was obtained as bright red solid. (500 mg, isolated yield = 87%, mp = 102-104 °C). FT-IR (KBr plate) $\nu = 3261, 2922, 1693, 1679, 1658, 1642, 1588, 1514, 1495, 1467, 1452, 1275, 1234, 1034, 837$. ^1H NMR (400 MHz, CDCl_3) δ 7.38 (d, $J = 4.2$ Hz, 1H),

7.32 (dt, $J = 8.5, 4.2$ Hz, 1H), 6.94 (d, $J = 8.5$ Hz, 1H), 6.90 – 6.75 (m, 1H), 6.73 – 6.60 (m, 1H), 6.31 – 6.12 (m, 1H), 4.61 (s, 1H), 3.84 (s, 1H). ^{13}C NMR (101 MHz, CDCl_3) δ 155.50, 155.39, 150.89, 144.16, 137.46, 133.76, 132.95, 128.73, 127.40, 127.25, 121.89, 120.85, 119.92, 114.76, 105.43, 55.47, 47.29. HRMS (ESI-TOF) m/z : $[\text{M}+\text{H}]^+$ calcd. for $\text{C}_{21}\text{H}_{20}\text{N}_2\text{O}$ 317.1648, found 317.1644.

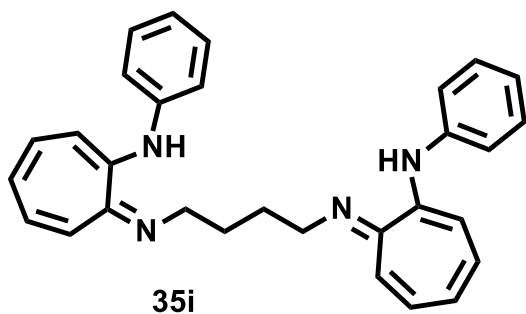
N-(phenyl)-2-(propergylamino)troponimine (**35h**):



The pure product was obtained as light red viscous liquid. (350 mg, isolated yield = 74%). FT-IR (KBr plate) $\nu = 3283, 2920, 2850, 1679, 1590, 1529, 1510, 1465, 1388, 1229, 697$. ^1H NMR (400 MHz, CDCl_3) δ 7.38 (t, $J = 7.7$ Hz, 2H), 7.08 (t, $J = 7.4$ Hz, 1H), 6.89 (t, $J = 9.8$ Hz, 3H),

6.75 (app d, $J = 12.0$ Hz, 1H), 6.69 – 6.64 (m, 1H), 6.35 – 6.28 (m, 1H), 6.26 (app d, $J = 9.9$ Hz, 1H), 4.17 (d, $J = 2.4$ Hz, 2H), 2.32 (t, $J = 2.2$ Hz, 1H). ^{13}C NMR (101 MHz, CDCl_3) δ 155.03, 150.74, 150.05, 133.64, 133.29, 129.44, 122.79, 121.42, 120.84, 105.97, 78.91, 71.96, 32.78. HRMS (ESI-TOF) m/z : $[\text{M}+\text{H}]^+$ calcd. for $\text{C}_{16}\text{H}_{14}\text{N}_2$ 235.1342, found 235.1230.

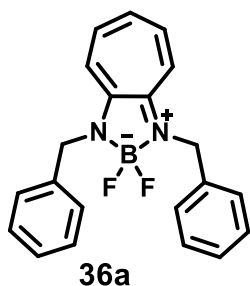
N,N-(diphenyl)-2-(1,4-diaminobutyl)ditroponimine (**35i**):



The pure product was obtained as yellow thick liquid, turned into soft solid after long standing. (70 mg, 20% yield,). ^1H NMR (400 MHz, CDCl_3) δ 7.35 (t, $J = 7.8$ Hz, 4H), 7.05 (t, $J = 7.4$ Hz, 2H), 6.86 (t, $J = 8.3$ Hz, 6H), 6.76 – 6.61 (m, 4H), 6.31 –

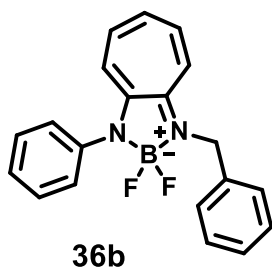
6.13 (m, 4H), 3.43 (t, $J = 5.8$ Hz, 4H), 1.96 (dd, $J = 5.9, 3.1$ Hz, 4H). ^{13}C NMR (101 MHz, CDCl_3) δ 154.95, 151.33, 150.93, 139.29, 133.97, 133.20, 129.31, 122.54, 121.04, 120.49, 119.57, 113.89, 105.16, 42.83, 26.47. HRMS (ESI-TOF) m/z : $[\text{M}+\text{H}]^+$ calcd. for $\text{C}_{30}\text{H}_{30}\text{N}_4$ 447.2543, found 447.2571.

Boron complex 36a:



The pure product was obtained as light green solid. (90 mg, isolated yield = 77%, mp = 159-161 °C). FT-IR (KBr plate) $\nu = 2922, 1599, 1546, 1495, 1469, 1452, 1439, 1415, 1351, 1298, 1248, 1144, 1096, 1075, 1056, 995, 733, 698$. ^1H NMR (400 MHz, CDCl_3) δ 7.40 (d, $J = 7.6$ Hz, 4H), 7.33 (t, $J = 7.5$ Hz, 4H), 7.26 – 7.21 (m, 4H), 6.81 – 6.65 (m, 3H), 4.85 (s, 4H). ^{13}C NMR (101 MHz, CDCl_3) δ 156.60, 138.50, 136.77, 128.71, 127.23, 127.18, 122.92, 113.93, 46.85. ^{11}B NMR (128 MHz, CDCl_3) δ 5.57 (t, $J = 30.8$ Hz). ^{19}F NMR (376 MHz, CDCl_3) δ -138.32 (q). HRMS (ESI-TOF) m/z : $[\text{M}+\text{H}]^+$ calcd. for $\text{C}_{21}\text{H}_{19}\text{BF}_2\text{N}_2$ 349.1686, found 349.1723.

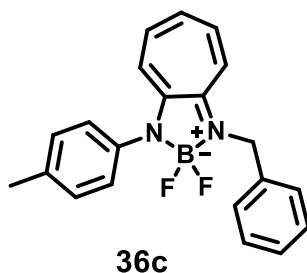
Boron complex 36b:



The pure compound was obtained as yellow thick liquid. (85 mg, isolated yield = 73%) FT-IR (KBr plate) $\nu = 2920, 2850, 1600, 1545, 1494, 1469, 1452, 1436, 1412, 1251, 1101, 1076$. ^1H NMR (400 MHz, CDCl_3) δ 7.49 (t, $J = 7.7$ Hz, 2H), 7.42 (d, $J = 5.0$ Hz, 4H), 7.37 - 7.29 (m, 4H), 7.27 - 7.24 (m, 2H), 7.02 (app d, $J = 10.7$ Hz, 1H), 6.84 - 6.76 (m, 2H), 4.86 (s, 2H).

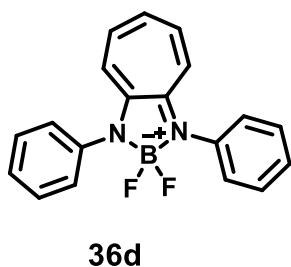
^{13}C NMR (101 MHz, CDCl_3) δ 156.55, 156.26, 139.05, 138.60, 138.55, 136.64, 129.68, 128.71, 127.27, 127.19, 126.15, 114.89, 114.70, 46.88. ^{11}B NMR (128 MHz, CDCl_3) δ 5.41 (t, J 29.8). ^{19}F NMR (376 MHz, CDCl_3) δ -135.68 – -136.02 (q). HRMS (ESI-TOF) m/z : $[\text{M}+\text{H}]^+$ calcd. for $\text{C}_{20}\text{H}_{17}\text{BF}_2\text{N}_2$ 335.1529, found 335.1546.

Boron complex 36c:



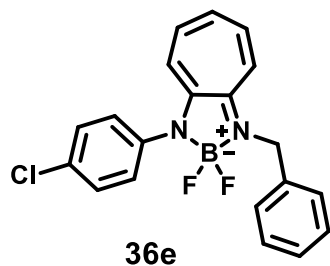
The pure product was obtained as yellow solid. (100 mg, isolated yield = 90%, mp = 149-149 °C) FT-IR (KBr plate) ν = 2923, 2852, 1599, 1544, 1512, 1468, 1437, 1414, 1350, 1251, 1099, 1075, 1000, 727. ^1H NMR (400 MHz, CDCl_3) δ 7.43 (d, J = 7.4 Hz, 2H), 7.38 – 7.22 (m, 9H), 7.03 (app d, J = 10.7 Hz, 1H), 6.82 - 6.75 (m, 2H), 4.86 (s, 2H), 2.41 (s, 3H). ^{13}C NMR (101 MHz, CDCl_3) δ 156.63, 156.22, 138.52, 138.42, 137.02, 136.73, 136.32, 130.31, 128.70, 127.27, 127.25, 125.87, 123.79, 114.74, 114.63, 46.89, 21.13. ^{11}B NMR (128 MHz, CDCl_3) δ 5.37 (t, J 29.7). ^{19}F NMR (376 MHz, CDCl_3) δ -135.88 – -136.31 (q). HRMS (ESI-TOF) m/z : $[\text{M}+\text{Na}]^+$ calcd. for $\text{C}_{21}\text{H}_{19}\text{BF}_2\text{N}_2$ 371.1505, found 371.1540.

Boron complex 36d:



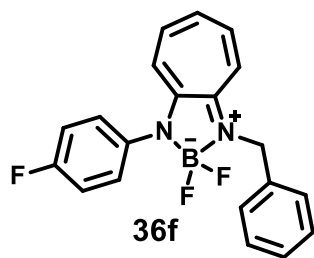
The pure product was obtained as yellow fine solid. (90 mg, isolated yield = 70%, mp = 165-167 °C) FT-IR (KBr plate) ν = 2919, 2850, 1592, 1542, 1493, 1474, 1453, 1434, 1405, 1250, 1097, 1060, 751, 694. ^1H NMR (400 MHz, CDCl_3) δ 7.55 – 7.47 (m, 4H), 7.44 (d, J = 7.2 Hz, 4H), 7.38 - 7.30 (m, 4H), 7.10 (app d, J = 10.6 Hz, 2H), 6.87 (t, J = 9.6 Hz, 1H). ^{13}C NMR (101 MHz, CDCl_3) δ 156.24, 138.93, 138.64, 129.73, 127.30, 126.24, 125.07, 115.66. ^{11}B NMR (128 MHz, CDCl_3) δ 5.21 (t, J 28.7). ^{19}F NMR (376 MHz, CDCl_3) δ -133.38 (q). HRMS (ESI-TOF) m/z : $[\text{M}+\text{Na}]^+$ calcd. for $\text{C}_{19}\text{H}_{15}\text{BF}_2\text{N}_2$ 343.1192, found 343.1048.

Boron complex 36e:



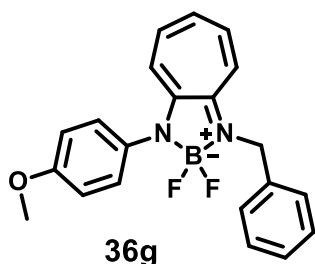
The pure product is obtained as yellow viscous liquid. (75 mg, isolated yield = 81%) FT-IR (KBr plate) ν = 2923, 2852, 1600, 1544, 1492, 1468, 1452, 1436, 1415, 1251, 1100. ^1H NMR (400 MHz, CDCl_3) δ 7.51 – 7.32 (m, 9H), 7.32 – 7.23 (m, 2H), 7.02 (app d, J = 10.7 Hz, 1H), 6.87 - 6.78 (m, 2H), 4.87 (s, 2H). ^{13}C NMR (101 MHz, CDCl_3) δ 156.35, 147.07, 138.86, 138.70, 137.63, 136.43, 132.71, 129.85, 128.72, 127.48, 127.32, 127.21, 124.42, 115.33, 114.49, 46.88. ^{11}B NMR (128 MHz, CDCl_3) δ 5.32 (t, J = 29.8 Hz). ^{19}F NMR (376 MHz, CDCl_3) δ -135.49 – -135.93 (q). HRMS (ESI-TOF) m/z : $[\text{M}+\text{H}]^+$ calcd. for $\text{C}_{20}\text{H}_{16}\text{ClBF}_2\text{N}_2$ 369.1139, found 369.1163.

Boron complex 36f:



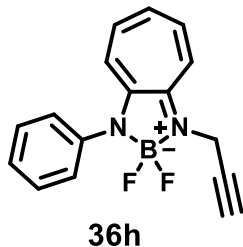
The pure product is obtained as yellow viscous thick liquid. (70 mg, isolated yield = 76%) FT-IR (KBr plate) ν = 2920, 2850, 1641, 1600, 1545, 1508, 1469, 1438, 1253, 1229, 1213, 1102, 815, 796, 732, 706. ^1H NMR (400 MHz, CDCl_3) δ 7.45 – 7.36 (m, 4H), 7.36 – 7.30 (m, 3H), 7.31 – 7.23 (m, 2H), 7.22 – 7.14 (m, 2H), 6.96 (app d, J = 10.7 Hz, 1H), 6.87 - 6.79 (m, 2H), 4.86 (s, 2H). ^{13}C NMR (101 MHz, CDCl_3) δ 162.77, 160.32, 156.63, 156.33, 138.75, 138.69, 136.53, 128.74, 127.97, 127.89, 127.33, 127.25, 124.17, 116.72, 116.49, 115.13, 114.47, 46.91. ^{11}B NMR (128 MHz, CDCl_3) δ 5.33 (t, J = 29.8 Hz). ^{19}F NMR (376 MHz, CDCl_3) δ -115.59 (s), -135.93 (q). HRMS (ESI-TOF) m/z : $[\text{M}+\text{H}]^+$ calcd. for $\text{C}_{20}\text{H}_{16}\text{BF}_3\text{N}_2$ 353.1435, found 353.1437.

Boron complex 36g:



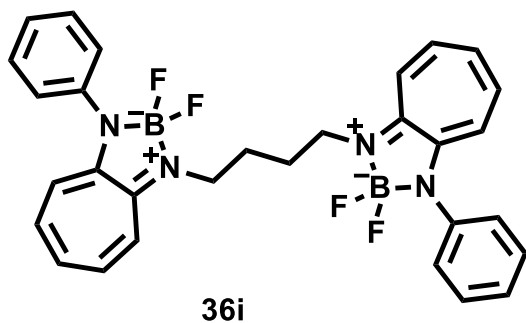
The pure product is obtained as yellow viscous thick liquid. (50 mg, isolated yield = 45%) FT-IR (KBr plate) ν = 2956, 2918, 2849, 1643, 1599, 1544, 1510, 1469, 1454, 1438, 1410, 1245, 1099. ^1H NMR (400 MHz, CDCl_3) δ 7.43 (d, J = 7.4 Hz, 2H), 7.38 – 7.30 (m, 4H), 7.30 – 7.22 (m, 3H), 7.05 – 6.97 (m, 3H), 6.78 (m, 2H), 4.86 (s, 2H), 3.86 (s, 3H). ^{13}C NMR (101 MHz, CDCl_3) δ 158.62, 156.93, 156.12, 147.07, 138.52, 138.41, 136.75, 131.68, 130.90, 128.71, 127.28, 127.26, 127.22, 124.45, 123.96, 123.71, 114.96, 114.70, 114.57, 55.51, 46.91. ^{11}B NMR (128 MHz, CDCl_3) δ 5.32 (t, J = 29.7 Hz). ^{19}F NMR (376 MHz, CDCl_3) δ -136.24 (dd, J = 59.3, 29.4 Hz). HRMS (ESI-TOF) m/z : $[\text{M}+\text{Na}]^+$ calcd. for $\text{C}_{20}\text{H}_{16}\text{BF}_3\text{N}_2$ 387.1454, found 387.1473.

Boron complex 36h:



(80 mg, isolated yield = 66%) FT-IR (KBr plate) ν = 2923, 2852, 1600, 1545, 1492, 1463, 1412, 1252, 1154, 1102, 1051, 995, 735, 695. ^1H NMR (400 MHz, CDCl_3) δ 7.57 - 7.51 (m, 1H), 7.47 (t, J = 7.7 Hz, 3H), 7.41 – 7.29 (m, 4H), 7.16 (app d, J = 10.7 Hz, 1H), 7.04 (app d, J = 10.8 Hz, 1H), 6.91 (t, J = 9.7 Hz, 1H), 4.38 (s, 2H), 2.29 (t, J = 2.5 Hz, 1H). ^{13}C NMR (101 MHz, CDCl_3) δ 156.79, 155.53, 147.05, 138.99, 138.81, 138.74, 129.68, 127.30, 126.08, 124.60, 115.44, 114.63, 77.66, 72.04, 14.07. ^{11}B NMR (128 MHz, CDCl_3) δ 4.93 (t, J = 29.7 Hz). ^{19}F NMR (376 MHz, CDCl_3) δ -136.06 – -139.11 (q). HRMS (ESI-TOF) m/z : $[\text{M}+\text{H}]^+$ calcd. for $\text{C}_{16}\text{H}_{13}\text{BF}_2\text{N}_2$ 283.1216, found 283.1204.

Boron complex 36i:



(30 mg, isolated yield = 40%) FT-IR (KBr plate) ν = 2923, 2852, 1599, 1544, 1492, 1468, 1453, 1436, 1415, 1251, 1101, 746, 701. ^1H NMR (400 MHz, CDCl_3) δ 7.50 - 7.45 (m, 6H), 7.38 - 7.33 (m, 6H), 7.31 - 7.22 (m, 3H), 7.04 (app d, J = 10.9 Hz, 2H), 6.95 (app d, J = 10.7 Hz, 2H), 6.83 (t, J = 9.6 Hz, 2H), 3.72 (s, 4H), 2.00 (s, 4H). ^{13}C NMR (101 MHz, CDCl_3) δ 156.31, 156.11, 139.10, 138.62, 138.33, 129.66, 127.11, 126.22, 123.71, 113.99, 42.87, 25.94. ^{11}B NMR (128 MHz, CDCl_3) δ 5.22 (t, J = 30.5 Hz). ^{19}F NMR (376 MHz, CDCl_3) δ -136.37 (q). HRMS (ESI-TOF) m/z : $[\text{M}+\text{Na}]^+$ calcd. for $\text{C}_{30}\text{H}_{28}\text{B}_2\text{F}_4\text{N}_4$ 565.2339, found 565.2302.

4.5 References and Notes

1. Pauson, P. L. *Chem. Rev.* **1955**, 55, 9.
2. Bentley, R. *Nat. Prod. Rep.* **2008**, 25, 118.
3. Liu, N.; Song, W.; Schienebeck, C. M.; Zhang, M. Tang, W. *Tetrahedron* **2014**, 70, 9281.
4. Cook, J. W.; Gibb, A. R.; Raphael, R. A.; Somerville, A. R. *J. Chem. Soc.* **1951**, 503.
5. Arai, T.; Okuyama, A. *Seikagaku.* **1973**, 45, 19.
6. Weisenberg, R. C.; Borisy, G. G.; Taylor, E. W. *Biochemistry* **1968**, 7, 4466.
7. Bhattacharyya, B.; Wolff, J. *Proc. Nat. Acad. Sci. USA*, **1974**, 71, 2627.
8. Bhattacharyya, B.; Wolff, J. *Biochemistry* **1976**, 15, 2283.
9. Tormos, R.; Bosca, F. *RSC Adv.*, **2013**, 3, 12031.
10. Croteau, R.; Leblanc, R.M. *Photochemistry and Photobiology* **1978**, 28, 33.
11. Hosoya, H.; Tanaka, J.; Nagakura, S. *Tetrahedron* **1962**, 18, 859.
12. Yamaguchi, H.; Amako, Y.; Azumi, H. *Tetrahedron* **1968**, 24, 267.
13. Croteau, R.; Leblanc, R.M. *Journal of Luminescence* **1977**, 15, 353.
14. Breheret, E.F.; Martin, M. M. *Journal of Luminescence* **1978**, 49.
15. Hojo, M.; Hasegawa, H.; Yoneda, H. *J. Chem. Soc. Perkin. Trans. 2.* **1994**, 1855.
16. De Sá, G.F., Malta, O.L., De Mello Donegá, C., Simas, A.M., Longo, R.L., Santa-Cruz, P.A., Da Silva Jr., E.F. *Coord. Chem. Rev.* **2000**, 196, 165.
17. Takagi, K.; Saiki, K.; Mori, K.; Yuki, Y.; Suzuki, M. *Polymer Journal* **2007**, 39, 813.
18. Sayapin, Y. A.; Tupaeva, I. O.; Kolodina, A. A.; Gusakov, E. A.; Komissarov, V. N.; Dorogan, I. V.; Makarova, N. I.; Metelitsa, A. V.; Tkachev, V. V.; Aldoshin, S. M.; Minkin, V. I. *Beilstein J. Org. Chem.* **2015**, 11, 2179–2188.

19. Zadeh, E. H. G.; Tang, S.; Woodward, A. W.; Liu, T.; Bondarc, M. V.; Belfield, K. D. *J. Mater. Chem. C* **2015**, *3*, 8495.
20. Ito, A.; Muratake, H.; Shudo, K. *J. Org. Chem.* **2013**, *78*, 5470.
21. Ito, A.; Muratake, H.; Shudo, K. *J. Org. Chem.* **2009**, *74*, 1275.
22. Roesky, P. W. *Chem. Soc. Rev.*, **2000**, *29*, 335.
23. Zulys, A.; Dochnahl, M.; Hollmann, D.; Löhnwitz, K.; Herrmann, J.-S.; Roesky, P. W.; Blechert, S. *Angew. Chem., Int. Ed.* **2005**, *44*, 7794.
24. Dochnahl, M.; Pissarek, J.-W.; Blechert, S.; Lohnwitz, K.; Roesky, P. W. *Chem. Commun.* **2006**, DOI: 10.1039/b607597e, 3405.
25. Davis, W. M.; Roberts, M. M.; Zask, A.; Nakanishi, K.; Nozoe, T.; Lippard, S. J. *J. Am. Chem. Soc.* **1985**, *107*, 3864.
26. Imajo, S.; Nakanishi, K.; Roberts, M.; Lippard, S. J.; Nozoe, T. *J. Am. Chem. Soc.* **1983**, *105*, 2071.
27. Villacorte, G. M.; Gibson, D.; Williams, I. D.; Lippard, S. J. *J. Am. Chem. Soc.* **1985**, *107*, 6732.
28. Holmquist, H. E.; Benson, R. E. *J. Am. Chem. Soc.* **1962**, *84*, 4720.
29. Crivat, G.; Taraska, J. W. *Trends in Biotechnology* **2012**, *30*, 8.
30. Kim, H. N.; Guo, Z.; Zhu, W.; Yoon, J. Tian, H. *Chem. Soc. Rev.* **2011**, *40*, 79.
31. Liu, S.; Shi, Z.; Xu, W.; Yang, H.; Xi, N. Liu, X.; Zhao, Q.; Huang, W. *Dyes and Pigments* **2014**, *103*, 145.
32. Fernandez-Suarez, M.; Ting, A. Y. *Nat Rev Mol Cell Biol*, **2008**, *9*, 929.
33. Zaumseil, J.; Sirringhaus, H. *Chem. Rev.* **2007**, *107*, 1296.
34. Bessette, A.; Hanan, G. S. *Chem. Soc. Rev.* **2014**, *43*, 3342.
35. Treibs, A.; Kreuzer, F.-H. *Justus Liebigs Annalen der Chemie* **1968**, *718*, 208.

36. Zaumseil, J.; Sirringhaus, H. *Chem. Rev.* **2007**, *107*, 1296.
37. Ulrich, G.; Ziessel, R.; Harriman, A. *Angew. Chem., Int.Ed.* **2008**, *47*, 1184.
38. Loudet, A.; Burgess, K. *Chem. Rev.* **2007**, *107*, 4891.
39. Lakshmi, V.; Lee, W.-Z.; Ravikanth, M. *Dalton Transactions* **2014**, *43*, 16006.
40. Basumatary, B.; Raja Sekhar, A.; Ramana Reddy R. V.; Sankar, J. *Inorg.Chem.* **2015**, *54*, 4257.
41. Swamy P. C. A.; Mukherjee, S.; Thilagar, P. *Inorg. Chem.* **2014**, *53*, 4813.
42. Fullagar, J. L.; Garner, A. L.; Struss, A. K.; Day, J. A.; Martin, D. P.; Yu, J.; Cai, X.; Janda, K. D.; Cohen, S. M. *Chem.Comm.* **2013**, *49*, 3197.
43. Hussein, L.; Purkait, N.; Biyikal, M.; Tausch, E.; Roesky, P. W.; Blechert, S. *Chem.Comm.* **2014**, *50*, 3862.
44. Potenziano, J.; Spitale, R.; Janik, M. E. *Synth.Comm.* **2005**, *35*, 2005.
45. Seganish, W. M.; Handy, C. J.; DeShong, P. *J. Org. Chem.* **2005**, *70*, 8948.
46. Dochnahl, M.; Löhnwitz, K.; Pissarek, J.-W.; Biyikal, M.; Schulz, S. R.; Schön, S.; Meyer, N.; Roesky, P. W.; Blechert, S. *Chem.-Eur.J.* **2007**, *13*, 6654.
47. Balachandra, C.; Sharma, N. K. *Tetrahedron* **2014**, *70*, 7464.
48. Balachandra, C.; Sharma, N. K. *Org. Lett.* **2015**, *17*, 3948.
49. Sanchez-Carrera, R. S.; Delgado, M. C. R.; Ferron, C. C.; Osuna, R. M.; Hernandez, V.; Navarrete, J. T. L. et al. *Org. Electron.* **2010**, *11*, 1701.
50. Morley, J. O.; Morley, R. M.; Fitton, A. L.; *J. Am. Chem. Soc* **1998**, *120*, 11479.
51. Brooker, L. G. S.; Keyes, G. H.; Sprague, R. H.; VanDyke, R. H.; VanLare, E.; VanZandt, G. et al. *J. Am. Chem. Soc.* **1951**, *73*, 5332.
52. Maar, R. R.; Barbon, S. M.; Sharma, N.; Groom, H.; Luyt, L. G.; Gilroy, J. B. *Chem. Eur- J* **2015**, *21*, 15589.

53. Barbon, S. M.; Price, J. T.; Reinkeluers, P. A.; Gilroy, J. B. *Inorg. Chem.* **2014**, *53*, 10585.
54. Lu, J.-s.; Ko, S.-B.; Walters, N. R.; Wang, S. *Org. Lett.* **2012**, *14*, 5660.
55. Cheng, C.; Gao, N.; Yu, C.; Wang, Z.; Wang, J.; Hao, E.; Wei, Y.; Mu, X.; Tian, Y.; Ran, C.; Jiao, L. *Org. Lett.* **2015**, *17*, 278.

4.6 Appendix-4

Contents

1. ^1H and ^{13}C NMR spectrum of 30	343
2. ^1H and ^{13}C NMR spectrum of 31a :	345
3. Mass spectrum of ligated product obtained through click reaction	347
4. ^1H and ^{13}C NMR spectrum of 31b	348
5. ^1H and ^{13}C NMR spectrum of 32 :	350
^1H and ^{13}C NMR spectrum of 32 in DMSO- d_6 :	351
6. NMR ($^1\text{H}/^{13}\text{C}$) and HRMS of N-(Benzyl)-2-(benzylamino)troponimine (35a)	353
7. NMR ($^1\text{H}/^{13}\text{C}$) and HRMS of N-(Phenyl)-2-(benzylamino)troponimine (35b)	355
8. NMR ($^1\text{H}/^{13}\text{C}$) and HRMS of N-(4-methylphenyl)-2-(benzylamino)troponimine (35c)	357
9. NMR ($^1\text{H}/^{13}\text{C}$) and HRMS of Imine N-(Phenyl)-2-(phenylamino)troponimine (35d)	359
10. NMR ($^1\text{H}/^{13}\text{C}$) and HRMS of N-(4-chlorophenyl)-2-(benzylamino)troponimine (35e)	361
11. NMR ($^1\text{H}/^{13}\text{C}$) and HRMS of N-(4-fluorophenyl)-2-(benzylamino)troponimine (35f)	363
12. NMR ($^1\text{H}/^{13}\text{C}$) and HRMS of N-(4-methoxyphenyl)-2-(benzylamino)troponimine (35g)	365
13. NMR ($^1\text{H}/^{13}\text{C}$) and HRMS of N-(phenyl)-2-(propergylamino)troponimine (35h)	367
14. NMR ($^1\text{H}/^{13}\text{C}$) and HRMS of N-(phenyl)-2-(diaminobutyl)ditroponimine (35i)	369
15. NMR ($^1\text{H}/^{13}\text{C}/^{11}\text{B}/^{19}\text{F}$) and HRMS of boron complex (36a)	371
16. NMR ($^1\text{H}/^{13}\text{C}/^{11}\text{B}/^{19}\text{F}$) and HRMS of boron complex (36b)	374
17. NMR ($^1\text{H}/^{13}\text{C}/^{11}\text{B}/^{19}\text{F}$) and HRMS of boron complex (36c):	377
18. NMR ($^1\text{H}/^{13}\text{C}/^{11}\text{B}/^{19}\text{F}$) and HRMS of boron complex (36d)	380
19. NMR ($^1\text{H}/^{13}\text{C}/^{11}\text{B}/^{19}\text{F}$) and HRMS of boron complex (36e):	383
20. NMR ($^1\text{H}/^{13}\text{C}/^{11}\text{B}/^{19}\text{F}$) and HRMS of boron complex (36f)	386
21. NMR ($^1\text{H}/^{13}\text{C}/^{11}\text{B}/^{19}\text{F}$) and HRMS of boron complex (36g)	389
22. NMR ($^1\text{H}/^{13}\text{C}/^{11}\text{B}/^{19}\text{F}$) and HRMS of boron complex (36h):	392
23. NMR ($^1\text{H}/^{13}\text{C}/^{11}\text{B}/^{19}\text{F}$) and HRMS of boron complex (36i):	395
24. Crystal data of Boron complex 36c :	398

1. ^1H and ^{13}C NMR spectrum of **30**

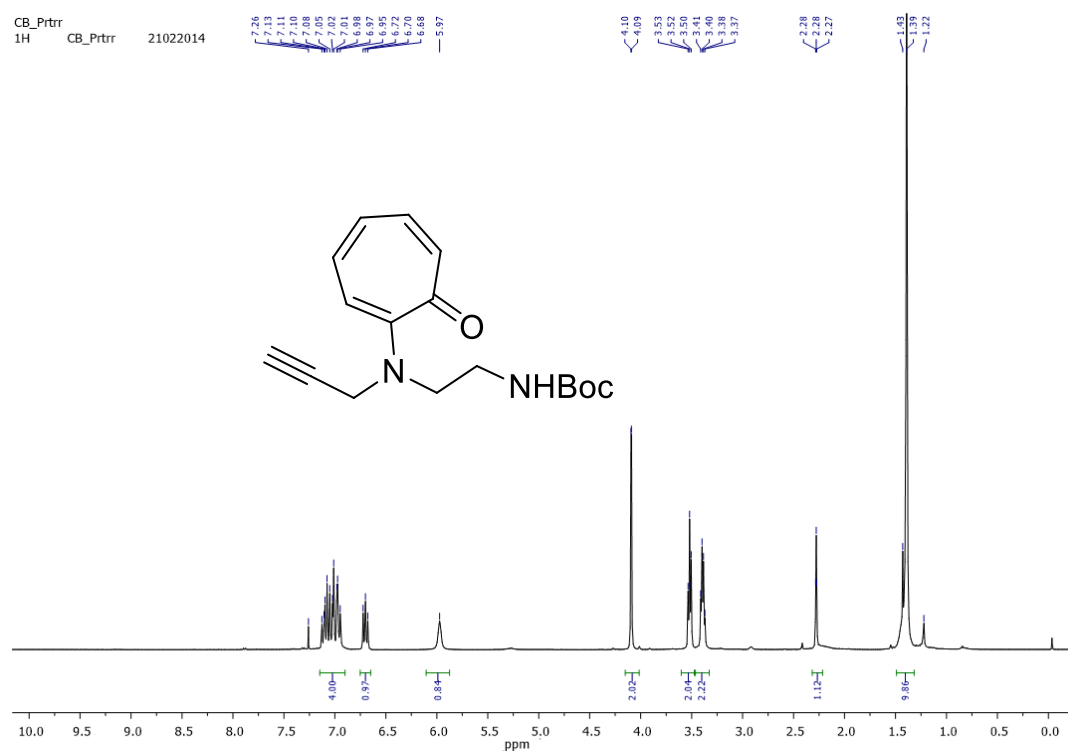


Figure A1. ^1H NMR spectrum of monomer **30** in CDCl_3

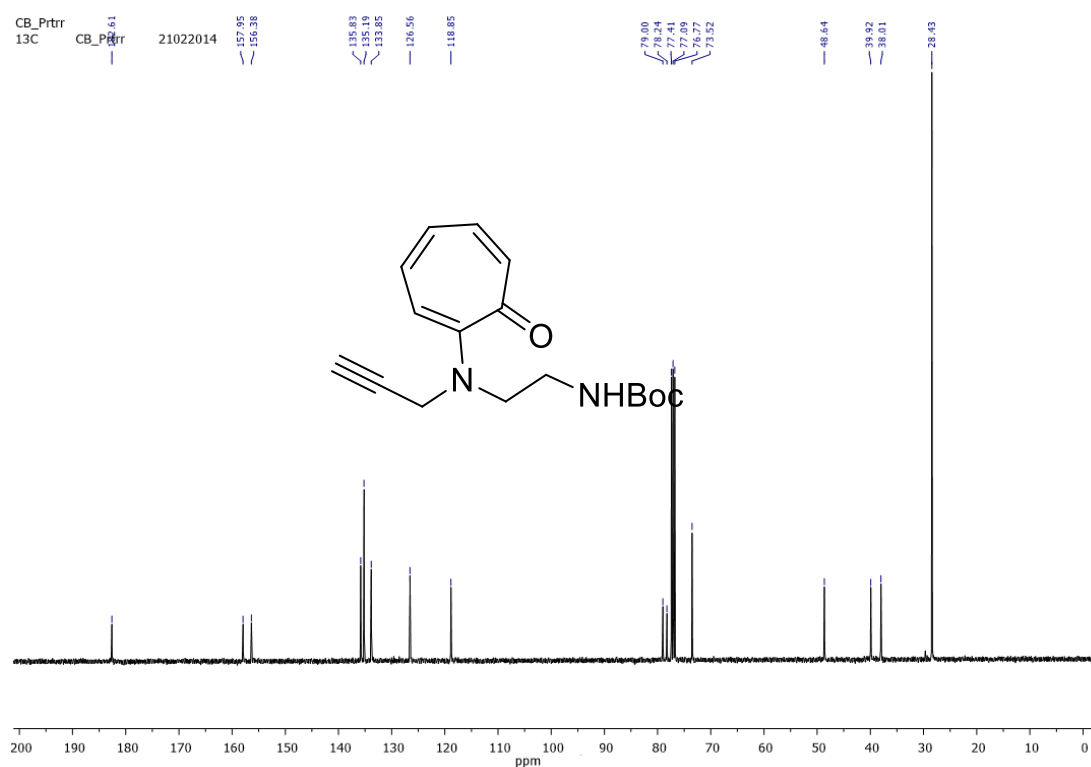


Figure A2. ^{13}C NMR spectrum of monomer **30** in CDCl_3

Display Report

Analysis Info

Analysis Name D:\Data\FEB-2014\NKS\21022014_NKS_CB_PRTR.d
Method Pos_tune_low.m
Sample Name ACN
Comment

Acquisition Date 2/21/2014 10:25:37 PM

Operator A.S.Sahu
Instrument micrOTOF-Q II 10337

Acquisition Parameter

Source Type	ESI	Ion Polarity	Positive	Set Nebulizer	0.4 Bar
Focus	Not active	Set Capillary	4500 V	Set Dry Heater	180 °C
Scan Begin	50 m/z	Set End Plate Offset	-500 V	Set Dry Gas	4.0 l/min
Scan End	3000 m/z	Set Collision Cell RF	130.0 Vpp	Set Divert Valve	Waste

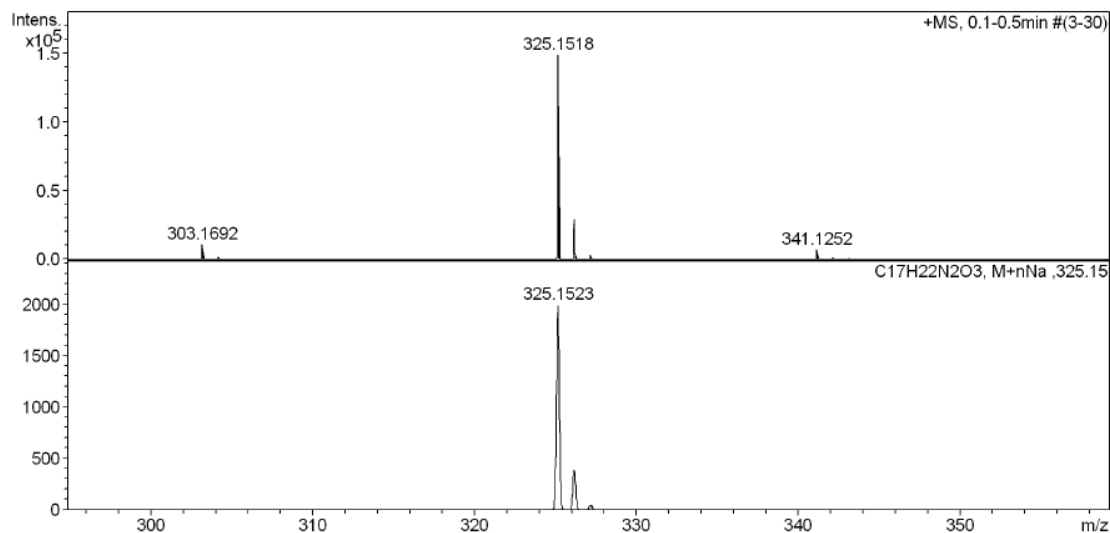
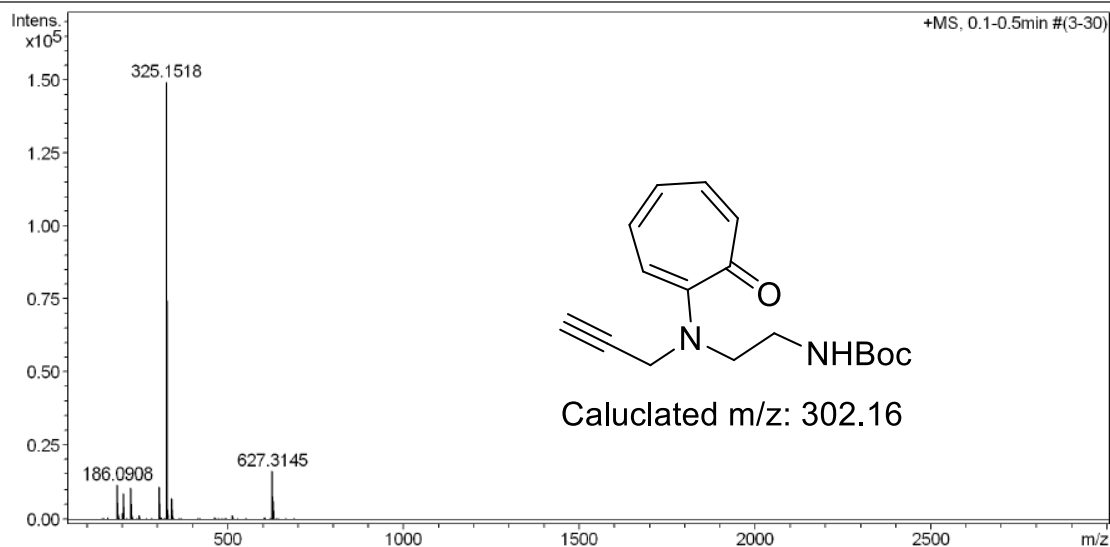


Figure A3. HRMS spectrum of **30**.

2. ^1H and ^{13}C NMR spectrum of **31a**:

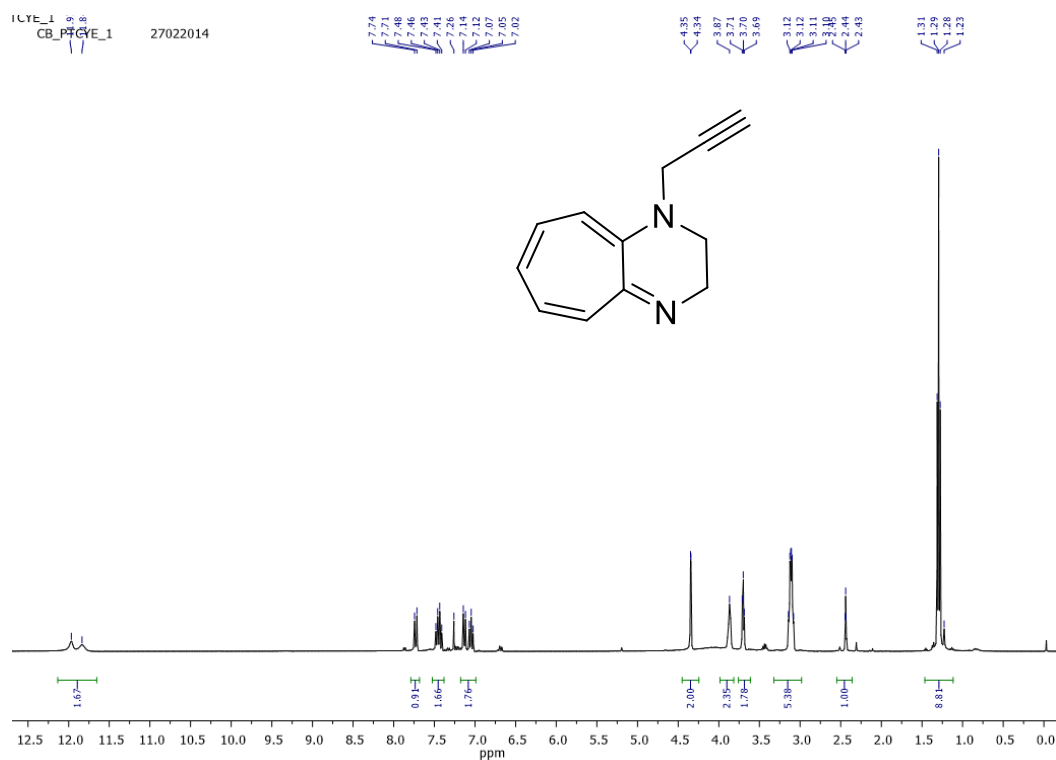


Figure A4. ^1H NMR spectrum of **31a** in CDCl_3

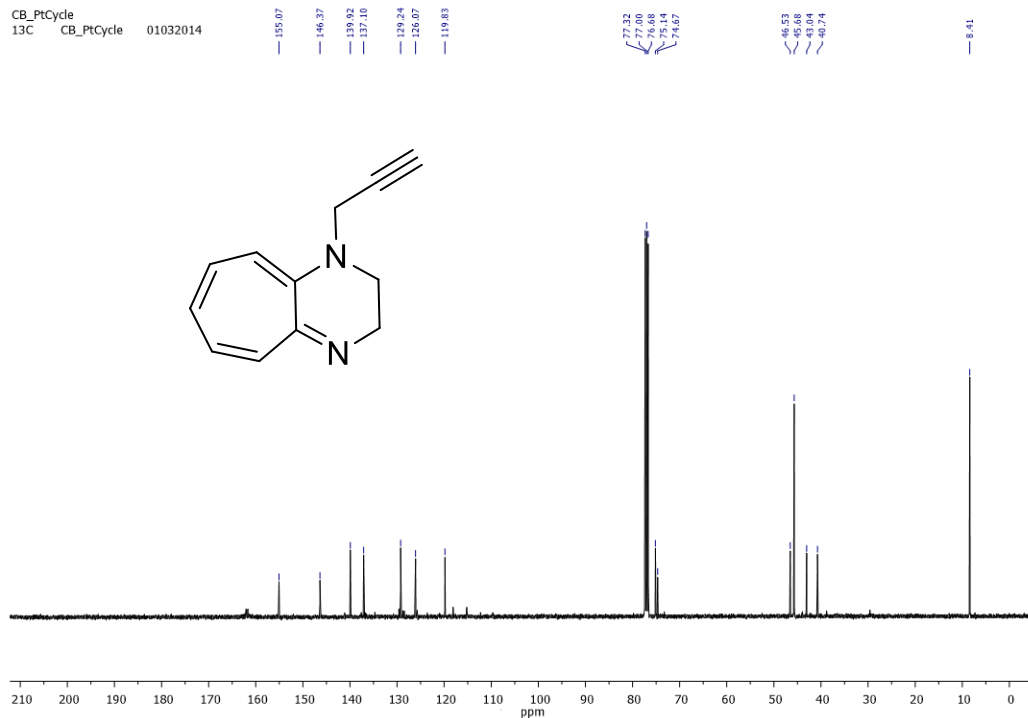


Figure A5. ^{13}C NMR spectrum of **31a** in CDCl_3

Display Report

Analysis Info

Analysis Name	D:\Data\FEB-2014\peru\22022014_NKS_CB_TRPRCYCAFEVA.d	Acquisition Date	2/22/2014 7:00:35 PM
Method	Pos_tune_low.m	Operator	A.S.Sahu
Sample Name	ACN	Instrument	microTOF-Q II 10337
Comment			

Acquisition Parameter

Source Type	ESI	Ion Polarity	Positive	Set Nebulizer	0.4 Bar
Focus	Not active	Set Capillary	4500 V	Set Dry Heater	180 °C
Scan Begin	50 m/z	Set End Plate Offset	-500 V	Set Dry Gas	4.0 l/min
Scan End	3000 m/z	Set Collision Cell RF	130.0 Vpp	Set Divert Valve	Waste

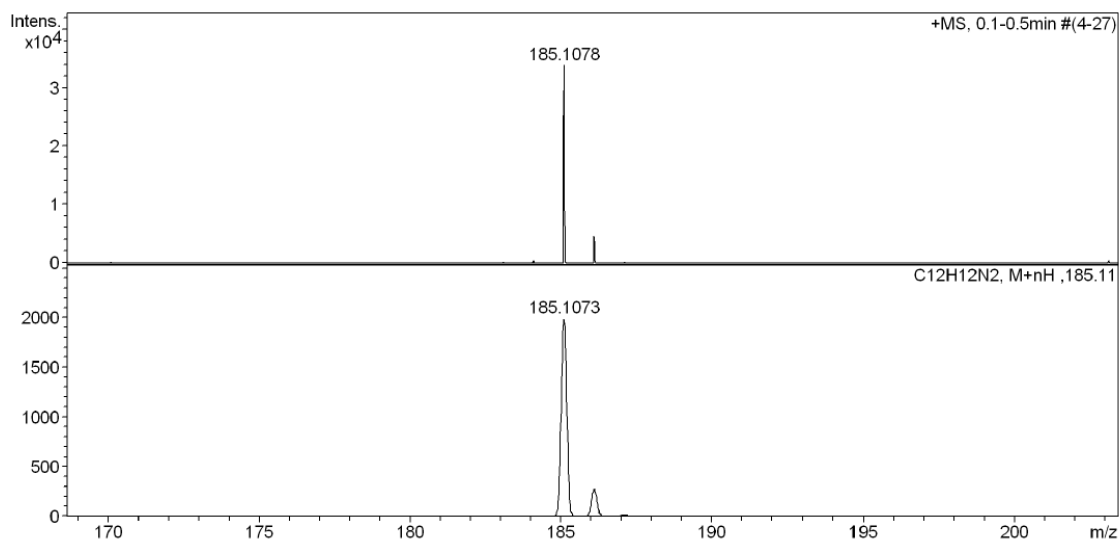
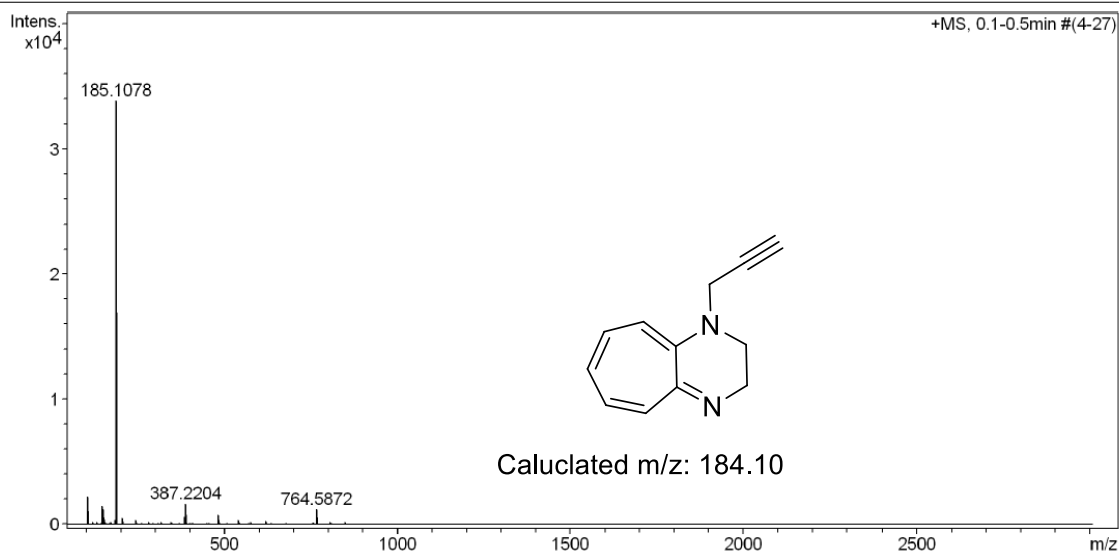


Figure A6. HRMS spectrum of **31a**

3. Mass spectrum of ligated product obtained through click reaction

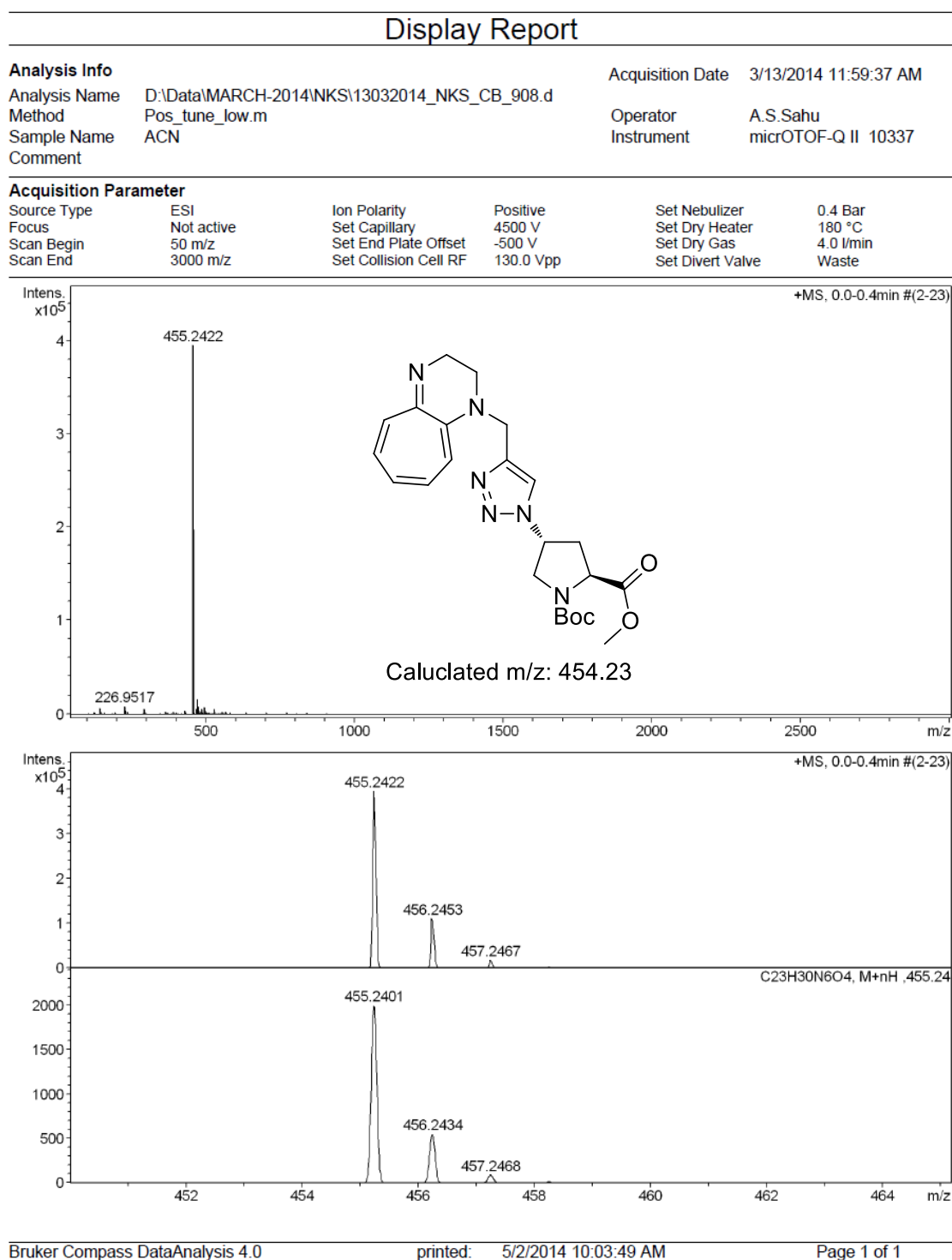


Figure A7. HRMS spectrum of ligated product obtained through click reaction.

4. ^1H and ^{13}C NMR spectrum of **31b**

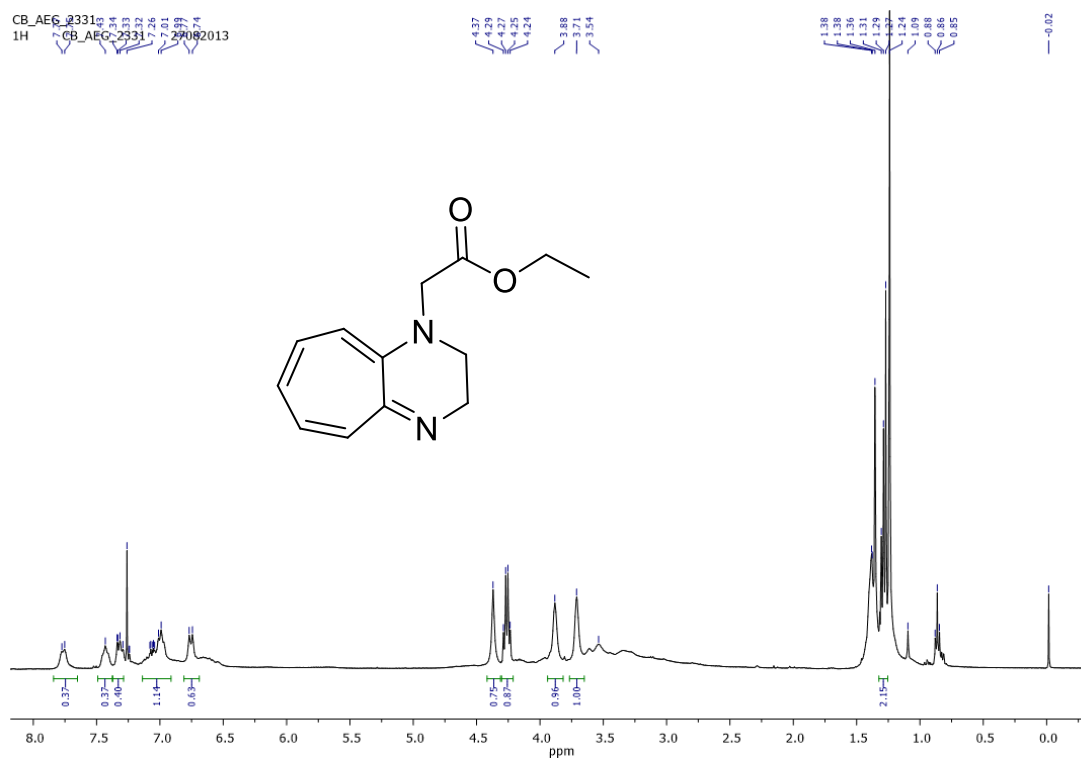


Figure A8. ^1H NMR spectrum of **31b** in CDCl_3

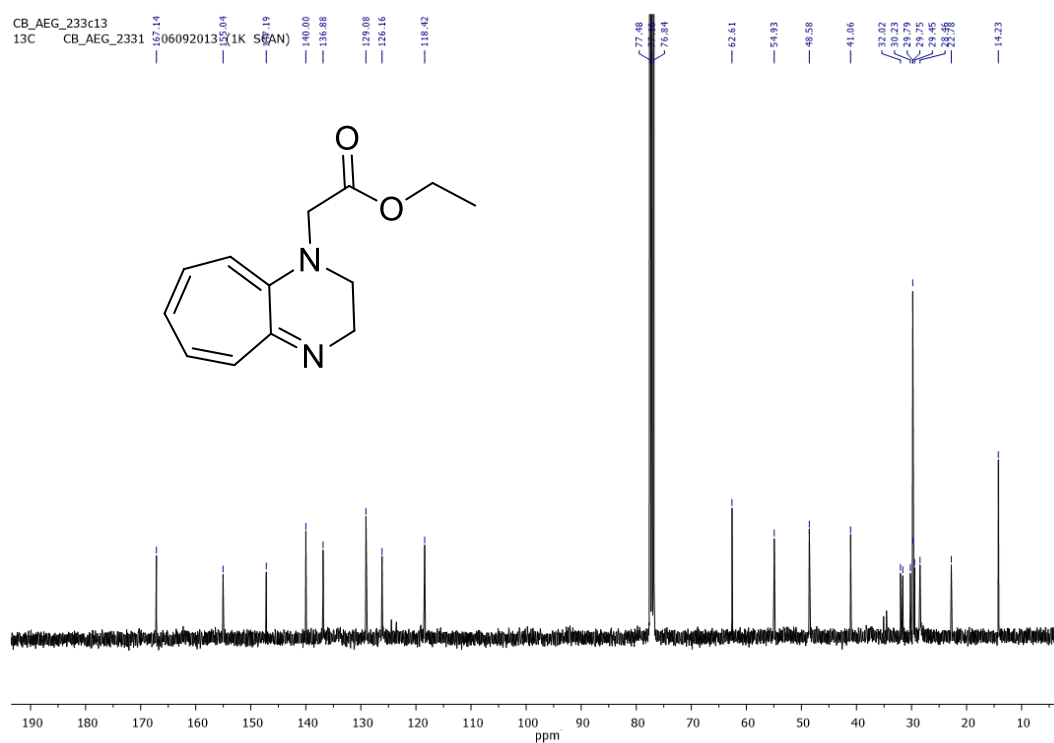


Figure A9. ^1H and ^{13}C NMR spectrum of **31b** in CDCl_3

Display Report

Analysis Info

Analysis Name D:\Data\AUG-2013\NKS\26082013_NKS_CB_aeg_233ETW.d
Method Pos_tune_low.m
Sample Name CH3CN
Comment

Acquisition Date 8/26/2013 2:34:18 PM

Operator CSREDDYG
Instrument micrOTOF-Q II 10337

Acquisition Parameter

Source Type	ESI	Ion Polarity	Positive	Set Nebulizer	0.4 Bar
Focus	Not active	Set Capillary	4500 V	Set Dry Heater	180 °C
Scan Begin	50 m/z	Set End Plate Offset	-500 V	Set Dry Gas	4.0 l/min
Scan End	3000 m/z	Set Collision Cell RF	130.0 Vpp	Set Divert Valve	Waste

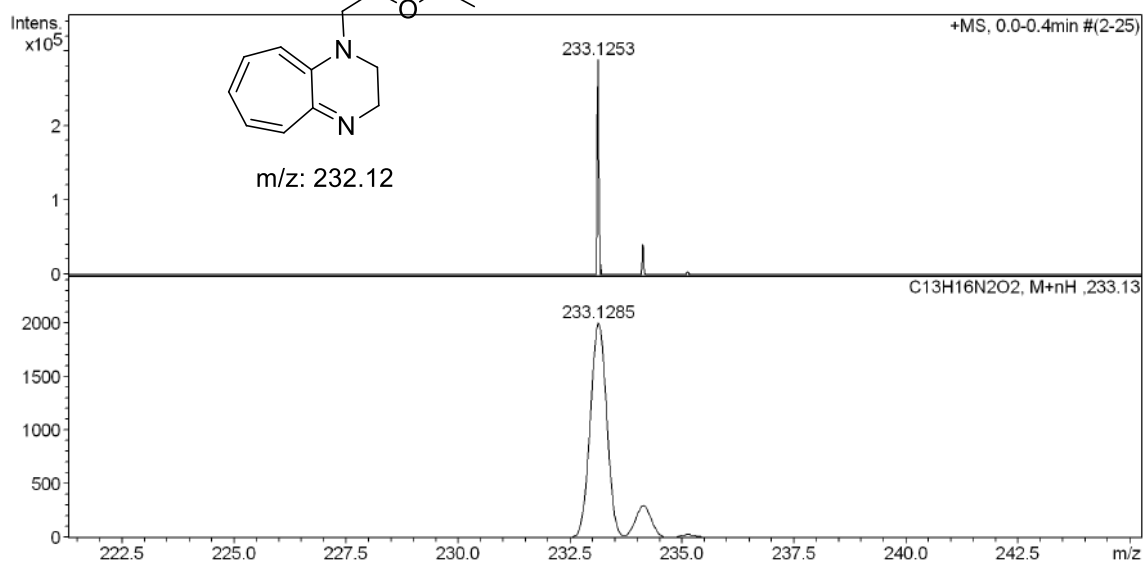
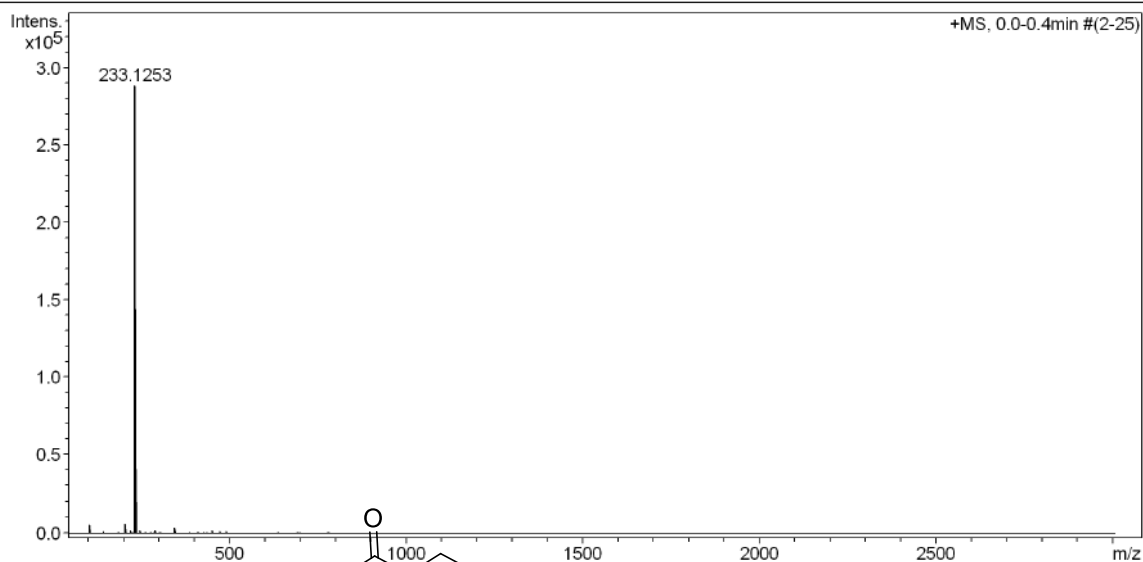


Figure A10. HRMS spectrum of **31b**

5. ^1H and ^{13}C NMR spectrum of **32**:

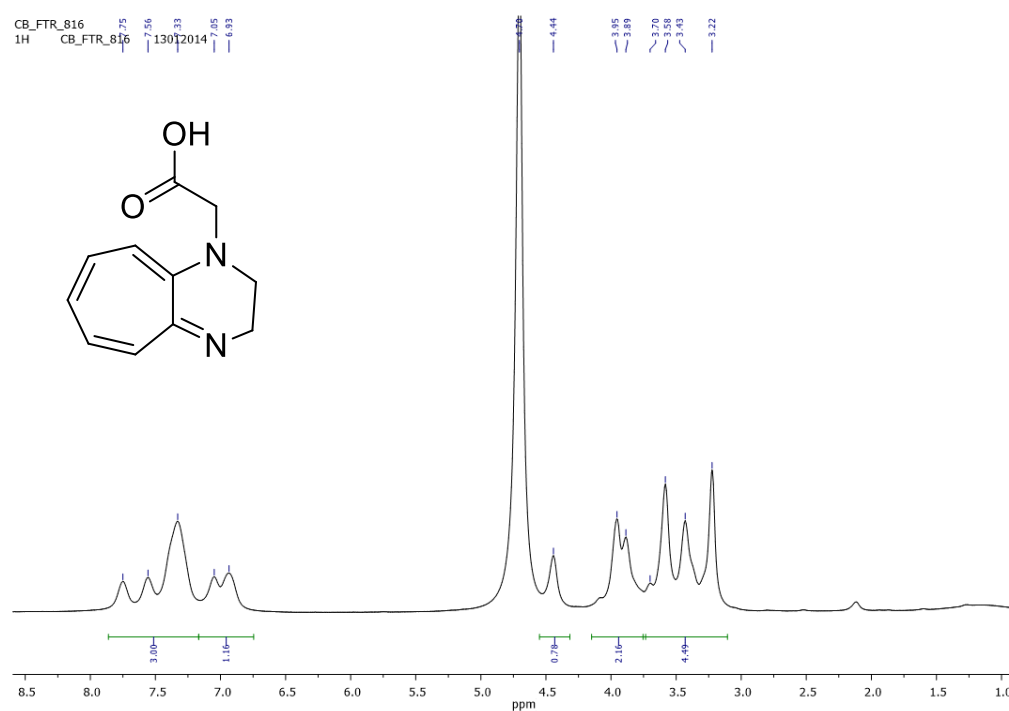


Figure A11. ^1H NMR spectrum of **32** in D_2O .

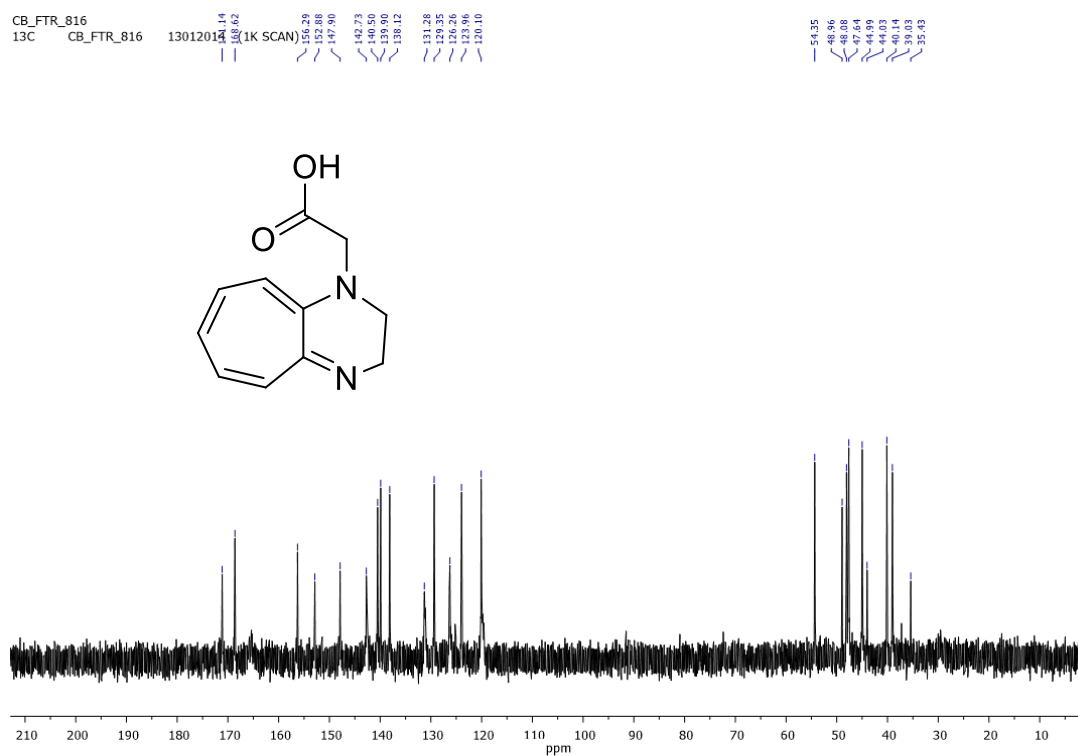


Figure A12. ^1H and ^{13}C NMR spectra of **32** in D_2O .

^1H and ^{13}C NMR spectrum of **32** in DMSO- d_6 :

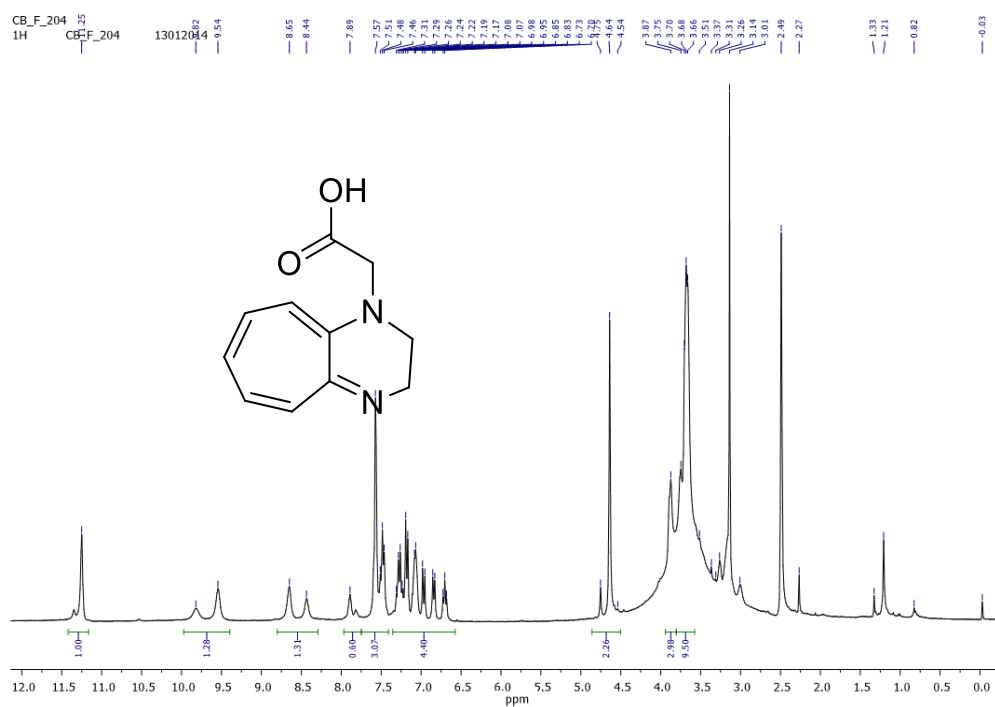


Figure A13. ^1H NMR spectrum of **32** in DMSO- d_6 .

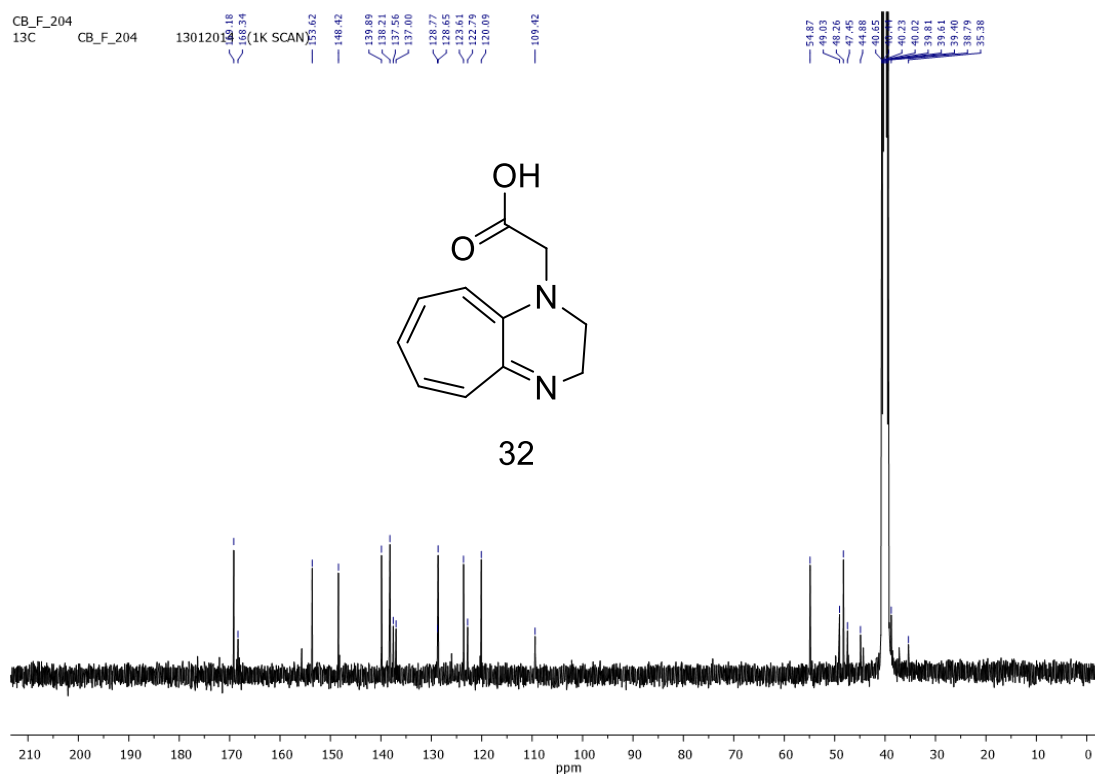


Figure A14. ^1H and ^{13}C NMR spectra of **32** in DMSO- d_6

Display Report

Analysis Info

Analysis Name D:\Data\SEP-2013\NKS\02092013_NKS_AEG204.d
Method Pos_tune_low.m
Sample Name CH3CN
Comment

Acquisition Date 9/2/2013 12:36:08 PM

Operator Rajkumar
Instrument microTOF-Q II 10337

Acquisition Parameter

Source Type	ESI	Ion Polarity	Positive	Set Nebulizer	0.4 Bar
Focus	Not active	Set Capillary	4500 V	Set Dry Heater	180 °C
Scan Begin	50 m/z	Set End Plate Offset	-500 V	Set Dry Gas	4.0 l/min
Scan End	3000 m/z	Set Collision Cell RF	130.0 Vpp	Set Divert Valve	Waste

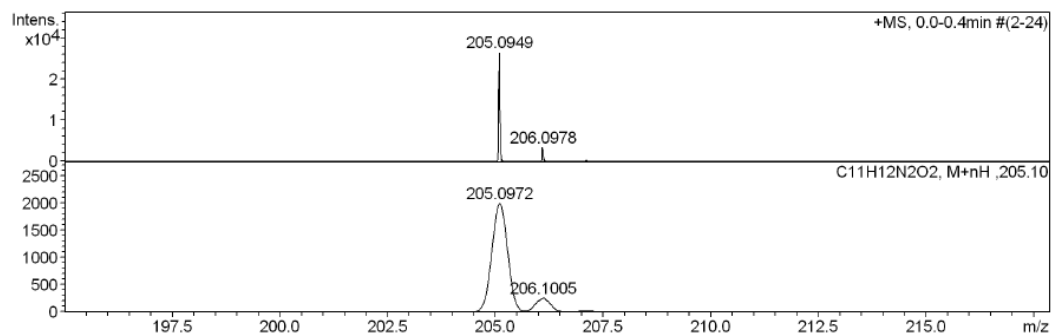
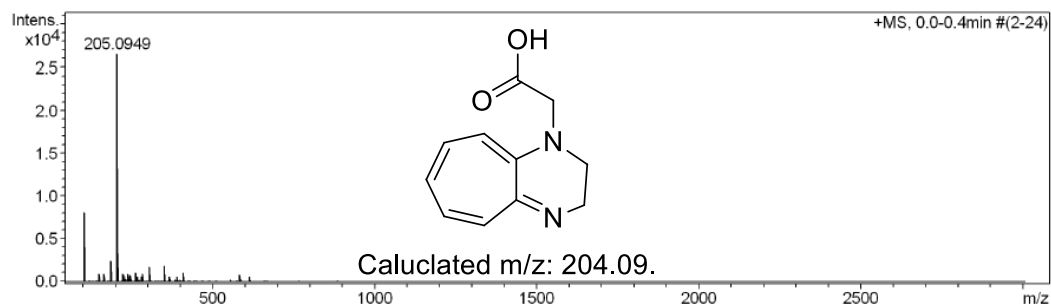
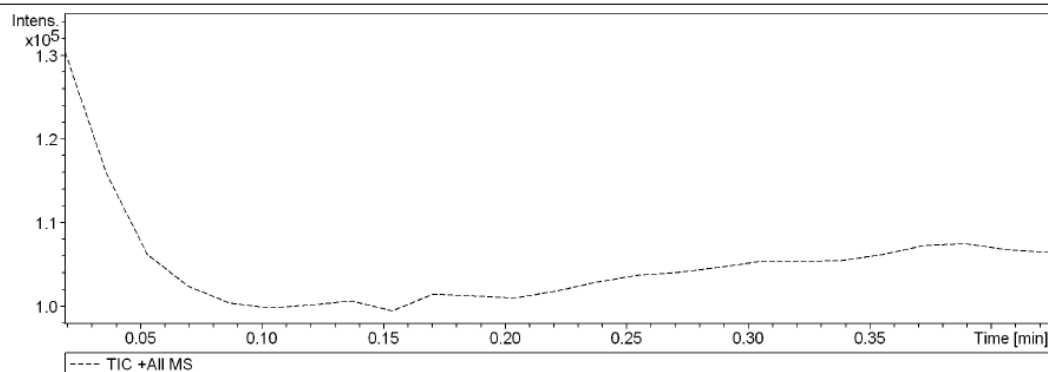


Figure A15. HRMS spectrum of **32**

6. NMR ($^1\text{H}/^{13}\text{C}$) and HRMS of N-(Benzyl)-2-(benzylamino)troponimine (**35a**)

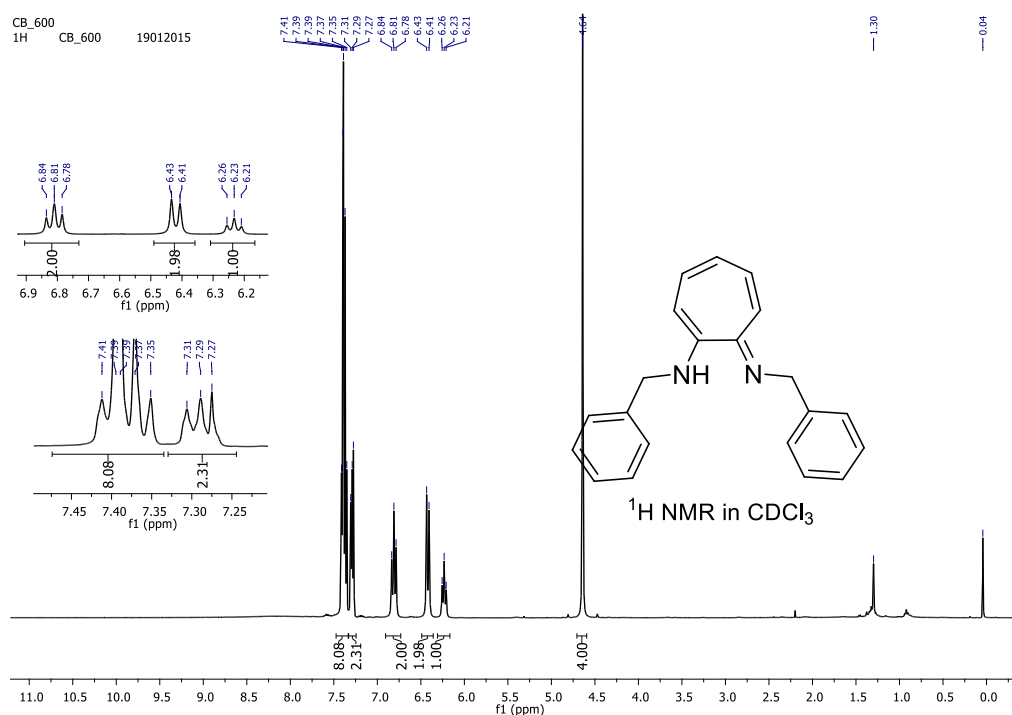


Figure A16. ^1H NMR spectrum of **35a** in CDCl_3

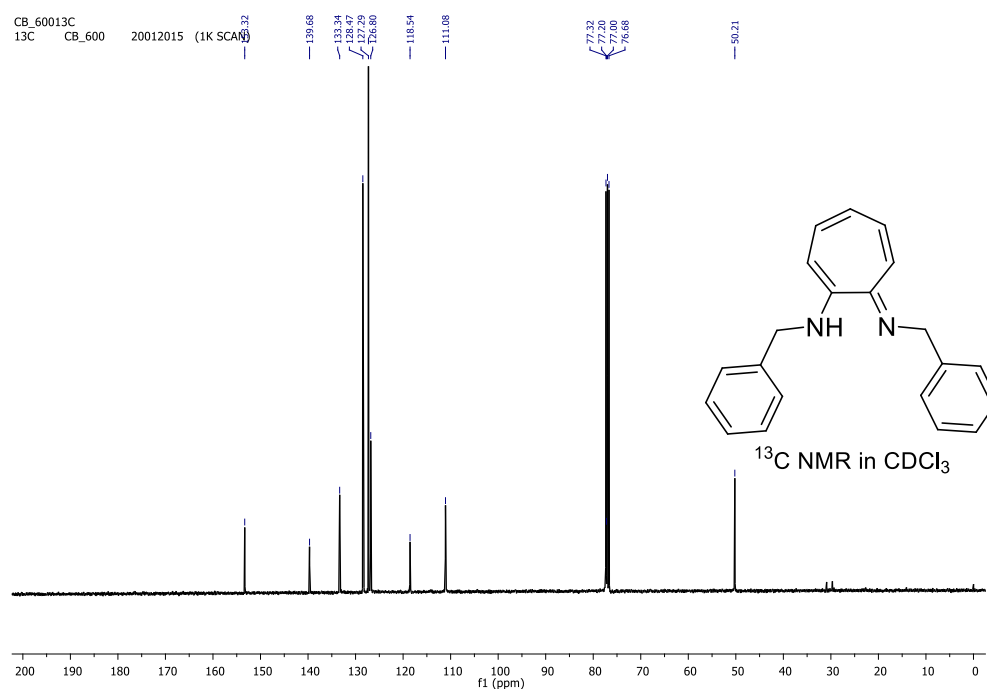


Figure A17. ^{13}C NMR spectrum of **35a** in CDCl_3

Generic Display Report

Analysis Info

Analysis Name D:\Data\JAN-2015\NKS\21012015_NKS_CB_600.d
Method Pos_tune_low.m
Sample Name NISER-LCMS
Comment

Acquisition Date 1/21/2015 3:59:23 PM

Operator NISER
Instrument micrOTOF-Q II

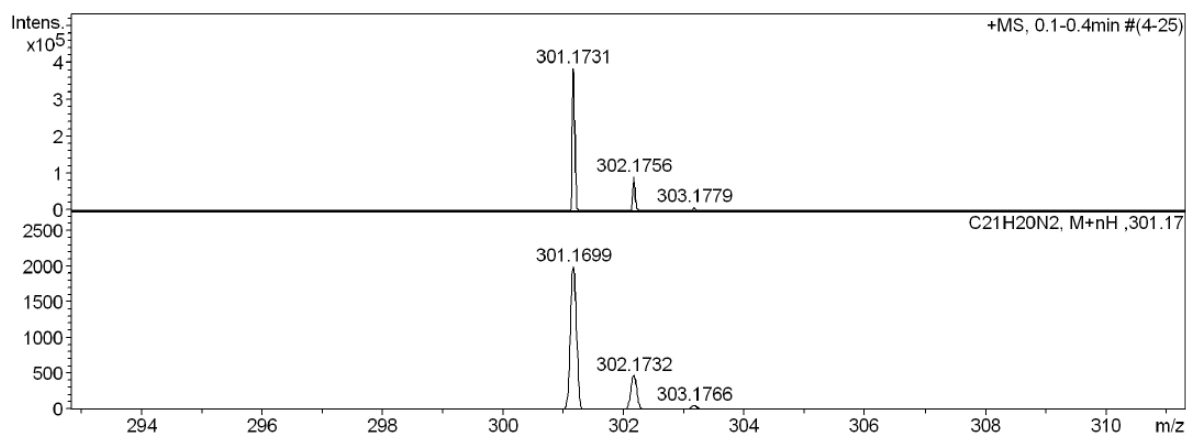
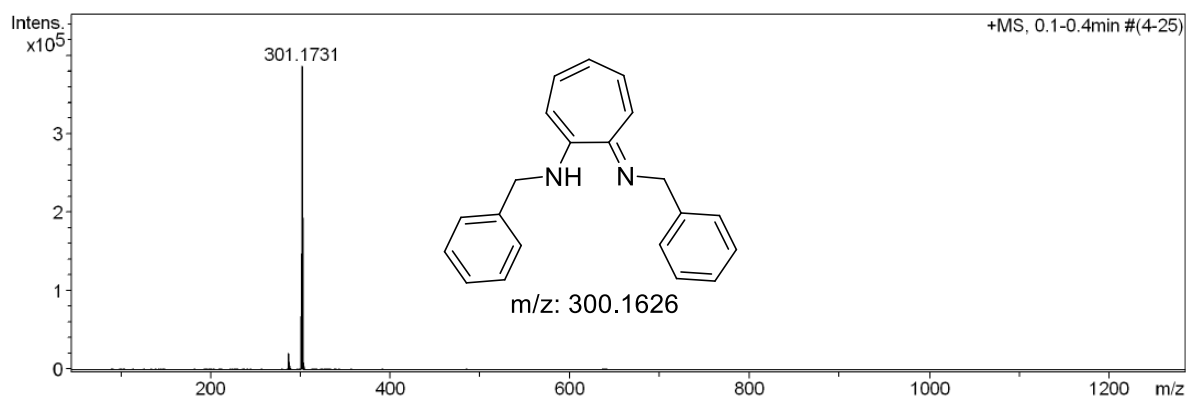
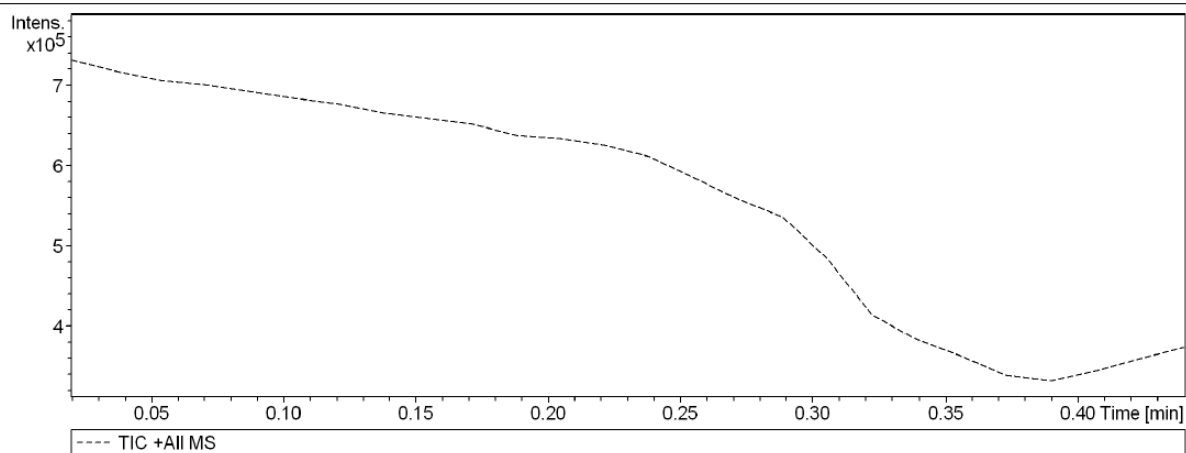


Figure A18. HRMS spectrum of aminotroponimine **35a**.

7. NMR ($^1\text{H}/^{13}\text{C}$) and HRMS of N-(Phenyl)-2-(benzylamino)troponimine (**35b**)

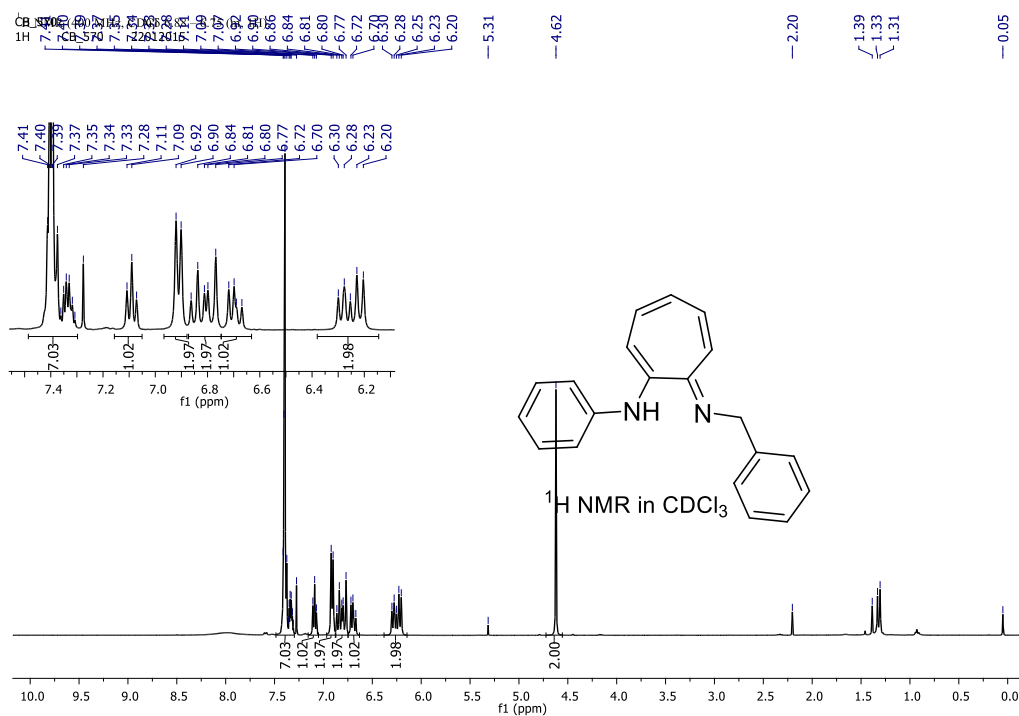


Figure A19. ^1H NMR of aminotroponimine **35b**.

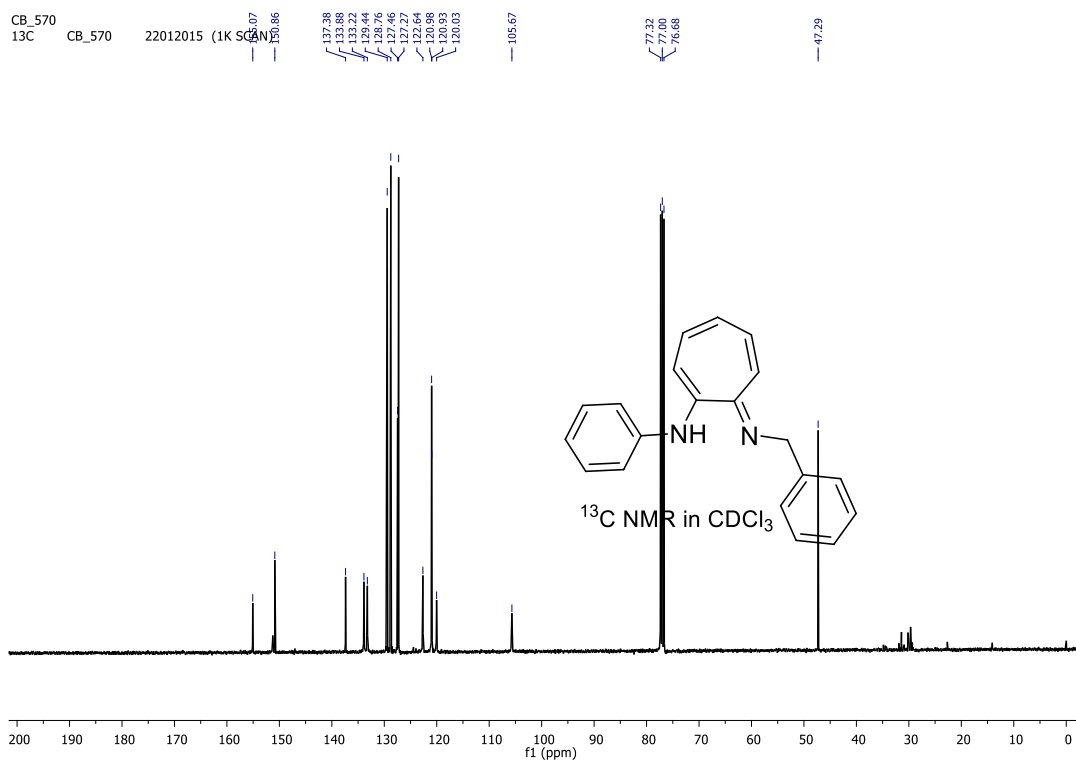


Figure A20. ^{13}C NMR of aminotroponimine **35b**.

Generic Display Report

Analysis Info

Analysis Name D:\Data\JAN-2015\NKS\21012015_NKS_CB_570.d
Method Pos_tune_low.m
Sample Name NISER-LCMS
Comment

Acquisition Date 1/21/2015 3:39:11 PM

Operator NISER
Instrument micrOTOF-Q II

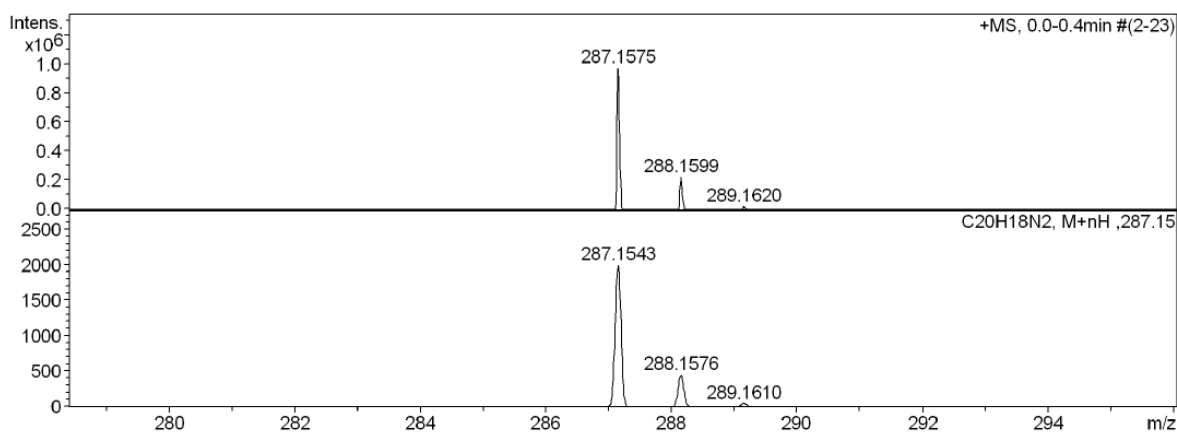
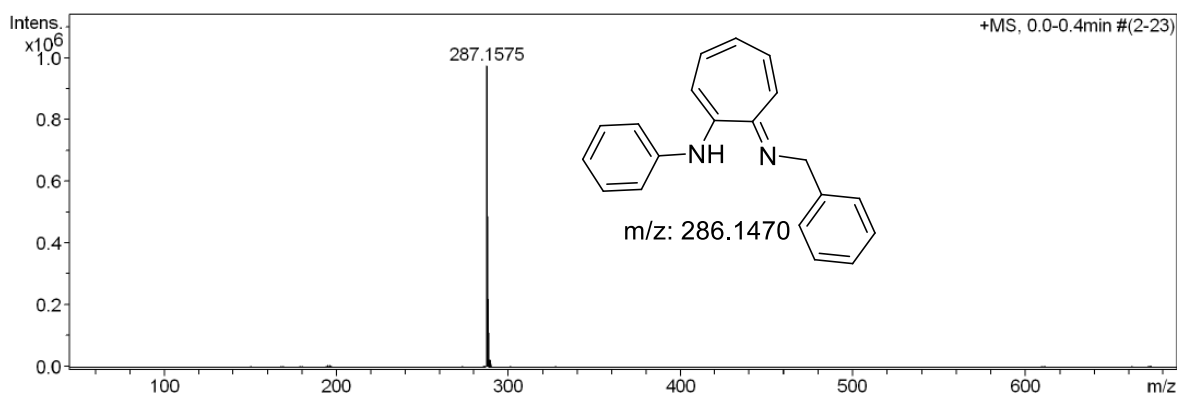
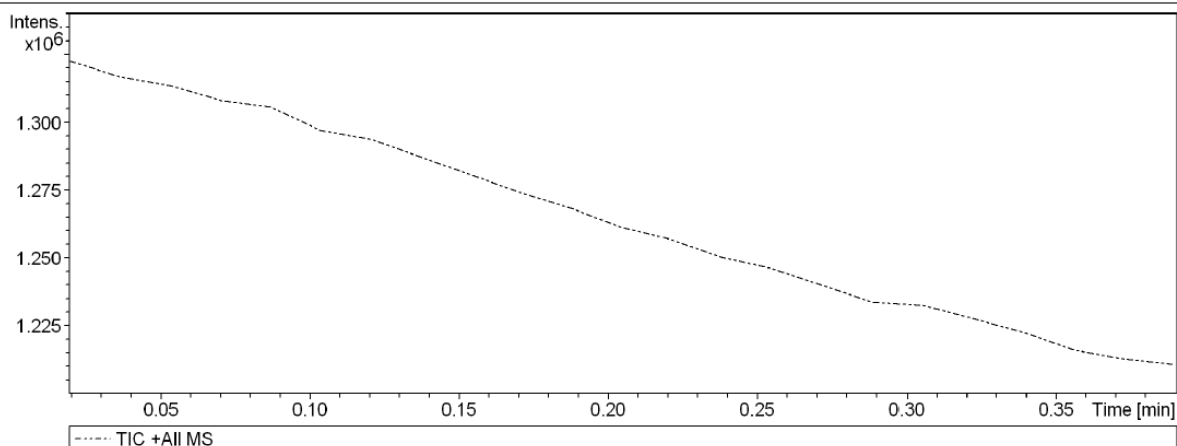


Figure A21. HRMS spectrum of aminotroponimine **35b**.

8. NMR ($^1\text{H}/^{13}\text{C}$) and HRMS of N-(4-methylphenyl)-2-(benzylamino)troponimine (**35c**)

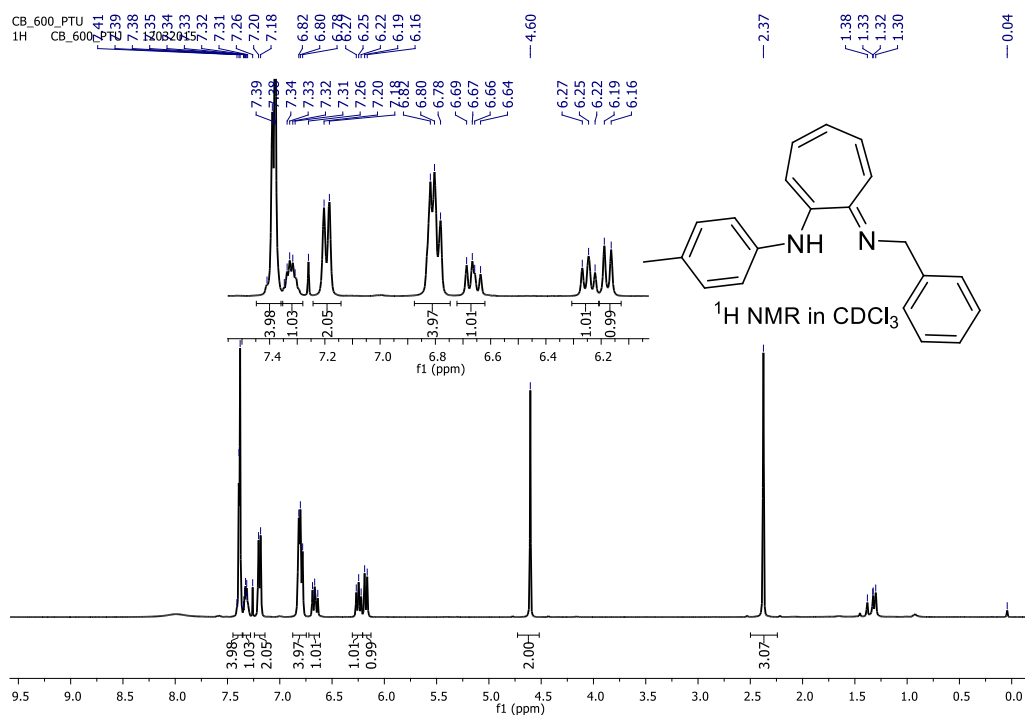


Figure A22. ^1H NMR spectrum of aminotroponimine **35c**

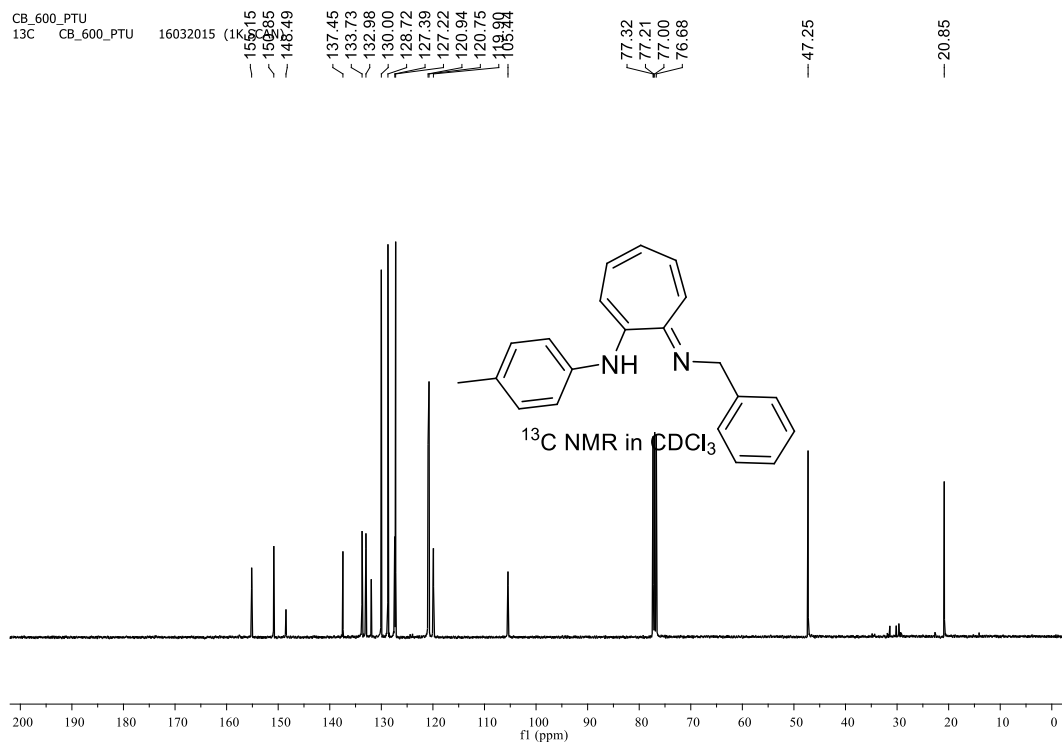


Figure A23. ^{13}C NMR spectrum of aminotroponimine **35c**.

Generic Display Report

Analysis Info

Analysis Name D:\Data\MAR-2015\NKS\11032015_NKS_CB_600_PTU.d
Method Pos_tune_low.m
Sample Name NISER-LCMS
Comment

Acquisition Date 3/11/2015 3:20:05 PM

Operator NISER
Instrument micrOTOF-Q II

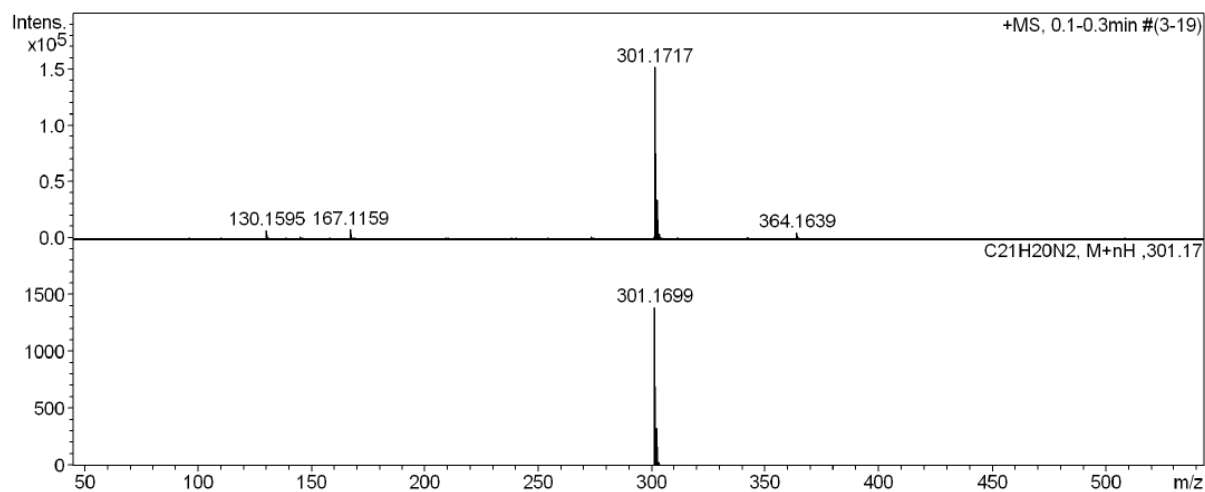
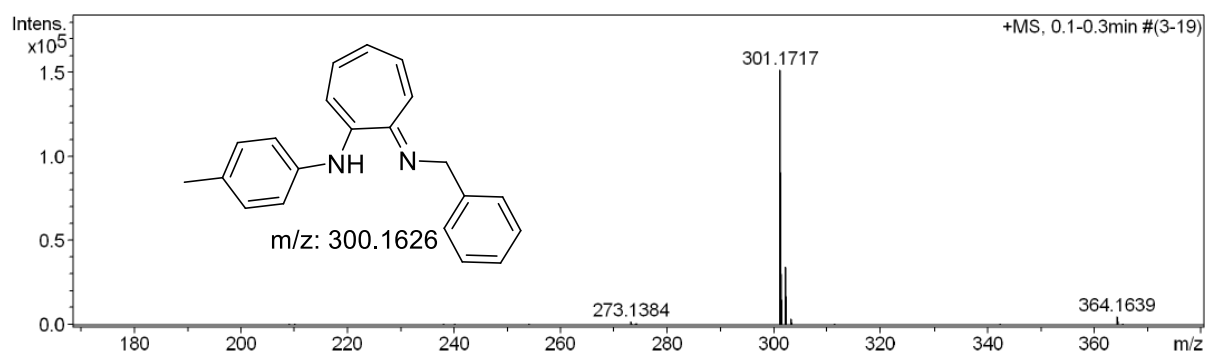
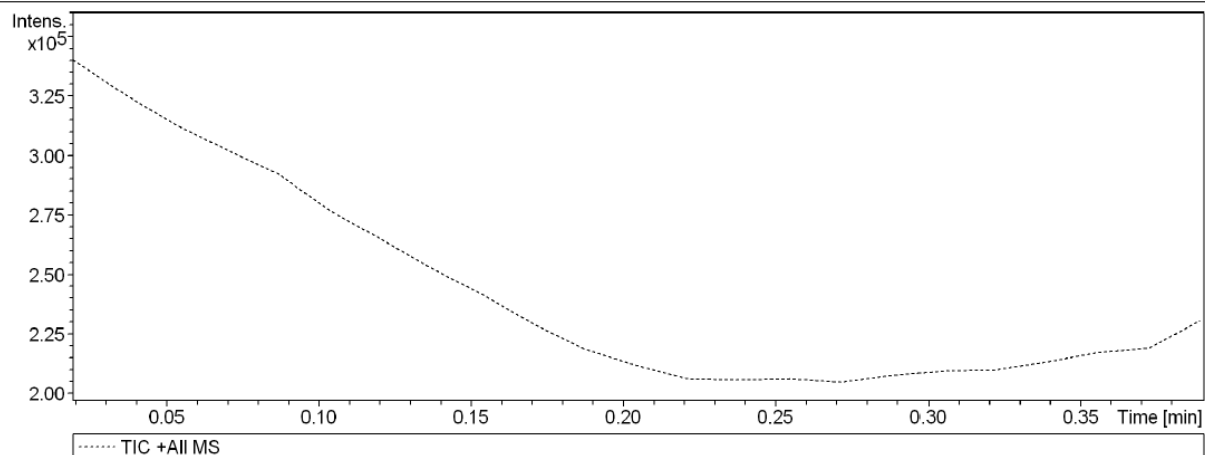


Figure A24. HRMS spectrum of aminotroponimine **35c**.

9. NMR ($^1\text{H}/^{13}\text{C}$) and HRMS of Imine N-(Phenyl)-2-(phenylamino)troponimine (**35d**)

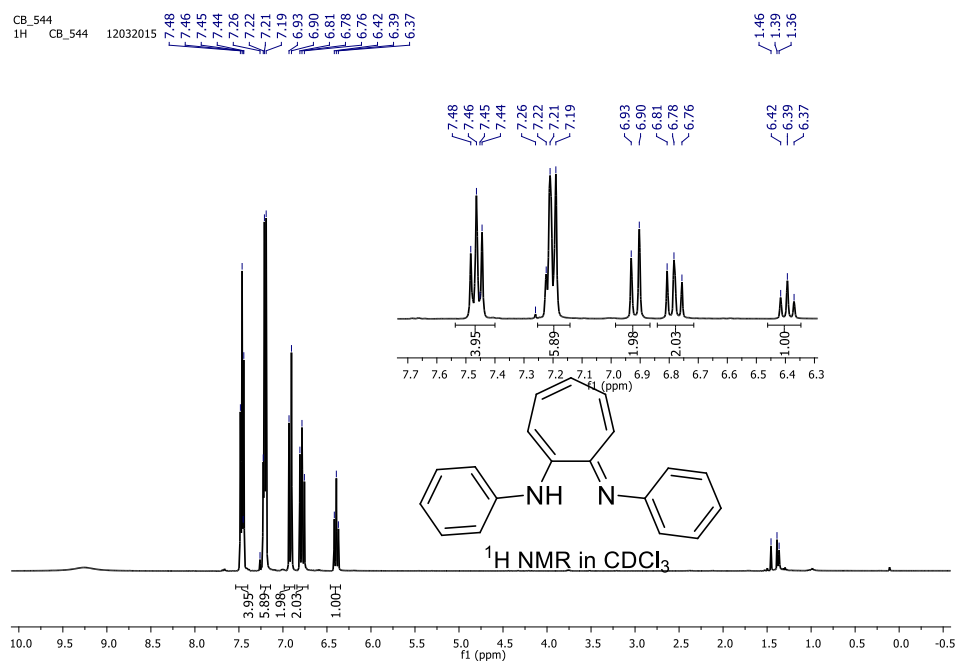


Figure A25. ^1H NMR spectrum of aminotroponimine **35d**.

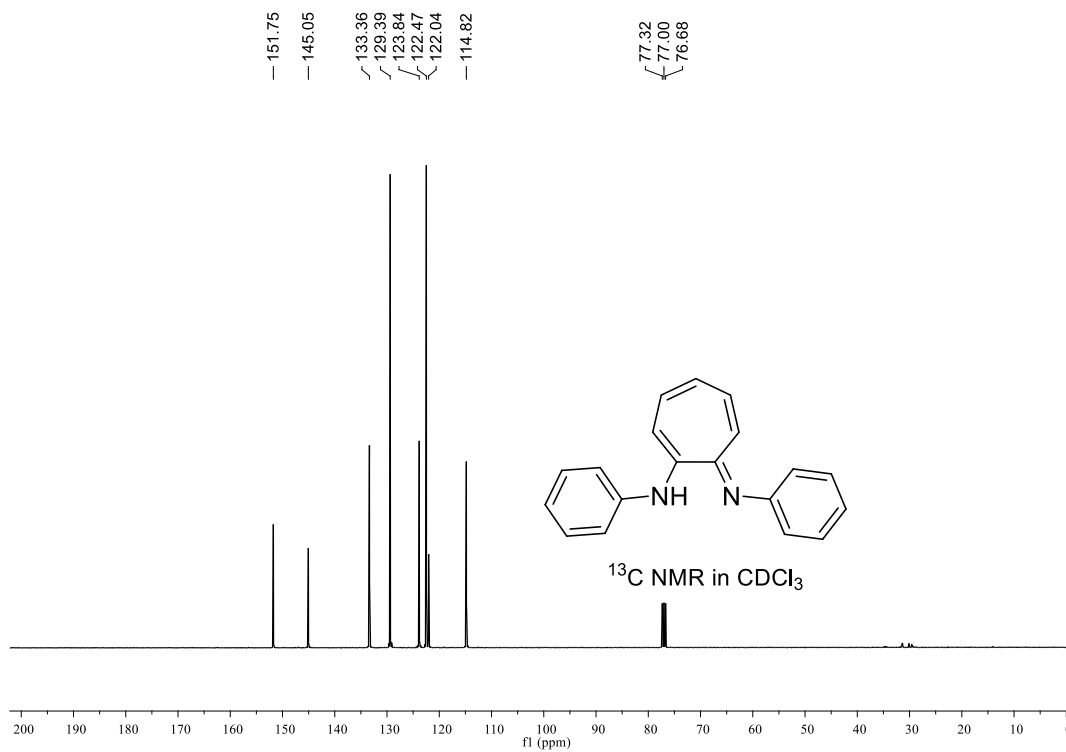


Figure A26. ^{13}C NMR spectrum of aminotroponimine **35d**.

Generic Display Report

Analysis Info

Analysis Name D:\Data\MAR-2015\NKS\11032015_NKS_CB-544.d
Method Pos_tune_low.m
Sample Name NISER-LCMS
Comment

Acquisition Date 3/11/2015 12:03:42 PM

Operator NISER
Instrument microTOF-Q II

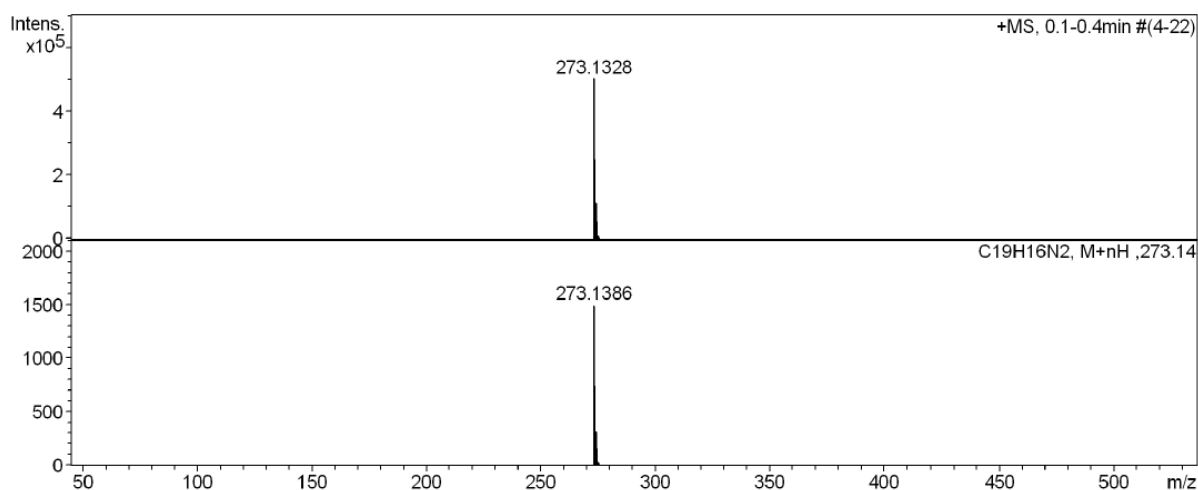
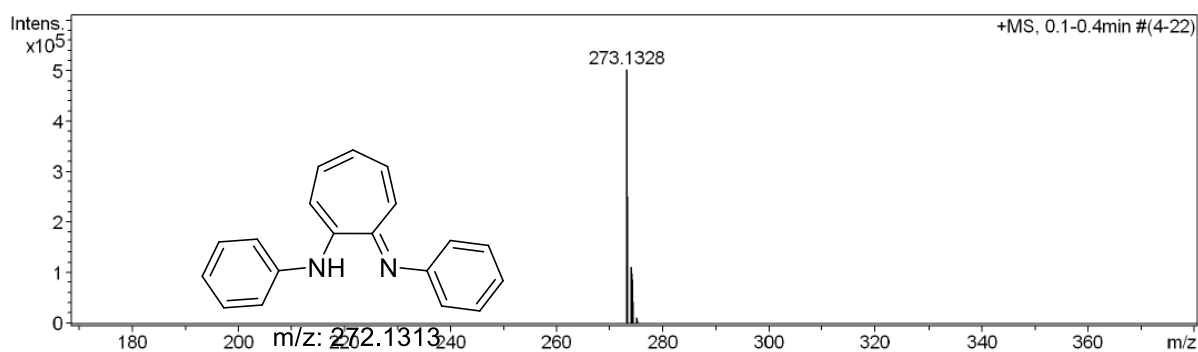
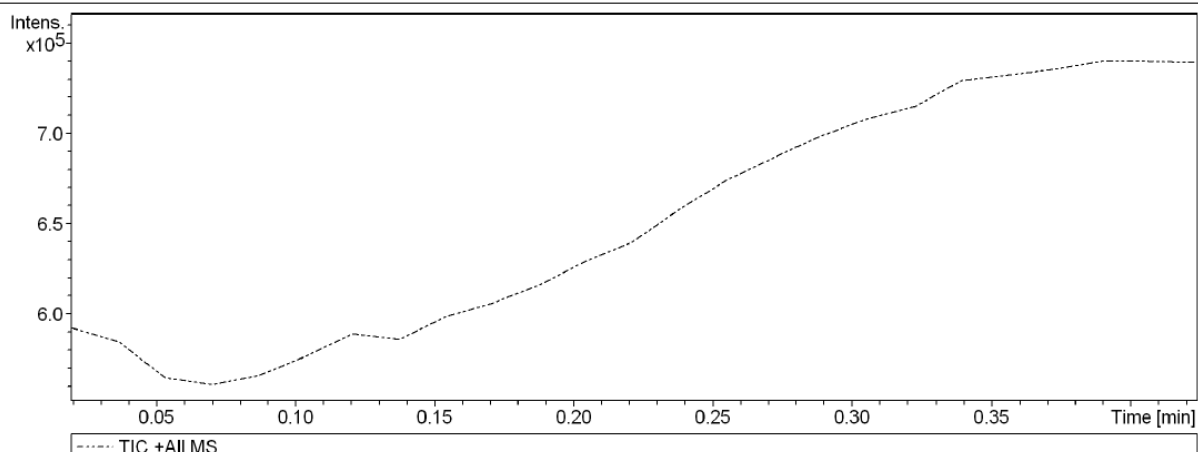


Figure A27. HRMS spectrum of aminotroponimine **35d**.

10. NMR ($^1\text{H}/^{13}\text{C}$) and HRMS of N-(4-chlorophenyl)-2-

(benzylamino)troponimine (**35e**)

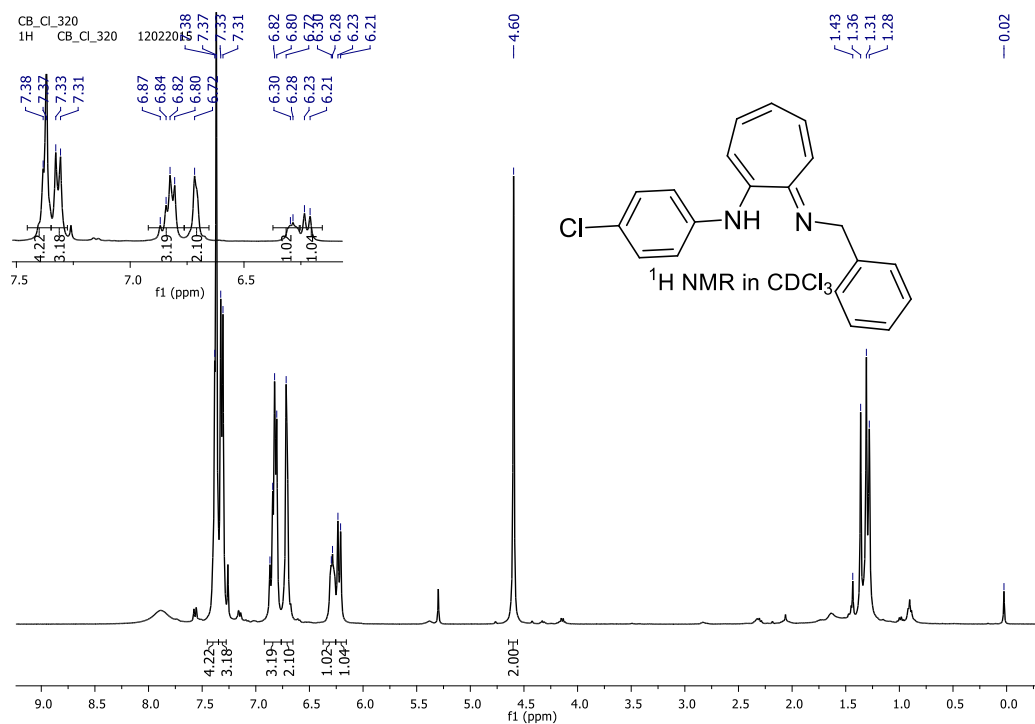


Figure A28. ^1H NMR spectrum of aminotroponimine **35e**

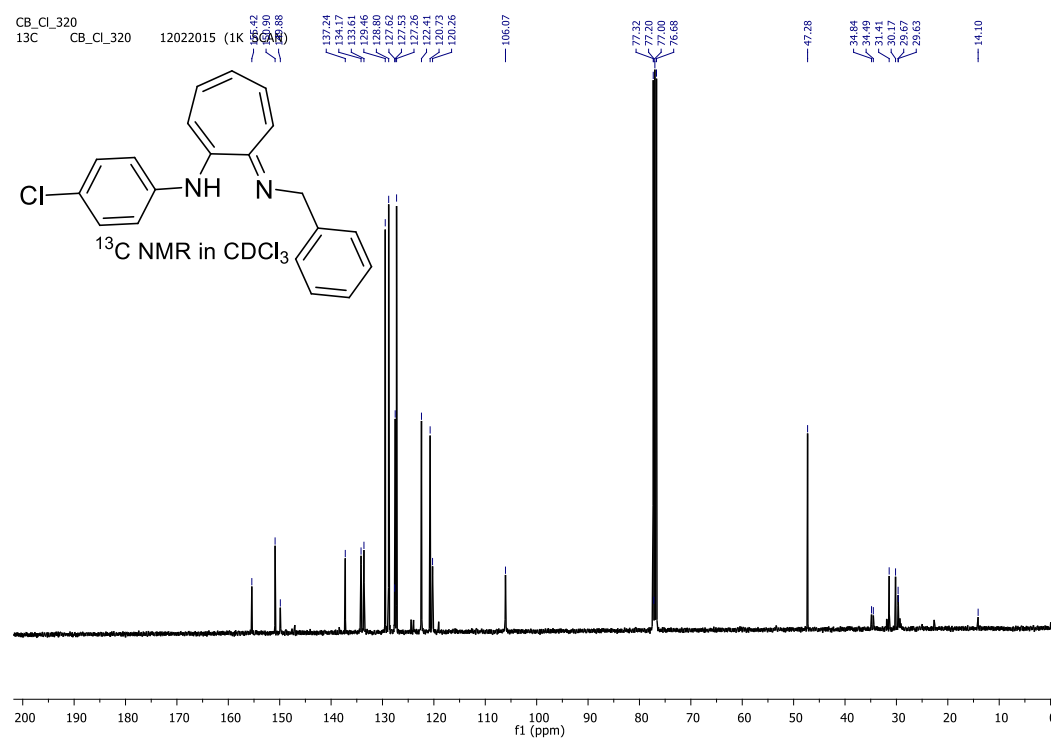


Figure A29. ^{13}C NMR spectrum of aminotroponimine **35e**

Generic Display Report

Analysis Info

Analysis Name D:\Data\FEB-2015\NKS\03022015_NKS_CB_4Cl640.d
Method Pos_tune_low.m
Sample Name NISER-LCMS
Comment

Acquisition Date 2/4/2015 9:25:07 AM

Operator NISER
Instrument microTOF-Q II

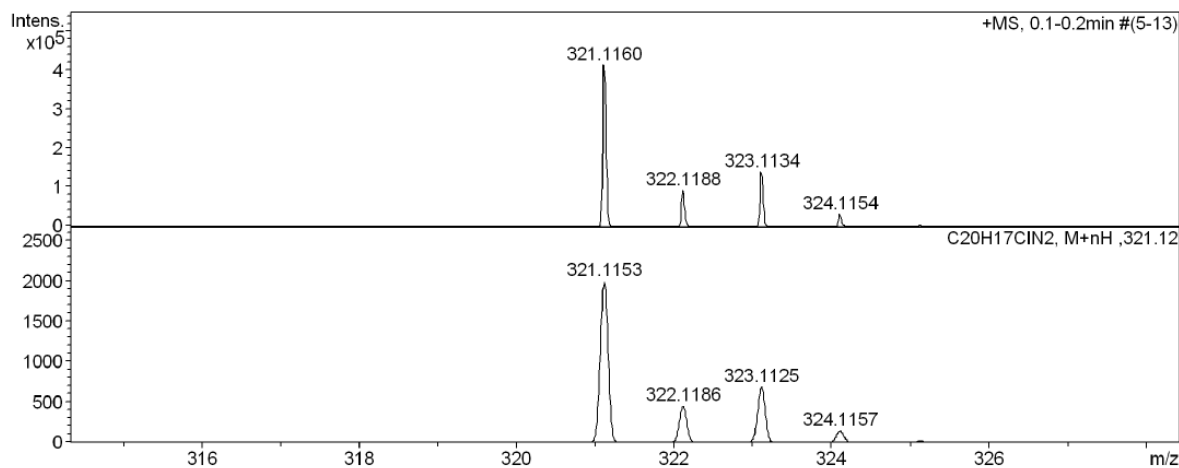
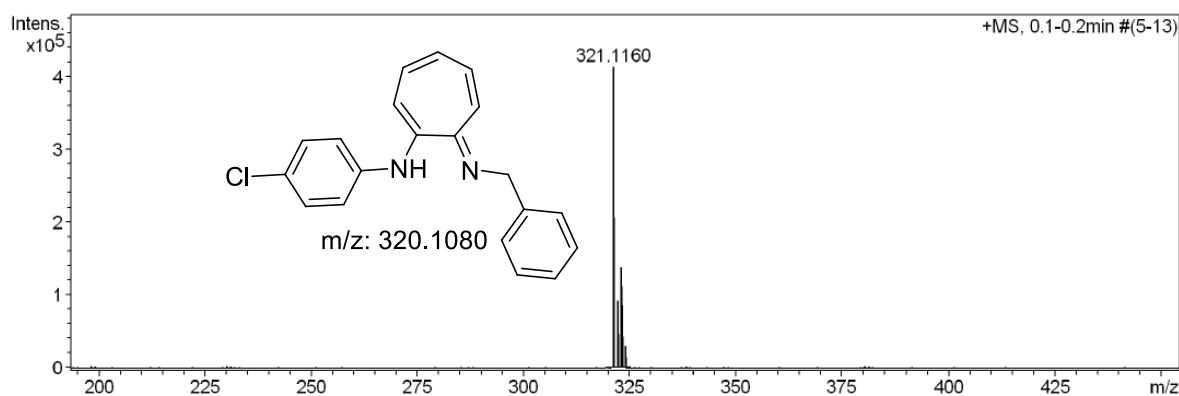
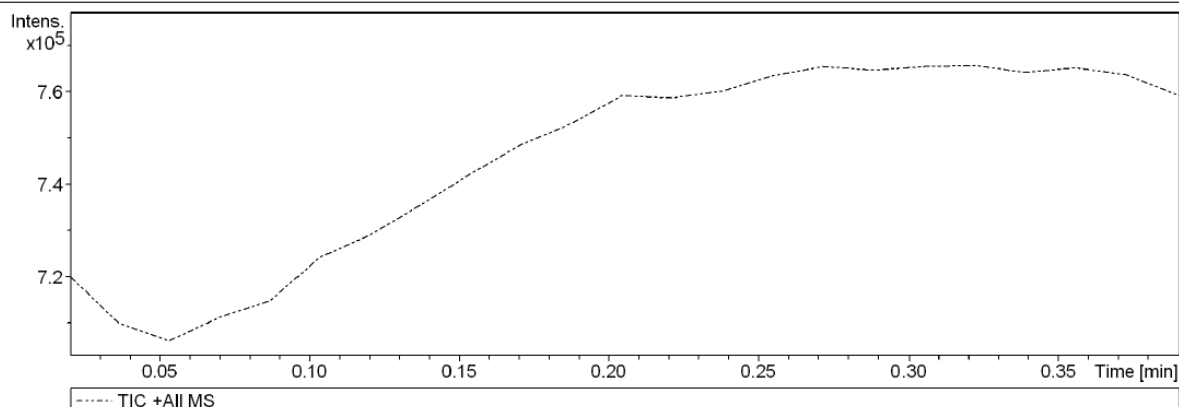


Figure A30. HRMS spectrum of aminotroponimine **31e**.

11. NMR ($^1\text{H}/^{13}\text{C}$) and HRMS of N-(4-fluorophenyl)-2-(benzylamino)troponimine (**35f**)

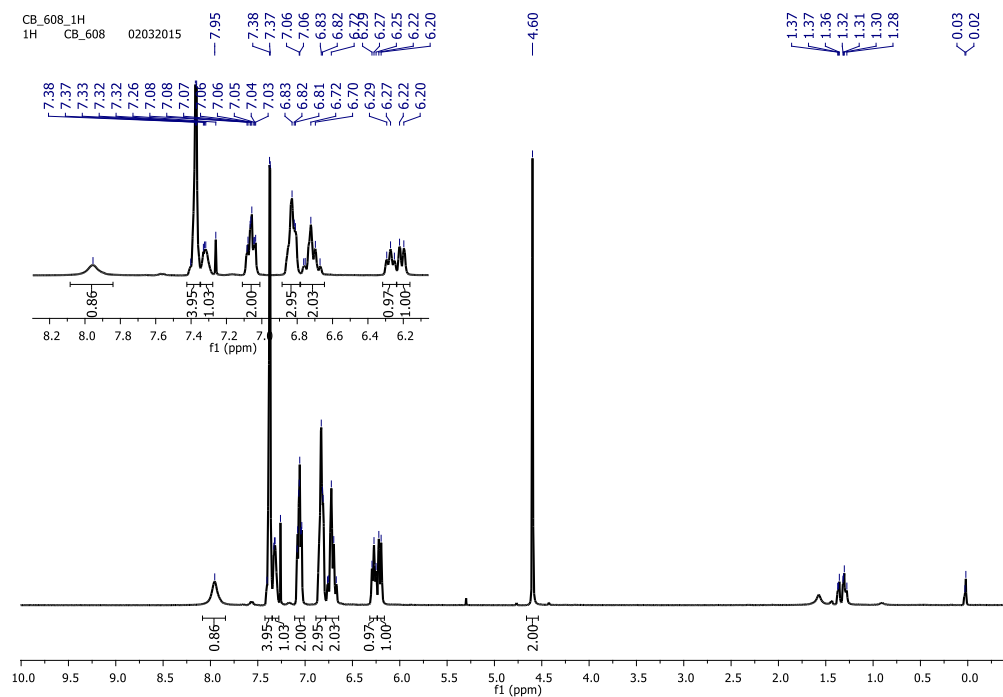


Figure A31. ^1H NMR spectrum of aminotroponimine **35f**.

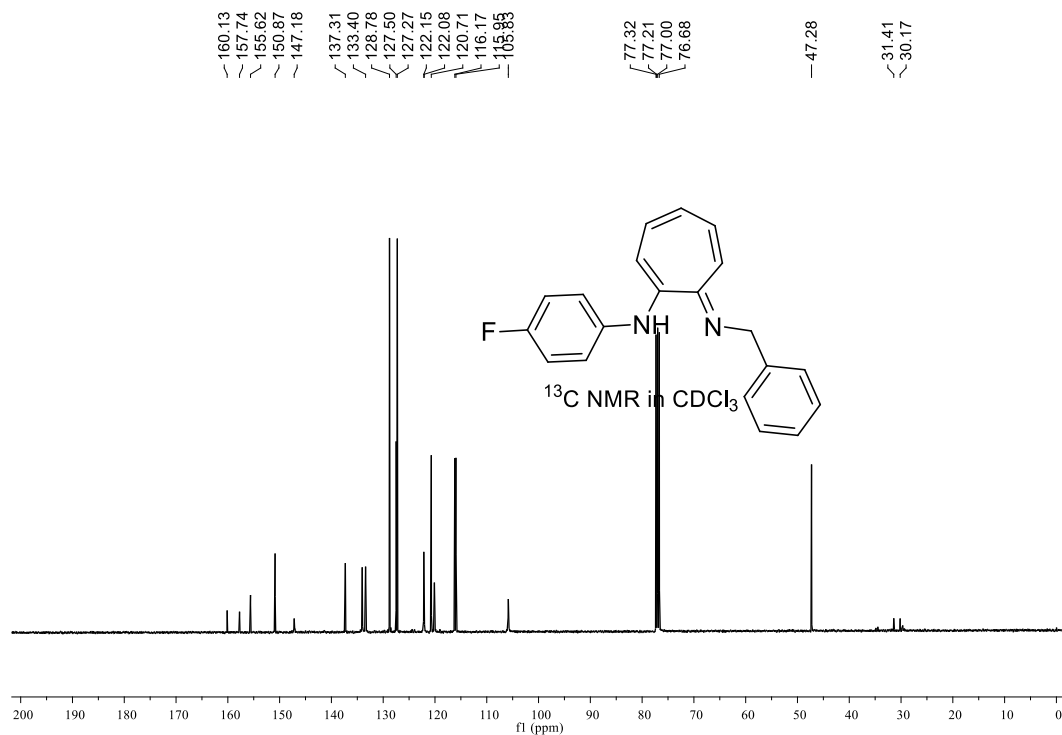


Figure A32. ^{13}C NMR spectrum of aminotroponimine **35f**

Generic Display Report

Analysis Info

Analysis Name D:\Data\MAR-2015\NKS\11032015_NKS_CB_608.d
Method Pos_tune_low.m
Sample Name NISER-LCMS
Comment

Acquisition Date 3/11/2015 3:33:42 PM

Operator NISER
Instrument micrOTOF-Q II

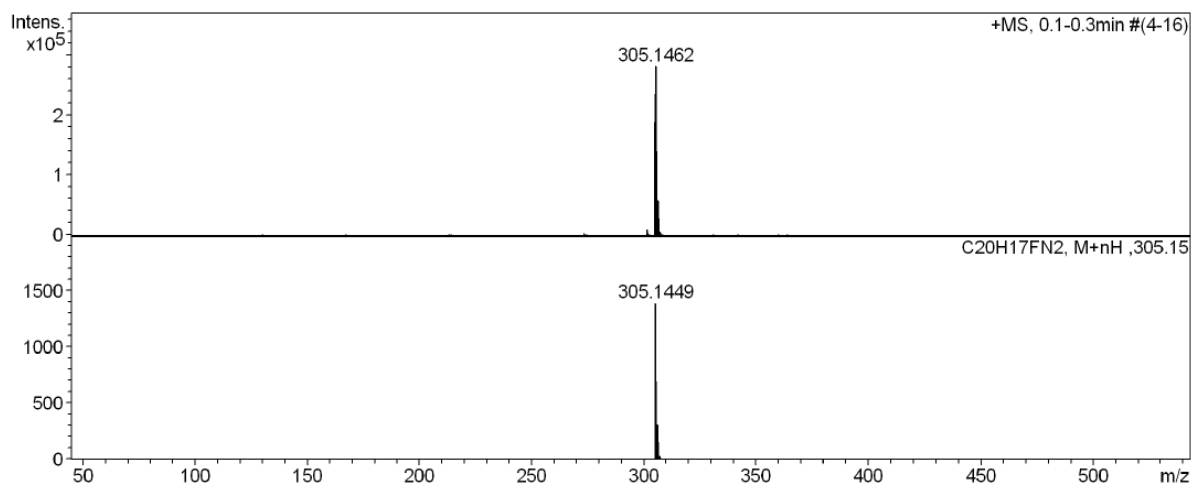
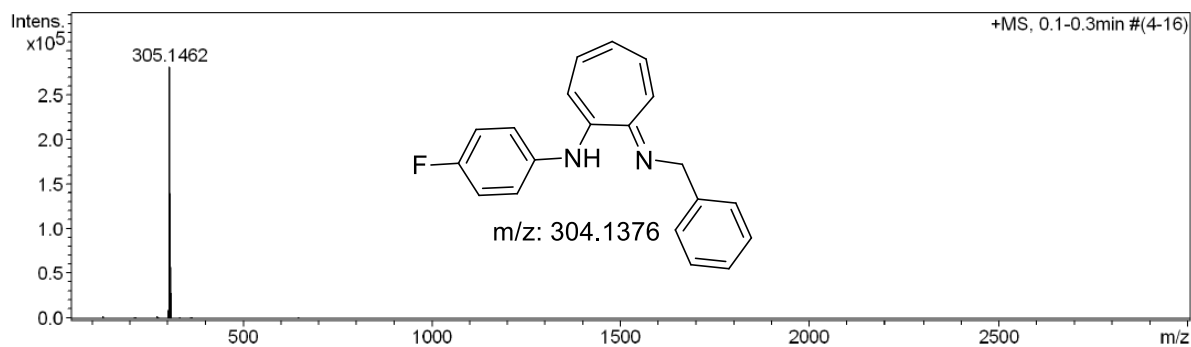
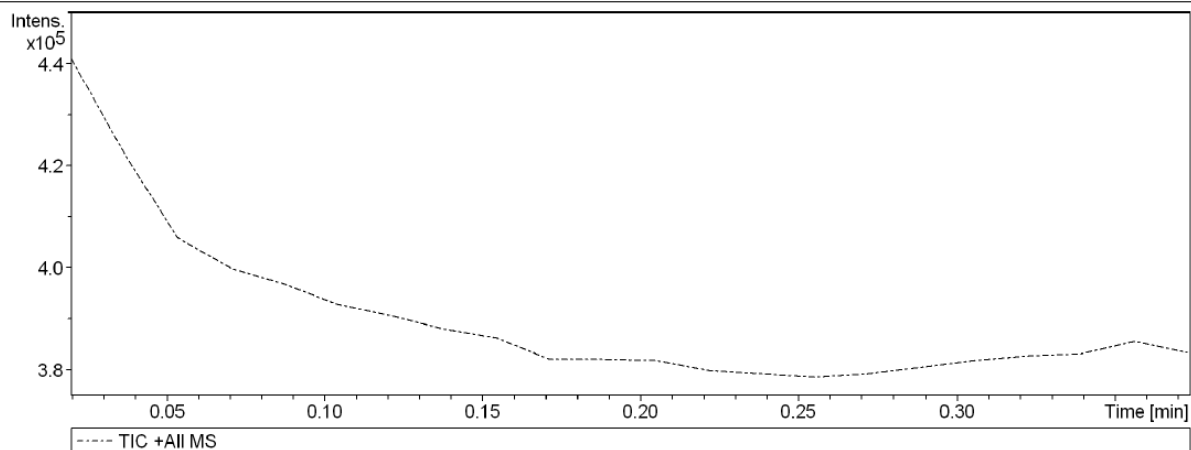
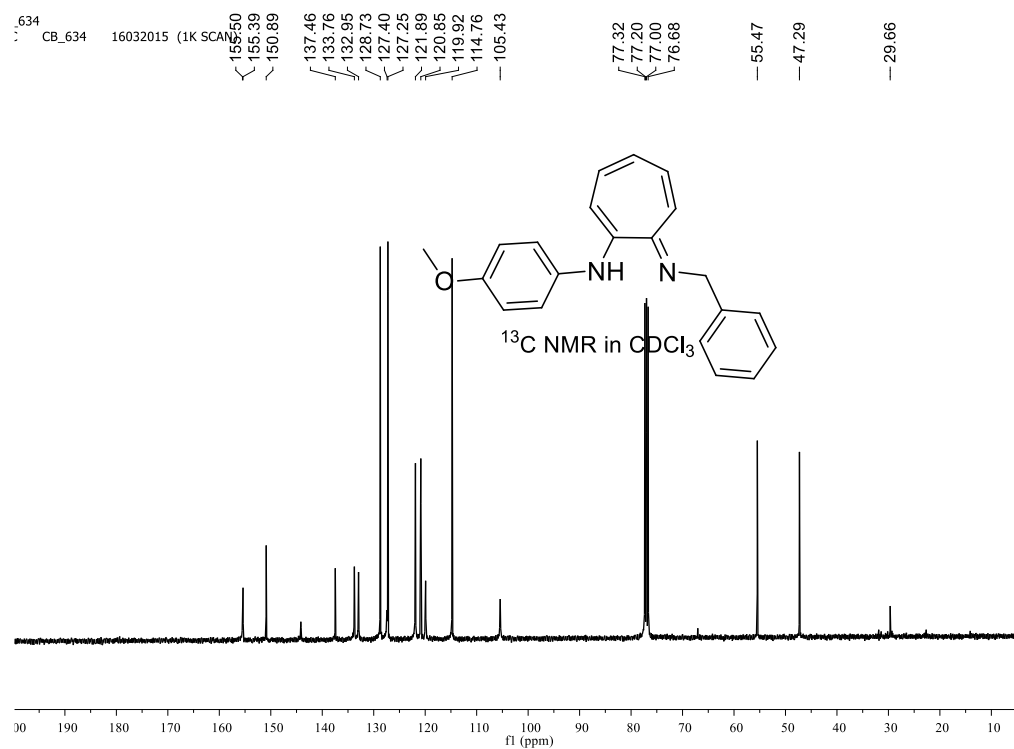
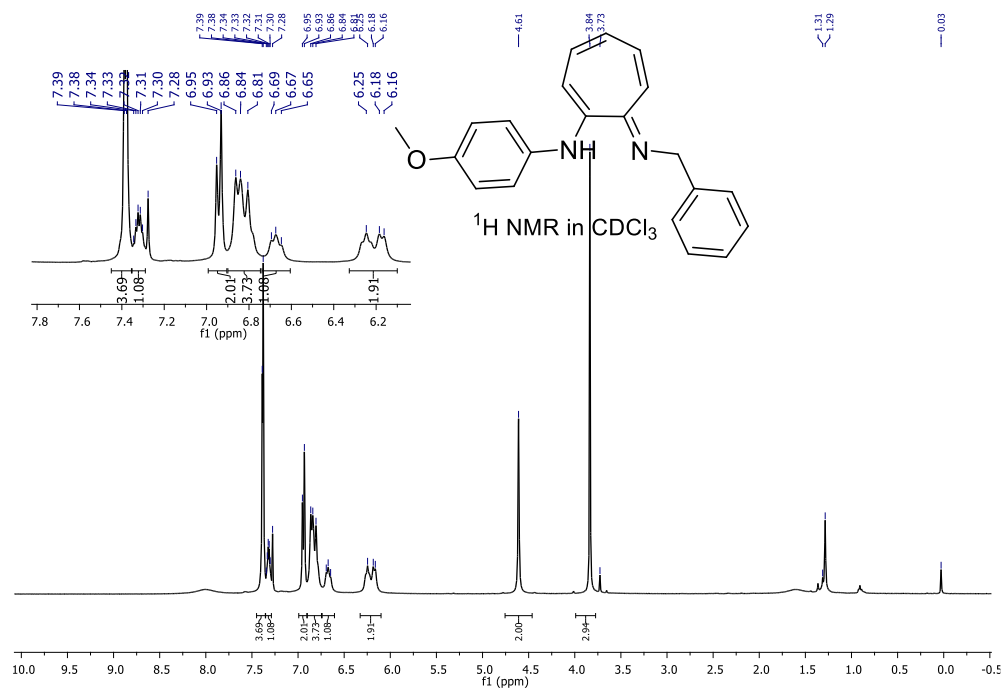


Figure A33. HRMS spectrum of aminotroponimine **35f**.

12. NMR ($^1\text{H}/^{13}\text{C}$) and HRMS of N-(4-methoxyphenyl)-2-(benzylamino)troponimine (**35g**)



Generic Display Report

Analysis Info

Analysis Name D:\Data\JAN-2015\NKS\27012015_NKS_CB_634.d
Method Pos_tune_low.m
Sample Name NISER-LCMS
Comment

Acquisition Date 1/27/2015 7:22:04 PM

Operator NISER
Instrument microTOF-Q II

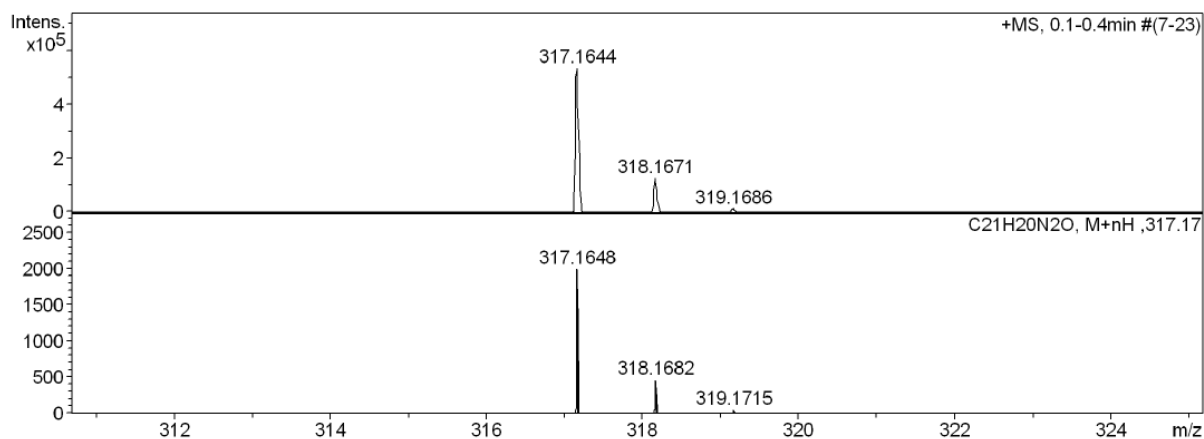
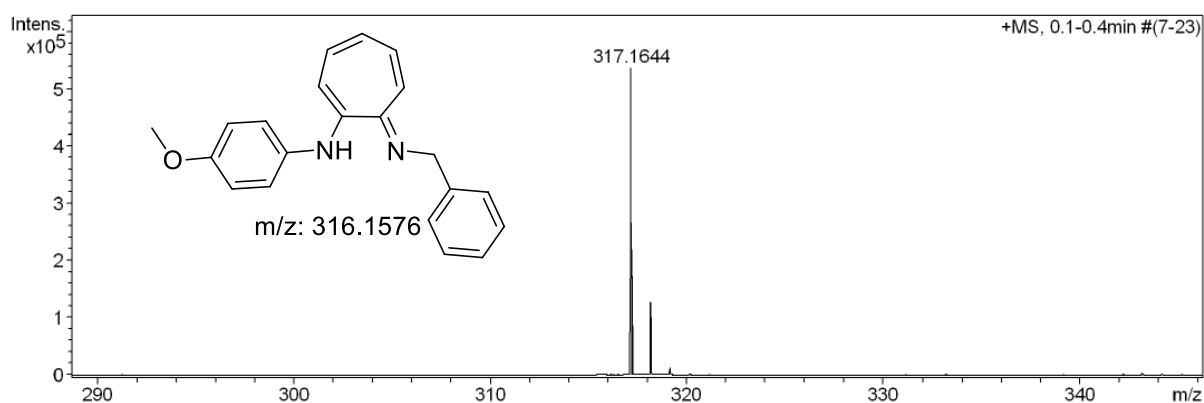
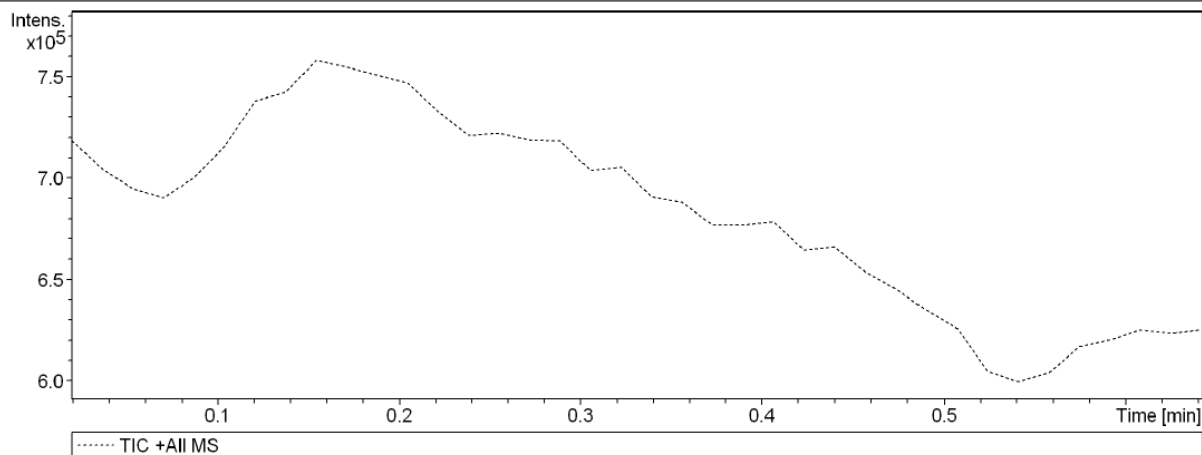


Figure A36. HRMS spectrum of aminotroponimine **35g**.

13.NMR ($^1\text{H}/^{13}\text{C}$) and HRMS of N-(phenyl)-2-(prop-1-yn-1-yl)troponimine

(35h)

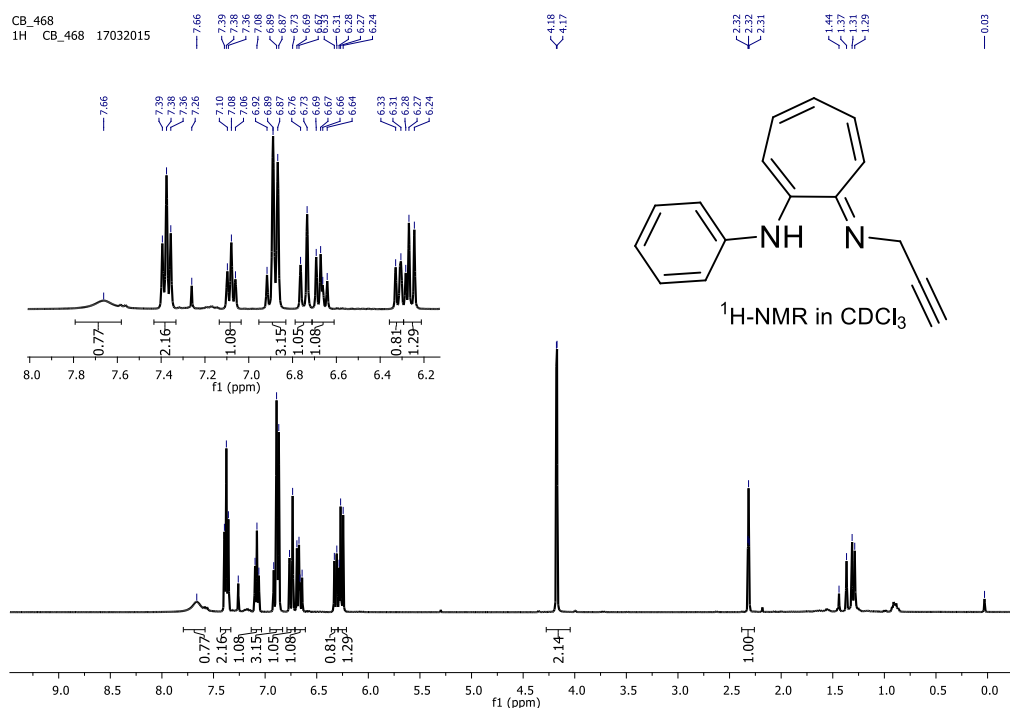


Figure A37. ^1H NMR spectrum of aminotroponimine 35h.

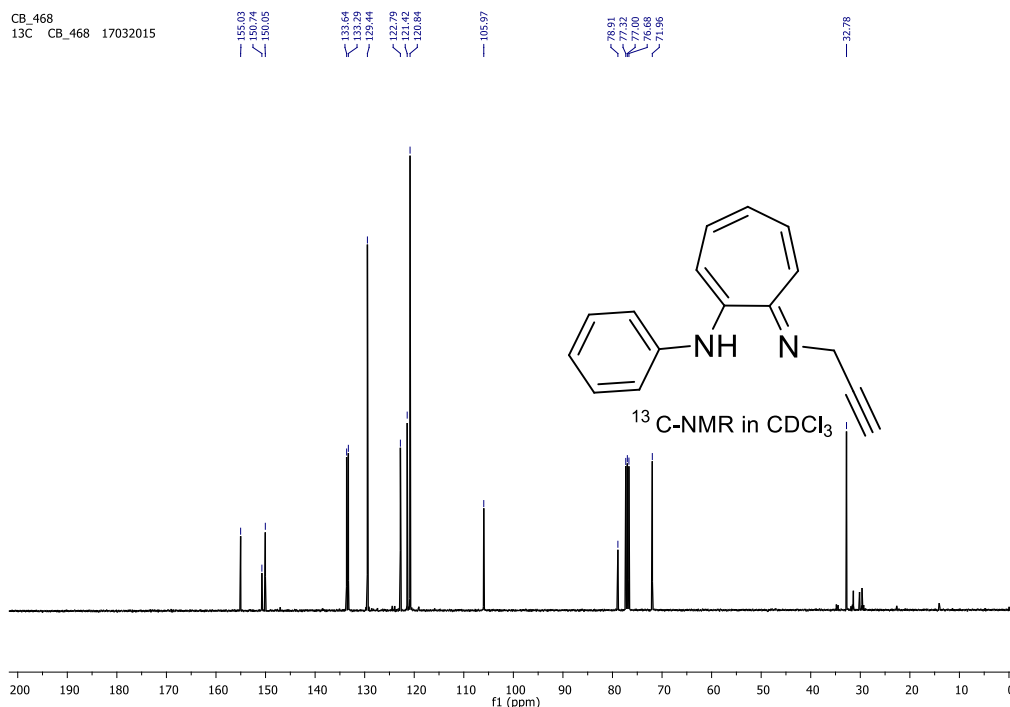


Figure A38. ^{13}C NMR spectrum of aminotroponimine 35h.

Generic Display Report

Analysis Info

Analysis Name D:\Data\MAR-2015\INKS\14032015_NKS-CB_470.d
Method Pos_tune_low.m
Sample Name NISER-LCMS
Comment

Acquisition Date 3/14/2015 6:31:39 PM

Operator NISER
Instrument micrOTOF-Q II

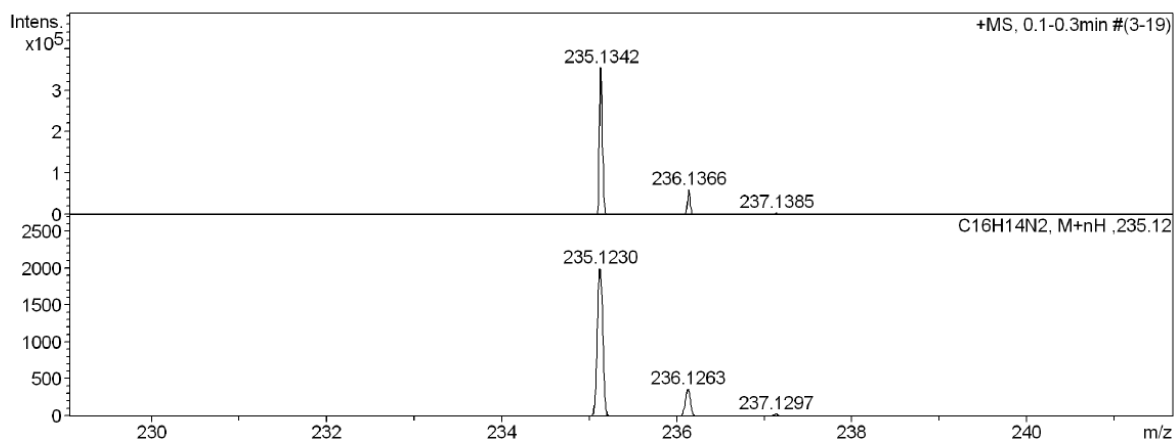
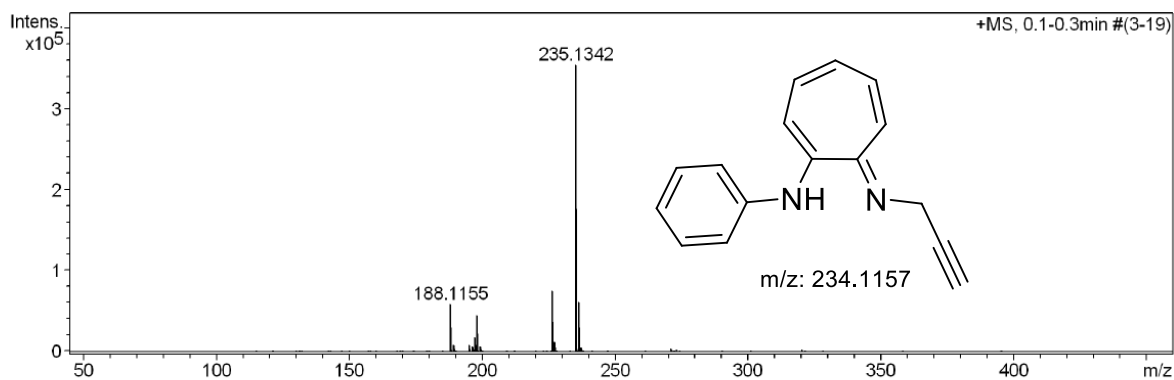
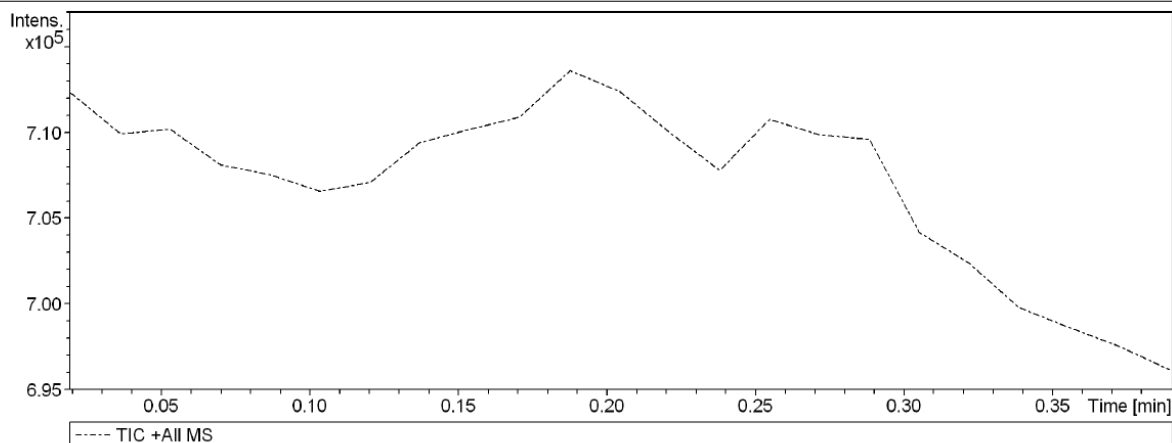


Figure A39. HRMS spectrum of aminotroponimine **35h**.

14. NMR ($^1\text{H}/^{13}\text{C}$) and HRMS of N-(phenyl)-2-(diaminobutyl)diprotonimine

(35i)

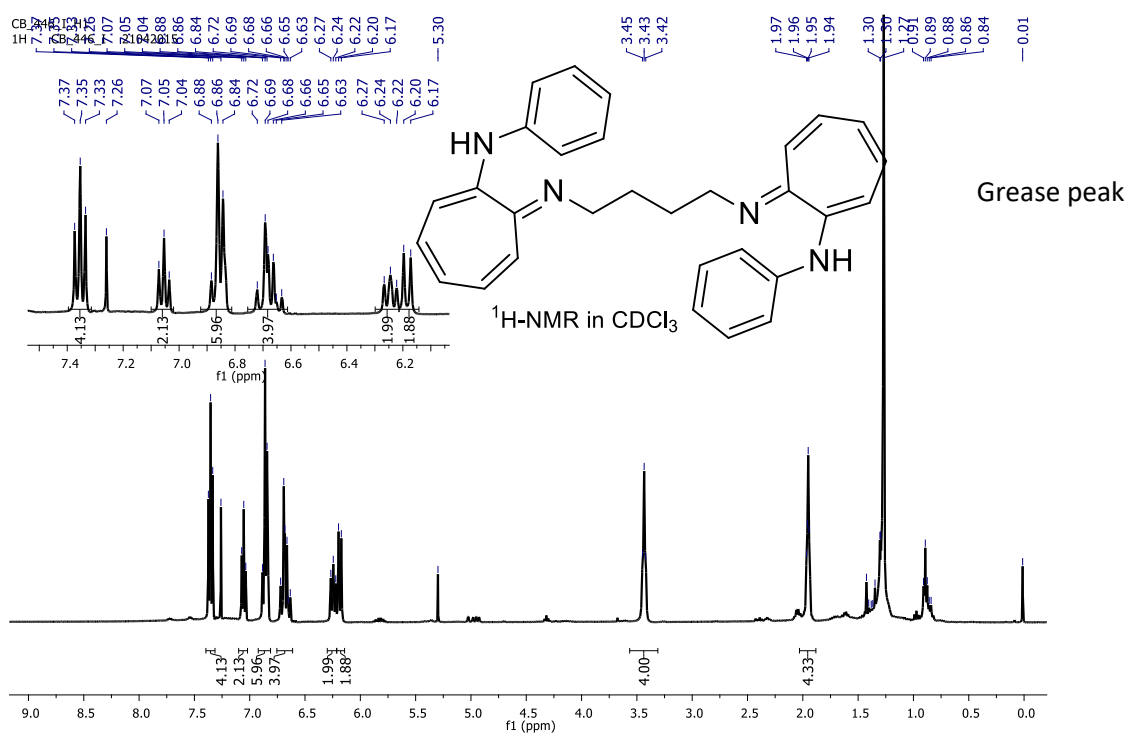


Figure A40. ^1H NMR spectrum of aminotroponimine 35i.

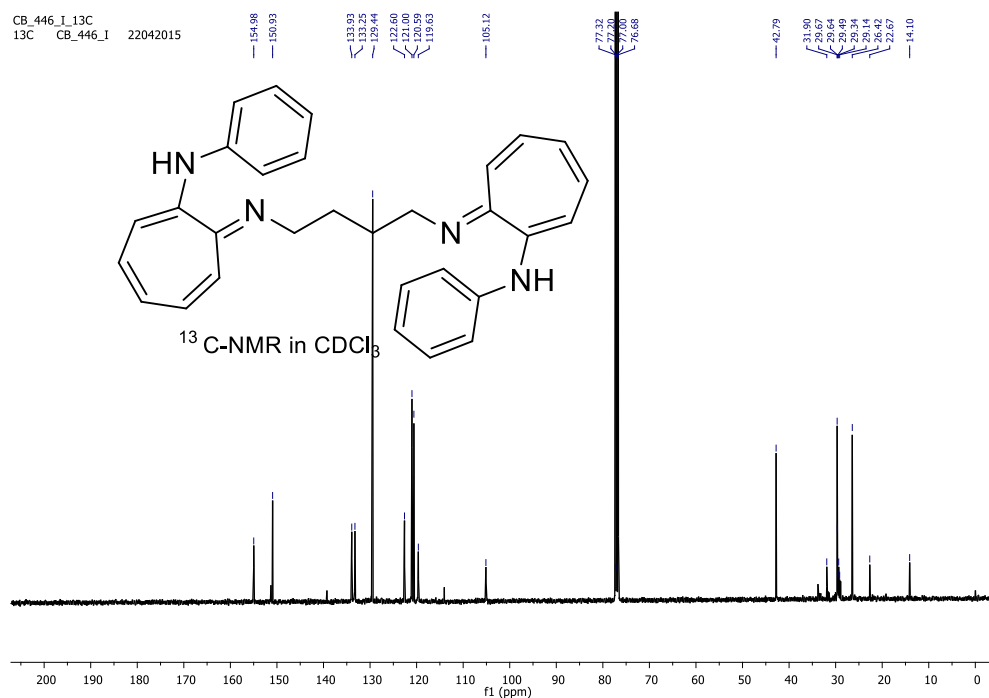


Figure A41. ^{13}C NMR spectrum of aminotroponimine 35i.

Generic Display Report

Analysis Info

Analysis Name D:\Data\APR-2015\NKS\21042015_NKS_CB_446T.d
Method Pso_tune_wide.m
Sample Name NISER-LCMS
Comment

Acquisition Date 4/21/2015 3:58:58 PM

Operator NISER
Instrument micrOTOF-Q II

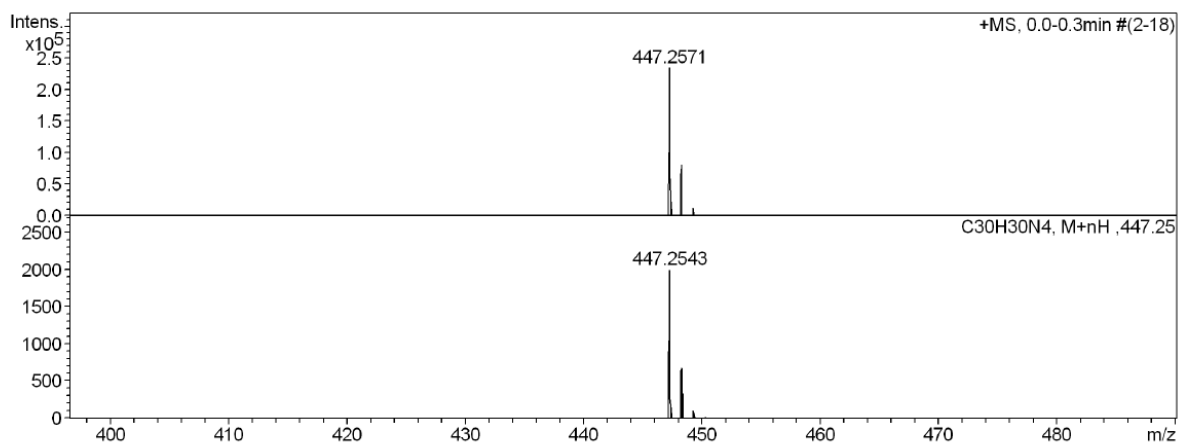
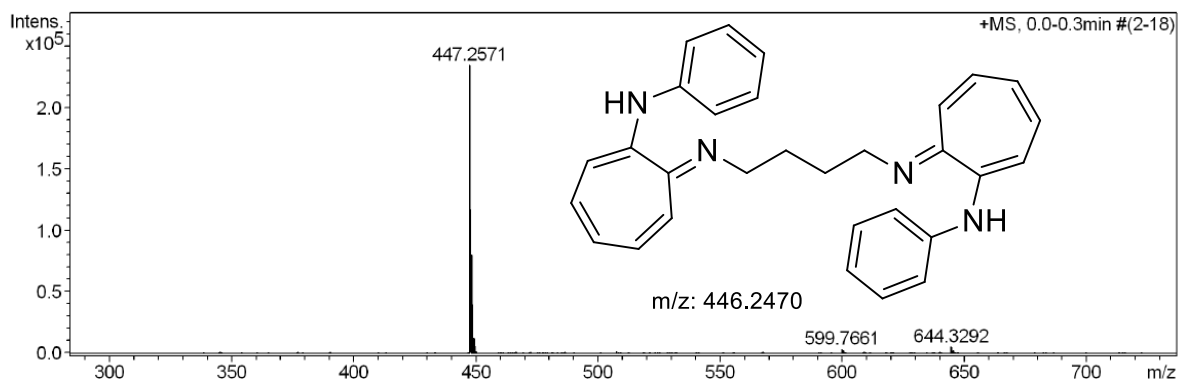
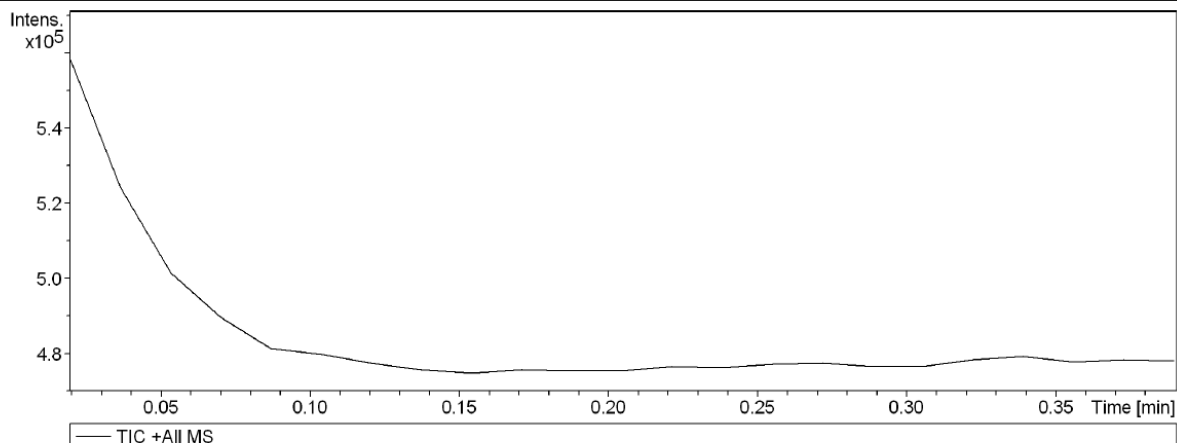


Figure A42. HRMS spectrum of aminotroponimine **35i**.

15.NMR ($^1\text{H}/^{13}\text{C}/^{11}\text{B}/^{19}\text{F}$) and HRMS of boron complex (**36a**)

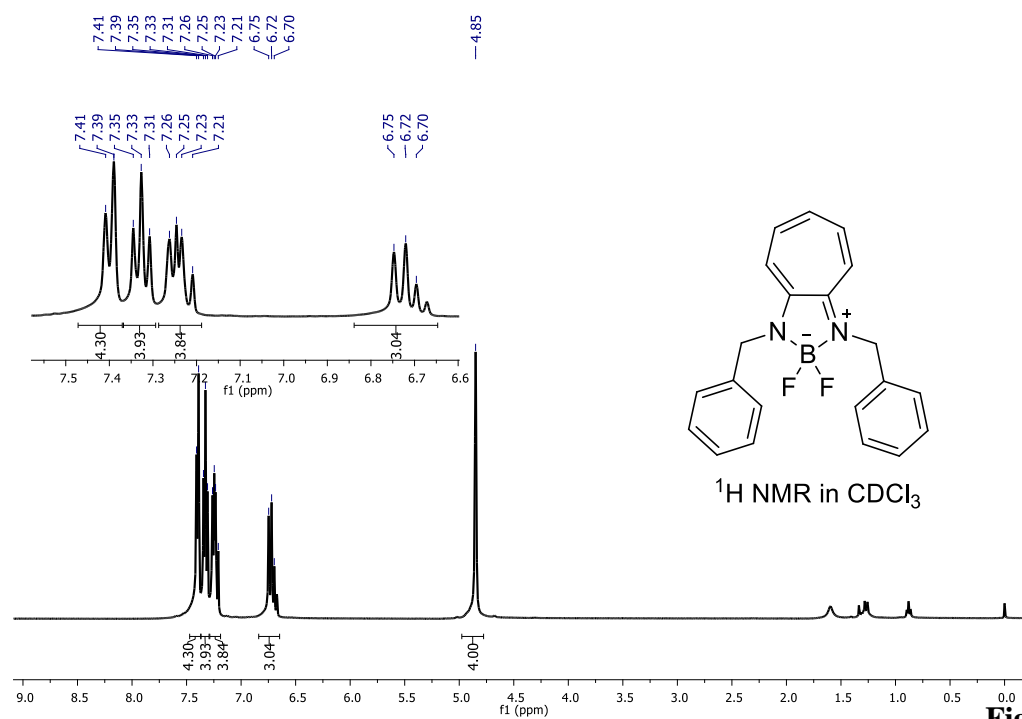


Figure A43. ^1H

NMR spectrum of boron complex **36a**

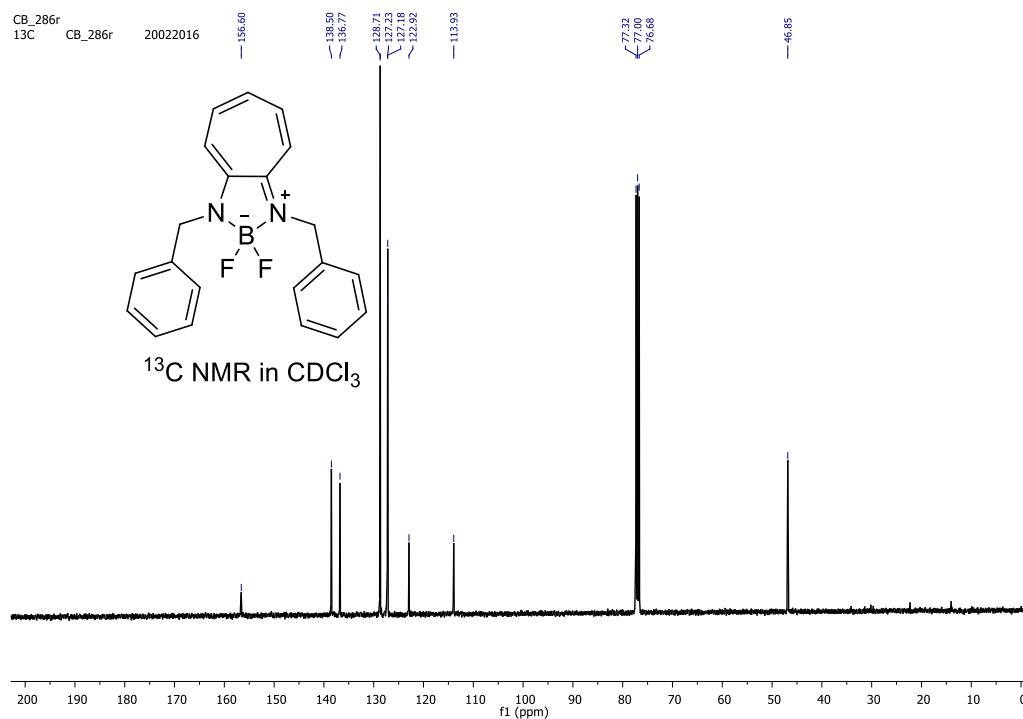


Figure A44. ^{13}C NMR spectrum of boron complex **36a**

CB_796_R
11B CB_796_R 22012015

5.82
5.57
5.33

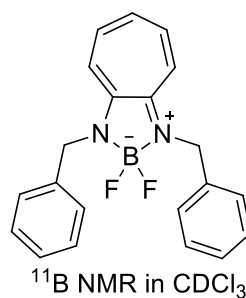
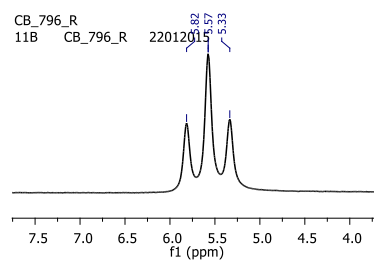


Figure A45. ^{11}B NMR spectrum of boron complex **36a**

CB_796_R
F19 CB_796_R 22012015

-138.20
-138.28
-138.36
-138.44

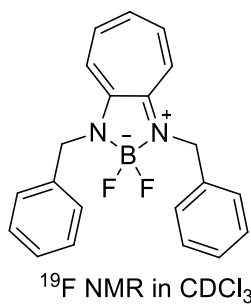
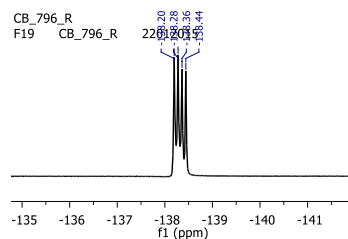


Figure A46. ^{19}F NMR spectrum of boron complex **36a**

Generic Display Report

Analysis Info

Analysis Name D:\Data\JAN-2015\NKS\21012015_NKS_CB_796R.d
Method Pos_tune_low.m
Sample Name NISER-LCMS
Comment

Acquisition Date 1/21/2015 6:24:57 PM

Operator NISER
Instrument microTOF-Q II

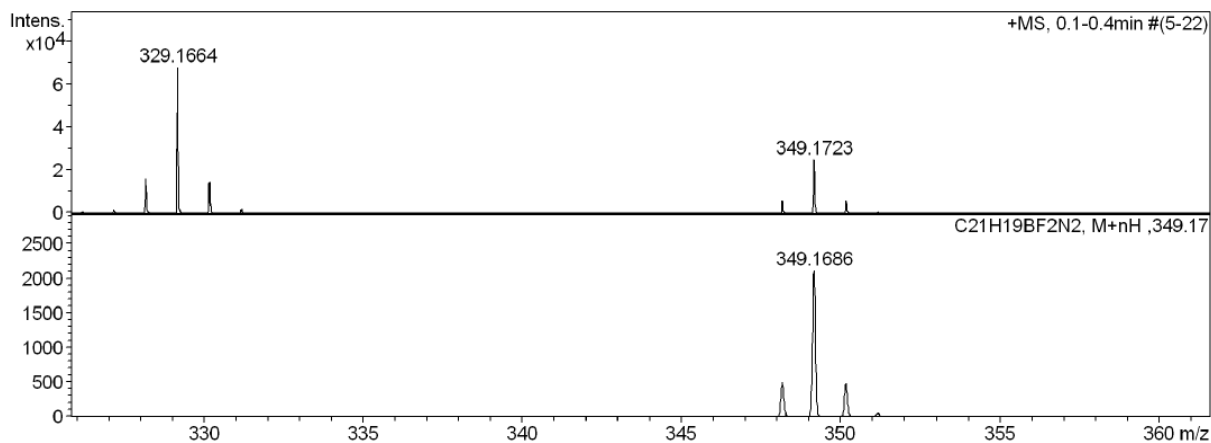
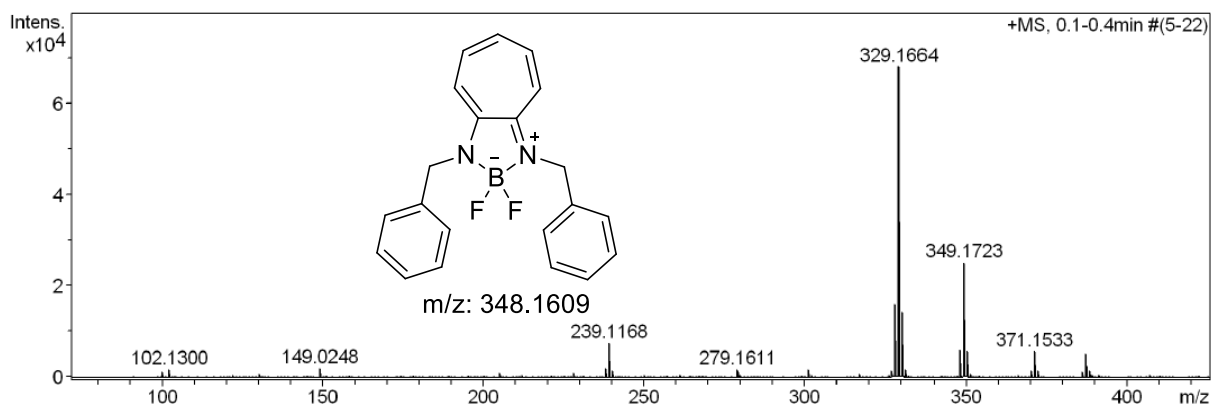
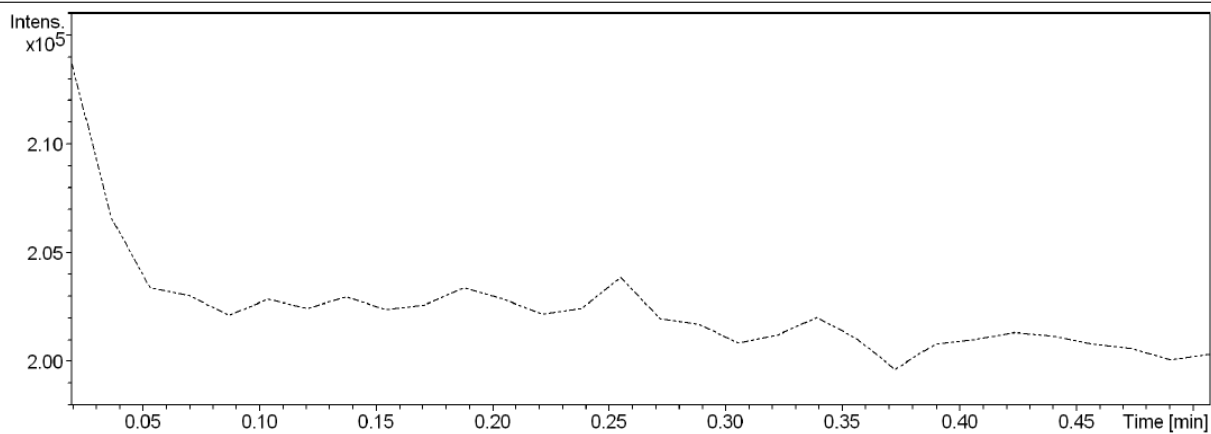


Figure A47. HRMS spectrum of boron complex **36a**

16. NMR ($^1\text{H}/^{13}\text{C}/^{11}\text{B}/^{19}\text{F}$) and HRMS of boron complex (**36b**)

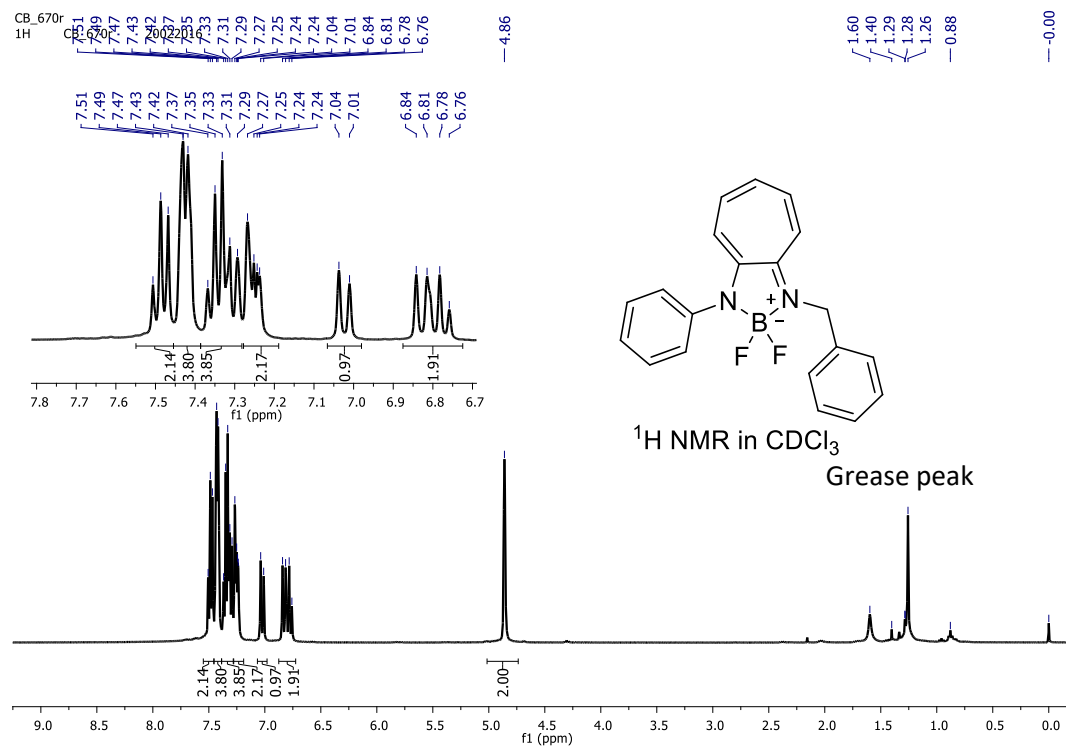


Figure A48. ^1H NMR spectrum of boron complex **36b**

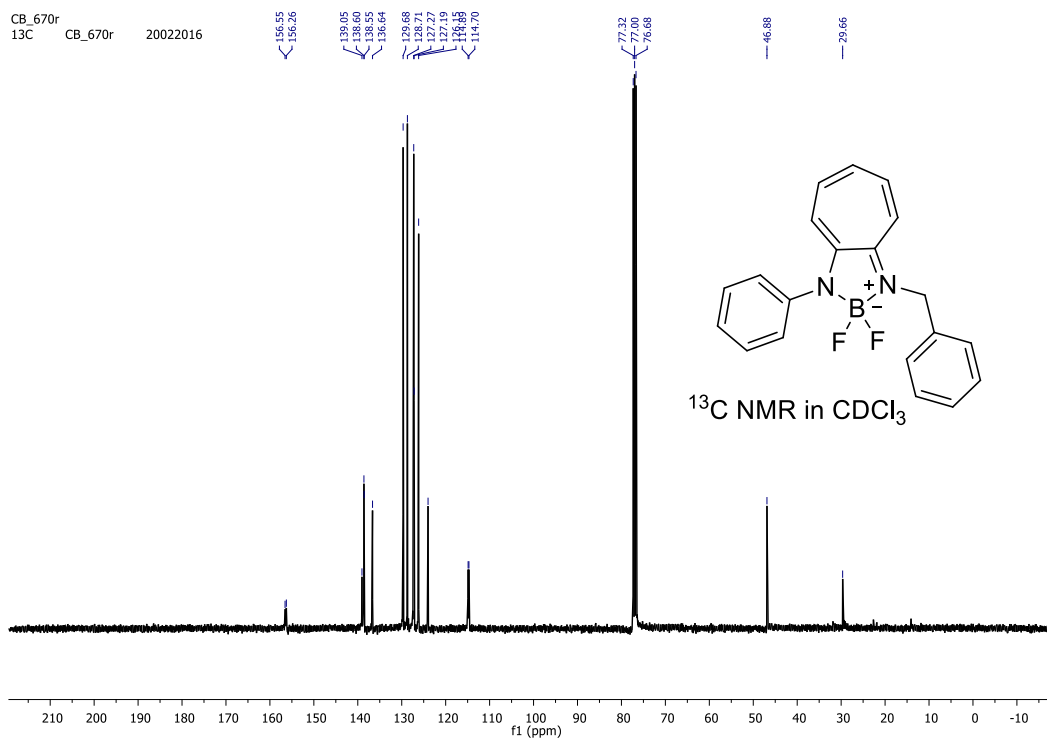


Figure A49. ^{13}C NMR spectrum of boron complex **36b**

CB_670_R
11B CB_670_R 22012015

5.64
5.41
5.18

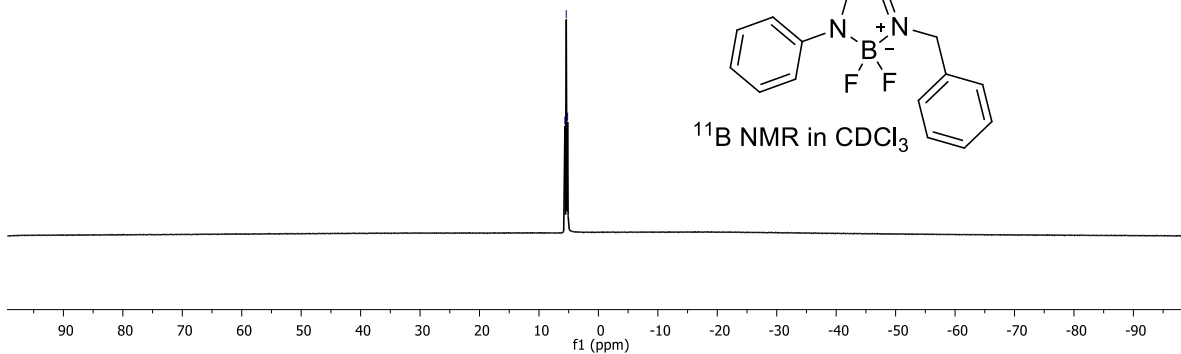
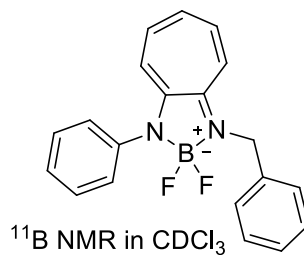
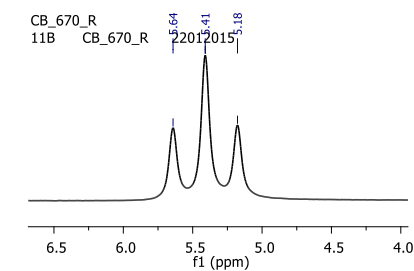


Figure A50. ¹¹B NMR spectrum of boron complex **36b**

CB_670_R
F19 CB_670_R 22012015

135.73
135.81
135.86
135.89
135.97

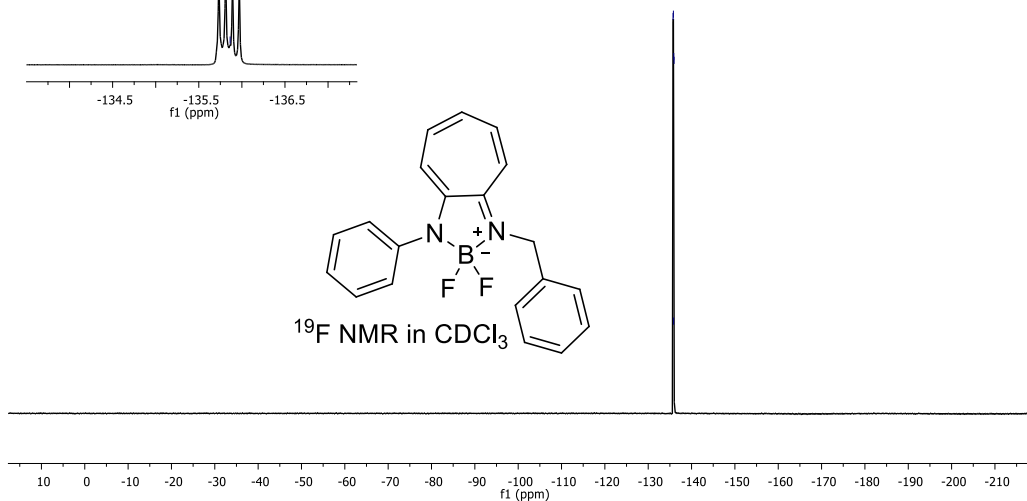
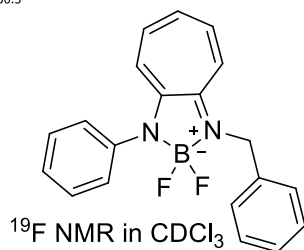
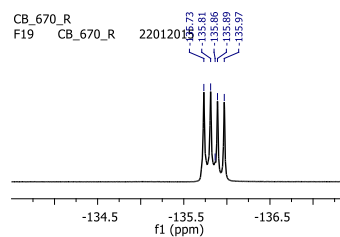


Figure A51. ¹⁹F NMR spectrum of boron complex **36b**.

Generic Display Report

Analysis Info

Analysis Name D:\Data\JAN-2015\NKS\21012015_NKS_CB_670.d
Method Pos_tune_low.m
Sample Name NISER-LCMS
Comment

Acquisition Date 1/21/2015 1:14:51 PM

Operator NISER
Instrument micrOTOF-Q II

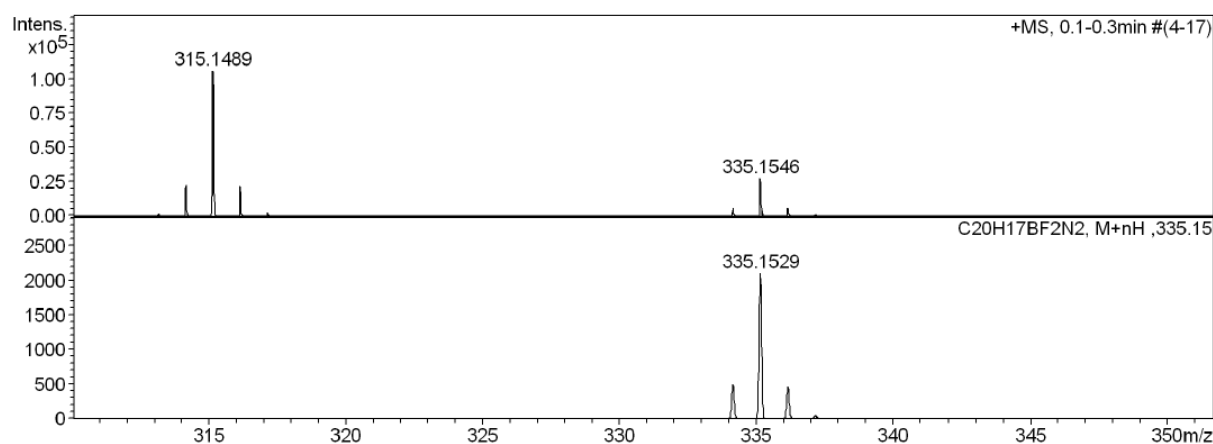
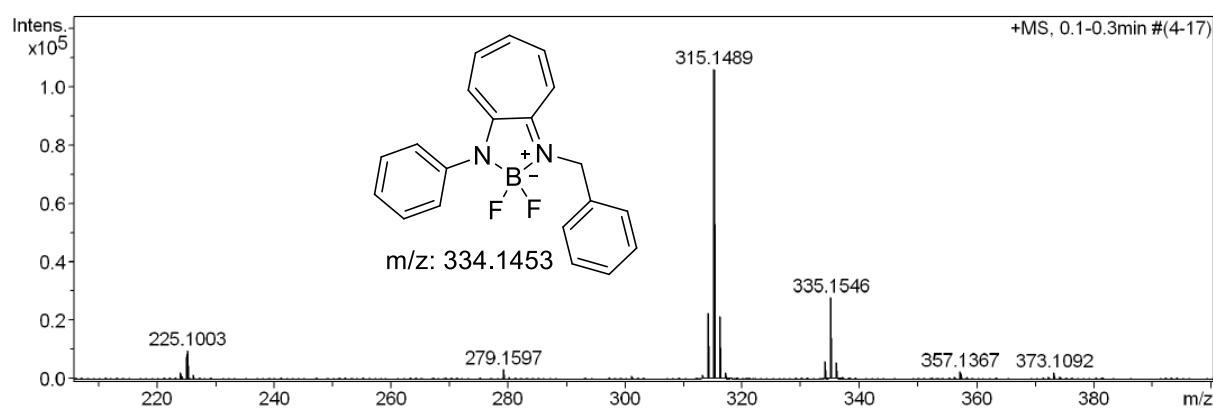
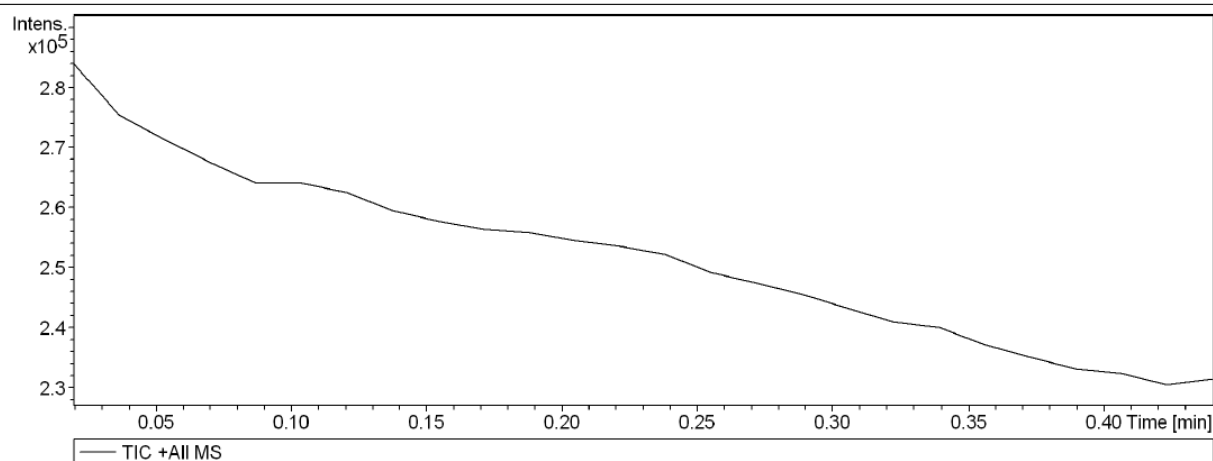


Figure A52. HRMS spectrum of boron complex **36b**

17. NMR ($^1\text{H}/^{13}\text{C}/^{11}\text{B}/^{19}\text{F}$) and HRMS of boron complex (**36c**):

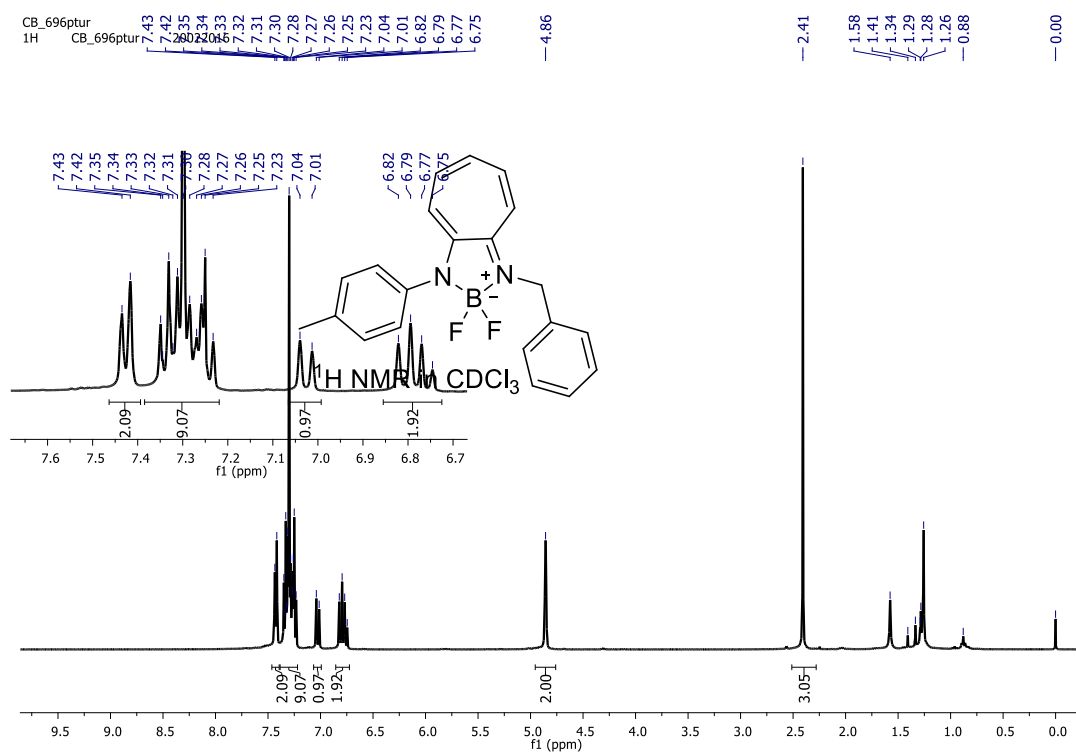


Figure A53. ^1H NMR spectrum of boron complex **36c**

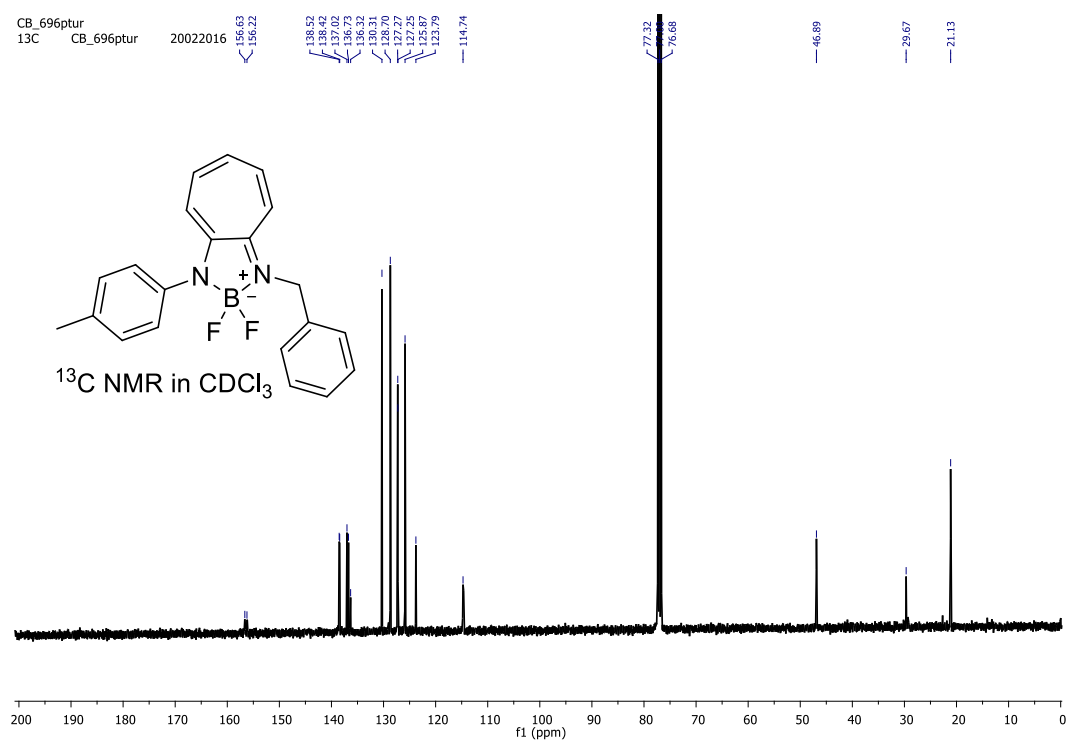


Figure A54. ^{13}C NMR spectrum of boron complex **36c**

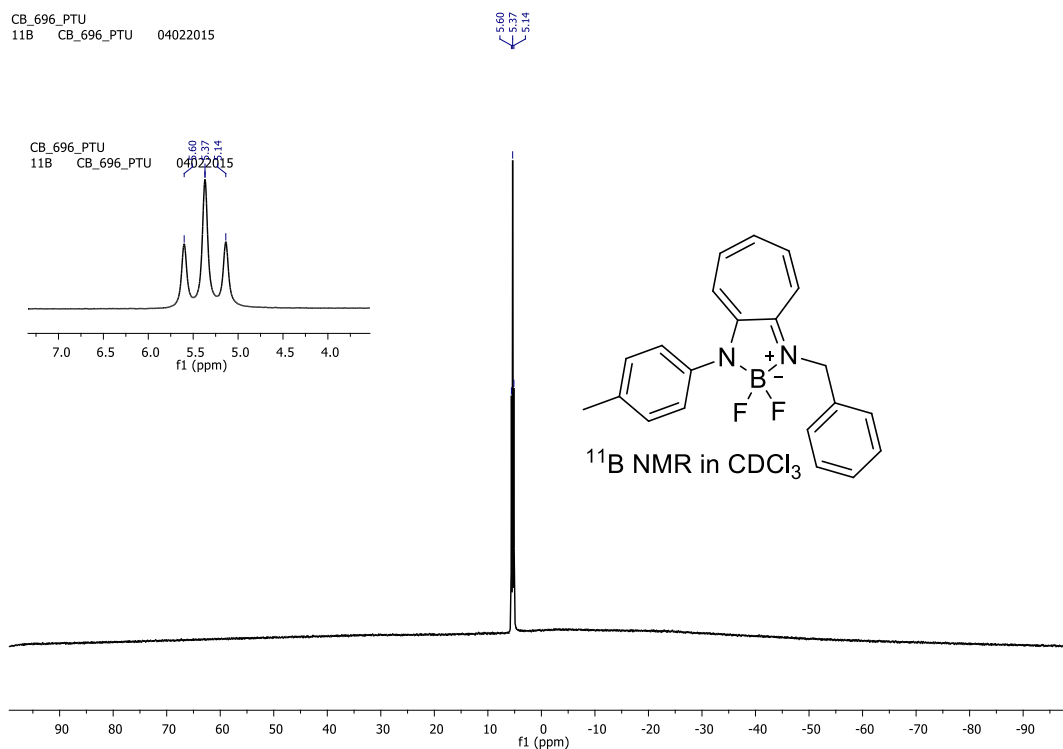


Figure A55. ^{11}B NMR spectrum of boron complex **36c**.

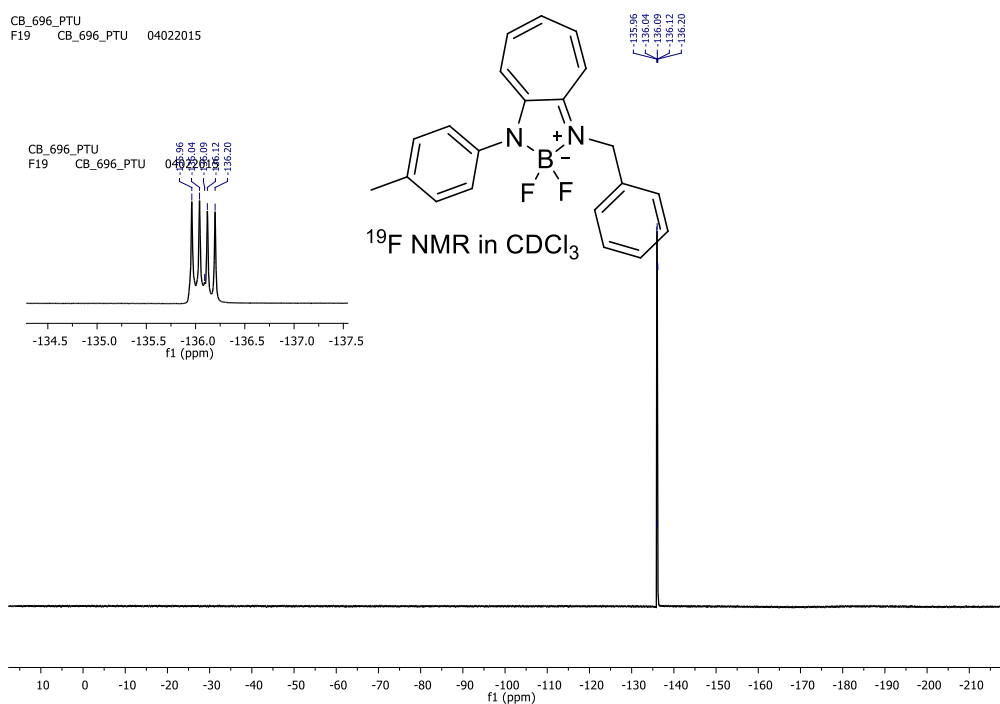


Figure A56. ^{19}F NMR spectrum of boron complex **36c**

Generic Display Report

Analysis Info

Analysis Name D:\Data\FEB-2015\NKS\11022015-NKS_CB_696PTU_1.d
Method Pos_tune_low.m
Sample Name NISER-LCMS
Comment

Acquisition Date 2/11/2015 11:35:02 AM

Operator NISER
Instrument microTOF-Q II

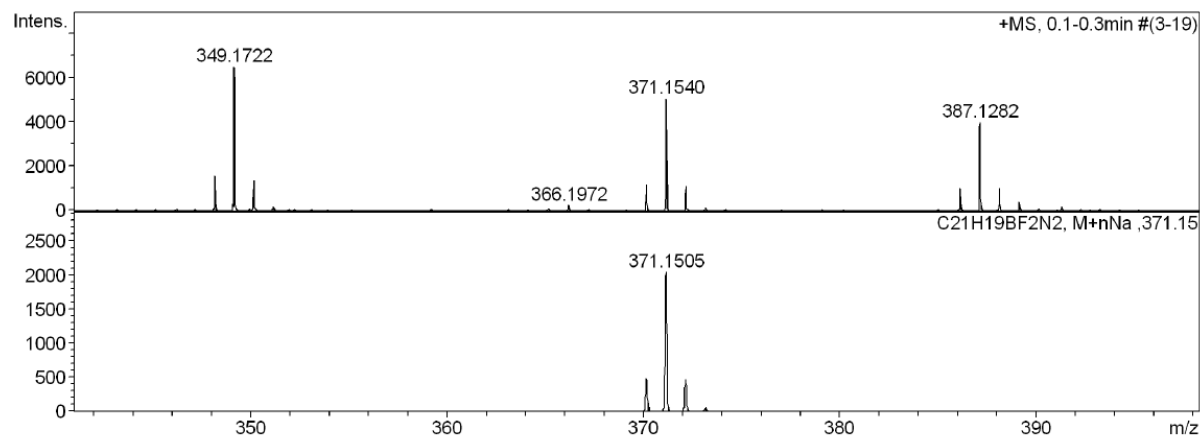
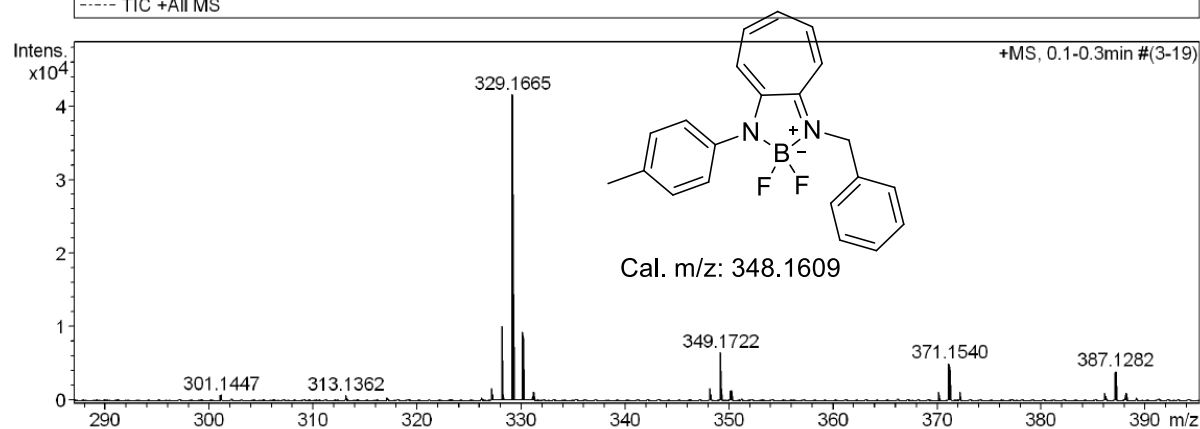
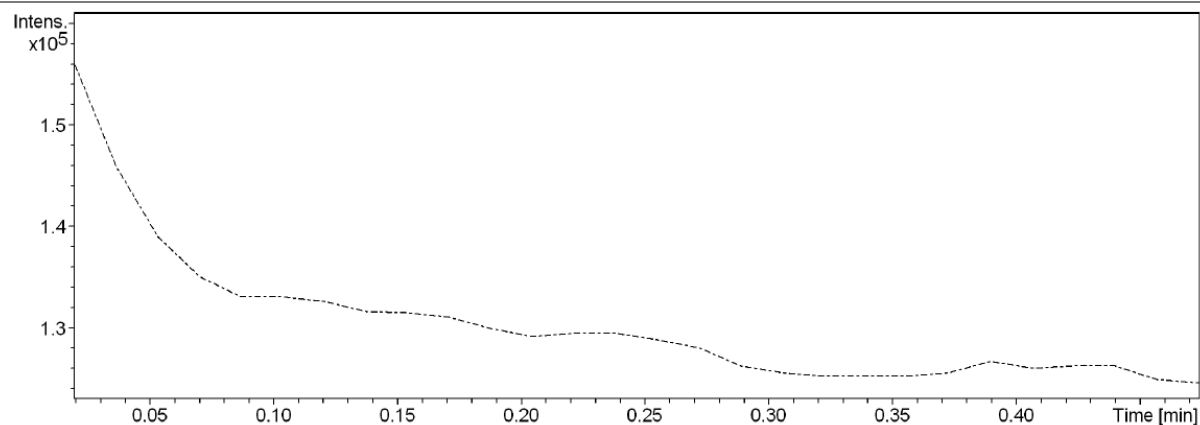


Figure A57. HRMS spectrum of boron complex **36c**

18.NMR ($^1\text{H}/^{13}\text{C}/^{11}\text{B}/^{19}\text{F}$) and HRMS of boron complex (**36d**)

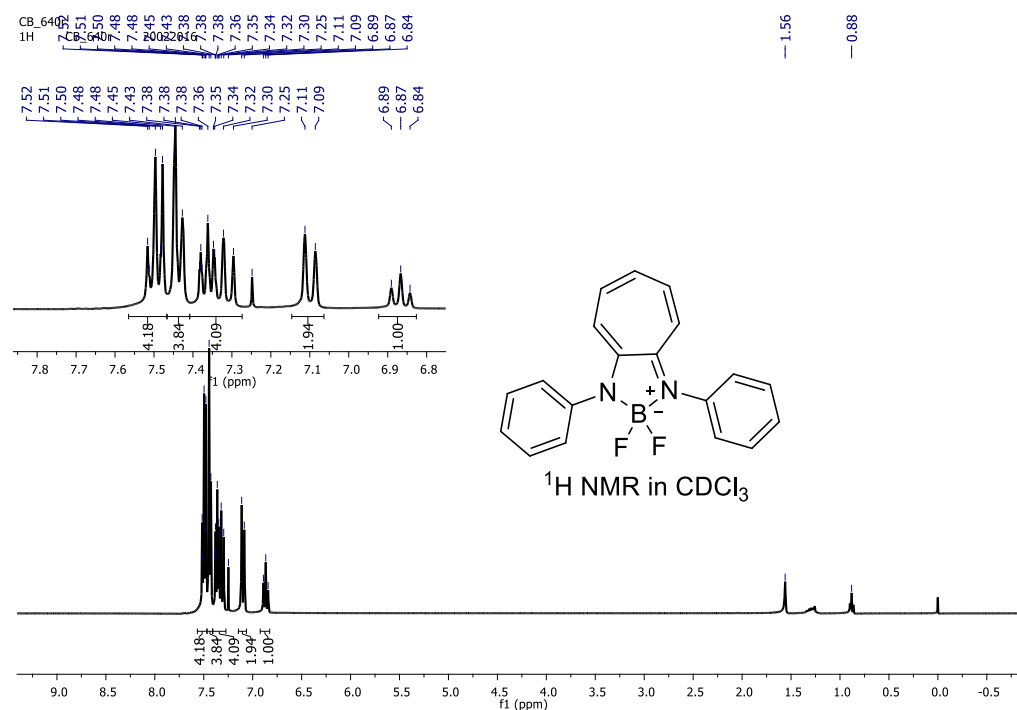


Figure A58. ^1H NMR spectrum boron complex **36d**

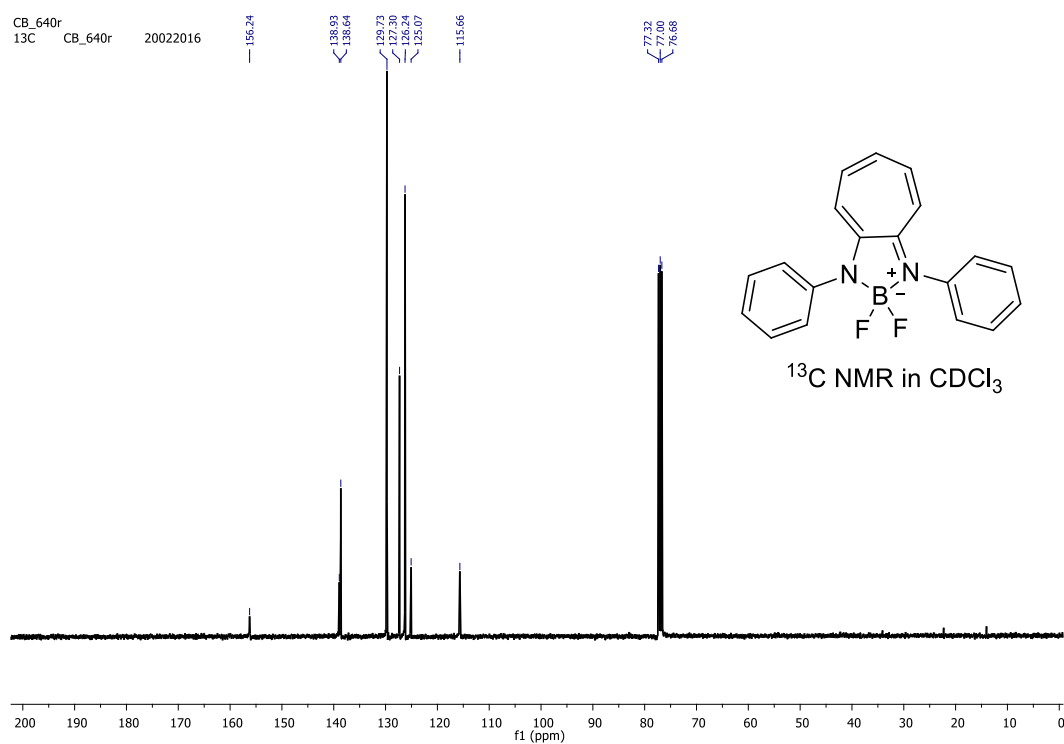


Figure A59. ^{13}C NMR spectrum of boron complex **36d**

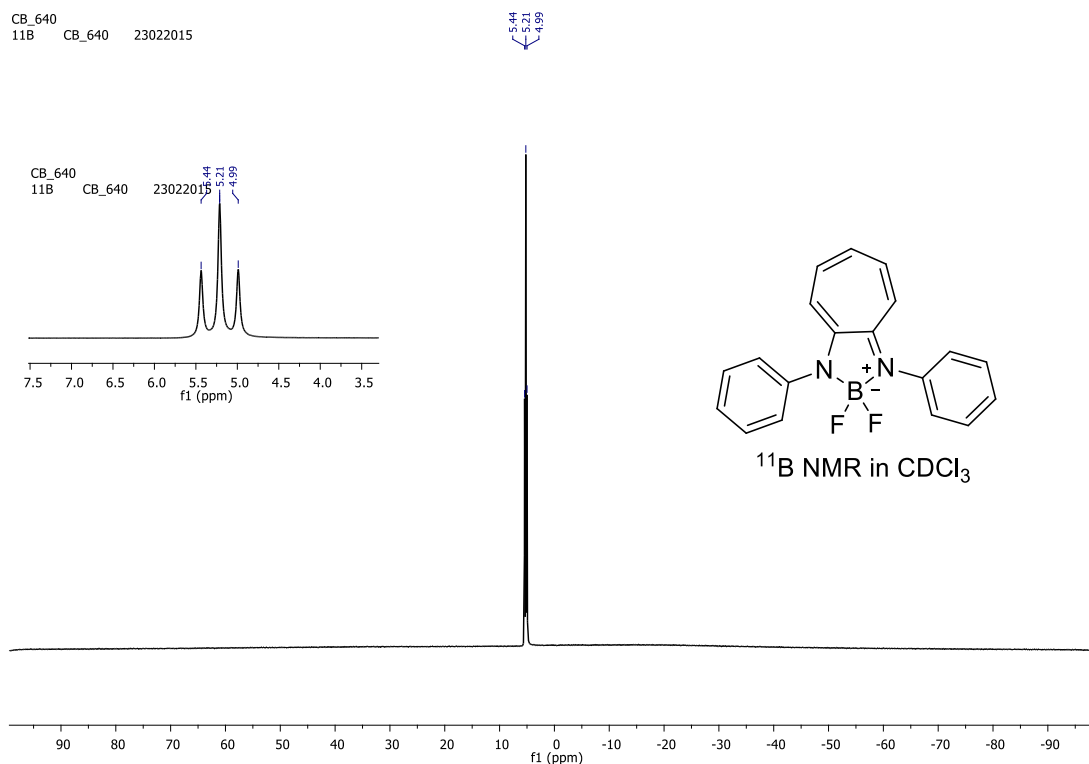


Figure A60. ¹¹B NMR spectrum of boron complex **36d**

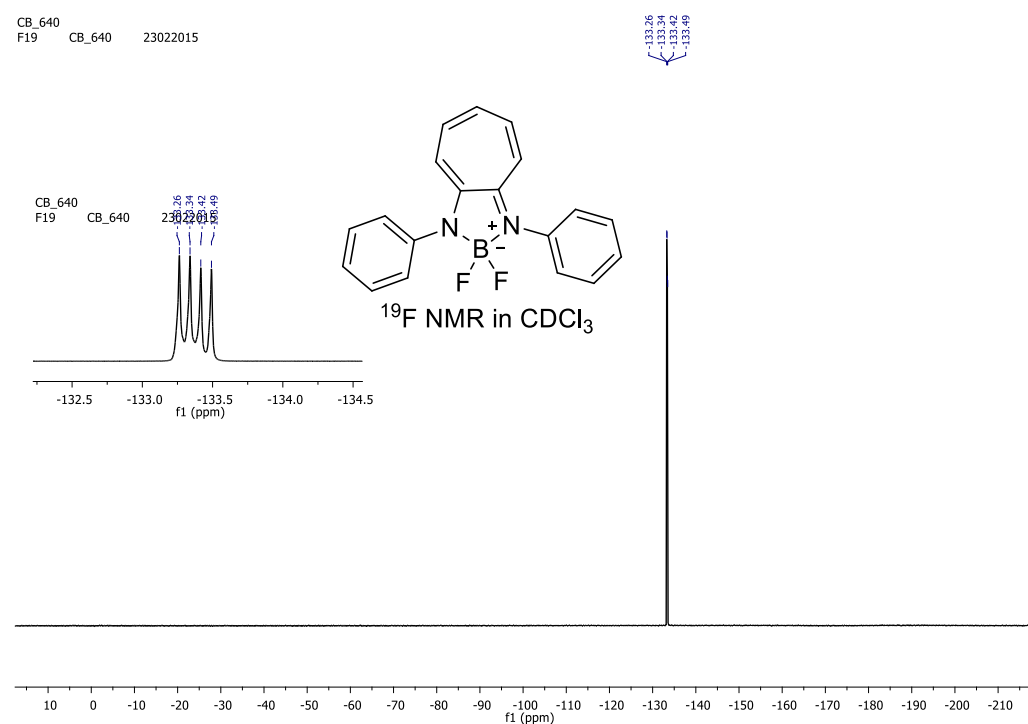


Figure A61. ¹⁹F NMR spectrum of boron complex **36d**

Generic Display Report

Analysis Info

Analysis Name D:\Data\FEB-2015\NKS\22022015_NKS_CB_640R.d

Method Pos_tune_low.m

Sample Name NISER-LCMS

Comment

Acquisition Date 2/23/2015 1:42:57 PM

Operator

NISER

Instrument

micrOTOF-Q II

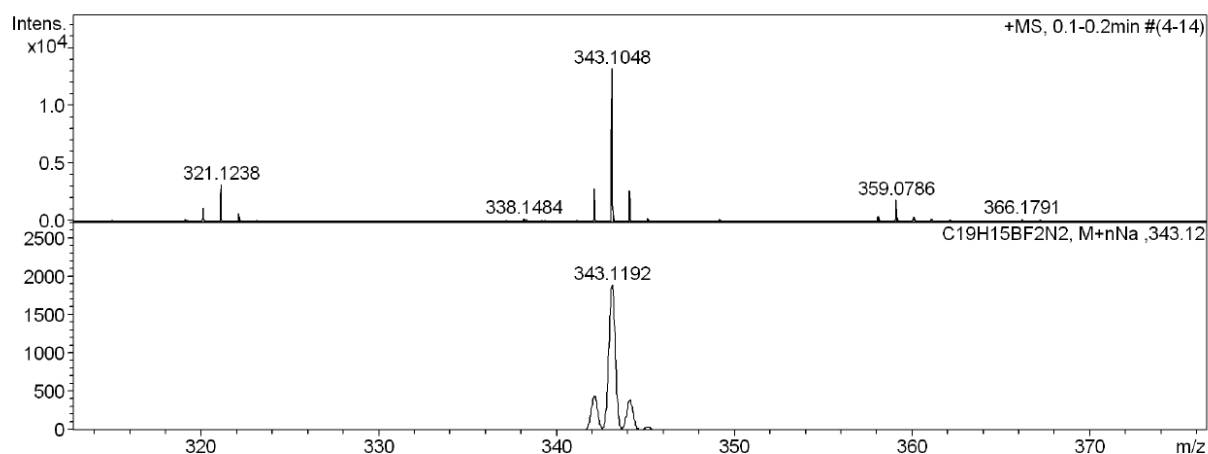
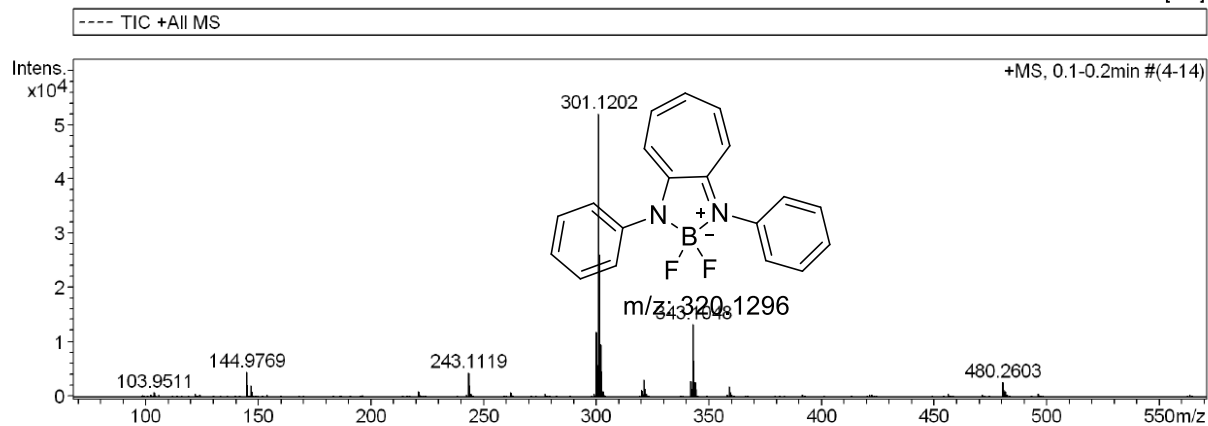
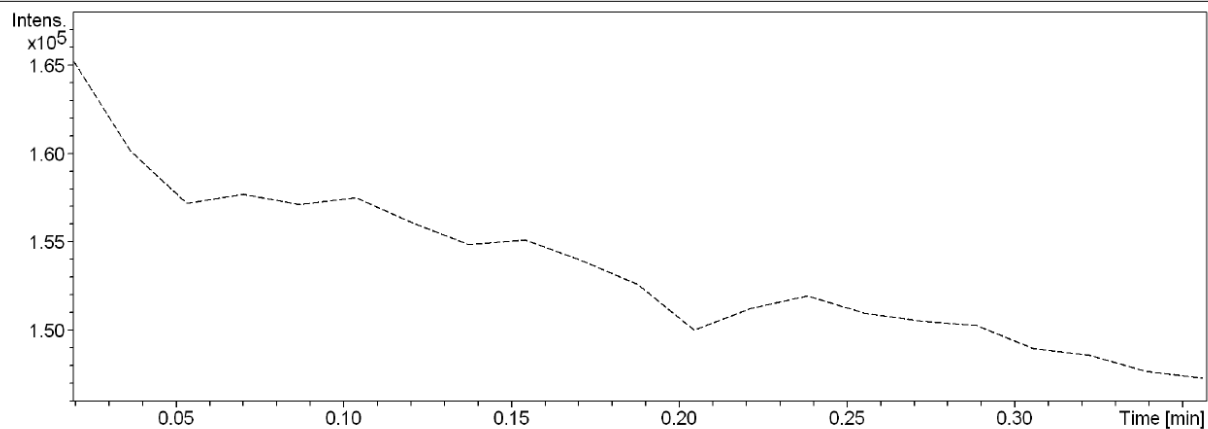


Figure A62. HRMS spectrum of boron aminotroponimine **36d**

19.NMR ($^1\text{H}/^{13}\text{C}/^{11}\text{B}/^{19}\text{F}$) and HRMS of boron complex (**36e**):

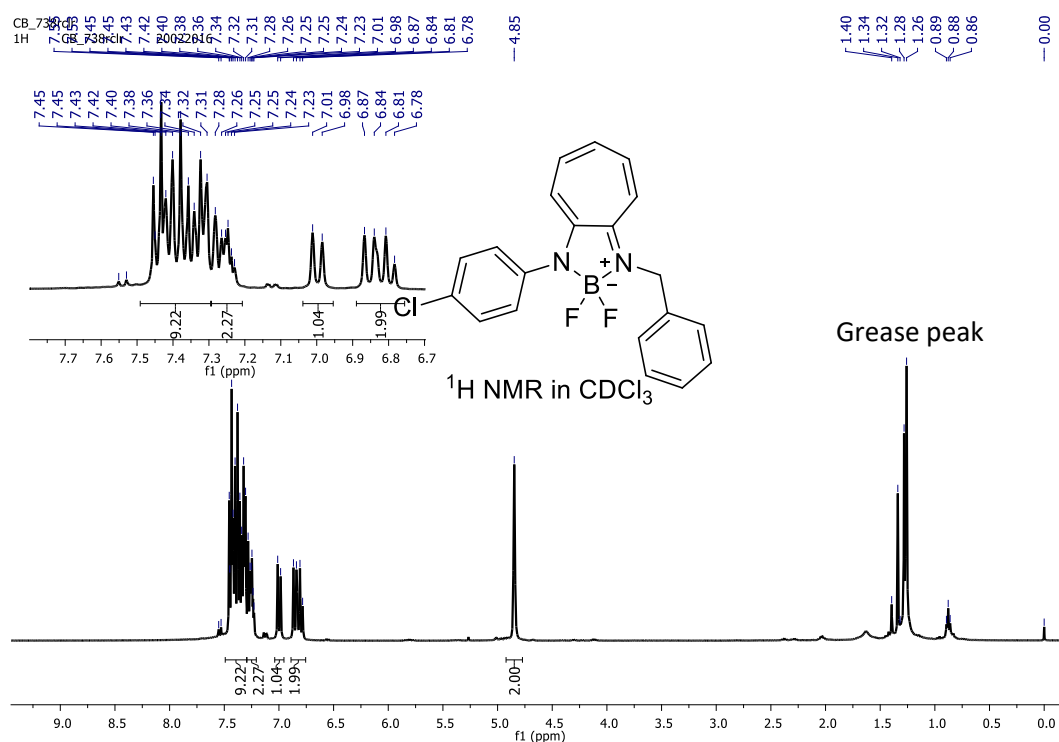


Figure A63. ^1H NMR spectrum of boron complex **36e**

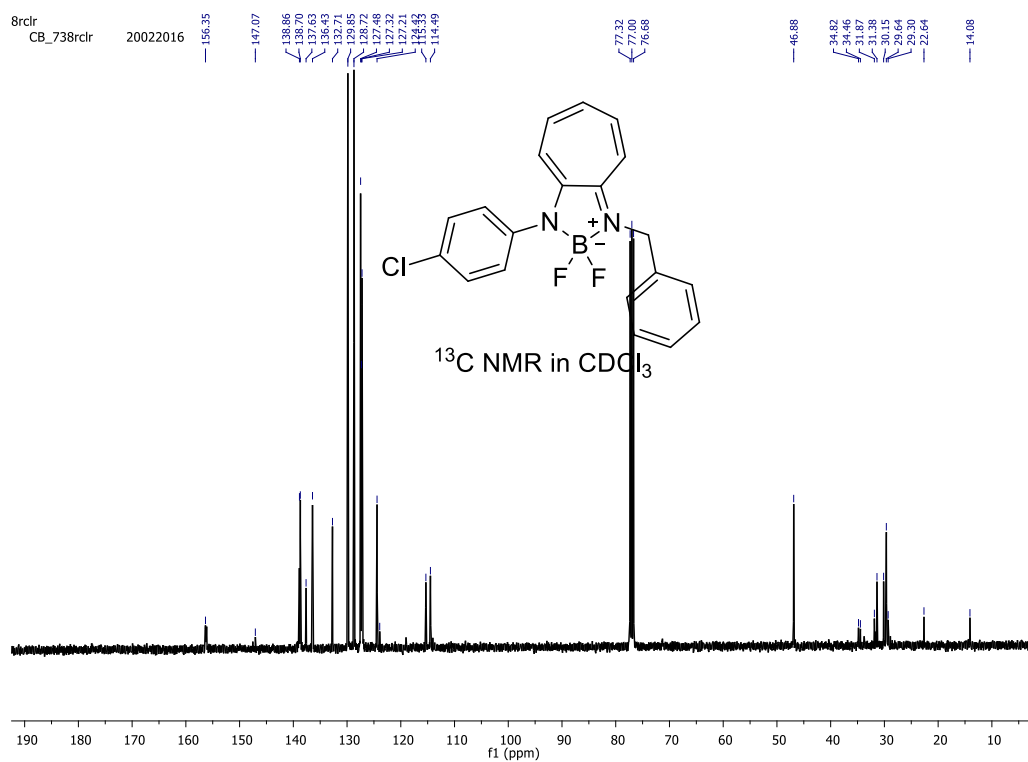


Figure A64. ^{13}C NMR spectrum of boron complex **36e**

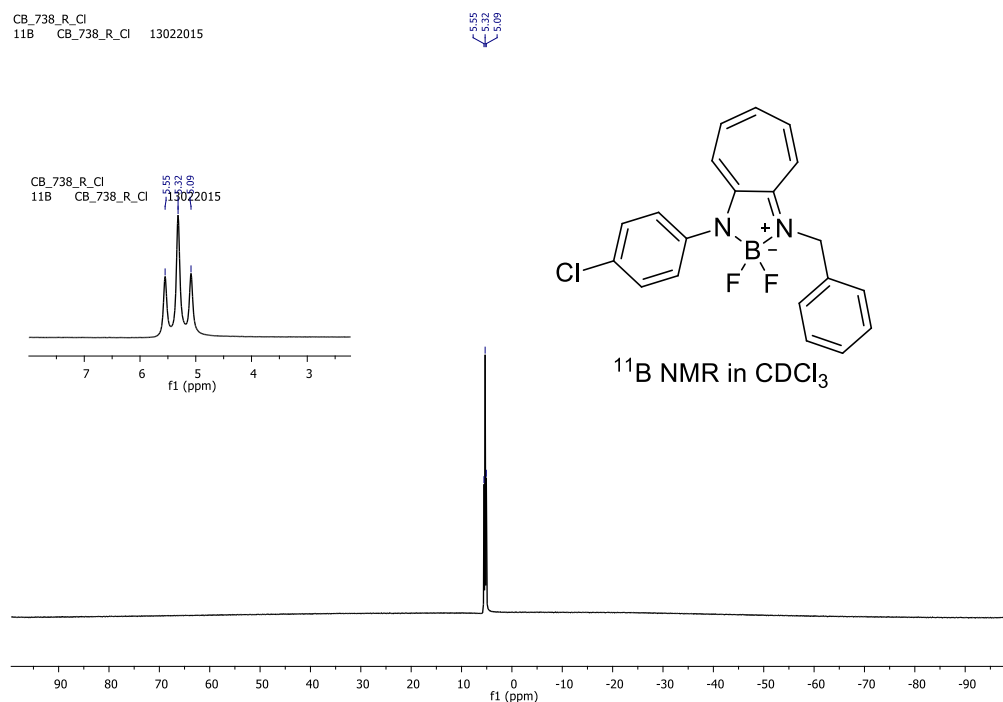


Figure A65. ¹¹B NMR spectrum of boron complex **36e**

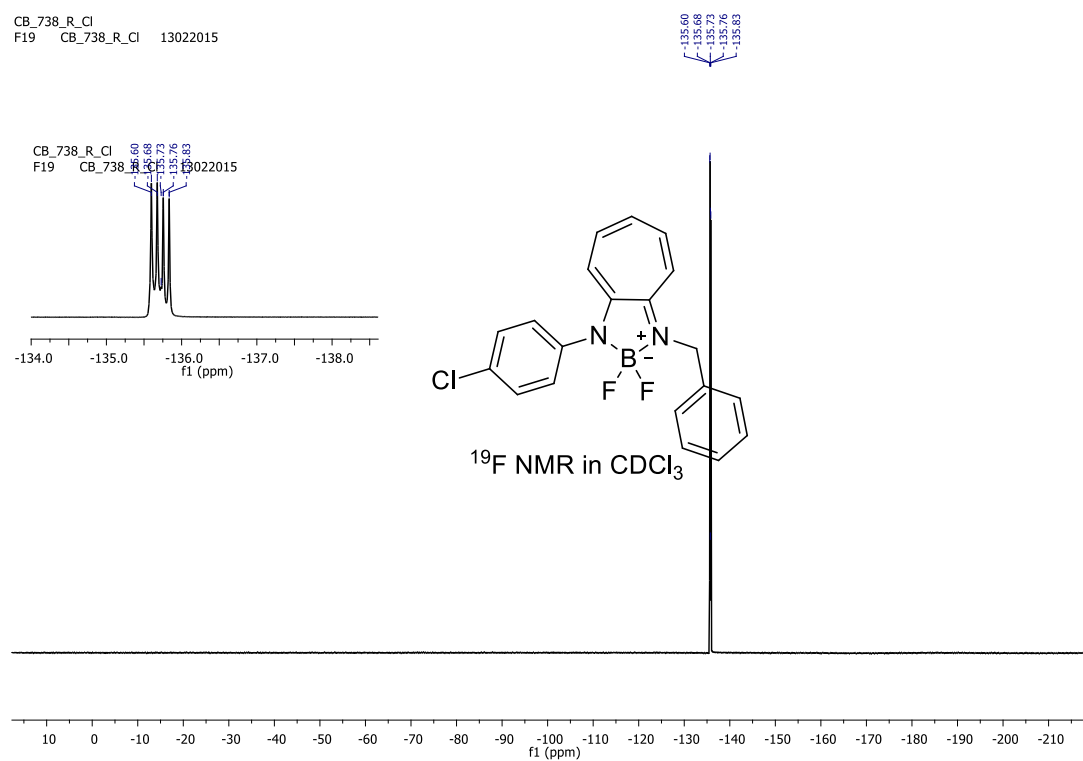


Figure A66. ¹⁹F NMR spectrum of boron complex **36e**

Generic Display Report

Analysis Info

Analysis Name D:\Data\FEB-2015\NKS\11022015-NKS_CB_7384_CL_1.d
Method Pos_tune_low.m
Sample Name NISER-LCMS
Comment

Acquisition Date 2/11/2015 11:26:55 AM

Operator NISER
Instrument micrOTOF-Q II

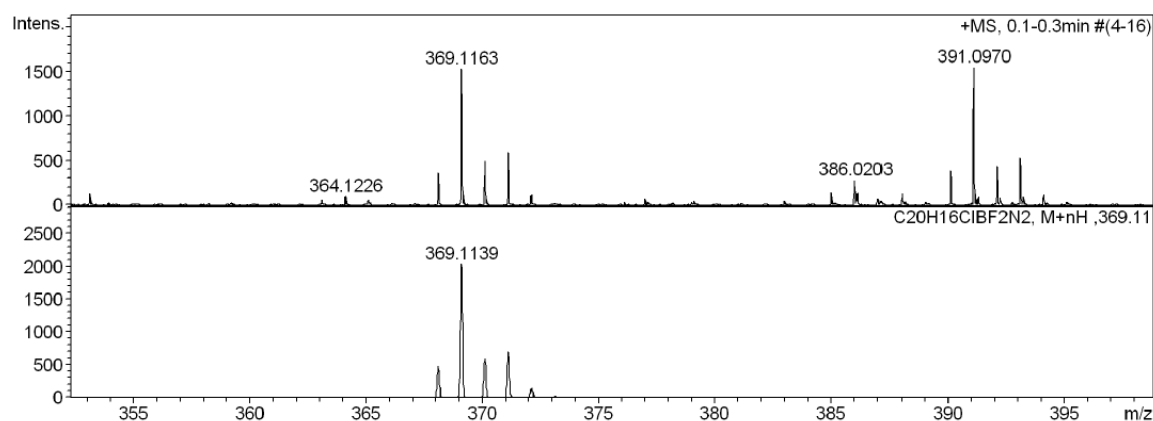
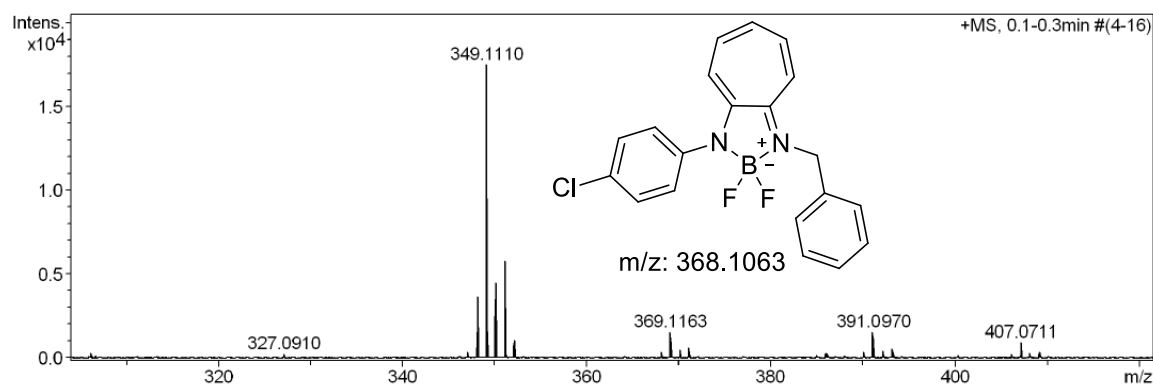
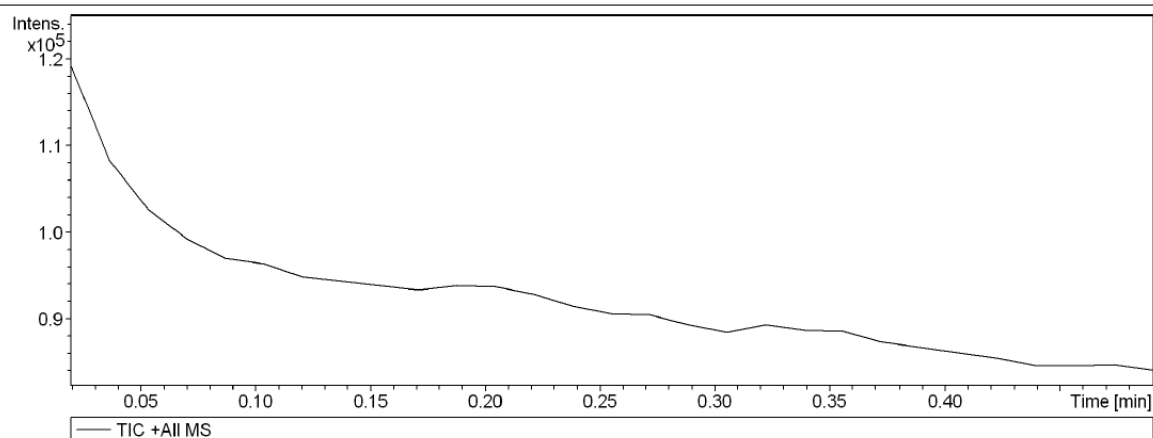


Figure A67. HRMS spectrum of boron complex **36e**

20. NMR ($^1\text{H}/^{13}\text{C}/^{11}\text{B}/^{19}\text{F}$) and HRMS of boron complex (**36f**)

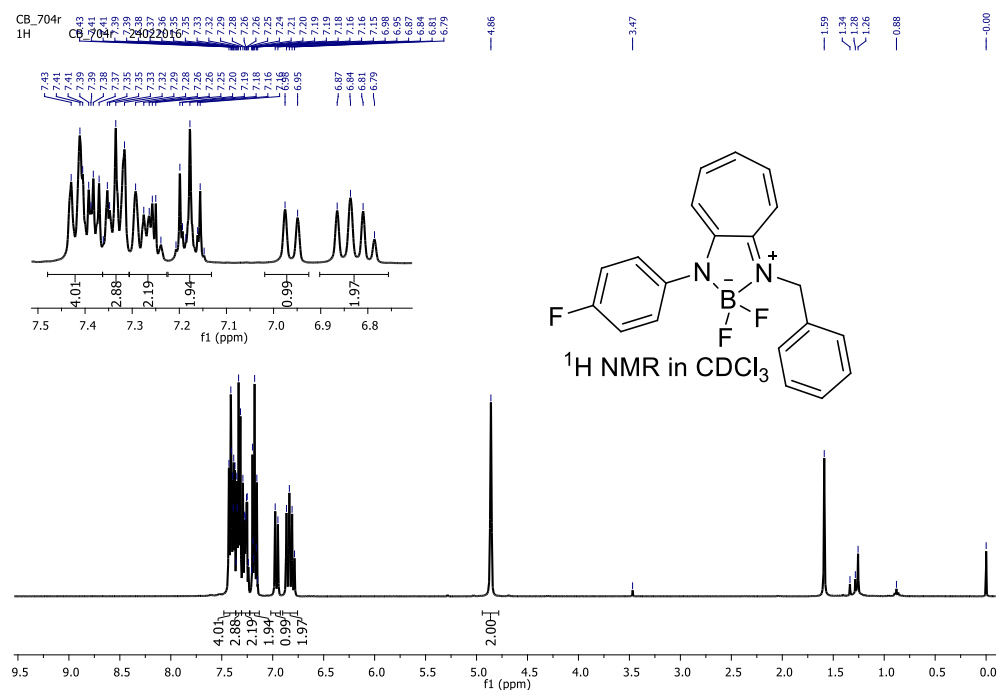


Figure A68. ^1H NMR spectrum of boron complex **36f**

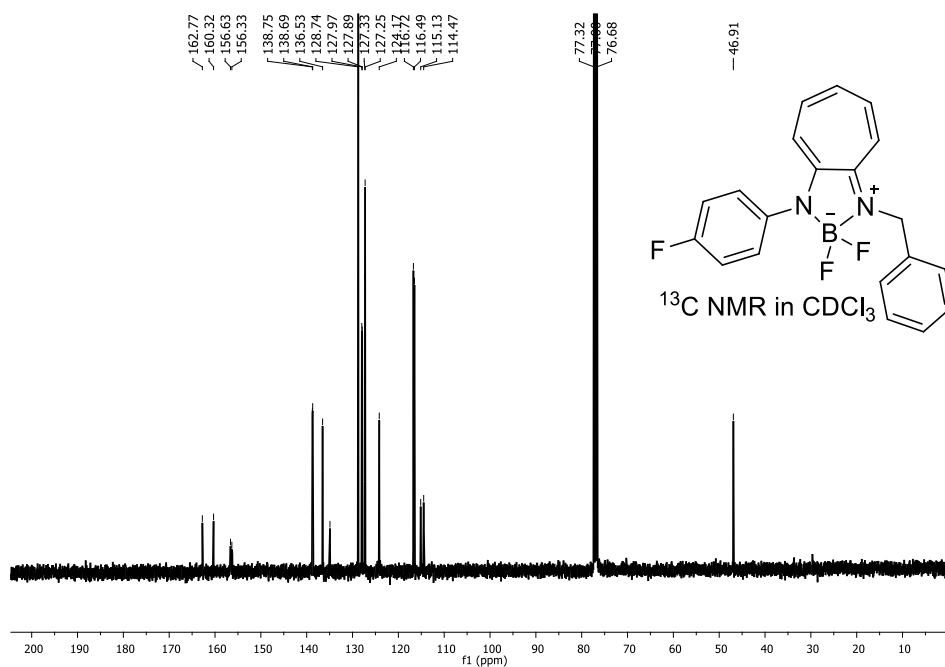


Figure A69. ^{13}C NMR spectrum of boron complex **36f**

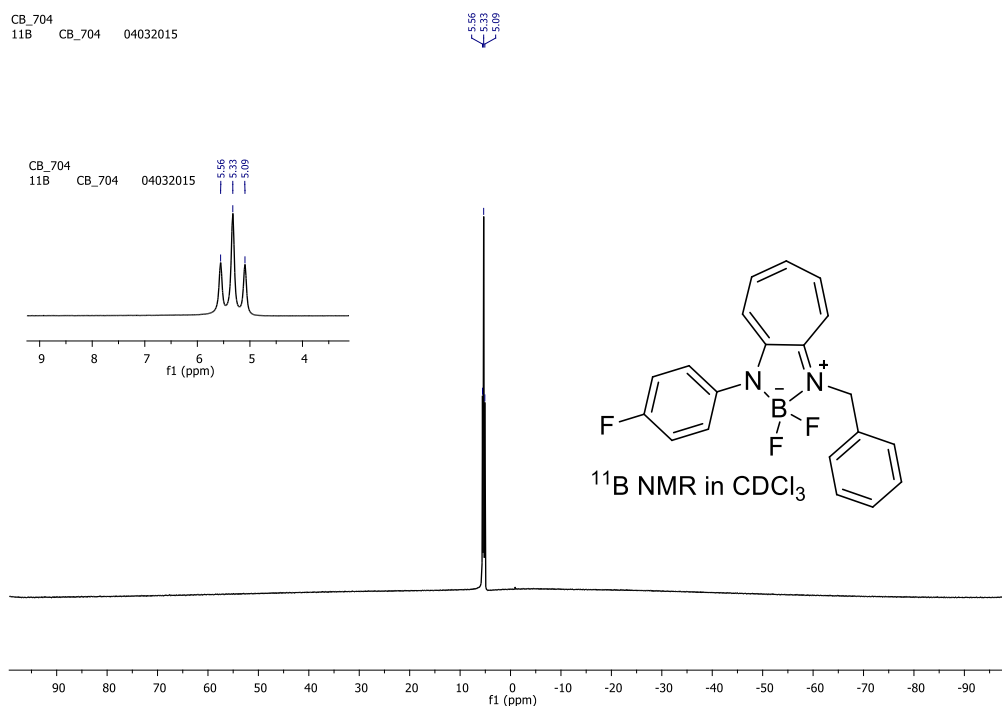


Figure A70. ¹¹B NMR spectrum of boron complex **36f**

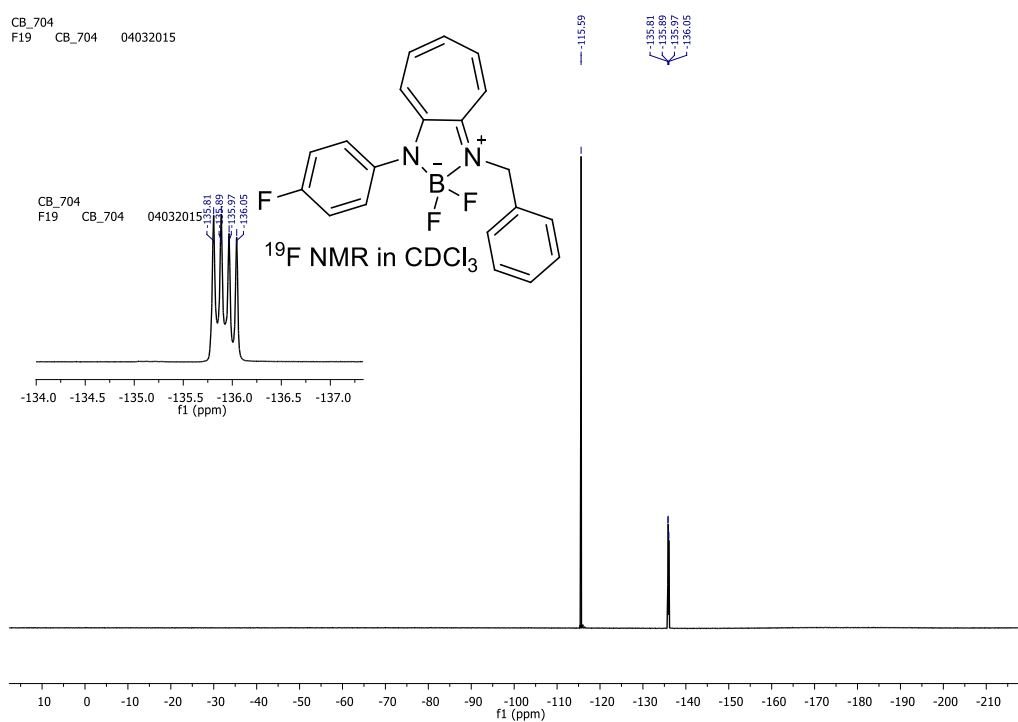


Figure A71. ¹⁹F NMR spectrum of boron complex **36f**

Generic Display Report

Analysis Info

Analysis Name D:\Data\FEB-2015\NKS\27022015_NKS_CB_704.d
Method Pos_tune_low.m
Sample Name NISER-LCMS
Comment

Acquisition Date 2/27/2015 9:46:31 PM

Operator NISER
Instrument micrOTOF-Q II

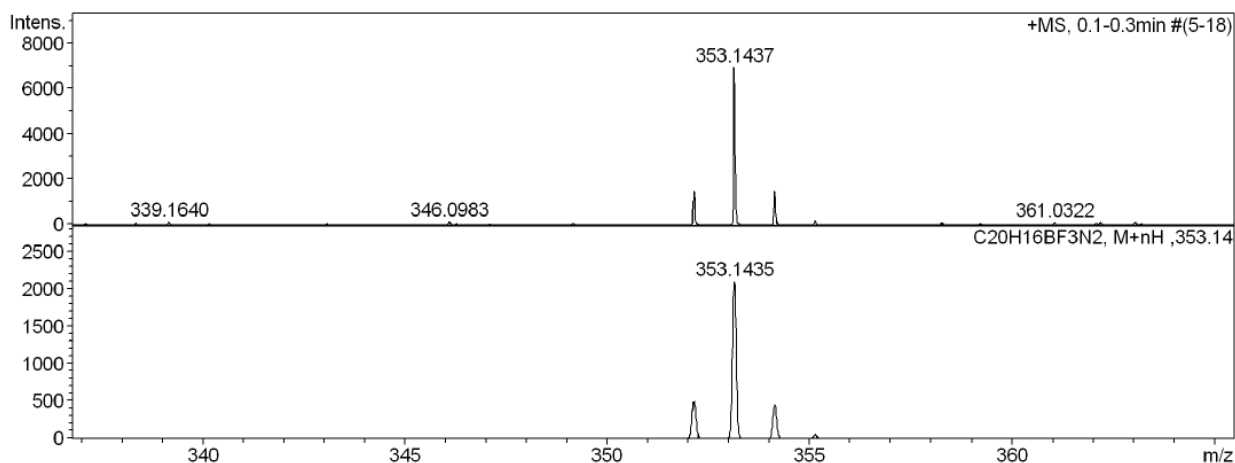
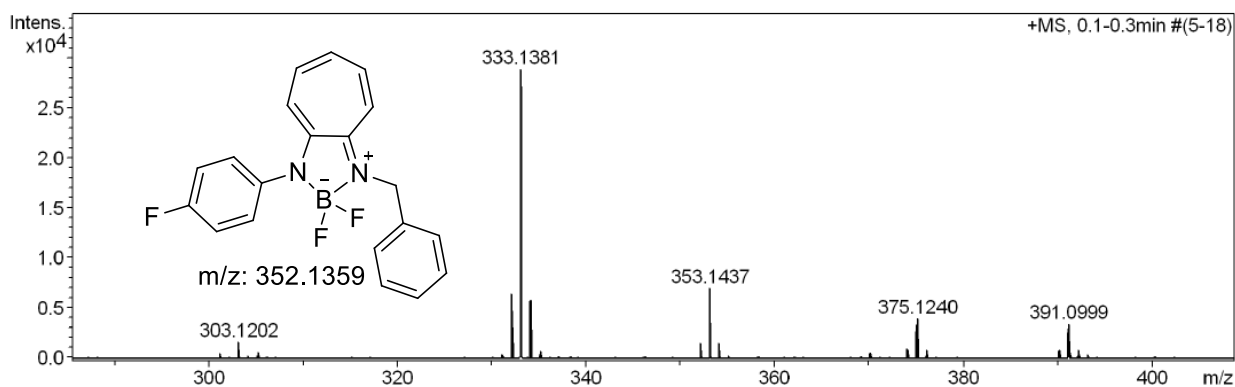
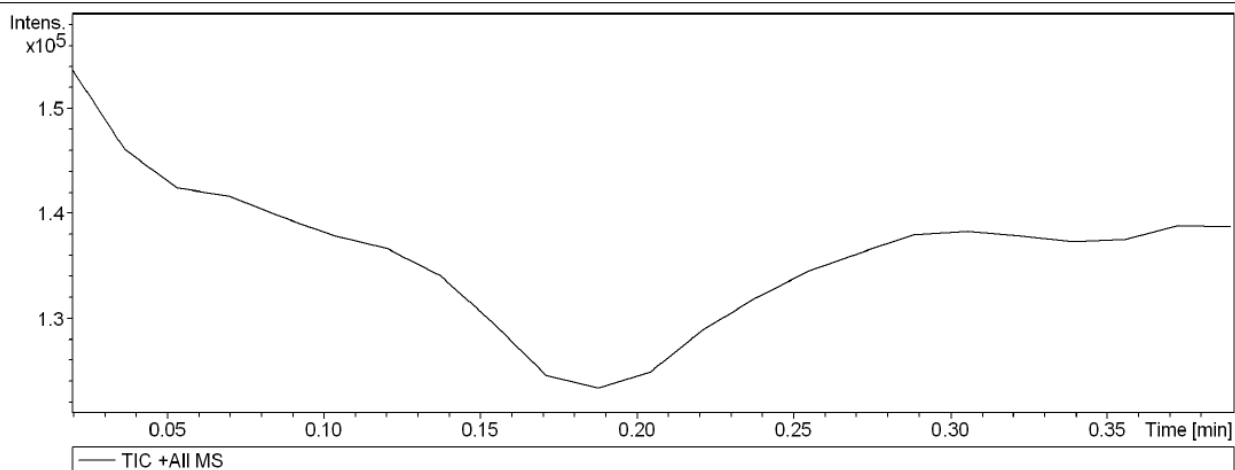


Figure A72. HRMS spectrum of boron complex **36f**

21. NMR ($^1\text{H}/^{13}\text{C}/^{11}\text{B}/^{19}\text{F}$) and HRMS of boron complex (**36g**)

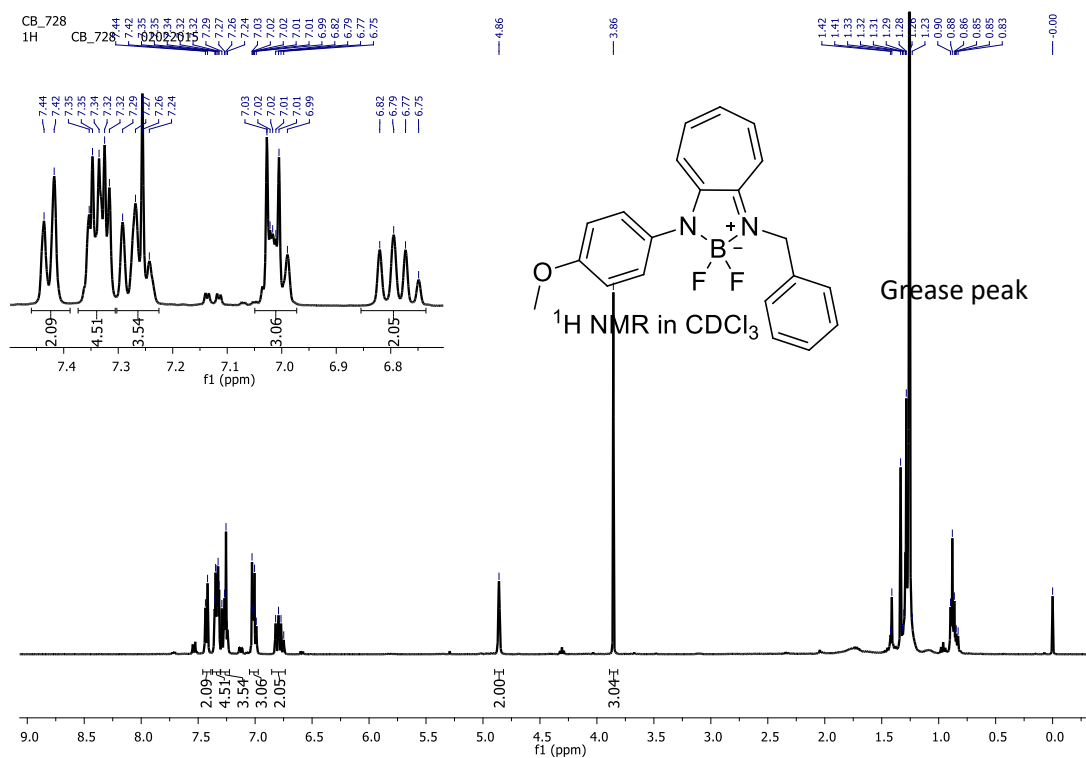


Figure A73. ^1H NMR spectrum of boron complex **36g**

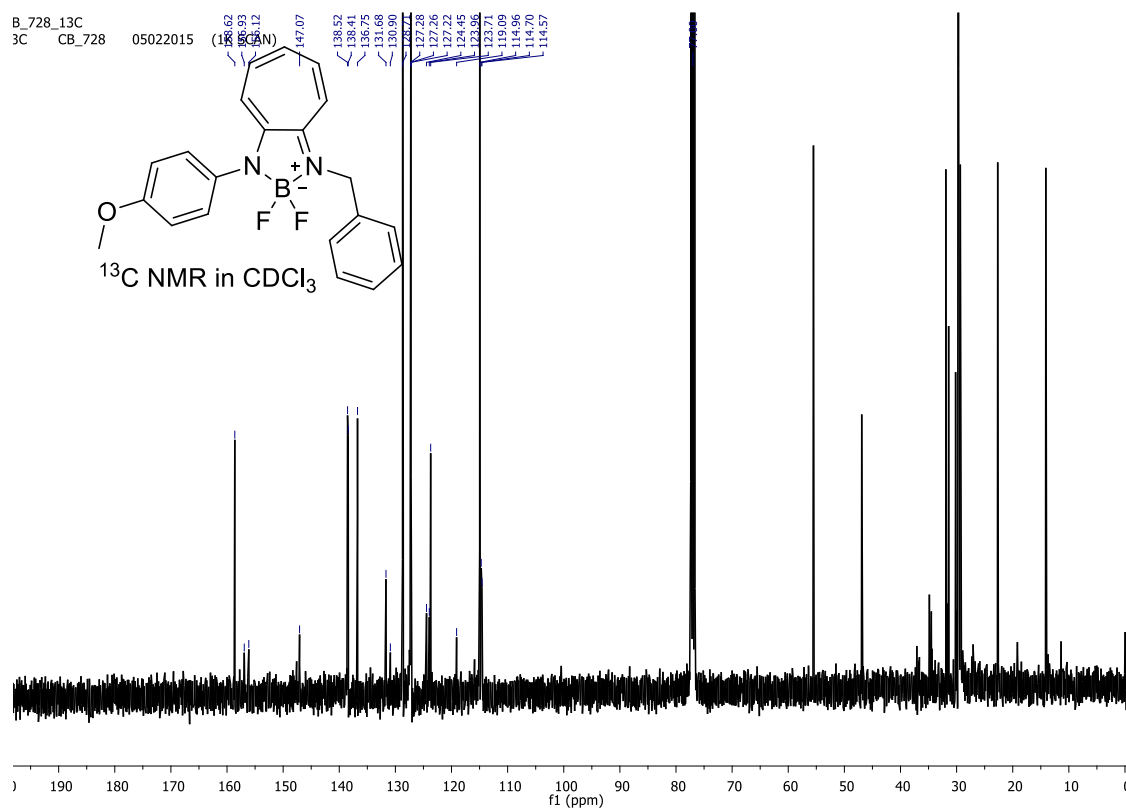


Figure A74. ^{13}C NMR spectrum of boron complex **36g**

3.728
1B CB_728 02022015

5.56
5.32
5.09

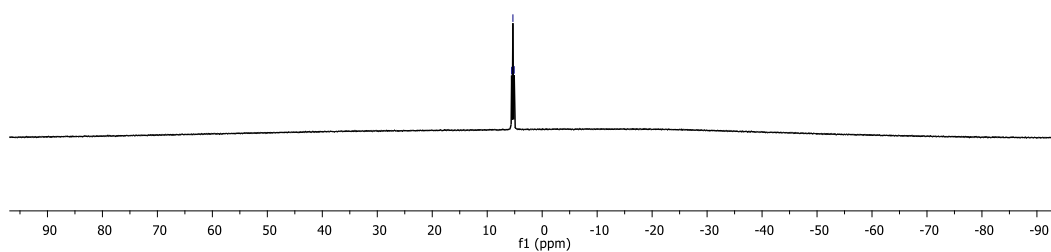
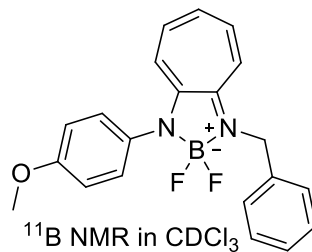
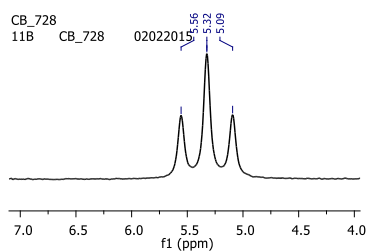


Figure A75. ^{11}B NMR spectrum boron complex **36g**

CB_728
F19 CB_728 02022015

-136.12
-136.20
-136.36
-136.36

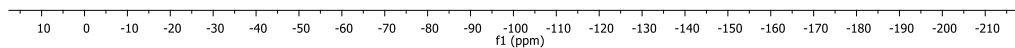
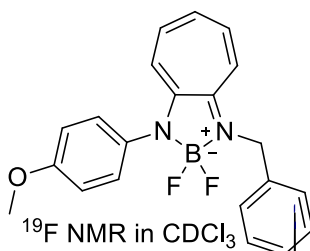
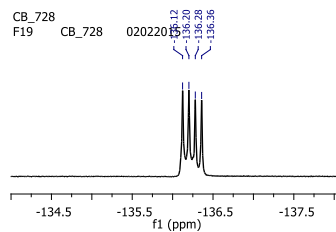


Figure A76. ^{19}F NMR spectrum of boron complex **36g**

Generic Display Report

Analysis Info

Analysis Name D:\Data\JAN-2015\NKS\03112015_NKS_CB_728B.d
Method Pso_tune_wide.m
Sample Name NISER-LCMS
Comment

Acquisition Date 2/2/2015 9:19:44 AM

Operator NISER
Instrument micrOTOF-Q II

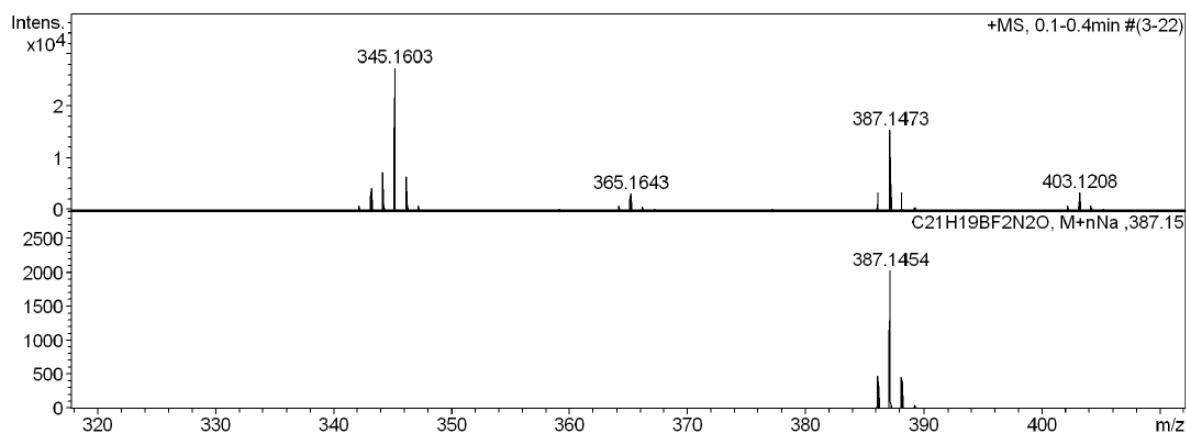
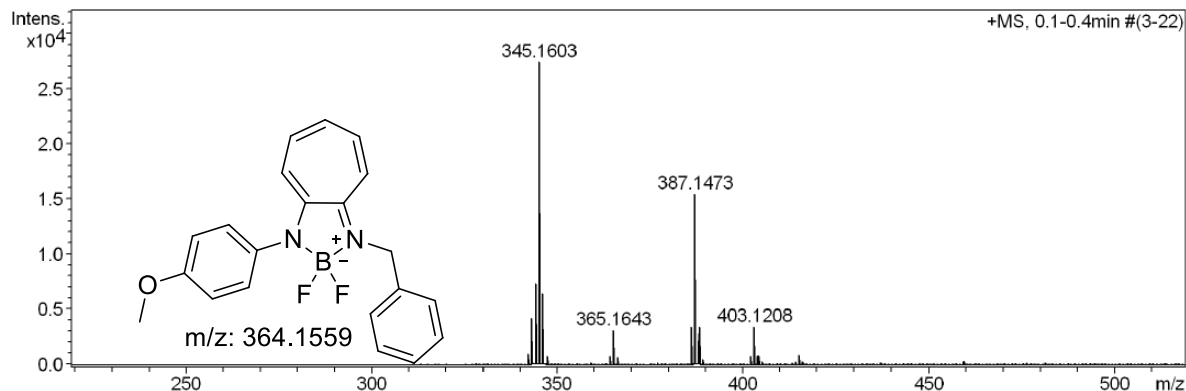
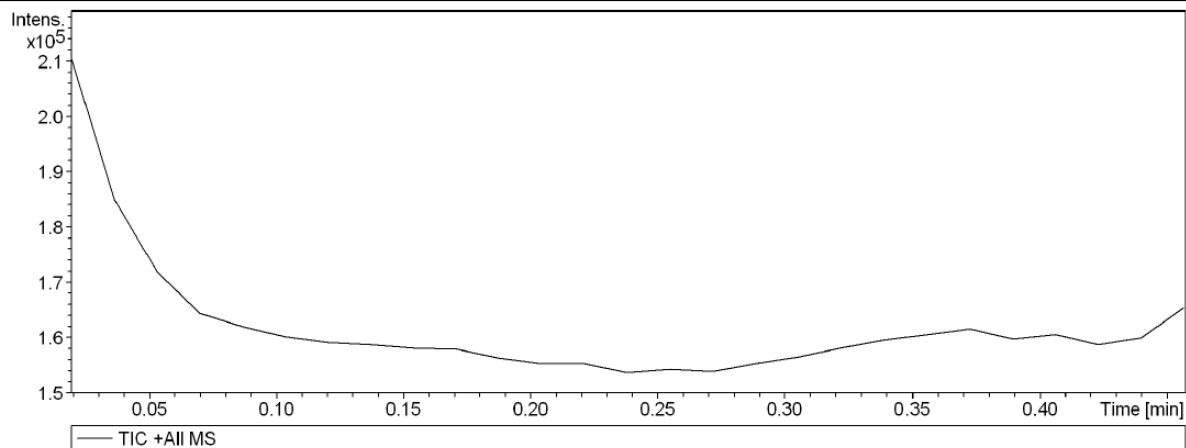


Figure A77. HRMS spectrum of boron complex **36g**.

22.NMR ($^1\text{H}/^{13}\text{C}/^{11}\text{B}/^{19}\text{F}$) and HRMS of boron complex (**36h**):

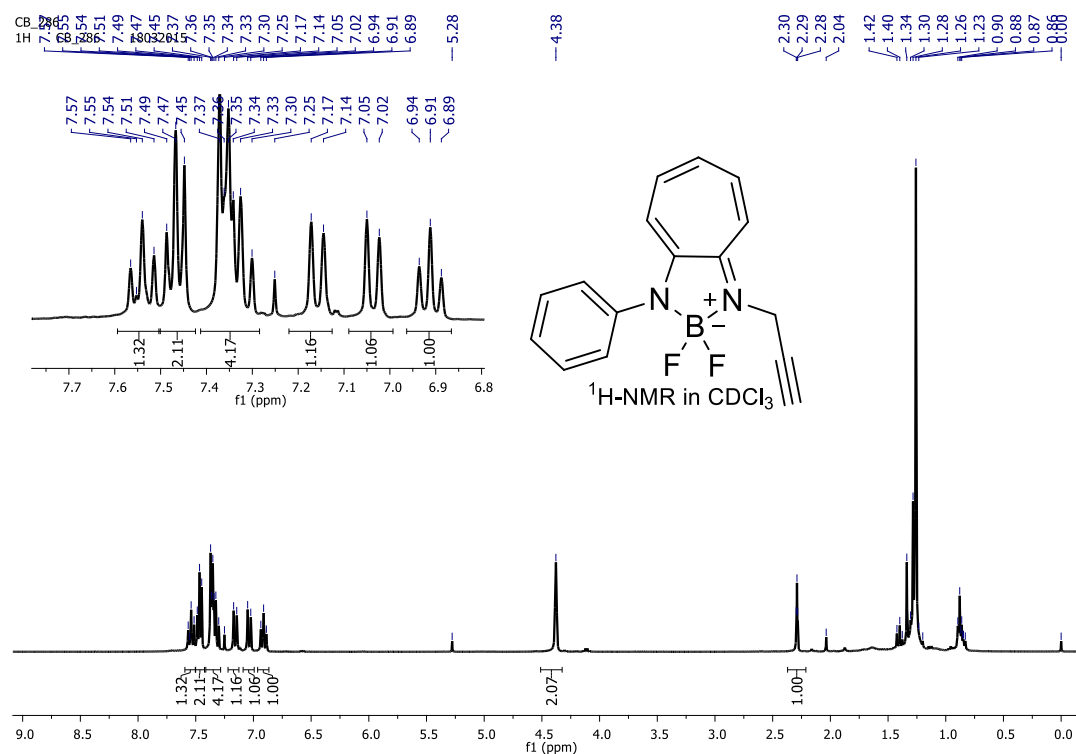


Figure A78. ^1H NMR spectrum of boron complex **36h**

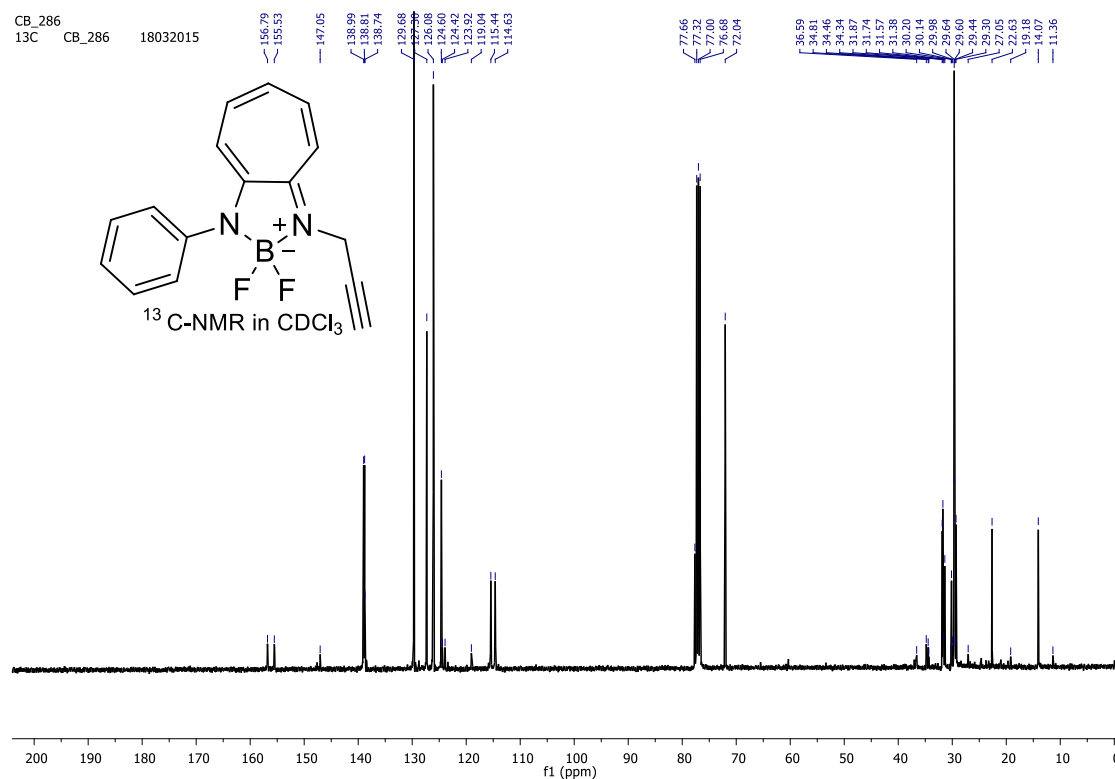


Figure A79. ^{13}C NMR spectrum of boron complex **36h**

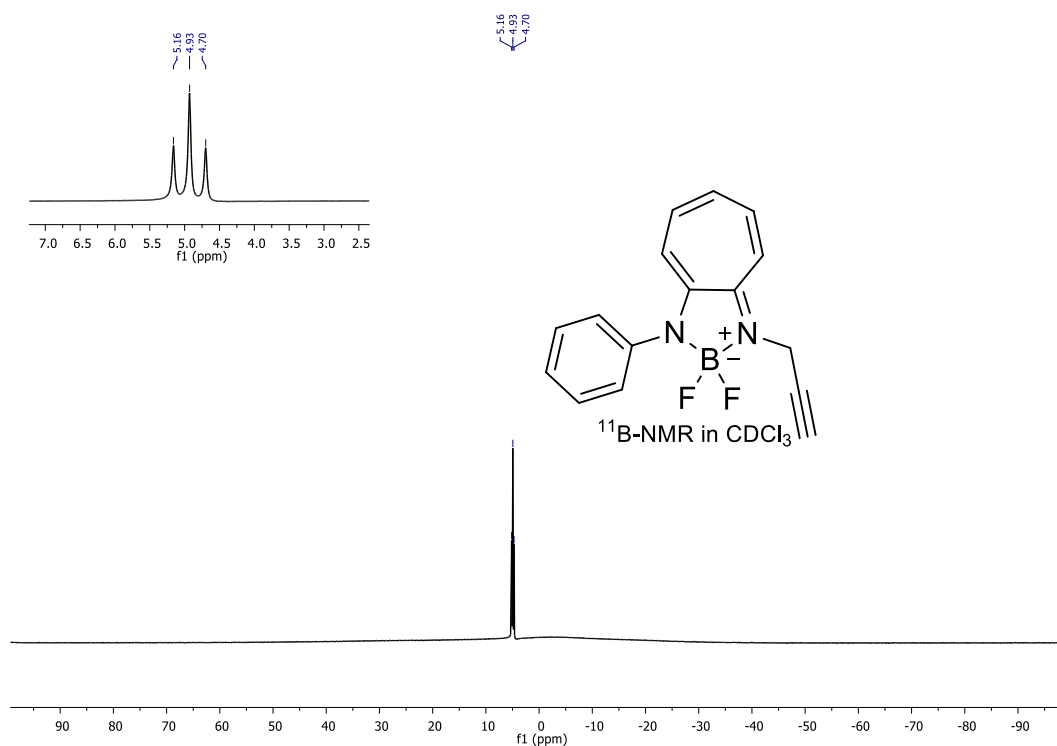


Figure A80. ^{13}C NMR spectrum of boron complex **36h**

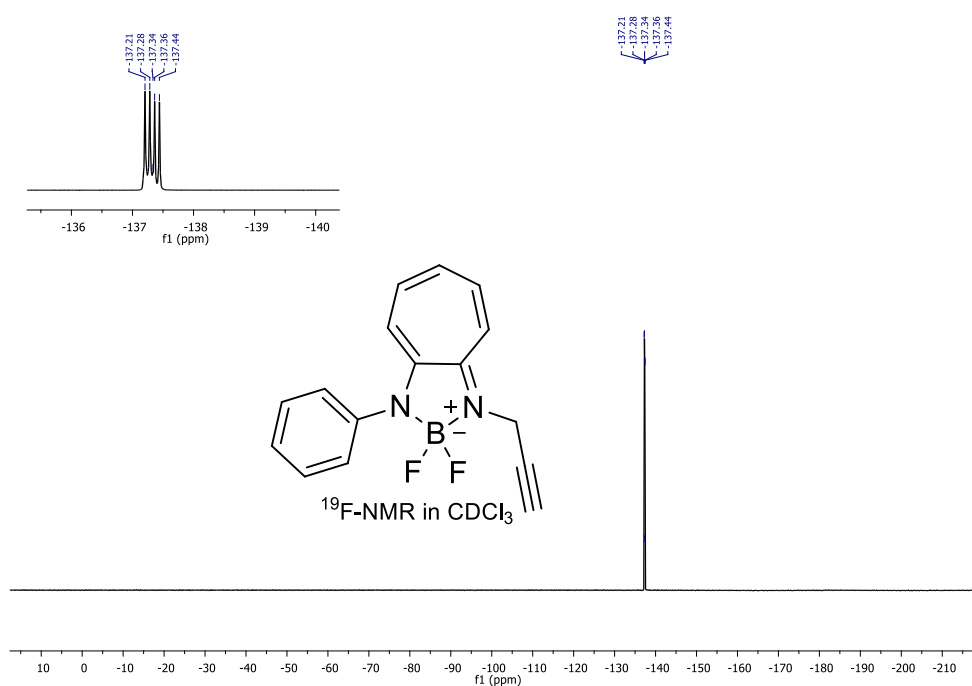


Figure A81. ^{19}F NMR spectrum of boron complex **36h**

Generic Display Report

Analysis Info

Analysis Name D:\Data\JUNE-2015\NKS\13062015_NKS_CB_286.d
Method Pos_tune_low.m
Sample Name NISER-LCMS
Comment

Acquisition Date 6/13/2015 7:26:40 PM

Operator AMIT
Instrument micrOTOF-Q II

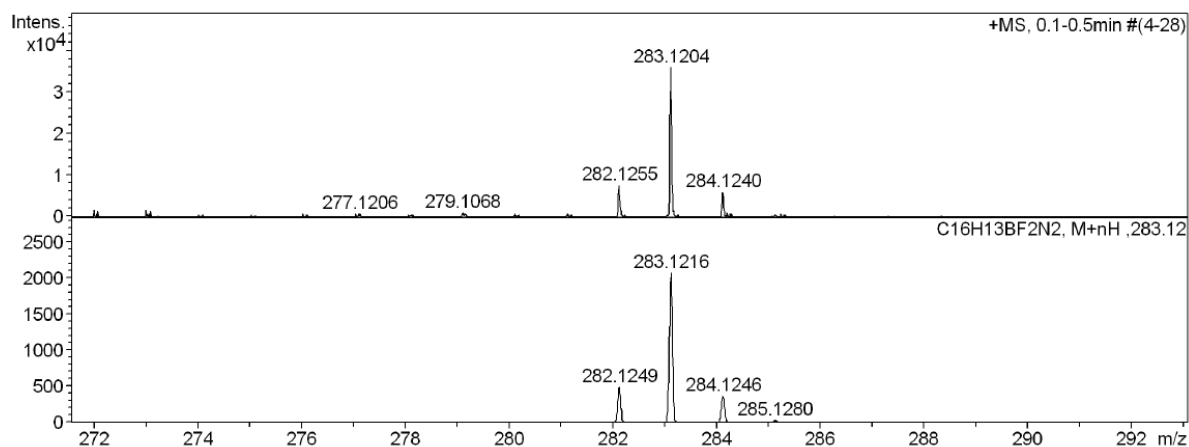
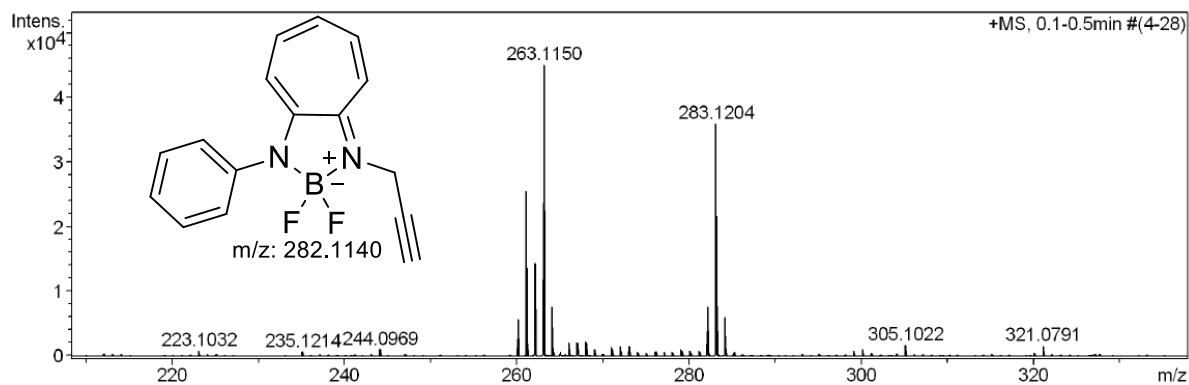
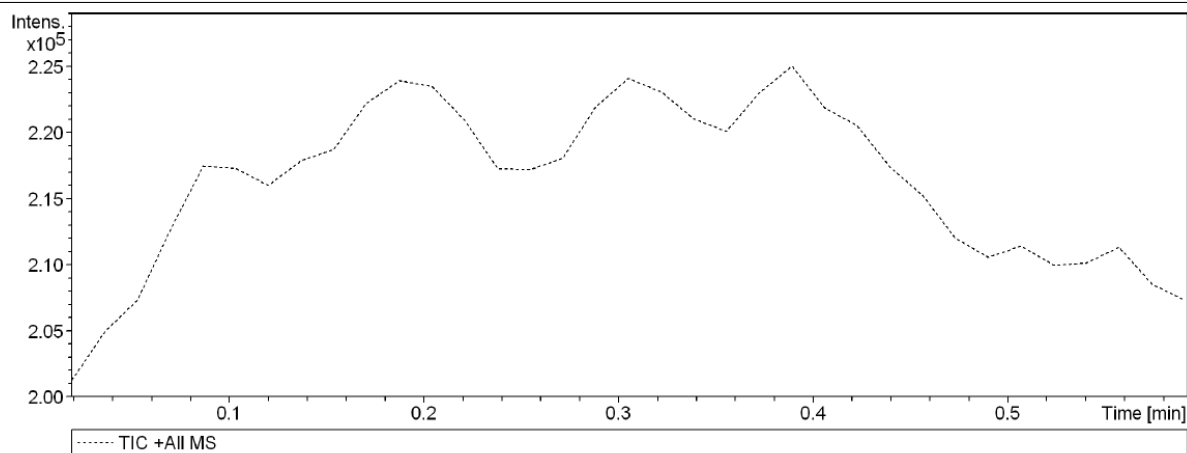


Figure A82. HRMS spectrum of boron complex **36h**

23.NMR ($^1\text{H}/^{13}\text{C}/^{11}\text{B}/^{19}\text{F}$) and HRMS of boron complex (**36i**):

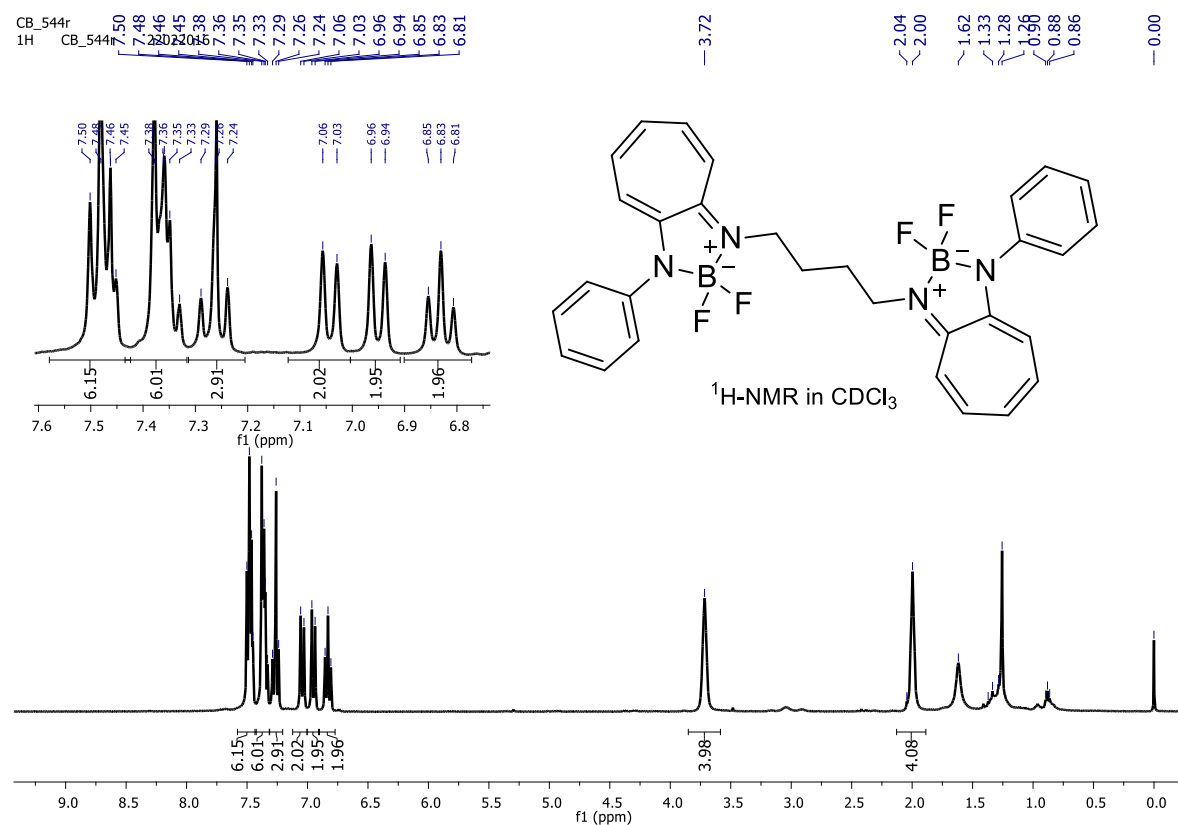


Figure A83. ^1H NMR spectrum of boron complex **36i**.

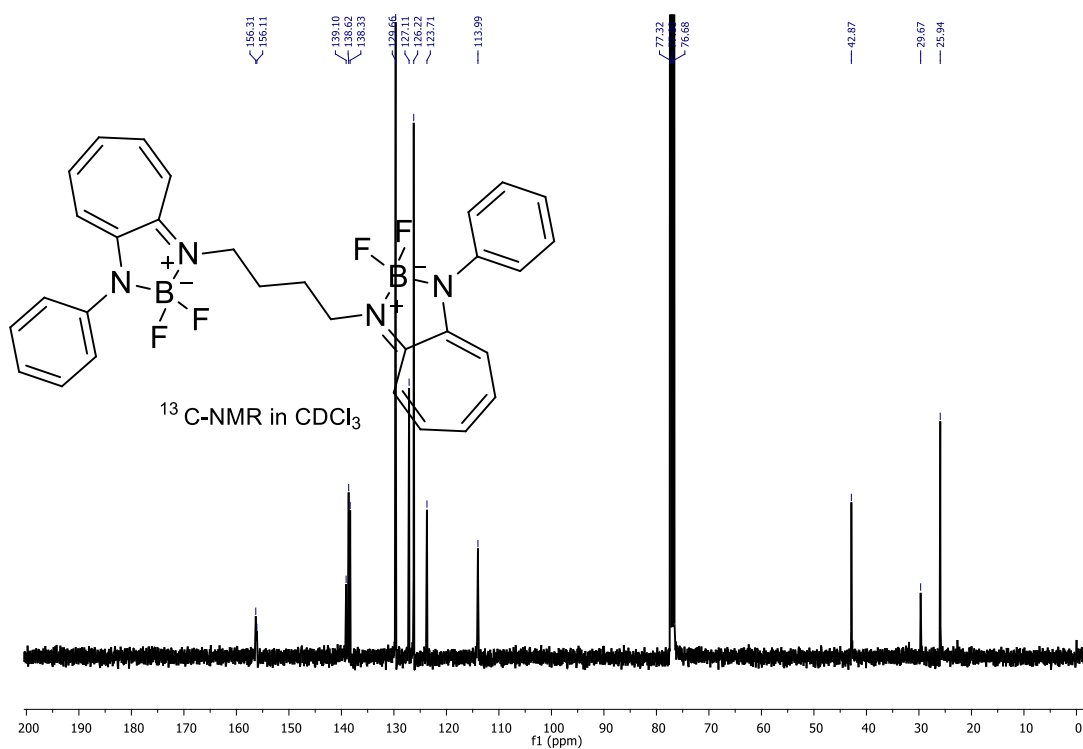


Figure A84. ^{13}C NMR spectrum boron complex **36i**

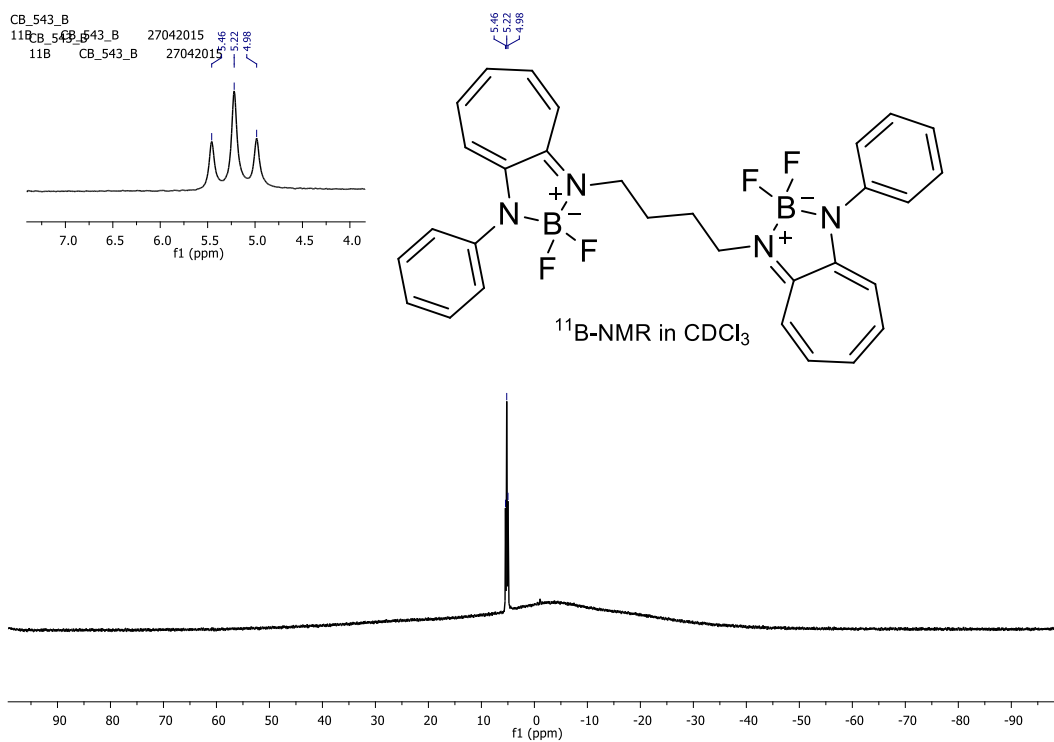


Figure A85. ^{11}B NMR spectrum of boron complex **36i**

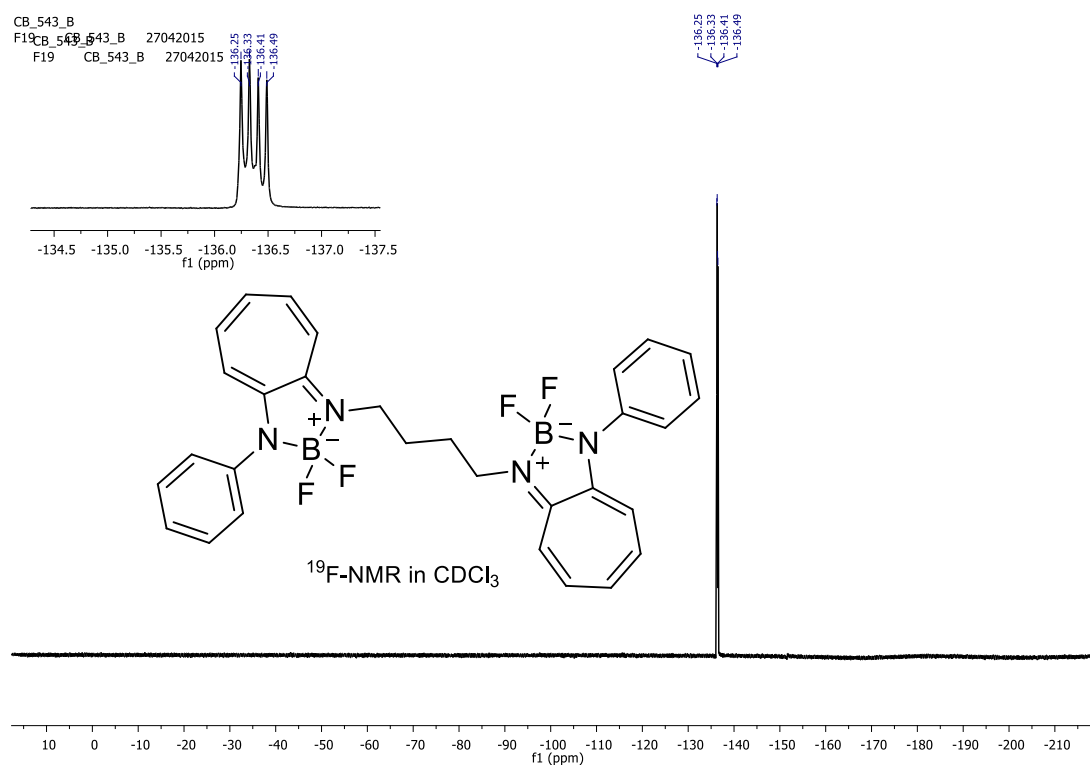


Figure A86. ^{19}F NMR spectrum of boron complex **36i**

Generic Display Report

Analysis Info

Analysis Name D:\Data\APR-2015\NKS\26042015NKS_CB_DIBF2.d
Method Pso_tune_wide.m
Sample Name NISER-LCMS
Comment

Acquisition Date 4/26/2015 8:14:28 PM

Operator NISER
Instrument micrOTOF-Q II

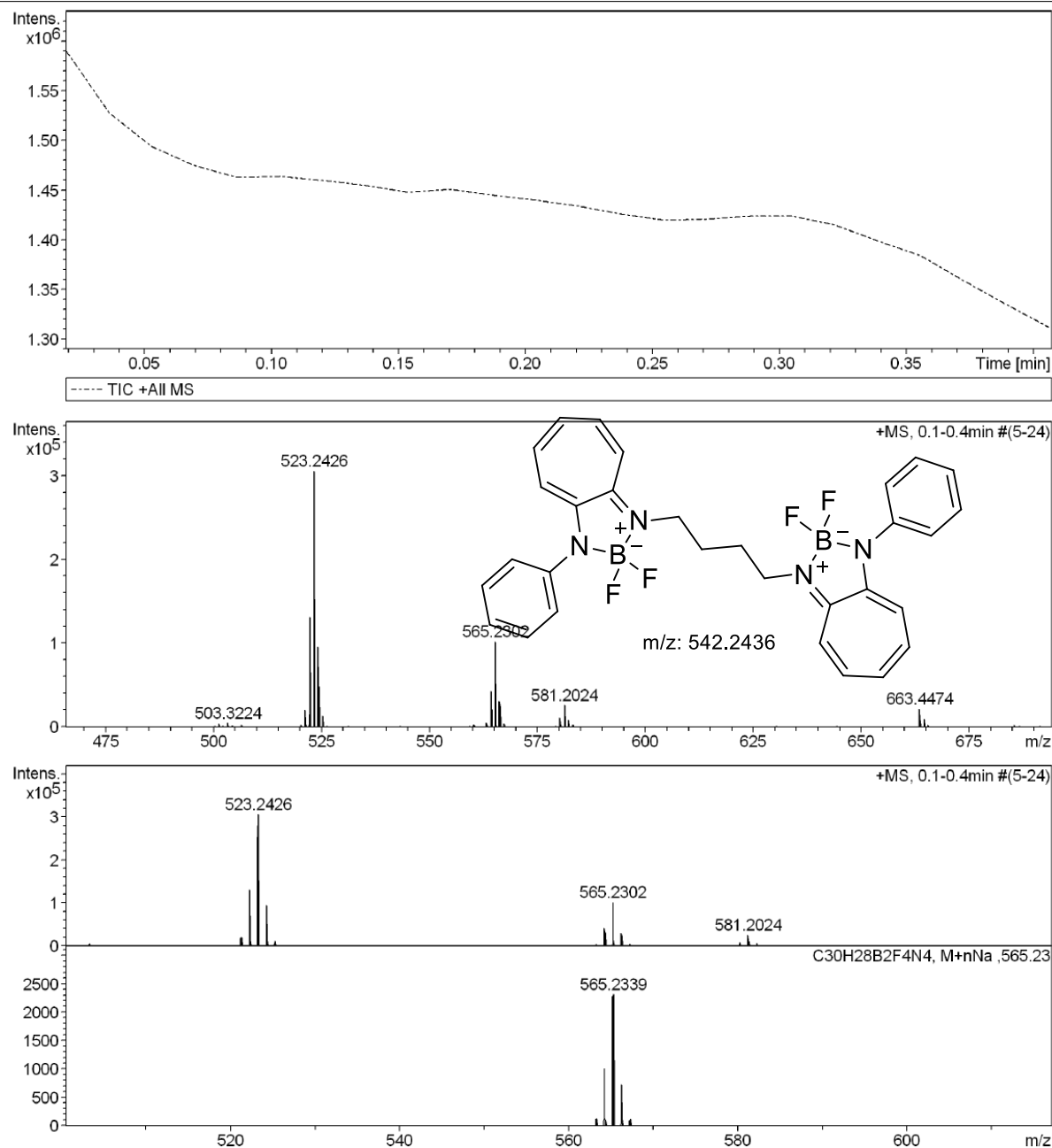


Figure A87. HRMS spectrum of boron complex **36i**.

24. Crystal data of Boron complex **36c**:

Table 5. Crystal data and structure refinement for cb_696.

Identification code	cb	
Empirical formula	C ₂₁ H ₁₉ B F ₂ N ₂	
Formula weight	348.19	
Temperature	293(2) K	
Wavelength	0.71073 Å	
Crystal system	Triclinic	
Space group	P-1	
Unit cell dimensions	a = 6.0730(2) Å	a = 89.941(3)°.
	b = 17.8979(6) Å	b = 86.476(2)°.
	c = 24.0942(9) Å	g = 85.239(2)°.
Volume	2604.90(16) Å ³	
Z	6	
Density (calculated)	1.332 Mg/m ³	
Absorption coefficient	0.093 mm ⁻¹	
F(000)	1092	
Crystal size	0.06 x 0.041 x 0.032 mm ³	
Theta range for data collection	2.43 to 28.37°.	
Index ranges	-7<=h<=8, -23<=k<=23, -32<=l<=32	
Reflections collected	39703	
Independent reflections	12866 [R(int) = 0.0834]	
Completeness to theta = 28.37°	98.8 %	
Refinement method	Full-matrix least-squares on F ²	
Data / restraints / parameters	12866 / 0 / 706	
Goodness-of-fit on F ²	0.967	

Final R indices [I>2sigma(I)]

R1 = 0.0563, wR2 = 0.1131

R indices (all data)

R1 = 0.1356, wR2 = 0.1435

Largest diff. peak and hole

0.225 and -0.280 e.Å⁻³

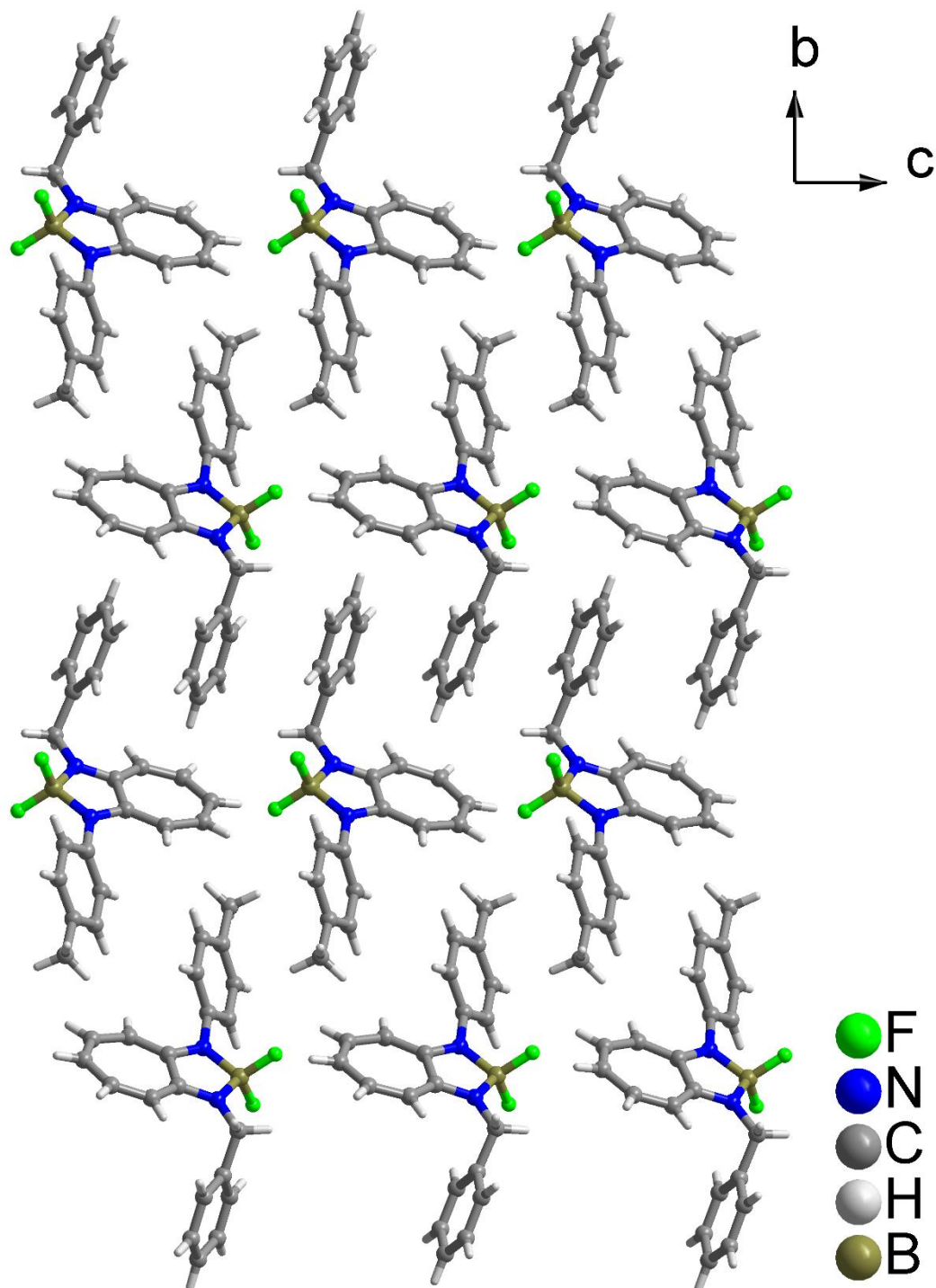


Figure A88. Molecular packing diagram of Boron complex 36c

CHAPTER FIVE

Syntheses of *Hexa*-Peptides *via* Alkyl Linkers

Chapter 5: Syntheses of *Hexa*-Peptides *via* Alkyl Linkers

5.1 Introduction

Proteins/peptides are one of the ubiquitous molecules occur in nature. They perform biological functions in the living system by adopting specific secondary structures.¹⁻⁷ Peptides adopt various secondary structures via co-operative conformational preference of individual amino acid residues in a sequence and non-covalent interactions such as hydrogen bonding, π - π stacking and vanderwaal's interactions.²⁻⁷ As described in chapter one, so far countless number of peptides have been synthesized to mimic the function of naturally occurring peptides and proteins with wide diversities in the sequence.²⁻⁷ The synthetic peptides have shown similar or enhanced biological properties. Synthetic peptides have been developed as therapeutic drugs, today, several peptide therapeutic drugs are available in the market for various diseases.^{9,10} Major disadvantages with the natural peptide therapeutic drugs are their proteolytic susceptibility and difficulties in oral administration.^{6,9,10} To overcome these issues, several structural modifications have been suggested in the literature, these include replacement of natural amino acid residues with unnatural amino acid residues, replacement of amide bond with different isosteric functional groups such as ester, thioamide, cyclization of peptides and linking peptides through carbon chain.²⁻¹⁰ Here, we have demonstrated the use of alkyl chain linkers in linking two proline *N*-terminus peptides via alkyl linkers.

5.1.1 Importance of proline and hydroxyproline in peptides

Proline (Pro) and hydroxyl proline (Hyp) amino acids are unique among all natural α -amino acids by having a cyclic backbone (**Figure 5.1A**).^{11-15,17-20} All natural amino acids except glycine contains acyclic substituents at α -carbon atom. Whereas, proline contains a *penta*-cyclic backbone, a propyl chain connecting α -carbon atom and amine functional group, as a results the primary amine group converts into secondary amine functional group.¹⁹ Proline and

hydroxyproline are the only amino acids containing secondary amine as amine functional group. Hence, the amide bond derived from proline amine and carboxylic acid of other amino acid is a tertiary amide bond and exists in *cis* and *trans* form (**Figure 5.1B**).^{11-15,19} In the nature, 95.0% of the proline amide bonds present in proteins are exists as *trans* amides and 5.0% exist in *cis* form.¹⁹ More interestingly, pyrrolidine ring of proline equilibrates between two ring conformers occurs due to ring puckering such as *C γ -exo* and *C γ -endo* conformers (**Figure 5.1C**).¹⁹ The *trans-Pro* amide form is favoured by electronic interactions such as *exo*-ring puckering, which facilitates strong $n \rightarrow \pi^*$ interactions (**Figure 5.1D**). Further, the presence of strong $n \rightarrow \pi^*$ interactions were demonstrated by crystal structure of *hexa*-oligoproline peptides which adopts PPII helix (left-handed helix).^{11-15,17-20}

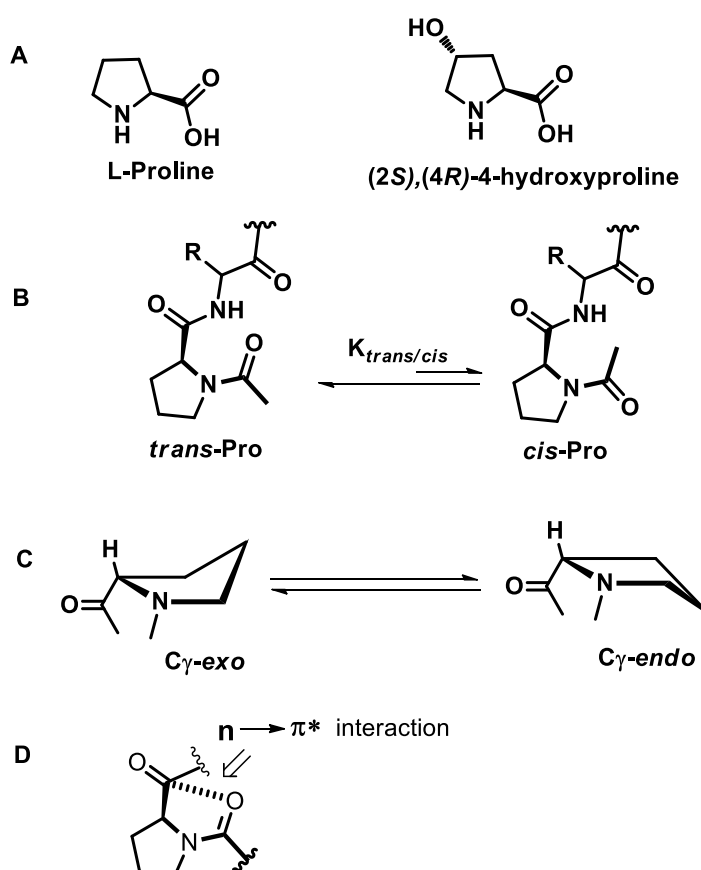


Figure 5.1 A) Chemical structures of L-proline and 4-hydroxyproline. B) Structural representation of *trans/cis*-Proline amide bond. C) Structural representation of *exo/endo* ring puckering. D) Representation of $n \rightarrow \pi^*$ interaction in *trans*-Pro amide.

Conformational constraint of pyrrolidine ring backbone of proline/hydroxyproline and absence of hydrogen bond donors in peptides derived from proline/hydroxyproline, made them as more preferable amino acid residues for constructing well-defined secondary structure peptides such as hairpins, loops and turns by using them as guiding residues (**Figure 5.2**).² For example, D-Pro and Gly/Aib or D-Pro and L-Pro respective sequence residues are well known for taking reverse turn to nucleate the formation of β -hairpin secondary structure.² In all these examples, proline residue is present, which is responsible for chain reversal of peptide and leads to the formation of turn segment. In the literature, so far, several β -hairpin peptides were synthesized containing proline as chain reversal residue.² Most importantly, it is well known that collagen, a most abundant human protein, consists of proline and hydroxyl proline residues as Xaa-Yaa-Gly repeating units. On the other hand, conformationally constrained prolyl peptide nucleic acids have also been synthesized from proline, which have shown nucleo-base dependent binding activities and relatively more stable *aep*-PNA:DNA duplexes when compare to *aeg*-PNA:DNA duplexes.¹⁶⁻¹⁸

Further, the *tri*-peptides derived from Pro-Pro-Asp-NH₂ are developed as catalysts for several enantioselective organic transformations.^{14,15} Most interestingly, proline itself acts as a catalyst for enantioselective aldol, Mannich and Michael addition reactions.³⁷

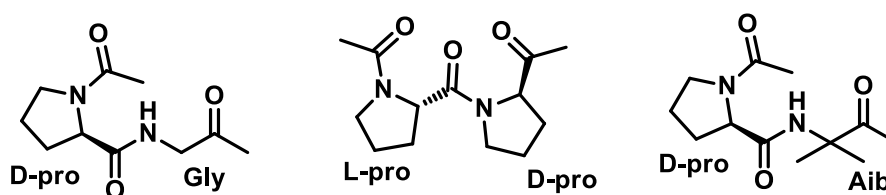


Figure 5.2 Reported hairpin nucleating sequence derived from L-Proline and D-Proline.

Overall, out of 20 natural α -amino acids, only proline/hydroxyl proline have characteristic properties such as conformationally constrained cyclic backbone, absence of hydrogen bond donors and high possibility of existence of $n \rightarrow \pi^*$ interactions via ring

puckering. All these exciting properties of proline and hydroxyl proline have led them to use in peptides as conformation controlling residues. And the application of proline in different fields of research as organocatalyst for selective organic transformations, for constructing conformationally constrained peptide nucleic acids and edited proline analogues in constructing biologically active peptides and so on.

5.1.2 Peptides as molecular building blocks in nanomaterial fabrication

Self-assembly of molecular building blocks *via* non-covalent interactions leads to the formation of supramolecular nano-architectures.²¹⁻²⁷ Peptide nanomaterials have wide range of applications in biomedical sciences, cosmetology and in nanotechnology.²¹⁻²⁷ Novel peptide nanomaterials are in huge demand for above mentioned applications.²¹⁻²⁷ Fabricating functional nanomaterials from peptides offer various advantages such as easy syntheses, characterization and opportunity to design the peptide sequence with wide chemical diversity from 20 natural amino acids.²¹⁻²⁷ Especially, these twenty amino acids have shown wide chemical diversity by having different substituents at α -carbon atom.²¹⁻²⁷ This feature further helps to design peptide sequence containing both hydrophilic and hydrophobic functional groups. Moreover, to date, the shortest peptide known for formation of nano-architectures is diphenylalanine peptide.²¹ Owing to their applications and advantages in syntheses, fabrication of functional nanomaterials from peptides become an active and exciting area of research.²¹⁻²⁷

5.1.3 Rational of Present Work

Inspired from the applications of peptides in various fields and importance of proline in design of peptides with well-defined secondary structures, we have designed a set of *tri*-peptides and *hexa*-peptides, they can be easily synthesized from *tri*-peptides by connecting two *tri*-peptides with alkyl linkers at nitrogen atom of the proline through C-N bond (**Figure 5.3**).

The followed synthetic method is known for the construction of chiral proline macrocyclic ligands, very few reports presented this method for macrocyclic ligand syntheses.³⁴⁻³⁵ However, so far there are no reports on the linking of two peptide units at proline amine by using alkyl linkers. The obtained peptides after linking two peptide units at proline *N*-terminus are sequence symmetric peptides, because they contain same residue sequence at two sides of the linkers. The advantage with these peptides is, they contain two tertiary amine nitrogens in the middle of the sequence, hence they may respond to pH of the medium. Moreover, as described above, fabrication of functional nanomaterials from peptides is one of the fast growing research area, hence, this methodology may provide opportunities to synthesize the peptides containing same duplicate sequence in the same molecule via linkers (ethyl/propyl). Recently, screening of different tripeptides for the hydrogel formation is reported, where Pro-Phe-Phe tripeptide is reported to form 0.70 μm aggregates.²⁷

Herein, we present the syntheses of *hexa*-peptides from *tri*-peptides *via* alkyl linkers and their initial structural properties examination by CD spectroscopy in different solvents.

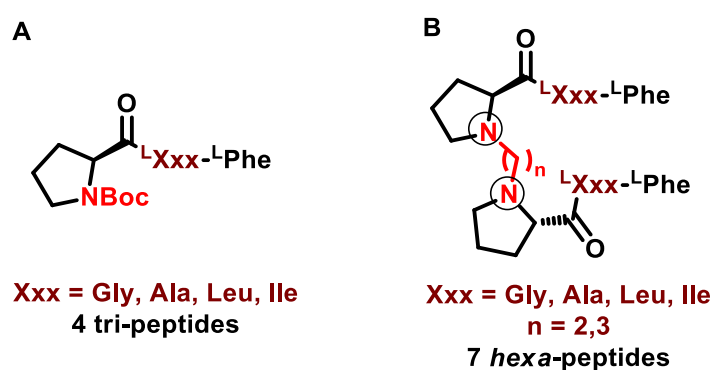


Figure 5.3 A) Designed *tri*-peptides for this work. B) Designed *hexa*-peptides containing alkyl linkers.

5.2 Results and discussion

5.2.1 Syntheses and characterization

The syntheses of *tri*-peptides were carried out through standard solution phase peptide syntheses and then Boc deprotected *tri*-peptides were allowed to *N*-alkylation with dibromo alkanes. First, the BocNH-AA-Phe-OMe (AA = Gly/Ala/Ile/Leu) *di*-peptides were synthesized by following the standard peptide coupling reaction conditions, diisopropylcarbodiimide (DIPCDI) or 1-Ethyl-3-(3-dimethylaminopropyl)carbodiimide (EDC.HCl) was used as coupling reagent along with hydroxyl benzotriazole (HOBt) as additive (**Scheme 5.1**). Next, these *di*-peptides were allowed to Boc-deprotection in presence of 30.0% TFA in DCM. The obtained free amine salt of *di*-peptides were coupled with Boc-L-Proline to obtain respective *tri*-peptides (**Figure 5.4**).

Further, these *tri*-peptides were allowed to Boc deprotection under above mentioned conditions to obtain free amine containing *tri*-peptides. After Boc deprotection, these L-proline free amine *tri*-peptides were linked via alkyl chains, to obtain *hexa*-peptides. The *N*-alkylation reaction of these *tri*-peptides was performed with dibromo alkanes in presence of K₂CO₃ in acetonitrile at 45 °C for 3 days. The desired *hexa*-peptides were isolated in 60-70% yields. These peptides were characterized by NMR and ESI-MS.

Here, we have rationally designed two types of *hexa*-peptides connected by two alkyl linkers such as ethyl and propyl linkers. With ethyl linkers four *hexa*-peptides were synthesized and with propyl linkers four *hexa*-peptides were synthesized. In case of all eight *hexa*-peptides, as mentioned above two *tri*-peptides were connected through free amine of L-proline. Hence, these peptides are symmetric peptides containing same amino acid sequence connected by alkyl linkers. Importantly, the two ends of these peptides contain carboxyl terminus. All the peptides contain phenyl alanine residues at two ends. Chemical structures of these *hexa*-peptides are

depicted in **Figure 5.5**. ^1H NMR and ESI-MS spectra of *hexa*-peptides **38a** and **39a** are depicted in **Figure 5.6**.

Scheme 5.1 Syntheses of *hexa*-peptides via alkyl linkers.

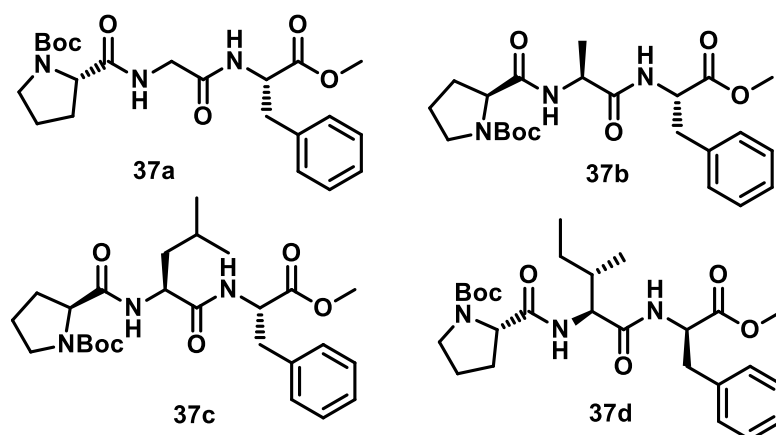
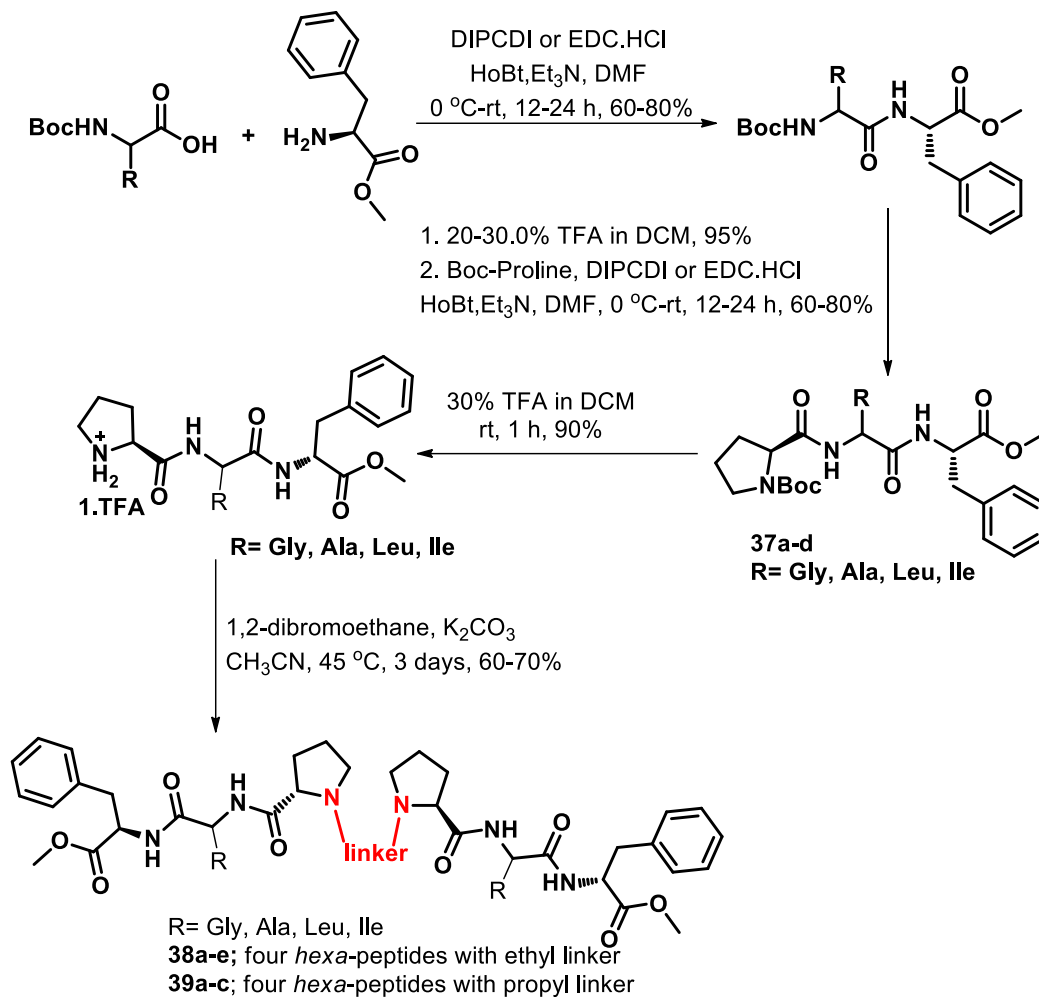


Figure 5.4 Synthesized *tri*-peptides.

The sequence of all these peptides is Phe-AA-Pro-*Linker*-Pro-AA-Phe. In all these peptides the residue at AA position is varied. Four different types of peptides were synthesized by varying the amino acid residue at AA position. These four residues are Glycine, Alanine, Leucine and Isoleucine.

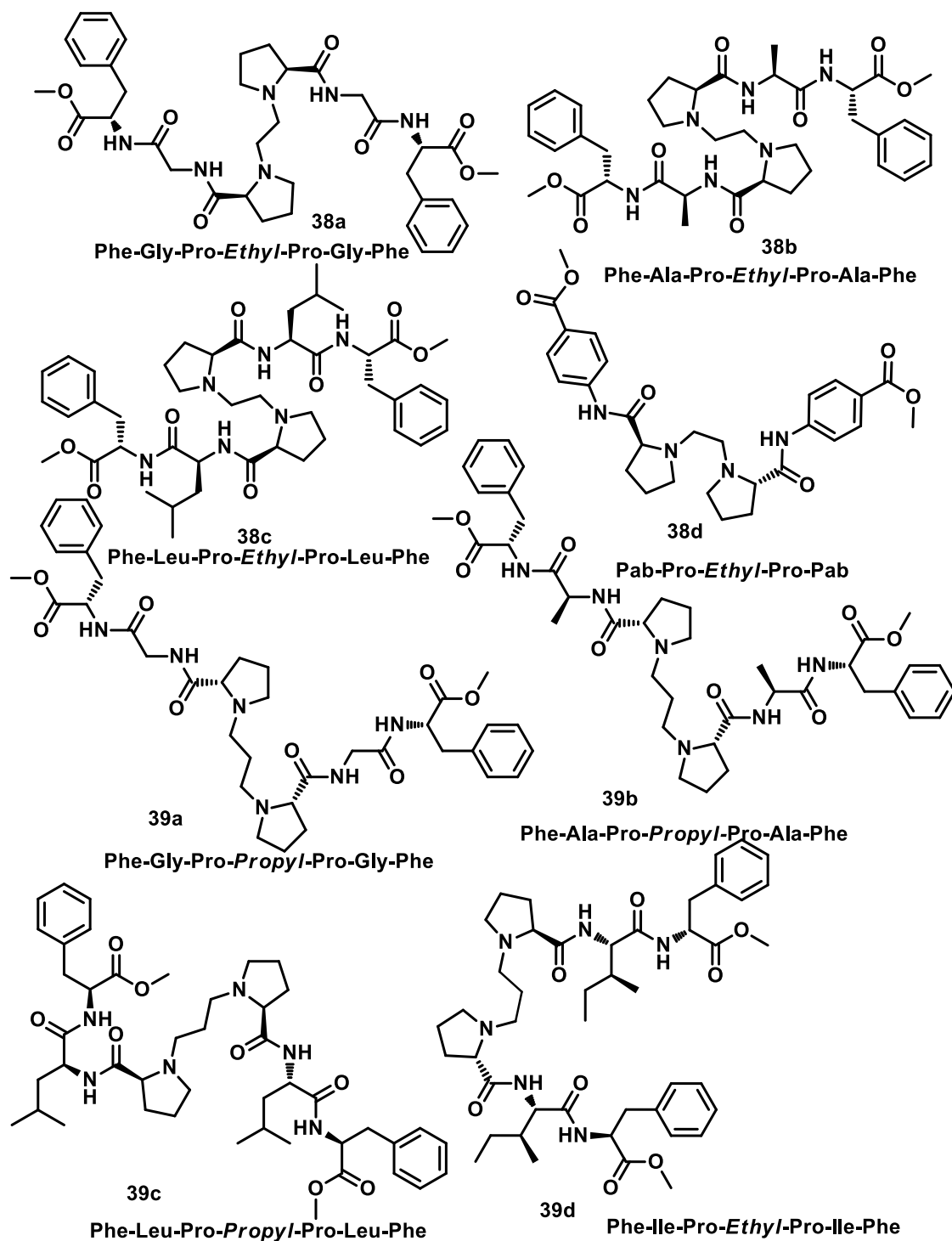


Figure 5.5 Chemical structures of synthesized peptides.

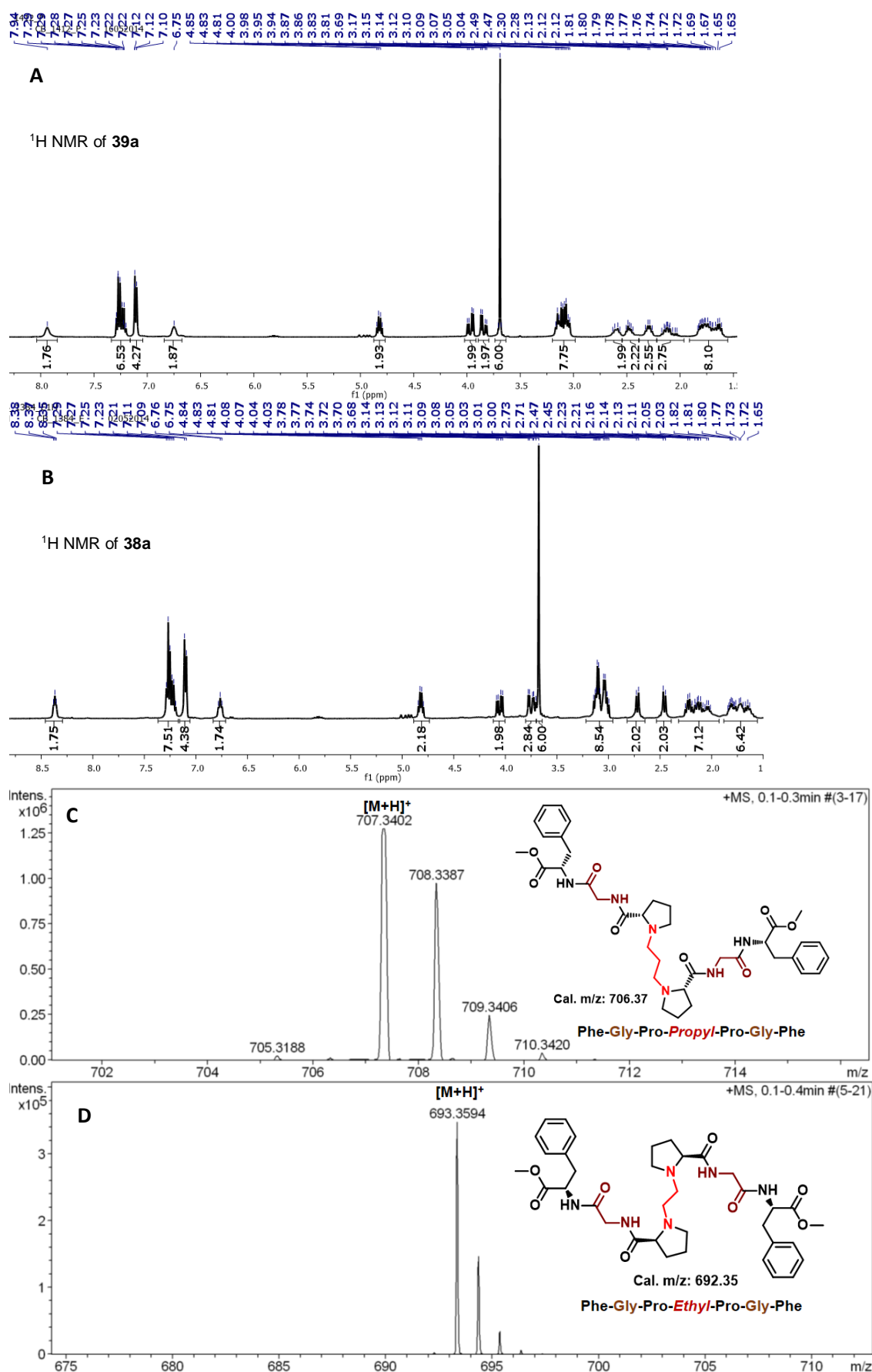


Figure 5. ^1H NMR and mass spectra of Phe-Gly-Pro-Propyl-Pro-Gly-Phe (**39a**) and Phe-Gly-Pro-Ethyl-Pro-Gly-Phe (**38a**), respectively.

5.2.2 NMR and Circular Dichroism (CD) spectroscopic studies

After successful syntheses of several *hexa*-peptides via ethyl and propyl linkers, we attempted to investigate their secondary structures by NMR and CD spectroscopic studies. For NMR experiments, first one of these *hexa*-peptides **39a** were dissolved in CDCl_3 and recorded COSY, ROESY spectra. Obtained spectra are provided in **Figure 5. 7/8**. After assigning cosy spectra of **39a**, we realized that due symmetrical sequence all protons represents two *tri*-peptides connected by linker are coming at same chemical shift value. However, we have

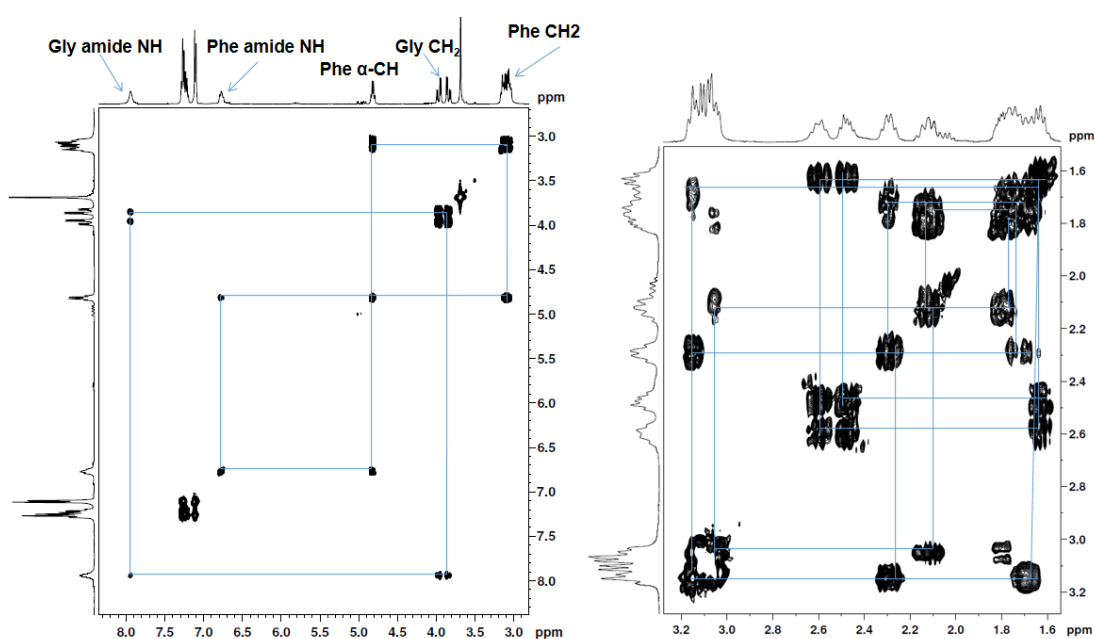


Figure 5.7 ^1H - ^1H NMR COSY spectra of *hexa*-peptide **38b** in CDCl_3

assigned the all protons of the molecule and their spatial interactions by using ROESY spectra. Later, from the ^1H NMR spectra of other peptides after integrating we realized that in all cases two tripeptide segments protons connected by linkers are resonating at same chemical shift value. Overall, from the NMR experiments we are unable to characterize the secondary structure of synthesized peptides.

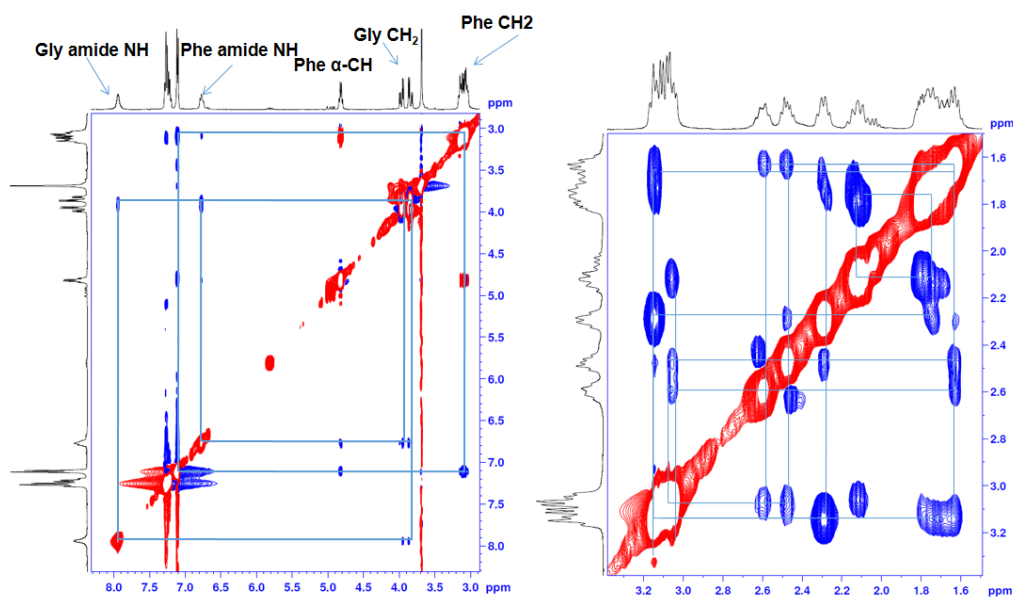


Figure 5.8 ^1H - ^1H NMR ROESY spectra of *hexa*-peptide **39a** in CDCl_3

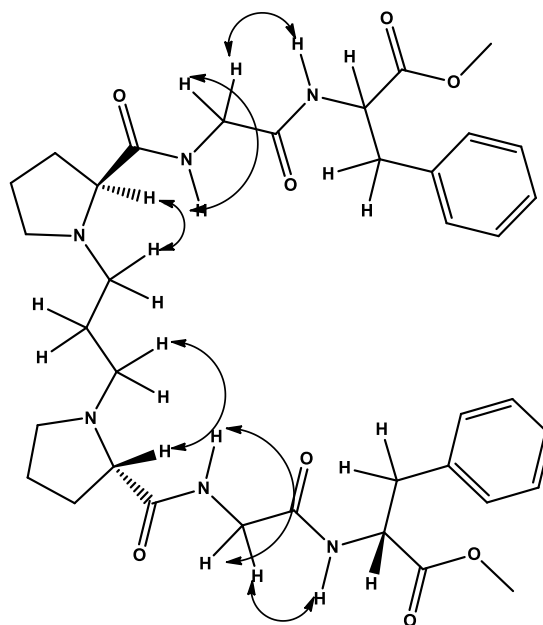


Figure 5.9 Observed ROESY interactions of *hexa*-peptide **39a** in CDCl_3

Circular Dichroism spectroscopy: Further, we attempted to examine the secondary structure of these peptides by using Circular Dichroism spectroscopy. For that reason, we recorded the CD spectra of all these peptides in methanol, acetonitrile and 2,2,2-trifluoroethanol at 0.33mM and 1.3 mM concentrations. The used solvents for CD studies are spectroscopic grade. The obtained spectra at 25 °C are depicted in the **Figures 5.10-12**.

CD spectra of tri and *hexa*-peptides exhibits positive peaks from 220 nm to 227 nm and 234 nm to 242 nm in all solvents at above mentioned concentrations. However, depends on concentration and solvent the CD spectra peptides has changed. Moreover, in same solvent also, at low and high concentrations CD spectra has shown noticeable changes.

First, it is important to correlate the CD spectra obtained in same solvent at different concentrations. The CD spectra of tri and *hexa*-peptides obtained in methanol at 0.3 mM concentration has shown more intense positive peaks from 220 to 227 nm than negative peaks (**Figure 5.10A**). Whereas, at 1.33 mM concentration the obtained spectra have shown interesting changes (**Figure 5.10B**). These are, positive peaks are observed for all tripeptides and 38/39c peptides, rest of the peptides have not shown any positive peak. Interestingly, relatively more intense negative peaks were observed at 1.33 mM concentration when compare to positive peaks and at low concentration.

In contrast, the CD spectra of these peptides in acetonitrile has shown more interesting changes. Unlike CD spectra at 0.33 mM concentration in methanol, the CD spectra at 0.33 mM concentration has shown very intense negative peaks for all the peptides than positive peaks (**Figure 5.11A**). And at 1.33 mM concentration positive peaks are disappeared for all peptides except **37a**. However, very high intense negative peaks were observed at 1.33 mM concentration in acetonitrile (**Figure 5.11B**).

The obtained CD spectra in 2,2,2-trifluoroethanol for all these peptides have shown relatively very less intensity at both negative and positive region at 0.33 mM and 1.33mM concentrations (**Figure 5.12**). Especially, at 0.33 mM concentration the obtained spectral intensity is very less, which is not considerable for analysis. However, at 1.33 mM more intense spectra was obtained compare to 0.33 mM concentration. More interestingly, all peptides have shown only negative peaks.

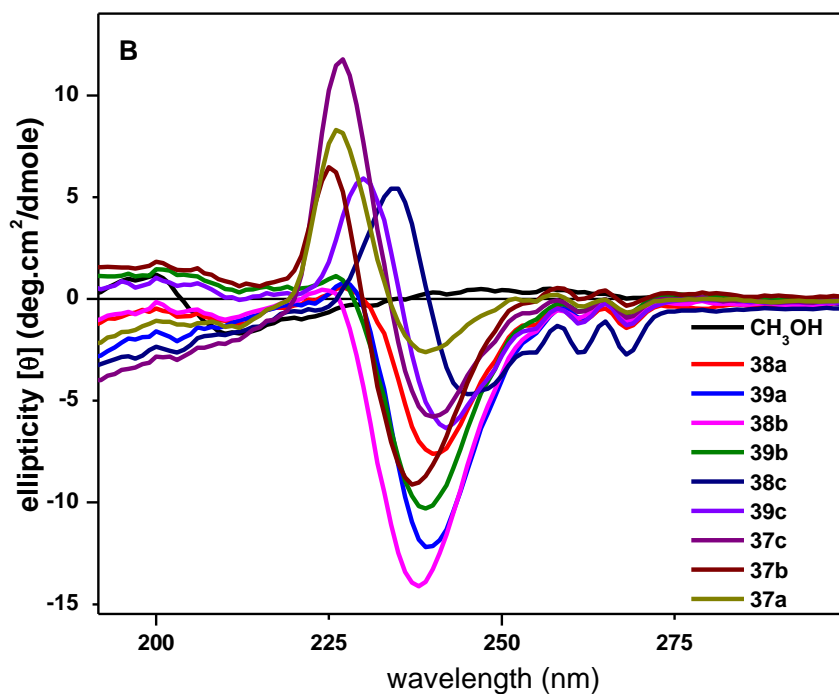
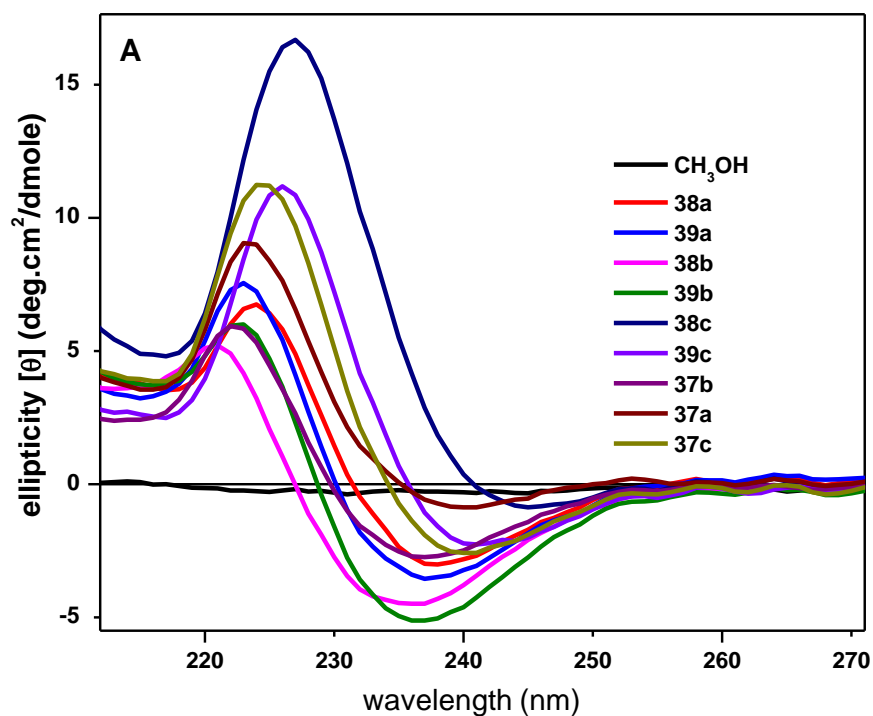


Figure 5.10 CD spectra of *tri*-peptides (**37**) and *hexa*-peptides (**38-39**) at 0.33 mM (A) and 1.33 mM (B) in methanol.

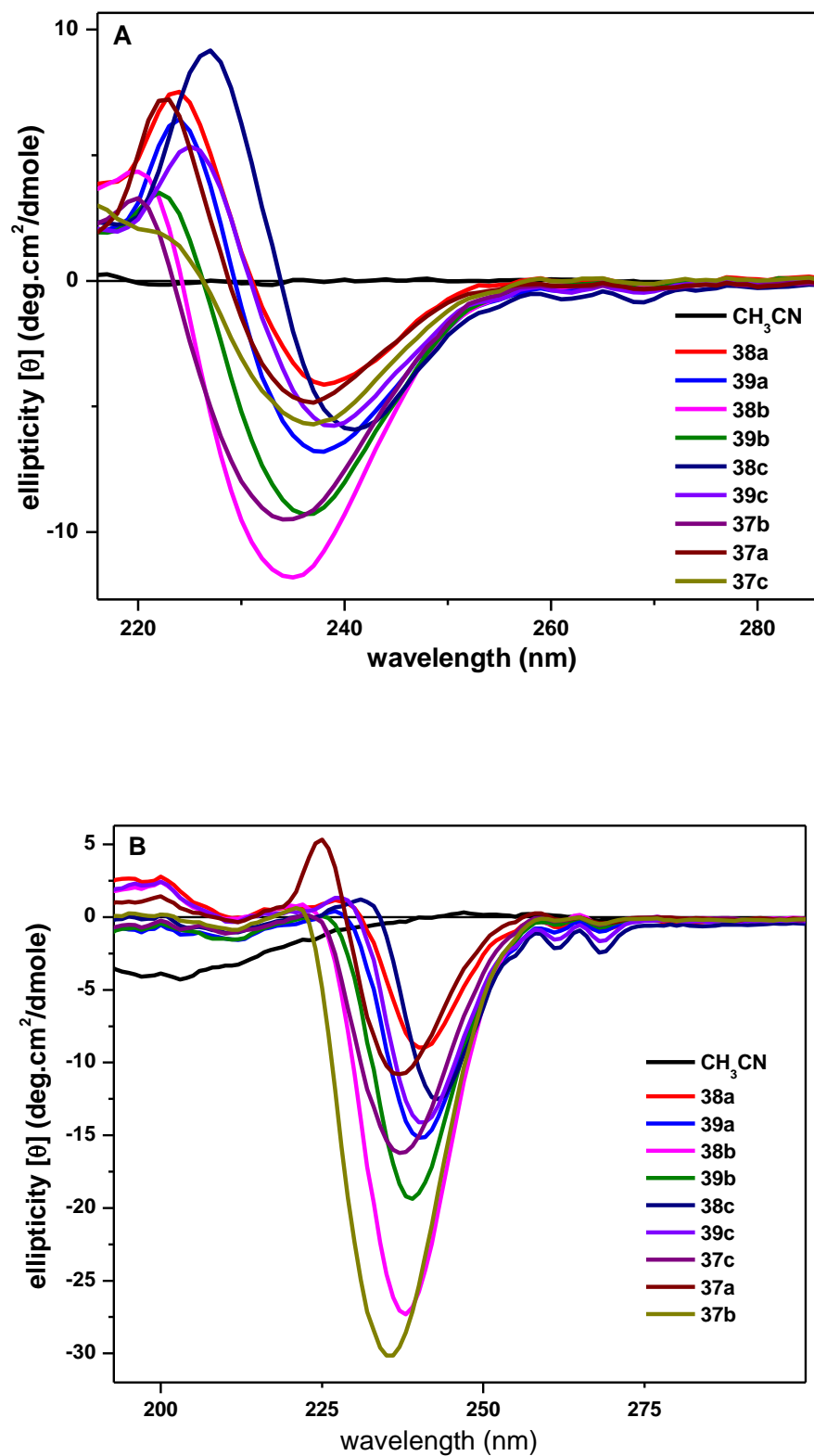


Figure 5.11 CD spectra of *tri*-peptides (37) and *hexa*-peptides (38-39) at 0.33 mM (A) and 1.33 mM (B) in acetonitrile.

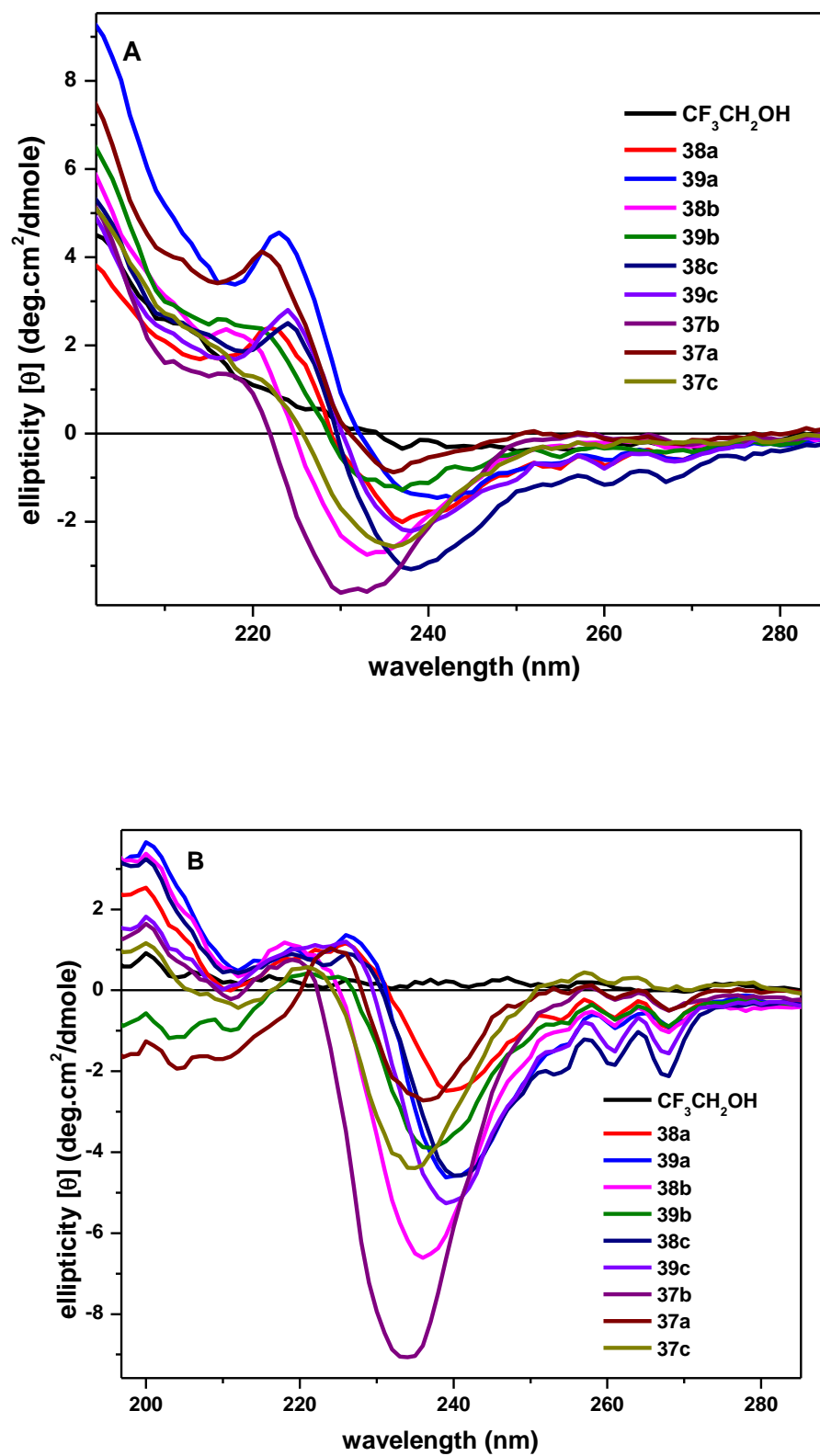


Figure 5.12 CD spectra of *tri*-peptides (**37**) and *hexa*-peptides (**38-39**) at 0.33 mM (A) and 1.33 mM (B) in 2,2,2-trifluoroethanol.

Overall, CD spectral analysis of these peptides revealed that they may be aggregating. Because, in the literature it is reported that, 2,2,2-trifluoroethanol (TFE) solvent promotes the formation of secondary structures of peptides.³⁶ Whereas, in case of synthesized *hexa*-peptides, the observed high intense peaks in methanol and acetonitrile at 0.33 mM and 1.33 mM concentration are appeared as very less intense in TFE. That means the appearing peaks are most probably due to aggregation of peptides. Further, at high concentration 1.33 mM, the intensity and peak pattern is changed. This further supports the aggregation of peptides in these particular solvents. In literature also, for some tri and *hexa*-peptides, it has been reported that the appearance of a negative peak after 230 nm is due to self-assembly of peptides.³⁰⁻³³ Moreover, a negative peak at ~230 and 235 nm is reported for self-assembly of peptide gelators and proteins.^{30,31} Overall, we assume that these peptides are most probably aggregating in methanol and acetonitrile at room temperature.

5.3 Conclusions

We have successfully demonstrated the use of ethyl and propyl linker for the syntheses of sequence symmetric *hexa*-peptides. Proline residue was used at *N*-terminus of *tri*-peptides for linking the two *tri*-peptides by using dibromoethane and dibromopropane via nucleophilic substitution. The advantage with proline residue is the presence of secondary amine which avoids the formation of *di*-alkylated products. Since the peptides are in huge demand for applications in nanomaterial fabrication, this method could be potential to construct the longer peptides by linking two proline free amine peptides at *N*-terminus through alkyl linkers.

We have also attempted to investigate the secondary structure of these peptides by using 2D NMR experiments in chloroform, but due to the symmetry in sequence of *hexa*-peptides, we unable to predict the non-spatial interaction in their ROESY spectra. We have also performed the CD spectroscopic experiments in different solvents, from this data it was realized that these molecules might be self-assembling in methanol and acetonitrile. Because,

in 2,2,2-trifluoroethanol, the intensity of the obtained spectra is very less when compare to spectra obtained in methanol and acetonitrile. Further, peak pattern was changed from low concentration to high concentration, which supports the aggregation of these peptides at high concentration.

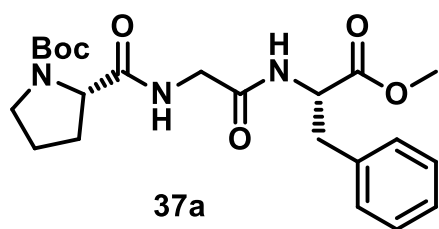
5.4 Experimental Section

General procedure for Boc deprotection: To the *tri*-peptides, a solution of 30.0% TFA in DCM is added at room temperature and allowed to stir. The reaction was monitored by TLC. After completion of the reaction all volatiles were evaporated and to the crude product saturated sodium bicarbonate was added and extracted with DCM thrice. The combined organic layers were dried over sodium sulphate and evaporated to obtain desired product. The obtained product was used for further step without any further purification.

General procedure for syntheses of *hexa*-peptides (**38**, **39**): The Boc-protected free amine *tri*-peptide was dissolved in anhydrous acetonitrile and to this 2.5 *equiv.* of anhydrous potassium carbonate was added. To the suspension, dibromo alkanes were added and allowed to stir at 45 °C for 3 days. After completion of the reaction, the reaction mixture was filtered through watman filter paper and washed the residue with acetonitrile. The obtained filtrate was evaporated and purified through silica gel column chromatography by using chloroform and methanol as mobile phase.

Analytical data:

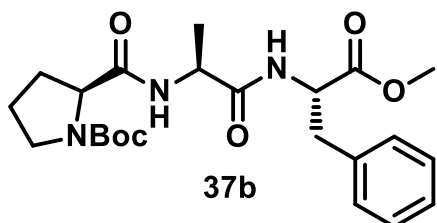
BocNH-Pro-Gly-Phe-OMe (37a):



2.0 gm (70%) of pure product was isolated as white needle like solid. ¹H NMR (400 MHz, CDCl₃) δ 7.28 – 7.11 (m, 3H), 7.04 (d, *J* = 7.0 Hz, 2H), 6.85 (s, 1H), 6.51 (s, 1H).

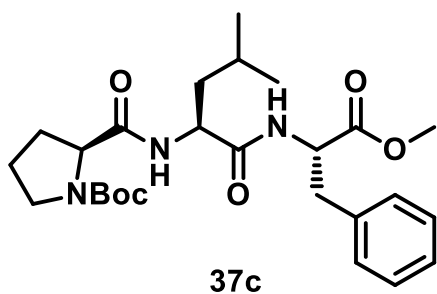
4.76 (d, *J* = 4.7 Hz, 1H), 4.16 (s, 1H), 3.97 (app dd, *J* = 16.7, 6.1 Hz, 1H), 3.74 (app dd, *J* =

16.7, 5.2 Hz, 1H), 3.62 (s, 3H), 3.34 (m, 2H), 3.07 (app dd, $J = 13.8, 5.9$ Hz, 1H), 2.99 (app dd, $J = 13.6, 6.1$ Hz, 1H). 2.23 – 1.70 (m, 5H), 1.38 (s, 9H). ^{13}C NMR (101 MHz, CDCl_3) δ 172.33, 171.15, 168.76, 155.67, 135.88, 129.24, 128.58, 127.09, 80.59, 60.35, 53.39, 52.30, 47.23, 43.01, 37.86, 31.92, 29.69, 29.36, 24.54, 22.69, 14.12.



BocNH-Pro-Ala-Phe-OMe (37b): 1.2 gm (67%) of pure product was isolated as white amorphous solid. ^1H NMR (400 MHz, CDCl_3) δ 7.40 – 7.18 (m, 3H), 7.11 (d, $J = 7.1$ Hz, 2H), 6.84 (s, 1H), 6.63 (s, 1H). 4.81 (dd, $J = 13.4, 6.6$

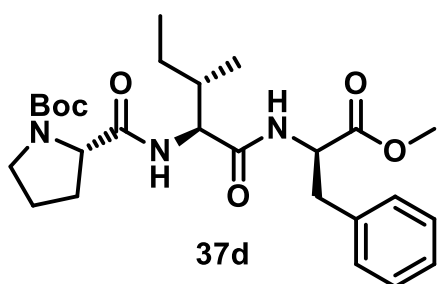
Hz, 1H), 4.40 (s, 1H), 4.30 – 4.09 (m, 1H), 3.70 (s, 3H), 3.39 (m, 2H), 3.13 (dd, $J = 13.8, 5.5$ Hz, 1H), 3.05 (dd, $J = 13.9, 6.3$ Hz, 1H), 2.34 – 2.05 (m, 3H), 1.87 (d, $J = 5.5$ Hz, 4H), 1.44 (s, 9H).



BocNH-Pro-Leu-Phe-OMe (37c): 1.8 gm (60%) of pure product was isolated as white solid. ^1H NMR (400 MHz, CDCl_3) δ 7.31 – 7.19 (m, 3H), 7.16 (t, $J = 7.8$ Hz, 2H), 6.75 (s, 2H), 4.90 – 4.64 (m, 1H), 4.61 – 4.47 (m, 1H), 4.33 – 4.10 (m, 1H), 3.67 (s, 3H), 3.28 (m, 2H), 3.07 (m,

2H), 2.06 (m, 3H), 1.37 (m, 9H), 1.01 – 0.77 (m, 6H). ^{13}C NMR (101 MHz, CDCl_3) δ : 172.74, 172.73, 170.57, 136.48, 129.45, 129.29, 129.25, 128.69, 128.58, 127.60, 80.03, 60.38, 58.10, 53.48, 52.20, 50.90, 47.27, 41.04, 37.85, 37.27, 33.40, 24.58, 22.72, 21.80, 21.01, 14.24.

BocNH-Pro-Ile-Phe-OMe (37d):

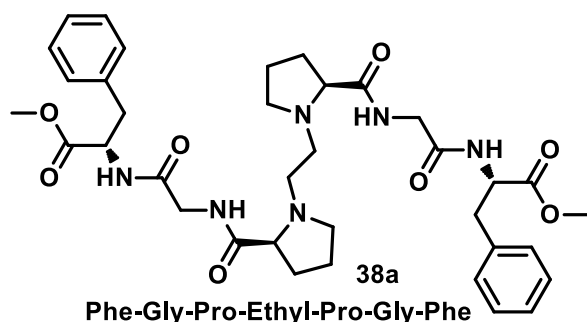


1.5 gm (80%) of pure product was isolated as white solid. ^1H NMR (400 MHz, CDCl_3) δ 7.45 – 7.20 (m, 3H), 7.12 (d, $J = 6.6$ Hz, 2H), 6.66 (s, 1H), 6.40 (s, 1H), 4.85 (dd, $J = 14.0, 6.2$ Hz, 1H), 4.45 – 4.12 (m, 2H), 3.69 (s, 3H), 3.38

(m, 2H), 3.09 (m, 2H), 2.32 (s, 1H), 2.20 – 1.71 (m, 5H), 1.40 (s, 9H), 0.85 (d, $J = 6.5$ Hz, 6H).

^{13}C NMR (101 MHz, CDCl_3) δ 172.22, 171.80, 170.82, 156.08, 136.02, 129.32, 128.68, 127.13, 80.73, 60.03, 58.09, 53.21, 52.35, 47.22, 37.99, 36.44, 29.77, 27.94, 24.76, 24.37, 15.56, 11.48.

Phe-Gly-Pro-Ethyl-Pro-Gly-Phe (**38a**): 70 mg of (60%) of pure product was isolated as



gelatinous colourless thick liquid. ^1H NMR

(400 MHz, CDCl_3) δ 8.37 (t, $J = 5.3$ Hz, 2H),

7.24 (m, 6H), 7.10 (d, $J = 7.3$ Hz, 4H), 6.76 (t,

$J = 7.0$ Hz, 2H), 4.82 (dd, $J = 13.3, 6.4$ Hz, 2H),

4.06 (dd, $J = 16.6, 6.5$ Hz, 2H), 3.80 – 3.70 (m,

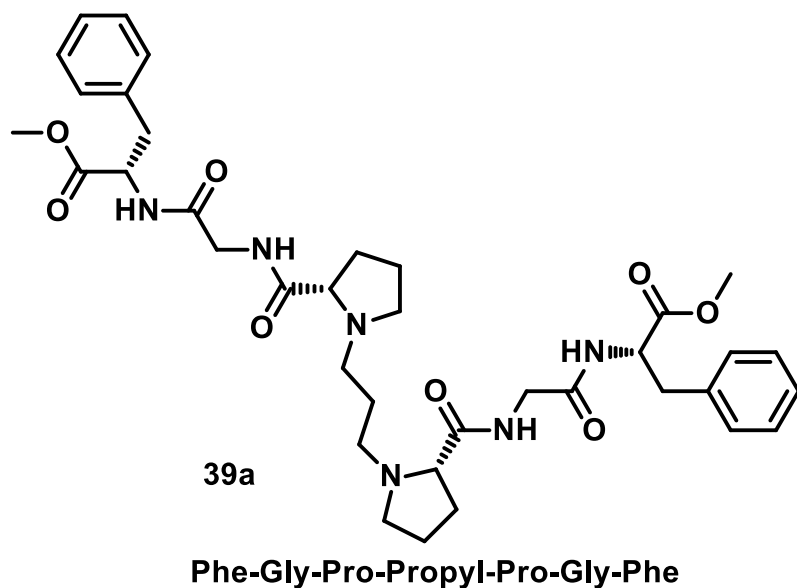
2H), 3.68 (s, 6H), 3.20 – 2.96 (m, 8H), 2.72 (d, $J = 8.6$ Hz, 2H), 2.46 (d, $J = 8.6$ Hz, 2H), 2.30

– 1.92 (m, 6H), 1.91 – 1.54 (m, 6H). ^{13}C NMR (101 MHz, CDCl_3) δ 175.63, 171.66, 168.86,

135.77, 129.21, 128.54, 127.03, 67.82, 54.97, 54.14, 53.18, 52.28, 42.92, 37.80, 31.87, 30.31,

29.56, 29.45, 29.30, 24.04, 22.64. Mass (ESI-TOF) m/z : found 693.3594.

Phe-Gly-Pro-propyl-Pro-Gly-Phe (**39a**): 90 mg of (62%) of pure product was isolated as



gelatinous colourless thick

liquid. ^1H NMR (400 MHz,

CDCl_3) δ 7.94 (s, 2H), 7.42 –

7.17 (m, 6H), 7.17 – 7.05 (m,

4H), 6.75 (s, 2H), 4.82 (dd, J

$= 13.6, 6.1$ Hz, 2H), 3.97 (dd,

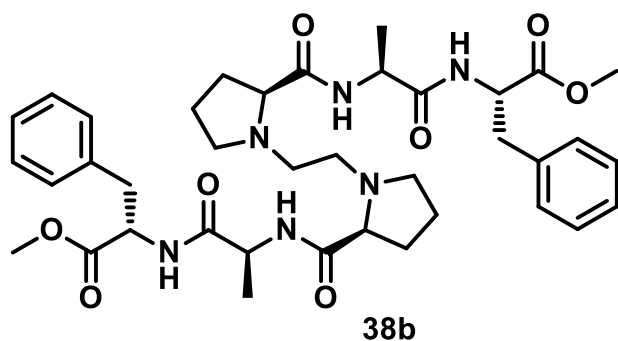
$J = 16.5, 5.9$ Hz, 2H), 3.84

(dd, $J = 16.5, 5.7$ Hz, 2H),

3.75 – 3.64 (m, 6H), 3.22 –

2.95 (m, 8H), 2.73 – 2.52 (m, 2H), 2.52 – 2.37 (m, 2H), 2.29 (m, 2H), 2.12 (m, 2H), 1.74 (m,

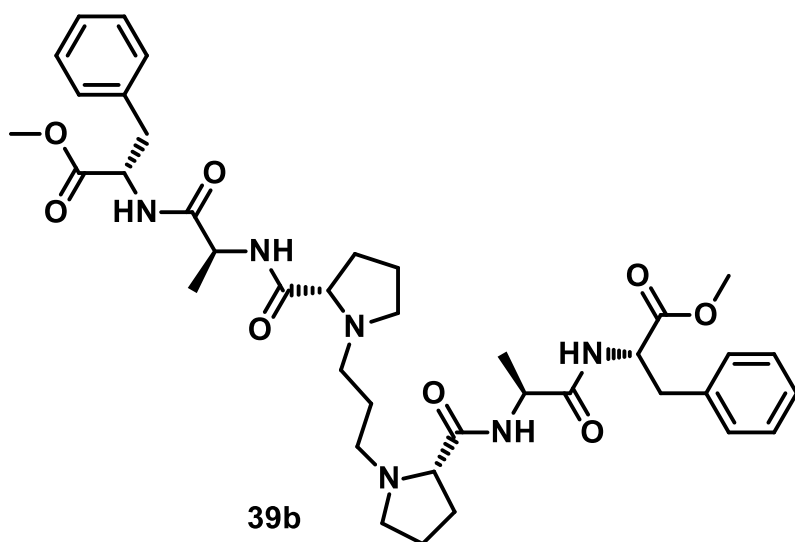
8H). ^{13}C NMR (101 MHz, CDCl_3) δ 175.37, 171.74, 168.91, 135.71, 129.20, 128.55, 127.06, 67.65, 53.78, 53.47, 53.32, 52.29, 42.66, 37.73, 30.30, 27.67, 23.94. Mass (ESI-TOF) m/z : found 707.3402



Phe-Ala-Pro-Ethyl-Pro-Ala-Phe

Phe-Ala-Pro-Ethyl-Pro-Ala-Phe (**38b**): 82 mg of (65%) of pure product was isolated as gelatinous colourless thick liquid. ^1H NMR (400 MHz, CDCl_3) δ 7.87 (d, $J = 7.2$ Hz, 2H), 7.33 – 7.16 (m, 6H), 7.13 (d, $J = 7.0$ Hz, 4H), 6.97 (d, $J = 7.0$ Hz, 2H), 4.71 (dd,

$J = 12.9, 7.7$ Hz, 2H), 4.49 – 4.31 (m, 2H), 3.69 (s, 6H), δ 3.12 (dd, $J = 13.9, 5.1$ Hz, 2H), 2.96 (dd, $J = 14.2, 7.5$ Hz, 3H), 2.88 (d, $J = 3.8$ Hz, 2H), 2.45 (d, $J = 9.2$ Hz, 2H), 2.21 (d, $J = 9.2$ Hz, 2H), 2.17 – 2.07 (m, 2H), 2.02 (dd, $J = 16.7, 8.4$ Hz, 3H), 1.89 – 1.77 (m, 2H), 1.76 – 1.62 (m, 3H). 1.37 – 1.20 (m, 6H). Mass (ESI-TOF) m/z : found 707.3402 721.4196

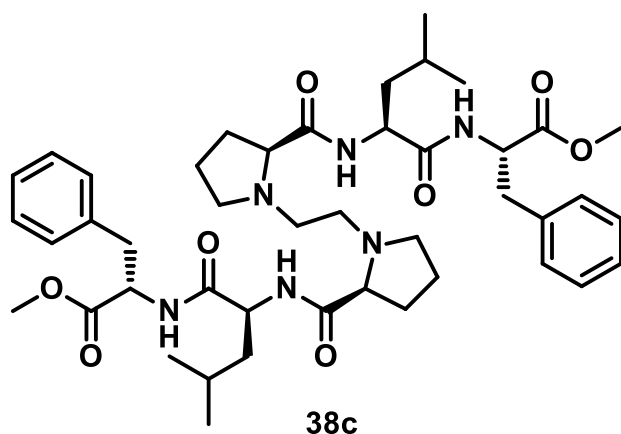


Phe-Ala-Pro-Propyl-Pro-Ala-Phe

Phe-Ala-Pro-Propyl-Pro-Ala-Phe (**39b**): 60 mg of (62%) of pure product was isolated as gelatinous colourless thick liquid. ^1H NMR (400 MHz, CDCl_3) δ 7.80 (d, $J = 6.8$ Hz, 2H), 7.36 – 7.15 (m, 6H), 7.09 (d, $J = 7.0$ Hz, 4H), 6.78 (d, $J = 4.4$

Hz, 2H), 4.74 (dd, $J = 13.5, 6.4$ Hz, 2H), 4.41 (dd, $J = 14.5, 7.2$ Hz, 2H), 3.67 (s, 6H), 3.13 (dd, $J = 16.8, 6.7$ Hz, 2H), 3.09 – 3.01 (m, 3H), 3.01 – 2.90 (m, 2H), 2.40 (d, $J = 7.3$ Hz, 3H), 2.32 – 2.19 (m, 3H), 2.13 (dd, $J = 20.5, 10.0$ Hz, 3H), 1.86 – 1.61 (m, 6H), 1.60 – 1.45 (m, 2H),

1.32 (t, $J = 7.4$ Hz, 6H). ^{13}C NMR (101 MHz, CDCl_3) δ 171.95, 171.68, 135.85, 129.15, 128.47, 126.98, 67.54, 53.80, 53.45, 52.21, 48.47, 37.83, 31.82, 30.25, 23.88, 23.39, 22.58, 17.97. Mass (ESI-TOF) m/z : found 735.4007

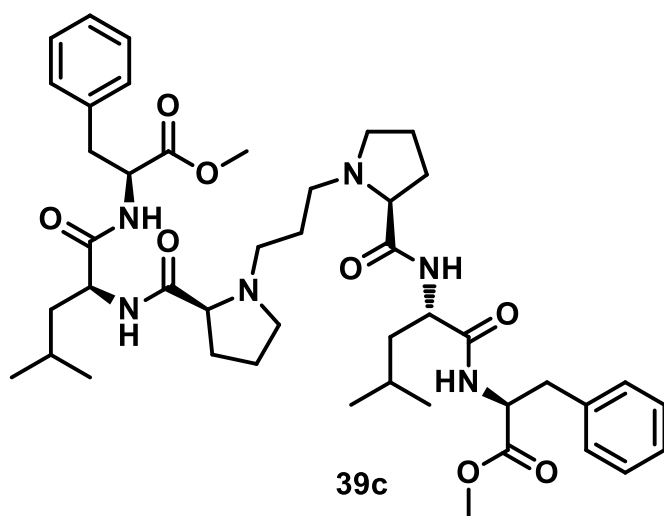


Phe-Leu-Pro-Ethyl-Pro-Leu-Phe

Phe-Leu-Pro-Ethyl-Pro-Leu-Phe (38c): 50 mg of (55%) of pure product was isolated as gelatinous colourless thick liquid. ^1H NMR (400 MHz, CDCl_3) δ 8.04 (d, $J = 8.3$ Hz, 2H), 7.24 – 7.14 (m, 10H), 6.76 (d, $J = 7.9$ Hz, 2H), 4.61 (dd, $J = 14.8, 8.4$ Hz, 2H), 4.50 (td, $J = 8.3, 5.4$ Hz, 3H), 3.64 (s, 6H),

3.12 (dd, $J = 13.9, 6.3$ Hz, 4H), 3.08 – 2.93 (m, 6H), 2.93 – 2.81 (m, 2H), 2.65 – 2.50 (m, 2H), 2.48 – 2.36 (m, 3H), 2.34 – 2.07 (m, 6H), 2.07 – 1.89 (m, 4H), 1.70 – 1.50 (m, 10H), 0.97 – 0.81 (m, 12H). ^{13}C NMR (101 MHz, CDCl_3) δ 175.17, 172.90, 170.86, 136.96, 129.30, 129.25, 128.53, 128.37, 126.73, 67.59, 54.75, 54.16, 53.49, 52.17, 50.83, 42.12, 41.23, 37.70, 33.76, 31.86, 30.34, 29.30, 29.10, 28.29, 28.30, 24.75, 23.94, 23.43, 22.64, 21.93. Mass (ESI-TOF) m/z : found 805.4806.

Phe-Leu-Pro-Propyl-Pro-Leu-Phe (39c):



Phe-Leu-Pro-Propyl-Pro-Leu-Phe

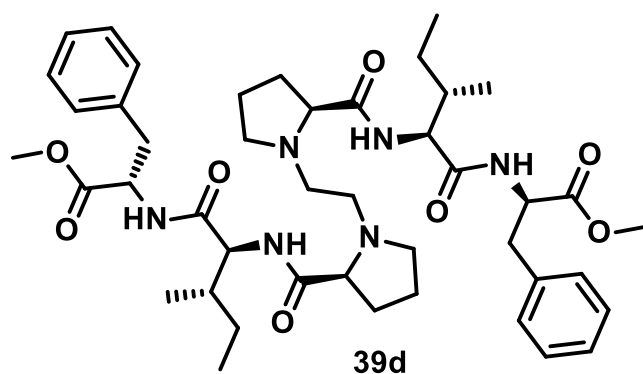
110 mg of (70%) of pure product was isolated as gelatinous colourless thick liquid. ^1H NMR (400 MHz, CDCl_3) δ 7.83 (d, $J = 7.9$ Hz, 2H), 7.32 – 7.12 (m, 10H), 6.86 (s, 2H), 4.61 (dd, $J = 14.7, 8.1$ Hz, 2H), 4.55 – 4.41 (m, 2H), 3.67 (s, 6H), 3.12 (dt, $J = 15.8, 8.0$ Hz, 2H), 3.01 (dd, $J = 23.0, 9.6$ Hz, 4H), 2.94 (d, $J = 20.0$ Hz, 2H), 2.36 (m, 5H), 2.20 (d,

$J = 5.5$ Hz, 2H), 2.07 – 1.88 (m, 2H), 1.78 – 1.42 (m, 10H), 0.87 (dd, $J = 18.5, 4.7$ Hz, 12H).

^{13}C NMR (101 MHz, CDCl_3) δ 175.36, 172.79, 171.61, 170.66, 136.74, 136.58, 129.40, 129.22, 129.14, 129.00, 128.42, 128.35, 126.92, 126.72, 67.37, 58.88, 53.58, 53.40, 52.11, 50.76, 41.12, 37.71, 37.47, 31.79, 30.32, 29.22, 24.77, 24.67, 24.01, 22.79, 22.66, 22.56, 21.83, 21.68. Mass (ESI-TOF) m/z : found 819.4842.

Phe-Ile-Pro-Propyl-Pro-Ile-Phe (**39d**):

40 mg of (50%) of pure product was isolated



Phe-Ile-Pro-Ethyl-Pro-Ile-Phe

as gelatinous colourless thick liquid. ^1H

NMR (400 MHz, CDCl_3) δ 10.39 (d, $J = 8.3$ Hz, 2H), 7.33 – 7.26 (m, 2H), 7.26 – 7.17 (m, 4H), 7.16 – 7.06 (m, 4H), 6.52 (d, $J = 8.0$ Hz, 2H), 4.88 (dd, $J = 14.1, 6.2$ Hz, 2H), 4.37 (dd, $J = 8.4, 6.0$ Hz, 1H), 4.24 (dd, $J = 11.3, 5.1$ Hz, 3H), 3.70 (s, 6H),

3.20 – 2.97 (m, 6H), 2.27 – 1.80 (m, 11H), 1.48 – 1.33 (m, 3H), 1.16 – 1.00 (m, 3H), 0.96 – 0.76 (m, 12H). Mass (ESI-TOF) m/z : found 819.4848

5.5 References and Notes

1. Alberts, B.; Johnson, A.; Lewis, J.; Raff, M.; Roberts, K.; Walter, P. *Molecular Biology of the Cell*, 4th ed.; Garland Science: New York, NY, 2002.
2. *Foldamer: Structure, Properties and Applications*; Hecht, S., Huc, I., Eds.; Wiley-VCH: Weinheim, Germany, **2007**.
3. Seebach, D.; Gardiner, J. *Acc. Chem. Res.* **2008**, *41*, 1366.
4. Horne, W. S.; Gellman, S. H. *Acc. Chem. Res.* **2008**, *41*, 1399.
5. Kotha, S. *Acc. Chem. Res.* **2003**, *36*, 342.
6. Avan, I.; Hall, C. D.; Katritzky, A. R. *Chem. Soc. Rev.* **2014**, *43*, 3575.
7. Pattabiraman, V. R.; Bode, J. W. *Nature*, **2011**, *480*, 471.
8. Choudhary, A.; Raines, R. T. *ChemBioChem*, **2011**, *12*, 1801.
9. Vlieghe, P.; Lisowski, V.; Martinez, J.; Khrestchatisky, M. *Drug Discov. Today* **2010**, *15*, 40.
10. Fosgerau, K.; Hoffmann, T. *Drug Discov. Today* **2015**, *20*, 122.
11. Erdmann, R. S.; Wennemers, H. *J. Am. Chem. Soc.* **2012**, *134*, 17117.
12. Wilhelm, P.; Lewandowski, B.; Trapp, N.; Wennemers, H. *J. Am. Chem. Soc.* **2014**, *136*, 15829.
13. Siebler, C.; Maryasin, B.; Kuemin, M.; Erdmann, R. S.; Rigling, C.; Grünenfelder, C.; Ochsenfeld, C.; Wennemers, H. *Chem. Sci.* **2015**, *6*, 6725.
14. Lewandowski, B.; Wennemers, H. *Curr. Opin. Chem. Biol.* **2014**, *22*, 40.
15. Duschmale, J.; Kohrt, S.; Wennemers, H. *Chem. Commun.* **2014**, *50*, 8109.

16. Nielsen, P. E.; Egholm, M.; Berg, R. H.; Buchardt, O. *Science*. **1991**, 254, 1497.
17. Sharma, N. K.; Ganesh, K. N. *Chem. Commun.* **2005**, 4330.
18. Kumar, V. A.; Ganesh, K. N.; *Acc. Chem. Res.* **2005**, 38, 404.
19. Pandey, A. K.; Naduthambi, D.; Thomas, K. M.; Zondlo, N. J. *J. Am. Chem. Soc.* **2013**, 135, 4333.
20. Newberry, R. W.; VanVeller, B.; Guzei, I. A.; Raines, R. T. *J. Am. Chem. Soc.* **2013**, 135, 7843.
21. Rechtes, M.; Gazit, E. *Science*, **2003**, 300, 625.
22. Langer, R.; Tirrell, D. A. *Nature*, **2004**, 428, 487.
23. Gazit, E. *Chem. Soc. Rev.* **2007**, 36, 1263.
24. Zelzer, M.; Ulijn, R. V. *Chem. Soc. Rev.*, 2010, **39**, 3351.
25. Adler-Abramovich, L.; Gazit, E. *Chem. Soc. Rev.* **2014**, 43, 6881.
26. Gazit, E. *Nat. Chem.* **2015**, 7, 14-15.
27. Frederix, P. W.; Scott, G. G.; Abul-Haija, Y. M.; Kalafatovic, D.; Pappas, C. G.; Javid, N.; Hunt, N. T.; Ulijn, R. V.; Tuttle, T. *Nat. Chem.* **2015**, 7, 30.
28. Marchesan, S.; Easton, C. D.; Kushkaki, F.; Waddington, L.; Hartley, P. G. *Chem. Commun.* **2012**, 48, 2195.
29. Roytman, R.; Adler-Abramovich, L.; Kumar, K. S. A.; Kuan, T.-C.; Lin, C.-C.; Gazit, E.; Brik, A. *Org. Biomol. Chem.* **2011**, 9, 5755.
30. Hauser, C. A. E.; Deng, R.; Mishra, A.; Loo, Y.; Khoe, U.; Zhuang, F.; Cheong, D. W.; Accardo, A.; Sullivan, M. B.; Riekel, C.; Ying, J. Y.; Hauser, U. A. *Proc. Natl. Acad. Sci. U. S. A.* **2011**, 108, 1361.

31. Javid, N.; Roy, S.; Zelzer, M.; Yang, Z.; Sefcik, J.; Ulijn, R. V. *Biomacromolecules* **2013**, *14*, 4368.
32. Thota, C. K.; Yadav, N.; Chauhan, V. S *Scientific Reports*. **2016**, *6*, 31167.
33. Dehsorkhi, A.; Castelletto, V.; Hamley, I. W. *J. Pept. Sci.* **2014**, *20*, 453.
34. Ligand syntheses, Yang, X.; Wu, X.; Fang, M.; Yuan, Q.; Fu, E. *Tetrahedron: Asymmetry* **2004**, *15*, 2491.
35. Yang, X.; Li, B.; Fu, E. *Synth. Commun.* **2005**, *35*, 271.
36. Roccatano, D.; Colombo, G.; Fioroni, M.; Mark, A. E. *Proc. Natl. Acad. Sci. U. S. A.* **2002**, *99*, 12179.

5.6 Appindix-5

Contents

1. NMR ($^1\text{H}/^{13}\text{C}$) and Mass spectra of <i>Phe-Gly-Pro-Ethyl-Pro-Gly-Phe</i> (38a):	426
2. NMR ($^1\text{H}/^{13}\text{C}$) and Mass spectra of <i>Phe-Gly-Pro-propyl-Pro-Gly-Phe</i> (39a):	428
3. NMR ($^1\text{H}/^{13}\text{C}$) and Mass spectra of <i>Phe-Ala-Pro-Ethyl-Pro-Ala-Phe</i> (38b):	430
4. NMR ($^1\text{H}/^{13}\text{C}$) and Mass spectra of <i>Phe-Ala-Pro-Propyl-Pro-Ala-Phe</i> (39b):	432
5. NMR ($^1\text{H}/^{13}\text{C}$) and Mass spectra of <i>Phe-Leu-Pro-Ethyl-Pro-Leu-Phe</i> (38c):	434
6. NMR ($^1\text{H}/^{13}\text{C}$) and Mass spectra of <i>Phe-Leu-Pro-Propyl-Pro-Leu-Phe</i> (39c):	436
7. Mass spectra of <i>Phe-Ile-Pro-Propyl-Pro-Ile-Phe</i> (39d):	438
8. NMR ($^1\text{H}/^{13}\text{C}$) and Mass spectra of <i>Pab-Pro-Ethyl-Pro-Pab</i> (38d):	439

1. NMR ($^1\text{H}/^{13}\text{C}$) and Mass spectra of *Phe-Gly-Pro-Ethyl-Pro-Gly-Phe* (**38a**):

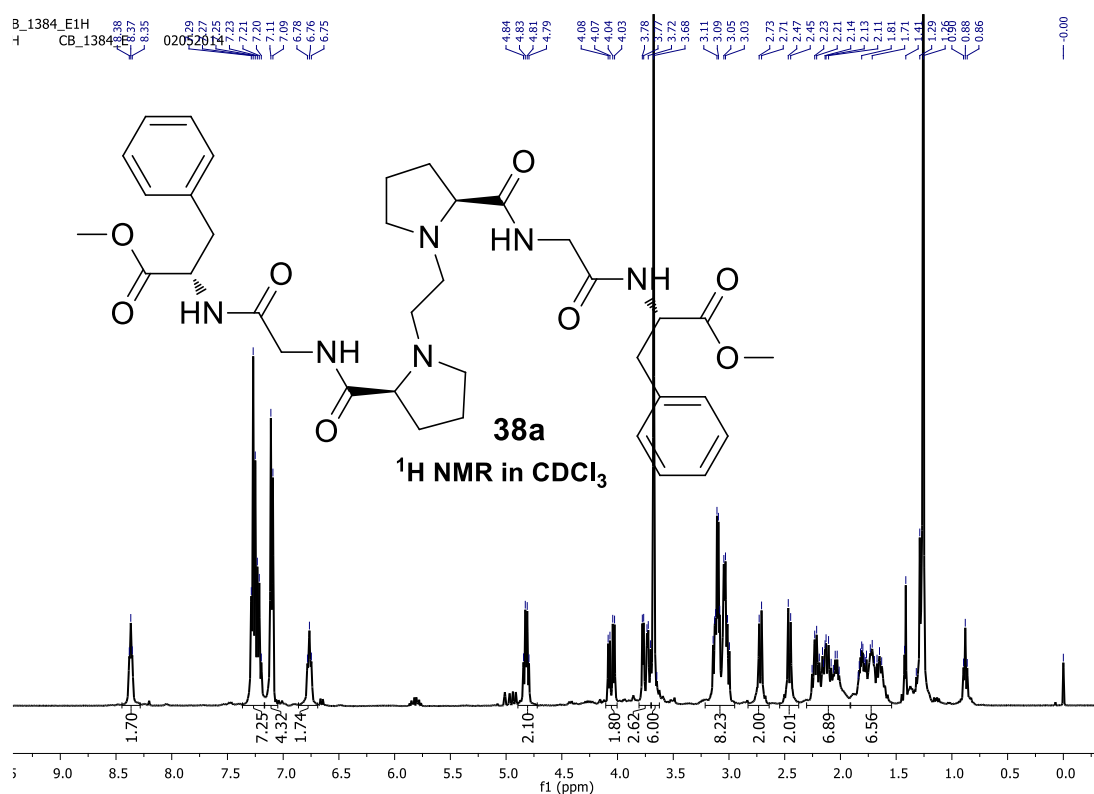


Figure A1. ^1H NMR of **38a** in CDCl_3

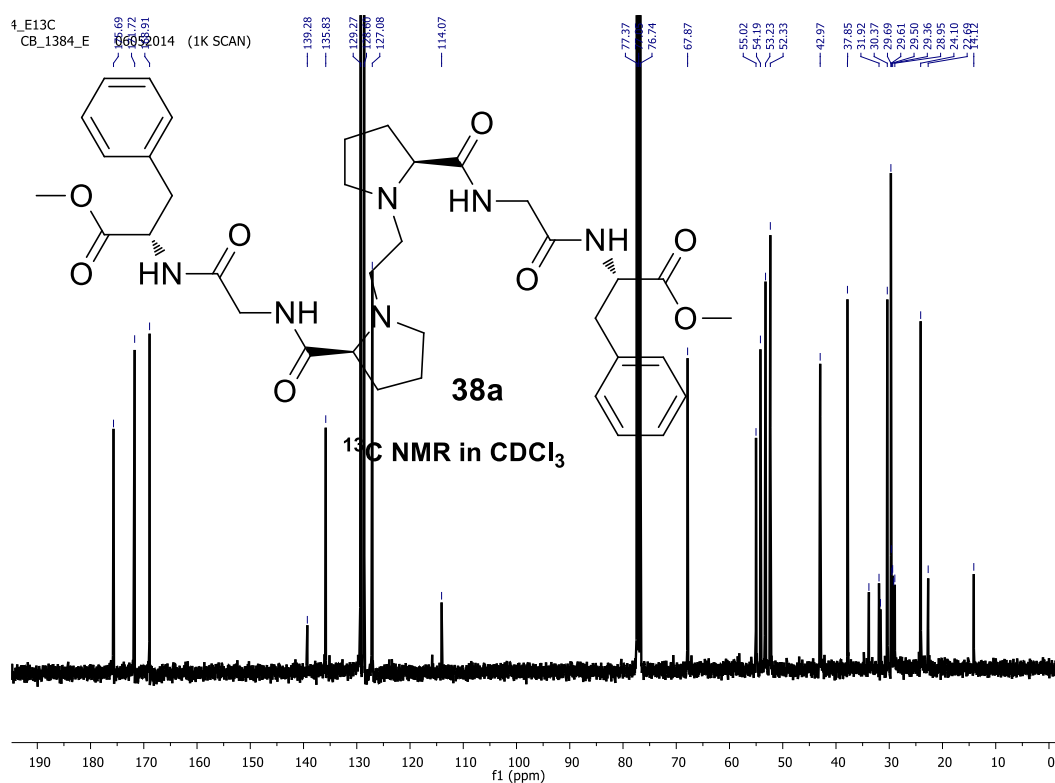


Figure A2. ^{13}C NMR of **38a** in CDCl_3

Generic Display Report

Analysis Info

Analysis Name D:\Data\FEB-2014\NKS\0602014_NKS_CB_ETHEX.d
Method Pos_tune_low.m
Sample Name ACN
Comment

Acquisition Date 2/6/2014 10:14:07 PM

Operator RAJKUMAR
Instrument microTOF-Q II

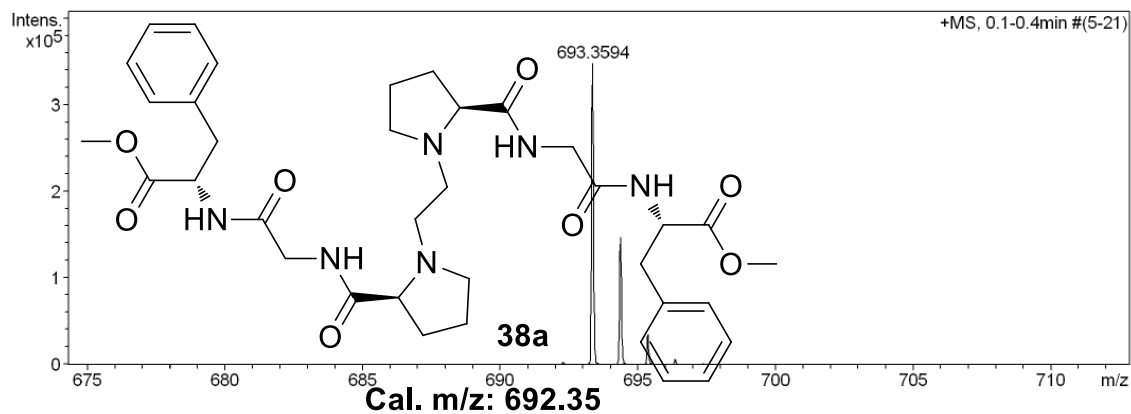
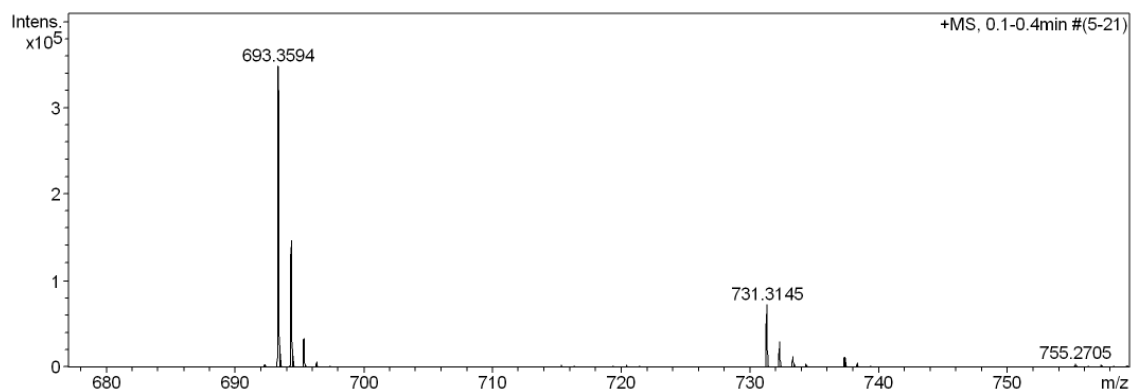
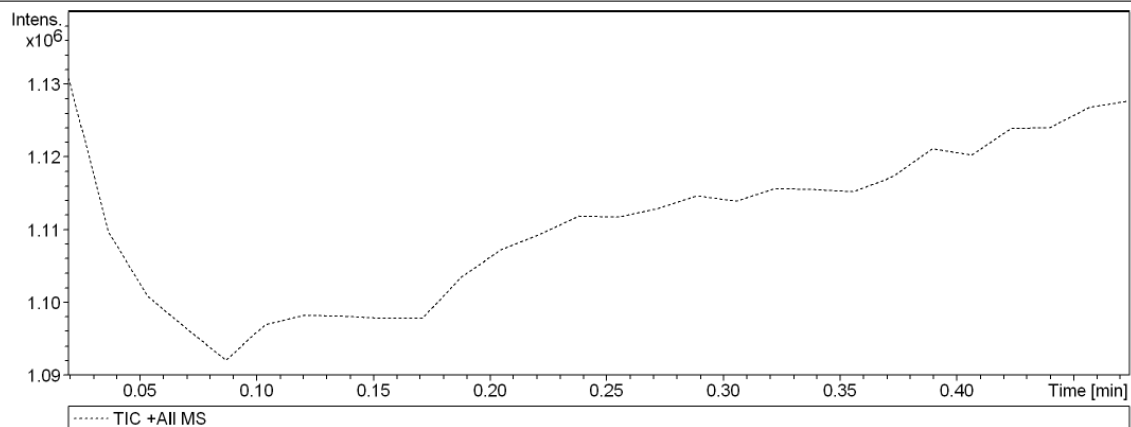


Figure A3. Mass spectrum of 38a

2. NMR ($^1\text{H}/^{13}\text{C}$) and Mass spectra of *Phe-Gly-Pro-propyl-Pro-Gly-Phe* (**39a**):

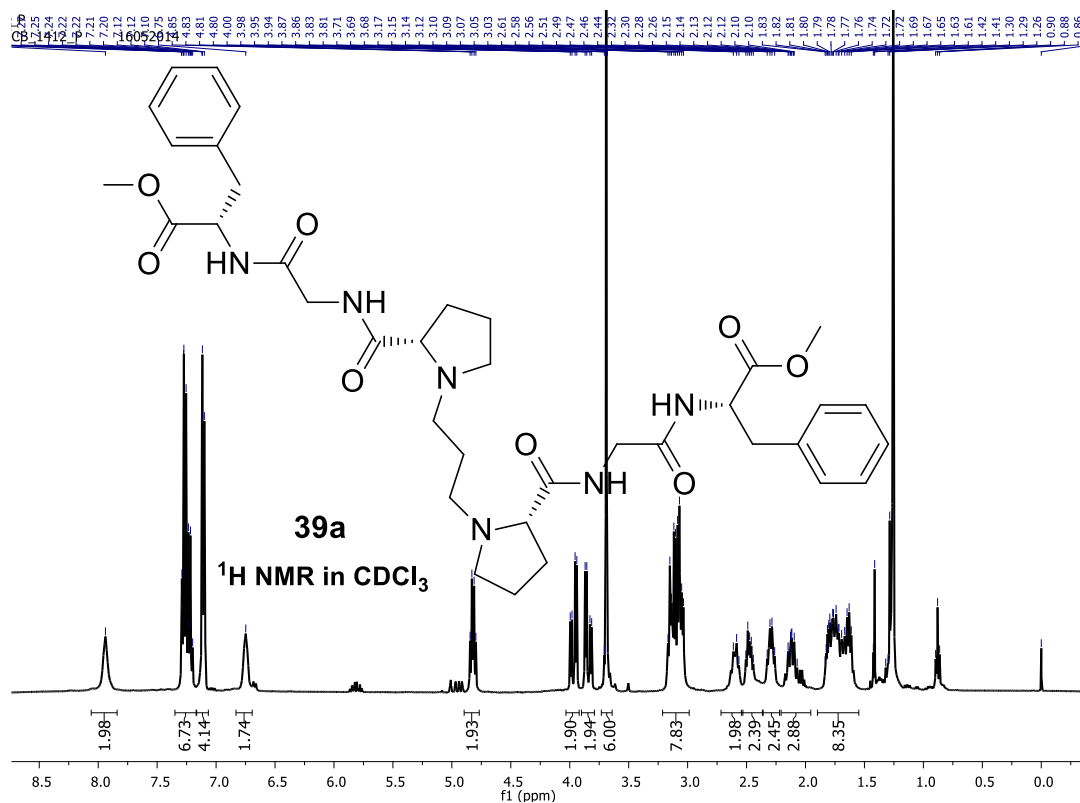


Figure A4. ^1H NMR of **39a** in CDCl_3

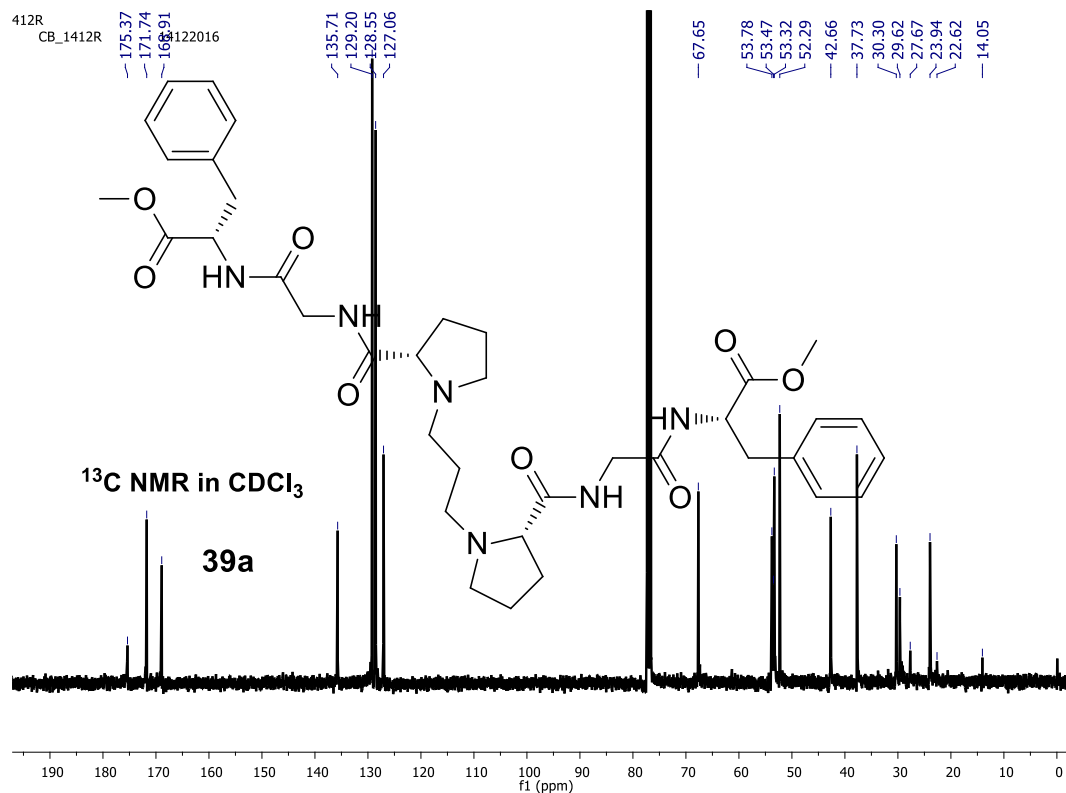


Figure A5. ^{13}C NMR of **39a** in CDCl_3

Generic Display Report

Analysis Info

Analysis Name D:\Data\APRIL-2014\INKS\29042014__NKS_CB_1412P.d
Method Pso_tune_wide.m
Sample Name
Comment

Acquisition Date 4/30/2014 9:34:18 AM

Operator A.S.Sahu
Instrument micrOTOF-Q II

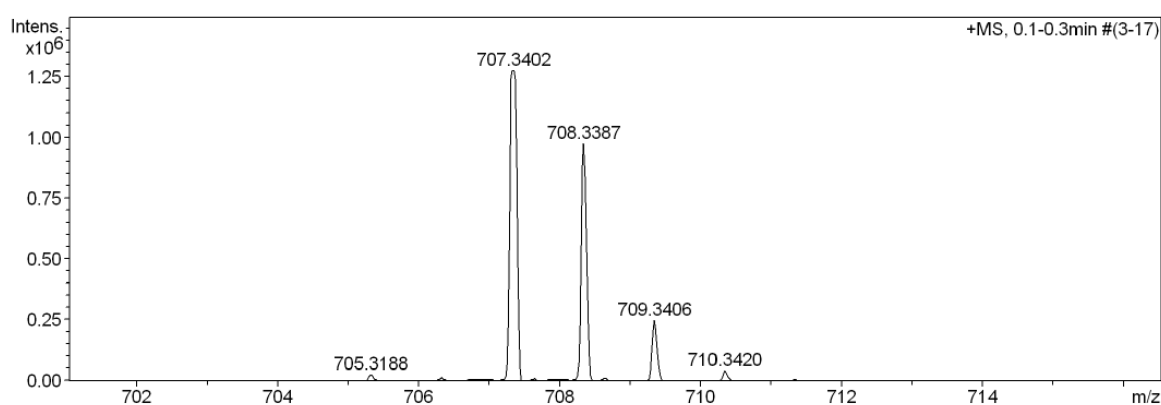
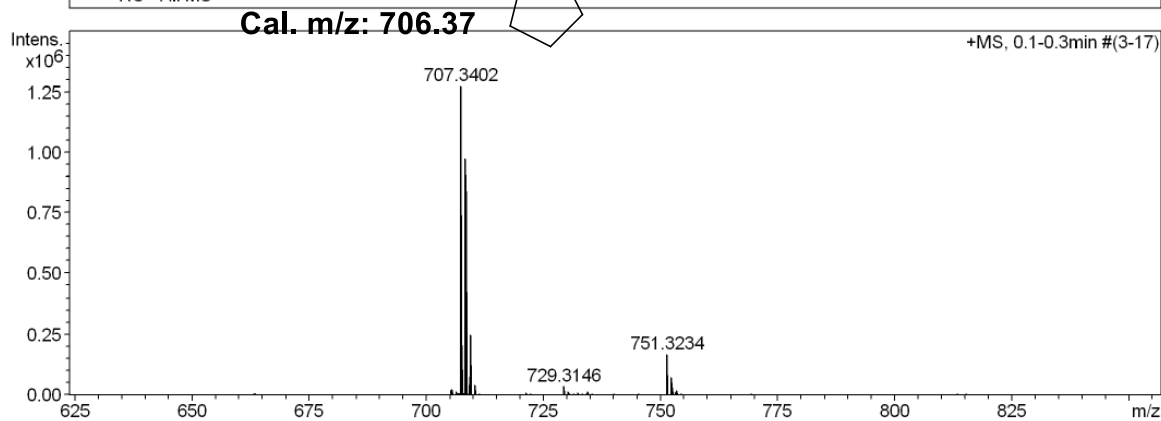
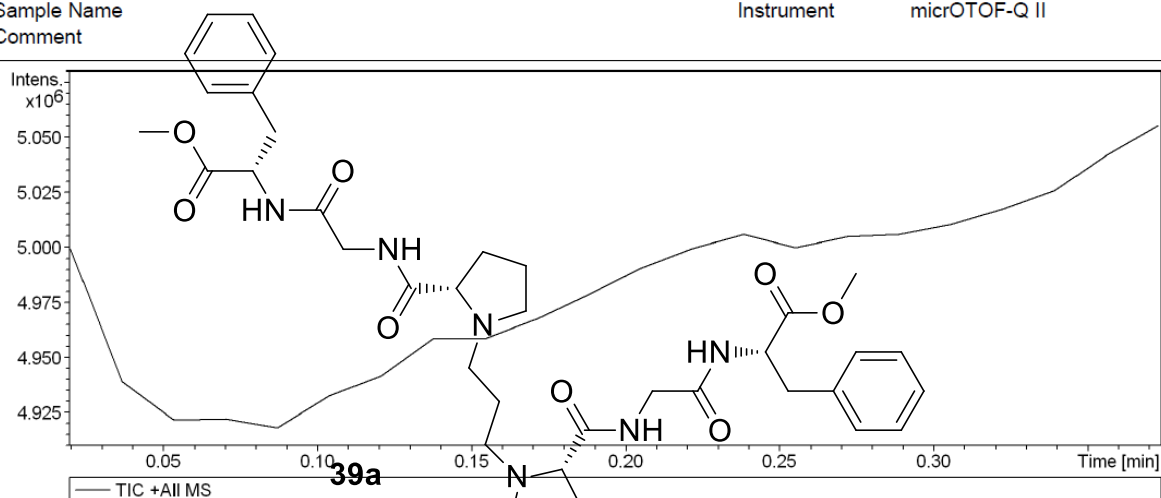


Figure A6. Mass spectrum of 39a

3. NMR ($^1\text{H}/^{13}\text{C}$) and Mass spectra of *Phe-Ala-Pro-Ethyl-Pro-Ala-Phe* (**38b**):

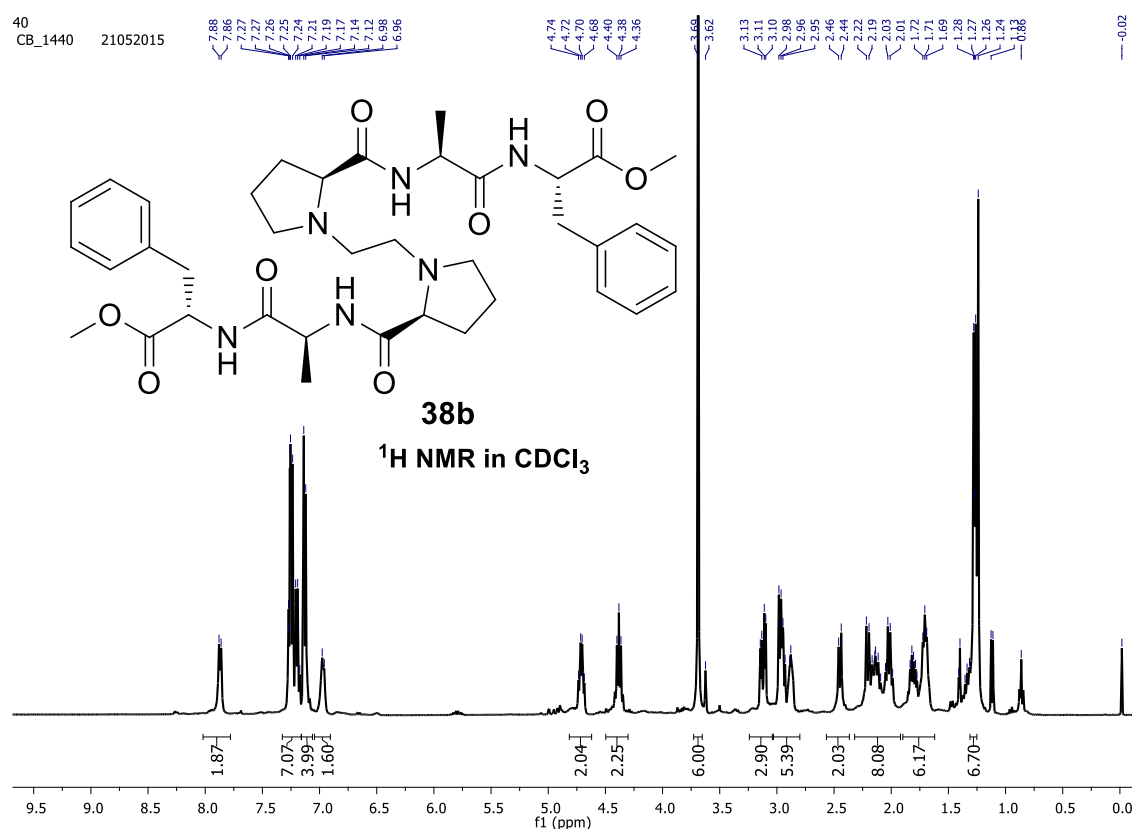


Figure A7. ^1H NMR of **38b** in CDCl_3

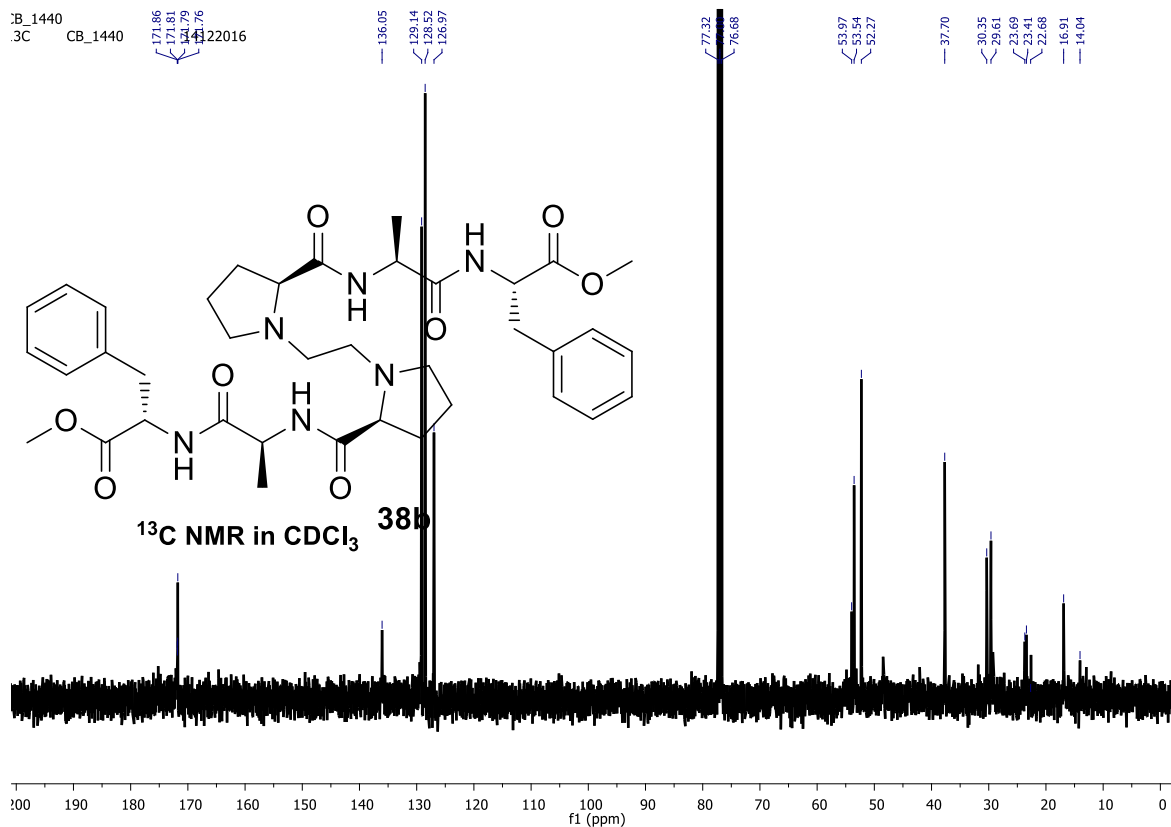


Figure A8. ^{13}C NMR of **38b** in CDCl_3

Generic Display Report

Analysis Info

Analysis Name D:\Data\MAY-2015\NKS\19052015_NKS_CB_PROALAPHEET.d
Method Pso_tune_wide.m
Sample Name NISER-LCMS
Comment

Acquisition Date 5/19/2015 1:26:48 PM

Operator NISER
Instrument micrOTOF-Q II

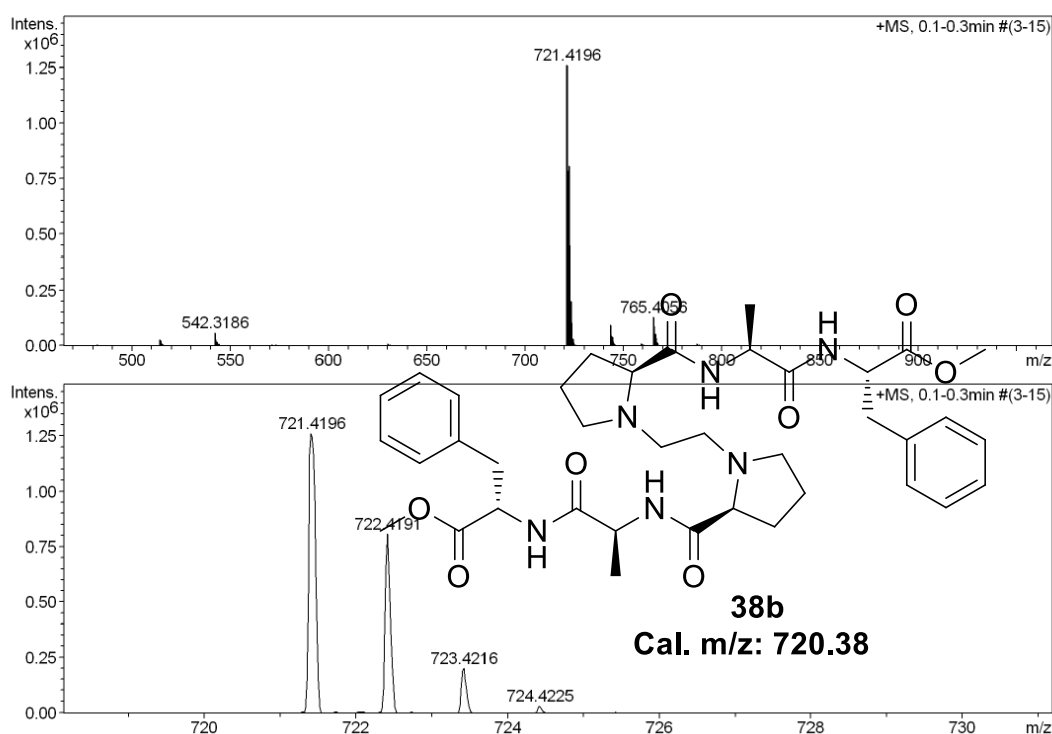
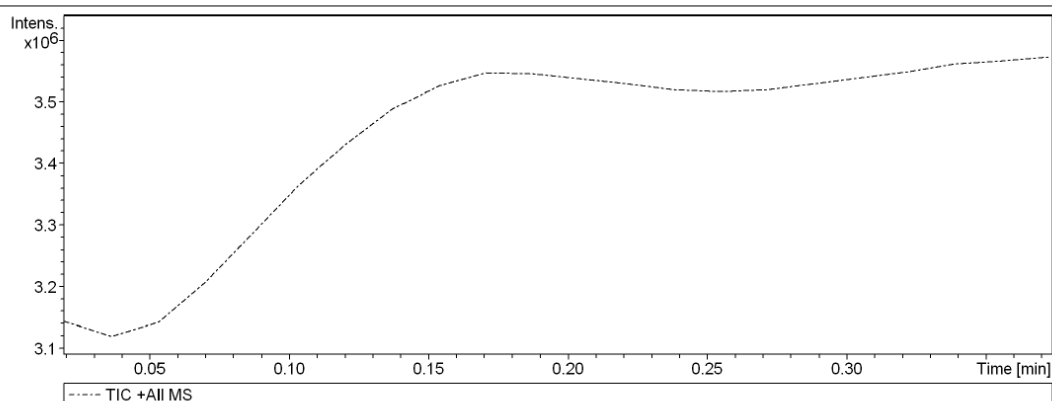


Figure A9. Mass spectrum of **38b**

4. NMR ($^1\text{H}/^{13}\text{C}$) and Mass spectra of *Phe-Ala-Pro-Propyl-Pro-Ala-Phe* (**39b**):

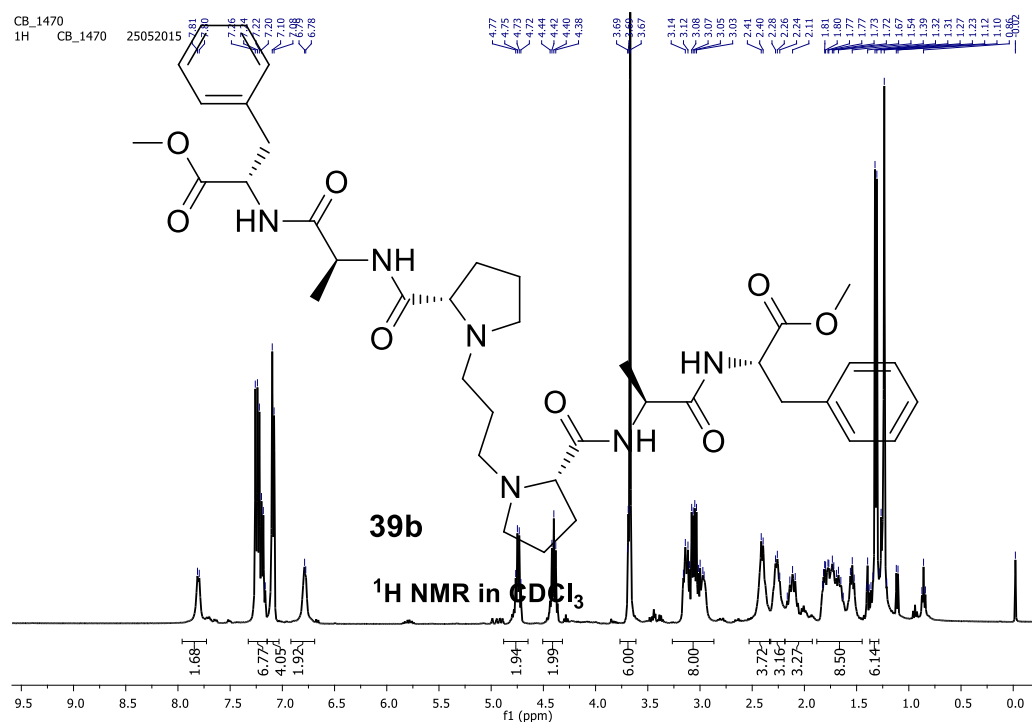


Figure A10. ^1H NMR of **39b** in CDCl_3

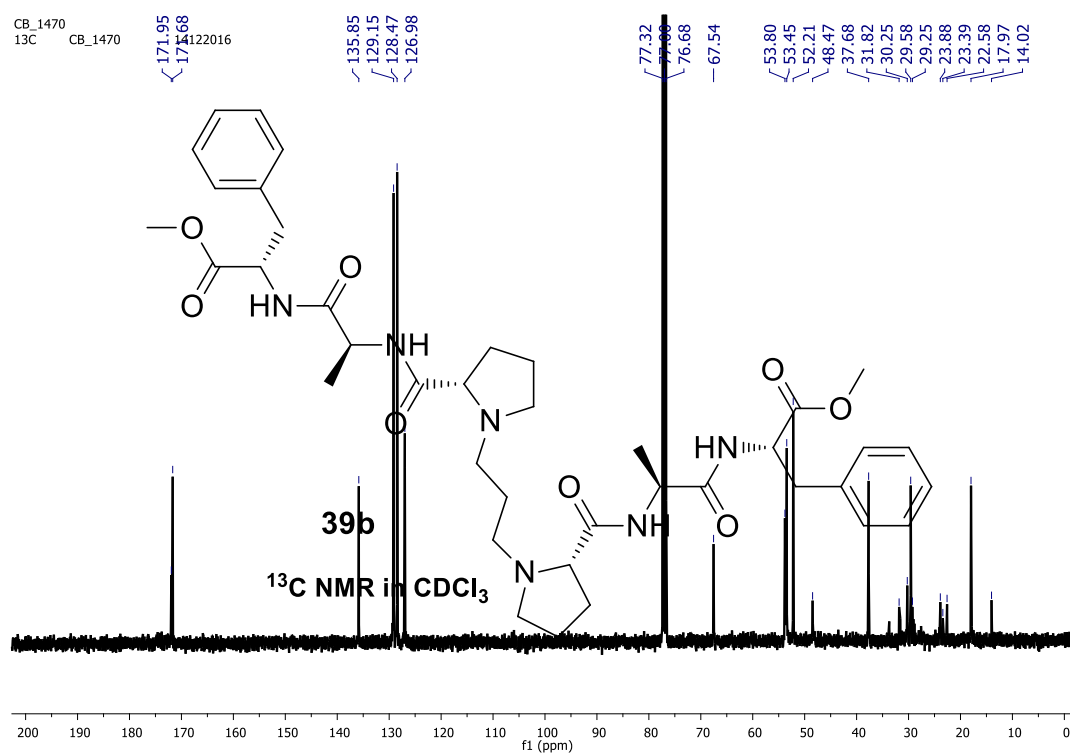


Figure A11. ^{13}C NMR of **39b** in CDCl_3

Generic Display Report

Analysis Info

Analysis Name D:\Data\MAY-2015\NKS\28052015_NKS_CB_1470.d
Method Pso_tune_wide.m
Sample Name NISER-LCMS
Comment

Acquisition Date 5/28/2015 1:30:26 PM

Operator NISER
Instrument micrOTOF-Q II

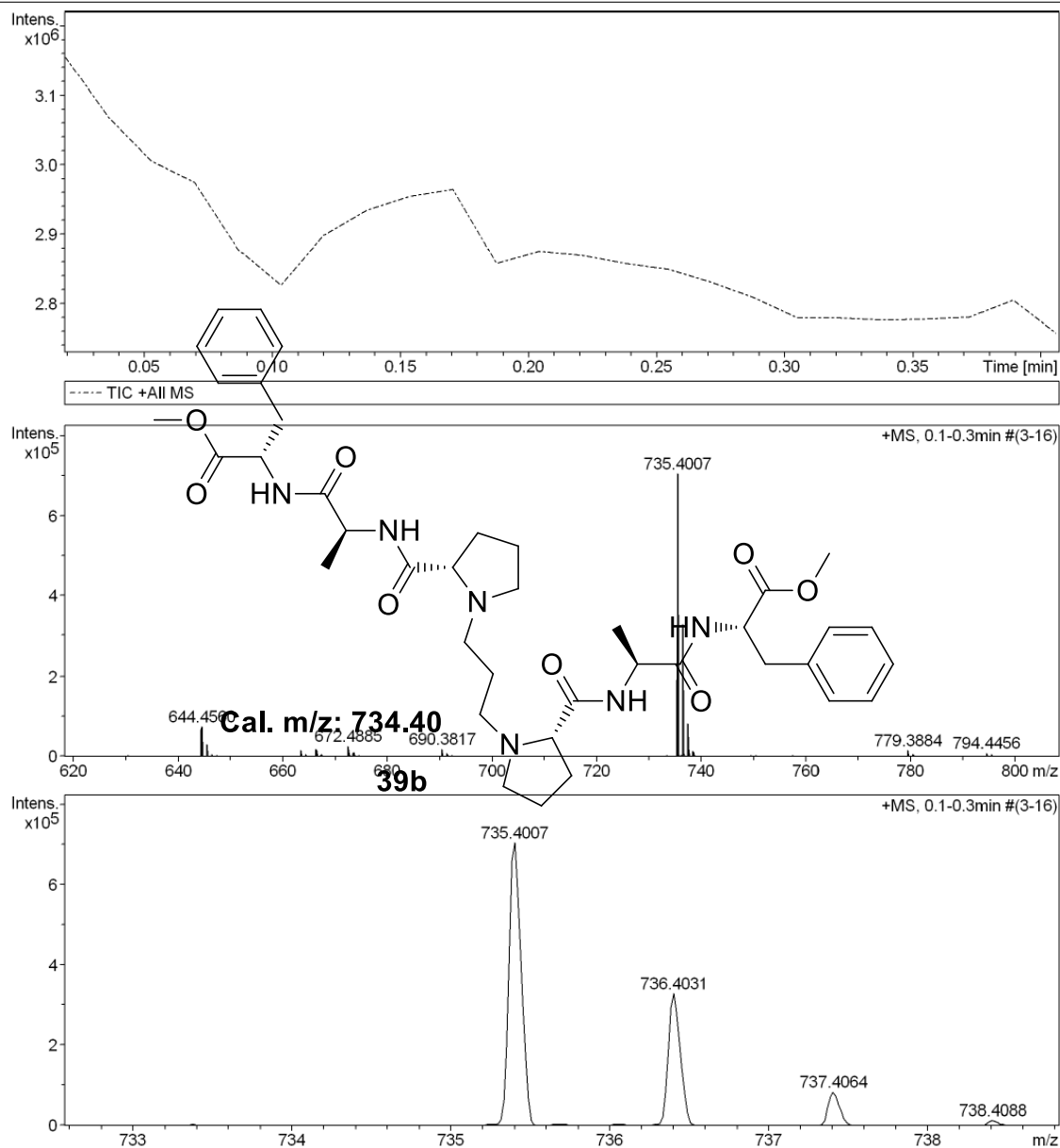


Figure A12. Mass spectrum of **39b**

5. NMR ($^1\text{H}/^{13}\text{C}$) and Mass spectra of *Phe-Leu-Pro-Ethyl-Pro-Leu-Phe* (**38c**):

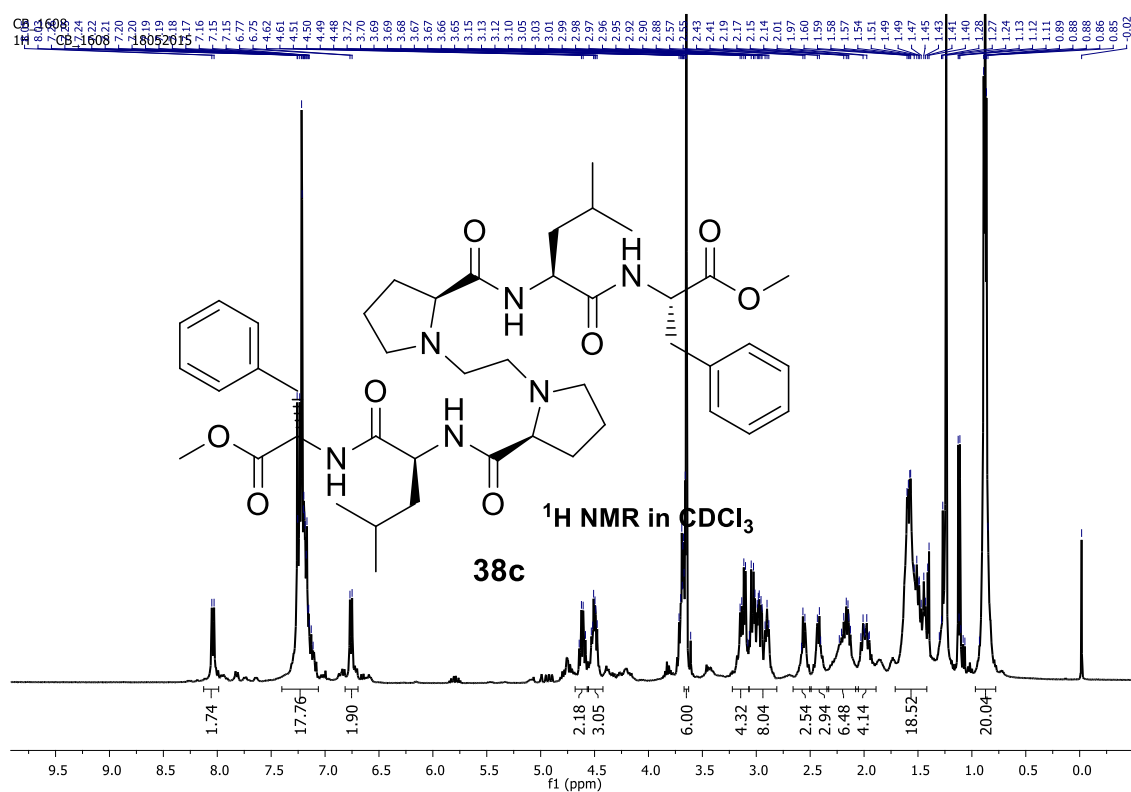


Figure A13. ^1H NMR of **38c** in CDCl_3

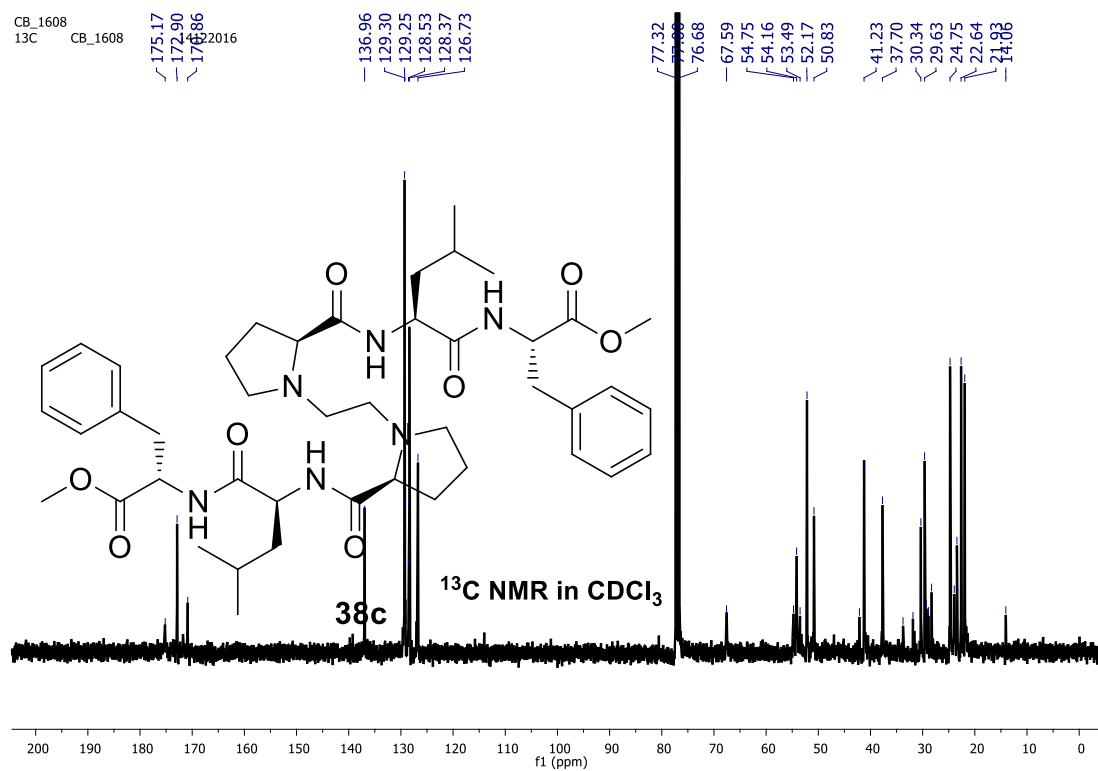


Figure A14. ^{13}C NMR of **38c** in CDCl_3

Generic Display Report

Analysis Info

Analysis Name D:\Data\MAY-2015\NKS\15052015_NKS_CB_PROLEUPHEET.d
Method Pso_tune_wide.m
Sample Name NISER-LCMS
Comment

Acquisition Date 5/15/2015 1:39:29 PM

Operator NISER
Instrument micrOTOF-Q II

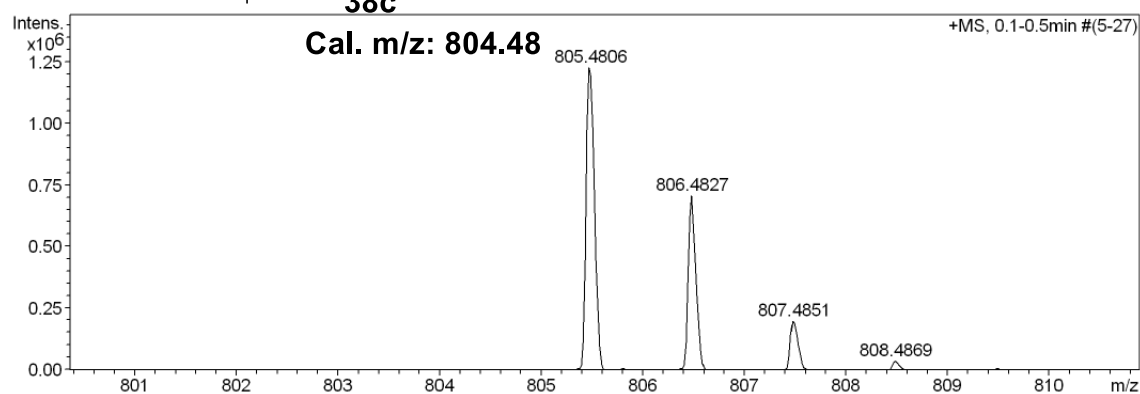
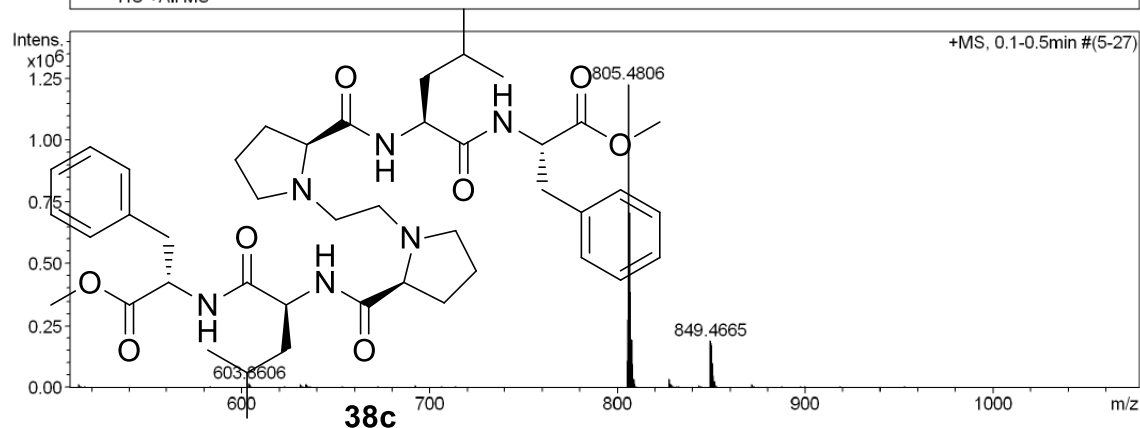
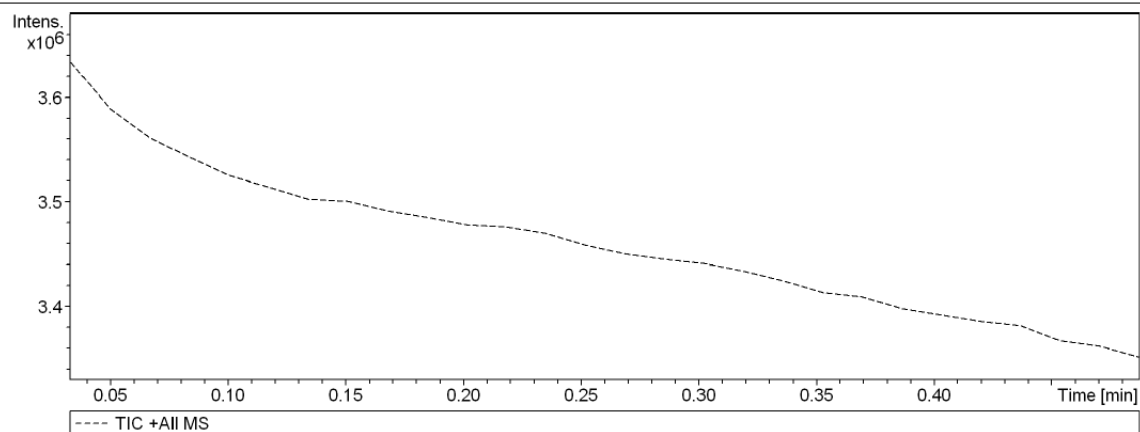


Figure A15. Mass spectrum of **38c**

6. NMR ($^1\text{H}/^{13}\text{C}$) and Mass spectra of *Phe-Leu-Pro-Propyl-Pro-Leu-Phe* (**39c**):

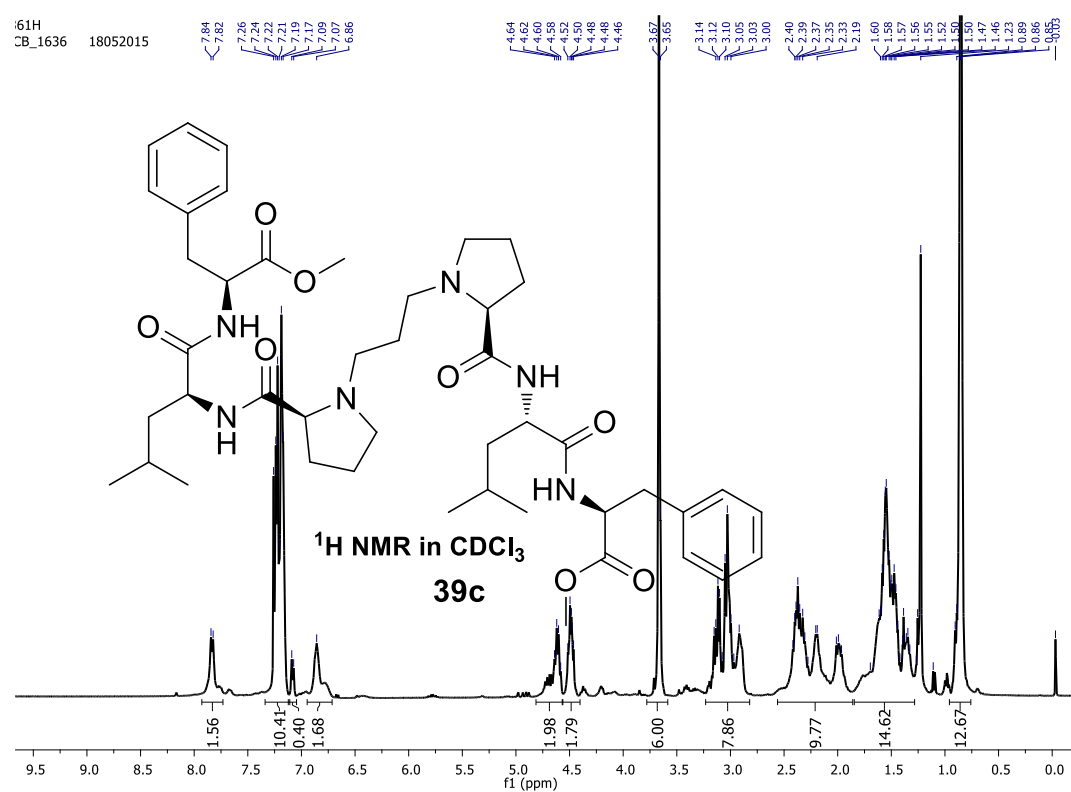


Figure A16. ^1H NMR of **39c** in CDCl_3

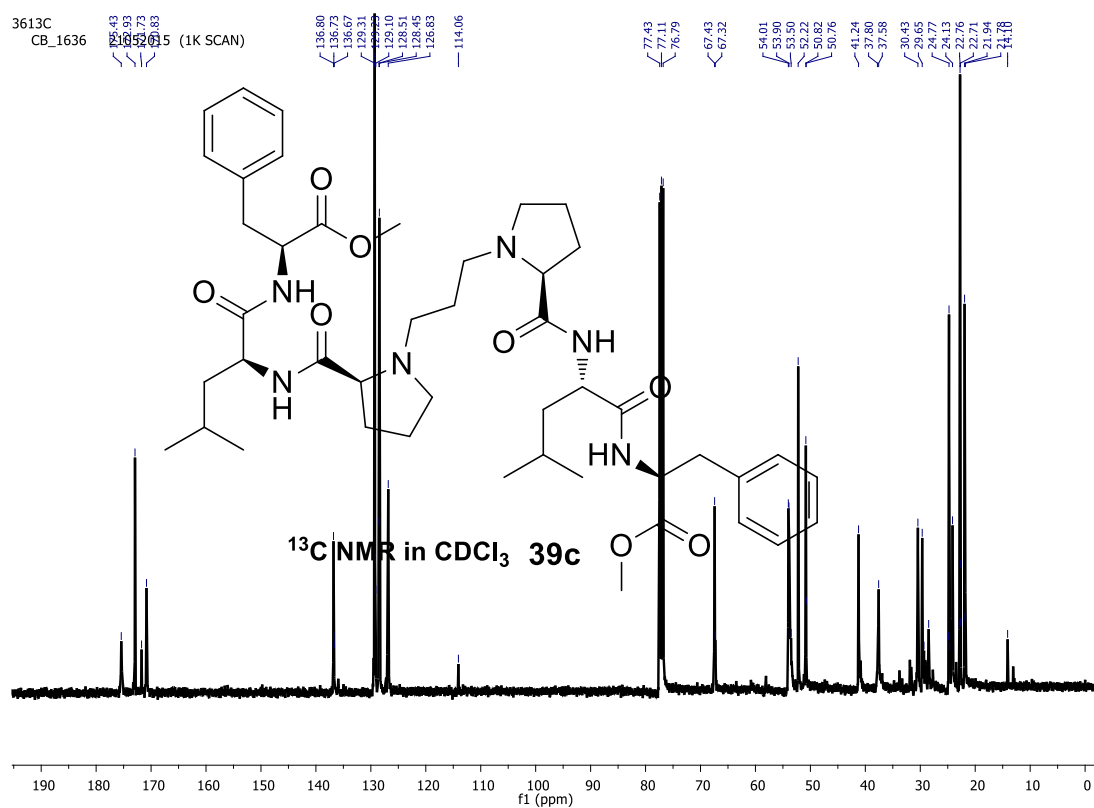


Figure A17. ^{13}C NMR of **39c** in CDCl_3

Generic Display Report

Analysis Info

Analysis Name D:\Data\MAY-2015\NKS\07052015_NKS_CB_PLEUPHEPROP.d
Method Pso_tune_wide.m
Sample Name NISER-LCMS
Comment

Acquisition Date 5/7/2015 4:40:50 PM

Operator NISER

Instrument microTOF-Q II

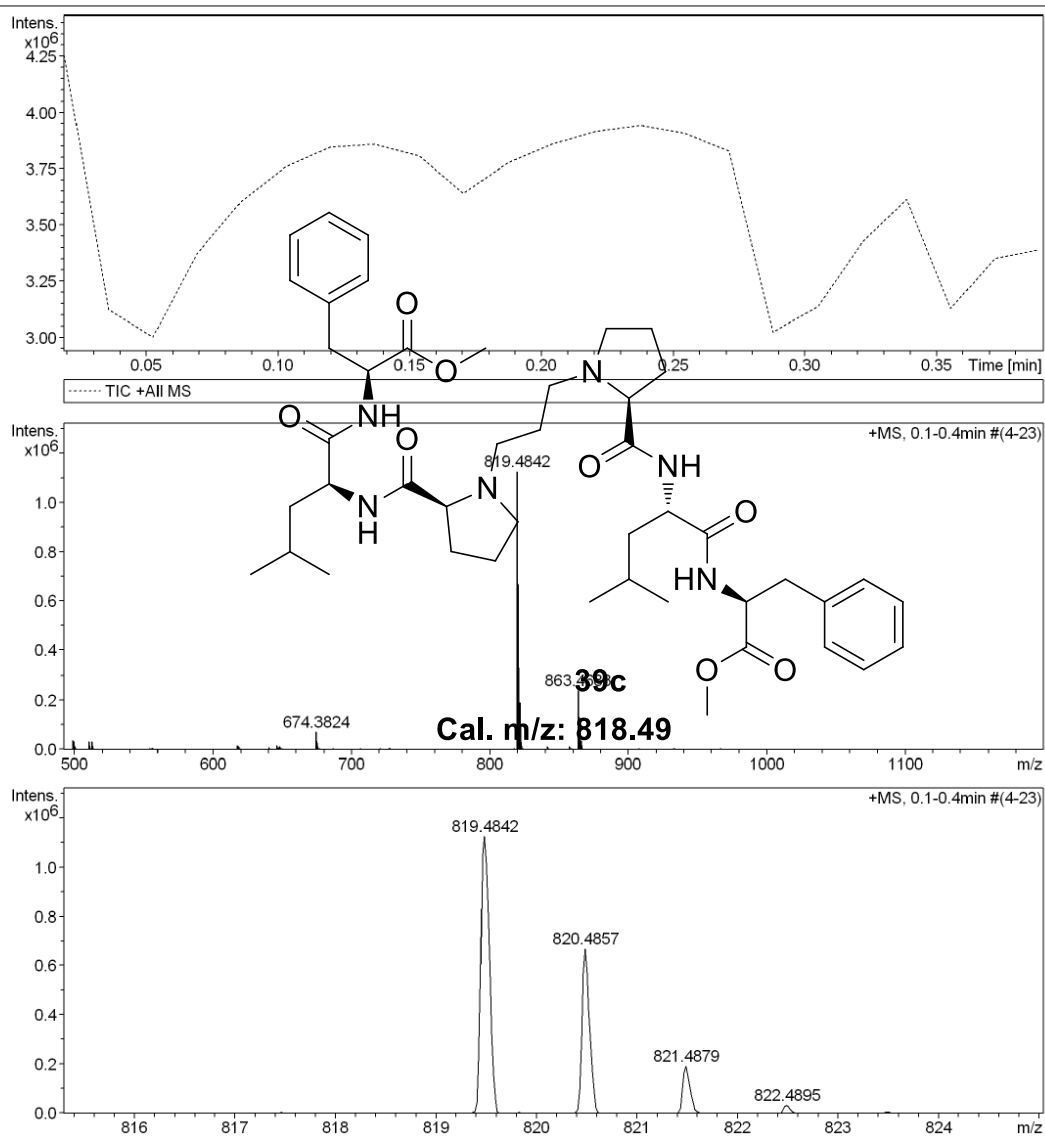


Figure A18. Mass spectrum of **39c**

7. Mass spectra of *Phe-Ile-Pro-Propyl-Pro-Ile-Phe* (**39d**):

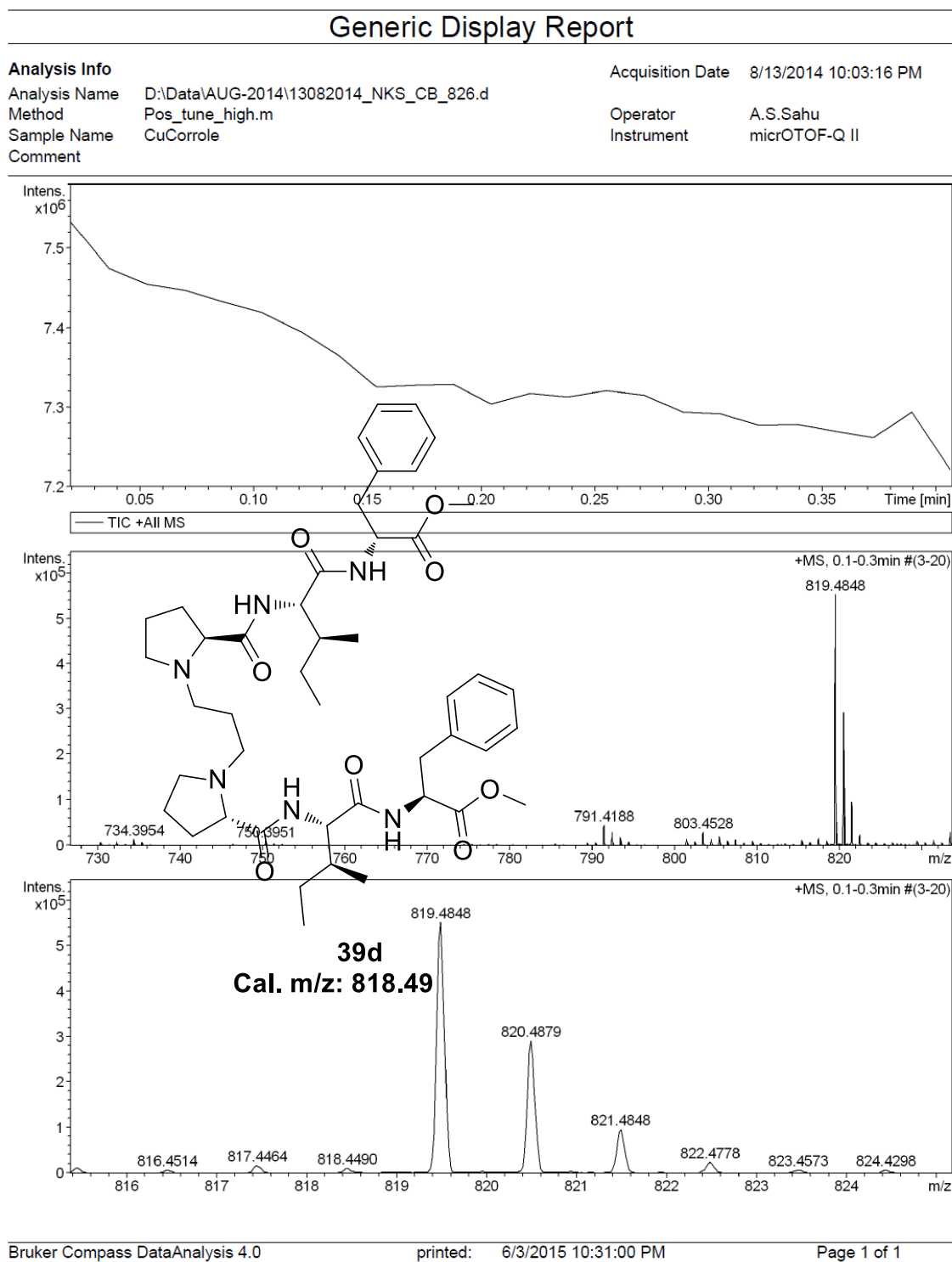


Figure A19. Mass spectrum of **39d**

8. NMR ($^1\text{H}/^{13}\text{C}$) and Mass spectra of *Pab-Pro-Ethyl-Pro-Pab* (**38d**):

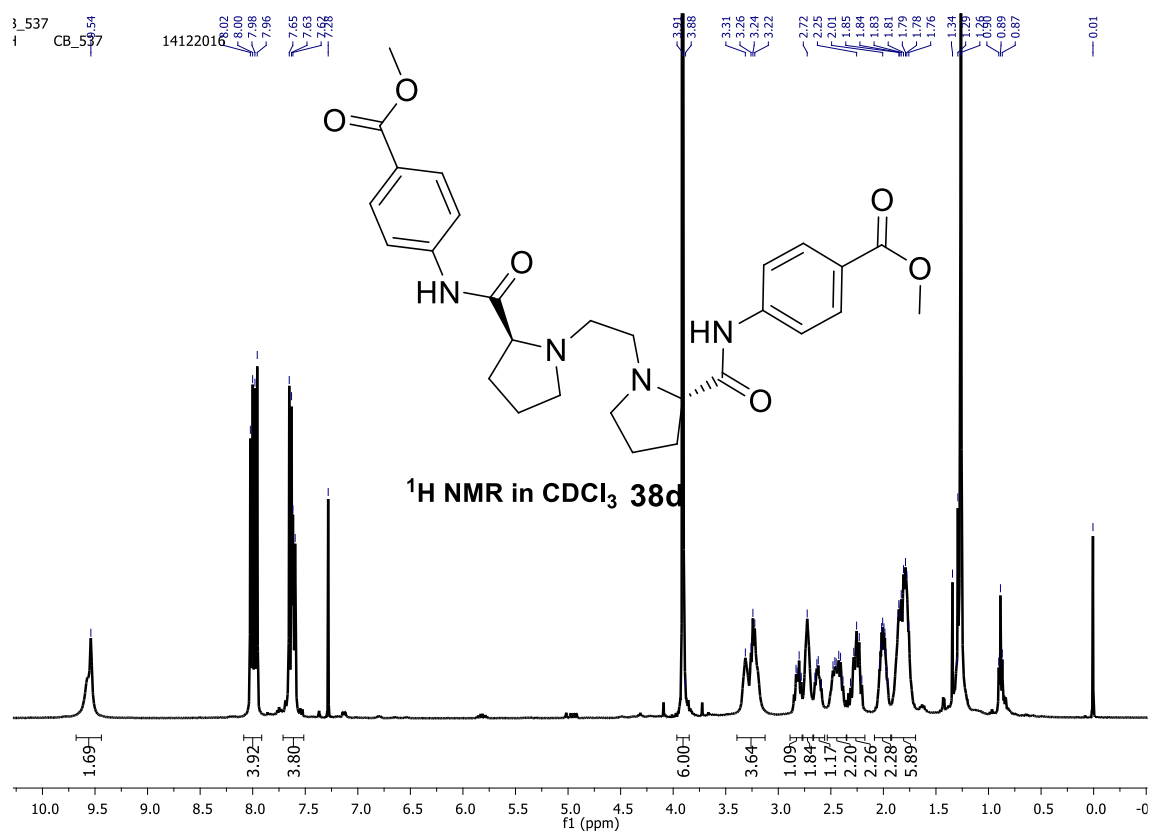


Figure A20. ^1H NMR of **38d** in CDCl_3

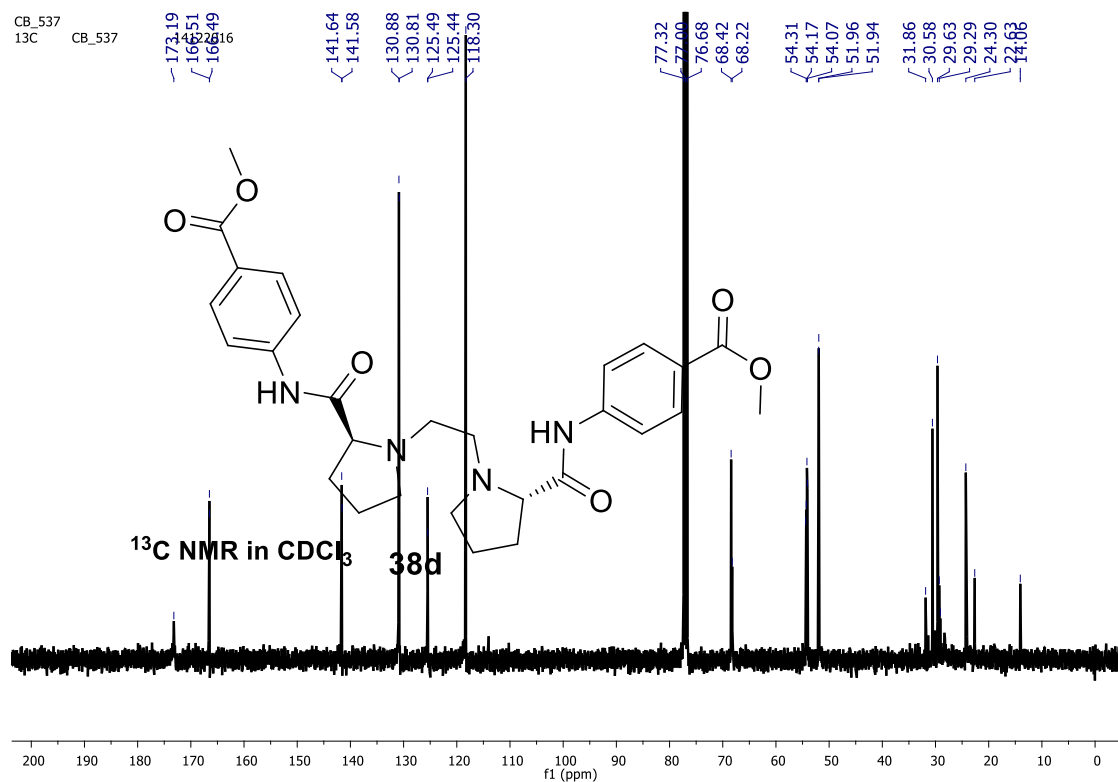


Figure A21. ^{13}C NMR of **38d** in CDCl_3

Thesis Summary

We have successfully synthesized the designed new unnatural δ -amino acid, Troponyl aminoethylglycine (*Traeg*) containing troponyl moiety as substituent on aminoethylglycine backbone. The formation of eight-membered ring hydrogen bonding between the troponyl carbonyl and adjacent amide NH is established.

An unusual cleavage of the amide bond derived from *Traeg*-aa under mild acidic conditions is established. The *Traeg* derived amide was cleaved into ester in alcoholic solvents and in acetonitrile, cationic troponyl lactone was obtained. In fact, the formation of cationic troponyl lactone from *Traeg* amide and other *N*-alkyl troponylglycinate amides is also an unusual and interesting transformation. Further, cationic troponyl lactone facilitated reversible amidation is established. So far, there no reports on such reversible amidation. Most interestingly, direct conversion of *N*-alkyl troponylglycinate esters into amides *via* cationic troponyl lactone without peptide coupling reagents is established at room temperature. The advantage with troponylglycinate esters is, they can be easily attached to free amine via amide bond and easily cleavable. Hence, *N*-alkyl troponylglycinates could be used as protecting groups for amine functionality of bioactive molecules.

Moreover, we have probed the *Traeg* derived amide and ester cleavage mechanism by suitable control experiments. Finally, the role of troponyl ring and glycinate methylene group is established by entrapping deuterium at glycinate methylene group.

Boron-aminotroponimines were successfully synthesized as novel fluorophores containing tropolonoid aromatic system. The photophysical properties of boron-aminotroponimines are examined. Syntheses of cyclic aminotroponimines and their fluorescent properties are also demonstrated.

Syntheses of sequence symmetric *hexa*-peptides by connecting proline tri-peptides at *N*-terminus through C-N bond by using alkyl linkers is established. Circular Dicroism studies revealed that these peptides are most probably aggregating at high concentration. Hence, this method could be useful for the syntheses of peptides for applications in nanomaterial fabrication.



Synthesis and conformational analysis of new troponyl aromatic amino acid



Chenikkayala Balachandra, Nagendra K. Sharma*

School of Chemical Sciences, National Institute of Science Education and Research (NISER) IOP Campus, Sachivalaya Marg, Sainik School (P.O), Bhubaneswar 751005, Odisha, India

ARTICLE INFO

Article history:

Received 28 May 2014

Received in revised form 22 July 2014

Accepted 8 August 2014

Available online 14 August 2014

Keywords:

Tropolone

Aminotropone

Conformational analysis

Aminoethylglycine (aeg)

δ -Amino acid, hybrid peptide

ABSTRACT

Synthetic peptides are in huge demand in expansion of potential peptide mimics, which may have improved or comparable function as natural one. With these concerns, phenyl bearing aromatic amino acids and peptides has extensively explored, because phenyl residue has high probability in forming stable secondary structure, owing to the presence of an extra stabilizing factor as π – π non-covalent interactions. Apart from phenyl bearing benzenoid aromatic amino acids, a few non-benzenoid aromatic derivatives such as tropolone and related compounds are also occurred in nature, but troponyl containing amino acids and peptides are very poorly understood. Tropolonyl derivatives also contain carbonyl functional group, which may play an important role to provide stable conformation in peptide. Herein we report the synthesis, and conformational analysis of rationally designed new unnatural δ -amino acid, troponyl aminoethylglycine (*Tr-aeg*), which contains troponyl residue as side chain in flexible aminoethylglycine (*aeg*) amino acid backbone. We also demonstrate the role of troponyl carbonyl of *Tr-aeg* residue in hydrogen bonding with adjacent amide NH of their hybrid di/tri-peptides with NMR methods and DFT calculations. In future, *Tr-aeg* amino acid would be a potential building block in development of promisable peptide mimics.

© 2014 Elsevier Ltd. All rights reserved.

1. Introduction

Conformational analysis of a molecule defines the type of structural organization, which explain the functional behavior of that molecule.¹ In case of macromolecules, the conformation of building blocks has crucial role in controlling the overall functionality of molecules.² For an instance, the function of protein and enzyme relay on favorable conformation of their building block such as amino acid residue. The side chain functionality of that amino acid residue having stable conformation is also responsible in modulation of non-covalent interactions for being functional respective protein/enzymes.^{3,4} Due to variable side chain of amino acids residue, various non-covalent interactions are present in functional protein and enzymes. Among them, hydrogen bonding, one of the important non-covalent interactions, plays an important role to acquire the well defined structural organization in protein/enzymes.^{4,5} To improve the structural and functional properties, many synthetic peptide mimics have been synthesized from natural and unnatural amino acids and nicely explored.⁶ Some of these

peptide mimics have shown exceptional functional properties and then considered as therapeutics drug candidate.⁷ For ideal peptide mimic, the presence of following secondary structural elements-helices, turns and sheets are required in target peptide to adopt protein-like conformations and folding pattern.^{5,8} To meet these requirements, many unnatural synthetic peptides from non-natural amino acid, including backbone expanded amino acids such as β -, γ -,^{8–10} and δ -amino acid^{12,13} were synthesized and studied extensively to find the interesting structurally folding behaviors. Some of these synthetic peptides have shown promiseable folding behavior with significant secondary structural elements. It is also learnt that the substituent of synthetic amino acids (β -, γ - and δ -amino acid) analogues also play an important role in acquiring secondary structure by restricting their allowed conformational space. For an instance, β -alanine peptide reportedly forms random structures in solution phase, while sheet like packing in its solid state.¹⁴ However, the substituted ring constrained β -amino acid analogues, containing cycloalkane ring, also facilitate the formation of helical type of secondary structure formation in solid state.¹⁵ Interestingly, the synthetic peptides, even with four appropriate residues, reportedly form stable secondary structures and inhibit protein-protein interactions and other biological events.^{10,16} Some of the synthetic peptides have also shown high stability towards

* Corresponding author. Tel.: +91 674 230 4130; fax: +91 674 230 2436; e-mail addresses: nagendrar@niser.ac.in, nagendra@niser.ac.in (N.K. Sharma).

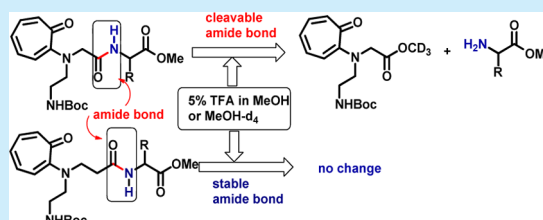
Instability of Amide Bond Comprising the 2-Aminotropone Moiety: Cleavable under Mild Acidic Conditions

Chenikkayala Balachandra and Nagendra K. Sharma*

School of Chemical Sciences, National Institute of Science Education and Research (NISER), IOP Campus, Sachivalaya Marg, Sainik School (P.O.), Bhubaneswar 751005, Odisha, India

S Supporting Information

ABSTRACT: An unusual hydrolysis/solvolysis of the classical acyclic amide bond, derived from *N*-troponylaminoethylglycine (*Traeg*) and α -amino acids, is described under mild acidic conditions. The reactivity of this amide bond is possibly owed to the protonation of the troponyl carbonyl functional group. The results suggest that the *Traeg* amino acid is a potential candidate for protecting and caging of the amine functional group of bioactive molecules via a cleavable amide bond.



The amide functional group has been known to be inert at neutral pH and room temperature for over 100 years.¹ However, enzymes (peptidases) hydrolyze the amide bond specifically and efficiently under physiological conditions. Hydrolysis of the amide bond requires drastic conditions such as elevated temperatures and extreme pH. At high pH, direct nucleophilic addition at the amide carbonyl followed by elimination of amine occurs, while at low pH, protonation of amide carbonyl is followed by nucleophilic addition with pronounced elimination of amine. In both cases, the reaction proceeds through a tetrahedral intermediate at the C atom of amide carbonyl.

Structurally, the classical acyclic amide bond (—NHCO—) is planar in nature, which is favorable for delocalization of nonbonding electrons of nitrogen toward the π -orbital of carbonyl.² As a result, the partial double bond character +N=C-O^- arises in the amide bond owing to resonance, which decreases the electrophilicity of the amide carbonyl group. In the case of ring-strained cyclic amides, the constituent atoms of the amide bond deviate from planarity, which results in poor delocalization of electrons and significantly decreases the partial double bond character of the amide bond. Subsequently, the reactivity of the amide carbonyl group increases toward nucleophilic addition reaction.

In the late 1990s, Kirby and co-workers reported the hydrolysis of the amide bond of 1-aza-2-adamantanone in the presence of water within 1 min, where the amide N-atom is at the bridgehead of the bicycle, which prevents amide resonance and diminishes the stability of the amide bond.³ The hydrolysis/solvolysis of bridged bicyclic lactams and acyclic distorted amides is influenced by the electronic and steric effects.

For two decades, there have been notable reports on metal-free⁴ and metal-mediated⁵ cleavage of acyclic amide bonds. The most fascinating among these is the Lloyd-Jones and Booker-Milburn activated acyclic amide (Figure 1A), which undergoes hydrolysis/solvolysis at room temperature in water/protic

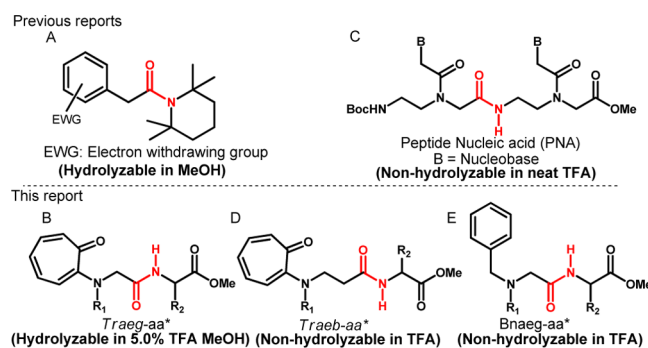


Figure 1. (A) Hydrolyzable amide bond (reported); (B) PNA with aeg-backbone (reported); (C, D) *Traeg* and *Traeb* peptides; (E) *Bnaeg* peptide.

solvents, respectively.^{1a,6} Importantly, the solvolysis of that acyclic amide reportedly relies on electron-withdrawing substituents at the α -C atom of amide carbonyl and steric crowding at the N-atom of amide amine. The hydrolyzable amide bond near physiological conditions could be applicable in protection/deprotection of carboxyl and amine functional groups in different environments. In the repertoire of unnatural aromatic amino acids/peptides, we explored the hydrogen bonding ability of troponyl carbonyl in unnatural peptides.⁸ In expansion of our previous studies, we have found an unusual instability of the amide bond containing 2-aminotropone moiety at α -C position of the amide carbonyl (Figure 1B).

Herein, we report the selective cleavage of the acyclic amide bond in peptide (*Traeg*-aa) under mild acidic conditions, which derived from *Traeg* and natural α -amino acid derivatives (Figure 1B). However, the amide bonds of structurally related peptides such as peptide nucleic acid (PNA) are stable like other acyclic amide bonds even in neat TFA (Figure 1C).⁷ For

Received: May 26, 2015

Published: August 7, 2015



Novel fluorophores: Syntheses and photophysical studies of boron-aminotroponimines

Chenikkayala Balachandra, Nagendra K. Sharma*

School of Chemical Sciences, National Institute of Science Education and Research (NISER), Jatani, 752050, Odisha, India



ARTICLE INFO

Article history:

Received 9 September 2016

Received in revised form

31 October 2016

Accepted 31 October 2016

Available online 1 November 2016

ABSTRACT

The syntheses and photophysical study of novel fluorescent boron-aminotroponimine complexes are described. The chemical structure of one of the boron complexes was confirmed by single crystal X-ray analysis, which shows the appearance of the distorted tetrahedral geometry at boron. The photophysical studies of these complexes revealed that the boron-aminotroponimines are fluorescent molecules with quantum yields ca. 0.17–0.28.

© 2016 Elsevier Ltd. All rights reserved.

1. Introduction

Troponone and tropolone chemical moieties are unique seven-membered ring non-benzenoid aromatic system present in many biologically active natural products [1]. The electronic structure of the tropolonoids is distinctive from the benzenoid aromatic compounds and have characteristic photophysical properties (absorption and emission) [2,4a–d]. However, notable fluorescence was observed with the bioactive tropolonoid natural product colchicine, comprising a methoxytroponone moiety, which has shown fluorescence after binding with the tubulin protein [3]. Later, fluorescent properties of tropolone were also explored, quantum yields of both tropolone and colchicine are very low at room temperature [4]. Moreover, substituted tropolone derivatives have shown fluorescence with enhanced quantum yields [5,6].

Aminotroponimines (Fig. 1A) are the synthetic aza-derivatives of tropolone, which are bidentate nitrogen chelating ligands [7a]. The aminotroponimine metal complexes are synthesized extensively and a few have been used as catalysts in selective organic transformation reactions [7,12]. Additionally, the synthesis of tropocoronands has also been elaborated, which are derived from cyclic aminotroponimines and metals [8]. However, the synthesis and hydrolytic stability of a few 2-bora-1,3-diazaazulene complexes have been reported in early 1962 but the fluorescent properties of these molecules are not explored so far [9]. On the other hand, Boron-Dipyrromethene (BODIPY, Fig. 1B) fluorescent dyes are widely explored [11,14e]. Importantly, organic fluorescent dyes are

enormously useful in different fields for many applications such as labeling agents [10a], chemical sensors [10b,c], cell imaging agents [10d] and energy related cassette entities [10e,f].

Overall, fluorescent molecules consisting of tropolonoid core structure are yet to be fully explored. Hence, it is important to develop the fluorescent molecules containing tropolonoid aromatic system.

The fluorescent properties of a few reported tropolonoids and boron-dipyrromethene complexes inspired us to design a set of novel organic fluorescent molecules, boron-aminotroponimines (Fig. 1C). These molecules are synthesized from aminotroponimine ligand, containing tropolonoid aromatic system, in place of dipyrromethene ligand of BODIPY complexes. However, boron-aminotroponimine core structure is a bicyclic core structure with the seven membered troponyl ring and a five membered ring, which is distinctive from BODIPY core structure. Herein, we report the syntheses of various boron-aminotroponimines and examine their photophysical properties.

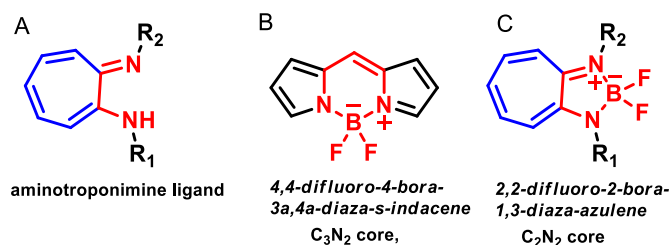


Fig. 1. Chemical structures of A) aminotroponimine ligand. B) boron dipyrromethene core. C) boron-aminotroponimine core (this work).

* Corresponding author.

E-mail address: nagendra@niser.ac.in (N.K. Sharma).